frontiers | Research Topics

Fungal wheat diseases: Etiology, breeding, and integrated management, volume II

Edited by
Maria Rosa Simon, Paul Christiaan Struik and Andreas Börner

Published in
Frontiers in Plant Science
Frontiers in Microbiology

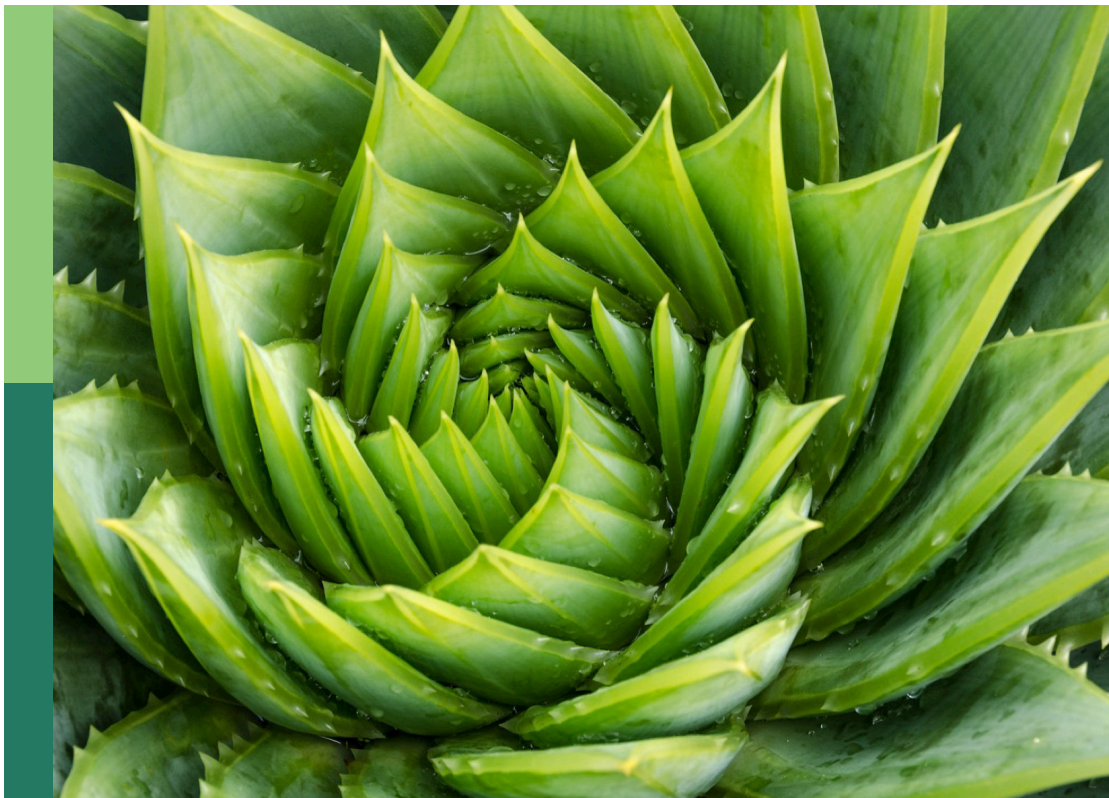

ISSN 1664-8714
ISBN 978-2-8325-3190-7
DOI 10.3389/978-2-8325-3190-7

About Frontiers

Frontiers is more than just an open access publisher of scholarly articles: it is a pioneering approach to the world of academia, radically improving the way scholarly research is managed. The grand vision of Frontiers is a world where all people have an equal opportunity to seek, share and generate knowledge. Frontiers provides immediate and permanent online open access to all its publications, but this alone is not enough to realize our grand goals.

Frontiers journal series

The Frontiers journal series is a multi-tier and interdisciplinary set of open-access, online journals, promising a paradigm shift from the current review, selection and dissemination processes in academic publishing. All Frontiers journals are driven by researchers for researchers; therefore, they constitute a service to the scholarly community. At the same time, the *Frontiers journal series* operates on a revolutionary invention, the tiered publishing system, initially addressing specific communities of scholars, and gradually climbing up to broader public understanding, thus serving the interests of the lay society, too.

Dedication to quality

Each Frontiers article is a landmark of the highest quality, thanks to genuinely collaborative interactions between authors and review editors, who include some of the world's best academicians. Research must be certified by peers before entering a stream of knowledge that may eventually reach the public - and shape society; therefore, Frontiers only applies the most rigorous and unbiased reviews. Frontiers revolutionizes research publishing by freely delivering the most outstanding research, evaluated with no bias from both the academic and social point of view. By applying the most advanced information technologies, Frontiers is catapulting scholarly publishing into a new generation.

What are Frontiers Research Topics?

Frontiers Research Topics are very popular trademarks of the *Frontiers journals series*: they are collections of at least ten articles, all centered on a particular subject. With their unique mix of varied contributions from Original Research to Review Articles, Frontiers Research Topics unify the most influential researchers, the latest key findings and historical advances in a hot research area.

Find out more on how to host your own Frontiers Research Topic or contribute to one as an author by contacting the Frontiers editorial office: frontiersin.org/about/contact

Fungal wheat diseases: Etiology, breeding, and integrated management, volume II

Topic editors

Maria Rosa Simon — National University of La Plata, Argentina

Paul Christiaan Struik — Wageningen University and Research, Netherlands

Andreas Börner — Leibniz Institute of Plant Genetics and Crop Plant Research (IPK), Germany

Citation

Simon, M. R., Struik, P. C., Börner, A., eds. (2023). *Fungal wheat diseases: Etiology, breeding, and integrated management, volume II*. Lausanne: Frontiers Media SA. doi: 10.3389/978-2-8325-3190-7

Table of contents

05 Editorial: Fungal wheat diseases: etiology, breeding, and integrated management, volume II
María Rosa Simón, Paul C. Struik and Andreas Börner

08 The haustorium: The root of biotrophic fungal pathogens
Johannes Mapuranga, Lirong Zhang, Na Zhang and Wenxiang Yang

23 A transcriptomic-guided strategy used in identification of a wheat rust pathogen target and modification of the target enhanced host resistance to rust pathogens
Bernard Nyamesorto, Hongtao Zhang, Matthew Rouse, Meinan Wang, Xianming Chen and Li Huang

37 Comparison of microscopic and metagenomic approaches to identify cereal pathogens and track fungal spore release in the field
Paola Pilo, Colleen Lawless, Anna M. M. Tiley, Sujit J. Karki, James I. Burke and Angela Feechan

52 Exploring and applying genes to enhance the resistance to Fusarium head blight in wheat
Haigang Ma, Yongjiang Liu, Xueyan Zhao, Suhong Zhang and Hongxiang Ma

63 Multi-peril pathogen risks to global wheat production: A probabilistic loss and investment assessment
Yuan Chai, Senait Senay, Diana Horvath and Philip Pardey

75 Key infection stages defending heat stress in high-temperature-resistant *Blumeria graminis* f. sp. *tritici* isolates
Meihui Zhang, Aolin Wang, Cheng Zhang, Fei Xu, Wei Liu, Jieru Fan, Zhanhong Ma and Yilin Zhou

88 Biocontrol and plant growth promotion by combined *Bacillus* spp. inoculation affecting pathogen and AMF communities in the wheat rhizosphere at low salt stress conditions
Chao Ji, Zhizhang Chen, Xuehua Kong, Zhiwen Xin, Fujin Sun, Jiahao Xing, Chunyu Li, Kun Li, Zengwen Liang and Hui Cao

104 Adapting to the projected epidemics of Fusarium head blight of wheat in Korea under climate change scenarios
Jin-Yong Jung, Jin-Hee Kim, Minju Baek, Chuloh Cho, Jaepil Cho, Junhwan Kim, Willingthon Pavan and Kwang-Hyung Kim

120 Genetics of spot blotch resistance in bread wheat (*Triticum aestivum* L.) using five models for GWAS
Sahadev Singh, Shailendra Singh Gaurav, Neeraj Kumar Vasistha, Uttam Kumar, Arun Kumar Joshi, Vinod Kumar Mishra, Ramesh Chand and Pushpendra Kumar Gupta

135 Role of seed infection for the near and far distance dissemination of wheat blast caused by *Magnaporthe oryzae* pathotype *Triticum*
Musrat Zahan Surovy, Tofazzal Islam and Andreas von Tiedemann

149 Genetics and breeding for resistance against four leaf spot diseases in wheat (*Triticum aestivum* L.)
Pushpendra Kumar Gupta, Neeraj Kumar Vasistha, Sahadev Singh and Arun Kumar Joshi

171 Defence-related metabolic changes in wheat (*Triticum aestivum* L.) seedlings in response to infection by *Puccinia graminis* f. sp. *tritici*
Mercy Maserumule, Molemi Rauwane, Ntakadzeni E. Madala, Efficient Ncube and Sandiswa Figlan

frontiers | Frontiers in Plant Science

TYPE Editorial
PUBLISHED 25 July 2023
DOI 10.3389/fpls.2023.1247327

OPEN ACCESS

EDITED AND REVIEWED BY
Brigitte Mauch-Mani,
Université de Neuchâtel, Switzerland

*CORRESPONDENCE
María Rosa Simón
mrsimon@agro.unlp.edu.ar

RECEIVED 25 June 2023
ACCEPTED 12 July 2023
PUBLISHED 25 July 2023

CITATION
Simón MR, Struik PC and Börner A (2023) Editorial: Fungal wheat diseases: etiology, breeding, and integrated management, volume II.
Front. Plant Sci. 14:1247327.
doi: 10.3389/fpls.2023.1247327

Editorial: Fungal wheat diseases: etiology, breeding, and integrated management, volume II

María Rosa Simón[1,2]*, Paul C. Struik[3] and Andreas Börner[4]

[1]Cerealicultura, Facultad de Ciencias Agrarias y Forestales, Universidad Nacional de La Plata, La Plata, Argentina, [2]Department of Agricultural and Forestry Technology, Laboratory of Extensive Agricultural Production (LAPROAGRE), Consejo Nacional de Investigaciones Científicas y Técnicas La Plata (CONICET), La Plata, Argentina, [3]Department of Plant Sciences, Centre for Crop System Analysis, Wageningen University & Research, Wageningen, Netherlands, [4]Genebank Department, Leibniz Institute of Plant Genetics and Crop Plant Research, Gatersleben, Germany

KEYWORDS

impact of wheat diseases, pathogen identification, infection structures, resistance of isolates to stresses, wheat defense mechanisms, integrated management

Editorial on the Research Topic
Fungal wheat diseases: etiology, breeding, and integrated management, volume II

Relevance of wheat and wheat diseases

Wheat is the most widely grown crop in the world in terms of area and is the major source of calories and plant-derived protein in human food. Advances in wheat yield rather than land expansion have been the main drivers of the steady growth of global wheat production (Erenstein et al., 2022), which is currently at 800 million tons (FAO, 2023). Wheat production is continuously threatened by factors such as a lack of suitable farmland, climate change and abiotic and biotic stressors. Future demand must be met by combining integrated disease and pest management, adaptation to warmer climates and abiotic stresses, and sparing use of water and other resources. A storm of newly emerging pathogens, caused by the loss of wheat's genetic diversity and the search for high-performing cultivars, has made diseases a serious concern (Figueroa et al., 2018).

In a first Research Topic on fungal wheat diseases, we brought together 26 papers, including reviews, original research papers and a methodological papers (Simón et al., 2021). This second volume on fungal wheat diseases consists of two reviews and 10 original papers. Advances on the probabilistic impact and identification of the main pathogens, functions of infection structures, the key infection stages of defense in high-temperature-resistant isolates, as well as metabolic changes in response to wheat pathogens are addressed. Aspects essential for proper integrated management, such as models to predict the risk infection index, mechanisms of seed transmission, genetics and breeding for resistance, and biological control are also considered.

Impact of wheat diseases

Pests and diseases are responsible for 21.5% of the current crop losses (Savary et al., 2019). Fungal diseases such as leaf and stripe rust, Fusarium head blight, Septoria leaf blotch, spot blotch, tan spot and powdery mildew cause the most significant losses out of the 31 pests and pathogens reported in wheat (Savary et al., 2019).

In this Research Topic, Chai et al. examined the probabilistic impact of five major fungal pathogens of wheat (leaf, stripe and stem rust, Septoria tritici blotch and Fusarium head blight) on wheat production. They determined that almost 90% of the wheat area is at risk from at least one of these diseases, resulting in annual losses of more than 62 million tons, and that more research on the subject is economically justified.

Identification of pathogens in wheat, infection structures and mechanisms of resistance of isolates to environmental stresses

To predict outbreaks, accurate pathogen identification is crucial. Fungal diseases can spread by releasing spores from infected plants or stubble (Suffert et al., 2011). Pilo et al. identified 150 species of fungal pathogens of cereals, using microscopy and two metagenomic-based methods useful for the forecasting of disease outbreaks without knowledge about which pathogens are present. They also found that some of the pathogens' spore release is correlated with environmental variables. Such correlations can be used to manage the diseases.

Fungal pathogens possess different infection structures. The haustorium is an infection structure present in biotrophic pathogens and is a key player in the establishment of pathogenesis (Jaswal et al., 2020). Mapuranga et al. assessed the state-of-the-art on the establishment and development of the haustorium, its structure, composition, gene expression, mode of nutrient acquisition and the haustorial effector secreted into the host cell, including the recent haustorial transcriptome investigations.

Plant pathogens have evolved the capacity to adapt to changing environments in order to survive (Knies and Kingsolver, 2010). Zhang et al. found that haustoria formation and hyphae expansion were the key infection stages when comparing high-temperature resistant with sensitive isolates of *Blumeria graminis* f.sp. *tritici*. Additionally, they discovered that high-temperature-resistance is related to the induction of heat shock protein genes in response to stress at those stages.

Defense mechanisms of wheat against pathogens

Numerous substances (from cell wall components to metabolic enzymes) that are crucial to the molecular and cellular signaling processes during pathogen infection, have been documented to shield plants from pathogen invasion and provide hosts with induced resistance (Kaur et al., 2022). Maserumule et al. analyzed the biochemical alterations in wheat metabolite expression in response to stem rust infection. They discovered biomarkers such as fatty and carboxylic acids, various sugars and phenolic chemicals, including flavonoids, hydrocinnamic acid derivatives, and polyphenols, linked to the interaction between wheat and *Puccinia graminis*. The most significant metabolic pathways linked to the metabolites regulating wheat defense were those involving riboflavin, cutin and suberin, thiamine, folate, and alpha-linolenic acid, as well as glyoxylate and dicarboxylate metabolism.

Integrated management of wheat diseases

Epidemic forecasting is relevant for effective integrated management strategies. Understanding how weather and heading dates affect diseases is crucial to preventing many epidemics (Simón et al., 2005). Jung et al. modeled prospective Fusarium head blight (FHB) epidemics in Korea using weather conditions during flowering. They showed that epidemics would gradually worsen and that the early-heading wheat cultivars would show decreases in FHB epidemics, highlighting the significance of taking adaptation measures to prevent a rise of the disease as a result of climate change.

Verifying the presence of pathogens in the seeds and their transmission to plants is crucial in the context of integrated management. Surovy et al. did not find evidence of systemic transfer of *Magnaporthe oryzae* pathotype *Triticum* (MoT), the causal agent of wheat blast, from infected seed to seedlings after tillering. However, the presence of MoT in seedlings may act as a source of inoculum, which might contaminate seeds by air-borne infection. Results highlight the dangers of the spread of wheat blast across continents through seeds and the significance of using healthy seeds.

Acceptable levels of resistance, adequate fertilization management, crop rotation, proper timing of planting and tillage that enhance residue decomposition, complemented with biological and/or chemical control, are also relevant strategies that can help minimize the severity of diseases (Simón et al., 2020).

Genetic resistance to wheat diseases

In this Research Topic, Gupta et al. reviewed the resistance to four relevant wheat pathogens causing Septoria nodorum blotch, tan spot, spot blotch and Septoria tritici blotch with emphasis on the necrotrophic effectors and sensitivity genes in the inverse gene for gene model. This contribution also includes recent information on the whole-genome sequences of the four pathogens.

Nyamesorto et al. identified and edited wheat genes that aid rust pathogens during infection to provide wheat with passive resistance to rust. They identified a wheat transcription factor as a rust

pathogen target. By altering it, the cultivars Chinese Spring and Cadenza became more resistant to stem rust and some races of the stem and stripe rust pathogens, respectively, and novel germplasm of wheat was also created.

Ma et al. summarized the genes conferring FHB resistance and mycotoxin detoxication discovered in common wheat and its relatives by using forward and reverse genetic approaches. They also discussed the effects of several resistance genes and the role of host induced gene silencing in enhancing the resistance to FHB as well as the molecular basis of the resistance and the use of the cloned genes for FHB management.

Singh et al. analyzed the genetic architecture of resistance to spot blotch in wheat using a genome-wide association study (GWAS) including 303 genotypes genotyped with 12,196 SNPs. They found 306 marker trait associations (MTAs), some of them significant with the five GWASs used, which were utilized for finding candidate genes. Seven MTAs were considered relevant for marker-assisted selection.

Biological control for wheat diseases

Biological control is a sustainable method for managing diseases. Plant growth-promoting rhizobacteria increase the control of soil-borne diseases; however, their effect on pathogenic fungi or arbuscular mycorrhizal fungi (AMF) is unclear. Ji et al. found that inoculation with some *Bacillus* strains enhanced rhizosphere soil chemical characteristics and wheat yield as well as lowered the incidence of diseases, rhizosphere fungus, and AMF fungal diversity.

Conclusion

This second volume on wheat fungal diseases creates an interesting supplement to the first Research Topic. The papers in this second volume highlight the rapid progress that can be made in knowledge with the latest research techniques, progress that is much needed to combat the ever-increasing threats caused by fungal diseases in wheat production across the globe.

Author contributions

MS prepared the draft. PS and AB revised the draft and approved the final submission. All authors contributed to the article and approved the final version.

Acknowledgments

We greatly thank all authors and reviewers for their contributions to this Research Topic as well as the support of the editorial office.

Conflict of interest

The authors declare that the research was conducted in the absence of any commercial or financial relationships that could be construed as a potential conflict of interest.

Publisher's note

References

Erenstein, O., Jaleta, M., Mottaleb, K. A., Sonder, K., Donovan, J., and Braun, H. J. (2022). "Global trends in wheat production, consumption and trade," in *Wheat Improvement*. Eds. M. P. Reynolds and H. J. Braun (Cham: Springer). doi: 10.1007/978-3-030-90673-3

FAO (2023). *World Food Situation*. Available at: https://www.fao.org/worldfoodsituation/csdb/en/#:~:text=FAO's%20first%20forecast%20puts%20world,the%20utilization%20of%20coarse%20grains (Accessed June 20, 2022).

Figueroa, M., Hammond-Kosack, K. E., and Solomon, P. S. (2018). A review of wheat diseases - a field perspective. *Mol. Plant Pathol.* 19 (6), 1523–1536. doi: 10.1111/mpp.12618

Jaswal, R., Kiran, K., Rajarammohan, S., Dubey, H., Singh, P. K., Sharma, Y., et al. (2020). Effector biology of biotrophic plant fungal pathogens: current advances and future prospects. *Microbiol. Res.* 241, 126567. doi: 10.1016/j.micres.2020.126567

Kaur, S., Samota, M. K., Choudhary, M., Choudhary, M., Pandey, A. K., Sharma, A., et al. (2022). How do plants defend themselves against pathogens - biochemical mechanisms and genetic interventions. *Physiol. Mol. Biol. Plants* 28 (2), 485–504. doi: 10.1007/s12298-022-01146-y

Knies, J. L., and Kingsolver, J. G. (2010). Erroneous Arrhenius: modified Arrhenius model best explains the temperature dependence of ectotherm fitness. *Am. Nat.* 176, 227–233. doi: 10.1086/653662

Savary, S., Willocquet, L., Pethybridge, S. J., Esker, P., Mc Roberts, N., and Nelson, A. (2019). The global burden of pathogens and pests on major food crops. *Nat. Ecol. Evol.* 3, 430–439. doi: 10.1038/s41559-018-0793-y

Simón, M. R., Börner, A., and Struik, P. C. (2021). Editorial: Fungal wheat diseases: etiology, breeding, and integrated management. *Front. Plant Sci.* 12. doi: 10.3389/fpls.2021.671060

Simón, M. R., Fleitas, M. C., Castro, A. C., and Schierenbeck, M. (2020). How foliar fungal diseases affect nitrogen dynamics, milling, and end-use quality of wheat. *Front. Plant Sci.* 11. doi: 10.3389/fpls.2020.569401

Simón, M. R., Perelló, A. E., Cordo, C. A., Larrán, S., van der Putten, P. E. L., and Struik, P. C. (2005). Association between Septoria tritici blotch, plant height, and heading date in wheat. *Agron. J.* 97 (4), 1072–1081. doi: 10.2134/agronj2004.0126

Suffert, F., Sache, I., and Lannou, C. (2011). Early stages of Septoria tritici blotch epidemics of winter wheat: Build-up, overseasoning, and release of primary inoculum. *Plant Pathol.* 60 (2), 166–177. doi: 10.1111/j.1365-3059.2010.02369.x

frontiers | Frontiers in Plant Science

TYPE Review
PUBLISHED 29 August 2022
DOI 10.3389/fpls.2022.963705

OPEN ACCESS

EDITED BY
Maria Rosa Simon,
National University of La Plata, Argentina

REVIEWED BY
Ramesh Amalraj,
Division of Crop Science (ICAR), India
Wen-Ming Wang,
Sichuan Agricultural University, China

*CORRESPONDENCE
Wenxiang Yang
wenxiangyang2003@163.com

SPECIALTY SECTION
This article was submitted to Plant Pathogen Interactions, a section of the journal Frontiers in Plant Science

RECEIVED 07 June 2022
ACCEPTED 15 August 2022
PUBLISHED 29 August 2022

CITATION
Mapuranga J, Zhang L, Zhang N and Yang W (2022) The haustorium: The root of biotrophic fungal pathogens. *Front. Plant Sci.* 13:963705. doi: 10.3389/fpls.2022.963705

The haustorium: The root of biotrophic fungal pathogens

Johannes Mapuranga, Lirong Zhang, Na Zhang and Wenxiang Yang*

College of Plant Protection, Technological Innovation Center for Biological Control of Plant Diseases and Insect Pests of Hebei Province, Hebei Agricultural University, Baoding, China

Biotrophic plant pathogenic fungi are among the dreadful pathogens that continuously threaten the production of economically important crops. The interaction of biotrophic fungal pathogens with their hosts necessitates the development of unique infection mechanisms and involvement of various virulence-associated components. Biotrophic plant pathogenic fungi have an exceptional lifestyle that supports nutrient acquisition from cells of a living host and are fully dependent on the host for successful completion of their life cycle. The haustorium, a specialized infection structure, is the key organ for biotrophic fungal pathogens. The haustorium is not only essential in the uptake of nutrients without killing the host, but also in the secretion and delivery of effectors into the host cells to manipulate host immune system and defense responses and reprogram the metabolic flow of the host. Although there is a number of unanswered questions in this area yet, results from various studies indicate that the haustorium is the root of biotrophic fungal pathogens. This review provides an overview of current knowledge of the haustorium, its structure, composition, and functions, which includes the most recent haustorial transcriptome studies.

KEYWORDS

haustorium, pathogen, host, nutrient uptake, effectors

Introduction

Naturally, the growth and development of plants is constantly threatened by various organisms including fungi, oomycetes, viruses, and bacteria. Biotrophic fungal pathogens are undisputedly among the most intriguing category of these organisms (Voegele et al., 2009; Dean et al., 2012). Various fungi use a variety of methods to infect and invade plants. Rusts and powdery mildews are among the 10 pathogens considered most significant internationally to plant pathology (Dean et al., 2012). Powdery mildews and rust fungi consist of approximately 900 species (Braun and Cook, 2012) and over 8,000 species, respectively (Aime et al., 2014; Lorrain et al., 2019). Biotrophic pathogenic fungi cause rust diseases, which significantly affect the production of economically important crops. Stem rust, leaf rust, and yellow rust, all caused by the rust pathogens *Puccinia graminis* f. sp. *tritici* (*Pgt*), *Puccinia triticina* (*Pt*), and *Puccinia striiformis* f. sp. *tritici* (*Pst*), respectively, continue to endanger worldwide wheat production on a year-round basis

(McIntosh et al., 1995; Dean et al., 2012; Hafeez et al., 2021; Kokhmetova et al., 2021). *Melampsora lini*, *Phakopsora pachyrhizi*, *Hemileia vastatrix*, and *Melampsora larici-populina*, cause flax rust, Asian soybean rust, coffee rust, and defoliating poplar rust disease, respectively (Lawrence et al., 2007; Kelly et al., 2015). During the course of an infection, plants are equipped with the ability to detect the presence of pathogens at many levels (Jones and Dangl, 2006), and as a consequence, the host defense system is activated. Pathogen-associated molecular patterns (PAMPs) are recognized by pattern-recognition receptors (PRRs) on the cell membrane, which in turn trigger PAMP-triggered immunity (PTI). Establishing a dynamic parasitic relationship between the biotrophic fungi and the host is the foundation for the development of the pathogen in host plant. In order to infect the host plant successfully, biotrophic fungal plant pathogens suppress PTI components by secreting virulence factors known as effectors through haustoria and hyphae into the host cells thereby causing diseases (Martel et al., 2021). The plants in response developed a second layer of innate immunity known as effector-triggered immunity (ETI), in which the plant resistance proteins recognize corresponding avirulence factors and set off a powerful defensive response (Jones and Dangl, 2006).

Although biotrophic pathogens like rusts and powdery mildews have unique life cycles, they both possess a sophisticated infection structure called the haustorium. The haustoria emerge after cell wall penetration and are surrounded by an invaginated plant plasma membrane (Mendgen and Deising, 1993). Fungal haustorium is widely accepted as a key player in the establishment of successful pathogenesis through nutrient acquisition from the host and delivery of effector proteins into the host cells for the manipulation of host defense response and other functions (Jones and Dangl, 2006; LoPresti et al., 2015; Jaswal et al., 2020). The expression of fungal pathogenicity is caused by differentiation-dependent gene activation, which then leads to the development of specialized hyphae that are armed with the mechanisms (enzymes, cell wall modifications) necessary to infect a host plant and cause diseases. Although the fungal haustorium was first described many years ago, many unexplained concerns persist. The major unanswered questions about haustorial biology include its establishment and composition, how it evades host recognition, how it acquires nutrients from the host cells, and how secreted effectors suppress host defense responses. Analysis of haustorial functions at molecular level is now feasible through the identification and characterization of haustorial genes and proteins. Studying haustoria function will improve our knowledge on biotrophic fungus pathogenesis. Transcriptome sequencing of haustoria, germinated spores, and urediospores may help understand the metabolic roles of infection structures and prioritize possible effector genes for subsequent functional research of this obligate biotrophic fungus. This review focuses on the establishment and development of the haustorium, its composition, gene expression, mode of nutrient acquisition, and the haustorial effectors secreted into the host cell.

Biotrophic fungal haustorium formation and development

The haustorium of biotrophic fungal plant pathogens adapt to the host cell's architecture due to its morphological features. The broad morphological spectrum of haustorium is best exemplified by rust fungi which possess monokaryotic and dikaryotic stages, all of which during their infection process produce haustoria of different morphologies (Mendgen et al., 2000). Dikaryotic haustoria arise from external haustorial mother cells and consist of a slender tubular neck that penetrates into host cell and a haustorial body that forms distally to the neck (Harder and Chong, 1984; Heath and Skalamera, 1997). The haustorial mother cells thus functionally resemble the appressoria. The dikaryotic nature of fungal rust implies that they harbor significant genetic variation that is shared between the two haplotypes (Figueroa et al., 2020). Monokaryotic haustoria are terminal intercellular hyphae without morphological differentiation and have a septum near the penetration site (Gold and Mendgen, 1984, 1991; Harder and Chong, 1984). Prior to the formation of haustorium, rust fungi dikaryotic urediospores germinate on host plant epidermis and form germ tubes which sense the host cuticle topography and develop appressoria above the stomata to penetrate the intercellular spaces of the mesophyll, potentially bypassing epidermal defense responses (Mapuranga et al., 2022). Penetration occurs through stomata by the penetration hyphae into the substomatal spaces where the fungus differentiates into substomatal vesicles and elongates into an intercellular hypha which comes into contact with the host mesophyll cells and develops haustorial mother cells (Mendgen et al., 2000; Voegele et al., 2009). Following this, haustorial formation is initiated, neckbands are formed around the site of penetration of the mesophyll cell and an extrahaustorial matrix (EHMA), a gel-like layer enriched in carbohydrates, develops between the haustoria cell wall and the cell plasma membrane (Figure 1A; Staples, 2001). The extrahaustorial matrix is responsible for two functions; first to acquire nutrients like sugar and amino acids into fungal cells, and second to secrete effectors into the host cell to suppress immunity and manipulate the host. The haustorium is not directly located in the cytoplasm, although it is within the host cell, instead, it is surrounded by an extrahaustorial membrane (EHM), usually a differentiated extension of the host plant cell cytoplasm.

During haustorial formation, the host cell wall is breached and the expanding haustorium invaginates the host plasma membrane, probably by synthesizing a new membrane (Voegele and Mendgen, 2011). As the haustorial body develops, a zone of separation essential for maintaining the biotrophic lifestyle is formed between the plasma membranes of the pathogen and the host (Hahn and Mendgen, 1997). The haustorium also contains its own nuclear genes and normal complement organelles. During haustorial formation in dikaryotic rusts, migration of haustorial mother cell cytoplasmic contents, including the two haploid nuclei, into the haustorium occurs through the neck structure leaving the haustorial mother cell highly vacuolated and

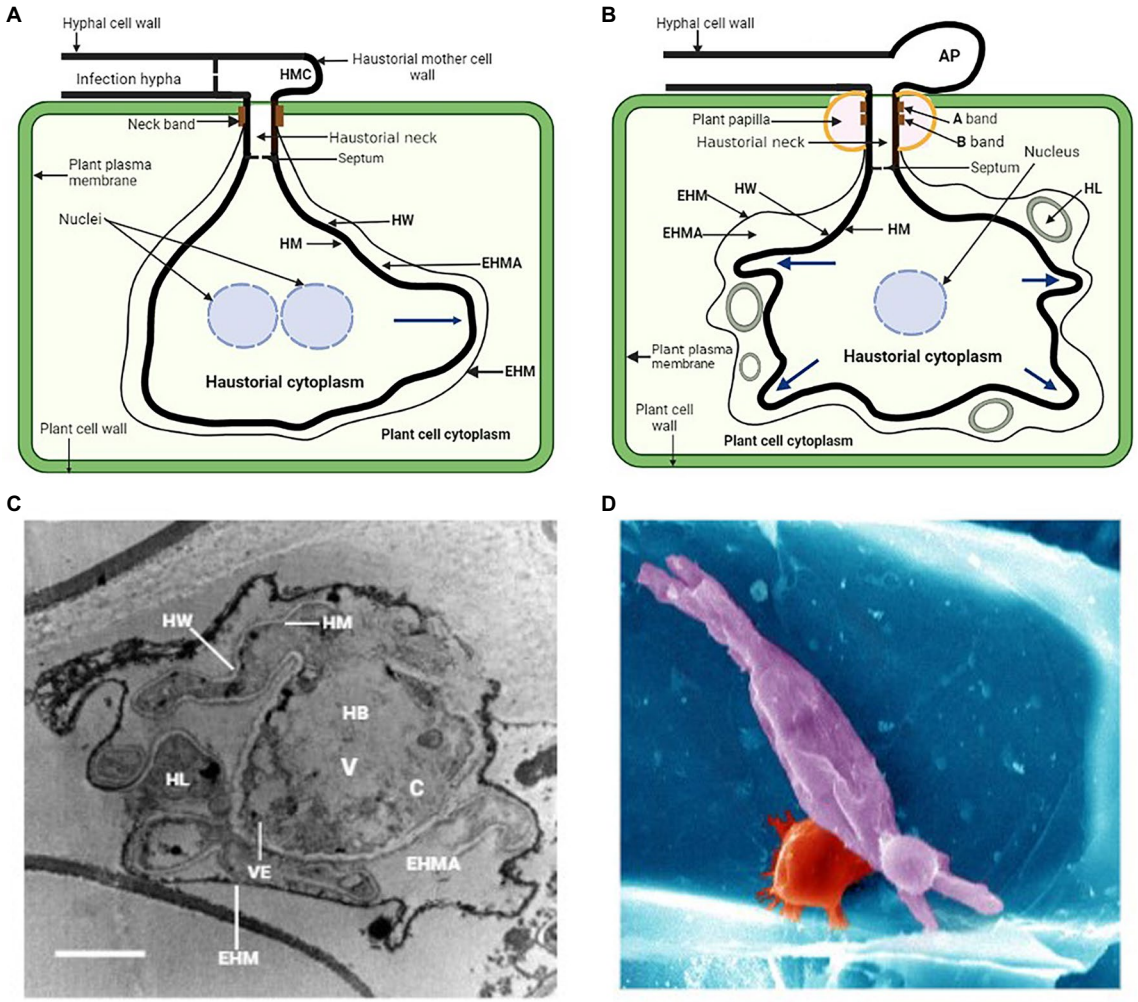

FIGURE 1
(A) General illustration of a rust fungus (dikaryon) haustorium and its association with the mesophyll cell of the host. HMC, haustorial mother cell; EHMA, extrahaustorial matrix; EHM, extrahaustorial membrane; HM, haustorial plasma membrane; HW, haustorial cell wall. **(B)** Schematic representation of a powdery mildew haustorial complex and its association with the epidermal cell of the host. AP, appressorium; HL, haustorial lobe. Blue arrows indicate secondary growth in these haustoria and direction of growth. **(C)** Transmission electron microscopy of a cross section of *P. xanthii* haustorial complex. The haustorial body (HB) is occupied by a large vacuole (V), a small cytoplasm (C) and many vesicles (VE). Bar, 2 µm. Picture was taken from Martínez-Cruz et al. (2014). **(D)** Scanning electron microscopy of leaf epidermal cell infected with the powdery mildew causal agent, *Blumeria* f. sp. *graminis* (false colored: barley cell wall, blue; papillae, red; fungal haustorium, purple). Picture was taken from Chowdhury et al. (2016).

enucleated (Mendgen et al., 2000). Throughout host cell wall penetration and haustorial maturation, complex changes like central pore occlusion occur to the haustorial mother cell septum, and this prevents continuity of contents of the cytoplasm throughout the hyphae (Mendgen et al., 2000; Voegele and Mendgen, 2003, 2011). This suggests the separation of the haustorial mother cell and haustorium from the hyphae which probably facilitates the development of independent transcriptional and metabolic programs in these cells (Polonio et al., 2021).

Most powdery mildew fungal species use their appressoria to directly penetrate into cuticle and cell wall of the host plant to colonize exclusively the epidermal cells of the host plant (Mapuranga et al., 2022). Successful penetration results in the development of a penetration peg that penetrates directly into the epidermal cuticle of the host plant leading to the formation of haustoria which invaginates the host plasma membrane (Bushell and Bergquist, 1974). This is followed by the complete development of the haustorial body with some prolongations called haustorial lobes emerging from it (Mackie et al., 1991; Martínez-Cruz et al., 2014). Since the process of the haustorium formation causes the invagination of the host plasma membrane, which remains surrounding the haustorium and gives rise to the so-called EHM (Gil and Gay, 1977; Mackie et al., 1991; Martínez-Cruz et al., 2014), the haustorium cannot be considered a true intracellular structure (Polonio et al., 2021). The haustoria of powdery mildew are established physically inside the epidermal cells of the host and are ultimate unicellular structures consisting

of a globular central body with projecting filamentous lobes (Figure 1B; Gil and Gay, 1977). There are two main morphologies of powdery mildew haustoria that have been described; the globular haustoria with projecting filamentous tubular lobes typical of Arabidopsis powdery mildew *Golovinomyces orontii* and *Podosphaera xanthii* a cucurbit powdery mildew (Figures 1B,C; Micali et al., 2011; Martínez-Cruz et al., 2014), and the highly branched multidigitate haustoria typical of barley powdery mildew *Blumeria graminis*. f. sp. *hordei* (Figure 1D; Lambertucci et al., 2019; Polonio et al., 2021). Powdery mildew appressorium and haustorium are separated by the haustorial neck where the EHM and the haustorial membrane (HM) are wrapped by two neckband regions termed A band and B band (Figure 1B; Stumpf and Gay, 1990; Mendgen et al., 2000; Martínez-Cruz et al., 2014). This neckband protects the extrahaustorial matrix (EHMA) against the bulk apoplast, resembling the endodermal Casparian strip (Heath, 1976). The haustorial cytoplasm and the appressorium are divided by a septum that has a hole and is the consequence of the rupture of a papilla (Mackie et al., 1991; Micali et al., 2011). This results in the formation of a space between the EHM and the HM that is referred to as the EHMA (Figures 1A,B; Gil and Gay, 1977). This space appears to be well-suited for the absorption of nutrition from the host and was regarded as a symplastic section (Mendgen et al., 2000; Micali et al., 2011). The haustorial body, haustorial lobes, HM, EHM, and EMHA make up the haustorial complex (HC; Mackie et al., 1991). This complex also includes the haustorial mesentery. Haustorial lobes form during haustorial maturity and the inner parts of haustorial complexes showed a haustorial body surrounded by irregular lobes (Gil and Gay, 1977; Micali et al., 2011; Martínez-Cruz et al., 2014). Transmission electron microscopy revealed an immature haustorium with a tiny haustorial body and no subcellular characteristics, and a bigger, highly organized mature haustorium (Martínez-Cruz et al., 2014). As in *G. orontii* and *B. graminis* f. sp. *hordei*, *P. xanthii* has lobes at both ends (Godfrey et al., 2009; Micali et al., 2011; Martínez-Cruz et al., 2014). Tiny lobes suggest young complexes, whereas wide lobes indicate mature complexes. Massive vacuoles and electron-dense vesicles dominated the haustorial core. Some lobes share the haustorial body's cytoplasm and cell wall. The haustorial body and lobes were separated from the plant cytoplasm by an electron-dense membrane (Martínez-Cruz et al., 2014). Haustorial lobes are involved in *P. xanthii*-host cell communication because they cover nearly the entire haustorial body, increasing contact area and facilitating material exchange. Furthermore, they probably facilitate vesicle secretion and transit because of their cell wall which is thinner than the haustorial body. (Eichmann and Hückelhoven, 2008; Rodrigues et al., 2008; Martínez-Cruz et al., 2014). In yeasts and filamentous fungi, the vesicular pathway has been extensively studied (Fischer-Parton et al., 2000), and in these species, vesicular trafficking involves different-sized vesicles. It is unknown whether vesicular trafficking occurs in rusts, powdery mildews, or haustorium function. The cytoskeleton of the host plant goes through a process of polarization alteration throughout the process of haustorial development, which is linked to the host's immune response (Henty-Ridilla et al., 2013; Polonio et al., 2021).

Changes in microtubule arrangement affect protein activity *via* direct or indirect transport (Schmidt and Panstruga, 2011). Papillae are one of the first plant structures that arise in response to a pathogen attack and they are made of cellulose and other polymers that curb pathogen proliferation (Wang et al., 2009; Eggert et al., 2014). This protective protein drives actin filament reorganization, which surrounds haustorial complexes and directs callose formation (Lipka and Panstruga, 2005; Eichmann and Hückelhoven, 2008). Actin filaments arrange themselves around the nucleus, bringing it closer to the point of entry in order to modify gene expression and facilitate a more rapid immune response (Eichmann et al., 2004). Fungal effectors affect plant cytoskeletons, whereas plant peptides target fungal cytoskeletons (Schmidt and Panstruga, 2007). Transmission electron microscopy (TEM) study demonstrated the very irregular shape of the EHM, which separates the EHMA of haustoria from the plant cell's cytoplasm. TEM examination showed haustoria-surrounding vesicles and electron-dense plaques which had been deposited on the *P. xanthii* haustoria, and it is most likely that these plaques originated from the plant host (Martínez-Cruz et al., 2014). Due to papilla development, callose deposition was limited to fungal penetration sites in colony perimeters. This clearly showed that haustorial maturity is associated with callose deposition (Martínez-Cruz et al., 2014).

Haustorial composition

The haustorium originated from a hypha as previously alluded, so it obviously appears to think that these two structures have the same composition. However, various haustorium distinct features have been explained (Mackie et al., 1991; Micali et al., 2011; Martínez-Cruz et al., 2014). For the vast majority of interactions with haustoria, where they are known as extrahaustorial matrices (EHMAs), they are also known as interfacial extracellular matrices (IFM), which refers to a specific subset of interactions. These matrices vary by organism. The homogeneous, amorphous appearance of these matrices reflects the uniform distribution of key components (Bracker and Littlefield, 1973). In haustoria, matrices are thickest around haustorial lobes and weakest, if existent, near the neck, where the host plasma membrane presses against the penetration peg cell wall (Bracker and Littlefield, 1973). There is a clear distinction between the fungal cell wall and the haustorial neckbands. Energy dispersive X-ray examination revealed a significant concentration of iron, phosphate, silicon, glucans, lipids, and proteins in the neckband of rust haustoria (Harder and Chong, 1991; Mendgen et al., 2000). The A band has a high concentration of 1,3-glucans, and the lipid molecules that make up this band are bonded to both chitin and 1,3-glucans. The B band has a high concentration of 1,4-glucans and the lipid molecules it contains are covalently bonded to its proteinaceous components (Stumpf and Gay, 1990;

Martínez-Cruz et al., 2014). Maintaining an effective seal between the EHMA and the plant's plasma membrane is thought to be critical for optimal nutrient transfer into haustoria (Hahn et al., 1997). The neckband creates a seal, hence EHMA is a contained entity, unlike apoplast (Bracker and Littlefield, 1973; Woods and Gay, 1983; Green et al., 1992). EHMA is a carbohydrate-rich layer between the haustorium and the EHM. A wide range of cytological approaches have been used to examine the EHMA composition surrounding the haustoria (Harder and Chong, 1991). *Erysiphe. pisi*'s EHMA expands in hypotonic solutions without rupturing the haustoria, indicating they are fluid (Gil and Gay, 1977). Small compounds like uranyl ions may get through the EHMA, but horse radish peroxidase cannot. The EHMA around *E. pisi* haustoria is gel-like, not a solution (Gay and Manners, 1987; Green et al., 1992).

The fungus may decrease plant cell wall formation and/or deposition at the invaginated plant plasma membrane (Green et al., 1995). EHMAs generated by obligate biotrophs infecting monocots include threonine-hydroxyproline-rich glycoproteins (THRGPs; Hippe-Sanwald et al., 1994), which may be plant-produced compounds that function as a fungal barrier (Hippe-Sanwald et al., 1994). A study of the EHMA around *Uromyces vignae* monokaryotic rust haustoria found plant hydroxyproline-rich glycoproteins (HRGPs), arabinogalactan proteins (AGPs), and callose (Stark-Urnau and Mendgen, 1995). Other components of the host cell wall such as cellulose and arabinogalactan proteins were also detected in the EHM using immunogold labeling. These findings established that the plant contributes to EHMA in certain obligatory biotrophic relationships but not in others (Stark-Urnau and Mendgen, 1995). Multivesicular bodies (MVBs) comprising lipid bilayers were discovered in the ultrastructure of *G. orontii* haustoria in another study (Micali et al., 2011). It was found that the delimitation membrane of each individual endosomal compartment is pushed inward, resulting in an increase in the volume of the endosomal lumens. In anatomically comparable haustorial lobes, there were more medium- and large-sized vesicles than in the body. MVBs have been proposed as the vehicles for transporting small vesicles to vacuoles or for the release of small vesicles called exosomes to the extracellular environment through fusion with the plasma membrane (Valadi et al., 2007; Rodrigues et al., 2008; Schorey and Bhatnagar, 2008; Théry, 2011). Small vesicles were found in the EHMA, at the EHM, and haustorial lobes, and prior findings suggested that these vesicles were exosomes discharged into the EHMA by MVB fusion with the haustorial membrane (Martínez-Cruz et al., 2014). Fungal effectors, proteins, microRNAs, and mRNAs can all be delivered by exosomes in powdery mildew haustoria, and this may be an effective method for the transport of these substances to the haustorium (Valadi et al., 2007).

The EHM is distinct from the non-invaginated section of the host plasma membrane by many utrastructural characteristics. In most cases, it is thicker than the plasma membrane and has a distinct color when stained. Cytological studies showed that the EHM has specific functional features (Harder, 1989). The EHM's genesis is uncertain, but two hypotheses have been proposed. First, EHM is caused by fungal activity altering the plant plasma membrane over time. The EHMA is a nutrition and information trading hub (Heath and Skalamera, 1997). Freeze fracture experiments demonstrated that EHMs generated by dikaryotic stage rusts and powdery mildews lack intramembrane particles and exhibit corrugations and protuberances that increase with haustoria age (Littlefield and Bracker, 1972; Harder and Mendgen, 1982; Harder and Chong, 1984). Convolutions in invaginated membranes may help the fungus to acquire nutrients by increasing surface area (Manners and Gay, 1983). Powdery mildew EHMs seem thicker than peripheral host plasma membranes, probably because of additional carbohydrates. EHM lacks ATPase activity, unlike plant plasma membranes (Polonio et al., 2021). Antibody labeling of *E. pisi* haustoria demonstrated that the EHM shares certain glycoproteins with the host plasma membrane but lacks others (Green et al., 1995). Invading fungi modify the invaginated plasma membrane for nutrition absorption (Woods et al., 1988; Smith and Smith, 1990).

The second hypothesis is that it developed from a *de novo* formation when the haustorium was still in the process of developing (Kim et al., 2014). Arabidopsis resistance protein RPMW8.2 was found to specifically target the EHM where it promotes haustorial encasement formation and onsite accumulation of H_2O_2 and triggers hypersensitive response (Wang et al., 2009; Ma et al., 2014; Berkey et al., 2017). It was also established that RPMW.2 precise targeting to EHM involves an EHM-oriented specific trafficking pathway (Wang et al., 2013; Kim et al., 2014). These findings indicated that the EHM is a critical host-pathogen battlefield and not only a cross-border trafficking. It was also demonstrated that the EHM is fixed at the haustorial neck and physically detachable from the papilla and plasma membrane (Berkey et al., 2017). The EHM and plasma membrane were suggested to be probably two unique membranes of different origins (Berkey et al., 2017), because RPW8.2 was exclusively present in the EHM (Wang et al., 2009) and there were no eight plasma membrane-localized proteins in the EHM (Koh et al., 2005). Recent research has also shown that the endoplasmic reticulum membrane and the endoplasmic reticulum heterogeneous membrane have similar properties. However, the EHM does not depend on normal secretion, which suggests that an unconventional secretory channel within the endoplasmic reticulum may supply the essential materials (Kwaaitaal et al., 2017). Isolated *E. pisi* haustorial complexes (haustoria encased in the EHM) have been studied by the development of monoclonal antibodies. There was one antibody that was able to identify the 62 kDa protein in the haustorial plasma membrane starting at the neckband area (Mackie et al., 1991). *U. fabae* plasma membrane vesicles from spores and germlings were found to have severalfold H^+-ATPase activity than vesicles from haustoria (Struck et al., 1996). This suggests that the haustorial H^+-ATPase plays a crucial function in nutrient absorption, presumably *via* activating carrier proteins for solute transport. One putative permease (PIG2) was only found in *U. fabae* haustoria plasma membranes (Hahn et al.,

1997a). It was therefore hypothesized that in rust haustoria, H^+-ATPase and transport proteins such as amino acid permeases collaborate in the energy-driven absorption of plant compounds (Hahn et al., 1997a). It was also established that 1,3-glucans and chitin are localized on the haustorium surface, and chitin may be converted into chitosan by fungi so that they can avoid being identified by their hosts (Micali et al., 2011). Chitosan has less eliciting power than chitin does (Polonio et al., 2021). The mechanism by which the haustorium prevents chitin identification, however, remains to be a mystery. Recently, a systematic subcellular localization analysis of 14 members of *Arabidopsis thaliana* monosaccharide sugar transporter protein (STP) family suggested that an endoplasmic reticulum-localized sugar transporter AtSTP8 maybe recruited to the EHM during haustorium biogenesis where it may assist sugar translocation across the haustorial interface by powdery mildew haustoria from Arabidopsis host cells (Liu et al., 2021). Transmembrane domain prediction showed that AtSTP8 possesses 12 transmembrane domains which conforms with a typical monosaccharide transporter structure (Doidy et al., 2012; Paulsen et al., 2019). It was also suggested that AtSTP8 is an energy-dependent wide monosaccharide transporter with a preference for glucose (Liu et al., 2021).

Molecular physiology of the haustorium

Gene expression

High-throughput sequencing has permitted extensive studies of gene expression in non-model species, increasing knowledge of haustorial cell gene expression. In order to discover the molecular physiology of the haustoria, efforts have been made to isolate the haustoria in rust and powdery mildew (Gil and Gay, 1977; Hahn and Mendgen, 1992; Cantrill and Deverall, 1993; Catanzariti et al., 2006). Due to the complexity of haustorial isolation techniques, only a few transcriptome studies of rust and powdery mildew haustoria have been reported so far. Transcriptome studies established that, rust haustoria are extremely active in acquiring amino acids, carbohydrates, phosphate, and nitrogen (Hahn et al., 1997a; Voegele, 2006). The vast majority of genes in rusts that are haustorially expressed play essential roles in the synthesis of proteins, generation of energy, and metabolic processes. Furthermore, several transcripts were found to encode nutrient transporters or secreted proteins (Yin et al., 2009). These studies, on the other hand, only looked at a small portion of the genes that are expressed in the haustorium. The haustorium comprises a typical balance of organelles and nuclear genes. One of the most numerous and uniquely expressed genes in rust haustorium encodes a hexose transporter (HTX1; Voegele et al., 2001). This gene was expressed in leaf haustoria but not in *in vitro* infection structures. *U. fabae* haustoria strongly expressed two genes involved in vitamin B1 production (Sohn et al., 2000). This is a co-factor for enzymes involved in carbohydrate, amino acid, and biosynthesis processes. Work on this rust fungus revealed that the haustorium is extremely metabolically active and vital in nutrient absorption (Voegele et al., 2001). Differential screening of cDNA libraries from purified *U. fabae* haustoria provided further evidence for plasma membrane specialization. Hahn and Mendgen (1997) found at least 31 *in planta*-induced genes (*PIGs*), single or low-copy number genomic genes that code for proteins involved in amino acid transport, thiamine biosynthesis, metallothioneins, cytochrome P-450 mono-oxygenases, and short-chain dehydrogenases. *PIG* genes are highly expressed in infected leaf haustoria but not in germlings (germinated spores) or infection structures created on artificial membranes. Studies on cDNA microarrays showed enhanced expression of glycolysis (energy) and protein production genes in *B. graminis* infected barley (Both et al., 2005, 2005a). In the latter fungus, a partial proteome of haustoria showed significant representation of proteins implicated in protein metabolic pathways and energy production (Godfrey et al., 2009), and a comparative proteomic analysis confirmed higher protein and energy metabolism in haustoria (Bindschedler et al., 2009). Four thousand and four hundred and 58 transcripts were annotated from *Pst* haustoria using a Percoll gradient (Garnica et al., 2013). Most of the identified genes were associated with pathogen proliferation and metabolism, including biosynthesis of thymine, sugar transporters, and cell wall modification enzymes. Digital expression analysis showed 295 predicted secreted proteins overexpressed in haustoria (Garnica et al., 2013).

Another transcriptome analysis found that, in haustoria, 3,524 genes were upregulated relative to urediospores and germ tubes (Garnica et al., 2013). Functional categories uncovered by gene annotation and pathway analysis help them understand how differentially expressed genes operate in haustoria formation and host-pathogen interactions. Biotrophic colonization requires haustoria, as shown by the presence of ATP and TCA-related genes being upregulated in *Pst* (Garnica et al., 2013). Jakupović and colleagues found higher expression of *in planta*-induced genes involved in metabolic processes in haustoria than in other structures or stages of *U. fabae* (Jakupović et al., 2006). *Pst_22758*, a ubiquitous heat shock protein containing a DnaJ domain, may be involved in protein folding, unfolding, transport, and degradation in haustoria (Qiu et al., 2006; Düppre et al., 2011). Cell wall biogenesis and DNA replication were shown to be increased in germinated urediniospores in a transcriptome study of RNAs extracted from *Pgt* haustoria and urediniospores (Upadhyaya et al., 2014). In another transcriptomics study, extracellular cell wall modifying enzymes like chitinases had a higher abundance in the haustorial transcriptome of *U. appendiculatus* (Polonio et al., 2019; Sharma et al., 2019). It was shown that enzymes that change extracellular cell walls may be detected in the haustorial transcriptomes of *E. pisi, G. orontii, and P. xanthii*. Overexpression of two chitin-binding/hydrolase/glycosylase proteins was found in the haustoria *of E. pisi*, while expression of a putative chitin lytic polysaccharide monooxygenase

was found in *P. xanthii* haustoria (Polonio et al., 2019; Sharma et al., 2019). This suggests that these enzymes are important for haustorial physiology.

Haustorium nutrient uptake and metabolism

Fungal haustoria are feeding structures that transfer sugars and amino acids into the fungal cells. A few fundamental questions about the haustorium's function remain unanswered. These include identifying pathways for bidirectional transport (nutrient import and effector export), pathogen and host proteins at the haustorium–host cell contact, and regulatory genes that determine haustorial identity. Detailed assessment of putative nutrient absorption processes is hindered by the fact that fully developed haustoria are generated only *in planta* and their purification leads to loss of function (Hahn and Mendgen, 1992). Hence, haustoria have been mostly studied cytologically. Cytological and molecular investigations unraveled indirect evidence of haustoria's function in nutrient absorption (Gil and Gay, 1977). Sugar transporters and potential amino acid transporters in the structure suggest a function in nutrition absorption. An active transport mechanism is likely required to maintain high rates of carbon fluxes toward pathogens from the host leaves, since haustoria serve as potent sinks for metabolites. The transfer of nutrients (glucose, fructose, amino acids) from the EHMA into the haustorium is powered by the generation of a proton gradient across the haustorial plasma membrane by a membrane H1-ATPase (Szabo and Bushnell, 2001). Establishing a proton gradient is achievable because the EHMA is a sealed compartment surrounded by the EHM on the plant side, the HM on the fungal side, and the neckband prevents it from communicating with the apoplast (Szabo and Bushnell, 2001; Voegele et al., 2001). The haustorial H^+-ATPase plays a crucial function in nutrient absorption, presumably *via* activating carrier proteins for solute transport. Electrochemical gradients may be generated by this enzyme, which combines ATP hydrolysis with proton extrusion (Figure 2A). Rust fungi lack crucial processes (nitrate and sulfate assimilation), which explains their reliance on nutrient intake from their hosts (Duplessis et al., 2011; Kemen et al., 2015). *E. pisi* powdery mildew has an ATPase activity that is linked to the haustorial plasma membrane, but not to the EHM, implying that the host cell has no control over solute fluxes (Baka et al., 1995). While the EHM enclosing monokaryotic haustoria displayed ATPase activity, the non-invaginated region of the host plasma membrane did not. As a result, the monokaryon's filamentous haustorium seems to be less remarkable than the dikaryon's haustorium (Baka et al., 1995).

Due to their ability to be separated from infected plant tissue, rust fungus haustoria provided the opportunity for the first study of haustorial gene expression in *U. fabae* (Hahn and Mendgen, 1997). The findings of this study uncovered genes that produce a hexose transporter known as HXT1 (Voegele et al., 2001) as well as three amino acid transporters known as AAT1, AAT2, and AAT3 (Mendgen et al., 2000; Struck et al., 2002, 2004). Immunolocalization studies indicated that HXT1 and AAT2 are at the haustorial plasma membrane (Mendgen et al., 2000; Voegele et al., 2001). The amino acid transporters AAT1 and AAT3 have selectivity for the amino acids L-histidine and L-lysine, as well as L-cysteine, L-methionine, and L-leucine (Struck et al., 2004). On the other hand, biochemical experiments demonstrated that AAT1 and AAT3 function as proton-dependent transporters with preferences for histidine/lysine and leucine/methionine/cysteine, respectively (Struck et al., 2002, 2004). These experiments provided the first evidence that haustoria are involved in the process of nutrient absorption. Homologs of haustorial AAT genes were found in different rust fungus (Hacquard et al., 2011; Garnica et al., 2013). Plasma membrane H^+-ATPases are an essential component in the process of active nutrient absorption in both fungi and plants (Sondergaard et al., 2004). It would seem that the HXT1 sugar transporter is a symport carrier that derives its energy from H^+-ATPase. Mendgen and colleagues provided a molecular analysis of the gene and its regulation, a functional characterization of HXT1, and exquisite cytological evidence that demonstrates HXT1 is localized solely in the haustorial plasma membrane (Voegele et al., 2001). It was proven by Voegele and colleagues that the HXT1 sugar transporter has a selectivity for D-glucose and D-fructose. This confirms that glucose and fructose, and not sucrose, are the major sugars that are imported by haustoria (Voegele et al., 2001). In addition, the authors demonstrated that the transfer of glucose takes place *via* a process known as proton symport. These findings provide credence to the hypothesis that nutrient transport at the haustorial interface is governed by a proton symport model (Figure 2A). Monokaryotic and dikaryotic haustoria, as shown by the location of AAT2p, showed identical molecular features while having significant morphological variations (Mendgen et al., 2000). Only the distal section of the monokaryotic haustorium and the dikaryotic haustorial body distal to the haustorial neck were found to have the putative amino acid transporter (Hahn et al., 1997a). The boundary of the fungal membrane that is delineated by the neckband is not the location where molecular differentiation takes place; rather, it takes place across domains of the membrane that are not morphologically distinct. Expression of AAT2p appears to occur only late after penetration of the host cell, particularly in monokaryotic haustoria, with negligible further lateral diffusion of the transport protein after that (Mendgen et al., 2000). However, in addition to its primary function of absorbing and using amino acids, the haustorium also plays a significant part in the metabolic processing of sugar. *In planta*-induced genes that are also induced in the biotrophic mycelium were identified from a cDNA library that was unique to the haustorium of the broad bean rust fungus, *U. fabae*. Thiamine, a cofactor for numerous metabolic enzymes, may increase resistance gene expression, and is involved in plants' H_2O_2 pathway (Boubakri et al., 2012). It was observed that all haustorium-forming pathogens acquire their thiamine from the host since they lack a biosynthetic pathway. This indicates that

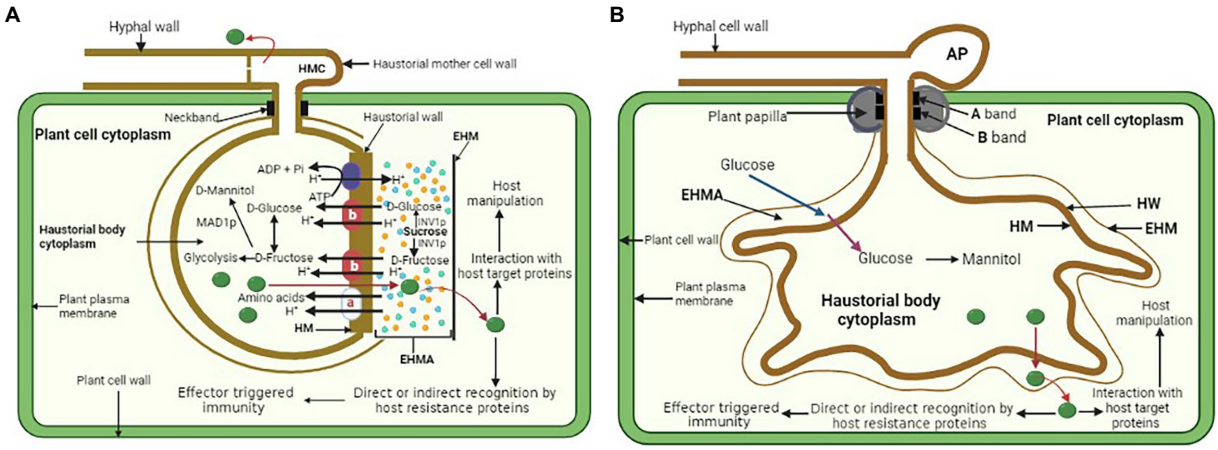

FIGURE 2
(A) General illustration of a rust fungus (dikaryon) haustorium and a proton symport model for the active uptake of amino acids and hexoses and redistribution from an infected leaf cell into a rust haustorium. EHMA, extrahaustorial matrix; EHM, extrahaustorial membrane; HM, haustorial plasma membrane. Haustorial plasma membrane H1-ATPase drives the uptake of nutrients by supplying protons. **a**—amino acid transporters AAT1 and AAT2; **b**—hexose transporter HXT1. Symport carriers utilize the resulting proton gradient between EHMA and haustorial cytoplasm to actively uptake amino acids and sugars. **(B)** General illustration of powdery mildew haustorium and its functions. HW, haustorial cell wall. Glucose passes through the EHM by facilitated diffusion (blue arrow) into EHMA where it is then actively transported (purple arrow) through the HM into the haustorial body cytoplasm. The glucose in the haustorium is converted to mannitol and then moves out to facilitate further mycelium growth. Both rust fungi and powdery mildew haustorium also secrete effectors (green) into the apoplast, including the EHMA and may pass through the EHM before entering the cytoplasm of the host plant where they are directly or indirectly recognized by the host disease resistance proteins resulting in effector triggered immunity, or they may target host proteins to manipulate host metabolism.

thiamine plays a critical role in both the metabolism of the haustorium and the formation of the hyphae (Kemen et al., 2011). Two genes involved in thiamine biosynthesis, known as *THI1* and *THI2*, were discovered to have the highest levels of expression in haustoria (Sohn et al., 2000). Together, they made up less than 5% of the mRNA detected in haustoria (Staples, 2001). The *THI1*-encoded protein was shown to have a strong preference for localization in the haustorial cytoplasm, as determined by immunocytology. Thiamine diphosphate, often known as vitamin B1, is a cofactor that is required by a number of enzymes involved in the metabolism of carbon and amino acids. Metallothioneins eliminate oxygen radicals by scavenging them (Ruttkay-Nedecky et al., 2013). Therefore, silencing *Pst_16188* may inhibit thiamine uptake from the host and thiamine metabolism in haustoria, which is consistent with obligate biotrophic fungus (Xu et al., 2020). Based on these findings, the haustoria are an important part of the main metabolic process (Sohn et al., 2000; Xu et al., 2020).

PIG2 is homologous to fungal amino acid permeases that act as symport carriers, transporting substrates using the energy of a proton gradient provided by a plasma membrane H^+-ATPase. There was an upregulation of the hydrolytic activity of a plasma membrane ATPase PMA1, in haustorial microsomal vesicles compared to germ tubes and ungerminated urediniospores (Struck et al., 1996). PMA1 molecular characterization established its autoregulation point and function in the process of nutrient absorption from host cells (Struck et al., 1998). PMA1 and MFL maltose transporter were both activated late in the fungal growth process (Weßling et al., 2012), but the absence of hexose transporters in the haustoria of *B. graminis* showed that powdery mildews make use of very few sugar transporters (Godfrey et al., 2009; Polonio et al., 2021). This may imply that, in contrast to rust haustoria, powdery mildew haustoria may make use of a variety of sources of carbohydrates. A major facilitator superfamily (MFS) sugar transporter was found to be among the top 50 expressed genes in a recent transcriptome study of *P. xanthii* haustoria. This study suggested that the powdery mildew fungi can use different methods for carbohydrate uptake (Figure 2B; Polonio et al., 2019). In addition to hexose and amino acid transporters, other nutrient transporters that are found in the haustoria have been characterized. *Pst* haustorial sulfate transporter (Yin et al., 2009), or the inorganic phosphate transporter among the top 50 expressed genes in the haustoria of Arabidopsis powdery mildew (Weßling et al., 2012), also showed that sulfur and phosphorus are taken up by the haustoria. The authors went on to demonstrate that this sugar transporter is localized in the haustorial membrane rather than in the membranes of the intercellular hyphae. This provided the first direct proof that sugar absorption takes place in the haustorium and indicated that it may be the sole site. Fourteen metabolism-related genes that were highly expressed in haustoria were silenced by host-induced gene silencing (Xu et al., 2020). It was shown that seven genes are involved in infection since silencing them in plants caused changes in the growth and development of *Pst*. The seven genes may have a

role in the differentiation of cells, the development of pathogens, as well as the production of carbohydrates, amino acids, and thiamine (Nowara et al., 2010).

Oligopeptide transporters (OPTs) are plasma membrane-localized transport systems involved in the import of oligopeptides (Lubkowitz, 2011). Different transcriptomic studies found that rust OPT genes are highly expressed *in planta* (Duplessis et al., 2011; Garnica et al., 2013; Lorrain et al., 2019). The *Pst* genome comprises of 12 amino acid and 7 sugar transporter genes, including two hexose transporters identical to the *HXT1* gene in *U. fabae* (Zheng et al., 2013). In addition, *Pgt* has 21 OPT genes, compared to 5 to 16 in other basidiomycete fungi (Duplessis et al., 2011), indicating greater peptide absorption in rust fungi. The enlarged transporter families in rust fungus and upregulated expression indicate functions in nutrient accumulation. *Pst* transcriptome sequencing found a gene encoding a transporter with strong homology to an S-methylmethionine permease (Garnica et al., 2013). This transporter was exclusively expressed in haustoria compared to germinated spores and may be important for sulfur absorption. However, genes encoding amino acid biosynthesis and metabolism enzymes were also found, showing possibility of metabolism of ammonia and amino acids from host plants. Recently, a comparative genomic analysis of a transportome (a complete collection of transporters in a given genome) was performed in Pucciniales and compared with other fungi in the Dikarya (Guerillot et al., 2022). It was found that the transportome of fungi in the order Pucciniales is distinguished by gene family expansions associated with metal transport and most notably, oligopeptide transport. Intriguingly, OPT genes are not constitutively expressed throughout the whole life cycle of poplar rust fungus *M. larici-populina*; instead, they are expressed either in the spores infecting each alternative host or directly during biotrophic growth and proliferation inside the hosts. The high expression of many OPT in *Pst* isolated haustoria, together with amino acid transporters clearly confirmed that the specialized structure serves as a nutritional hub during pathogen-host interactions (Garnica et al., 2013; Lorrain et al., 2019). OPT genes exhibited dynamic expression patterns throughout the rust fungus life cycle, and especially during infection of the poplar host tree, suggesting a specialization for nitrogen and sulfur acquisition through oligopeptides transportation from the host during biotrophic growth (Guerillot et al., 2022). *In vitro* analysis of the bean rust *U. fabae* infection structures identified various extracellular proteases including metalloproteases (Rauscher et al., 1995). The proteases were suggested to release oligopeptides from degrading proteins within this compartment. The source of oligopeptides transported by rust fungi during their interactions with the hosts however remains a mystery. Therefore, it would be very interesting to try to determine the flux of the oligopeptides derived from the host plant and the material that serves as a source for such oligopeptides. Although OPTs are mainly responsible for the transport of oligopeptides, it cannot be ruled out that some specific OPTs may convey perception of signals during the interactions (Lubkowitz, 2006).

Other rusts, such as *Uromyces appendiculatus* and *Phakopsora pachyrhizi* (Link et al., 2014) and *Pgt* (Duplessis et al., 2011; Upadhyaya et al., 2014), have comparable haustorial transcriptomes, indicating they use similar processes to utilize host-derived resources. In contrast, rust fungal genomes lack nitrate/nitrite transporters and nitrate reductases in the NH_4^+ assimilation pathway (Duplessis et al., 2011; Zheng et al., 2013). This indicates nitrate absorption inability and amino acid absorption from host cells. Since the host provides the activities that are needed for mandatory biotrophy, the lack of sulfite reductase in *Pgt* shows that there is no sulfate assimilation pathway in mandatory biotrophy (Duplessis et al., 2011). Recently, the invertase PsINV was studied in wheat rust *Pst* and exhibited great sucrose hydrolysis efficiency and boosted wheat infection expression (Chang et al., 2017). Other genes from *U. fabae* that have to do with metabolism, like glucokinase GLK1p, mannitol dehydrogenase 1 (MAD1p), and $NADH^+$ dependent D-arabitol dehydrogenase (ARD1p), have shown how this rust fungus stores and uses carbon (Voegele et al., 2005; Voegele and Mendgen, 2011). Homologs of these genes were discovered in other rust fungi and exhibited strong expression after infection, validating the processes of glucose absorption in rust fungus (Hacquard et al., 2010; Duplessis et al., 2011, 2011a; Garnica et al., 2013; Zheng et al., 2013). No sucrose transporter has been found in rust fungus, suggesting that hexose transport may be necessary in haustoria (Duplessis et al., 2011). Furthermore, findings from powdery mildew feeding experiments (Sutton et al., 1999) and rust fungi studies (Voegele et al., 2001; Voegele, 2006; Duplessis et al., 2011; Voegele and Mendgen, 2011; Zheng et al., 2013; Chang et al., 2017, 2020), collectively suggest that these pathogens mainly uptake hexose as the major carbohydrate source in the EHMA, where the hexose is either directly transported from host cells and/or converted from sucrose to hexose by a fungal invertase secreted into the EHMA (Liu et al., 2021). However, analysis of key haustorial genes of rust fungi only cannot enable conclusions regarding haustorial metabolism.

Biotrophic fungal pathogens are thought to strategically manipulate sugar transport in host cells to facilitate their access to carbohydrates. It was previously demonstrated that rust fungi or powdery mildew infection might cause an increased capacity for sugar acquisition in the infected host cells (Sutton et al., 2007; Chang et al., 2013). The increased sugar capacity may be due to enhanced activity of existing transporters or synthesis of new transporters in the infected host cells, which ultimately results in an increase in the amount of glucose available to the invading biotrophic fungal pathogens (Doidy et al., 2012). A sugar transporter *TaSTP6* was upregulated during rust infection and contributed to the susceptibility of wheat, most probably by enhancing cytoplasmic hexose concentration (Huai et al., 2019). Furthermore, a hexose transporter *Ps*HXT1 was recently found to have typical features of an MFS symporter with 12 membrane-spanning segments (Chang et al., 2020). *Ps*HXT1 was shown to be different from other rust fungal glucose transporters that have been characterized so far, and it only shared 26% similarity with

*Uf*HXT1. *Ps*HXT1 was confirmed to be localized on the plasma membrane and this showed that it could function as a transporter like *Uf*HXT1 (Voegele et al., 2001). In addition, *Ps*HXT1 biochemical characterization using *Saccharomyces cerevisiae* mutant strain lacking 20 hexose transporters revealed that it has a substrate preference of glucose. This was also further confirmed by competition experiments which showed that *Ps*HXT1 only has a high affinity for glucose (Chang et al., 2020). Silencing of *PsHXT1* significantly restricted normal growth and development of *Pst* during wheat infection, resulting in reduced disease symptoms and fungal biomass. These findings clearly demonstrated that *Ps*HXT1 is a glucose-proton symporter (Chang et al., 2020). Taken together with the previous *Ps*INV study (Chang et al., 2017), it can be ascertained that sugar starvation does not only impair *Pst* invasive growth and development, but also slackens pathogen proliferation and virulence without possible muddle with signaling effects. Genes/proteins involved in sugar uptake are promising targets for disease control novel strategies because they are very conserved compared to effectors (Oliva and Quibod, 2017; Chang et al., 2020).

Haustorial effectors

The fact that rusts and powdery mildews contain a high amount of transcripts encoding putative secreted proteins (Weßling et al., 2012; Garnica et al., 2013; Link et al., 2014; Polonio et al., 2019; Sharma et al., 2019; Xu et al., 2020), suggests that the haustorium might directly release effectors into the host cells, highlighting its importance not only in nutrients acquisition but also in pathogenesis, such as in the manipulation of host physiology and defense responses (Duplessis et al., 2012; Garnica et al., 2014; Polonio et al., 2021). For rust and powdery mildews, haustoria produce, secrete, and distribute virulence components, called effectors, that affect host physiology and immunity (Jones and Dangl, 2006). Several transcriptome studies focused on haustorial proteins to find haustorial effectors, and most of the identified proteins were novel candidates (Garnica et al., 2014; Link et al., 2014; Tao et al., 2017; Polonio et al., 2019; Elmore et al., 2020; Xu et al., 2020). Transcriptomic and genomic data from rust fungi found RTP1 homologs in at least 13 species, suggesting that this protein may play a role in biotrophic interactions (Pretsch et al., 2013). In the genomes of *Pgt*, *Pst*, *M. larici-populina*, and *M. lini* (Cantu et al., 2011; Duplessis et al., 2011; Nemri et al., 2014), approximately 8% of the predicted proteomes match the potential effectors that meet these requirements. Infection tissue-specific transcriptomes of these pathogens (Duplessis et al., 2011; Cantu et al., 2013; Garnica et al., 2013) and other rusts, notably *U. fabae* (Link and Voegele, 2008), have found multiple *in plant*-expressed effectors. Recently, haustoria-specific transcriptome data found 58% of the effector complement expected *in planta* in *Pgt* (Upadhyaya et al., 2014), supporting the hypothesis that the haustorium is the principal source of effector proteins. Proteome studies established that *Pt* has six effector protein signatures (peptidase and proteases, glucan-1,3-glucosidase and chitinases, protein disulfide isomerases, subtilisin-like serine proteases, cyclophilins, and carboxypeptidase; Song et al., 2011). *Pst* haustorial transcriptome analysis found an excess of cysteine-rich proteins among potential haustorial effectors and the majority of the secreted proteins produced in haustoria were expressed in a distinct manner from how they were expressed in germinating spores (Garnica et al., 2013). This is consistent with the fact that the majority of effector candidate genes are expressed in the haustoria, which is where they have the ability to operate directly by influencing the activities of host cells. A monoclonal antibody in mice was created using purified haustoria isolated from *Pt*-infected leaves. Purified haustoria contained 1,192 proteins, including 140 candidate secreted effector proteins (Rampitsch et al., 2015). In the haustorial transcriptome of *Pgt*, 520 secreted proteins were found, including 430 haustorially elevated secreted proteins and 90 genes expressed in germinated spores and haustoria as well as in haustoria alone (Cuomo et al., 2017). Research including transcriptome sequencing of isolated haustoria of stripe rust CYR31 race discovered 1,197 secreted proteins in haustoria, 69 of which suppressed cell death in tobacco and 49 decreased callose deposition in wheat, showing their critical roles in *Pst* infection (Xu et al., 2020). Six hundred and thirty-five candidate effectors of *P. triticina* were discovered through the RNA-seq of the interaction between *P. triticina* and wheat (Zhang et al., 2020).

Recent transcriptomics studies on powdery mildew haustoria established that there were some exclusively haustorially secreted proteins that included a SnodProt1 protein and many other putative adhesion proteins. The proteins had many ribonucleases and were also thought to be involved in protection against reactive oxygen species, phosphorous acquisition, and haustorial accommodation (Polonio et al., 2019; Sharma et al., 2019). Knockdown of some of the genes enhanced infection by powdery mildew (Sharma et al., 2019). Based on these findings, there may be a connection between the role of haustorium, its secreted proteins, and the proliferation of the pathogen. Since Y/F/WxC proteins account for 20% of the *B. graminis* haustorial transcriptome, it may be deduced that, this domain may play the key role in the physiological processes of powdery mildew (Polonio et al., 2021). The majority of the fungal haustorium cell's proteins are either host-translocated or function at the EHMA since the fungal haustorium cell is located inside the plant cell. The presence of transcripts encoding putatively secreted proteins in rust and powdery mildew haustoria suggests that the haustorium is involved in the release of effectors directly into host cells, underlining the importance of this structure not only for nutrient uptake but also for how effectors enter plant cells, which is unknown (Polonio et al., 2021). RTP1 and Avr proteins indicate a class of rust effectors that are transported into host cells *via* haustoria, some of which could become targets of immune receptors. The first fungal proteins to enter host cells were RTP1ps from *Uromyces* spp (Kemen et al., 2005). The proteins were

localized in host cells and then in the nucleus, suggesting a specific transport mechanism to their final location. Four different *M. lini* Avr proteins were successfully transported into their host cells (Rafiqi et al., 2010). All of these *M. lini* Avr proteins encode tiny secreted proteins that are produced in haustoria and found in the cytoplasm of the host, showing that they are delivered during infection. This was confirmed by direct visualization of the AvrM effectors (Rafiqi et al., 2010). Because AvrM and AvrL567 were expressed by tobacco cells, which were targeted to the plant secretory system, this work provided evidence that certain effectors may be taken up into the host cytosol regardless of a specific pathogen delivery mechanism. This was demonstrated by the fact that both of these effectors accumulated in the cytosol. AvrM is a membrane-binding protein that consists of two subunits, each of which has a hydrophobic surface patch that is essential for pathogen-independent internalization (Rafiqi et al., 2010; Ve et al., 2013). However, the mechanisms by which biotrophic fungal plant pathogens deliver their effectors into host cells are still a mystery.

Conclusion and perspectives

The growth of biotrophic fungal pathogens needs an important structure, the haustorium, formed inside the cells of a living host plant. The haustorium is essential for nutrient acquisition, as well as secretion and delivery of effectors into the host cells. The development of transformation techniques, methods for isolating haustoria and intracellular hyphae, genome sequencing, and EST analysis help us to understand the function of haustorium in biotrophic fungal pathogens. Many genes involved in the production of energy, host defense suppression, and pathogenicity are expressed in haustoria, and gene expression analysis data has indicated that this structure is the root of biotrophic fungal pathogens. Nevertheless, there is limited knowledge on the signaling pathways involved in the development of haustoria and intracellular hyphae; the involvement of the fungus and the plant in assembly; the molecular foundation for their activities; and how they establish and sustain a biotrophic interaction with a suitable host. In the near future, the rapidly expanding collections of genes obtained through large-scale sequencing projects, as well as the application of gene-expression profiling and functional genomics, will make it possible to conduct in-depth research on a variety of regulatory and functional phenomena. Future studies need to focus on the mechanisms underlying EHM biogenesis and functions, whether immune signaling occurs at the pathogen interface or not, and also EMH manipulation by the pathogens for their own benefit. There is still a great deal of fundamental issues unanswered. How does pathogen infection affect EHM content? How are symbiotic interfaces formed, and what signals drive their formation? How exactly does the movement of metabolites and minerals through the membranes of donor cells take place? Which characteristics (for example, the secretion of enzymes and toxins, interface components, and signaling mechanisms) differentiate biotrophic pathogens from endophytes, hemibiotrophs, and necrotrophs? In order to guarantee a steady supply of nutrients from the host plant, how can fungal symbionts cause metabolic sinks to form at the sites of infection? In the process of sink induction and the symbiotic differentiation of the fungus, what functions do sugars and enzymes that metabolize sugar (like invertases) play? Answers to these questions will reveal complicated molecular and cellular processes at the haustorial interface. Our understanding is limited to transporters strongly expressed in various phases of rust fungi, leading us to believe that they are essential nutrient transporters. Future research should also identify all nitrogen transporters. Also, rust fungi's nutrition signaling and amino acid absorption regulatory components must be identified. Thus, functional investigations of predicted haustorial proteins are essential. These components might help us to understand how biotrophic fungal plant pathogens evolved to affect their hosts.

Author contributions

JM and WY: conceptualization and literature search. JM: writing—original draft preparation. JM, WY, LZ, and NZ: writing—review and editing. WY: supervision and funding acquisition. All authors contributed to the article and approved the submitted version.

Funding

This work was funded by the Natural Science Foundation of China (nos. 301871915 and 32172367), National Key R&D Research Program of China (nos. 2013CB127702 and 2017YFD0201707), Natural Science Foundation of Hebei Province (no. C2020204071), and Modern Agricultural Industry System of Wheat Industry in Hebei Province (no. HBCT2018010204).

Conflict of interest

The authors declare that the research was conducted in the absence of any commercial or financial relationships that could be construed as a potential conflict of interest.

Publisher's note

References

Aime, M., Toome-Heller, M., and McLaughlin, D. (2014). "Pucciniomycotina" in *The Mycota VII Part A*. eds. D. MacLaughlin and J. W. Spatafora (Berlin: Springer), 271–294.

Baka, Z. A., Larous, L., and Lösel, D. M. (1995). Distribution of ATPase activity at the host-pathogen interfaces of rust infections. *Physiol. Mol. Plant Pathol.* 47, 67–82. doi: 10.1006/pmpp.1995.1043

Berkey, R., Zhang, Y., Ma, X., King, H., Zhang, Q., Wang, W., et al. (2017). Homologues of the RPW8 resistance protein are localized to the extrahaustorial membrane that is likely synthesized *de novo*. *Plant Physiol.* 173, 600–613. doi: 10.1104/pp.16.01539

Bindschedler, L. V., Burgis, T. A., Mills, D. J., Ho, J. T., Cramer, R., and Spanu, P. D. (2009). In planta proteomics and proteogenomics of the biotrophic barley fungal pathogen Blumeria graminis f. sp. hordei. *Mol. Cell. Proteomics* 8, 2368–2381. doi: 10.1074/mcp.M900188-MCP200

Both, M., Csukai, M., Stumpf, M. P. H., and Spanu, P. D. (2005). Gene expression profiles of *Blumeria graminis* indicate dynamic changes to primary metabolism during development of an obligate biotrophic pathogen. *Plant Cell* 17, 2107–2122. doi: 10.1105/tpc.105.032631

Both, M., Eckert, S. E., Csukai, M., Müller, E., Dimopoulos, G., and Spanu, P. D. (2005a). Transcript profiles of *Blumeria graminis* development during infection reveal a cluster of genes that are potential virulence determinants. *Mol. Plant-Microbe Interact.* 18, 125–133. doi: 10.1094/mpmi-18-0125

Boubakri, H., Wahab, M. A., Chong, J., Bertsch, C., Mliki, A., and Soustre-Gacougnolle, I. (2012). Thiamine induced resistance to *Plasmopara viticola* in grapevine and elicited host-defense responses, including HR like-cell death. *Plant Physiol. Biochem.* 57, 120–133. doi: 10.1016/j.plaphy.2012.05.016

Bracker, C. E., and Littlefield, L. J. (1973). "Structural concepts of host–pathogen interfaces," in *Fungal Pathogenicity and the Plant's Response*. eds. R. J. W. Byrde and C. V. Cutting (Academic Press), 159–317.

Braun, U., and Cook, R. (2012). *Taxonomic Manual of the Erysiphales (Powdery Mildews)*. CBS-KNAW Fungal Biodiversity Centre, Utrecht, Netherlands.

Bushell, W. R., and Bergquist, S. E. (1974). Aggregation of host cytoplasm and the formation of papillae and haustoria in powdery mildew of barley. *Phytopathology* 65, 310–318.

Cantrill, L. C., and Deverall, B. J. (1993). Isolation of haustoria from wheat leaves infected by the leaf rust fungus. *Physiol. Mol. Plant Pathol.* 42, 337–343.

Cantu, D., Govindarajulu, M., Kozik, A., Wang, M., Chen, X., Kojima, K. K., et al. (2011). Next generation sequencing provides rapid access to the genome of *Puccinia striiformis* f. sp. *tritici*, the causal agent of wheat stripe rust. *PLoS One* 6:e24230. doi: 10.1371/journal.pone.0024230

Cantu, D., Segovia, V., MacLean, D., Bayles, R., Chen, X., Kamoun, S., et al. (2013). Genome analyses of the wheat yellow (stripe) rust pathogen *Puccinia striiformis* f. sp. *tritici* reveal polymorphic and haustorial expressed secreted proteins as candidate effectors. *BMC Genomics* 14:270. doi: 10.1186/1471-2164-14-270

Catanzariti, A.-M., Dodds, P. N., Lawrence, G. J., Ayliffe, M. A., and Ellis, J. G. (2006). Haustorially expressed secreted proteins from flax rust are highly enriched for avirulence elicitors. *Plant Cell* 18, 243–256. doi: 10.1105/tpc.105.035980

Chang, Q., Lin, X., Yao, M., Liu, P., Guo, J., Huang, L., et al. (2020). Hexose transporter PsHXT1-mediated sugar uptake is required for pathogenicity of wheat stripe rust. *Plant Biotechnol. J.* 18, 2367–2369. doi: 10.1111/pbi.13398

Chang, Q., Liu, J., Lin, X., Hu, S., Yang, Y., Li, D., et al. (2017). A unique invertase is important for sugar absorption of an obligate biotrophic pathogen during infection. *New Phytol.* 215, 1548–1561. doi: 10.1111/nph.14666

Chang, Q., Liu, J., Wang, Q., Han, L., Liu, J., Li, M., et al. (2013). The effect of *Puccinia striiformis* f. sp. *tritici* on the levels of water-soluble carbohydrates and the photosynthetic rate in wheat leaves. *Physiol. Mol. Plant Pathol.* 84, 131–137. doi: 10.1016/j.pmpp.2013.09.001

Chowdhury, J., Schober, M. S., Shirley, N. J., Singh, R. R., Jacobs, A. K., Douchkov, D., et al. (2016). Down-regulation of the glucan synthase-like 6 gene (*HvGsl6*) in barley leads to decreased callose accumulation and increased cell wall penetration by *Blumeria graminis* f. sp. *hordei*. *New Phytol.* 212, 434–443. doi: 10.1111/nph.14086

Cuomo, C. A., Bakkeren, G., Khalil, H. B., Panwar, V., Joly, D., Linning, R., et al. (2017). Comparative analysis highlights variable genome content of wheat rusts and divergence of the mating loci. *G3* 7, 361–376. doi: 10.1534/g3.116.032797

Dean, R., Van Kan, J. A. L., Pretorius, Z. A., Hammond-Kosack, K. E., Di Pietro, A., Spanu, P. D., et al. (2012). The top 10 fungal pathogens in molecular plant pathology. *Mol. Plant Pathol.* 13, 414–430. doi: 10.1111/j.1364-3703.2011.00783.x

Doidy, J., Grace, E., Kühn, C., Simon-Plas, F., Casieri, L., and Wipf, D. (2012). Sugar transporters in plants and in their interactions with fungi. *Trends Plant Sci.* 17, 413–422. doi: 10.1016/j.tplants.2012.03.009

Duplessis, S., Cuomo, C. A., Lin, Y.-C., Aerts, A., Tisserant, E., Veneault-Fourrey, C., et al. (2011). Obligate biotrophy features unraveled by the genomic analysis of rust fungi. *Proc. Natl. Acad. Sci.* 108, 9166–9171. doi: 10.1073/pnas.1019315108

Duplessis, S., Hacquard, S., Delaruelle, C., Tisserant, E., Frey, P., Martin, F., et al. (2011a). *Melampsora larici-Populina* transcript profiling during germination and timecourse infection of poplar leaves reveals dynamic expression patterns associated with virulence and biotrophy. *Mol. Plant-Microbe Interact.* 24, 808–818. doi: 10.1094/MPMI-01-11-0006

Duplessis, S., Joly, D. L., and Dodds, P. N. (2012). "Rust effectors," in *Effectors in plant-microbe Interactions*. eds. F. Martin and S. Kamoun (Oxford, UK: John Wiley & Sons).

Düppre, E., Rupprecht, E., and Schneider, D. (2011). Specific and promiscuous functions of multiple DnaJ proteins in Synechocystis sp. PCC 6803. *Microbiology* 157, 1269–1278. doi: 10.1099/mic.0.045542-0

Eggert, D., Naumann, M., Reimer, R., and Voigt, C. A. (2014). Nanoscale glucan polymer network causes pathogen resistance. *Sci. Rep.* 4, 1–6. doi: 10.1038/srep04159

Eichmann, R., and Hückelhoven, R. (2008). Accommodation of powdery mildew fungi in intact plant cells. *J. Plant Physiol.* 165, 5–18. doi: 10.1016/j.jplph.2007.05.004

Eichmann, R., Schultheiss, H., Kogel, K. H., and Hückelhoven, R. (2004). The barley apoptosis suppressor homologue BAX inhibitor-1 compromises nonhost penetration resistance of barley to the inappropriate pathogen *Blumeria graminis* f. sp. *tritici*. *Mol. Plant-Microbe Interact.* 17, 484–490. doi: 10.1094/mpmi.2004.17.5.484

Elmore, M. G., Banerjee, S., Pedley, K. F., Ruck, A., and Whitham, S. A. (2020). *De novo* transcriptome of Phakopsora pachyrhizi uncovers putative effector repertoire during infection. *Physiol. Mol. Plant Pathol.* 110:101464. doi: 10.1016/j.pmpp.2020.101464

Figueroa, M., Dodds, P. N., and Henningsen, E. C. (2020). Evolution of virulence in rust fungi - multiple solutions to one problem. *Curr. Opin. Plant Biol.* 56, 20–27. doi: 10.1016/j.pbi.2020.02.007

Fischer-Parton, S., Parton, R. M., Hickey, P. C., and Dijksterhuis, J. (2000). HA 545 Atkinson, and ND read. 2000. Confocal microscopy of FM4-64 as a tool for 546 analysing endocytosis and vesicle trafficking in living fungal hyphae. *J. Microsc.* 547, 246–259. doi: 10.1046/j.1365-2818.2000.00708.x

Garnica, D. P., Nemri, A., Upadhyaya, N. M., Rathjen, J. P., and Dodds, P. N. (2014). The ins and outs of rust haustoria. *PLoS Pathog.* 10:e1004329. doi: 10.1371/journal.ppat.1004329

Garnica, D. P., Upadhyaya, N. M., Dodds, P. N., and Rathjen, J. P. (2013). Strategies for wheat stripe rust pathogenicity identified by transcriptome sequencing. *PLoS One* 8:e67150. doi: 10.1371/journal.pone.0067150

Gay, J. L., and Manners, J. M. (1987). Permeability of the haustorium-host interface in powdery mildews. *Physiol. Mol. Plant Pathol.* 30, 389–399. doi: 10.1016/0885-5765(87)90019-1

Gil, F., and Gay, J. L. (1977). Ultrastructural and physiological properties of the host interfacial components of haustoria of *Erysiphe pisi in vivo* and in vitro. *Physiol. Plant Pathol.* 10, 1–12. doi: 10.1016/0048-4059(77)90002-9

Godfrey, D., Zhang, Z., Saalbach, G., and Thordal-Christensen, H. (2009). A proteomics study of barley powdery mildew haustoria. *Proteomics* 9, 3222–3232. doi: 10.1002/pmic.200800645

Gold, R. E., and Mendgen, K. (1984). Cytology of basidiospore germination, penetration, and early colonization of *Phaseolus vulgaris* by *Uromyces appendiculatus* var. appendiculatus. *Can. J. Bot.* 62, 1989–2002. doi: 10.1139/b84-271

Gold, R. E., and Mendgen, K. (1991). "Rust basidiospore germlings and disease initiation," in *The Fungal spore and Disease Initiation in Plants and Animals*. eds. G. T. Cole and H. C. Hoch (Boston, MA: Springer US), 67–99.

Green, J. R., Mackie, A. J., Roberts, A. M., and Callow, J. A. (1992). "Molecular differentiation and development of the host–parasite interface in powdery mildew of pea," in *Perspectives in plant cell Recognition*. eds. J. A. Callow and J. R. Green, Society for Experimental Biology Seminar Series (Cambridge: Cambridge University Press), 193–212.

Green, J. R., Pain, N. A., Cannell, M. E., Leckie, C. P., McCready, S., Mitchell, A. J., et al. (1995). Analysis of differentiation and development of the specialized infection structures formed by biotrophic fungal plant pathogens using monoclonal antibodies. *Canad. J. Bot.* 73, 408–417. doi: 10.1139/b95-277

Guerillot, P., Salamov, A., Louet, C., Morin, E., Frey, P., Grigoriev, I. V., et al. (2022). A remarkable expansion of oligopeptide transporter genes in rust fungi (Pucciniales) suggests a specialization in nutrients acquisition for obligate biotrophy. bioRxiv [preprint]. pp. 2022.04.20.488971.

Hacquard, S., Delaruelle, C., Legué, V., Tisserant, E., Kohler, A., Frey, P., et al. (2010). Laser capture microdissection of uredinia formed by *Melampsora larici-*

Populina revealed a transcriptional switch between biotrophy and sporulation. *Mol. Plant-Microbe Interact.* 23, 1275–1286. doi: 10.1094/mpmi-05-10-0111

Hacquard, S., Petre, B., Frey, P., Hecker, A., Rouhier, N., and Duplessis, S. (2011). The poplar-poplar rust interaction: insights from genomics and transcriptomics. *J. Pathog.* 2011:716041. doi: 10.4061/2011/716041

Hafeez, A. N., Arora, S., Ghosh, S., Gilbert, D., Bowden, R. L., and Wulff, B. B. H. (2021). Creation and judicious application of a wheat resistance gene atlas. *Mol. Plant* 14, 1053–1070. doi: 10.1016/j.molp.2021.05.014

Hahn, M., Deising, H., Struck, C., and Mendgen, K. (1997). "Fungal morphogenesis and enzyme secretion during pathogenesis," in *In Resistance of Crop Plants against Fungi*. eds. H. Hartleb, R. Heitefuss and H. H. Hoppe (Jena: Gustav Fischer), 33–57.

Hahn, M., and Mendgen, K. (1992). Isolation by ConA binding of haustoria from different rust fungi and comparison of their surface qualities. *Protoplasma* 170, 95–103. doi: 10.1007/BF01378785

Hahn, M., and Mendgen, K. (1997). Characterization of in planta-induced rust genes isolated from a haustorium-specific cDNA library. *Mol. Plant-Microbe Interact.* 10, 427–437. doi: 10.1094/mpmi.1997.10.4.427

Hahn, M., Neef, U., Struck, C., Göttfert, M., and Mendgen, K. (1997a). A putative amino acid transporter is specifically expressed in haustoria of the rust fungus Uromyces fabae. *Mol. Plant-Microbe Interact.* 10, 438–445. doi: 10.1094/mpmi.1997.10.4.438

Harder, D. E. (1989). Rust fungal haustoria -past, present, future. *Can. J. Plant Pathol.* 11, 91–99. doi: 10.1080/07060668909501154

Harder, D. E., and Chong, J. (1984). "Structure and physiology of haustoria," in *The Cereal Rusts, vol 1, Origins, Specificity, Structure and Physiology*. eds. W. R. Bushell and A. R. Roelfs (Orlando, FL: Academic Press), 431–476.

Harder, D. E., and Chong, J. (1991). "Rust haustoria," in *Electron Microscopy of plant Pathogens*. eds. K. Mendgen and D.-E. Lesemann (Berlin, Heidelberg: Springer), 235–250.

Harder, D. E. R., and Mendgen, K. (1982). Filipin-sterol complexes in bean rust- and oat crown rust-fungal/plant interactions: freeze-etch electron microscopy. *Protoplasma* 112, 46–54. doi: 10.1007/BF01280214

Heath, M. C. (1976). Ultrastructural and functional similarity of the haustorial neckband of rust fungi and the Casparian strip of vascular plants. *Can. J. Bot.* 54, 2484–2489. doi: 10.1139/b76-266

Heath, M. C., and Skalamera, D. (1997). "Cellular interactions between plants and biotrophic fungal parasites," in *Advances in Botanical Research*. eds. J. H. Andrews, I. C. Tommerup and J. A. Callow (Academic Press), 195–225.

Henty-Ridilla, J. L., Shimono, M., Li, J., Chang, J. H., Day, B., and Staiger, C. J. (2013). The plant actin cytoskeleton responds to signals from microbe-associated molecular patterns. *PLoS Pathog.* 9:e1003290. doi: 10.1371/journal.ppat.1003290

Hippe-Sanwald, S., Marticke, K. H., Kieliszewski, M. J., and Somerville, S. C. (1994). Immunogold localization of THRGP-like epitopes in the haustorial interface of obligate, biotrophic fungi on monocots. *Protoplasma* 178, 138–155. doi: 10.1007/BF01545964

Huai, B., Yang, Q., Qian, Y., Qian, W., Kang, Z., and Liu, J. (2019). ABA-induced sugar transporter TaSTP6 promotes wheat susceptibility to stripe rust. *Plant Physiol.* 181, 1328–1343. doi: 10.1104/pp.19.00632

Jakupović, M., Heintz, M., Reichmann, P., Mendgen, K., and Hahn, M. (2006). Microarray analysis of expressed sequence tags from haustoria of the rust fungus Uromyces fabae. *Fungal Genet. Biol.* 43, 8–19. doi: 10.1016/j.fgb.2005.09.001

Jaswal, R., Kiran, K., Rajarammohan, S., Dubey, H., Singh, P. K., Sharma, Y., et al. (2020). Effector biology of biotrophic plant fungal pathogens: current advances and future prospects. *Microbiol. Res.* 241:126567. doi: 10.1016/j.micres.2020.126567

Jones, J. D., and Dangl, J. L. (2006). The plant immune system. *Nature* 444, 323–329. doi: 10.1038/nature05286

Kelly, H. Y., Dufault, N. S., Walker, D. R., Isard, S. A., Schneider, R. W., Giesler, L. J., et al. (2015). From select agent to an established pathogen: the response to Phakopsora pachyrhizi (soybean rust) in North America. *Phytopathology* 105, 905–916. doi: 10.1094/phyto-02-15-0054-fi

Kemen, A. C., Agler, M. T., and Kemen, E. (2015). Host-microbe and microbe-microbe interactions in the evolution of obligate plant parasitism. *New Phytol.* 206, 1207–1228. doi: 10.1111/nph.13284

Kemen, E., Gardiner, A., Schultz-Larsen, T., Kemen, A. C., Balmuth, A. L., Robert-Seilaniantz, A., et al. (2011). Gene gain and loss during evolution of obligate parasitism in the white rust pathogen of Arabidopsis thaliana. *PLoS Biol.* 9:e1001094. doi: 10.1371/journal.pbio.1001094

Kemen, E., Kemen, A. C., Rafiqi, M., Hempel, U., Mendgen, K., Hahn, M., et al. (2005). Identification of a protein from rust fungi transferred from haustoria into infected plant cells. *Mol. Plant-Microbe Interact.* 18, 1130–1139. doi: 10.1094/mpmi-18-1130

Kim, H., O'Connell, R., Maekawa-Yoshikawa, M., Uemura, T., Neumann, U., and Schulze-Lefert, P. (2014). The powdery mildew resistance protein RPW8.2 is carried on VAMP721/722 vesicles to the extrahaustorial membrane of haustorial complexes. *Plant J.* 79, 835–847. doi: 10.1111/tpj.12591

Koh, S., André, A., Edwards, H., Ehrhardt, D., and Somerville, S. (2005). Arabidopsis thaliana subcellular responses to compatible Erysiphe cichoracearum infections. *Plant J.* 44, 516–529. doi: 10.1111/j.1365-313X.2005.02545.x

Kokhmetova, A., Rsaliyev, A., Malysheva, A., Atishova, M., Kumarbayeva, M., and Keishilov, Z. (2021). Identification of stripe rust resistance genes in common wheat cultivars and breeding lines from Kazakhstan. *Plan. Theory* 10:2303. doi: 10.3390/plants10112303

Kwaaitaal, M., Nielsen, M. E., Böhlenius, H., and Thordal-Christensen, H. (2017). The plant membrane surrounding powdery mildew haustoria shares properties with the endoplasmic reticulum membrane. *J. Exp. Bot.* 68, 5731–5743. doi: 10.1093/jxb/erx403

Lambertucci, S., Orman, K. M., Das Gupta, S., Fisher, J. P., Gazal, S., Williamson, R. J., et al. (2019). Analysis of barley leaf epidermis and extrahaustorial proteomes during powdery mildew infection reveals that the PR5 thaumatin-like protein TLP5 is required for susceptibility towards *Blumeria graminis* f. sp. hordei. *Front. Plant Sci.* 10:1138. doi: 10.3389/fpls.2019.01138

Lawrence, G. J., Dodds, P. N., and Ellis, J. G. (2007). Rust of flax and linseed caused by Melampsora lini. *Mol. Plant Pathol.* 8, 349–364. doi: 10.1111/j.1364-3703.2007.00405.x

Link, T. I., Lang, P., Scheffler, B. E., Duke, M. V., Graham, M. A., Cooper, B., et al. (2014). The haustorial transcriptomes of Uromyces appendiculatus and Phakopsora pachyrhizi and their candidate effector families. *Mol. Plant Pathol.* 15, 379–393. doi: 10.1111/mpp.12099

Link, T. I., and Voegele, R. T. (2008). Secreted proteins of *Uromyces fabae*: similarities and stage specificity. *Mol. Plant Pathol.* 9, 59–66. doi: 10.1111/j.1364-3703.2007.00448.x

Lipka, V., and Panstruga, R. (2005). Dynamic cellular responses in plant–microbe interactions. *Curr. Opin. Plant Biol.* 8, 625–631. doi: 10.1016/j.pbi.2005.09.006

Littlefield, L. J., and Bracker, C. E. (1972). Ultrastructural specialization at the host-pathogen interface in rust-infected flax. *Protoplasma* 74, 271–305. doi: 10.1007/BF01282533

Liu, J., Liu, M., Tan, L., Huai, B., Ma, X., Pan, Q., et al. (2021). AtSTP8, an endoplasmic reticulum-localised monosaccharide transporter from *Arabidopsis*, is recruited to the extrahaustorial membrane during powdery mildew infection. *New Phytol.* 230, 2404–2419. doi: 10.1111/nph.17347

LoPresti, L., Lanver, D., Schweizer, G., Tanaka, S., Liang, L., Tollot, M., et al. (2015). Fungal effectors and plant susceptibility. *Annu. Rev. Plant Biol.* 66, 513–545. doi: 10.1146/annurev-arplant-043014-114623

Lorrain, C., Gonçalves dos Santos, K. C., Germain, H., Hecker, A., and Duplessis, S. (2019). Advances in understanding obligate biotrophy in rust fungi. *New Phytol.* 222, 1190–1206. doi: 10.1111/nph.15641

Lubkowitz, M. (2006). The OPT family functions in long-distance peptide and metal transport in plants. *Genet. Eng.* 27, 35–55. doi: 10.1007/0-387-25856-6_3

Lubkowitz, M. (2011). The oligopeptide transporters: A small gene family with a diverse group of substrates and functions? *Mol. Plant* 4, 407–415. doi: 10.1093/mp/ssr004

Ma, X. F., Li, Y., Sun, J. L., Wang, T. T., Fan, J., Lei, Y., et al. (2014). Ectopic expression of RESISTANCE TO POWDERY MILDEW8.1 confers resistance to fungal and oomycete pathogens in *Arabidopsis*. *Plant Cell Physiol.* 55, 1484–1496. doi: 10.1093/pcp/pcu080

Mackie, A. J., Roberts, A. M., Callow, J. A., and Green, J. R. (1991). Molecular differentiation in pea powdery-mildew haustoria. *Planta* 183, 399–408. doi: 10.1007/BF00197739

Manners, J. M., and Gay, J. L. (1983). The host-parasite interface and nutrient transfer in biotrophic parasitism. *Biochem. Plant Pathol.* 163:195.

Mapuranga, J., Zhang, N., Zhang, L., Chang, J., and Yang, W. (2022). Infection strategies and pathogenicity of biotrophic plant fungal pathogens. *Front. Microbiol.* 13:799396. doi: 10.3389/fmicb.2022.799396

Martel, A., Ruiz-Bedoya, T., Breit-McNally, C., Laflamme, B., Desveaux, D., and Guttman, D. S. (2021). The ETS-ETI cycle: evolutionary processes and metapopulation dynamics driving the diversification of pathogen effectors and host immune factors. *Curr. Opin. Plant Biol.* 62:102011. doi: 10.1016/j.pbi.2021.102011

Martínez-Cruz, J., Romero, D., Dávila, J. C., and Pérez-García, A. (2014). The Podosphaera xanthii haustorium, the fungal Trojan horse of cucurbit-powdery mildew interactions. *Fungal Genet. Biol.* 71, 21–31. doi: 10.1016/j.fgb.2014.08.006

McIntosh, R. A., Wellings, C. R., and Park, R. F. (1995). *Wheat rusts: An atlas of resistance genes*. East Melbourne, Australia: CSIRO Publishing.

Mendgen, K., and Deising, H. (1993). Infection structures of fungal plant pathogens – a cytological and physiological evaluation. *New Phytol.* 124, 193–213. doi: 10.1111/j.1469-8137.1993.tb03809.x

Mendgen, K., Struck, C., Voegele, R., and Hahn, M. (2000). Biotrophy and rust haustoria. *Physiol. Mol. Plant Pathol.* 56, 141–145. doi: 10.1006/pmpp.2000.0264

Micali, C. O., Neumann, U., Grunewald, D., Panstruga, R., and O'Connell, R. (2011). Biogenesis of a specialized plant-fungal interface during host cell internalization of *Golovinomyces orontii* haustoria. *Cell. Microbiol.* 13, 210–226. doi: 10.1111/j.1462-5822.2010.01530.x

Nemri, A., Saunders, D., Anderson, C., Upadhyaya, N., Win, J., Lawrence, G., et al. (2014). The genome sequence and effector complement of the flax rust pathogen Melampsora lini. *Front. Plant Sci.* 5:98. doi: 10.3389/fpls.2014.00098

Nowara, D., Gay, A., Lacomme, C., Shaw, J., Ridout, C., Douchkov, D., et al. (2010). HIGS: host-induced gene silencing in the obligate biotrophic fungal pathogen *Blumeria graminis*. *Plant Cell* 22, 3130–3141. doi: 10.1105/tpc.110.077040

Oliva, R., and Quibod, I. L. (2017). Immunity and starvation: new opportunities to elevate disease resistance in crops. *Curr. Opin. Plant Biol.* 38, 84–91. doi: 10.1016/j.pbi.2017.04.020

Paulsen, P. A., Custódio, T. F., and Pedersen, B. P. (2019). Crystal structure of the plant symporter STP10 illuminates sugar uptake mechanism in monosaccharide transporter superfamily. *Nat. Commun.* 10:407. doi: 10.1038/s41467-018-08176-9

Polonio, Á., Pérez-García, A., Martínez-Cruz, J., Fernández-Ortuño, D., and de Vicente, A. (2021). "The haustorium of phytopathogenic fungi: A short overview of a specialized cell of obligate biotrophic plant parasites," in *Progress in Botany*. eds. F. M. Cánovas, U. Lüttge, M.-C. Risueño and H. Pretzsch, vol. *82* (Cham: Springer International Publishing), 337–355.

Polonio, Á., Seoane, P., Claros, M. G., and Pérez-García, A. (2019). The haustorial transcriptome of the cucurbit pathogen *Podosphaera xanthii* reveals new insights into the biotrophy and pathogenesis of powdery mildew fungi. *BMC Genomics* 20:543. doi: 10.1186/s12864-019-5938-0

Pretsch, K., Kemen, A., Kemen, E., Geiger, M., Mendgen, K., and Voegele, R. (2013). The rust transferred proteins-a new family of effector proteins exhibiting protease inhibitor function. *Mol. Plant Pathol.* 14, 96–107. doi: 10.1111/j.1364-3703.2012.00832.x

Qiu, X. B., Shao, Y. M., Miao, S., and Wang, L. (2006). The diversity of the DnaJ/Hsp 40 family, the crucial partners for Hsp 70 chaperones. *Cell. Mol. Life Sci.* 63, 2560–2570. doi: 10.1007/s00018-006-6192-6

Rafiqi, M., Gan, P. H., Ravensdale, M., Lawrence, G. J., Ellis, J. G., Jones, D. A., et al. (2010). Internalization of flax rust avirulence proteins into flax and tobacco cells can occur in the absence of the pathogen. *Plant Cell* 22, 2017–2032. doi: 10.1105/tpc.109.072983

Rampitsch, C., Günel, A., Beimcik, E., and Mauthe, W. (2015). Proteome of monoclonal antibody-purified haustoria from *Puccinia triticina* Race-1. *Proteomics* 15, 1307–1315. doi: 10.1002/pmic.201400241

Rauscher, M., Mendgen, K., and Deising, H. (1995). Extracellular proteases of the rust fungus Uromyces viciae-fabae. *Exp. Mycol.* 19, 26–34. doi: 10.1006/emyc.1995.1004

Rodrigues, M. L., Nimrichter, L., Oliveira, D. L., Nosanchuk, J. D., and Casadevall, A. (2008). Vesicular trans-cell wall transport in fungi: a mechanism for the delivery of virulence-associated macromolecules? *Lipid Insights* 2:LPI.S1000. doi: 10.4137/lpi.s1000

Ruttkay-Nedecky, B., Nejdl, L., Gumulec, J., Zitka, O., Masarik, M., Eckschlager, T., et al. (2013). The role of metallothionein in oxidative stress. *Int. J. Mol. Sci.* 14, 6044–6066. doi: 10.3390/ijms14036044

Schmidt, S. M., and Panstruga, R. (2007). Cytoskeleton functions in plant–microbe interactions. *Physiol. Mol. Plant Pathol.* 71, 135–148. doi: 10.1016/j.pmpp.2008.01.001

Schmidt, S. M., and Panstruga, R. (2011). Pathogenomics of fungal plant parasites: what have we learnt about pathogenesis? *Curr. Opin. Plant Biol.* 14, 392–399. doi: 10.1016/j.pbi.2011.03.006

Schorey, J. S., and Bhatnagar, S. (2008). Exosome function: from tumor immunology to pathogen biology. *Traffic* 9, 871–881. doi: 10.1111/j.1600-0854.2008.00734.x

Sharma, G., Aminedi, R., Saxena, D., Gupta, A., Banerjee, P., Jain, D., et al. (2019). Effector mining from the *Erysiphe pisi* haustorial transcriptome identifies novel candidates involved in pea powdery mildew pathogenesis. *Mol. Plant Pathol.* 20, 1506–1522. doi: 10.1111/mpp.12862

Smith, S. E., and Smith, F. A. (1990). Structure and function of the interfaces in biotrophic symbioses as they relate to nutrient transport. *New Phytol.* 114, 1–38. doi: 10.1111/j.1469-8137.1990.tb00370.x

Sohn, J., Voegele, R. T., Mendgen, K., and Hahn, M. (2000). High level activation of vitamin B1 biosynthesis genes in haustoria of the rust fungus *Uromyces fabae*. *Mol. Plant-Microbe Interact.* 13, 629–636. doi: 10.1094/MPMI.2000.13.6.629

Sondergaard, T. E., Schulz, A., and Palmgren, M. G. (2004). Energization of transport processes in plants. Roles of the plasma membrane H^+-ATPase. *Plant Physiol.* 136, 2475–2482. doi: 10.1104/pp.104.048231

Song, X., Rampitsch, C., Soltani, B., Mauthe, W., Linning, R., Banks, T., et al. (2011). Proteome analysis of wheat leaf rust fungus, *Puccinia triticina*, infection structures enriched for haustoria. *Proteomics* 11, 944–963. doi: 10.1002/pmic.201000014

Staples, R. (2001). Nutrients for a rust fungus: The role of haustoria. *Trends Plant Sci.* 6, 496–498. doi: 10.1016/S1360-1385(01)02126-4

Stark-Urnau, M., and Mendgen, K. (1995). Sequential deposition of plant glycoproteins and polysaccharides at the host-parasite interface of *Uromyces vignae* and Vigna sinensis. *Protoplasma* 186, 1–11. doi: 10.1007/BF01276929

Struck, C., Ernst, M., and Hahn, M. (2002). Characterization of a developmentally regulated amino acid transporter (AAT1p) of the rust fungus *Uromyces fabae*. *Mol. Plant Pathol.* 3, 23–30. doi: 10.1046/j.1464-6722.2001.00091.x

Struck, C., Hahn, M., and Mendgen, K. (1996). Plasma membrane H^+-ATPase activity in spores, germ tubes, and haustoria of the rust fungus *Uromyces viciae-fabae*. *Fungal Genet. Biol.* 20, 30–35. doi: 10.1006/fgbi.1996.0006

Struck, C., Mueller, E., Martin, H., and Lohaus, G. (2004). The *Uromyces fabae UfAAT3* gene encodes a general amino acid permease that prefers uptake of in planta scarce amino acids. *Mol. Plant Pathol.* 5, 183–189. doi: 10.1111/j.1364-3703.2004.00222.x

Struck, C., Siebels, C., Rommel, O., Wernitz, M., and Hahn, M. (1998). The plasma membrane H^+-ATPase from the biotrophic rust fungus *Uromyces fabae*: molecular characterization of the gene (PMA1) and functional expression of the enzyme in yeast. *Mol. Plant-Microbe Interact.* 11, 458–465. doi: 10.1094/mpmi.1998.11.6.458

Stumpf, M. A., and Gay, J. L. (1990). The composition of *Erysiphe pisi* haustorial complexes with special reference to the neckbands. *Physiol. Mol. Plant Pathol.* 37, 125–143. doi: 10.1016/0885-5765(90)90004-H

Sutton, P. N., Gilbert, M. J., Williams, L. E., and Hall, J. (2007). Powdery mildew infection of wheat leaves changes host solute transport and invertase activity. *Physiol. Plantarum.* 129, 787–795. doi: 10.1111/j.1399-3054.2007.00863.x

Sutton, P. N., Henry, M. J., and Hall, J. L. (1999). Glucose, and not sucrose, is transported from wheat to wheat powdery mildew. *Planta* 208, 426–430. doi: 10.1007/s004250050578

Szabo, L. J., and Bushnell, W. R. (2001). Hidden robbers: the role of fungal haustoria in parasitism of plants. *Proc. Natl. Acad. Sci.* 98, 7654–7655. doi: 10.1073/pnas.151262398

Tao, S.-Q., Cao, B., Tian, C.-M., and Liang, Y.-M. (2017). Comparative transcriptome analysis and identification of candidate effectors in two related rust species (*Gymnosporangium yamadae* and *Gymnosporangium asiaticum*). *BMC Genomics* 18:651. doi: 10.1186/s12864-017-4059-x

Théry, C. (2011). Exosomes: secreted vesicles and intercellular communications. *F1000 Biol. Rep.* 3:15. doi: 10.3410/B3-15

Upadhyaya, N. M., Garnica, D. P., Karaoglu, H., Sperschneider, J., Nemri, A., Xu, B., et al. (2014). Comparative genomics of Australian isolates of the wheat stem rust pathogen *Puccinia graminis* f. sp. *tritici* reveals extensive polymorphism in candidate effector genes. *Front. Plant Sci.* 5:759. doi: 10.3389/fpls.2014.00759

Valadi, H., Ekström, K., Bossios, A., Sjöstrand, M., Lee, J. J., and Lötvall, J. O. (2007). Exosome-mediated transfer of mRNAs and micro RNAs is a novel mechanism of genetic exchange between cells. *Nat. Cell Biol.* 9, 654–659. doi: 10.1038/ncb1596

Ve, T., Williams Simon, J., Catanzariti, A.-M., Rafiqi, M., Rahman, M., Ellis Jeffrey, G., et al. (2013). Structures of the flax-rust effector Avr M reveal insights into the molecular basis of plant-cell entry and effector-triggered immunity. *Proc. Natl. Acad. Sci.* 110, 17594–17599. doi: 10.1073/pnas.1307614110

Voegele, R. T. (2006). *Uromyces fabae*: development, metabolism, and interactions with its host *Vicia faba*. *FEMS Microbiol. Lett.* 259, 165–173. doi: 10.1111/j.1574-6968.2006.00248.x

Voegele, R. T., Hahn, M., Lohaus, G., Link, T., Heiser, I., and Mendgen, K. (2005). Possible roles for mannitol and mannitol dehydrogenase in the biotrophic plant pathogen *Uromyces fabae*. *Plant Physiol.* 137, 190–198. doi: 10.1104/pp.104.051839

Voegele, R., Hahn, M., and Mendgen, K. (2009). "The uredinales: cytology, biochemistry, and molecular biology" in *The Mycota, V. Plant Relationships*. ed. H. Deising (Berlin: Springer Verlag), 69–98.

Voegele, R. T., and Mendgen, K. (2003). Rust haustoria: nutrient uptake and beyond. *New Phytol.* 159, 93–100. doi: 10.1046/j.1469-8137.2003.00761.x

Voegele, R. T., and Mendgen, K. W. (2011). Nutrient uptake in rust fungi: how sweet is parasitic life? *Euphytica* 179, 41–55. doi: 10.1007/s10681-011-0358-5

Voegele, R. T., Struck, C., Hahn, M., and Mendgen, K. (2001). The role of haustoria in sugar supply during infection of broad bean by the rust fungus *Uromyces fabae*. *Proc. Natl. Acad. Sci. U. S. A.* 98, 8133–8138. doi: 10.1073/pnas.131186798

Wang, W., Wen, Y., Berkey, R., and Xiao, S. (2009). Specific targeting of the *Arabidopsis* resistance protein RPW8.2 to the interfacial membrane encasing the fungal haustorium renders broad-spectrum resistance to powdery mildew. *Plant Cell* 21, 2898–2913. doi: 10.1105/tpc.109.067587

Wang, W., Zhang, Y., Wen, Y., Berkey, R., Ma, X., Pan, Z., et al. (2013). A comprehensive mutational analysis of the Arabidopsis resistance protein RPW8.2 reveals key amino acids for defense activation and protein targeting. *Plant Cell* 25, 4242–4261. doi: 10.1105/tpc.113.117226

Weßling, R., Schmidt, S. M., Micali, C. O., Knaust, F., Reinhardt, R., Neumann, U., et al. (2012). Transcriptome analysis of enriched *Golovinomyces orontii* haustoria by deep 454 pyrosequencing. *Fungal Genet. Biol.* 49, 470–482. doi: 10.1016/j.fgb.2012.04.001

Woods, A. M., Didehvar, F., Gay, J. L., and Mansfield, J. W. (1988). Modification of the host plasmalemma in haustorial infections of *Lactuca sativa* by Bremia lactucae. *Physiol. Mol. Plant Pathol.* 33, 299–310. doi: 10.1016/0885-5765(88)90030-6

Woods, A. M., and Gay, J. L. (1983). Evidence for a neckband delimiting structural and physiological regions of the host plasma membrane associated with haustoria of Albugo candida. *Physiol. Plant Pathol.* 23, 73–88. doi: 10.1016/0048-4059(83)90035-8

Xu, Q., Tang, C., Wang, L., Zhao, C., Kang, Z., and Wang, X. (2020). Haustoria – arsenals during the interaction between wheat and Puccinia striiformis f. sp. tritici. *Mol. Plant Pathol.* 21, 83–94. doi: 10.1111/mpp.12882

Yin, C., Chen, X., Wang, X., Han, Q., Kang, Z., and Hulbert, S. H. (2009). Generation and analysis of expression sequence tags from haustoria of the wheat stripe rust fungus Puccinia striiformis f. sp. tritici. *BMC Genomics* 10:626. doi: 10.1186/1471-2164-10-626

Zhang, Y., Wei, J., Qi, Y., Li, J., Amin, R., Yang, W., et al. (2020). Predicating the effector proteins secreted by *Puccinia triticina* through transcriptomic analysis and multiple prediction approaches. *Front. Microbiol.* 11:538032. doi: 10.3389/fmicb.2020.538032

Zheng, W., Huang, L., Huang, J., Wang, X., Chen, X., Zhao, J., et al. (2013). High genome heterozygosity and endemic genetic recombination in the wheat stripe rust fungus. *Nat. Commun.* 4:2673. doi: 10.1038/ncomms3673

frontiers | Frontiers in Plant Science

TYPE Original Research
PUBLISHED 02 September 2022
DOI 10.3389/fpls.2022.962973

OPEN ACCESS

EDITED BY
Maria Rosa Simon,
National University of La Plata, Argentina

REVIEWED BY
Yulin Cheng,
Chongqing University, China
Klára Kosová,
Crop Research Institute (CRI), Czechia

*CORRESPONDENCE
Bernard Nyamesorto
bernard.nyamesorto@montana.edu
Li Huang
lhuang@montana.edu

SPECIALTY SECTION
This article was submitted to Plant Pathogen Interactions, a section of the journal Frontiers in Plant Science

RECEIVED 07 June 2022
ACCEPTED 15 August 2022
PUBLISHED 02 September 2022

CITATION
Nyamesorto B, Zhang H, Rouse M, Wang M, Chen X and Huang L (2022) A transcriptomic-guided strategy used in identification of a wheat rust pathogen target and modification of the target enhanced host resistance to rust pathogens. *Front. Plant Sci.* 13:962973. doi: 10.3389/fpls.2022.962973

A transcriptomic-guided strategy used in identification of a wheat rust pathogen target and modification of the target enhanced host resistance to rust pathogens

Bernard Nyamesorto[1]*, Hongtao Zhang[1], Matthew Rouse[2], Meinan Wang[3], Xianming Chen[3,4] and Li Huang[1]*

[1]Department of Plant Sciences and Plant Pathology, Montana State University, Bozeman, MT, United States, [2]USDA-ARS, Cereal Disease Laboratory, Department of Plant Pathology, University of Minnesota, Saint Paul, MN, United States, [3]Department of Plant Pathology, Washington State University, Pullman, WA, United States, [4]Wheat Health, Genetics, and Quality Research Unit, United State Department of Agriculture-Agriculture Research Service, Pullman, WA, United States

Transcriptional reprogramming is an essential feature of plant immunity and is governed by transcription factors (TFs) and co-regulatory proteins associated with discrete transcriptional complexes. On the other hand, effector proteins from pathogens have been shown to hijack these vast repertoires of plant TFs. Our current knowledge of host genes' role (including TFs) involved in pathogen colonization is based on research employing model plants such as *Arabidopsis* and rice with minimal efforts in wheat rust interactions. In this study, we begun the research by identifying wheat genes that benefit rust pathogens during infection and editing those genes to provide wheat with passive resistance to rust. We identified the wheat *MYC4* transcription factor (TF) located on chromosome 1B (*TaMYC4-1B)* as a rust pathogen target. The gene was upregulated only in susceptible lines in the presence of the pathogens. Down-regulation of *TaMYC4-1B* using barley stripe mosaic virus-induced gene silencing (BSMV-VIGS) in the susceptible cultivar Chinese Spring enhanced its resistance to the stem rust pathogen. Knockout of the *TaMYC4-1BL* in Cadenza rendered new resistance to races of stem, leaf, and stripe rust pathogens. We developed new germplasm in wheat via modifications of the wheat *TaMYC4–1BL* transcription factor.

KEYWORDS

***MYC4* Transcription factor, *Triticum aestivum* (bread wheat), rust, (*Puccinia*), BSMV-VIGS, kallisto program, wheat-tilling, enhanced resistance**

Introduction

Plants employ a complex network of signaling pathways to defend themselves against pathogen attacks. Signal integration is dictated by transcription factor (TF) regulatory networks. Transcriptional reprogramming is a major component of plant immunity and is administered by TFs and co-regulatory proteins connected within distinct transcriptional complexes (Moore et al., 2011). Over a couple of decades, studies have uncovered numerous TF family members mostly in *Arabidopsis thaliana* and rice that are critical in regulating proper defense responses when plants are confronted by pathogens. Many of these TFs have been categorized into AP2/ERF, bHLH, bZIP, MYB, NAC and WRKY families. *MYC*, a basic-helix-loop-helix (bHLH) family TFs were initially discovered from a homology study between an oncogene carried by the Avian *v*irus, *My*elocytomatosis (*v-MYC*) and a human gene overexpressed in different cancers, *c*ellular *MYC* (*c-MYC*). They have a DNA binding domain made of 50–60 amino acids, which allows for homo- or heterodimerization to their DNA consensus hexamer sequence CANNTG (Finver et al., 1988). The bHLH TFs have been shown to be key regulators in Jasmonic Acid (JA)-mediated defense responses and in mediating crosstalk with other phytohormones, including salicylic acid (SA), abscisic acid (ABA), gibberellins (GA), and auxin (Kazan and Manners, 2013).

Co-evolved with host defense systems in plants, pathogens are also continually developing counter mechanisms to overcome host defenses. It has become evident that one component of their arsenal is manipulating host cellular processes using effector proteins, including exploiting pathogen susceptible host genes. Efforts in modifying these pathogen targeted host genes to increase resistance against pathogens have become a go-to approach for disease-resistant breeding in model crops such as rice. For example, alteration of rice promoters *OsSWEET14* and *OsSWEET11* and the *OsMPK5* gene enhanced resistance to bacterial blight (caused by *Xanthomonas oryzae* pv. *oryzae*), bacterial panicle blight (*Burkholderia glumae*) and blast (caused by fungus *Magnaporthe grisea*) of rice (Li et al., 2012; Jiang et al., 2013; Xie and Yang, 2013). Similarly, alteration of wheat *TaMLO* and *TaEDR1* genes (three homeologs) enhanced resistance to powdery mildew (caused by *Blumeria graminis* f. sp. *tritici*) (Shan et al., 2013; Wang et al., 2014; Zhang et al., 2017). Identifying host targets of pathogen effectors and modifying these sites to abolish the effector-target interactions would be a quick approach to generate new resistance.

Upon the release of the complete genome sequence of hexaploid wheat (*Triticum aestivum* L.) by the International Wheat Genome Sequencing Consortium (Appels et al., 2018), it has become apparent that of the over 107,891 high-confidence genes identified, more than 35,000 are transcriptional factors categorized into 40 families and 84 subfamilies (Appels et al., 2018). This genome resource makes gene identification in wheat from a short sequence read possible. In a pilot transcriptomic study on the interaction between wheat and the leaf rust pathogen (*Puccinia triticina; Pt*) using a pair of near isogenic lines (NILs) of mnr220/MNR220 (the Alpowa background) (Campbell et al., 2012), the expression patterns of some wheat genes were found to be upregulated starting at 5-days post-*Pt* inoculation (data not shown), a critical rust *Pt* development stage when the rust has established infection sites in susceptible wheat cultivars. Among those upregulated expressed genes, five of them are transcriptional factors (TFs). Among the five TFs, one of them is 97% similar to a cDNA of *TaMYC4* -like sequence named TRIUR3_32014 from *Triticum urartu* (a close wild relative of wheat) after BLAST search in NCBI. MYC2/MYC3/MYC4 were identified as a core of TFs regulating jasmonic acid (JA) and JA-isoleucine accumulation through a positive amplification loop in Arabidopsis (Van Moerkercke et al., 2019). This observation suggested a hypothesis that some rust pathogens upregulate host JA production to suppress SA-mediated defense by manipulating host MYC transcription factors. The wheat *MYC4* genes (*TaMYC4*) are the targets of the rust pathogen during infection. In this study, we have demonstrated that the *TaMYC4* homeolog in the long arm of chromosome 1B (*TaMYC4−1BL*) is upregulated upon pathogen infection and that modification of the *TaMYC4−1BL* enhanced resistance to wheat against rust pathogens.

Materials and methods

Plant and pathogen materials

Spring wheat cultivar Alpowa (PI 566596) was obtained from the USDA National Plant Germplasm System (NPGS), and Chinese Spring (CS) was obtained from Dr. Evans Lagudah at Commonwealth Scientific and Industrial Research Organization (CSIRO). Cadenza, spring wheat, was obtained from the SeedStor *via* http://www.seedstor.ac.uk.

The *Puccinia graminis* f. sp. *tritici* (*Pgt*) races QFCSC (isolate 10UML6-1) and TPMKC (isolate 07MT137-2) were provided by Dr. Yue Jin from Cereal Disease Laboratory, USDA-ARS, St. Paul, MN. The *P. triticina* (*Pt*) race PBJJG (isolate 09KSAL1-6) was provided by Dr. Robert Bowden (USDA-ARS, Manhattan, KS, USA). A *P. striiformis* f. sp. *tritici* (*Pst*) culture (race and isolate unknown) was collected from the Bozeman Agricultural Research and Teaching Farm of Montana State University (MSU).

Plant growth conditions

For rust screenings, wheat seeds were directly planted into 4-inch small pots (5 seeds/pot) containing SunGro Horticulture Sunshine mix (HeavyGardens Company, Denver, CO). For seed

propagation and crosses, wheat seeds were first germinated in Petri dishes on filter paper at room temperature. At root radical emergence, the seeds were transferred to 8-inch pots (one seedling/pot) containing a 1:1 ratio mixture of local soil: Sunshine mix. Growth conditions were set at 22/14°C Day/night temperatures and a 16 h photoperiod in a greenhouse at the Plant Growth Center, MSU. Plants were watered and fertilized every day with Peters General Purpose Plant Food (Scotts-Miracle-Gro Company, Marysville, OH, USA) at a concentration of 150 ppm.

Rust pathogen inoculation and assessment

All rust screenings were completed at the two-leaf seedling stage. Rust inoculations were conducted as described in Campbell et al. (2012). In brief, plants were inoculated with rust pathogen urediniospores in Soltrol170 oil suspensions. Inoculated plants were then transferred to a Percival I-60D dew chamber (Percival Scientific Inc., Perry, IA, USA) pre-conditioned to an internal air temperature between 15 and 17°C for *Pt* and *Pst*, 19-20°C for *Pgt* for 24 h. An additional step of 4 h exposure to light prior to removing the plants from a dew chamber for stem rust inoculation. *Pgt* races QFCSC and TMLKC, *Pt* race PBJJG and *Pst* evaluations were conducted at Montana State University in the greenhouse of the Plant Growth Center. Assays with TTKSK (isolate 04KEN156/04) and TKTTF (isolate 13GER10-5) were completed in the Cereal Disease Laboratory, USDA-ARS, St. Paul, MN, following the procedure described by Jin et al. (2007). The tests with other *Pst* races were conducted at the Wheat Health, Genetics, and Quality Research Unit, USDA-ARS, Pullman, WA, according to the procedure described by Line and Qayoum (1992) and infections types (IT) recorded 18–20 days after inoculation.

Infection types of seedlings to leaf and stem rusts were assessed using the 0-4 IT scale (McIntosh et al., 1995) at 8 and 13–14 days post inoculation (dpi) for *Pt* and *Pgt*, respectively, when the symptoms and signs of susceptible controls were fully expressed. Stripe rust was assessed at 14 dpi based 0 (immune)—9 scale (highest susceptible) (Line and Qayoum, 1992).

Sample collection and treatments

For RNA extraction, leaf samples were taken from three plants separately per treatment. Each sample was frozen in liquid nitrogen and stored at −80°C. RNA extractions were completed when all the samples at different time points were collected. Sample collection times ranged from 0 to 10 dpi, depending on the experiment. The samples at 0 dpi were taken immediately after inoculation before placing the inoculated plants in a dew chamber. For DNA extraction, leaf samples were taken and immediately used for extraction.

RNA and DNA extraction

Total RNAs were isolated and treated with DNase I on columns using the Qiagen RNeasy Plant Mini Kit (Qiagen, Valencia, CA) following the manufacturer's instructions. Genomic DNA extraction for conventional PCR was done using the QIAGEN DNeasy Plant Mini Kit (Qiagen Sciences Inc, Germantown, MD, USA). For KASP assays, DNA was extracted from 96 plants using the 96-well plate extraction procedure modified from Holleley and Sutcliffe (2022). The quality and concentration of total RNA/DNA were assessed using 260/280ABS measurements on a NanoDrop 1,000 spectrophotometer (Thermo Fisher Scientific Inc., Wilmington, DE, USA). The integrity of DNA or RNA was checked *via* agarose gel electrophoresis with 2 μl of a sample, 4 μl of water, 1 μl loading buffer (98% formamide, 10 mM EDTA, 0.25% bromophenol blue, and 0.25% xylene cyanol) on a 0.8–1% gel stained by GelRed (Bio-Rad, Hercules, CA) at 125 volts for 25 min.

qRT-PCR, conventional PCR and KASP assays

qRT-PCR was performed using the iScript One-Step RT-PCR Kit with SYBR Green (Bio-Rad, Hercules, CA) on a CFX96 real-time PCR detection system (Bio-Rad, Hercules, CA) following the manufacturer's procedure with 100–150 μg sample RNA at annealing temperatures of 56/57°C depending on the primers. ACTB (β-actin) (Kozera and Rapacz, 2013) was used as the housekeeping gene for normalization of transcript abundance (Supplementary Table 1). qRT-PCR was conducted in triplicate.

PCR amplifications were conducted in 20 μl reactions containing 25 mM $MgCl_2$, 10 mM dNTP, 2 μM of each primer (BN1BL primers, Table 2), 50 ng genomic DNA and 1 unit Go Taq Flexi DNA polymerase (Promega, Madison, Wisconsin). Amplifications were performed at 95°C for 7 min, followed by 35 cycles at 95°C for 45 s, 55°C for 45 s, and 68/72°C for 40 s (depending on primers), with a final extension at 68/72°C for 10 min.

KASP genotyping was conducted using the KASP genotyping trial kit following the manufacturer's protocol (Biosearch Technologies Genomic analysis by LGC) using manually designed KASP primers (Supplementary Table 1) on a CFX96 real-time PCR detection system. Products from qRT-PCR, PCR and KASP were checked using gel electrophoresis as described previously.

Barley stripe mosaic virus-induced gene silencing assay

Gene knockdown was conducted *via* a BSMV-VIGS assay. The original BSMV vectors were obtained from Dr. Andrew O. Jackson (UC Berkeley, CA, USA). The target fragment for the silencing assay was inserted into the modified γ vector ready for direct PCR cloning as described by Campbell and Huang (2010). BSMV RNA transcripts were synthesized *in vitro* using the T7 RNA polymerase (New England Biolabs, Ipswich, MA, USA) from linearized α, β, and γ plasmids. The BSMV inoculum was prepared with 3 μL of BSMV RNAs (1:1:1 ratio of α, β, and γ) and 22.5 μL of the inoculation buffer. The inoculum was then rub-inoculated onto the first leaf of two-leaf-stage plants. Leaf tissue was sampled 9 days after virus inoculation to test the silencing efficiency. Stem rust inoculations were done 14 days post virus inoculation when BSMV-induced target gene silencing reached the highest level.

Mutant search and validation

Cadenza mutants were identified from the wheat-tilling database using the sequence of candidate genes as a query. Wheat-tilling is a resource TILLING population consisting of 2,700 individuals developed *via* ethyl methanesulfonate (EMS) mutagenesis in tetraploid durum cv "Kronos" and the hexaploid wheat cv "Cadenza" backgrounds (Rakszegi et al., 2010). The genome of each mutant has been completely sequenced. Mutations of requested mutants were validated *via* sequencing of the target regions after PCR amplification from the wild-type Cadenza and mutants using gene-specific primers.

Genetic analysis

Genetic analysis was conducted to test the genotype-phenotype association using 150 seeds from a self-pollinated heterozygote mutant plant at the selected locus. Also, 96 F_4 individuals were used for genotyping and phenotyping *via* KASP assay using the designed KASP primers. For mutant L683F, the single nucleotide polymorphism (SNP) was a C-T nucleotide change from the wild-type to the L683F mutant. The forward oligos were designed as: Allele 1 with wild-type nucleotide (C) and Allele 2, which has the mutant nucleotide (T). A common reverse primer was designed for both allele oligos. A combination of the three oligos was used in the assay (Supplementary Table 1).

Pathogenesis-related genes expression

During the time courses of the *Pgt* TMLKC infections, *PR* gene expression was assayed at 0, 1, and 2 dpi in both the wild-type Cadenza and mutant. Leaf samples were collected from three biological replicates per dpi for the wild-type and mutant and pretreated under recommended conditions for RNA extraction. Using the corresponding *PR* gene primers (Supplementary Table 1), *PR* genes were quantified using extracted RNA *via* real-time-qPCR as described earlier. The PR gene primers were according to Desmond et al. (2005).

Databases and *in silico* sequence analysis

All BLAST and sequence downloads were completed using the International Wheat Genome Sequence Consortium (IWGSC) resources at https://wheat-urgi.versailles.inra.fr/Seq-Repository/BLAST. Initially, sequence downloads were completed from IWGSC RefSeq v1.0 (2017-08-07) and later from IWGSC RefSeq v2.1 (2019-02-20). Multiple sequence alignments were conducted using ClustalW Omega at https://www.ebi.ac.uk/Tools/msa/clustalo/. Gene and conserved domain predictions were performed using Softberry at http://www.softberry.com/berry.phtml?topic=fgenesh&group=programs&subgroup=gfind and Pfam at http://pfam.xfam.org/. Primers were designed either manually or using the PrimerQuest® tool at https://www.idtdna.com/pages/tools/primerquest, and primer specificity was assessed by BLAST search of the IWGSC database. RNA-seq data quality was checked using FastQC Version 0.11.6 (Babraham Bioinformatics, Cambridge, CB22 3AT, UK).

The RNA sequence data from the Sequence Read Archive (SRA) of the National Center for Biotechnology Information (NCBI) accession number (PRJEB12497: http://www.ebi.ac.uk/ena/data/view/PRJEB12497) (Dobon et al., 2016) were used to quantify the expression levels of homeologs at different time points *via* Kallisto software (Bray et al., 2016). The wheat transcriptome downloaded from IWGSC was indexed and reads of RNA-seq were also assessed for quality *via* FastQC High Throughput Sequence QC Report (version: 0.11.7) in interactive mode. Paired-end sequences were split using Fastq-dump prior to transcript quantification. The paired-end reads were run using default parameters with 100 bootstraps (-b 100). Refer to Kallisto Manual-Pachter Lab (https://pachterlab.github.io/kallisto/manual) for more details to run Kallisto on bulk RNA-seq data.

Statistical analysis

Data assessment and analysis were conducted in Microsoft Excel and R-studio software version 1.1.453.0. For real-time

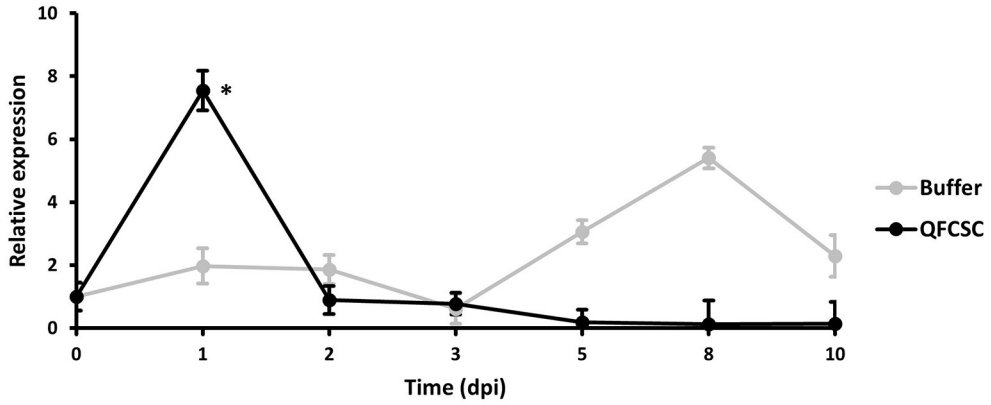

FIGURE 1
Relative expression of *TaMYC4* in wheat cultivar Alpowa inoculated with buffer (control) and the *Puccinia graminis* f. sp. *tritici* (*Pgt*) pathogen (race QFCSC). Alpowa cultivar were inoculated with *Pgt* urediniospore at 2-leaf stage. RNA samples were extracted from the leaf samples collected at seven time points. Real-time PCR was used to quantify transcript abundances of *TaMYC4* genes in both buffer and *Pgt* inoculated samples. Expression of *TaMYC4* genes at each time point was computed relative to the level at 0-dpi. Error bars represent standard deviation computed as the square root of pooled variance between groups and * denote statistical significance at the $P \leq 0.05$ levels calculated between each time point compared with 0 dpi.

PCR assays, data were used only if the Ct standard deviation among the triplets was ≤0.2 and the mean of the triplet's Ct was used for downstream analysis. Relative expression was calculated using the ΔΔCt method as described in the CFX96 manual (Bio-Rad, Hercules, CA), where fold change = $2^{-\Delta\Delta Ct}$. Expression measurement of genes was conducted in three technical replicates for each of three biological replicates. Standard deviations were calculated among three biological replicates or using pooled standard deviation formula when comparing two different groups (ΔCt values). Student's *t*-tests were performed to test whether the expression levels at different time points were significantly different. The *p*-values were calculated based on an unpaired two-tailed distribution. Expression patterns were graphically represented using averages of the three biological replicates.

Results

Conserved domains of *TaMYC4* genes in wheat

To address our question of *TaMYC4*'s possible negative role in wheat plant defense against rust pathogens, we began with further investigation of *TaMYC4* conserved domains to relate its structure to function. We identified three copies of the *TaMYC4* gene in bread wheat using the cDNA of *TaMYC4* -like sequence of TRIUR3_32014 from *T. urartu* to BLAST search the International Wheat Genomic Sequence Consortium (IWGSC) database. *TaMYC4*-like genes were identified on 1AL, 1BL, and 1DL chromosomes with 97–99% similarities on the DNA level or the amino acid level with an Expect Value of 0.0. The three homeologs were predicted to have conserved basic-helix-loop-helix (bHLH) and helix-loop-helix (HLH) domains at E-values approximately 0.0. A Leucine-zipper domain was predicted on only the 1BL homeolog at an E-value of 0.31. Each of these domains is a classical *MYC4* conserved domain (Supplementary Figure 1, Supplementary File 2). The bHLH/HLH and leucine zipper motifs allow binding of MYC proteins to DNA and dimerization with other bHLH TFs (including Max). Based on a ClustalW Omega multiple sequence alignment of the sequences, the percent identity matrix indicated that the three homeologs had over 95% identity at the DNA, mRNA, and protein levels. These insights gave additional validity that the sequence we were interested in is a TF of *MYC4*.

Expression profiles of the *TaMYC4* genes by qRT-PCR

To further confirm the expression pattern of the *TaMYC4* genes observed in the pilot study (data not shown), we conducted a time-course study in Alpowa, the genetic background of the NILs used in the wheat-*Pt* transcriptomics pilot study. Alpowa was inoculated with *Pt* race PBJJG and *Pgt* race QFCSC or buffer Soltrol 170 isoparaffin as a mock inoculated control. An RNA collection time course was set at 0-, 1-, 2-, 3-, 4-, 5-, 8-, and 10-days post-inoculation (dpi). The expression level of *TaMYC4* was assayed *via* qRT-PCR using the BN4RT primers that measured all three homeologs of the *TaMYC4* genes (Supplementary Table 1, Supplementary File 1). We did not observe any significant changes in the expression profile of *TaMYC4* at any of the time points for the PBJJG-inoculated Alpowa (Supplementary Figure 2). When

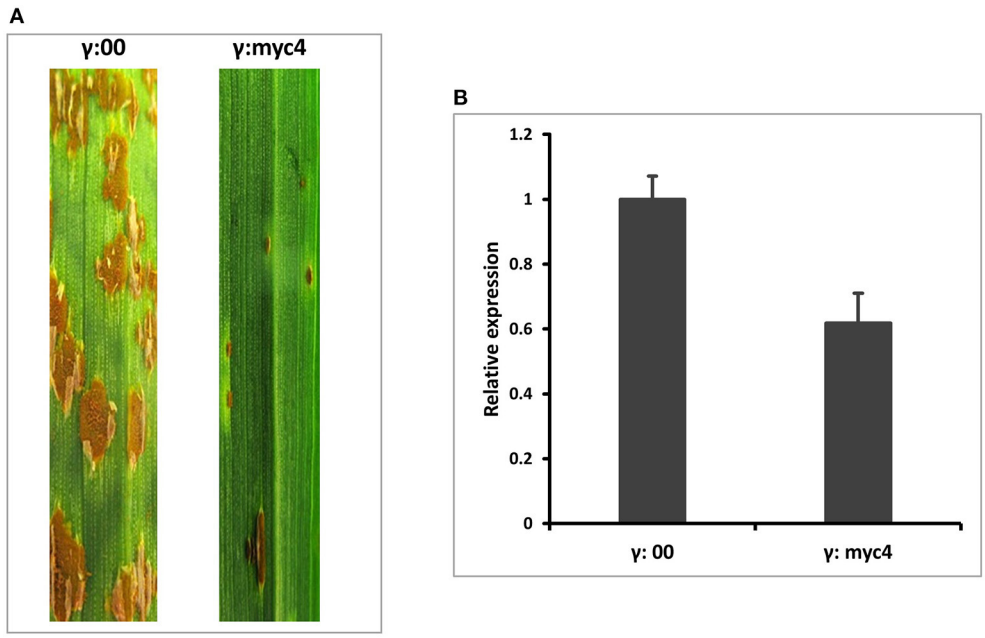

FIGURE 2
BSMV-VIGS of *TaMYC4* in wheat cultivar Chinese Spring (CS). The first leaf of each plant was rub inoculated with the indicated BSMV constructs at the two-leaf stage and then spray inoculated with *Pgt* race QFCSC at 10 days after BSMV inoculation. The disease was assessed and photographed at 14 dpi. CS without any viral inoculation, used as a rust inoculation control; γ:00, CS inoculated with BSMV: *MYC4*; γ:*myc4*. RNA was extracted from viral-free leaf samples taken from γ:00 and γ:*myc4* plants prior to pathogen inoculation. Transcript abundance was quantified via RT-qPCR. Error bars represent standard deviation among three biological reps. **(A)** Infection types of *MYC4*-silenced plants **(B)** Relative expression of *TaMYC4* in γ:00 and γ:*myc4* silenced plants.

Alpowa was inoculated with the *Pgt* race QFCSC, the expression levels of *TaMYC4* were similar in samples taken at 0 dpi between *Pgt*-inoculated Alpowa and the control. However, a significant increase in *TaMYC4* transcript abundance was detected at 1 dpi in *Pgt* infected Alpowa compared to the control plants. The *TaMYC4* expression level returned to an undetectable level at 2 dpi and stayed unchanged during the rest of the time points (Figure 1). The expression level of *TaMYC4* in buffer inoculated Alpowa showed minor and insignificant changes along from 1 to 3 dpi but showed an increase from 5 to 8 dpi that then declined at 10 dpi. This increase was, however, statistically insignificant. A significantly higher expression of *TaMYC4* occurred after rust infection and only in the susceptible host revealed in the pilot study. These observations encouraged us to investigate whether *Pgt*-induced *TaMYC4* upregulation is beneficial to the pathogen during colonization of wheat.

Silencing of the *TaMYC4* genes

To quickly determine the function of *TaMYC4* regarding stem rust resistance, we downregulated the *TaMYC4* genes and examined the infection types on the host. We knocked down all three endogenous copies of *TaMYC4* (to avoid functional redundancy) in a rust susceptible wheat cultivar Chinese Spring (CS) using a BSMV-VIGS assay. We used CS instead of Alpowa for the silencing assay for two reasons. One is that BSMV-VIGS is homolog-based, and the sequences of the three *TaMYC4* genes obtained from the IWGSC database are from CS. The other reason was to validate our hypothesis in a different cultivar background to study if the pathogen uses the same strategy to infect different cultivars. A construct containing a 247-bp fragment conserved among the gene homeologs after multiple sequence alignment (Supplementary File 1) was obtained *via* PCR amplification using primers VIGS-F/R (Supplementary Table 1) and used to silence each homoeolog on the three chromosomes (labeled as BSMV:*MYC4*) (see also Supplementary File 1). A construct carrying only the BSMV genome was used as a no-target control and labeled as BSMV:00. For short, the BSMV-derived construct with no insert was named as γ00, and each BSMV silencing construct was named after the target gene, for example, γ*MYC4*. The concurrent silencing of BSMV inoculum was made by combining the α: β: γ target transcripts in an equal ratio with excess inoculation buffer (FES). In each assay, 20 wheat seedlings were inoculated with γ*MYC4* or γ00, as a control. At 6 days post BSMV inoculations (dpbi), viral symptoms were visualized on the newly emerged

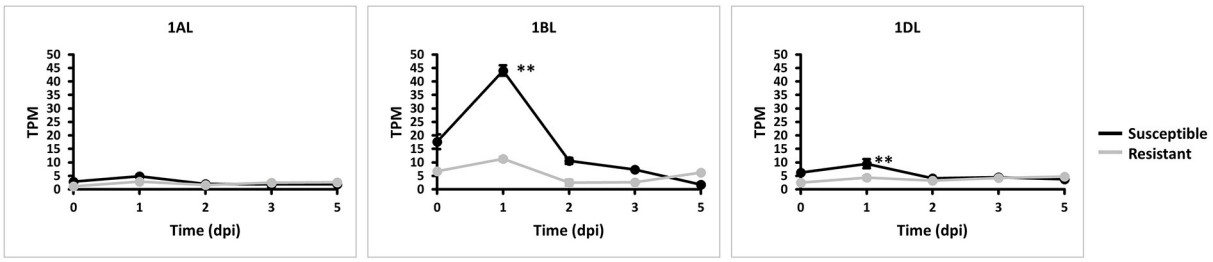

FIGURE 3
Expression of *TaMYC4* (1AL, 1BL and 1DL) homeologs during stripe rust–Avocet Yr5 (resistant) and Vuka (susceptible) interactions. TPM is transcript per million. Error bars represent standard deviation among three biological reps and ** denote statistical significance at the $P \leq 0.01$ levels calculated between each time point and 0 dpi.

TABLE 1 Summary of identified TaMYC4–1BL Cadenza mutants.

Chromosome	Nucleotide change	Mutated amino acid position	Amino acid changes	Type of mutation	SIFT score[a]	Mutated ID[b]
1BL	G to A	683	L to F	Homozygote	0	L683F-MYC4–1BL
1BL	C to T	635	M to I	Heterozygote	0	M635I-MYC4–1BL

[a]SIFT score predicts whether an amino acid substitution affects protein function, and ranges from 0 to 1. The amino acid substitution is predicted to be damaging if the score is ≤0.05 and tolerated if the score is >0.05. [b]Gene IDs were based on amino acid change and position of change, gene name and chromosome.

leaves of plants inoculated with BSMV. At nine dpbi, plants inoculated with BSMV constructs showed viral-symptom-free leaf segments, indicating that BSMV induced gene silencing had occurred. Three viral-symptom-free leaf segments were randomly sampled from plants inoculated with γ00 and γ*MYC4* construct for RT-qPCR. The plants were inoculated with *Pgt* race QFCSC immediately. Infection type (IT) observed 14 dpi showed enhanced disease resistance in plants that had *TaMYC4* silenced. Non-silenced plants were susceptible (Figure 2A. Transcript abundances of *TaMYC4* were measured through qRT-PCR using primers BN4RTF/R (Supplementary Table 1), which confirmed a 40% reduction of *TaMYC4* in silenced plants relative to the control (Figure 2B). Though the reduction in the expression of the three *TaMYC4* homeologous genes resulted in enhanced resistance to *Pgt* QFCSC, we do not know which homeolog or if all three of them are critical for the rust fungus to colonize the wheat host successfully.

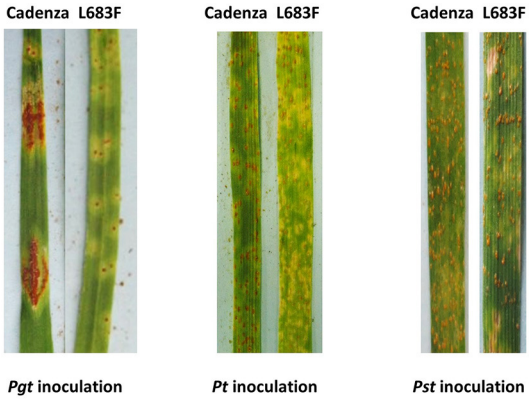

FIGURE 4
Reactions of the wild-type Cadenza and the *TaMYC4* mutant L683F after inoculation with *Puccinia graminis* f. sp. *tritici* (*Pgt*), *P. triticina* (*Pt*) and *P. striiformis* f. sp. *tritici* (*Pst*) inoculation. Infection types (IT) of Cadenza: L683F in each pair of images were, *Pgt* (4: 1+), *Pt* (3: 2-;) and *Pst* (4: 3c) Photos of *Pgt* and *Pst* inoculated plants were taken 14 days post inoculation. Photos of *Pt* inoculated plants were taken 9 days post inoculation.

Expression of *TaMYC4* homeologs during the *Pst* infection

We explored whether all three *TaMYC4* homeologs are negatively involved in the plant's defense mechanism based on their expressions. We quantified each *TaMYC4* homeolog *via* Kallisto software using the RNA sequence data generated from a previous study (Dobon et al., 2016) involving Avocet *Yr5* (resistant) and Vuka (susceptible) inoculated with *Pst* pathogen at 0, 1, 2, 3, and 5 dpi and accessed from the NCBI. We used just the *Pst*-wheat data set since we could not find readily available *Pgt*-wheat RNAseq data for the specific time-course study of our interest. Also, the *Pst*-wheat study helped us to assess the *TaMYC4* expression pattern in the wheat-*Pst* interaction, which we already examined beforehand

10.3389/fpls.2022.962973

TABLE 2 Rust evaluations of Cadenza L683F mutant and wild-type Cadenza.

			Infection type (IT)			
Pathogen	**Race**	**Isolate**	**Alpowa**	**Avocet**	**Mutant**	**Cadenza**
Pgt	QFCSC	10UML6-1	3+	N	1	2
	TPMKC	07MT137-2	3+	N	;1-	3+
	TTKSK	04KEN156/04	N	N	3+	2+3
	TRTTF	06YEM34-1	N	N	3+	3+
Pt	PBJJG	09KSAL1-6	N	N	;1	3
Pst	NK	18Field Collection	N	N	3	7
	PSTv-4	19WA-200-YrSP	N	8	3	3
	PSTv-37	19ID-11	N	8	8	8
	PSTv-41	19WA-193	N	8	8	8
	PSTv-47	19ID-32	N	8	8	8

Pgt, P. graminis f. sp. tritici; Pt, P. triticina; Pst, P. striiformis f. sp. tritici. For infection type, higher the number, more susceptible plant with a "+" (more than average) or a "–" (less than average) to further quantify the level. A semicolon (;) symbolizes the presence of hypersensitive flecks. N means not tested. Wheat cultivar Alpowa was used as a stem rust susceptible control, and Avocet was used as stripe rust susceptible control. The race of the field collected stripe rust used is unknown (NK).

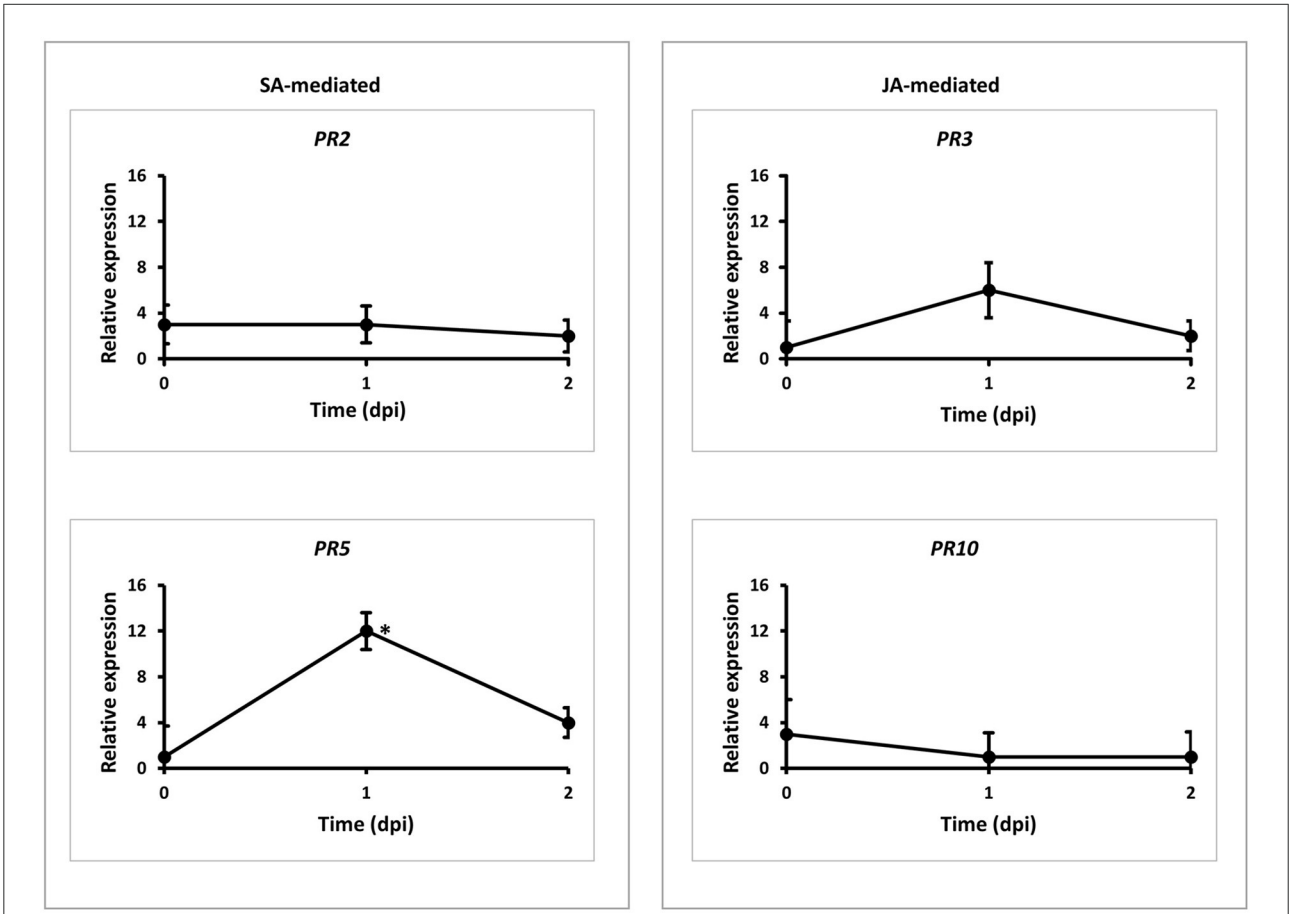

FIGURE 5
Expressions of pathogen related (PR) genes responding to *Pgt* (race TMLKC) in the wild-type and mutant wheat lines. Wild-type Cadenza and mutant *L683F-MYC4-1BL* were inoculated with the *Pgt* pathogen at 2-leaf stage. RNA samples were extracted from the leaf samples collected at three time points. Real-time PCR was used to quantify transcript abundances of the four *PR* genes. Expression of PR genes at each time point was expressed in the mutant relative to the level in the wild-type. * denote statistical significance at the $P \leq 0.05$ levels compared between wildtype and mutant at each time point. Error bars represent standard deviation computedas the square root of pooled variance between groups.

in *Pgt*/*Pt*-wheat (Supplementary Figures 2; Figure 1). FastQC is a quality control tool for high throughput sequence data. Overall, FastQC checks on the RNA-seq data indicated good quality features such as per base sequence quality and overrepresented sequences. The RNA-seq was pseudo-aligned and quantified *via* Kallisto software (Bray et al., 2016). The output of transcript abundance was recorded in transcript per million (tpm). The transcript abundances of the genes of interest (1AL, 1BL, and 1DL) were imported using the gene IDs; TRIAE_CS42_1AL_TGACv1_000298_AA0008240.1, TRIAE_CS42_1BL_TGACv1_726352_AA2170300.1, TRIAE_CS42_1DL_TGACv1_061684_AA0201690.1, respectively. Pre-examination of the transcript data for abundance satisfied normality requirement in the R studio. A graph of expression of the gene was plotted using the averages of biological replicates at each time point.

Homeolog *TaMYC4-1BL* was significantly upregulated in the susceptible cultivar at 1 dpi compared with the resistant cultivar. It was also the most expressed of the three homeologs (Figure 3). This result led us to the search for permanent alteration (mutants) of *TaMYC4-1BL*.

Identification of *TaMYC4* mutants and their response to the rust pathogens

Using the *TaMYC4-1BL* cDNA sequence as a query, a BLAST search for matches in the database of wheat-tilling mutant lines revealed more than 40 lines carrying a mutation on the *TaMYC4-1BL* gene in the wheat cv Cadenza background. We selected three mutants that had a Sorting Intolerant from Tolerant (SIFT) score of 0.0. Two of the three mutations were confirmed after genotyping with *TaMYC4−1BL* specific primers (Supplementary Table 1). One is a homozygote with a missense mutation at the protein position 683, changing amino acid L to F, hereafter identified as L683F-MYC4−1BL or L683F. The other is a heterozygote with a missense mutation from M to I at position 635, designated as M635I-MYC4-1BL or M635I (Table 1).

The Cadenza L683F mutant showed enhanced resistance to *Pgt* race TPMKC, *Pt* race PBJJG, and one field-collected race of *Pst* (Figure 4; Table 2). The L683F mutant was then tested using additional races of *Pgt* and *Pst* (Table 2). The mutant showed higher levels of resistance to *Pgt* QFCSC and *Pst* race PSTv-4. However, the mutant was as susceptible as Cadenza to *Pgt* races TTKSK and TRTTF, and *Pst* races PSTv-37, PSTv-41 and PSTv-47. The rust screening results indicated the resistance conferred by the mutation L683F in *TaMYC4-1B* is race-specific.

Genetic analysis of the mutations

To confirm the new rust resistance in the mutant due to the mutation in *TaMYC4-1B* and not due to other mutations in the background, we crossed the mutant L683F with a susceptible cultivar Alpowa. F_1 plants were self-pollinated to produce F_2 segregating populations. Out of the 150 individuals in the first genetics analysis, infection types of 148 plants with clear phenotypes were scored. A resistant to susceptible ratio of 35:113 was observed, fitting the 1:3 ratio, [χ^2 (1, N = 148) = 0.14, p = 0.70], indicating that resistance was a recessive phenotype. The genotyping results from 12 susceptible and 3 resistant plants confirmed the resistant plants had the mutant nucleotide (T/A) and the susceptible plants had the (C/G) base. The second step of confirmation was to design a KASP assay to detect the SNP for mutant L683F using the design primers (Supplementary Table 1) based on the *TaMYC4-1BL* scaffold sequence (Supplementary File 1). The result of the KASP assay from 94 F_2 individuals and the two parental lines showed that all 35 resistant plants had a monomorphic SNP marker of L683F. Among the 58 susceptible plants, 17 were heterozygotes of the SNP, and 42 were homozygotes of the wild-type SNP.

Molecular mechanism of the new rust resistance

To understand the genetic mechanism of the new rust resistance, we tested the expressions of four *PR* genes, including SA-dependent *PR2* and *PR5* and JA-dependent *PR3* and *PR10* (Van Loon and Van Strien, 1999) in a time-course study in the wild-type Cadenza and mutant L683F with *Pgt* TPMKC infection. The level of each *PR* gene was monitored at three-time points with qRT-PCR using *PR* gene-specific primers (Supplementary Table 1). The basal expression of the *PR* genes at 0 dpi was at a similar level between the wild-type Cadenza and mutant L683F (Figure 5), about 0-0.5 relative to the expression of the reference gene *actin* (data not shown). The result suggested that these four *PR* genes had minimal expression in the absence of *Pgt*. However, *PR5* was highly upregulated (12-fold) at 1 dpi in L683F relative to its expression in the wild-type Cadenza (Figure 5), suggesting that the mutation in L683F permitted an elevated level of an SA-mediated *PR* gene. Meanwhile, *PR2*, *PR3*, and *PR10* had no significant differences compared to the wild-type Cadenza across the three-time points. This result suggested that the mutation in L683F did not affect the two JA-mediated *PR* genes in the defense response to *Pgt* TPMKC infection.

Discussion

Wheat *TaMYC4* gene aids rust pathogens in host colonization

The first evidence that supports the hypothesis that the *TaMYC4* genes are targets of the pathogen for assistance

in colonization is the upregulation of *TaMYC4* only in rust inoculated but not in the mock-inoculated wheat plants. This provided initial evidence that differentially expressed *TaMYC4* TF was due to the presence of rust pathogens (Figure 1). Secondly, the upregulation of *TaMYC4-1B* occurred only in a susceptible host (Figure 3). The expression trajectory indicated that the targeting of the *TaMYC4-1B* gene happened at the early stage of pathogen colonization. Also, down-regulation of all three copies of *TaMYC4* reduced the susceptibility of a susceptible host to *Pgt* race QFCSC (Figure 2A). The relative reduction in *TaMYC4* transcript abundance in the silenced plants (Figure 2B) indicated that the observed enhanced resistance was attributable to the *TaMYC4* knockdown. The silencing assay suggested that the effect of the *TaMYC4* upregulation was a benefit to the pathogen and negative to the wheat host. *Arabidopsis MYC4* has been shown positively involved in JA and JA-isoleucine accumulation (Van Moerkercke et al., 2019). JA and ABA are positive regulators of stomatal closure (Sarwat and Tuteja, 2017). Bacterial pathogen *Pseudomonas syringae* secret coronatine (COR), a structural and functional analog of the active form of JA, to open host stomata during infection (Zhou et al., 2015). We hypothesize that rust pathogens upregulate *TaMYC4-1B* to increase the JA level to open up host stomata because rust fungal germ tubes enter the host through the stomata. Additional support of this hypothesis is a study of *PR* gene expression during rust pathogen infections. JA-mediated *PR* gene expressions were low in resistant lines, suggesting a low JA level at the early time point post-inoculation (Zhang et al., 2018). Finally, a recessive loss-of-function mutation in *TaMYC4−1BL* conferred resistance to rust pathogens (Figure 4), supporting our claim that the *TaMYC4-1B* gene facilitated infection by rust pathogens in a compatible wheat host.

The three homeologs of *TaMYC4* have bHLH/HLH conserved domains characteristic of *MYC* transcription factors. Nonetheless, an LZ domain is only found in the *TaMYC4-1B* protein (Supplementary Figure 1), suggesting a possible non-redundancy function under different conditions. Most literature have provided evidence of the positive contribution of the leucine zipper TFs to biotic (Milligan et al., 1998; Ballvora et al., 2002; Alves et al., 2013) and abiotic stresses (Yu et al., 2020). Generally, LZ TFs heterodimerize with other proteins involved in cell proliferation, survival, and metabolism (Adhikary and Eilers, 2005). These functions could be hijacked by pathogens for their benefit with enhanced host susceptibility, as observed with the mutation of *TaMYC4-1B* resulting in enhanced resistance to the rust pathogens. More research is however needed to arrive at this conclusion. Indeed, several studies (Shitsukawa et al., 2007; Hovav et al., 2008; Chaudhary et al., 2009; Chen et al., 2011) have revealed transcriptional divergence among homeologs. However, non-redundancy can also arise due to different expression patterns, not due to the protein sequence. Therefore, we suggest that the *TaMYC4−1BL* gene acts as a rust pathogen susceptibility gene such that it acts as a factor needed by the pathogens to colonize the host.

The segregation ratio of resistant to susceptible phenotypes confirmed that *TaMYC4−1BL* confers a recessive phenotype for resistance or a dominant phenotype for susceptibility. At 24 h post-inoculation, development of haustorial mother cells of a wheat rust fungus commences (Serfling et al., 2016). Haustoria are known to play a vital role in cellular communication between pathogen and host (Heath, 1997), nutrient acquisition (Hahn and Mendgen, 2001), manipulation of host metabolism, and the suppression of host defenses (Voegele and Mendgen, 2003). This knowledge further strengthens our claim that *TaMYC4-1BL* was a target to manipulate host defense to benefit the pathogen at the early pathogenesis stage.

Indeed, the higher level of *TaMYC4−1BL* transcripts at 1-day post *Pgt* inoculation (Figure 1) resulted in lower *PR5* expression in Cadenza L683F mutant (Figure 5), suggesting that *PR5* expression was hampered when the TF was increased in the presence of *Pgt*. *PR* genes are involved in host defense under different wheat-pathogen race interactions (Zhang et al., 2018). *PR5* is an SA-dependent thaumatin-like protein (Van Loon, 1982) and has been shown to inhibit the growth of various fungi (Muthukrishnan et al., 2001). Strategies of bacteria hijacking plant hormones to manipulate host defense has been well studied. For example, *Agrobacterium tumefaciens* uses its T-DNA to facilitate production of host auxin and cytokinin hormones in the formation of crown galls. Various strains of *P. syringae* produces coronatine (COR) phytotoxin to manipulate host hormones to enhance bacterial growth and symptom development (Mittal and Davis, 1995). It was later shown that COR is structurally similar to JA isoleucine hence functioning in antipathy to the SA pathway, which plays a crucial role in defense against this bacterial (Brooks et al., 2005; Browse, 2009). Zheng et al. (2012) demonstrated that COR targets host NAC TFs to case stomata reopening and systemically induced susceptibility. We suspect that *PR5* might have been suppressed by rust pathogen effectors using *TaMYC4−1BL* as a host target gene. The insignificant expression of *PR10* (the other SA-related proteins) in this interaction (Figure 5) suggested that for specific signal transduction, separate *PR* proteins may be involved during different plant-pathogen interactions. Also, it has been established that a cross-communication between SA- and JA-dependent defense pathways exists (Felton and Korth, 2000; Pieterse et al., 2001). The relatively lower and insignificant expression levels of the JA-pathway associated *PR* proteins (*PR2* and *PR3*) at 1 dpi (Figure 5) allude to this crosstalk that enables plants to fine-tune their defense reactions depending on the type of stress they encounter.

The bHLH superfamily of transcription factors, including *TaMYC4*, have essential regulatory components in transcriptional networks of many developmental pathways (Atchley and Fitch, 1997). In *Arabidopsis*, *MYC4* TFs are known to bind to the G-box of promoters and are involved in JA

gene regulation (Niu et al., 2011). Collectively, *MYC4*, *MYC2* and *MYC3* were shown to control JA-dependent responses (Fernández-Calvo et al., 2011). It was demonstrated that *MYC4* could form complexes with glucosinolate-related MYBs to regulate glucosinolate biosynthesis (Schweizer et al., 2013). A recent study unraveled that an *MYC2*/*MYC3*/*MYC4*-controlled positive-feedback loop transcriptionally regulated spray-induced jasmonate accumulation (Van Moerkercke et al., 2019). These activities of *MYC4* in *Arabidopsis* give additional credence to our hypothesis that *TaMYC4* is beneficial to pathogens in suppressing host defense in the early stages of wheat rust interaction. However, contrary to its implication in JA-pathways in *Arabidopsis*, we found its negative function in the SA-dependent pathway implicated in *PR5* suppression. This emphasizes our knowledge that a gene could function in different pathways in different species and under varying conditions. At this point, this study has not ascertained if this mechanism is similar for all the three rust pathogens and has also not uncovered the detailed mode of action of *TaMYC4-1BL* during the compatible wheat-rust interactions. Hence further study is necessary to elucidate these unknowns.

Cadenza L683F mutant showed race-specific resistance

The Cadenza L683F mutant showed resistance to *Pt* race PBJJG, *Pgt* race TPMKC, but not to *Pgt* races TTKSK (Ug99) and TRTTF. Also, the mutant was susceptible to all the *Pst* races tested except for a field-collected uncharacterized *Pst* isolate and race PSTv-4 (Table 2). The race-specific resistance was shown by hypersensitive reaction and moderate resistance at the seedling stage during their interaction with the pathogens. The resulting infection types range from 1 to 3 in seedlings. The wild-type Cadenza had a moderate resistance level to *Pgt* race QFCSC, but the mutant L683F had enhanced resistance to the pathogen. Furthermore, the same mutation enhanced resistance to three rusts, suggesting a common target in a host used by the rust pathogens as a strategy.

We also noticed that down-regulation of the *TaMYC4* genes in wheat cv. CS enhanced resistance to *Pgt* race TPMKC, and mutated *TaMYC4-1BL* in different wheat cultivars could enhance resistance to the same rust pathogen race, suggesting a rust pathogen race used the same strategy targeting the same genes in different genetic backgrounds of the same host.

An approach to creating new resistant germplasm

Over the years, wheat rust resistance breeding has been focused on using adult-plant resistance (APR) and all-stage resistance (R) genes from wheat and related species. At the same time, this is very resource-consuming because these resistance genes are continually overcome by evolving virulent races of rust pathogens, mainly because most of these genes confer race-specific resistance. There have been considerations for the building resistance gene cassettes to confer efficient resistances against different rust pathogens or races. However, this effort requires the availability of effective resistance genes as resources.

Due to the limitations of natural existing resistance genes in wheat or its relatives, scientists are looking for strategies to generate new resistance genes *via* mutagenesis or genome editing. Decades of studies on plant-pathogen interactions revealed that when pathogens successfully colonize host plants, some of the host genes are reprogrammed by the pathogens. Those host genes could be transcriptionally activated by the pathogen transcription activator-like effectors (TALEs), interact with the pathogen effectors to suppress the plant defense response (Fukuoka et al., 2009), or redirect the host nutrient sinks to the host-pathogen interfaces (Chen et al., 2010). In nature, a single mutation of one of those host genes could happen and make the host less desirable to the pathogen, therefore less severity of the disease. For example, rice *xa13*-mediated resistance is due to a mutation of the effector binding site (EBE) in the promoter of the host glucose transporter gene OsSWEET11 (*Xa13*). The mutation leads to the loss of the bacterial pathogen *Xanthomonas oryzae pathovar oryzae* (Xoo) strain PXO99 *PthXo1*-mediated induction of the *SWEET* gene and reduced bacterial growth (Chen et al., 2010). In wheat, changes of only two amino acids in a conserved region of a hexose transporter at the *Lr67* locus between *lr67* and *Lr67* reduce the growth of multiple biotrophic pathogen species (Moore et al., 2015). Understanding the specificity of pathogen targeting DNA sequences has enabled the development of new host resistance in rice (Hummel et al., 2012; Zeng et al., 2015), pepper (Romer et al., 2009), and resistance against *Ralstonia solanacearum* in a broad host range (de Lange et al., 2013).

Our study demonstrated an effective scheme of using a transcriptomic-guided approach in wheat to select candidates of pathogen targets, a BSMV-induced gene silencing assay to identify and confirm the targets, and phenotype and genetic analysis of mutations on selected targets to develop new resistant germplasm. *TaMYC4*-1BL was selected because the upregulation of the gene was only detected in susceptible lines in the presence of rust pathogens. A reverse genetic approach using BSMV-induced gene silencing revealed that the host demonstrated improved resistance when the *TaMYC4-1BL* was downregulated. With the known DNA sequence of *TaMYC4-1BL* and an EMS mutagenized population, we were able to identify mutations in the gene. Phenotype and genetic analysis of the L683F mutation in *TaMYC4-1BL* of Cadenza confirmed a new resistance to rust pathogens in wheat. This approach provides a means of navigating the challenges associated with germplasm creation and studying gene function in wheat, low efficiency in wheat

transformation, and concerns with detrimental effects of a host gene mutation.

Data availability statement

The datasets presented in this study can be found in online repositories. The names of the repository/repositories and accession number(s) can be found in the article/Supplementary material.

Author contributions

Conceptualization and funding acquisition: LH. Methodology: BN, LH, HZ, MR, MW, and XC. Investigation and formal analysis: BN. Writing—original draft: BN and LH. Writing—review and editing: BN, LH, MR, MW, and XC. All authors contributed to the article and approved the submitted version.

Funding

This research was supported by the NSF BREAD program (Grant No. IOS-0965429).

Acknowledgments

Our sincere gratitude to Dr. Evans Lagudah, for providing us with Chinese Spring wheat; to Rothamsted Research and JIC for providing the Cadenza mutants, to Dr. Yue Jin, for providing *Pgt* races QFCSC (isolate 10UML6-1) and TPMKC (isolate 07MT137-2); to Dr. Robert Bowden for providing *Pt* race PBJJG (isolate 09KSAL1-6) and the USDA National Plant Germplasm System (NPGS) for spring wheat cultivar Alpowa (PI 566596).

Conflict of interest

The authors declare that the research was conducted in the absence of any commercial or financial relationships that could be construed as a potential conflict of interest.

Publisher's note

All claims expressed in this article are solely those of the authors and do not necessarily represent those of their affiliated organizations, or those of the publisher, the editors and the reviewers. Any product that may be evaluated in this article, or claim that may be made by its manufacturer, is not guaranteed or endorsed by the publisher.

Supplementary material

The Supplementary Material for this article can be found online at: https://www.frontiersin.org/articles/10.3389/fpls.2022.962973/full#supplementary-material

References

Adhikary, S., and Eilers, M. (2005). Transcriptional regulation and transformation by Myc proteins. *Nat. Rev. Mol. Cell. Biol.* 6, 635–645. doi: 10.1038/nrm1703

Alves, M. S., Dadalto, S. P., Gonçalves, A. B., De Souza, G. B., Barros, V. A., and Fietto, L. G. (2013). Plant bZIP transcription factors responsive to pathogens: a review. *Int. J. Mol. Sci.* 14, 7815–7828. doi: 10.3390/ijms14047815

Appels, R., Eversole, K., Stein, N., Feuillet, C., Keller, B., Rogers, J., et al. (2018). Shifting the limits in wheat research and breeding using a fully annotated reference genome. *Science* 361, eaar7191. doi: 10.1126/science.aar7191

Atchley, W. R., and Fitch, W. M. (1997). A natural classification of the basic helix-loop-helix class of transcription factors. *Proc. Natl. Acad. Sci. U. S. A.* 94, 5172–5176. doi: 10.1073/pnas.94.10.5172

Ballvora, A., Ercolano, M. R., Wei,ß, J., Meksem, K., Bormann, C. A., Oberhagemann, P., et al. (2002). The R1 gene for potato resistance to late blight (Phytophthora infestans) belongs to the leucine zipper/NBS/LRR class of plant resistance genes. *Plant J.* 30, 361–371. doi: 10.1046/j.1365-313X.2001.01292.x

Bray, N. L., Pimentel, H., Melsted, P., and Pachter, L. (2016). Near-optimal probabilistic RNA-seq quantification. *Nat. Biotechnol.* 34, 525–527. doi: 10.1038/nbt.3519

Brooks, D. M., Bender, C. L., and Kunkel, B. N. (2005). The *Pseudomonas syringae* phytotoxin coronatine promotes virulence by overcoming salicylic acid-dependent defences in Arabidopsis thaliana. *Mol. Plant. Pathol.* 6, 629–639. doi: 10.1111/j.1364-3703.2005.00311.x

Browse, J. (2009). Jasmonate passes muster: a receptor and targets for the defense hormone. *Ann. Rev. Plant Biol.* 60, 183–205. doi: 10.1146/annurev.arplant.043008.092007

Campbell, J., and Huang, L. (2010). Silencing of multiple genes in wheat using Barley stripe mosaic virus. *J. Biotech. Res.* 2, 12

Campbell, J., Zhang, H., Giroux, M. J., Feiz, L., Jin, Y., Wang, M., et al. (2012). A mutagenesis-derived broad-spectrum disease resistance locus in wheat. *Theor. Appl. Genet.* 125, 391–404. doi: 10.1007/s00122-012-1841-7

Chaudhary, B., Flagel, L., Stupar, R. M., Udall, J. A., Verma, N., Springer, N. M., et al. (2009). Reciprocal silencing, transcriptional bias and functional divergence of homeologs in polyploid cotton (*Gossypium*). *Genetics* 182, 503–517. doi: 10.1534/genetics.109.102608

Chen, C., Costa, M. G., Yu, Q., Moore, G. A., and Gmitter, F. G. (2010). Identification of novel members in sweet orange carotenoid biosynthesis gene families. *Tree Genet. Genomes* 6, 905–914. doi: 10.1007/s11295-010-0300-3

Chen, X., Truksa, M., Snyder, C. L., El-Mezawy, A., Shah, S., and Weselake, R. J. (2011). Three homologous genes encoding sn-glycerol-3-phosphate acyltransferase 4 exhibit different expression patterns and functional divergence in Brassica napus. *Plant Physiol.* 155, 851–865. doi: 10.1104/pp.110.169482

de Lange, O., Schreiber, T., Schandry, N., Radeck, J., Braun, K. H., Koszinowski, J., et al. (2013). Breaking the DNA-binding code of Ralstonia solanacearum TAL effectors provides new possibilities to generate plant resistance genes against bacterial wilt disease. *New Phytologist* 199, 773–786. doi: 10.1111/nph.12324

Desmond, O. J., Edgar, C. I., Manners, J. M., Maclean, D. J., Schenk, P. M., and Kazan, K. (2005). Methyl jasmonate induced gene expression in wheat delays symptom development by the crown rot pathogen Fusarium pseudograminearum. *Physiol. Mol. Plant Pathol.* 67, 171–179. doi: 10.1016/j.pmpp.2005.12.007

Dobon, A., Bunting, D. C. E., Cabrera-Quio, L. E., Uauy, C., and Saunders, D. G. O. (2016). The host-pathogen interaction between wheat and yellow rust induces temporally coordinated waves of gene expression. *BMC Genomics* 17, 380–380. doi: 10.1186/s12864-016-2684-4

Felton, G. W., and Korth, K. L. (2000). Trade-offs between pathogen and herbivore resistance. *Curr. Opin. Plant Biol.* 3, 309–314. doi: 10.1016/S1369-5266(00)00086-8

Fernández-Calvo, P., Chini, A., Fernández-Barbero, G., Chico, J. -M., Gimenez-Ibanez, S., Geerinck, J., et al. (2011). The Arabidopsis transcription factors MYC3 and MYC4 are targets of JAZ repressors and act additively with MYC2 in the activation of jasmonate responses. *Plant Cell* 23, 701. doi: 10.1105/tpc.110.080788

Finver, S. N., Nishikura, K., Finger, L. R., Haluska, F. G., Finan, J., Nowell, P. C., et al. (1988). Sequence analysis of the MYC oncogene involved in the t chromosome translocation in a human leukemia T-cell line indicates that putative regulatory regions are not altered. *Proc. Natl. Acad. Sci.* 85, 3052–3056. doi: 10.1073/pnas.85.9.3052

Fukuoka, S., Saka, N., Koga, H., Ono, K., Shimizu, T., Ebana, K., et al. (2009). Loss of function of a proline-containing protein confers durable disease resistance in rice. *Science* 325, 998–1001. doi: 10.1126/science.1175550

Hahn, M., and Mendgen, K. (2001). Signal and nutrient exchange at biotrophic plant–fungus interfaces. *Curr. Opin. Plant Biol.* 4, 322–327. doi: 10.1016/S1369-5266(00)00180-1

Heath, M. C. (1997). Signalling between pathogenic rust fungi and resistant or susceptible host plants. *Ann. Botany* 80, 713–720. doi: 10.1006/anbo.1997.0507

Holleley, C., and Sutcliffe, A. (2022). *3.12 96 Well DNA Extraction Protocol*. Available online at: https://www.researchgate.net/profile/Clare-Holleley-2/publication/242744494_96_Well_DNA_Extraction_Protocol/links/0f317531d650ba76a1000000/96-Well-DNA-Extraction-Protocol.pdf

Hovav, R., Udall, J. A., Chaudhary, B., Rapp, R., Flagel, L., and Wendel, J. F. (2008). Partitioned expression of duplicated genes during development and evolution of a single cell in a polyploid plant. *Proc. Natl. Acad. Sci.* 105, 6191–6195. doi: 10.1073/pnas.0711569105

Hummel, A. W., Doyle, E. L., and Bogdanove, A. J. (2012). Addition of transcription activator-like effector binding sites to a pathogen strain-specific rice bacterial blight resistance gene makes it effective against additional strains and against bacterial leaf streak. *New Phytologist* 195, 883–893. doi: 10.1111/j.1469-8137.2012.04216.x

Jiang, W., Zhou, H., Bi, H., Fromm, M., Yang, B., and Weeks, D. P. (2013). Demonstration of CRISPR/Cas9/sgRNA-mediated targeted gene modification in Arabidopsis, tobacco, sorghum and rice. *Nucleic. Acids Res.* 41, e188–e188. doi: 10.1093/nar/gkt780

Jin, Y., Singh, R., Ward, R., Wanyera, R., Kinyua, M., Njau, P., et al. (2007). Characterization of seedling infection types and adult plant infection responses of monogenic *Sr* gene lines to race TTKS of *Puccinia graminis* f. sp. tritici. *Plant Dis.* 91, 1096–1099. doi: 10.1094/PDIS-91-9-1096

Kazan, K., and Manners, J. M. (2013). MYC2: The master in action. *Mol. Plant* 6, 686–703. doi: 10.1093/mp/sss128

Kozera, B., and Rapacz, M. (2013). Reference genes in real-time PCR. *J. Appl. Genet.* 54, 391–406. doi: 10.1007/s13353-013-0173-x

Li, T., Liu, B., Spalding, M. H., Weeks, D. P., and Yang, B. (2012). High-efficiency TALEN-based gene editing produces disease-resistant rice. *Nat. Biotechnol.* 30, 390. doi: 10.1038/nbt.2199

Line, R. F., and Qayoum, A. (1992). *Virulence, Aggressiveness, Evolution, and Distribution of Races of Puccinia Striiformis (the cause of stripe rust of wheat) in North America, 1968-87. Technical bulletin-United States Department of Agriculture* (1788)

McIntosh, R. A., Wellings, C. R., and Park, R. F. (1995). *Wheat Rusts: An Atlas of Resistance Genes*. Kluwer Academic *Publishers*. doi: 10.1071/9780643101463

Milligan, S. B., Bodeau, J., Yaghoobi, J., Kaloshian, I., Zabel, P., and Williamson, V. M. (1998). The root knot nematode resistance gene Mi from tomato is a member of the leucine zipper, nucleotide binding, leucine-rich repeat family of plant genes. *Plant Cell* 10, 1307–1319. doi: 10.1105/tpc.10.8.1307

Mittal, S., and Davis, K. R. (1995). Role of the phytotoxin coronatine in the infection of Arabidopsis thaliana by Pseudomonas syringae pv. tomato. *Mol. Plant Microbe Interact.* 8, 165–171. doi: 10.1094/MPMI-8-0165

Moore, J. W., Herrera-Foessel, S., Lan, C., Schnippenkoetter, W., Ayliffe, M., Huerta-Espino, J., et al. (2015). A recently evolved hexose transporter variant confers resistance to multiple pathogens in wheat. *Nat. Genet.* 47, 1494–1498. doi: 10.1038/ng.3439

Moore, J. W., Loake, G. J., and Spoel, S. H. (2011). Transcription dynamics in plant immunity. *Plant Cell* 23, 2809–2820. doi: 10.1105/tpc.111.087346

Muthukrishnan, S., Liang, G. H., Trick, H. N., and Gill, B. S. (2001). Pathogenesis-related proteins and their genes in cereals. *Plant Cell Tissue Organ Culture* 64, 93. doi: 10.1023/A:1010763506802

Niu, Y., Figueroa, P., and Browse, J. (2011). Characterization of JAZ-interacting bHLH transcription factors that regulate jasmonate responses in Arabidopsis. *J. Exp. Bot.* 62, 2143–2154. doi: 10.1093/jxb/erq408

Pieterse, C. M., Ton, J., and Van Loon, L. (2001). Cross-talk between plant signalling pathways: boost or burden. *Ag. Biotech. Net.* 3, 1–8.

Rakszegi, M., Kisgyörgy, B., Tearall, K., Shewry, P., Láng, L., Phillips, A., et al. (2010). Diversity of agronomic and morphological traits in a mutant population of bread wheat studied in the Healthgrain program. *Euphytica* 174, 409–421. doi: 10.1007/s10681-010-0149-4

Romer, P., Strauss, T., Hahn, S., Scholze, H., Morbitzer, R., Grau, J., et al. (2009). Recognition of AvrBs3-like proteins is mediated by specific binding to promoters of matching pepper Bs3 alleles. *Plant Physiol.* 150, 1697–1712. doi: 10.1104/pp.109.139931

Sarwat, M., and Tuteja, N. K. (2017). Hormonal signaling to control stomatal movement during drought stress. *Plant Genet.* 11, 143–153. doi: 10.1016/j.plgene.2017.07.007

Schweizer, F., Fernández-Calvo, P., Zander, M., Diez-Diaz, M., Fonseca, S., Glauser, G., et al. (2013). Arabidopsis basic helix-loop-helix transcription factors MYC2, MYC3, and MYC4 regulate glucosinolate biosynthesis, insect performance, and feeding behavior. *Plant Cell* 25, 3117. doi: 10.1105/tpc.113.115139

Serfling, A., Templer, S. E., Winter, P., and Ordon, F. (2016). Microscopic and molecular characterization of the prehaustorial resistance against wheat leaf rust (*Puccinia triticina*) in einkorn (*Triticum monococcum*). *Front. Plant Sci.* 7, 1668. doi: 10.3389/fpls.2016.01668

Shan, Q., Wang, Y., Li, J., Zhang, Y., Chen, K., Liang, Z., et al. (2013). Targeted genome modification of crop plants using a CRISPR-Cas system. *Nat. Biotechnol.* 31, 686doi: 10.1038/nbt.2650

Shitsukawa, N., Tahira, C., Kassai, K. -i., Hirabayashi, C., Shimizu, T., Takumi, S., et al. (2007). Genetic and epigenetic alteration among three homoeologous genes of a class E MADS box gene in hexaploid wheat. *Plant Cell* 19, 1723–1737. doi: 10.1105/tpc.107.051813

Van Loon, L. (1982). *Regulation of changes in proteins and enzymes associated with active defence against virus infection. In Active defense mechanisms in plants*. Springer, 247–273. doi: 10.1007/978-1-4615-8309-7_14

Van Loon, L. C., and Van Strien, E. A. (1999). The families of pathogenesis-related proteins, their activities, and comparative analysis of PR-1 type proteins. *Physiol. Mol. Plant Pathol.* 55, 85–97. doi: 10.1006/pmpp.1999.0213

Van Moerkercke, A., Duncan, O., Zander, M., Šimura, J., Broda, M., Vanden Bossche, R., et al. (2019). A MYC2/MYC3/MYC4-dependent transcription factor network regulates water spray-responsive gene expression and jasmonate levels. *Proc. Natl. Acad. Sci.* 116, 23345. doi: 10.1073/pnas.1911758116

Voegele, R. T., and Mendgen, K. (2003). Rust haustoria: nutrient uptake and beyond. *New Phytol.* 159, 93–100. doi: 10.1046/j.1469-8137.2003.00761.x

Wang, Y., Cheng, X., Shan, Q., Zhang, Y., Liu, J., Gao, C., et al. (2014). Simultaneous editing of three homoeoalleles in hexaploid bread wheat confers heritable resistance to powdery mildew. *Nat. Biotechnol.* 32, 947. doi: 10.1038/nbt.2969

Xie, K., and Yang, Y. (2013). RNA-guided genome editing in plants using a CRISPR–Cas system. *Mol. Plant* 6, 1975–1983. doi: 10.1093/mp/sst119

Yu, Y., Qian, Y., Jiang, M., Xu, J., Yang, J., Zhang, T., et al. (2020). Regulation mechanisms of plant basic leucine zippers to various abiotic stresses. *Front. Plant Sci.* 11, 1258. doi: 10.3389/fpls.2020.01258

Zeng, X., Tian, D., Gu, K., Zhou, Z., Yang, X., Luo, Y., et al. (2015). Genetic engineering of the Xa10 promoter for broad-spectrum and durable resistance to Xanthomonas oryzae pv. *oryzae. Plant Biotechnol. J.* 13, 993–1001. doi: 10.1111/pbi.12342

Zhang, H., Qiu, Y., Yuan, C., Chen, X., and Huang, L. (2018). Fine-tuning of PR genes in wheat responding to different *Puccinia* rust species. *J. Plant Physiol. Pathol.* 06, 178. doi: 10.4172/2329-955X.1000178

Zhang, Y., Bai, Y., Wu, G., Zou, S., Chen, Y., Gao, C., et al. (2017). Simultaneous modification of three homoeologs of Ta EDR 1 by genome editing enhances powdery mildew resistance in wheat. *Plant J.* 91, 714–724. doi: 10.1111/tpj.13599

Zheng, X.-Y., Spivey, N. W., Zeng, W., Liu, P.-P., Fu, Z. Q., Klessig, D. F., et al. (2012). Coronatine promotes Pseudomonas syringae virulence in plants by activating a signaling cascade that inhibits salicylic acid accumulation. *Cell Host Microbe* 11, 587–596. doi: 10.1016/j.chom.2012.04.014

Zhou, Z., Wu, Y., Yang, Y., Du, M., Zhang, X., Guo, Y., et al. (2015). An Arabidopsis plasma membrane proton ATPase modulates JA signaling and is exploited by the *Pseudomonas syringae* effector protein AvrB for stomatal invasion. *Plant Cell* 27, 2032–2041. doi: 10.1105/tpc.15.00466

frontiers | Frontiers in Plant Science

TYPE Original Research
PUBLISHED 20 October 2022
DOI 10.3389/fpls.2022.1039090

OPEN ACCESS

EDITED BY
Paul Christiaan Struik,
Wageningen University and Research,
Netherlands

REVIEWED BY
Erik Lysøe,
Norwegian Institute of Bioeconomy
Research (NIBIO), Norway
Livio Torta,
Università di Palermo,
Italy

*CORRESPONDENCE
Angela Feechan
angela.feechan@ucd.ie;
angela.feechan@hw.ac.uk

SPECIALTY SECTION
This article was submitted to
Plant Pathogen Interactions,
a section of the journal
Frontiers in Plant Science

RECEIVED 07 September 2022
ACCEPTED 06 October 2022
PUBLISHED 20 October 2022

CITATION
Pilo P, Lawless C, Tiley AMM, Karki SJ, Burke JI and Feechan A (2022) Comparison of microscopic and metagenomic approaches to identify cereal pathogens and track fungal spore release in the field.
Front. Plant Sci. 13:1039090.
doi: 10.3389/fpls.2022.1039090

Comparison of microscopic and metagenomic approaches to identify cereal pathogens and track fungal spore release in the field

Paola Pilo[1], Colleen Lawless[2], Anna M. M. Tiley[3], Sujit J. Karki[1], James I. Burke[1] and Angela Feechan[1,4]*

[1]School of Agriculture & Food Science and UCD Earth Institute, University College Dublin, Belfield, Ireland, [2]School of Biology and Environmental Science and UCD Earth Institute, University College Dublin, Belfield, Ireland, [3]Department of Agriculture, Food and the Marine, Celbridge, Ireland, [4]Institute for Life and Earth Sciences, School of Energy, Geosciences, Infrastructure and Society, Heriot-Watt University, Edinburgh, United Kingdom

Wheat is one of the main staple food crops, and 775 million tonnes of wheat were produced worldwide in 2022. Fungal diseases such as Fusarium head blight, Septoria tritici blotch, spot blotch, tan spot, stripe rust, leaf rust, and powdery mildew cause serious yield losses in wheat and can impact quality. We aimed to investigate the incidence of spores from major fungal pathogens of cereals in the field by comparing microscopic and metagenomic based approaches for spore identification. Spore traps were set up in four geographically distinct UK wheat fields (Carnoustie, Angus; Bishop Burton, Yorkshire; Swindon, Wiltshire; and Lenham, Kent). Six major cereal fungal pathogen genera (*Alternaria* spp., *Blumeria graminis, Cladosporium* spp., *Fusarium* spp., *Puccinia* spp., and *Zymoseptoria* spp.) were found using these techniques at all sites. Using metagenomic and BLAST analysis, 150 cereal pathogen species (33 different genera) were recorded on the spore trap tapes. The metagenomic BLAST analysis showed a higher accuracy in terms of species-specific identification than the taxonomic tool software Kraken2 or microscopic analysis. Microscopic data from the spore traps was subsequently correlated with weather data to examine the conditions which promote ascospore release of *Fusarium* spp. and *Zymoseptoria* spp. This revealed that *Zymoseptoria* spp. and *Fusarium* spp. ascospore release show a positive correlation with relative humidity (%RH). Whereas air temperature (°C) negatively affects *Zymoseptoria* spp. ascospore release.

KEYWORDS

Spore trap, ascospore, microscopy, metagenomic, fungal pathogen, *Zymoseptoria tritici*, *Fusarium* spp., wheat

Introduction

Every year approximately 15 – 20% of wheat yields are lost due to fungal pathogens (FAO, 2022; Figueroa et al., 2018). Yield losses in the UK due to Septoria tritici blotch (STB) caused by *Zymoseptoria tritici* are around 20% on average (Fones and Gurr, 2015). In addition to yield loss Fusarium head blight (FHB) also contaminates grain with deoxynivalenol that is harmful to human and animal health (Rocha et al., 2005). One of the ways which cereal fungal pathogens can spread to new hosts is *via* spore release into the atmosphere from infected plants or stubble (Eversmeyer and Kramer, 1987; Suffert et al., 2011).

Aerobiology studies applied to plant pathology have focused on fungal spore dispersal in the air by using passive or active spore traps as a sampling method (Calderon et al., 1995; Cordo et al., 2017; Aguayo et al., 2018; Schiro et al., 2018; Woo et al., 2018). Passive spore traps include filter papers or microscope slides coated with an adhesive matrix, mounted onto a support. The spores in the air naturally land on the sampling surface by gravity or wind (Cordo et al., 2017; Aguayo et al., 2018; Schiro et al., 2018; Woo et al., 2018). In contrast, active spore traps use a mechanical and electrical system to draw a constant volume of air inside the mechanism. This allows spores to adhere to adhesive tape, a microscope slide, a micro tube, or a filter, depending on the type of machine in use (Calderon et al., 1995; Grinn-Gofroń and Rapiejko, 2009; Jackson and Bayliss, 2011)

The analysis following spore trap sampling ranges from more "traditional" approaches such as microscopy for spore counting and identification (Calderon et al., 1995; Cordo et al., 2017; Schiro et al., 2018) to molecular techniques such as Polymerase Chain Reaction (PCR) and New Generation Sequencing (NGS), often involving analysis of the ribosomal internal transcribed space (ITS) region (Woo et al., 2018; Aguayo et al., 2018). Metagenomics utilises NGS to analyse the genomes of all the organisms from an environmental sample. This type of environmental sampling in the field can allow the detection of a wide range of crop and plant pathogens since no prior knowledge of the pathogens present is required (Yang et al., 2022). Microscopy of airborne spores is a well-established technique and, despite being time consuming, provides detailed information. For example, timing of spore release can be correlated with external factors such as the time of day (dawn and dusk) (Calderon et al., 1995) and changes in weather conditions (Cordo et al., 2017; Schiro et al., 2018).

PCR based methods have also been used for correlation with weather data where gene copy numbers obtained by qPCR analysis were statistically compared with average weather data (Choudhury et al., 2016). Molecular based approaches for the study of airborne spores can be very useful in terms of identification at the species level. Previous research by Woo et al. (2018) used weekly DNA extractions, and sequencing of the ITS region amplicons to determine which species were present in the atmosphere between two different collection conditions (dry and wet). Whereas, Aguayo et al. (2018) assessed high-throughput sequencing with metabarcoding to compare different types of passive spore trap samples and DNA extraction methods.

In this study the presence of airborne spores from fungal pathogens of cereals were assessed and compared using microscopy and two metagenomic based methods (BLAST based and Kraken2) (Wood et al., 2019). Examples of cereal pathogens identified include *Alternaria* spp., *Cladosporium* spp., *Blumeria graminis*, *Fusarium* spp., *Puccinia* spp., and *Zymoseptoria tritici*. The samples were collected from volumetric spore traps over four UK wheat field sites (Carnoustie, Angus; Bishop Burton, Yorkshire; Swindon, Wiltshire and Lenham, Kent). Weather data such as air temperature (°C), rainfall (mm), relative humidity (%RH), and wind speed (Km/h) were correlated with bi–hourly time points of spore release for the Ascomycete fungal pathogens of wheat *Zymoseptoria* spp. and *Fusarium* spp., using microscopy. This provided an overview of the fungal pathogens present at the different field sites and revealed that spore release is positively correlated with relative humidity (%RH) but negatively correlated with air temperature (°C).

Methods

Spore trap set-up

Spore traps were installed at each of the four UK sites 1) Carnoustie, Angus; 2) Bishop Burton, Yorkshire; 3) Swindon, Wiltshire; and 4) Lenham, Kent (Figure 1). A volumetric Pollen and Particle Sampler (VPPS® 2010, by LANZONI srl) was installed at the Carnoustie and Bishop Burton field sites (Figure 1A). A Seven-Day Recording Volumetric Spore Trap (©Burkard Manufacturing Co Ltd) was installed at the Swindon and Lenham field sites (Figure 1B). Both type of spore traps record volumetric samples for seven days. Each machine is equipped with a rotating drum where a SILKOSTRIP (Lanzoni), a polyester pre–siliconed sampling tape, is mounted for each week of collection. A clockwork mechanism rotates the drum clockwise while air enters through the orifice allowing spores to be deposited on the tape, with a progression of 2 mm every 2 hours (h). Each spore trap is powered by a 12–Volt battery. The flow rate is checked after installation with a flowmeter provided by the manufacturer, as spore traps operate with an airflow of 10 $Lmin^{-1}$. The spore traps were set up in each of the four UK wheat fields, and air samples were collected consecutively for seven days, every two weeks, from 4th May 2018 until 17th of August 2018.

10.3389/fpls.2022.1039090

FIGURE 1
UK spore traps locations at wheat fields in: **(1)** Carnoustie, Angus (North-East); **(2)** Bishop Burton, Yorkshire (Central-East); **(3)** Swindon, Wiltshire (South-West); and **(4)** Lenham, Kent (South-East). Volumetric Pollen and Particle Sampler, VPPS® 2010 by LANZONI srl in Carnoustie and Bishop Burton; Seven-Day Recording Volumetric Spore Trap by ©Burkard Manufacturing Co Ltd in Swindon and Lenham.

Spore trap tape preparation

Following collection, insects and large debris were removed and trap tapes were stored at 4°C prior to preparation. Each of the spore trap tapes were divided into two longitudinal halves; the first half of the tape was used for downstream microscopy and the second half used for DNA extraction and metagenomic analysis (Figure 2A). A total of eight half tapes corresponding to eight weeks (two weeks each from the months of May, June, July, and August) from 2018, were used to perform microscopy analysis, and a total of six half tapes corresponding to six weeks (two weeks from the months of June, July, and August) were used for metagenomic analysis for all sites (Figure 2).

Microscopy

For microscopic analysis, each of the half tapes were divided into seven segments, each measuring 48 x 7 mm (L X W) and representing each of the seven days of collection (Figure 2B). Individual segments were then placed on a microscope slide. A solution of 10% Trypan – blue – lactophenol (Boedijn, 1956) and 90% colorless glycerin (100%) (~300µl *per* slide) was evenly distributed over the tape to stain the fungal spores. The tapes were then covered with a glass slide and left to dry. Once dry, a marker pen was used to divide the slides into 12 x 2 mm transverse sections, each one corresponding to 2-hour (2 h) time points, so that one slide represents 24 hours of sampling (Figure 2C).

Spore sampling was undertaken over two weeks per month over four months (MayA-August) in 2018. Therefore, two spore trap tapes were collected per month per site. A total of 14 slides (one for each day of the two weeks) were analyzed *per* month *per* site. For each site, there was therefore a total of 56 slides, representing a total of 56 days.

Microscopy was performed using a Leica DM5500B microscope equipped with a Leica DFC 310 FX Camera. Fungal taxa were identified *via* visual assessment based on spore morphology and appearance (Figure 2D) (Lacey and West, 2007). Spores were counted for three random fields of view (1 field = 321 x 240 µm) *per* each of the 12 x 2 mm transverse sections with X40 magnification. The number and type of spores available was recorded. The fungal spores were adjusted to the concentration of spores per cubic meter of air using the following formula:

$$N \times CF = N \times \frac{0.28}{width\ of\ \ one\ traverse\ (mm)}$$

Where (N) is the daily total number of spores, multiplied by the Correction Factor (CF) where the combination of microscope/lens, used will give the daily mean concentration of fungal spores per cubic meter (Lacey and West, 2007). In this

10.3389/fpls.2022.1039090

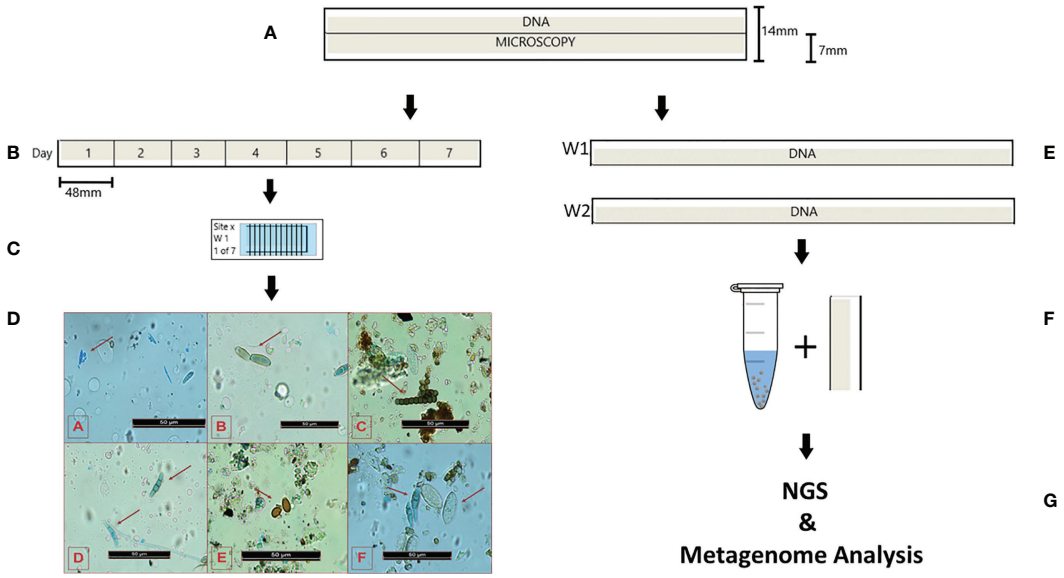

FIGURE 2
Schematic summarizing the preparation of the spore trap tapes for microscopy and metagenomic analysis. **(A)** the full tape was split longitudinally and divided ½ for microscopy and ½ for DNA extraction; **(B)** the microscopy half was divided into 7 sections (48 mm wide), each representing one day of collection; **(C)** tape sections were stained with solution of 10% Trypan-blue-lactophenol 90% colorless glycerin, and mounted on microscope slides, which were segmented in 12 parts 2mm wide. Each 2mm section represents 2 hours of collection; **(D)** Representative images of different fungal spores from the spore trap tape microscope slides. Red arrows indicate: [A] *Zymoseptoria* spp. ascospores, [B] *Cladosporium* spp., [C] *Torula herbarum* [D] *Fusarium* spp. Ascospores, [E] *Puccinia* spp. [F] *Alternaria* spp. (left), *Blumeria graminis* (right); **(E)** Two half tapes from two consecutive weeks of collection were used for monthly DNA extraction; **(F)** tape sections were used for DNA extraction using the Qiagen DNeasy Soil Kit and 400 – 600 µm acid – washed beads; **(G)** DNA extracted was sent for NGS and DNA reads analyzed for metagenomic of fungal pathogens.

case a Leica DM5500B microscope with a DFC 310 FX Camera, and X40 lens magnification corresponds to a width of 321 µm (0.321 mm). The results from each day of sampling were summed to obtain a weekly count of fungal spores per cubic meter (Figure 3). Percentages of each spore type were calculated weekly *per* site (Table 1).

Microscopic results for spores from the ascomycete fungal pathogens, *Zymoseptoria* spp. and *Fusarium* spp., from all four

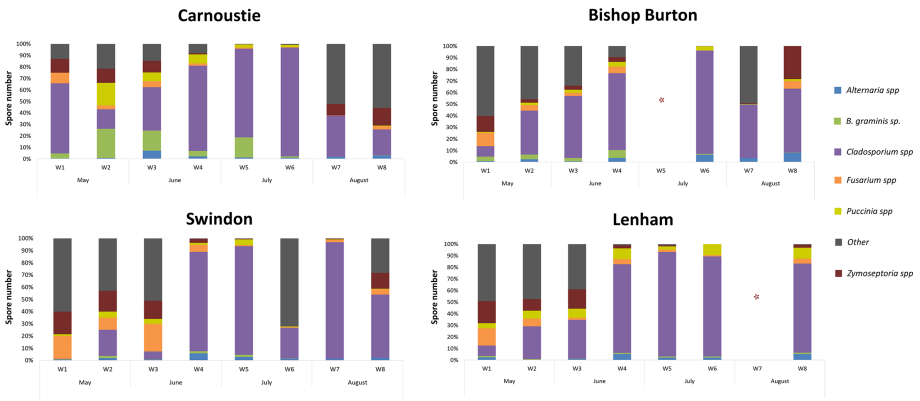

FIGURE 3
Weekly percentages of spores from the six major pathogens recognized and detected with the microscopic analysis at the four sites. Asterisk (*) denotes missing data in week 5 from the Bishop Burton field site and at week 7 at the Lenham field site due to mechanical failure of the spore trap.

sites were analyzed based on 2 h time points. The spore release data were correlated to weather data, specifically air temperature (°C), rainfall (mm), relative humidity (%RH), and wind speed (Km/h), to elucidate whether there was a correlation between spore release and weather conditions. The weather data was provided by Origin Enterprises plc. Weather stations were located at each of the four sites and data was collected every 15 minutes.

DNA extraction and processing

DNA extraction for Whole Genome Sequencing (WGS), was performed using a Qiagen DNeasy Soil Kit with the addition of 400–600 µm acid washed beads. Two half – tapes from the two weeks of collection for each month were pooled to generate a monthly sample from June to August for all four sites (Figure 2E). This therefore resulted in a total of 12 DNA samples per site. DNA extraction from May samples was unsuccessful.

Each tape was cut into 7 mm x 40 mm (W x L) sections and placed into a 2 ml screw – lid tube provided with the DNeasy Soil Kit, in which 300mg of 400–600 µm acid – washed beads were added. Each tube containing the tape was vortexed for five minutes, the processed tape was then exchanged for a new piece and vortexing was repeated for each month.

Once all tape segments were processed, the DNeasy Soil Kit protocol was followed using the manufacturer's instructions (Figure 2F). WGS was performed by Eurofins Genomics using a pipeline for low yield samples (DNA yield< 10 ng/µl). A metagenomic library was constructed, using Illumina® sequencing technology with 2 x 150 bp reads and with a minimum of 5 million reads per sample.

TABLE 1 Microscopy results displayed as weekly, week 1 (W1) to week 8 (W8) percentage of fungal cereal pathogen abundances.

Site	*Cereal Fungal Pathogen*	W1	W2	W3	W4	W5	W6	W7	W8
Car	*Alternaria* spp.	0.41%	0.80%	7.13%	2.20%	1.21%	0.97%	1.81%	3.09%
BB	*Alternaria* spp.	0.77%	2.39%	0.64%	3.63%		6.28%	3.65%	8.01%
SW	*Alternaria* spp.	0.58%	1.95%	0.73%	5.83%	2.91%	1.26%	1.23%	2.06%
Len	*Alternaria* spp.	2.28%	0.22%	0.99%	5.23%	2.14%	2.13%		5.26%
Car	*Blumeria graminis*	4.31%	25.46%	17.48%	4.67%	17.57%	1.24%	0.04%	0.14%
BB	*Blumeria graminis*	3.94%	4.13%	3.01%	6.85%		0.80%	0.02%	0.34%
SW	*Blumeria graminis.*	0.32%	1.65%	0.10%	1.68%	1.58%	0.14%	0.06%	0.05%
Len	*Blumeria graminis*	1.16%	0.61%	0.14%	1.09%	0.99%	1.06%		1.10%
Car	*Cladosporium* spp.	61.04%	16.95%	37.70%	74.08%	77.08%	94.51%	35.79%	22.47%
BB	*Cladosporium* spp.	9.09%	37.87%	53.47%	66.22%		89.05%	45.95%	55.05%
SW	*Cladosporium* spp.	0.32%	21.42%	6.53%	81.46%	89.13%	25.24%	95.62%	51.78%
Len	*Cladosporium* spp.	9.13%	28.37%	33.49%	76.34%	90.15%	86.17%		76.75%
Car	*Fusarium* spp.	9.17%	3.21%	5.17%	2.08%	0.95%	0.48%	0.14%	2.64%
BB	*Fusarium* spp.	11.37%	4.68%	2.79%	5.65%		0.12%	0.12%	6.50%
SW	*Fusarium* spp.	18.82%	9.88%	22.47%	5.65%	0.89%	0.58%	1.84%	4.51%
Len	*Fusarium* spp.	14.80%	6.54%	1.95%	4.37%	1.75%	1.06%		4.39%
Car	*Puccinia* spp.	0.00%	19.68%	7.76%	7.87%	2.64%	1.83%	0.13%	0.64%
BB	*Puccinia* spp.	0.88%	2.18%	2.36%	4.02%		3.53%	0.39%	1.56%
SW	*Puccinia* spp.	1.36%	5.06%	4.21%	1.73%	4.62%	0.49%	0.50%	0.25%
Len	*Puccinia* spp.	4.45%	6.89%	7.65%	9.30%	3.03%	9.57%		9.35%
Car	*Zymoseptoria* spp.	12.06%	12.45%	9.87%	1.01%	0.18%	0.38%	9.85%	15.35%
BB	*Zymoseptoria* spp.	13.70%	2.94%	3.62%	4.04%		0.06%	0.46%	28.53%
SW	*Zymoseptoria* spp.	18.49%	16.96%	14.75%	3.11%	0.34%	0.01%	0.47%	13.14%
Len	*Zymoseptoria* spp.	18.95%	9.87%	16.82%	2.54%	0.80%	0.00%		2.55%
Car	Other	13.02%	21.45%	14.89%	8.10%	0.37%	0.59%	52.25%	55.67%
BB	Other	60.25%	45.81%	34.10%	9.58%		0.15%	49.42%	0.00%
SW	Other	60.09%	43.08%	51.21%	0.54%	0.53%	72.28%	0.30%	28.22%
Len	Other	49.23%	47.50%	38.95%	1.12%	1.13%	0.00%		0.59%

Same genera/species clustered together for the 4 sites (Car = Carnoustie; BB = Bishop Burton; Sw = Swindon; Len = Lenham). The color scheme in each of the names follow the same color distribution of Figure 3 for comparison.

Metagenomics

DNA reads were analyzed using the bioinformatic OmicsBox Software by Bioinformatics and Valencia, 2019 (Figure 2G). Quality control of the reads and pre–processing was done using FASTQ. Metagenomic assembly of the reads was performed by MEGAHIT (Li et al., 2015). Gene and protein prediction from the assembled contigs was performed with FragGeneScan (Rho et al., 2010). Once obtained, protein prediction FASTA files were used for a Basic Local Alignment Search Tool (BLAST – p) search against non-redundant protein database using the OmicsBox online cloud. BLAST Species Hits from the predicted protein sequences were retrieved, characterized, and classified for species recognition based on the first five highest hits with an e – value ≤ 0.01 and Sim mean ≥ 60%. BLAST results were then analyzed with MEGAN Community Edition (version 6.21.10, built 29 Jul 2021) (Huson et al., 2007; Huson et al., 2016) to determine taxonomic relative abundances, in each site *per* each month.

As a control method for the BLAST analysis, the taxonomic classification tool Kraken2 was used, from OmicsBox. Kraken2 is a taxonomic classification system using exact *k – mer* matches to achieve high accuracy and fast classification speeds. This classifier matches each *k – mer* within a query sequence to the lowest common ancestor (LCA) of all genomes containing the given *k – mer* (Wood et al., 2019). This analysis was performed using the raw cleaned FASTQ reads. To compare both taxonomic systems, species diversity indexes (Shannon – Wiener and Simpson's) were calculated for both methods (Peet, 1975).

Statistical analysis

Statistical analysis for the comparison of results from both metagenomic methods were performed on results from BLAST and Kraken2. Species diversity indexes Shannon-Wiener and Simpson's were calculated for both methods (Peet, 1975). A two – way ANOVA test was performed using GraphPad Prism version 8.0.0 for Windows, GraphPad Software, San Diego, California USA (www.graphpad.com), to determine the difference between the Indexes means for the two methods.

Correlation between weather data from the four sites and M spore release data at two hour time points were analyzed using Prism – GraphPad (www.graphpad.com), and IBM SPSS Statistics 26 (IBM-Corp, 2019). The non – parametric Spearman's rho correlation coefficient (Spearman's Rank, 2008) was used to assess *Zymoseptoria* spp. and *Fusarium* spp. ascospore release against the air temperature (°C), rainfall (mm), relative humidity (%RH), and wind speed (Km/h).

Results

Abundance of fungal cereal pathogen spores across UK wheat field sites using microscopy

Approximately 20 taxa were identified using microscopy (*Alternaria spp., Aspergillus spp., Blumeria graminis, Cladosporium spp., Claviceps purpurea, Cochliobolus/Bipolaris spp., Epicoccum spp., Fusarium spp., Gaeumannomyces tritici, Helicomyces spp., Myxomycetes, Penicillium spp., Pithomycetes, Pleospores, Puccinia spp., Tilletiopsis spp., Torula spp., Trichotechium roseum, Zymoseptoria spp.*). Microscopy classification of spores in the *Fusarium* or *Alternaria*, *Cladosporium*, and *Puccinia* genus were counted as a unit at the genus level. However, microscopy was impacted by the malfunction of the spore traps at Bishop Burton in week five (July) and Lenham week seven (August) and as a result only DNA extraction was possible for these weeks.

Microscopic analysis revealed a broad diversity in the fungal species present on the spore trap tapes. Of these, cereal pathogens belonging to six genera (*Alternaria* spp., *Blumeria graminis, Cladosporium* spp., *Fusarium* spp., *Puccinia* spp. and *Zymoseptoria* spp.*)* were consistently identified throughout the sampling season at every site and these were selected for downstream spore counting. The remaining fungal spores were recorded as "*Other*". The percentage of spore abundance for each fungal cereal pathogen genera was recorded per site *per* week (Figure 3). The percentage of the total amount of spores *per* sample by pathogen genera are shown in Table 1.

A high percentage of *Blumeria graminis* conidia were identified at the Carnoustie field site followed by the Bishop Burton field site throughout the sampling season (Figure 3). Carnoustie had the highest percentage of *B. graminis* conidia, with 25.46% in week 2 (May), 17.48% in week 3 (June) and 17.47% in week 5 (July). The percentage of *B. graminis* conidia decreased at the Carnoustie and Bishop Burton sites towards the end of the season in week 6 (July), week 7 and week 8 (August), where values registered were between 0.02% and 1.24% (Table 1). Low percentage levels of *B. graminis* were identified at the Swindon and Lenham field sites throughout the sampling season. For example, at Swindon, the percentage of *B. graminis* was highest in week 4 (June) 1.68% and lowest in week 8 (August) 0.05%. At Lenham, the percentage of *B. graminis* was highest in week 1 (May) at 1.16% and lowest in week 3 (June) 0.14% (Figure 3, Table 1).

The presence of *Zymoseptoria* spp. ascospores was detected throughout the season at all four sites. In week 1 (May) there was a high percentage of *Zymoseptoria* spp. at all sites (Carnoustie 12.06%, Bishop Burton 13.70%, Swindon and Lenham >18%).

Presence of *Zymoseptoria* spp. ascospores decreased at the Bishop Burton site to 2.94% in week 2 (May) and to 3.62% in week 3 (June). The abundance *of Zymoseptoria* spp. ascospores at the remaining sites were between ~10% to ~17% (Figure 3, Table 1). A decrease in the percentage of *Zymoseptoria* spp. ascospores at all sites from week 4 (June) to week 7 (August) was recorded. This was with the exception of Carnoustie, where there was an increase from ~0.4% in week 6 (July) to ~10% in week 7 (August) (Table 1). The percentage of *Zymoseptoria* spp. ascospores increased at the end of August (week 8) at all sites. The highest percentage of *Zymoseptoria* spp. ascospores was registered at week 8 in Bishop Burton at 28.53% and the lowest percentage was registered at week 8 in Lenham at 2.55% (Table 1, Figure 3).

Fusarium spp. ascospore release followed a similar pattern to *Zymoseptoria* spp. ascospore release (Figure 3). Higher ascospore percentages were recorded at the beginning of the sampling season in week 1, from 9.17% in Carnoustie to 18.82% in Swindon (Table 1). This followed a decrease by the end of June (week 4) in all the sites, with percentages of *Fusarium* spp. between 2.08% and 5.65% (Table 1). Percentages of *Fusarium* spp. ascospores remained low across the four sites in weeks 6 and 7 ($0.12\% \leq X \leq 1.84\%$). A slight increase was recorded by the end of August (week 8) with percentages between 2.64% and 6.50% (Table 1).

Monthly results from microscopic analysis for the whole season demonstrated that spores belonging to the *Cladosporium* spp. genus were the most abundant spore type at all four sites. The maximum percentage of *Cladosporium* spp. spores were registered at Carnoustie in July (90.72%) and the lowest percentage were registered at Swindon in May (11.19%) (Table S1). *Zymoseptoria* spp. was the second most abundant single pathogen over the four sites. The highest percentage presence of *Zymoseptoria* spp. ascospores was recorded at Swindon in May (17.70%) and the lowest percentage presence was observed at Bishop Burton in July (0.06%). Generally, the month of May registered the highest percentage of *Zymoseptoria* spp. ascospores across all sites (Table S1). The monthly percentages of *Fusarium* spp. ascospores also showed a higher percentage presence in May for all sites (6.66% in Carnoustie, 9.63% in Bishop Burton, 14.21% in Swindon, and 10.21% in Lenham). However, the highest presence of *Fusarium* spp. ascospores was found in Swindon in June (20.93%) (Table S1). While the lowest percentage of *Fusarium* spp. was found in July over the four sites (0.58% at Carnoustie, 0.12% in Bishop Burton, 0.68% in Swindon, and 1.74% in Lenham) (Table S1).

Correlation between weather conditions and *Zymoseptoria* spp. and *Fusarium* spp. spore release using microscopy

Zymoseptoria spp. and *Fusarium* spp. ascospore release data from the microscopy were correlated with weather data to establish any connection between spore release and weather conditions. The 2h spore release data for both ascomycetes were correlated with air temperature (°C), rainfall (mm), relative humidity (%RH), and wind speed (Km/h) using the Spearman's rho statistical tool (Table S2). The air temperature (°C) was negatively correlated to *Zymoseptoria* spp. spore release at all the sites, according to the p – values (> 0.05) and the correlation coefficients (r = - n). Whereas the *Fusarium* spp. ascospore release was only found to negatively correlate with air temperature (°C) at the Lenham site, and no significance was registered for the other sites. Significant (p – value > 0.05) positive correlation coefficients (r = + n) were observed for percentage relative humidity (%RH) with both *Zymoseptoria* spp. and *Fusarium* spp. ascospores across all sites (Table S2). For the remaining categories of rainfall (mm) and wind speed (Km/h), the Spearman's correlations revealed a significant positive correlation between both spore type and rainfall (mm) only at the Carnoustie site. While only at Lenham spore release was found to be significantly, negatively correlated with wind speed (Km/h) data (Table S2). The spore abundance over the whole sampling season at 2h intervals for *Zymoseptoria* spp. and *Fusarium* spp. with air temperature (°C) and relative humidity (%RH) are shown on Figure 4A. The correlations found between *Zymoseptoria* spp. and *Fusarium* spp. spore release and air temperature (°C), and relative humidity over the four sites plotted by time of the day are shown in Figures 4B, C. Negative correlations are indicated when the two lines in the graph bend in opposite directions (e.g., *Zymoseptoria* spp. and air temperature °C). When both lines follow the same curve, the correlation between the two data sets is positive (Figures 4B, C, Table S2, Table S3). These results together suggest that %RH has an impact on the spore release of these two pathogens.

Metagenomic BLAST taxonomic classification from UK wheat field spore traps

DNA was extracted from the spore trap samples across all sites for the months of June, July, and August followed by WGS. Taxonomic classification was carried out using BLAST followed by phylogenetic analysis (Figure S1). The overall taxonomic results from the BLAST metagenomic analysis for the 12 monthly samples are shown as a cladogram tree (Figure S1). Most of the BLAST species hits for cellular organisms belonged to the Eukaryote domain, specifically in the Opisthokonta supergroup. Of these, the kingdom Fungi was the most represented in all of the samples. Within the *Ascomycota* phylum, the *Saccharomyceta* clade was present in all samples, with a maximum presence of hits found at Carnoustie in August (80 – 90%). Comparison with the *Basidiomycota* phylum show a division of the classification of reads, into *Agaricomycotina*, *Pucciniomycotina* and *Ustilaginomycotina* with the percentage

of hits predominantly in the latter. In the *Pucciniomycotina*, a higher percentage of hits were registered for the Lenham field site in June/August (25–30%), and Swindon in July/August (10–15%). In the *Ustilaginomycotina*, most of the hits (10 – 15%) were identified for Carnoustie in July/August.

Metagenomic identification of fungal cereal pathogens across UK wheat fields

Using the BLAST species hits, a total of 150 species (33 different genera) of fungal cereal pathogens were recorded on the spore trap tapes (Figure 5; Figure S2). Within these, the presence of the six genera previously identified with the microscopy were confirmed (Figure 5). A heatmap produced with MEGAN calculated relative abundances between the samples for each species as z-score (-3/+3) (Figure 5). The same taxonomic dataset is also shown as a cladogram tree of the species built with MEGAN 6. Which shows the percentage of BLAST hit abundances for each sample in a white (0%) to green (100%) color shade scale (Figure S2).

For example, nine species were recognized in the *Alternaria* genus which can infect cereals or impact cereal product quality due to mycotoxin production (Figure 5). The highest presence of the *Alternaria* genus was registered at Bishop Burton in June, while the most abundant species amongst all the sites and months was *Alternaria solani* found at Swindon in June (Figure 5).

Two *formae speciales* of *Blumeria graminis* were identified: *B. graminis f.* sp. *hordei*, known to be the causal agent of powdery mildew on barley, and *B. graminis f.* sp. *tritici* the causal agent of powdery mildew on wheat. Results from Carnoustie in June and July, and Bishop Burton in July for both *B. graminis f.* sp. shows a higher presence of these pathogens compared to the other months and sites (Figure 5).

Hits belonging to the *Cladosporium* genus were divided between seven species that are identified as cereal pathogens. However, from the BLAST analysis the *Rachicladosporium antarcticum* species was recognized as an ubiquitous fungus closely related to plant pathogens belonging to the *Cladosporium* genus (Kang et al., 2019). It was not possible to distinguish the spores of these phylogenetically close species (Figure S2) from microscopic analysis. No pattern was observed in the relative abundance between sites or months for these fungi (Figure 5).

Within the *Fusarium* genus BLAST species hits, a total of 18 species were recognized as cereal pathogens. The samples from Swindon in June recorded the highest abundance compared to the other samples for the *Fusarium* genus (Figure 5). The most abundant species were *F. acuminatum*, *F. culmorum, F. gerlachii, F. graminearum, F. pseudograminearum*, and *F. solani*. BLAST species hits for the *Puccinia* genus, showed the presence of five cereal pathogen species across all sites. The sample from Lenham in June had the highest abundance of *Puccinia* sp., in particular *Puccinia coronata* var. *avenae f.* sp. *avenae* species (Figure 5).

Finally, *Z. tritici* relative abundance from the BLAST species hits results appeared to have the same pattern between the sites of Carnoustie and Lenham. A higher abundance of the pathogen was observed in June and July at these sites. In contrast, Swindon had a higher abundance of *Z. tritici* in the months of July and August. At Bishop Burton, the highest *Z. tritici* ascospore abundance was found in July (Figure 5).

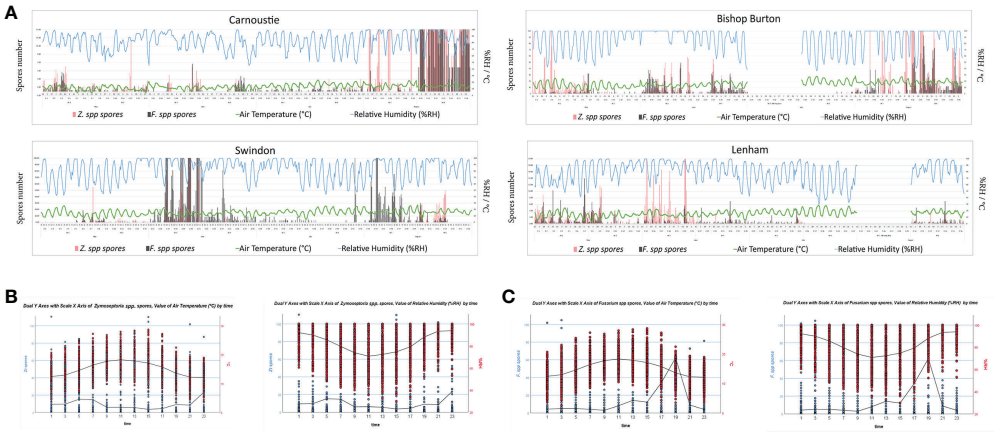

FIGURE 4
(A) Temporal distribution of *Z.* spp. (*Zt*, Pink bars) and *Fusarium* spp. (*F.*spp. Grey bars) ascospore release, plotted on the primary Y axis, against air temperature (Green line) and relative humidity (Blue line), plotted on the secondary Y axis; for all the four sites. **(B)** Dual Y axis with scale X axis of *Zymoseptoria* spp. or *Fusarium* spp. ascospores and value of air temperature by 2h timepoints. Values for all the 4 sites were used to generate the negative correlation curve. Graphs with IBM SPSS Statistics 26. **(C)** Dual Y axis with scale X axis of *Zymoseptoria* spp. or *Fusarium* spp. ascospores and value of relative humidity by the 2h timepoints. Values for all the 4 sites were used to generate the positive correlation curve. Graphs with IBM SPSS Statistics 26.

A larger number of hits were identified that belonged to other fungal species not previously identified from microscopy and classified as major cereal pathogens. These pathogens include: *Aspergillus* spp., *Botrytis cinerea, Colletotrichum* spp., *Epicoccum nigrum, Parastagonospora nodorum* (*Septoria nodorum*), *Penicillium* spp., *Pyrenophora tritici–repentis, Ramularia collo–cygni, Stagonospora* spp. and *Ustilago maydis* (etc.) (Figure 5, Figure S2). These species are known to be causal

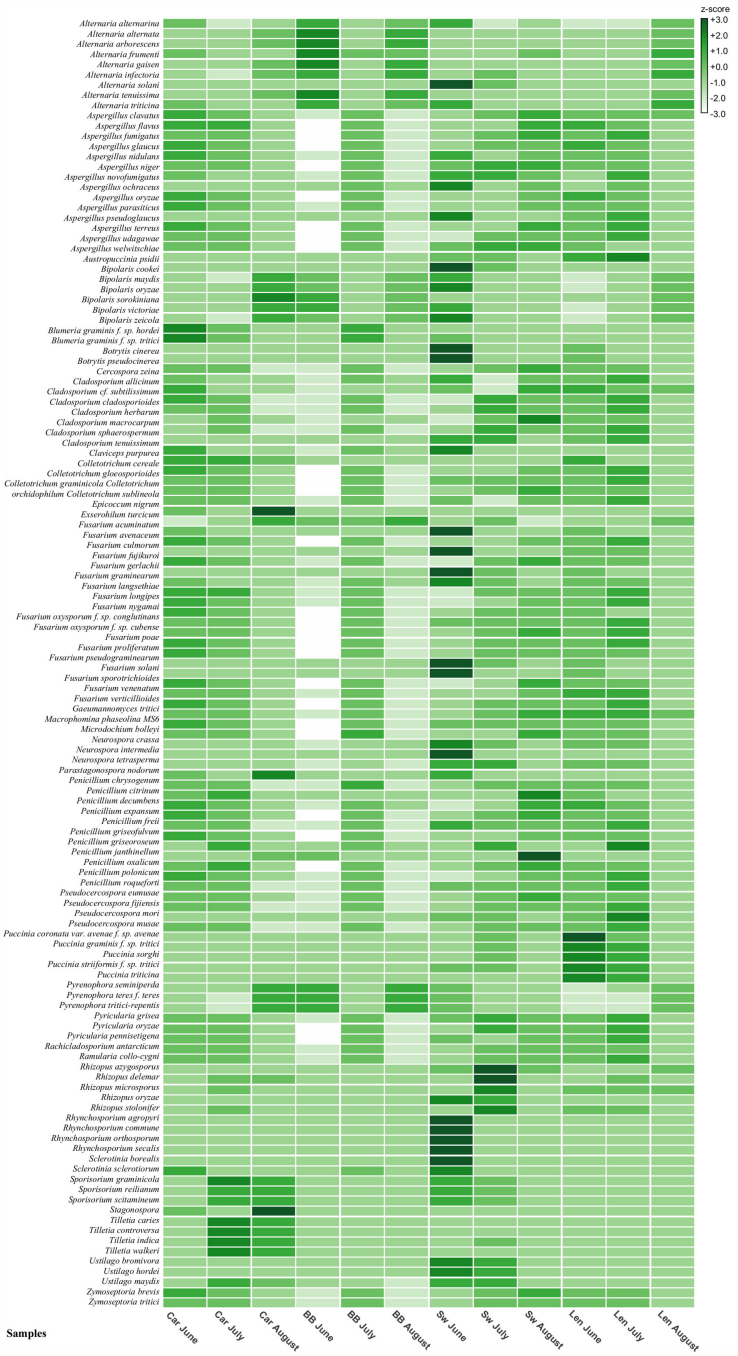

FIGURE 5
Heat map built in MEGAN 6 summarizing the 150 cereal fungal pathogens species hits recognized by BLAST metagenomic analysis. Species names are on the left-hand side of the map and field site samples names are located on the bottom. Z-scores range: +3/-3. Car, Carnoustie; BB, Bishop Burton; SW, Swindon; Len, Lenham.

agents of major diseases in cereals and other plants (Sweeney and Dobson, 1998; Freeman et al., 1998; Boudra and Morgavi, 2005; Dean et al., 2012; Różewicz et al., 2021).

Comparison of metagenomic analysis and microscopy for the identification of fungal cereal pathogens

Fungal species recognized by the BLAST analysis were compared and validated by cross referencing the data with the microscopy analysis, and also using the Kraken2 taxonomic classification tool (Wood et al., 2019) (Figure S3; Table 2). The methods were compared for the identification of the presence of 20 selected fungal taxa which are cereal pathogens (Table 2). For each one of the specific fungal pathogens the presence (+); absence (-); or not – recognized (/) was recorded for each of the methods (Microscopy, BLAST species hits, and Kraken2). All the nine taxa of fungal pathogen within the 20 listed in Table 2 that were recognized by microscopy were also recognized by the BLAST analysis (*Alternaria* spp., *Aspergillus* spp., *Blumeria graminis, Claviceps purpurea, Cladosporium* spp., *Epicoccum nigrum, Fusarium* spp., *Puccinia* spp., *Zymoseptoria tritici)*. Only three species out of the nine were recognized by the Kraken2 taxonomy tool (specifically *Aspergillus fumigatus/oryzae, Fusarium graminearum, Zymoseptoria tritici)* (Table 2). In contrast, the presence of five fungal taxa (*Botrytis cinerea, Cercospora* spp., *Colletotrichum* spp., *Neurospora crassa, Sporisorium* spp.*)* were recognized by both Kraken2 and BLAST analysis, but were not identified by microscopy (Table 2). The eight fungal pathogens identified by Kraken2 (*Aspergillus fumigatus/oryzae, Fusarium graminearum, Z. tritici, Botrytis cinerea, Cercospora* spp., *Colletotrichum* spp., *Neurospora crassa, Sporisorium* spp.*)* (Table 2), were the only fungal hits of the 66 most recognized genera using this method (Figure S3). A total of six fungal pathogens, from the 20 selected species, were recognized only using the BLAST analysis (*Parastagonospora nodorum, Pyrenophora teres f. teres, Pyrenophora tritici-repentis, Ramularia collo-cygni, Stagonospora* sp., *Ustilago maydis)*.

Comparison between the two metagenomic methods revealed that BLAST analysis is a more efficient method for the recognition of fungal pathogens. The percentages of reads classified from the raw FASTQ reads files from the Kraken2 were between 3% and 8% compared to between 26% and 38% using BLAST, obtained from the same FASTQ reads (Table S4). These results were confirmed by the statistical analysis on species diversity indexes. Simpson's, and Shannon – Wiener indexes were calculated for both methods, and a two – way ANOVA test was used to determine if there was a difference between the methods for each of the diversity indexes. The species diversity for the two metagenomics methods is compared in Figure 6. This includes: 1) monthly values, *per* each of the four sites, for the Shannon – Wiener index, the Evenness, and the Simpson's Index, from the BLAST analysis and from the Kraken2

TABLE 2 Recorded presence (+); absence (-); or not – recognized (/) of 20 selected cereal fungal pathogens genera / species from each of the methods of analysis (Microscopy, BLAST, Kraken2).

Cereal Fungal Pathogens	Microscopic Analysis	Blast Analysis	Kraken2 Analysis
Alternaria spp.	+	+	–
Aspergillus spp. *(fumigatus / oryzae)*	+	+	+
Blumeria graminis	+	+	–
Botrytis cinerea	/	+	+
Cercospora spp.	/	+	+
Cladosporium spp.	+	+	–
Claviceps purpurea	+	+	–
Colletotrichum spp.	/	+	+
Epicoccum nigrum	+	+	–
Fusarium spp. *(graminearum)*	+	+	+
Neurospora crassa	/	+	+
Parastagonospora nodorum	/	+	–
Puccinia spp.	+	+	–
Pyrenophora teres f. teres	/	+	–
Pyrenophora tritici-repentis	/	+	–
Ramularia collo-cygni	/	+	–
Sporisorium spp.	/	+	+
Stagonospora sp.	/	+	–
Ustilago maydis	/	+	–
Zymoseptoria spp.	+	+	+

analysis (Figure 6A); 2) analysis of the variances between the two methods, using the monthly samples, for both diversity indexes *per* all the four sites (Figure 6B). The diversity indexes related to the BLAST analysis are consistently higher than the variances of the Kraken2 diversity indexes for all the sites (Figure 6B), indicating that the BLAST tool can recognize a greater diversity of species than Kraken2. Furthermore, the two – way ANOVA analysis conducted on these data, confirmed that the differences between the two methods are statistically significant with a Column Factor p – value<0.0001 for both, Shannon – Wiener index, and Simpson's index.

Discussion

Different types of approaches have been used for the analysis of spore trap samples. The most traditional approach is microscopic analysis and this uses the size, shape and colour to identify and quantify spores. On the other hand, in the last decade molecular based analysis has become more frequent (Jackson and Bayliss, 2011). The various trapping mechanisms and their possible applications in plant biosecurity were reviewed by Jackson and Bayliss (2011), including the advantages and disadvantages of nine types of spore traps and the variety of analyses that can be performed on the samples obtained from each type.

In this work we analyzed air samples from volumetric spore traps, focusing specifically on the presence of cereal fungal pathogen spores present in the air at four UK wheat field sites. To compare the results from each analysis, the same samples were analyzed with both microscopic and metagenomic methods.

Microscopic analysis was performed on spore trap tapes, for the identification and quantification of fungal spores. Approximately 20 morphologically distinct spore types were recognized. Six of these taxa (*Alternaria* spp., *Blumeria graminis, Cladosporium* spp. *Fusarium* spp., *Puccinia* spp., *Zymoseptoria* spp.*)* were frequently found in all samples, making them the most ubiquitous genera present across the sites. The presence of ubiquitous pathogens such as *Cladosporium* spp. and *Alternaria* spp., (D'Amato et al., 1997; Grinn-Gofroń and Rapiejko, 2009) were recorded during the whole season for all the sites. We also used a metagenomic approach where DNA extraction was carried out monthly from June, July, and August, followed by NGS sequencing and classification of BLAST species hits taxonomically (Figure S1). For all the four wheat field sites, the majority of the species hits belonged to the fungal kingdom. A total of 33 different genera, which included 150 species of cereal pathogens, were identified by BLAST analysis (Figure 5, Figure S2). This compares to 63 operational taxonomic units (OTUs) identified from rice fields using DNA metabarcoding of the fungal ITS region (Ortega et al., 2020). Air sampling in the city of Seoul, South Korea identified 80-300 OTUs by sequencing of the fungal ITS region depending on the sampling conditions (dry or wet) and time of the year (Woo et al., 2018). Therefore, the BLAST analysis allows more detailed information on which species are present at each site.

Blumeria graminis, was recorded mostly in the first half of the season, which correlates with the life cycle of this pathogen

A

Site_Month	BLAST Analysis			Kraken2 Analysis		
	Shannon Index (H)	Evenness (EH) (H / LN(N))	Simpson's Index (D)	Shannon Index (H)	Evenness (EH) (H / LN(N))	Simpson's Index (D)
BB_June	4.744	0.560	0.959	3.269	0.422	0.870
BB_July	4.839	0.575	0.964	4.495	0.568	0.944
BB_August	4.569	0.574	0.963	3.593	0.457	0.876
Car_June	4.761	0.554	0.962	3.840	0.477	0.913
Car_July	4.832	0.563	0.967	2.835	0.366	0.818
Car_August	5.105	0.591	0.980	2.827	0.366	0.809
Len_June	5.255	0.564	0.973	3.611	0.444	0.841
Len_July	5.317	0.591	0.977	4.090	0.504	0.923
Len_August	4.565	0.536	0.967	3.735	0.469	0.913
Sw_June	6.480	0.707	0.991	2.859	0.364	0.763
Sw_July	5.632	0.607	0.977	3.275	0.401	0.758
Sw_August	4.543	0.538	0.961	3.500	0.445	0.872

B

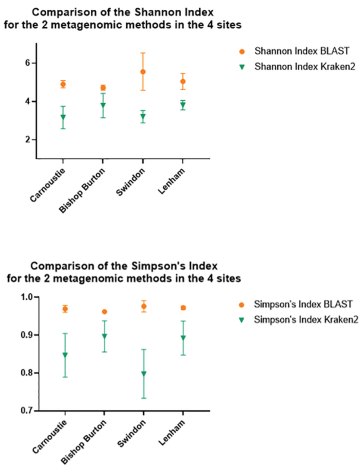

FIGURE 6
Comparison of the two metagenomic methods, BLAST and Kraken2. **(A)** Table with the monthly values for all the sites of Shannon – Wiener diversity index, its Evenness, and the Simpson's Index for both methods. Car, Carnoustie; BB, Bishop Burton; SW, Swindon; Len, Lenham; **(B)** XY Plots of variances for the Indexes values between the two methods (BLAST in Orange; Kraken2 in Green) by site.

(Dean et al., 2012; Troch et al., 2012). The differences noticeable between the sites could be due to the weather, since *B. graminis* infection occurs in cool and humid weather conditions (Parry, 1990; Dean et al., 2012). This may explain the high presence of *Blumeria graminis* in northern sites where weather conditions are more favorable to its growth. In fact, Carnoustie and Bishop Burton show a higher presence of *Blumeria graminis*, than Lenham and Swindon. These sites are situated in Scotland and the north of England, where weather conditions in summertime are more suitable for this pathogen than in the south of England (Figure 1). In this case results from the microscopy analysis, weekly (Table 1) and monthly percentages (Table S1) for *B. graminis* (both *formae speciales)* agree with the metagenomic results from the BLAST analysis (Figure 5) confirming the highest relative abundance at Carnoustie for June and July.

The trend for *Zymoseptoria* spp. ascospores observed using microscopy was the same across all the sites. A high abundance of *Zymoseptoria* spp. ascospores was registered in the first three weeks (May and beginning of June) of sampling followed by a decrease in ascospores in the middle of the sampling season. An increase was then observed in the last week (August) for three of the sites (Carnoustie, Bishop Burton, and Swindon). The production of ascospores from *Z. tritici* comes from sexual reproduction and occurs throughout the growing season (Hunter et al., 1999; Cordo et al., 2017). The *Z. tritici* ascospores are released from stubble present in the field from the previous year. These, ascospores are then carried *via* the wind to land on wheat leaves. Following leaf infection, the pathogen produces asexual pycnidiospores reducing the production of ascospores (Suffert et al., 2019). Sexual reproduction generally increases again at the end of the infection season. This allows the fungus to overwinter, resulting in an increase of ascospore production from August throughout the autumn season (Suffert et al., 2011; Cordo et al., 2017). This life cycle of *Z. tritici* corresponds with the observed airborne ascospore patterns at the four sites. However, the pattern of *Zymoseptoria* spp. ascospore release found from the microscopy analysis was not mirrored from the BLAST analysis for the four sites. For instance, the Lenham and Carnoustie field sites shared a high relative abundance of *Z. tritici* BLAST hits in June and July rather than June and August as suggested by the microscopy. The differences in the results from the two methods, could be due to the uneven distribution of spores on the tapes, which might impact the accuracy of microscopy scoring (Jackson and Bayliss, 2011), this could be further impacted by using a half tape for the analysis.

An example of strong similarity in the results, from both microscopy and metagenomic BLAST analysis, is the high presence of the *Fusarium* genus in the sample from Swindon in June (week 3). *Fusarium* spp. spore counts in week 3 of microscopy were the highest registered in the genus amongst all the samples at 22.47% (Table 1) and in terms of the monthly percentage abundances 20.93% (Table S1). The same results were also obtained by the metagenomic BLAST analysis (Figure 5), which show the highest z-score for five out of 18 *Fusarium* species recognized (*F. acuminatum; F. culmorum; F. graminearum; F. pseudograminearum; F. solani*), supporting that the sample from Swindon June has the highest presence of *Fusarium* spp. Compared to other samples. Generally, the spores belonging to the *Fusarium* species, are known to be present in the air throughout the whole season (Karlsson et al., 2021).

Volumetric spore traps used in this experiment allowed data to be obtained at two-hour time points (2 h) which was compared to weather data to understand if any correlation between spore release and climate conditions was present. Weather conditions such as humidity can influence the infectivity rate of *Z. tritici* (Fones et al., 2017). Air humidity and air velocity are known as factors which can influence spore release in the atmosphere (Pasanen et al., 1991). Comparison of *Zymoseptoria* spp. and *Fusarium* spp. Ascospore types with relative humidity (%RH) performed in this study, showed a consistent and strong positive correlation, these results were identical for all 4 sites. In contrast, air temperature (°C) negatively affects *Zymoseptoria* spp. spore release, the data from the 4 sites show a significant negative correlation for the Spearman's rank (Table S2). *Z. tritici* ascospore release in Argentina was previously found to be positively corelated with %RH and negatively correlated with temperature which is in agreement with our findings (Cordo et al., 2017). Trail et al., 2002 also found *F. graminearum* ascospore discharge to increase at %RH greater than 92% under light conditions (TrailKeller et al., 2014). Previous studies found the optimum temperature for *F. graminearum* ascospore release was at 16.6°C (Tschanz et al., 1976). In contrast, our results identified a negative correlation with temperature only at Lenham, which was the most Southern UK site. Therefore, microscopy can be useful to understand the relative concentration of fungal pathogens in the air and to identify external factors that impact spore release. This information may be used to inform the timing and application of fungicides for disease control.

Overall, microscopy allows the presence and concentration of specific airborne pathogens present in the area to be recorded. However, microscopic analysis is time consuming and requires trained personnel able to recognize a broad range of genera or species. Furthermore, the microscopy from spore trap tapes can be affected by a variety of factors including types of adhesive. These can influence the microscope focus plane where the spores appear, or their ability to adhere in one/multiple layers or aggregate due to humidity and water drops (Jackson and Bayliss, 2011). Microscopic analysis rely exclusively on manual counting of spores, in which error can vary depending on the counting technique used by the operator (Comtois et al., 1999; Sterling et al., 1999). No method is completely reliable unless the whole slide is counted (Comtois et al., 1999). In this work, the 12 transverses (representative of the 2 h sampling) (Lacey and West, 2007) gave the closest results to when the whole slide is counted with small error in comparison to other counting

methods, giving a better estimation of spore presence in a shorter time.

In order to evaluate the efficiency of the BLAST analysis, a second taxonomy tool was employed. The same samples FASTQ reads were run with the Kraken2 software, which was included in the OmicsBox package. The two metagenomic methods were inconsistent with each other for fungal species recognition. In fact, Kraken2 recognized only some of the fungal species present in the metagenome, within the top 66 genera recognized only eight were fungal pathogens (Figure S3; Table 2). The two methods have a difference in efficiency demonstrated by the percentage of the total reads classified (Table S4). Percentages of reads classified by the BLAST analysis are between three and 12 times greater than the reads classified by Kraken2. Another significant difference between the two methods can be observed from the two Diversity indexes, Shannon – Wiener, and Simpson's (Figure 6). A major difference in the cereal fungal pathogens' presence registered from the Microscopy, BLAST and Kraken2 analysis is shown in Table 2. Which displays spores from 20 major cereal fungal pathogens as; not recognized (/); presence (+); absence (-). This demonstrates that pathogens such as *Alternaria* spp., *Puccinia* spp., *Blumeria graminis, Cladosporium* spp., and *Claviceps purpurea*, are not found in the Kraken2 database, but are recognized by both Microscopy and BLAST analysis (Table 2). Only three pathogens out of the 20 listed in Table 2 are recognized by all three methods, these are *Aspergillus* spp. *(fumigatus/oryzae), Fusarium* spp. *(graminearum)*, and *Zymoseptoria* spp. *(tritici)*. BLAST taxonomic analysis registered the presence for all of the 20 selected cereal pathogens, these results are for the most part supported by either the microscopy results or/and the Kraken2 analysis. Similar results were recently published by Jo et al. (2020) where the authors use both, Kraken2 and a BLASTx metagenomic analysis for peach. The authors come to similar conclusions that the Kraken2 database for *Fungi* is not as extensive as the NCBI database used in the BLAST analysis (Jo et al., 2020).

Various metagenomic approaches can be applied to spore trap tapes, some of which can deliver different types of information. For instance, the method applied in this study focused on presence/absence of specific cereal pathogens in the field. Methods such as NGS with subsequent BLAST taxonomic classification may have implications for identification of pathogens important for plant biosecurity (Jackson and Bayliss, 2011). With which, the presence of specific Quarantine Pests could be easily and quickly identified. While recognizing the presence of specific species with methods such as microscopic analysis is difficult and time consuming. Moreover, alternative methods that use metagenomic solutions can be used to determine the quantity and type of the pathogens in the field (Aguayo et al., 2018; Woo et al., 2018). This can be performed through quantitative PCR evaluating the gene copy number (Woo et al., 2018) or with metabarcoding (Aguayo et al., 2018). It would be interesting in future studies to compare metagenomics and metabarcoding using ITS sequencing of the spore trap tapes to determine if metabarcoding is more sensitive since it is also cheaper than the WGS, used here. These approaches can substitute the traditional, time consuming, microscopy approach.

Microscopy gives detailed information on abundance and timing of fungal spores present. In contrast, the metagenomic approach coupled with BLAST analysis provides a more rapid, accurate recognition and estimate of abundances of the fungal cereal pathogens. Results from the Kraken2 taxonomic classification were instead less accurate and many species were not present in the software database and therefore not recognized.

Future approaches using metagenomics may be useful for the identification of crop pathogens and prediction of disease outbreaks without bias or knowledge of which pathogens are present. For example, 150 cereal pathogens were detected here using metagenomic BLAST analysis. The future development of the method to correlate the abundance of pathogens identified by metagenomic BLAST analysis to weather data could possibly be used to inform the timing and application of fungicides for disease control.

Data availability statement

The datasets presented in this study can be found in online repositories. The names of the repository/repositories and accession number(s) can be found below: https://www.ncbi.nlm.nih.gov/, PRJNA872486.

Author contributions

PP and AF designed the experiment. PP and CL carried out sampling and microscopic and metagenomic experiments. AT contributed to the sampling and microscopic analysis. PP carried out the analysis of the results. PP and AF wrote the manuscript. SK, JB, and AF revised the manuscript. All authors contributed to the article and approved the submitted version.

Funding

This work was supported by the SFI Strategic Partnerships Programme (16/SPP/3296) and SFI Career Development Award (15/CDA/3451).

Acknowledgments

The authors want to thank Agrii plc and Origin enterprises plc for providing access to the UK field sites. Special thanks to Francesca Salinari and David Langton for the help with the sample collection.

Conflict of interest

The authors declare that the research was conducted in the absence of any commercial or financial relationships that could be construed as a potential conflict of interest.

Publisher's note

All claims expressed in this article are solely those of the authors and do not necessarily represent those of their affiliated organizations, or those of the publisher, the editors and the reviewers. Any product that may be evaluated in this article, or claim that may be made by its manufacturer, is not guaranteed or endorsed by the publisher.

Supplementary material

The Supplementary Material for this article can be found online at: https://www.frontiersin.org/articles/10.3389/fpls.2022.1039090/full#supplementary-material

SUPPLEMENTARY FIGURE 1
Cladogram tree of BLAST species hits distribution; each node contains 12 boxes representing the 12 samples (3 monthly samples for the four UK wheat field sites). Color shading of the boxes indicates the percentage of BLAST hits relative abundance in that specific clade for the specific sample. The white colour represents 0% increasing through green shading to dark green representative of 100%. Tree built with MEGAN 6.

SUPPLEMENTARY FIGURE 2
BLAST species hits for 150 cereal fungal pathogen species, distributed in a cladogram tree; each node contains 12 boxes representing the 12 samples (3 monthly samples for the four UK wheat field sites). Colour shading of the boxes indicates the percentage of BLAST hits relative abundance in that specific clade for the specific sample. The white color represents 0% increasing through green shading to dark green representative of 100%. Tree built with MEGAN 6.

SUPPLEMENTARY FIGURE 3
Stacked taxa bar chart showing the relative abundance at the general level from the Kraken2 tool, only eight out of the most abundant 66 genera recognized were fungal organisms. Bar chart was built using OmicsBox (BioBam).

References

Aguayo, J., Fourrier-Jeandel, C., Husson, C., and Ioos, R. (2018). Assessment of passive traps combined with high-throughput sequencing to study airborne fungal communities. *Appl. Environ. Microbiol.* 84, e02637-17. doi: 10.1128/AEM.02637-17

Bioinformatics, B., and Valencia, S. (2019). OmicsBox-bioinformatics made easy. *BioBam Bioinf.* 2019, 3. Available at: https://www.biobam.com/omicsbox/

Boedijn, K. B. (1956). Trypan blue as a stain for fungi. *Stain Technol.* 31, 115–116. doi: 10.3109/10520295609113788

Boudra, H., and Morgavi, D. P. (2005). Mycotoxin risk evaluation in feeds contaminated by aspergillus fumigatus. *Anim. Feed Sci. Technol.* 120, 113–123. doi: 10.1016/j.anifeedsci.2005.01.006

Calderon, C., Lacey, J., McCartney, H., and Rosas, I. (1995). Seasonal and diurnal variation of airborne basidiomycete spore concentrations in Mexico city. *Grana* 34, 260–268. doi: 10.1080/00173139509429055

Choudhury, R. A., Koike, S. T., Fox, A. D., Anchieta, A., Subbarao, K. V., Klosterman, S. J., et al. (2016). Season-long dynamics of spinach downy mildew determined by spore trapping and disease incidence. *Phytopathology®* 106, 1311–1318. doi: 10.1094/PHYTO-12-15-0333-R

Comtois, P., Alcazar, P., and Néron, D. (1999). Pollen counts statistics and its relevance to precision. *Aerobiologia* 15, 19–28. doi: 10.1023/A:1007501017470

Cordo, C. A., Mónaco, C. I., Altamirano, R., Perelló, A. E., Larrán, S., Kripelz, N. I., et al. (2017). Weather conditions associated with the release and dispersal of zymoseptoria tritici spores in the Argentine pampas region. *Int. J. Agron.* 1468580. doi: 10.1155/2017/1468580

D'Amato, G., Chatzigeorgiou, G., Corsico, R., Gioulekas, D., Jäger, L., Jäger, S., et al. (1997). Evaluation of the prevalence of skin prick test positivity to alternaria and cladosporium in patients with suspected respiratory allergy: a European multicenter study promoted by the Subcommittee on Aerobiology and Environmental Aspects of Inhalant Allergens of the European Academy of Allergology and Clinical Immunology. *Allergy* 52, 711–716. doi: 10.1111/j.1398-9995.1997.tb01227.x

Dean, R., Van Kan, J. A. L., Pretorius, Z. A., Hammond-Kosack, K. E., Di Pietro, A., Spanu, P. D., et al. (2012). The top 10 fungal pathogens in molecular plant pathology. *Mol. Plant Pathol.* 13, 414–430. doi: 10.1111/j.1364-3703.2011.00783.x

Eversmeyer, M. G., and Kramer, C. L. (1987). Vertical concentrations of fungal spores above wheat fields. *Grana* 26, 97–102. doi: 10.1080/00173138709428909

FAO (2022) *FAOSTAT*. Available at: http://www.fao.org/faostat/en/#data/QC/visualize.

Figueroa, M., Hammond-Kosack, K. E., and Solomon, P. S. (2018). A review of wheat diseases-a field perspective. *Mol. Plant Pathol.* 19, 1523–1536. doi: 10.1111/mpp.12618

Fones, H. N., Eyles, C. J., Kay, W., Cowper, J., and Gurr, S. J. (2017). A role for random, humidity-dependent epiphytic growth prior to invasion of wheat by zymoseptoria tritici. *Fungal Genet. Biol.* 106, 51–60. doi: 10.1016/j.fgb.2017.07.002

Fones, H., and Gurr, S. (2015). The impact of septoria tritici blotch disease on wheat: An EU perspective. *Fungal Genet. Biol.* 79, 3–7. doi: 10.1016/j.fgb.2015.04.004

Freeman, S., Katan, T., and Shabi, E. (1998). Characterization of colletotrichum species responsible for anthracnose diseases of various fruits. *Plant Dis.* 82, 596–605. doi: 10.1094/PDIS.1998.82.6.596

Grinn-Gofroń, A., and Rapiejko, P. (2009). Occurrence of cladosporium spp. and alternaria spp. spores in Western, northern and central-Eastern Poland in 2004–2006 and relation to some meteorological factors. *Atmospheric Res.* 93, 747–775. doi: 10.1016/j.atmosres.2009.02.014

Hunter, T., Coker, R., and Royle, D. (1999). The teleomorph stage, mycosphaerella graminicola, in epidemics of septoria tritici blotch on winter wheat in. *Plant Pathol.* 48, 51–57. doi: 10.1046/j.1365-3059.1999.00310.x

Huson, D. H., Auch, A. F., Qi, J., and Schuster, S. C. (2007). MEGAN analysis of metagenomic data. *Genome Res.* 17, 377–386. doi: 10.1101/gr.5969107

Huson, D. H., Beier, S., Flade, I., Górska, A., El-Hadidi, M., Mitra, S., et al. (2016). And analysis of Large-scale microbiome sequencing data. *PloS Comput. Biol.* 12, e1004957. doi: 10.1371/journal.pcbi.1004957

IBM-Corp (2019). *IBM SPSS Statistics for windows, version 26.0* (Armonk, NY: IBM Corp).

Jackson, S. L., and Bayliss, K. L. (2011). Spore traps need improvement to fulfil plant biosecurity requirements. *Plant Pathol.* 60, 801–810. doi: 10.1111/j.1365-3059.2011.02445.x

Jo, Y., Back, C.-G., Choi, H., and Cho, W. K. (2020). Comparative microbiome study of mummified peach fruits by metagenomics and metatranscriptomics. *Plants* 9, 1052. doi: 10.3390/plants9081052

Kang, Y.-N., So, K.-K., Kim, D.-W., Kim, D.-H., and Lee, T.-H. (2019). Draft genome sequencing of the pathogenic fungus cladosporium phlei ATCC 36193 identifies candidates of novel polyketide synthase genes involved in perylenequinone-group pigment production. *Evolutionary Bioinf.* 15, 117693431983130. doi: 10.1177/1176934319831306

Karlsson, I., Persson, P., and Friberg, H. (2021). Fusarium head blight from a microbiome perspective. *Front. Microbiol.* 12, 628373. doi: 10.3389/fmicb.2021.628373

Keller, M. D., Bergstrom, G. C., and Shields, E. J. (2014). The aerobiology of Fusarium graminearum. *Aerobiologia* 30, 123–136.

Lacey, M. E., and West, J. S. (2007). *The air spora: a manual for catching and identifying airborne biological particles* (Springer Science & Business Media).

Li, D., Liu, C.-M., Luo, R., Sadakane, K., and Lam, T.-W. (2015). MEGAHIT: an ultra-fast single-node solution for large and complex metagenomics assembly *via* succinct de bruijn graph. *Bioinformatics* 31, 1674–1676. doi: 10.1093/bioinformatics/btv033

Ortega, S. F., Ferrocino, I., Adams, I., Silvestri, S., Spadaro, D., Gullino, M. L., et al. (2020). Monitoring and surveillance of aerial mycobiota of rice paddy through DNA metabarcoding and qPCR. *J. Fungi* 6, 372. doi: 10.3390/jof6040372

Parry, D. W. (1990). *Plant pathology in agriculture* (CUP Archive).

Pasanen, A.-L., Pasanen, P., Jantunen, M., and Kalliokoski, P. (1991). Significance of air humidity and air velocity for fungal spore release into the air. *Atmospheric Envi. Part A. Gen. Top.* 25, 459–462. doi: 10.1016/0960-1686(91)90316-Y

Peet, R. K. (1975). Relative diversity indices. *Ecology* 56, 496–498. doi: 10.2307/1934984

Rho, M., Tang, H., and Ye, Y. (2010). FragGeneScan: predicting genes in short and error-prone reads. *Nucleic Acids Res.* 38, e191–e191. doi: 10.1093/nar/gkq747

Rocha, O., Ansari, K., and Doohan, F. M. (2005). Effects of trichothecene mycotoxins on eukaryotic cells: A review. *Food Additives Contaminants* 22, 369–378.

Różewicz, M., Wyzińska, M., and Grabiński, J. (2021). The most important fungal diseases of cereals–problems and possible solutions. *Agronomy* 11, 714. doi: 10.3390/agronomy11040714

Schiro, G., Verch, G., Grimm, V., and Müller, M. E. (2018). Alternaria and fusarium fungi: differences in distribution and spore deposition in a topographically heterogeneous wheat field. *J. Fungi* 4, 63. doi: 10.3390/jof4020063

Spearman's Rank (2008). *Spearman rank correlation coefficient* (New York: Springer).

Sterling, M., Rogers, C., and Levetin, E. (1999). An evaluation of two methods used for microscopic analysis of airborne fungal spore concentrations from the burkard spore trap. *Aerobiologia* 15, 9–18. doi: 10.1023/A:1007561201541

Suffert, F., Delestre, G., and Gélisse, S. (2019). Sexual reproduction in the fungal foliar pathogen *Zymoseptoria tritici is* driven by antagonistic density dependence mechanisms. *Microbial Ecol.* 77, 110–123. doi: 10.1007/s00248-018-1211-3

Suffert, F., Sache, I., and Lannou, C. (2011). Early stages of septoria tritici blotch epidemics of winter wheat: build-up, overseasoning, and release of primary inoculum. *Plant Pathol.* 60, 166–177. doi: 10.1111/j.1365-3059.2010.02369.x

Sweeney, M. J., and Dobson, A. D. (1998). Mycotoxin production by aspergillus, fusarium and penicillium species. *Int. J. Food Microbiol.* 43, 141–158. doi: 10.1016/S0168-1605(98)00112-3

Trail, F., Xu, H., Loranger, R., and Gadoury, D. (2002). Physiological and environmental aspects of ascospore discharge in Gibberella zeae (anamorph Fusarium graminearum). *Mycologia* 94, 181–189.

Troch, V., Audenaert, K., Bekaert, B., Höfte, M., and Haesaert, G. (2012). Phylogeography and virulence structure of the powdery mildew population on its' new'host triticale. *BMC Evolutionary Biol.* 12, 1–12. doi: 10.1186/1471-2148-12-76

Tschanz, A. T., Horst, R. K., and Nelson, P. E. (1975). Ecological aspects of ascospore discharge in Gibberella zeae. *Phytopathology* 65, 597–599.

Woo, C., An, C., Xu, S., Yi, S.-M., and Yamamoto, N. (2018). Taxonomic diversity of fungi deposited from the atmosphere. *ISME J* 12, 2051–2060. doi: 10.1038/s41396-018-0160-7

Wood, D. E., Lu, J., and Langmead, B. (2019). Improved metagenomic analysis with kraken 2. *Genome Biol.* 20:1–13. doi: 10.1186/s13059-019-1891-0

frontiers | Frontiers in Plant Science

TYPE Review
PUBLISHED 27 October 2022
DOI 10.3389/fpls.2022.1026611

OPEN ACCESS

EDITED BY
Maria Rosa Simon,
National University of La Plata,
Argentina

REVIEWED BY
Cong Jiang,
Northwest A&F University, China
Yueqiang Leng,
North Dakota State University,
United States

*CORRESPONDENCE
Haigang Ma
mhg@yzu.edu.cn
Hongxiang Ma
mahx@yzu.edu.cn

SPECIALTY SECTION
This article was submitted to Plant Pathogen Interactions, a section of the journal Frontiers in Plant Science

RECEIVED 24 August 2022
ACCEPTED 13 October 2022
PUBLISHED 27 October 2022

CITATION
Ma H, Liu Y, Zhao X, Zhang S and Ma H (2022) Exploring and applying genes to enhance the resistance to Fusarium head blight in wheat. *Front. Plant Sci.* 13:1026611. doi: 10.3389/fpls.2022.1026611

Exploring and applying genes to enhance the resistance to Fusarium head blight in wheat

Haigang Ma*, Yongjiang Liu, Xueyan Zhao, Suhong Zhang and Hongxiang Ma*

Jiangsu Co-Innovation Center for Modern Production Technology of Grain Crops/Jiangsu Key Laboratory of Crop Genomics and Molecular Breeding, Yangzhou University, Yangzhou, China

Fusarium head blight (FHB) is a destructive disease in wheat worldwide. *Fusarium graminearum* species complex (FGSC) is the main causal pathogen causing severe damage to wheat with reduction in both grain yield and quality. Additionally, mycotoxins produced by the FHB pathogens are hazardous to the health of human and livestock. Large numbers of genes conferring FHB resistance to date have been characterized from wheat and its relatives, and some of them have been widely used in breeding and significantly improved the resistance to FHB in wheat. However, the disease spreads rapidly and has been severe due to the climate and cropping system changes in the last decade. It is an urgent necessity to explore and apply more genes related to FHB resistant for wheat breeding. In this review, we summarized the genes with FHB resistance and mycotoxin detoxication identified from common wheat and its relatives by using forward- and reverse-genetic approaches, and introduced the effects of such genes and the genes with FHB resistant from other plant species, and host-induced gene silencing (HIGS) in enhancing the resistance to FHB in wheat. We also outlined the molecular rationale of the resistance and the application of the cloned genes for FHB control. Finally, we discussed the future challenges and opportunities in this field.

KEYWORDS

wheat disease, *Fusarium graminearum*, Fusarium head blight, genetics, breeding

Introduction

Fusarium head blight (FHB), which is also known as head scab and ear blight, caused by *Fusarium graminearum* (teleomorph *Gibberella zeae*) species complex is a fungal disease responsible for severe yield losses and poor grain quality in wheat (*Triticum aestivum* L.) (Bai and Shaner, 2004; Xu and Nicholson, 2009). The pathogen also produces mycotoxins such as trichothecenes and zearalenone contaminating infected wheat grains, which are harmful to humans and animals (Chen et al., 2019). Due to the

warm temperature, abundant rainfall, and maize/wheat and rice/wheat rotations, the disease has been frequent and severe for the last decade worldwide, especially in China (Bai et al., 2018; Ma et al., 2019).

The most effective and economical solution for reducing FHB damage is to identify genes related to FHB resistance and apply them to breed disease-resistant varieties. The resistance to FHB is quantitative in wheat and no immune genes have been found so far (Bai et al., 2018). To date, a substantial number of quantitative trait loci (QTL) or genes conferring FHB resistance have been reported (Liu et al., 2009; Zheng et al., 2021). Previously, strategies and progress of wheat breeding for FHB resistance have been reviewed (Ma et al., 2019; Zhu et al., 2019). Here, we summarize advances in wheat resistance to FHB with the main focus on the characterized genes related to FHB resistance and their function in genetic improvement for the FHB resistance in wheat.

Cloning resistance genes from common wheat using forward genetic approaches

Cloning and utilization of *Fhb1*

Of the hundreds of QTL identified for FHB resistance by molecular mapping in common wheat, *Fhb1*, a QTL located on the short arm of chromosome 3B with the largest explanation of phenotype variation, provides durable and stable resistance to FHB. *Fhb1* candidate genes have been cloned recently using the map-based cloning approach. In 2016, a pore-forming toxin-like (*PFT*) gene was firstly cloned as the candidate of *Fhb1* (Rawat et al., 2016). However, this gene was also found in some susceptible accessions without *Fhb1* (Yang et al., 2005; He et al., 2018a; Jia et al., 2018). Before long, another gene named *HRC* or *His* was cloned as an *Fhb1* candidate by two independent studies (Li et al., 2019; Su et al., 2019). *HRC/His* encoded histidine-rich calcium-binding protein located in the nucleus. In comparison to that in the susceptible lines (*HRC/His-S*), the gene in the resistant lines carrying *Fhb1* (*HRC/His-R*) had a deletion in its genome, which is responsible for FHB resistance (Li et al., 2019; Su et al., 2019). The function of *TaHRC* was validated by using a BSMV-mediated gene editing system in Bobwhite and Everest (Chen et al., 2022a; Chen et al., 2022b).

It was recently found that *HRC/His-S* from *Leymus chinensis* (named *LcHRC* in the original article), which showed identical amino acid sequence to wheat HRC/His-S, bound calcium and zinc ion *in vitro* (Yang et al., 2020). *Arabidopsis thaliana* seedlings overexpressing *LcHRC* showed sensitivity to abscisic acid (ABA) (Yang et al., 2020). A protein that participates in heterochromatin silencing was identified as an LcHRC interactor through the screening of *Arabidopsis* yeast cDNA library (Yang et al., 2020). These results suggest a potential role of *LcHRC* in the regulation of genes involved in abiotic stress response. In wheat, HRC-S interacting proteins were identified through the screening of wheat yeast cDNA library (Chen et al., 2022b). One of the interactors, TaCAXIP4 [a cation exchanger (CAX)-interacting protein 4], was further validated to physically interact with HRC-S *in planta* (Chen et al., 2022b). The interaction with HRC-S suppressed TaCAXIP4-mediated calcium cation (Ca^{2+}) transporting in yeast cells and resulted in reduced reactive oxygen species (ROS) triggered by chitin (Chen et al., 2022b), leading to the hypothesis that Ca^{2+} signaling-mediated ROS burst is essential for wheat FHB resistance. However, the details on how *HRC/His* affects FHB resistance remain equivocal, and more efforts are needed to elucidate their biological function and the regulatory network they mediated in defense response.

In fact, *Fhb1* locus has been widely used for FHB resistance breeding prior to the gene cloning. A large number of wheat varieties worldwide carried *Fhb1* locus, which confers moderate FHB resistance with the reduction of at most 50% in FHB severity (Bai et al., 2018; Zhu et al., 2019), which further confirmed the solid role of this locus in FHB resistance.

Other resistance genes from common wheat

Besides *Fhb1*, many other QTL conferring FHB resistance of wheat have been reported, but the majority of their candidate genes remain unidentified. *QFhb.mgb-2A*, a major QTL located on chromosome 2A, was found in a recombinant inbred line (RIL) population, obtained by crossing an hexaploid line derived from a resistant cultivar Sumai3 and a susceptible durum cv. Saragolla (Giancaspro et al., 2016). Several genes, including *Fatty Acyl-CoA Reductase 1*, *Wall-associated receptor kinase 2* (*WAK2*), *Arginine decarboxylase*, *SWI/SNF-related matrix-associated actin-dependent regulator of chromatin subfamily A member 3*, and *Ubiquitin thioesterase otubain* genes, were detected in the QTL region (Gadaleta et al., 2019). The homeolog of *WAK2* in common wheat, which was named *TaWAK2A-800*, was identified later as a positive regulator of wheat resistance to FHB (Guo et al., 2021). Knocking down *TaWAK2A-800* in wheat using the virus-induced gene silencing (VIGS) method compromised FHB resistance, which may be attributed to the impaired defense pathway induced by chitin (Guo et al., 2021).

Cloning genes with FHB resistance or mycotoxin detoxication from wheat using reverse genetic approaches

Decades of efforts in plant immunity have led to the development of plant resistance gene pool and the

understanding of the mechanisms of plant disease resistance. The completion of wheat genome sequencing provides great convenience for the identification of the homologs of resistance genes in wheat through genome-wide homologous sequence analysis. Moreover, a variety of omics methods including transcriptomics, proteomics, and metabolomics will aid in identifying wheat resistance genes. A number of reverse genetics techniques are applied subsequently to overexpress and/or knock out/knock down the identified genes with the aim to verify their function. The widely used approaches in wheat include clustered regularly interspaced short palindromic repeats (CRISPR)/CRISPR-associated protein 9 (Cas9)-based genome editing, VIGS, and RNA interference (RNAi). They have been invaluable in analyzing gene function in wheat FHB resistance.

Genes with FHB resistance in wheat

Many classes of genes have been implicated in the resistance to FHB in wheat. One group of them is referred to as pathogenesis-related (*PR*) genes. Increased expression of *PR* genes is a hallmark of plant defense response to pathogen attack. Based on gene sequence homology, two wheat *PR* genes, encoding chitinase (*PR3*) and β-1,3-glucanase (*PR2*), respectively, have been separately overexpressed in wheat and enhanced FHB resistance was observed in greenhouse but not in the field when using inoculated corn kernels (Anand et al., 2003). In another study, transgenic wheat lines with overexpression of wheat α-1-purothionin gene (a *PR* gene) exhibited increased FHB resistance in the field condition when using the spaying inoculation method (Mackintosh et al., 2007).

The essential role of plant hormones in the disease resistance is also a global consensus. Several genes involved in wheat phytohormone biosynthesis or signaling have been identified for FHB resistance. *EIN2* is a central regulator of ethylene (ET) signaling (Alonso et al., 1999). RNA interference (RNAi)-mediated *EIN2* silencing in wheat (Travella et al., 2006) reduced FHB symptoms (Chen et al., 2009), implying that ET signaling may promote wheat susceptibility to *F. graminearum*. Likewise, auxin was also implicated in FHB susceptibility of wheat. The expression of an auxin receptor gene *TaTIR1* was found to be downregulated during *F. graminearum* infection (Su et al., 2021). Knockdown of *TaTIR1* in wheat using RNAi technology increased FHB resistance (Su et al., 2021).

In addition to phytohormones, wheat metabolites are also essential for FHB resistance. Using a metabolomics approach, a research group identified several genes conferring resistance to FHB, including *TaACT* encoding agmatine coumaroyl transferase (Kage et al., 2017a), *TaLAC4* encoding laccase (Soni et al., 2020), and *TaWRKY70* and *TaNAC032* both encoding transcription factors (Kage et al., 2017b; Soni et al., 2021). These genes are all involved in the biosynthesis of hydroxycinnamic acid amides and phosphotidic acid, the major metabolites accumulated in wheat rachis after *F. graminearum* invasion. Suppressing the expression of these genes respectively using VIGS reduced FHB resistance.

Transcriptomics are powerful in identifying genes related to FHB resistance. Lots of genes whose expression are induced by *F. graminearum* have been identified by different methods, such as Genechips and RNA sequencing, and some of them have been validated to be effective in FHB control. A wheat orphan gene named *T. aestivum* Fusarium Resistance Orphan Gene (*TaFROG*), which is a taxonomically restricted gene specific to the grass subfamily *Pooideae*, was identified as an *F. graminearum*-responsive gene and promoted wheat resistance to FHB (Perochon et al., 2015). *TaFROG* encodes a protein with unknown function but binds to TaSnRK1α, which is a wheat α subunit of the Sucrose Non-Fermenting1 (SNF1)-Related Kinase1 and plays central roles in plant energy and stress signaling (Perochon et al., 2015). Another TaFROG interactor, *T. aestivum* NAC-like D1 (*TaNACL-D1*), which is a NAC [No apical meristem (NAM), *Arabidopsis* transcription activation factor (ATAF), Cup-shaped cotyledon (CUC)] transcription factor, was identified by using yeast two-hybrid screening (Perochon et al., 2019). *TaNACL-D1* was also responsive to *F. graminearum* and enhanced wheat resistance to FHB with unclarified mechanisms (Perochon et al., 2019).

Plant lectins, a class of proteins binding reversibly to mono- or oligosaccharides, are often associated with biotic and abiotic responses. Wheat genes encoding lectins have been shown to improve FHB resistance. *TaJRLL1* and *Ta-JA1/TaJRL53* are two genes in wheat encoding jacalin-related lectins. Suppressing their expression in wheat separately using VIGS compromised the disease resistance to FHB, while overexpressing *TaJRL53* in wheat enhanced FHB resistance (Ma et al., 2010a; Xiang et al., 2011; Chen et al., 2021).

Other genes, including *TaLRRK-6D* encoding a leucine-rich repeat receptor-like kinase (Thapa et al., 2018), *TaMPT* encoding a mitochondrial phosphate transporter responsible for transporting inorganic phosphate (Pi) into the mitochondrial matrix (Malla et al., 2021), *TaSAM* encoding an S-adenosyl methionine (SAM)-dependent methyltransferase that catalyzes the transfer of methyl groups from SAM to a large variety of acceptor substrates (Malla et al., 2021), *TaPIEP1* encoding transcription factor (Liu et al., 2011), and *TaSHMT3A-1* encoding serine hydroxymethyltransferase (Hu et al., 2022), are also identified to contribute to FHB resistance.

The abovementioned genes with FHB resistance are listed in Table 1. They varied enormously in gene products and biochemical functions. It seems that wheat utilizes extensive biological processes to defend against *F. graminearum* attack. As no immune genes were found in FHB resistance, a deep understanding of the signaling pathway mediated by these resistance genes will help to optimize wheat FHB resistance in breeding.

Wheat genes whose products are targets of *F. graminearum* effectors

Plant pathogenic microbes always secrete proteins that act as effectors into host cells to evade or inhibit host immunity, leading to enhanced pathogen virulence and facilitated pathogen growth (Dou and Zhou, 2012). The secreted effectors bind host proteins to modify their native biological functions. Some of the host targets are key regulators of plant immunity and therefore could be deployed for disease control.

Secreted proteome of *F. graminearum* has been obtained, with the protein numbers varied in different studies (Yang et al., 2012; Rampitsch et al., 2013; Yang et al., 2013; Lowe et al., 2015). However, their host targets are largely unknown.

It has been found that *F. graminearum* produces orphan secretory proteins (OSPs), and one of them, Osp24, functions as an effector (Jiang et al., 2020). After being secreted into wheat cells, Osp24 binds wheat protein TaSnRK1α (Jiang et al., 2020). The binding by Osp24 accelerates TaSnRK1α degradation, which may suppress host defense responses including cell death and is thus beneficial for pathogen infection; however, physical interaction with TaFROG, a wheat orphan protein, prevents TaSnRK1α from degradation and helps in wheat defense (Jiang et al., 2020). The interplay between the two orphan genes, OSP24 and TaFROG, may be indicative of co-evolution of *F. graminearum* and the host wheat, and the distinctive defense response of wheat to *F. graminearum*.

Detoxication genes in wheat

The mycotoxins such as deoxynivalenol (DON, a type B trichothecene) produced by the pathogen are toxic to humans and animals. They cause emesis, feed refusal, and even death (Eriksen and Pettersson, 2004). In addition, DON is considered as a virulence factor capable to facilitate disease spread on wheat (Proctor et al., 1995; Bai et al., 2002). *F. graminearum* deficient in DON biosynthesis was able to infect wheat spikelets but failed to spread in spikelets, thus causing diminished disease symptoms (Bai et al., 2002). Therefore, decreasing the amount of DON of wheat grain during pathogen infection is not only necessary for food security, but also one goal of breeding for FHB resistance.

Proteins encoded by various genes have been identified with the ability to detoxify DON (Table 1). Among them, uridine diphosphate (UDP)-glycosyltransferases (UGTs) have been widely reported to be able to detoxify DON through glucosylation. These enzymes transfer a glycosyl group from UDP-glucose to DON to conjugate DON into deoxynivalenol-3-O-glucose (D3G), which is nontoxic for animals. As DON can promote disease spreading, glucosylation of DON to D3G is an important plant defense mechanism. He et al. (2018b) systematically analyzed family-1 UGTs and identified 179 putative UGT genes in a reference genome of wheat, Chinese Spring. Among them, *TaUGT3* (Ma et al., 2010b; Pei, 2011; Chen, 2013), *TaUGT5* (Zhao et al., 2018), and *TaUGT6* (He et al., 2020) were validated to be effective in reducing DON content in wheat. Wheat lines overexpressing the three genes respectively showed resistance to DON treatment and the resultant disease resistance to FHB, implying the potential of *TaUGT* as useful disease resistance genes in breeding for FHB resistance.

Adenosine triphosphate (ATP)-binding cassette (ABC) transporters have been implicated in DON detoxication. They may export DON from the cytoplasm to reduce the damage caused by mycotoxin. *TaABCC3*, encoding an ABC transporter responsible for substance transport across cell membrane, was cloned from DON-treated wheat transcripts (Walter et al., 2015). Inhibition of *TaABCC3* expression by VIGS increased wheat sensitivity to DON (Walter et al., 2015). However, the effect of *TaABCC3* on FHB resistance was not analyzed. *TaPDR1* and *TaPDR7*, two wheat genes encoding the pleiotropic drug resistance (PDR) subfamily of ABC transporters, were upregulated by DON treatment and *F. graminearum* infection; knockdown of *TaPDR7* in wheat by VIGS compromised FHB resistance (Shang et al., 2009; Wang et al., 2016).

Cytochrome P450, membrane-bound enzymes that can perform several types of oxidation–reduction reactions, was also reported to possess the ability to catabolize DON (Ito et al., 2013). A wheat P450 gene, *TaCYP72A*, was found to be activated by DON treatment and *F. graminearum* infection (Gunupuru et al., 2018). Suppressing *TaCYP72A* through VIGS reduced wheat resistance to DON (Gunupuru et al., 2018). However, whether this gene confers FHB resistance is not identified.

Exploration and utilization of alien genes in *Triticeae* with FHB resistance

There are over 300 species classified under more than 20 genera in *Triticeae* (Dewey, 1984), which represent an invaluable gene pool for wheat improvement. The wild relatives of wheat are an important source for wheat improvement with FHB resistance. Many genes with FHB resistance have been identified and verified *in vivo* (Table 2). They show unique features as well as shared characteristics with those identified in hexaploidy wheat.

Genes from *Thinopyrum*

Of the QTL that showed a stable major effect on FHB resistance, *Fhb7* was transferred from wheatgrass *Thinopyrum* (Fu et al., 2012; Guo et al., 2015), and was cloned recently using

TABLE 1 Genes identified with FHB resistance in various common wheat variety.

Gene name	Wheat variety	Accession number	Gene products	References
PFT	Sumai3	included in KX907434.1[a]	pore-forming toxin-like protein	Rawat et al., 2016
HRC	Sumai3	MK450312[a]	histidine-rich calcium-binding-protein	Su et al., 2019
His	Wangshuibai	KX022629[a]	histidine-rich calcium-binding-protein	Li et al., 2019
TaWAK2A-800	Chinese Spring	TraesCS2A02G071800[b]	wall-associated kinase	Guo et al., 2021
PR2	Sumai3	undisclosed	β-1,3-glucanase	Anand et al., 2003
PR3	Sumai3	undisclosed	chitinase	Anand et al., 2003
PR	Undisclosed	X70665.1[a]	α-1-purothionin	Mackintosh et al., 2007
TaEIN2	Mercia	AL816731[a]	endoplasmic reticulum membrane-localized Nramp homolog	Travella et al., 2006 Chen et al., 2009
TaTIR1	Sumai 3	TraesCS1A02G091300[b]	putative auxin receptor	Su et al., 2021
TaACT	Wuhan-1	KT962210[a]	agmatine coumaroyl transferase	Kage et al., 2017a
TaLAC4	Sumai 3	MT587562[a]	laccase	Soni et al., 2020
TaFROG	CM82036	KR611570[a]	orphan protein with unknown function	Perochon et al., 2015
TaSnRK1α	CM82036, Xiaoyan 22	KR611568[a], TraesCS1A02G350500[b]	SNF1-related kinase 1	Perochon et al., 2015 Jiang et al., 2020
TaJRLL1	CM82036	HQ317136[a]	jacalin-related lectin	Xiang et al., 2011
Ta-JA1/TaJRL53	H4564, Chinese Spring	AY372111[a]	jacalin-related lectin	Ma et al., 2010a Chen et al., 2021
TaLRRK-6D	Chinese Spring	TraesCS6D02G206100[b]	receptor-like kinase	Thapa et al., 2018
TaMPT	Chinese Spring	TraesCS5A02G236700[b]	mitochondrial phosphate transporter	Malla et al., 2021
TaSAM	Chinese Spring	TraesCS2A02G048600[b]	methyltransferase	Malla et al., 2021
TaSHMT3A-1	Chinese Spring	TraesCS3A02G385600[b]	serine hydroxymethyltransferase	Hu et al., 2022
TaWRKY70	Wuhan-1	KU562861[a]	WRKY transcription factor	Kage et al., 2017b
TaWRKY45	Chinese spring	AB603888[a]	WRKY transcription factor	Bahrini et al., 2011
TaNAC032	Sumai 3	MT512636[a]	NAC transcription factor	Soni et al., 2021
TaPIEP1	Shannong0431	EF583940[a]	ERF transcription factor	Dong et al., 2010; Liu et al., 2011
TaNACL-D1	CM82036	MG701911[a]	NAC transcription factor	Perochon et al., 2019
TaUGT3	Wangshuibai	FJ236328[a]	uridine diphosphate-glycosyltransferase	Ma et al., 2010b; Pei, 2011 Chen, 2013
TaUGT5	Sumai 3	TraesCS2B02G184000[b]	uridine diphosphate-glycosyltransferase	Zhao et al., 2018
TaUGT6	Sumai 3	TraesCS5B02G436300[b]	uridine diphosphate-glycosyltransferase	He et al., 2020
Traes_2BS_14CA35D5D	Apogee	MK166044[a]	uridine diphosphate-glycosyltransferase	Gatti et al., 2018
TaABCC3	CM82036	KM458975[a], KM458976[a]	ATP-binding cassette (ABC) transporters	Walter et al., 2015
TaPDR1	Wangshuibai	FJ185035[a], FJ858380[a]	pleiotropic drug resistance (PDR) type ABC transporter	Shang et al., 2009
TaPDR7	Ning 7840	undisclosed	PDR type ABC transporter	Wang et al., 2016
TaCYP72A	CM82036	TraesCS3A01G532600[b]	cytochrome P450	Gunupuru et al., 2018
TaLTP5	Shannong 0431	JQ652457[a]	lipid transfer protein	Zhu et al., 2012

[a]GenBank accession number (https://www.ncbi.nlm.nih.gov/nucleotide/).
[b]Ensembl Plants accession number (http://plants.ensembl.org/Triticum_aestivum/Info/Index).

the map-based cloning approach (Wang et al., 2020a). *Fhb7* was mapped to chromosome 7E of *Th. elongatum* (Fu et al., 2012; Guo et al., 2015). The underpinning gene of the locus was identified that encodes a glutathione S-transferase (GST) with the prominent ability to detoxify trichothecene toxins produced by the pathogens (Wang et al., 2020a). The expression of the gene was increased at the late stage of infection and was also induced by trichothecene treatment (Wang et al., 2020a), implying an active role of *Fhb7* in the response to mycotoxins. How *Fhb7* is regulated at the molecular level remains obscure and needs to be determined. This may help to increase the expression of *Fhb7* in wheat cultivars for further enhanced FHB resistance. Notably, wheat lines with *Fhb7* locus showed increased resistance to FHB without growth defect and yield penalty (Wang et al., 2020a), making *Fhb7* a promising potential for wheat resistance breeding.

TABLE 2 Genes identified with FHB resistance in wheat relatives.

Species	Gene name	Accession number	Gene products	References
Thinopyrum elongatum	*Fhb7*	Tel7E01T1020600.1[a]	glutathione S-transferase	Wang et al., 2020a
Hordeum vulgare	*tlp-1*	AM403331[b]	thaumatin-like protein	Mackintosh et al., 2007
	PR2	M62907.1[b]	β-1,3-glucanase	Mackintosh et al., 2007
	HvWIN1	KT946819[b]	ethylene-responsive transcription factor	Kumar et al., 2016
	HvLRRK-6H	MLOC_12033.1[c]	receptor like kinase	Thapa et al., 2018
	chitinase gene	M62904[b]	chitinase	Shin et al., 2008
	HvUGT13248	GU170355[b]	uridine diphosphate-glycosyltransferase	Schweiger et al., 2010; Shin et al., 2012; Li et al., 2015; Li et al., 2017; Mandalà et al., 2019
	HvUGT-10W1	undisclosed	uridine diphosphate-glycosyltransferase	Xing et al., 2017
Brachypodium distachyon	*Bradi5g03300*	Bradi5g03300	uridine diphosphate-glycosyltransferase	Schweiger et al., 2013; Pasquet et al., 2016; Gatti et al., 2019
	BdCYP711A29	Bradi1g75310	cytochrome P450 monooxygenase	Changenet et al., 2021
Haynaldia villosa	*CERK1-V*	Dv07G125800	chitin-recognition receptor	Fan et al., 2022

[a]WheatOmics accession (http://wheatomics.sdau.edu.cn).
[b]GenBank accession number (https://www.ncbi.nlm.nih.gov/nucleotide/).
[c]IPK Barley Blast Server (http://webblast.ipk-gatersleben.de/barley).

Genes from *Hordeum vulgare*

Barley (*Hordeum vulgare*) *PR* genes also contributed to FHB resistance. Transgenic wheat lines separately overexpressing barley *tlp-1* and *PR2* gene showed increased resistance to FHB (Mackintosh et al., 2007). Two other genes, *HvWIN1* encoding a transcriptional regulator of cuticle biosynthetic genes and *HvLRRK-6H* encoding a leucine-rich receptor-like kinase, were identified as positive regulators of FHB resistance (Kumar et al., 2016; Thapa et al., 2018). Knockdown of the two genes individually by VIGS increased the disease severity of barley (Kumar et al., 2016; Thapa et al., 2018). Wheat lines overexpressing a barley chitinase gene improved wheat resistance to FHB (Shin et al., 2008).

UGT genes responsible for DON detoxication have also been identified in barley. *HvUGT13248* played an effective role in DON detoxication when expressed in yeast (Schweiger et al., 2010), *Arabidopsis* (Shin et al., 2012), durum (Mandalà et al., 2019), and wheat (Li et al., 2015; Li et al., 2017; Mandalà et al., 2019). Wheat lines constitutively expressing *HvUGT13248* showed improved FHB resistance (Li et al., 2015; Li et al., 2017; Mandalà et al., 2019).

Recombinant HvUGT-10W1 purified from bacterium cells inhibited hypha growth of *F. graminearum* in the PDA (potato/dextrose/agar) media. Furthermore, suppressing *HvUGT-10W1* expression in a barley variety 10W1, which showed resistance to FHB, using the VIGS approach reduced the resistance to FHB (Xing et al., 2017), implying the positive role of *HvUGT-10W1* in barley resistance to FHB.

Genes from *Haynaldia villosa*

CERK1-V (Dv07G125800), the chitin-recognition receptor of *Haynaldia villosa*, was recently cloned and introduced into wheat under the drive of maize ubiquitin promoter (Fan et al., 2022). The overexpression lines showed enhanced FHB resistance, implying that the perception of chitin is an important step to initiate FHB resistance. Therefore, it has potential to identify the genes involved in chitin signaling and develop them for FHB resistance.

Genes from *Brachypodium distachyon*

Brachypodium distachyon has been developed for FHB resistance analysis (Peraldi et al., 2011). Several genes from *B. distachyon* have been characterized by FHB resistance. *Bradi5g03300 UGT* gene has been introduced into *B. distachyon* Bd21-3 and the wheat variety Apogee, both of which are susceptible to FHB (Schweiger et al., 2013; Pasquet et al., 2016; Gatti et al., 2019). Enhanced resistance to FHB and strong reduction of DON content in infected spikes were observed in the transgenic lines. Promisingly, some of the transgenic lines with high *Bradi5g03300* transcripts showed normal growth or phenotype compared with the wild type.

BdCYP711A29 (Bradi1g75310) encoding cytochrome P450 monooxygenase involved in orobanchol (one form of strigolactones) biosynthesis was identified to negatively regulate FHB resistance. Overexpression of *BdCYP711A29* in

B. distachyon increases susceptibility to FHB, while the TILLING mutants showed disease symptoms similar to those of the wild type (Changenet et al., 2021).

FHB resistance genes from plant species beyond *Triticeae* species

Genes from *Arabidopsis thaliana*

Arabidopsis has been exploited for the analysis of the scientific rationale of plant resistance to *F. graminearum* because the fungi can infect *Arabidopsis* flowers (Urban et al., 2002; Brewer and Hammond-Kosack, 2015). Many genes that have been identified from *A. thaliana* showed potential for resistance against these pathogenic fungi.

NPR1 is an ankyrin repeat-containing protein involved in the regulation of systemic acquired resistance. Wheat lines overexpressing NPR1 showed enhanced resistance to FHB (Makandar et al., 2006).

AtALA1 and AtALA7, two members of *Arabidopsis* P-type ATPases, contributes to plant resistance to DON through cellular detoxification of mycotoxins (Wang et al., 2021). They mediated the vesicle transport of toxins from the plasma membrane to vacuoles. Transgenic *Arabidopsis* or maize plants overexpressing *AtALA1* enhanced resistance to DON and disease caused by *F. graminearum*. It remains unknown whether *AtALA1* homologous genes exist in wheat genome and have the same detoxification function.

Genes from rice and maize

F. graminearum also infects other crops, such as rice (*Oryza sativa* L.) and maize (*Zea mays* L.). In rice plants, a UGT OsUGT79 expressed and purified from bacterium cells was reported to be effective in conjugating DON into D3G *in vitro* (Michlmayr et al., 2015; Wetterhorn et al., 2017) and could be used as a promising candidate for FHB resistance breeding. Additionally, overexpression of rice *PR5* gene encoding thaumatin-like protein in wheat reduced FHB symptoms (Chen et al., 1999).

In maize, *RIP* gene *b-32* encoding ribosome inactive protein promotes FHB resistance when overexpressed in wheat (Balconi et al., 2007).

Host-induced and spray-induced gene silencing of genes in *Fusarium graminearum*

Host-induced gene silencing (HIGS) was recently developed to control fungal diseases, in which transgenic host plants produce small interference RNAs (siRNAs) that match important genes of the invading pathogen to silence fungal genes during infection (Machado et al., 2018). Koch et al. (2013) reported that detached leaves of both transgenic *Arabidopsis* and barley plants expressing double-stranded RNA from cytochrome P450 lanosterol C-14a-demethylase genes exhibited resistance to *F. graminearum*. HIGS transgenic wheat targeting the chitin synthase 3b also confers resistance to FHB (Cheng et al., 2015). HIGS targeting multiple genes involving *FgSGE1*, *FgSTE12*, and *FgPP1* of the fungus is effective and can be used as an alternative approach for developing FHB- and mycotoxin-resistant crops (Wang et al., 2020b).

Spray-induced gene silencing (SIGS), mechanistically similar to HIGS, is also effective to fungal disease control. In this approach, sprayed siRNAs or noncoding double-stranded (ds) RNAs onto plant surfaces targeting key genes of pathogens are taken up by the pathogens and in turn inhibit pathogen gene expression, leading to inhibited pathogen growth in plants (Koch et al., 2016; Song et al., 2018). SIGS targeting *F. graminearum* genes has been reported to effectively inhibit the pathogen growth in barley, providing the potential for FHB control (Koch et al., 2019; Werner et al., 2020; Rank and Koch, 2021).

Challenges and perspectives

Compared with agronomic practices, chemical control, and biological control, genetic resistance is the best and most cost-effective strategy that could provide meaningful, consistent, and durable FHB control (Shude et al., 2020). There are variations in the susceptibility of different host plant species to FHB; however, no wheat varieties possess immunity against FHB (Dweba et al., 2017). Though hundreds of QTL have been reported in wheat, only two, *Fhb1* and *Fhb7*, have been cloned through years of hard work (Rawat et al., 2016; Li et al., 2019; Su et al., 2019; Wang et al., 2020a); thus, the FHB resistance genes that can be used for breeding is obviously limited. How to improve FHB resistance to a high level in wheat using the limited genes is a fundamental ongoing challenge. Pyramiding resistance genes to increase FHB resistance is feasible and popularized. However, the strategy is highly dependent on the adequate resistance genes. The majority of the QTL identified usually show a minor effect on FHB resistance and have no diagnostic markers. Therefore, sustained and continuous efforts are still needed in cloning and validating resistance genes from hundreds of QTL associated with FHB resistance in wheat. The integration of various forward- and reverse-genetic approaches will be an important means to explore the genes of FHB resistance in wheat, with the development of plant–pathogen interaction mechanism in model plants (Figure 1).

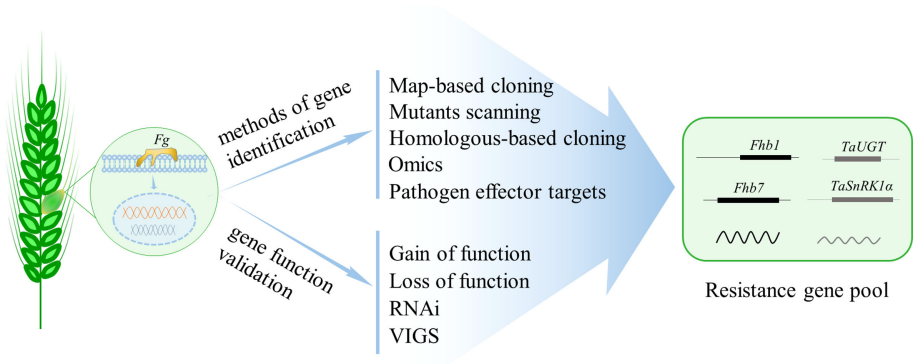

FIGURE 1
Methods to identify and validate genes that show resistance to *Fusarium graminearum* (*Fg*) and compose the resistance gene pool for wheat FHB resistance breeding. Map-based cloning and mutants scanning are two widely used approaches in gene identifying, while the latter is rarely applied in the analysis of wheat FHB resistance partially due to the functional redundancy among homeologs in polyploid wheat. With the completion of wheat genome sequencing, the popularized reverse-genetic approaches such as homologous-based cloning and omics technology are capable of identifying FHB resistance genes. Additionally, identifying the targets of pathogen effectors is also effective in wheat resistance gene identification. Finally, various gene gain- or loss-of-function technologies, or gene knockdown approaches such as RNAi and VIGS, are applicable to validate gene function in wheat FHB resistance.

In contrast to FHB resistance genes, modification of the susceptibility (S) genes will be an alternative option for controlling FHB. S factors or resistance suppressors have already been located on different chromosomes in wheat, yet, to date, they have not received much attention (Ma et al., 2006). In plants, some host factors encoded by S genes are always hijacked by pathogens through the secreted effectors to promote disease development. Mutations of these S genes evade the manipulation by pathogens and have been successfully utilized in crop disease control including wheat resistance to fungal pathogen (Garcia-Ruiz et al., 2021; Koseoglou et al., 2022). As secreted proteome of *F. graminearum* has been obtained, in depth analysis of the interaction between host and *F. graminearum* would facilitate the understanding of the function of S genes in wheat. Genes encoding resistance suppressors that always inhibit plant immune responses fall into another category of S genes (Garcia-Ruiz et al., 2021; Koseoglou et al., 2022). Mutations of these genes with abolished or reduced gene expression generally result in enhanced and durable disease resistance. These genes are significant components of crop disease resistance gene pool, while in FHB resistance, no such genes have been isolated so far. With the development of wheat mutant libraries, identification of such S genes will be facilitated.

Though some genes with FHB resistance have been identified, the signaling pathway that wheat perceives and responds to *F. graminearum* attack remains obscure. Plant immunity involves large-scale changes in gene expression. Intensive investigation of the role of those genes responsive to *F. graminearum* in wheat FHB resistance will contribute to the cloning of practical resistance genes. With the completion of wheat genome sequencing, the initiation of pan-genomic research for tribe *Triticeae*, and the rapid development in biotechniques, breakthrough will be made in the field in the future.

Author contributions

HGM and HXM wrote the manuscript. YL, XZ and SZ collected some data. All authors contributed to the article and approved the submitted version.

Funding

This research was funded by the Jiangsu Key Project for the Research and Development (BE2022337) and the Seed Industry Revitalization Project of Jiangsu Province (JBGS2021047).

Conflict of interest

The authors declare that the research was conducted in the absence of any commercial or financial relationships that could be construed as a potential conflict of interest.

Publisher's note

All claims expressed in this article are solely those of the authors and do not necessarily represent those of their affiliated

organizations, or those of the publisher, the editors and the reviewers. Any product that may be evaluated in this article, or claim that may be made by its manufacturer, is not guaranteed or endorsed by the publisher.

References

Alonso, J., Hirayama, T., Roman, G., Nourizadeh, S., and Ecker, J. (1999). EIN2, a bifunctional transducer of ethylene and stress responses in arabidopsis. *Science* 284, 2148–2152. doi: 10.1126/science.284.5423.2148

Anand, A., Zhou, T., Trick, H., Gill, B., Bockus, W., and Muthukrishnan, S. (2003). Greenhouse and field testing of transgenic wheat plants stably expressing genes for thaumatin-like protein, chitinase and glucanase against fusarium graminearum. *J. Exp. Bot.* 54, 1101–1111. doi: 10.1093/jxb/erg110

Bahrini, I., Sugisawa, M., Kikuchi, R., Ogawa, T., Kawahigashi, H., Ban, T., et al. (2011). Characterization of a wheat transcription factor, TaWRKY45, and its effect on fusarium head blight resistance in transgenic wheat plants. *Breed. Sci.* 61, 121–129. doi: 10.1270/jsbbs.61.121

Bai, G., Desjardins, A., and Plattner, R. (2002). Deoxynivalenol-nonproducing fusarium graminearum causes initial infection, but does not cause disease spread in wheat spikes. *Mycopathologia* 153, 91–98. doi: 10.1023/a:1014419323550

Bai, G., and Shaner, G. (2004). Management and resistance in wheat and barley to fusarium head blight. *Annu. Rev. Phytopathol.* 42, 135–161. doi: 10.1146/annurev.phyto.42.040803.140340

Bai, G., Su, Z., and Cai, J. (2018). Wheat resistance to fusarium head blight. *Can. J. Plant Pathol.* 40, 336–346. doi: 10.1080/07060661.2018.1476411

Balconi, C., Lanzanova, C., Conti, E., Triulzi, T., Forlani, F., Cattaneo, M., et al. (2007). Fusarium head blight evaluation in wheat transgenic plants expressing the maize b-32 antifungal gene. *Eur. J. Plant Pathol.* 117, 129–140. doi: 10.1007/s10658-006-9079-3

Brewer, H. C., and Hammond-Kosack, K. E. (2015). Host to a stranger: Arabidopsis and fusarium ear blight. *Trends Plant Sci.* 20, 651–663. doi: 10.1016/j.tplants.2015.06.011

Changenet, V., Macadré, C., Boutet-Mercey, S., Magne, K., Januario, M., Dalmais, M., et al. (2021). Overexpression of a cytochrome P450 monooxygenase involved in orobanchol biosynthesis increases susceptibility to fusarium head blight. *Front. Plant Sci.* 12. doi: 10.3389/fpls.2021.662025

Chen, Q. (2013). *Research on transformation of wheat resistance-related genes TaUGT3 and TaPRP to fusarium head blight into common wheat* (Nanjing, China, Nanjing Agricultural University).

Chen, W., Chen, P., Liu, D., Kynast, R., Friebe, B., Velazhahan, R., et al. (1999). Development of wheat scab symptoms is delayed in transgenic wheat plants that constitutively express a rice thaumatin-like protein gene. *Theor. Appl. Genet.* 99, 755–760. doi: 10.1007/s001220051294

Cheng, W., Song, X. S., Li, H. P., Cao, L. H., Sun, K., Qiu, X. L., et al. (2015). Host-induced gene silencing of an essential chitin synthase gene confers durable resistance to fusarium head blight and seedling blight in wheat. *Plant Biotechnol. J.* 13, 1335–1345. doi: 10.1111/pbi.12352

Chen, Y., Kistler, H. C., and Ma, Z. (2019). Fusarium graminearum trichothecene mycotoxins: Biosynthesis, regulation, and management. *Annu. Rev. Phytopathol.* 57, 15–39. doi: 10.1146/annurev-phyto-082718-100318

Chen, T., Luo, Y., Zhao, P., Jia, H., and Ma, Z. (2021). Overexpression of TaJRL53 enhances the fusarium head blight resistance in wheat. *Acta Agron. Sin.* 47, 19–29. doi: 10.3724/SP.J.1006.2021.01050

Chen, X., Steed, A., Travella, S., Keller, B., and Nicholson, P. (2009). Fusarium graminearum exploits ethylene signalling to colonize dicotyledonous and monocotyledonous plants. *New Phytol.* 182, 975–983. doi: 10.1111/j.1469-8137.2009.02821.x

Chen, H., Su, Z., Tian, B., Hao, G., Trick, H. N., and Bai, G. (2022a). TaHRC suppresses the calcium-mediated immune response and triggers wheat head blight susceptibility. *Plant Physiol.* doi: 10.1093/plphys/kiac352

Chen, H., Su, Z., Tian, B., Liu, Y., Pang, Y., Kavetskyi, V., et al. (2022b). Development and optimization of a barley stripe mosaic virus-mediated gene editing system to improve fusarium head blight resistance in wheat. *Plant Biotechnol. J.* 20, 1018–1020. doi: 10.1111/pbi.13819

Dewey, D. R. (1984). "The genomic system of classification as a guide to intergeneric hybridization with the perennial triticeae," in *Gene manipulation in plant improvement*, vol. 209–279 . Ed. J. P. Guastafson (New York: Lenum Press).

Dong, N., Liu, X., Lu, Y., Du, L., Xu, H., Liu, H., et al. (2010). Overexpression of TaPIEP1, a pathogen-induced ERF gene of wheat, confers host-enhanced resistance to fungal pathogen bipolaris sorokiniana. *Funct. Integr. Genomics* 10, 215–226. doi: 10.1007/s10142-009-0157-4

Dou, D., and Zhou, J. M. (2012). Phytopathogen effectors subverting host immunity: different foes, similar battleground. *Cell Host Microbe* 12, 484–495. doi: 10.1016/j.chom.2012.09.003

Dweba, C. C., Figlan, S., Shimelis, H. A., Motaung, T. E., Sydenham, S., Mwadzingeni, L., et al. (2017). Fusarium head blight of wheat: Pathogenesis and control strategies. *Crop Prot.* 91, 114–122. doi: 10.1016/j.cropro.2016.10.002

Eriksen, G. S., and Pettersson, H. (2004). Toxicological evaluation of trichothecenes in animal feed. *Anim. Feed Sci. Technol.* 114, 205–239. doi: 10.1016/j.anifeedsci.2003.08.008

Fan, A., Wei, L., Zhang, X., Liu, J., Sun, L., Xiao, J., et al. (2022). Heterologous expression of the haynaldia villosa pattern-recognition receptor CERK1-V in wheat increases resistance to three fungal diseases. *Crop J.* doi: 10.1016/j.cj.2022.02.005

Fu, S., Lv, Z., Qi, B., Guo, X., Li, J., Liu, B., et al. (2012). Molecular cytogenetic characterization of wheat–thinopyrum elongatum addition, substitution and translocation lines with a novel source of resistance to wheat fusarium head blight. *J. Genet. Genomics* 39, 103–110. doi: 10.1016/j.jgg.2011.11.008

Gadaleta, A., Colasuonno, P., Giove, S. L., Blanco, A., and Giancaspro, A. (2019). Map-based cloning of QFhb.mgb-2A identifies a WAK2 gene responsible for fusarium head blight resistance in wheat. *Sci. Rep.* 9, 6929. doi: 10.1038/s41598-019-43334-z

Garcia-Ruiz, H., Szurek, B., and Van den Ackerveken, G. (2021). Stop helping pathogens: engineering plant susceptibility genes for durable resistance. *Curr. Opin. Biotechnol.* 70, 187–195. doi: 10.1016/j.copbio.2021.05.005

Gatti, M., Cambon, F., Tassy, C., Macadre, C., Guerard, F., Langin, T., et al. (2019). The brachypodium distachyon UGT Bradi5gUGT03300 confers type II fusarium head blight resistance in wheat. *Plant Pathol.* 68, 334–343. doi: 10.1111/ppa.12941

Gatti, M., Choulet, F., Macadré, C., Guérard, F., Seng, J. M., Langin, T., et al. (2018). Identification, molecular cloning, and functional characterization of a wheat UDP-glucosyltransferase involved in resistance to fusarium head blight and to mycotoxin accumulation. *Front. Plant Sci.* 9. doi: 10.3389/fpls.2018.01853

Giancaspro, A., Giove, S. L., Zito, D., Blanco, A., and Gadaleta, A. (2016). Mapping QTL for fusarium head blight resistance in an interspecific wheat population. *Front. Plant Sci.* 7. doi: 10.3389/fpls.2016.01381

Gunupuru, L. R., Arunachalam, C., Malla, K. B., Kahla, A., Perochon, A., Jia, J., et al. (2018). A wheat cytochrome P450 enhances both resistance to deoxynivalenol and grain yield. *PLoS One* 13, e0204992. doi: 10.1371/journal.pone.0204992

Guo, F., Wu, T., Xu, G., Qi, H., Zhu, X., and Zhang, Z. (2021). TaWAK2A-800, a wall-associated kinase, participates positively in resistance to fusarium head blight and sharp eyespot in wheat. *Int. J. Mol. Sci.* 22, 11493. doi: 10.3390/ijms222111493

Guo, J., Zhang, X., Hou, Y., Cai, J., Shen, X., Zhou, T., et al. (2015). High-density mapping of the major FHB resistance gene Fhb7 derived from thinopyrum ponticum and its pyramiding with Fhb1 by marker-assisted selection. *Theor. Appl. Genet.* 128, 2301–2316. doi: 10.1007/s00122-015-2586-x

He, Y., Ahmad, D., Zhang, X., Zhang, Y., Wu, L., Jiang, P., et al. (2018b). Genome-wide analysis of family-1 UDP glycosyltransferases (UGT) and identification of UGT genes for FHB resistance in wheat (Triticum aestivum l.). *BMC Plant Biol.* 18, 67. doi: 10.1186/s12870-018-1286-5

He, Y., Wu, L., Liu, X., Jiang, P., Yu, L., Qiu, J., et al. (2020). TaUGT6, a novel UDP-glycosyltransferase gene enhances the resistance to FHB and DON accumulation in wheat. *Front. Plant Sci.* 11. doi: 10.3389/fpls.2020.574775

He, Y., Zhang, X., Zhang, Y., Ahmad, D., Wu, L., Jiang, P., et al. (2018a). Molecular characterization and expression of PFT, an FHB resistance gene at the Fhb1 QTL in wheat. *Phytopathology* 108, 730–736. doi: 10.1094/PHYTO-11-17-0383-R

Hu, P., Song, P., Xu, J., Wei, Q., Tao, Y., Ren, Y., et al. (2022). Genome-wide analysis of serine hydroxymethyltransferase genes in triticeae species reveals that TaSHMT3A-1 regulates fusarium head blight resistance in wheat. *Front. Plant Sci.* 13. doi: 10.3389/fpls.2022.847087

Ito, M., Sato, I., Ishizaka, M., Yoshida, S., Koitabashi, M., Yoshida, S., et al. (2013). Bacterial cytochrome P450 system catabolizing the fusarium toxin

deoxynivalenol. *Appl. Environ. Microbiol.* 79, 1619–1628. doi: 10.1128/AEM.03227-12

Jiang, C., Hei, R., Yang, Y., Zhang, S., Wang, Q., Wang, W., et al. (2020). An orphan protein of fusarium graminearum modulates host immunity by mediating proteasomal degradation of TaSnRK1α. *Nat. Commun.* 11, 4382. doi: 10.1038/s41467-020-18240-y

Jia, H., Zhou, J., Xue, S., Li, G., Yan, H., Ran, C., et al. (2018). A journey to understand wheat fusarium head blight resistance in the Chinese wheat landrace wangshuibai. *Crop J.* 6, 48–59. doi: 10.1016/j.cj.2017.09.006

Kage, U., Karre, S., Kushalappa, A. C., and McCartney, C. (2017a). Identification and characterization of a fusarium head blight resistance gene TaACT in wheat QTL-2DL. *Plant Biotechnol. J.* 15, 447–457. doi: 10.1111/pbi.12641

Kage, U., Yogendra, K. N., and Kushalappa, A. C. (2017b). TaWRKY70 transcription factor in wheat QTL-2DL regulates downstream metabolite biosynthetic genes to resist fusarium graminearum infection spread within spike. *Sci. Rep.* 7, 42596. doi: 10.1038/srep42596

Koch, A., Biedenkopf, D., Furch, A., Weber, L., Rossbach, O., Abdellatef, E., et al. (2016). An RNAi-based control of fusarium graminearum infections through spraying of long dsRNAs involves a plant passage and is controlled by the fungal silencing machinery. *PLoS Pathog.* 12, e1005901. doi: 10.1371/journal.ppat.1005901

Koch, A., Höfle, L., Werner, B. T., Imani, J., Schmidt, A., Jelonek, L., et al. (2019). SIGS vs HIGS: a study on the efficacy of two dsRNA delivery strategies to silence fusarium FgCYP51 genes in infected host and non-host plants. *Mol. Plant Pathol.* 20, 1636–1644. doi: 10.1111/mpp.12866

Koch, A., Kumar, N., Weber, L., Keller, H., Imani, J., and Kogel, K. H. (2013). Host-induced gene silencing of cytochrome P450 lanosterol C14 alphademethylase-encoding genes confers strong resistance to fusarium species. *Proc. Natl. Acad. Sci. U.S.A.* 110, 19324–19329. doi: 10.1073/pnas.1306373110

Koseoglou, E., van der Wolf, J. M., Visser, R. G. F., and Bai, Y. (2022). Susceptibility reversed: modified plant susceptibility genes for resistance to bacteria. *Trends Plant Sci.* 27, 69–79. doi: 10.1016/j.tplants.2021.07.018

Kumar, A., Yogendra, K. N., Karre, S., Kushalappa, A. C., Dion, Y., and Choo, T. M. (2016). WAX INDUCER1 (HvWIN1) transcription factor regulates free fatty acid biosynthetic genes to reinforce cuticle to resist fusarium head blight in barley spikelets. *J. Exp. Bot.* 67, 4127–4139. doi: 10.1093/jxb/erw187

Li, X., Michlmayr, H., Schweiger, W., Malachova, A., Shin, S., Huang, Y., et al. (2017). A barley UDP-glucosyltransferase inactivates nivalenol and provides fusarium head blight resistance in transgenic wheat. *J. Exp. Bot.* 68, 2187–2197. doi: 10.1093/jxb/erx109

Li, X., Shin, S., Heinen, S., Dill-Macky, R., Berthiller, F., Nersesian, N., et al. (2015). Transgenic wheat expressing a barley UDP-glucosyltransferase detoxifies deoxynivalenol and provides high levels of resistance to fusarium graminearum. *Mol. Plant Microbe Interact.* 28, 1237–1246. doi: 10.1094/MPMI-03-15-0062-R

Liu, X., Cai, S., Zhang, B., Zhou, M., and Zhang, Z. (2011). Molecular detection and identification of TaPIEP1 transgenic wheat with enhanced resistance to sharp eyespot and fusarium head blight. *Acta Agron. Sin.* 37, 1144–1150. doi: 10.3724/SP.J.1006.2011.01144

Liu, S., Hall, M. D., Griffey, C. A., and McKendry, A. L. (2009). Meta-analysis of QTL associated with fusarium head blight resistance in wheat. *Crop Sci.* 49, 1955–1968. doi: 10.2135/cropsci2009.03.0115

Li, G., Zhou, J., Jia, H., Gao, Z., Fan, M., Luo, Y., et al. (2019). Mutation of a histidine-rich calcium-binding-protein gene in wheat confers resistance to fusarium head blight. *Nat. Genet.* 51, 1106–1112. doi: 10.1038/s41588-019-0426-7

Lowe, R. G., McCorkelle, O., Bleackley, M., Collins, C., Faou, P., Mathivanan, S., et al. (2015). Extracellular peptidases of the cereal pathogen fusarium graminearum. *Front. Plant Sci.* 6. doi: 10.3389/fpls.2015.00962

Ma, H., Bai, G., Gill, B., and Patrick, H. (2006). Deletion of a chromosome arm altered wheat resistance to fusarium head blight and deoxynivalenol accumulation in Chinese spring. *Plant Dis.* 90, 1545–1549. doi: 10.1094/PD-90-1545

Machado, A. K., Brown, N. A., Urban, M., Kanyuka, K., and Hammond-Kosack, K. E. (2018). RNAi as an emerging approach to control fusarium head blight disease and mycotoxin contamination in cereals. *Pest Manage. Sci.* 74, 790–799. doi: 10.1002/ps.4748

Mackintosh, C. A., Lewis, J., Radmer, L. E., Shin, S., Heinen, S. J., Smith, L. A., et al. (2007). Overexpression of defense response genes in transgenic wheat enhances resistance to fusarium head blight. *Plant Cell Rep.* 26, 479–488. doi: 10.1007/s00299-006-0265-8

Makandar, R., Essig, J. S., Schapaugh, M. A., Trick, H. N., and Shah, J. (2006). Genetically engineered resistance to fusarium head blight in wheat by expression of arabidopsis NPR1. *Mol. Plant Microbe Interact.* 19, 123–129. doi: 10.1094/MPMI-19-0123

Malla, K. B., Thapa, G., and Doohan, F. M. (2021). Mitochondrial phosphate transporter and methyltransferase genes contribute to fusarium head blight type II disease resistance and grain development in wheat. *PLoS One* 16, e0258726. doi: 10.1371/journal.pone.0258726

Mandalà, G., Tundo, S., Francesconi, S., Gevi, F., Zolla, L., Ceoloni, C., et al. (2019). Deoxynivalenol detoxification in transgenic wheat confers resistance to fusarium head blight and crown rot diseases. *Mol. Plant Microbe Interact.* 32, 583–592. doi: 10.1094/MPMI-06-18-0155-R

Ma, L., Shang, Y., Cao, A., Qi, Z., Xing, L., Chen, P., et al. (2010b). Molecular cloning and characterization of an up-regulated UDP-glucosyltransferase gene induced by DON from triticum aestivum l. cv. wangshuibai. *Mol. Biol. Rep.* 37, 785–795. doi: 10.1007/s11033-009-9606-3

Ma, Q., Tian, B., and Li, Y. (2010a). Overexpression of a wheat jasmonate-regulated lectin increases pathogen resistance. *Biochimie* 92, 187–193. doi: 10.1016/j.biochi.2009.11.008

Ma, H., Zhang, X., Yao, J., and Cheng, S. (2019). Breeding for the resistance to fusarium head blight of wheat in China. *Front. Agr. Sci. Eng.* 6, 251–264. doi: 10.15302/J-FASE-2019262

Michlmayr, H., Malachová, A., Varga, E., Kleinová, J., Lemmens, M., Newmister, S., et al. (2015). Biochemical characterization of a recombinant UDP-glucosyltransferase from rice and enzymatic production of deoxynivalenol-3-O-β-D-glucoside. *Toxins* 7, 2685–2700. doi: 10.3390/toxins7072685

Pasquet, J. C., Changenet, V., Macadré, C., Boex-Fontvieille, E., Soulhat, C., Bouchabké-Coussa, O., et al. (2016). A brachypodium UDP-glycosyltransferase confers root tolerance to deoxynivalenol and resistance to fusarium infection. *Plant Physiol.* 172, 559–574. doi: 10.1104/pp.16.00371

Pei, H. (2011). *Construction of the expression vector and transformation of TaUGT3 gene into common wheat* (Nanjing, China, Nanjing Agricultural University).

Peraldi, A., Beccari, G., Steed, A., and Nicholson, P. (2011). Brachypodium distachyon: a new pathosystem to study fusarium head blight and other fusarium diseases of wheat. *BMC Plant Biol.* 11, 100. doi: 10.1186/1471-2229-11-100

Perochon, A., Jianguang, J., Kahla, A., Arunachalam, C., Scofield, S. R., Bowden, S., et al. (2015). TaFROG encodes a pooideae orphan protein that interacts with SnRK1 and enhances resistance to the mycotoxigenic fungus fusarium graminearum. *Plant Physiol.* 169, 2895–2906. doi: 10.1104/pp.15.01056

Perochon, A., Kahla, A., Vranić, M., Jia, J., Malla, K. B., Craze, M., et al. (2019). A wheat NAC interacts with an orphan protein and enhances resistance to fusarium head blight disease. *Plant Biotechnol. J.* 17, 1892–1904. doi: 10.1111/pbi.13105

Proctor, R. H., Hohn, T. M., and McCormick, S. P. (1995). Reduced virulence of gibberella zeae caused by disruption of a trichothecene toxin biosynthetic gene. *Mol. Plant Microbe Interact.* 8, 593–601. doi: 10.1094/mpmi-8-0593

Rampitsch, C., Day, J., Subramaniam, R., and Walkowiak, S. (2013). Comparative secretome analysis of fusarium graminearum and two of its non-pathogenic mutants upon deoxynivalenol induction *in vitro*. *Proteomics* 13, 1913–1921. doi: 10.1002/pmic.201200446

Rank, A. P., and Koch, A. (2021). Lab-To-field transition of RNA spray applications–how far are we? *Front. Plant Sci.* 12. doi: 10.3389/fpls.2021.755203

Rawat, N., Pumphrey, M. O., Liu, S., Zhang, X., Tiwari, V. K., Ando, K., et al. (2016). Wheat Fhb1 encodes a chimeric lectin with agglutinin domains and a pore-forming toxin-like domain conferring resistance to fusarium head blight. *Nat. Genet.* 48, 1576–1580. doi: 10.1038/ng.3706

Schweiger, W., Boddu, J., Shin, S., Poppenberger, B., Berthiller, F., Lemmens, M., et al. (2010). Validation of a candidate deoxynivalenol-inactivating UDP-glucosyltransferase from barley by heterologous expression in yeast. *Mol. Plant Microbe Interact.* 23, 977–986. doi: 10.1094/MPMI-23-7-0977

Schweiger, W., Pasquet, J. C., Nussbaumer, T., Paris, M. P., Wiesenberger, G., Macadré, C., et al. (2013). Functional characterization of two clusters of brachypodium distachyon UDP-glycosyltransferases encoding putative deoxynivalenol detoxification genes. *Mol. Plant Microbe Interact.* 26, 781–792. doi: 10.1094/MPMI-08-12-0205-R

Shang, Y., Xiao, J., Ma, L., Wang, H., Qi, Z., Chen, P., et al. (2009). Characterization of a PDR type ABC transporter gene from wheat (Triticum aestivum l.). *Chin. Sci. Bull.* 54, 3249–3257. doi: 10.1007/s11434-009-0553-0

Shin, S., Mackintosh, C. A., Lewis, J., Heinen, S. J., Radmer, L., Dill-Macky, R., et al. (2008). Transgenic wheat expressing a barley class II chitinase gene has enhanced resistance against fusarium graminearum. *J. Exp. Bot.* 59, 2371–2378. doi: 10.1093/jxb/ern103

Shin, S., Torres-Acosta, J. A., Heinen, S. J., McCormick, S., Lemmens, M., Paris, M. P., et al. (2012). Transgenic arabidopsis thaliana expressing a barley UDP-glucosyltransferase exhibit resistance to the mycotoxin deoxynivalenol. *J. Exp. Bot.* 63, 4731–4740. doi: 10.1093/jxb/ers141

Shude, S. P. N., Yobo, K. S., and Mbili, N. C. (2020). Progress in the management of fusarium head blight of wheat: An overview. *S. Afr. J. Sci.* 116, 7854. doi: 10.17159/sajs.2020/7854

Song, X. S., Gu, K. X., Duan, X. X., Xiao, X. M., Hou, Y. P., Duan, Y. B., et al. (2018). Secondary amplification of siRNA machinery limits the application of

spray-induced gene silencing. *Mol. Plant Pathol.* 19, 2543–2560. doi: 10.1111/mpp.12728

Soni, N., Altartouri, B., Hegde, N., Duggavathi, R., Nazarian-Firouzabadi, F., and Kushalappa, A. C. (2021). TaNAC032 transcription factor regulates lignin-biosynthetic genes to combat fusarium head blight in wheat. *Plant Sci.* 304, 110820. doi: 10.1016/j.plantsci.2021.110820

Soni, N., Hegde, N., Dhariwal, A., and Kushalappa, A. C. (2020). Role of laccase gene in wheat NILs differing at QTL-Fhb1 for resistance against fusarium head blight. *Plant Sci.* 298, 110574. doi: 10.1016/j.plantsci.2020

Su, Z., Bernardo, A., Tian, B., Chen, H., Wang, S., Ma, H., et al. (2019). A deletion mutation in TaHRC confers Fhb1 resistance to fusarium head blight in wheat. *Nat. Genet.* 51, 1099–1105. doi: 10.1038/s41588-019-0425-8

Su, P., Zhao, L., Li, W., Zhao, J., Yan, J., Ma, X., et al. (2021). Integrated metabolo-transcriptomics and functional characterization reveals that the wheat auxin receptor TIR1 negatively regulates defense against fusarium graminearum. *J. Integr. Plant Biol.* 63, 340–352. doi: 10.1111/jipb.12992

Thapa, G., Gunupuru, L. R., Hehir, J. G., Kahla, A., Mullins, E., and Doohan, F. M. (2018). A pathogen-responsive leucine rich receptor like kinase contributes to fusarium resistance in cereals. *Front. Plant Sci.* 9. doi: 10.3389/fpls.2018.00867

Travella, S., Klimm, T. E., and Keller, B. (2006). RNA Interference-based gene silencing as an efficient tool for functional genomics in hexaploid bread wheat. *Plant Physiol.* 142, 6–20. doi: 10.1104/pp.106.084517

Urban, M., Daniels, S., Mott, E., and Hammond-Kosack, K. (2002). Arabidopsis is susceptible to the cereal ear blight fungal pathogens fusarium graminearum and fusarium culmorum. *Plant J.* 32, 961–973. doi: 10.1046/j.1365-313x.2002.01480.x

Walter, S., Kahla, A., Arunachalam, C., Perochon, A., Khan, M. R., Scofield, S. R., et al. (2015). A wheat ABC transporter contributes to both grain formation and mycotoxin tolerance. *J. Exp. Bot.* 66, 2583–2593. doi: 10.1093/jxb/erv048

Wang, G., Hou, W., Zhang, L., Wu, H., Zhao, L., Du, X., et al. (2016). Functional analysis of a wheat pleiotropic drug resistance gene involved in fusarium head blight resistance. *J. Integr. Agric.* 15, 2215–2227. doi: 10.1016/S2095-3119(16)61362-X

Wang, F., Li, X., Li, Y., Han, J., Chen, Y., Zeng, J., et al. (2021). Arabidopsis P4 ATPase-mediated cell detoxification confers resistance to fusarium graminearum and verticillium dahliae. *Nat. Commun.* 12, 6426. doi: 10.1038/s41467-021-26727-5

Wang, H., Sun, S., Ge, W., Zhao, L., Hou, B., Wang, K., et al. (2020a). Horizontal gene transfer of Fhb7 from fungus underlies fusarium head blight resistance in wheat. *Science* 368, eaba5435. doi: 10.1126/science.aba5435

Wang, M., Wu, L., Mei, Y., Zhao, Y., Ma, Z., Zhang, X., et al. (2020b). Host-induced gene silencing of multiple genes of fusarium graminearum enhances resistance to fusarium head blight in wheat. *Plant Biotechnol. J.* 18, 2373–2375. doi: 10.1111/pbi.13401

Werner, B. T., Gaffar, F. Y., Schuemann, J., Biedenkopf, D., and Koch, A. M. (2020). RNA-Spray-mediated silencing of fusarium graminearum AGO and DCL genes improve barley disease resistance. *Front. Plant Sci.* 11. doi: 10.3389/fpls.2020.00476

Wetterhorn, K. M., Gabardi, K., Michlmayr, H., Malachova, A., Busman, M., McCormick, S. P., et al. (2017). Determinants and expansion of specificity in a trichothecene UDP-glucosyltransferase from oryza sativa. *Biochemistry* 56, 6585–6596. doi: 10.1021/acs.biochem.7b01007

Xiang, Y., Song, M., Wei, Z., Tong, J., Zhang, L., Xiao, L., et al. (2011). A jacalin-related lectin-like gene in wheat is a component of the plant defence system. *J. Exp. Bot.* 62, 5471–5483. doi: 10.1093/jxb/err226

Xing, L., He, L., Xiao, J., Chen, Q., Li, M., Shang, Y., et al. (2017). An UDP-glucosyltransferase gene from barley confers disease resistance to fusarium head blight. *Plant Mol. Biol. Rep.* 35, 224–236. doi: 10.1007/s11105-016-1014-y

Xu, X., and Nicholson, P. (2009). Community ecology of fungal pathogens causing wheat head blight. *Annu. Rev. Phytopathol.* 47, 83–103. doi: 10.1146/annurev-phyto-080508-081737

Yang, J., Bai, G., and Shaner, G. E. (2005). Novel quantitative trait loci (QTL) for fusarium head blight resistance in wheat cultivar chokwang. *Theor. Appl. Genet.* 111, 1571–1579. doi: 10.1007/s00122-005-0087-z

Yang, F., Jacobsen, S., Jørgensen, H. J., Collinge, D. B., Svensson, B., and Finnie, C. (2013). Fusarium graminearum and its interactions with cereal heads: Studies in the proteomics era. *Front. Plant Sci.* 4. doi: 10.3389/fpls.2013.00037

Yang, F., Jensen, J. D., Svensson, B., Jørgensen, H. J., Collinge, D. B., and Finnie, C. (2012). Secretomics identifies fusarium graminearum proteins involved in the interaction with barley and wheat. *Mol. Plant Pathol.* 13, 445–453. doi: 10.1111/j.1364-3703.2011.00759.x

Yang, J., Zhang, T., Mao, H., Jin, H., Sun, Y., and Qi, Z. (2020). A leymus chinensis histidine-rich Ca2+-binding protein binds Ca2+/Zn2+ and suppresses abscisic acid signaling in arabidopsis. *J. Plant Physiol.* 252, 153209. doi: 10.1016/j.jplph.2020.153209

Zhao, L., Ma, X., Su, P., Ge, W., Wu, H., Guo, X., et al. (2018). Cloning and characterization of a specific UDP-glycosyltransferase gene induced by DON and fusarium graminearum. *Plant Cell Rep.* 37, 641–652. doi: 10.1007/s00299-018-2257-x

Zheng, T., Hua, C., Li, L., Sun, Z., Yuan, M., Bai, G., et al. (2021). Integration of meta-QTL discovery with omics: towards a molecular breeding platform for improving wheat resistance to fusarium head blight. *Crop J.* 9, 739–749. doi: 10.1016/j.cj.2020.10.006

Zhu, Z., Hao, Y., Mergoum, M., Bai, G., Humphreys, G., Cloutier, S., et al. (2019). Breeding wheat for resistance to fusarium head blight in the global north: China, USA and Canada. *Crop J.* 7, 730–738. doi: 10.1016/j.cj.2019.06.003

Zhu, X., Li, Z., Xu, H., Zhou, M., Du, L., and Zhang, Z. (2012). Overexpression of wheat lipid transfer protein gene TaLTP5 increases resistances to cochliobolus sativus and fusarium graminearum in transgenic wheat. *Funct. Integr. Genomics* 12, 481–488. doi: 10.1007/s10142-012-0286-z

frontiers | Frontiers in Plant Science

TYPE Original Research
PUBLISHED 31 October 2022
DOI 10.3389/fpls.2022.1034600

OPEN ACCESS

EDITED BY
Maria Rosa Simon,
National University of La Plata, Argentina

REVIEWED BY
Marcelo Anibal Carmona,
University of Buenos Aires, Argentina
Daniel Bebber,
University of Exeter, United Kingdom

*CORRESPONDENCE
Yuan Chai
chaix026@umn.edu

SPECIALTY SECTION
This article was submitted to Plant Pathogen Interactions, a section of the journal Frontiers in Plant Science

RECEIVED 01 September 2022
ACCEPTED 12 October 2022
PUBLISHED 31 October 2022

CITATION
Chai Y, Senay S, Horvath D and Pardey P (2022) Multi-peril pathogen risks to global wheat production: A probabilistic loss and investment assessment.
Front. Plant Sci. 13:1034600.
doi: 10.3389/fpls.2022.1034600

Multi-peril pathogen risks to global wheat production: A probabilistic loss and investment assessment

Yuan Chai[1,2]*, Senait Senay[2,3], Diana Horvath[4] and Philip Pardey[1,2]

[1]Department of Applied Economics, University of Minnesota, St. Paul, MN, United States, [2]GEMS (Genetics x Environment x Management x Socio-economics) Informatics Center, University of Minnesota, St. Paul, MN, United States, [3]Department of Plant Pathology, University of Minnesota, St. Paul, MN, United States, [4]2Blades, Evanston, IL, United States

Crop diseases cause significant food and economic losses. We examined the joint, probabilistic, long-term, bio-economic impact of five major fungal pathogens of wheat on global wheat production by combining spatialized estimates of their climate suitability with global wheat production and modeled distributions of potential crop losses. We determined that almost 90% of the global wheat area is at risk from at least one of these fungal diseases, and that the recurring losses attributable to this set of fungal diseases are upwards of 62 million tons of wheat production per year. Our high-loss regime translates to around 8.5% of the world's wheat production on average—representing calories sufficient to feed up to 173 million people each year. We estimate that a worldwide research expenditure of $350-$974 million (2018 prices) annually on these five fungal diseases of wheat, let alone other pathogens, can be economically justified, equivalent to 2 to 5 times more than the amount we estimate is currently spent on *all* wheat disease-related public R&D.

KEYWORDS

wheat, fungal diseases, biotic risks, disease losses, R&D investment

Introduction

Crops are food not just for people and animals, but also for numerous microbial pathogens and insect pests. Often the impacts of a specific pathogen on a particular plant host are examined individually, but the reality is that agro-ecological regions more typically have conditions favorable for multiple pathogens. For many human diseases such as the most recent SARS-CoV2 outbreaks, access to real-time data on the movement and variation of pathogen strains has helped prioritize responses to the pandemic. However, the data on most plant diseases are fragmented and often out of date, making it

difficult to accurately assess the impacts of crop diseases and appropriately allocate resources for mitigation efforts. In this study, we use a probabilistic, multi-peril approach to examine the worldwide risks and impacts of the most significant fungal pathogens affecting wheat, and explore their policy implications in terms of the economically justifiable research and development investments globally to mitigate the wheat losses attributable to these pathogens.

Wheat is an especially critical component of global food supplies. This single crop accounts for about one-fifth of the total calories and total protein consumed by the planet's 7.9 billion people each and every year (FAO, 2020). United Nations (2022) projections have global population approaching 10 billion people by 2050. This inexorably growing population, coupled with increasing per capita incomes, will continue to push the global demand for food ever higher (Pardey et al., 2014). Against these stark food consumption futures is an equally stark agricultural production reality. Crop yields are intrinsically variable due to fluctuating and sometimes extreme weather, and doubly so given the losses from a range of biological threats, i.e., diseases, insects, animals, and weeds—collectively "pests,"—that can compromise yields and reduce quality, taste, nutrition, and food safety (see, e.g., Reynolds et al., 2007).

The pests that impact wheat crops are representative of the problem, which results in significant, albeit temporally and spatially variable, damage—ostensibly accounting for 10-50% (on average) of wheat crop losses worldwide (e.g., Oerke, 2006; Savary et al., 2019). In the U.S., $209 million was paid out to wheat farmers on insurance claims for crop losses attributable to insects, diseases, and weeds between 2010-2020 (USDA-RMA, 2021, authors' calculation), even *after* farmers had taken preventive steps by applying herbicides to 71% of their wheat acreage, fungicides to 30%, and insecticides to 7% of the cropped area (in 2017) (USDA-NASS, 2018, authors' calculations). For smallholder farmers in developing countries, crop pest losses are also likely large, especially given the limited uptake of modern seed varieties and the even more limited use of agricultural chemicals that can mitigate these losses (Sheahan and Barrett, 2017; Pardey et al., 2022). Furthermore, climate change is amplifying these issues by increasing plant stress and expanding the natural ranges of pathogens, as well as the geographical risk exposure to the consequences of crop pests (Bebber et al., 2013). Chaloner et al. (2021) projected that infection risks from 80 plant pathogens are likely to increase at higher latitudes in the future, exerting even greater burden for securing global crop production under climate change challenges.

The substantial and continuing economic loss and damage to livelihoods from crop pests present a *prima facie* case for investing in innovations that address these pervasive and perennial crop-pest problems. Determining how much to invest and how to prioritize investments among the many pests that affect wheat (and other crops) is difficult. Getting a sense of the magnitude of the losses is key to estimating the amount of investment that a hard-nosed economic assessment would support to avoid these losses. However, the prior bio-economic evidence is patchy—particularly at geographical scale (such as a country, and especially worldwide)—and is less useful for making strategic innovation investment choices. Losses attributable to pests vary seasonally and geographically. Where credible long-run loss data exist—e.g., Pardey et al. (2013) in the case of wheat stem rust losses affecting U.S. farmers for over a century—they reveal that even for this problematic pest, in numerous years the losses are negligible. Thus, it is an overstatement to consider losses for a particular pest in a given year and locale (especially a localized extreme loss) as being representative of the longer-run average annual losses at scale (say for a country or the world). Furthermore, farmers are subject to the yield-reducing effects of multiple pests, and so estimates of the combined losses arising from these multiple threats is required to properly calibrate the overall magnitude of the investments justified to deal with these multi-peril pest problems.

In this study we examined the economic impacts of five fungal pathogen threats to wheat by taking into consideration the complex interactions among environment-pathogen-host in disease-related crop losses. We focused on estimating potential losses caused by five fungal diseases, namely stem rust (*Puccinia graminis*), stripe rust (*Puccinia striiformis*), leaf rust (*Puccinia triticina*), fusarium head blight (FHB) (*Fusarium graminearum*), and septoria tritici blotch (STB) (*Zymoseptoria tritici*), that afflict wheat producers in rich and poor countries alike (see, e.g., Figueroa et al., 2018). We combine spatially-explicit estimates of each pathogen's climate suitability with global wheat production and modeled potential loss distributions to jointly assess the long-term impact of this crop disease complex and their policy implications. Our novel, multi-peril pest approach accounts for the location-to-location and season-to-season variation in pest-related damage to crops. We consider the risk profile faced by farmers worldwide from this portfolio of pests and extend the probabilistic loss methodology—hitherto used on a pest-by-pest basis (e.g., Pardey et al. (2013) for stem rust, Beddow et al. (2015) for stripe rust, and Chai et al. (2020) for leaf rust)—to assess the overall losses jointly attributable to the five fungal diseases. We then used the losses to estimate the implied research and development (R&D) investments worldwide that are economically justified to mitigate these losses under both high- and low-loss regimes.

Results

Global wheat vulnerability to fungal diseases

Wheat was planted on 219 million acres globally in 2020, equal to about one-third of the world's total area for cereal

agriculture. Strikingly, we find that 80% or more of that global wheat area is at risk from four fungi: FHB, and leaf, stripe, and stem rust infection (Table 1). In addition to these four pathogens, around half the wheat area is climate-suitable for STB.

Rows with values in bold represent the aggregated values for countries in "Developed World", "Developing World" and all "World", respectivelyThese pathogens co-evolved over centuries in tandem with wheat, and thus it is of little surprise that the same climate also sustains these fungi (Thompson and Burdon, 1992). However, wheat has moved well beyond its ancestral center of origin in the Fertile Crescent that spans modern countries of Israel, Jordan, Syria, Lebanon, eastern Turkey, western Iran, and northern Iraq (see, e.g., Khoury et al., 2016). It now grows in latitudes stretching from 67° north in Norway, Finland, and Russia to 45° south in Argentina (Joglekar et al., 2016; Yu et al., 2020). Different varieties of wheat are more or less suitable for different climatic conditions, and similarly fungal diseases vary by climate and locale. These spatial sensitivities are reflected in the regional data summarized in Table 1. Our analysis shows that even in more recently farmed or minor wheat growing areas, all five diseases pose a significant threat, with many capable of occurring on more than 90% of the wheat areas in sub-Saharan Africa and Latin America. The geographic extent of wheat areas deemed climate-suitable for fungal infections is generally of comparable magnitude in North America and Western Europe. The Former Soviet Union countries collectively account for about one-fifth of the world's wheat area, much of it in more northerly latitudes, however in this region the climate suitability for all five fungal diseases is more restricted. Our results suggest that the most significant risk to the world supply of wheat comes from production that occurs in Asia. This region accounted for 30.9% of the world's wheat harvested area in 2020, and wheat there is vulnerable to infection from several fungi, with climate-suitable area shares ranging from 92.2%-99.0% for stem rust, leaf rust and FHB diseases.

Within the spatial extent of global wheat production, Figure 1 maps 10 arc minute pixelated spatial grids with climates that can sustain various fungi for at least one life cycle of the disease, differentiating between those pixels that are climate suitable for none, one, and so on up to five of the pests. The shading in Figure 1 thus represents the multi-peril risk exposure for the five wheat fungal diseases at each location. The darker the shading, the more pests that can be sustained at a given pixel. Most of the map tends toward the darker end of the spectrum, consistent with the summary of this co-suitability phenomenon in Supplementary Table S1. Starkly, only 11.4% of the world's wheat area occurs in locales that none of the five pests find climate suitable. More than 75% of the world's wheat will sustain at least four of the pests, and more than half (54.0%) of the area is susceptible to all five diseases.

Notably, the more-developed countries grow their wheat in locations that tend to have less multi-peril risk exposure than countries throughout the developing world. Nonetheless, developed countries are by no means free of these risks. We estimate that well over half (56.4%) of the wheat area in developed countries is threatened by all five fungi. In the developing world, wheat crops in sub-Saharan Africa and Latin America are especially vulnerable to infestations from multiple fungi; more than 90% of the wheat area in both regions are at risk from at least four fungi, while in Asia 92% of the area is vulnerable to at least three pests. Moreover, many of the poorer wheat producers in these areas have less access to

TABLE 1 Share of regional wheat growing areas at risk from fungal disease.

Region	Harvested Wheat area		Wheat fungal disease suitable area share				
	Amount *(million hectares)*	Global share *(percent)*	FHB	Leaf Rust	Stripe Rust *(percent)*	Stem Rust	STB
Developed World	**138.0**	**57.6**	**80.3**	**80.6**	**81.5**	**73.2**	**56.9**
Former Soviet Union	51.9	21.7	54.4	54.7	56.6	44.3	22.3
Western Europe	50.4	21.0	97.0	97.2	98.6	96.8	79.6
North America	25.3	10.5	95.3	95.4	92.0	85.4	83.5
Australasia	10.4	4.4	82.2	83.2	87.3	66.8	43.8
Developing World	**101.6**	**42.4**	**98.9**	**94.8**	**80.0**	**92.5**	**50.7**
Asia	89.4	37.3	99.0	94.6	78.0	92.2	46.1
Latin America	9.4	3.9	98.6	97.1	92.7	94.7	80.5
sub-Saharan Africa	2.8	1.2	97.1	94.1	90.6	93.7	74.5
World	**239.6**	**100.0**	**86.8**	**85.5**	**80.9**	**79.9**	**54.7**

Source: Developed by authors.
For ease of exposition, we aggregated some of the Beddow et al. (2013) zones when reporting the results in this table. Specifically, the Latin America and the Caribbean (LAC) figures represent an aggregation of the estimates formed for the Central America & Caribbean, Andean and Eastern South America zones. Sub-Saharan Africa (SSA) is an aggregation of the East Central Africa, West Central Africa and Southern Africa zones. Asia groups together the Southeast Asia, Southwest Asia and Northeast Asia zone estimates. Western Europe includes all countries on the European Continent from the North Africa & West Europe and Eurasian zones. FSU is the Former Soviet Union countries.
Rows with values in bold represent the aggregated values for countries in "Developed World", "Developing World" and all "World", respectively.

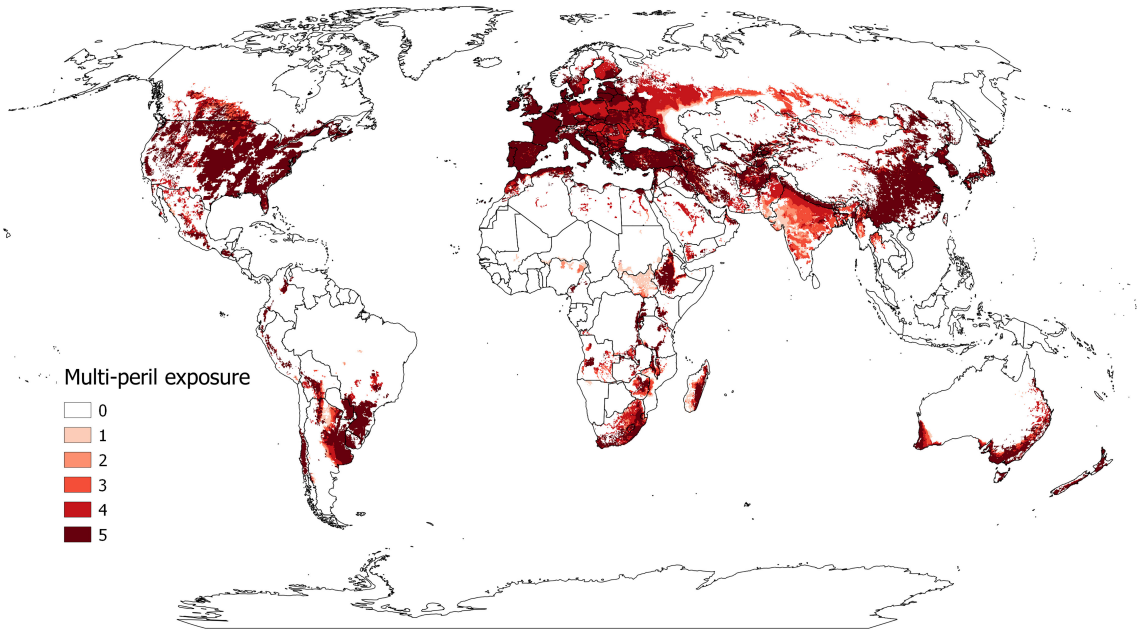

FIGURE 1
Modeled global climate-based multi-peril exposure for selected wheat fungal diseases. This map reports the climate-based multi-peril exposure (pest suitability count) of modeled CLIMEX annual growth indexes (GI) for the following wheat fungal diseases: stem rust, stripe rust, leaf rust, FHB, and septoria tritici blotch. The map shows the count of disease suitability (i.e., GI > 5) within the global wheat production areas reported by the Spatial Allocation Model (SPAM) (Yu et al., 2020).

resistant varieties, fungicides, and information about best management practices.

Global wheat loss estimates

The occurrence and magnitude of crop losses due to disease depends on several factors. Locations that are climate-suitable for a particular pest certainly put farmers at risk from that pest, but it does not necessarily mean in any particular cropping season they incur crop losses from it. The odds of a crop being infected, the severity and timing of an infection, and the dispersal mechanisms that can spread the disease well beyond its initial site of infection are part of the complex epidemiological processes that affect the geographic extent and magnitude of pest-induced crop losses. Figure 2 provides a conceptual (and empirically tractable) visualization of the effects of pests on crop yields that is especially useful for impact assessment purposes. The with- and without-disease threat construct in this framing provides the basis for the counterfactual underpinnings of our loss assessment approach, which in principle can be applied at any spatial scale (be it an experimental plot, a farm field, a country, etc.). In addition, the loss likelihood functions we estimated based on reported historical observations (see Methods and Supplementary Figure S1, and visualized as the respective green, red and blue yield distributions in Figure 2) capture the highly variable nature of the crop losses associated with a particular disease from year-to-year at any particular location. Differences in each disease's epidemiological characteristics result in different modeled yield loss distributions. Climate has played a role in the historic year-to-year variability, just as it does in the location-to-location variability of disease-induced crop losses, thus, this analysis factors in impacts of climate variability. Facing uncertain climate change challenges, future impacts may be even more variable.

In our analysis, we use historical data to derive high- and low-loss regimes. We introduced two counterfactual regimes to help bound the range of likely global (or regional) losses, by applying these constructs on a pixelated basis at scale, across more- or less-advanced wheat farming practices throughout the world. The notes to Figure 2 describe details of the (typically unobserved) "without" and (observed) "with" disease threat counterfactual construct. In farmers' fields, all factors in the environment-pathogen-host disease triangle can affect the actual loss experienced by farmers. In constructing our high- and low-loss regimes, the goal is not to predict the loss that will occur in any particular season at a particular location. Rather, our assumption is that, within the wheat areas that are climatically suitable for these wheat fungal diseases, the *probabilistic loss distribution* of wheat fungal diseases derived from long-term historical data across the U.S. can serve as proxy loss scenarios for wheat growers elsewhere in the world.

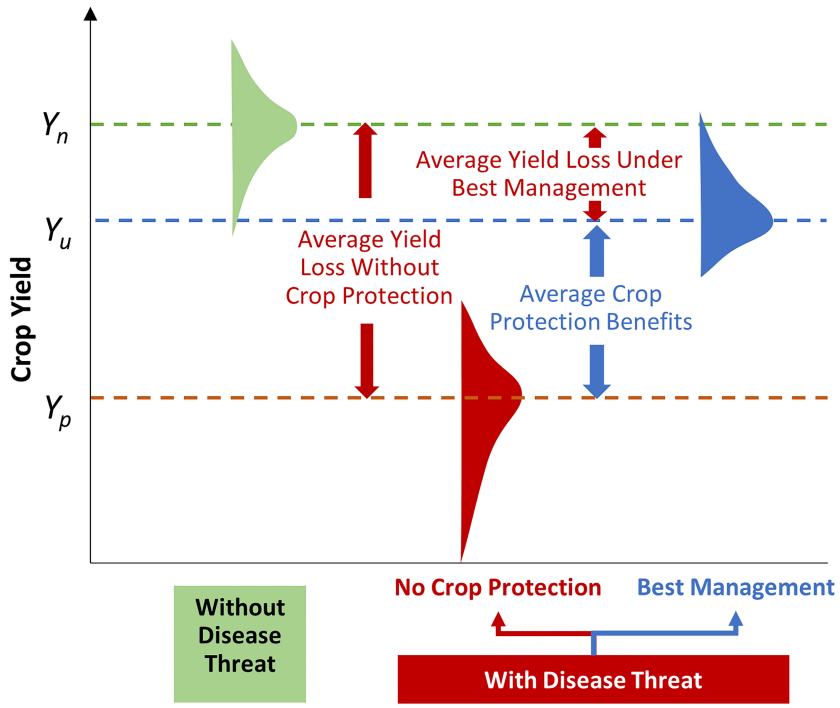

FIGURE 2
Raising crop productivity and derisking farmers' yields. The green distribution reflects variation in (field-scale) crop yields around an average yield, Y_n, that is free of any pest threats. Here the distribution in yields represents the effects of season-to-season variation in local weather. Y_p represents the average yield for the same crop in the same agroecology, but now yields vary in response to both local weather and pests. This red-shaded distribution has a long downside tail stretching to zero to indicate low probability but nonetheless severe (and in rare cases, total) loss events arising from a pest infestation. The difference in yields ($Y_p - Y_n$) represents the losses, *on average*, attributable to pest threats. Through deployment of best pest management and mitigation practices, the yield losses due to crop pests can be restored, and if *fully effective*, would raise yields (or conversely reduce unit costs of production), on average, from Y_p to Y_n. A *cost-effective* approach to dealing with crop pests is unlikely to fully restore yields (and thus household food and nutrition access, and perhaps farm incomes) *on average*, or eliminate yield risk entirely. Rather it would involve protecting yields and reducing risks up to the point that the marginal (or incremental) benefits equals the marginal costs of ameliorating the crop damage consequences of pests. This is indicated by the shift from the red to blue yield distribution profiles, where average yields are increased from Y_p to Y_u (the average yield under the no-disease-threat regime), that is largely, but not fully, restored and the dispersion in yields around the average is reduced. This reduction in risk is visually represented in terms of the more peaked yield distribution (blue) when farmers use pest-reducing innovations versus when they do not (red), such that reducing the variability in yields de-risks cropping for farmers and others in the supply chain.

Climate conditions, disease pressure, and wheat production practices vary greatly across locations. These result in spatially-variable wheat yields that are intrinsic to the spatially-explicit loss estimation procedure we describe below. To reflect variation in the use of genetics and fungicides and other factors that can influence the magnitude of the *percentage* losses (relative to spatially-variable yield *levels*) we use our yield-loss *distribution* evidence to construct both high- and low-loss regimes that plausibly bound our probabilistic loss estimates. Our high-loss regime represents a situation where disease pressures are high and/or farmers failed to implement effective disease management practices, while the low-loss regime represents a situation where disease pressures are low and/or well-managed in farmers' fields. While our spatially-sensitive, probabilistic estimation methodology can be applied at different spatial scales (fields vs regions vs globally) spanning different time periods (within season or spanning multiple seasons, past or future), in this instance we use longer-term (historical) data to gain a bounded and strategic sense of the loss profiles at scale for each of the five fungal diseases separately and in aggregate to guide longer-term investment decisions concerning crop breeding or other methods to mitigate and manage these crop loss risks.

Table 2 summarizes all this loss estimation complexity into three policy and investment related metrics—namely, the likely quantitative loss in global wheat production associated with each of the diseases one-by-one (columns 2-6), and the diseases as a multi-peril complex of diseases (column 1); the production losses expressed in U.S. dollar values (2018 prices); and the share of average annual wheat production likely lost to each of the diseases and the five diseases in total.

We estimate that the *average annually recurring* loss of global wheat production from this complex of five fungal

TABLE 2 Estimates of global annual losses in wheat production from fungal diseases.

	Total (1)	FHB (2)	STB (3)	Stem Rust (4)	LeafRust (5)	StripeRust (6)
Production loss (million metric tons)						
Low-loss regime						
Mean	24.3	16.9	1.9	0.9	3.6	1.0
Range	(20.7-29.5)	(13.5-21.7)	(1.3-2.7)	(0.7-1.2)	(3.4-3.9)	(0.3-2.5)
High-loss regime						
Mean	62.0	28.5	10.6	9.9	8.9	4.1
Range	(56.4-70.0)	(23.4-35.9)	(9.7-11.7)	(8.7-11.6)	(8.2-9.8)	(3.5-4.9)
Production loss (billion US$, 2018 prices)						
Low-loss regime						
Mean	4.2	2.9	0.3	0.2	0.6	0.2
Range	(3.6-5.1)	(2.3-3.8)	(0.2-0.5)	(0.1-0.2)	(0.6-0.7)	(0.05-0.4)
High-loss regime						
Mean	10.8	4.9	1.8	1.7	1.5	0.7
Range	(9.8-12.1)	(4.1-6.2)	(1.7-2.0)	(1.5-2.0)	(1.4-1.7)	(0.6-0.8)
Percentage of global average annual wheat production						
Low-loss regime						
Mean	3.3	2.3	0.3	0.1	0.5	0.1
Range	(2.8-4.0)	(1.8-3.0)	(0.2-0.4)	(0.1-0.2)	(0.47-0.53)	(0.04-0.3)
High-loss regime						
Mean	8.5	3.9	1.4	1.4	1.2	0.6
Range	(7.7-8.5)	(3.2-4.9)	(1.3-1.6)	(1.2-1.6)	(1.1-1.3)	(0.5-0.7)

Source: Developed by authors.
Table entries represent estimates of average annual losses per year during the period 2020-2050.
Range (in brackets) represents the values between 5%-90% probability of loss.

diseases lies in the range of 24.3 to 62.0 million metric tons, depending on the counterfactual loss regime. The intrinsic year-to-year variability in losses associated with crop pests and diseases is masked by the annual averages, but are revealed in the range entries. Thus, for example, while the high-loss regime projects average losses of 62.0 million metric tons per year, we estimate there is a 90% chance these global annual losses will exceed 56.4 million metric tons on average over the period 2020-2050, and a 5% chance the losses could be as high as 70.0 million metric tons per year. In dollar terms the overall losses are sizable, ranging from an annual average of $4.2 billion (2018 prices) worldwide in the low-loss scenario to $10.8 billion in the high-loss scenario. With estimated global wheat production projected to total $127.0 billion per year on average during 2020-2050, our estimates translate to annual losses that constitute between 3.3 and 8.5% of global wheat production.

Complementing Table 2, Figure 3 also provides information on the losses attributable to each of the fungal diseases. Complicating factors, the rank ordering of crop damages associated with each disease is sensitive to the counterfactual loss regime under consideration. For example, based on these estimates, FHB stands out as the dominant source of wheat losses in both the high- and low-loss regime. STB and stem rust are the next most damaging diseases. Under the high-loss regime, STB, stem and leaf rust have comparable loss profiles, whereas for the low-loss regime leaf rust slightly dominates the STB loss profile while stem rust losses are on par with those observed for stripe rust.

The investment bottom line

Because R&D for innovation and the development of resilient crop varieties is an established and environmentally sound approach to avert crop losses from disease, the development of effective breeding solutions hinges on the question "*how much should be spent on innovative efforts to mitigate the crop losses attributable to fungal diseases of wheat*?" A defensible answer to this question requires recognizing the opportunity cost of these funds. That is, funds spent, say, on wheat fungal R&D cannot be spent on other types of R&D, or other means of ameliorating the crop losses due to fungal infections. Our investment estimation method explicitly factors in these opportunity costs by using the concept of the Modified Internal Rate of Return (MIRR) to calculate *the economically justifiable* R&D investments for the joint control of these five wheat fungal diseases.

We estimate that to achieve a 10% per year return on investment (the economic benchmark for public agricultural

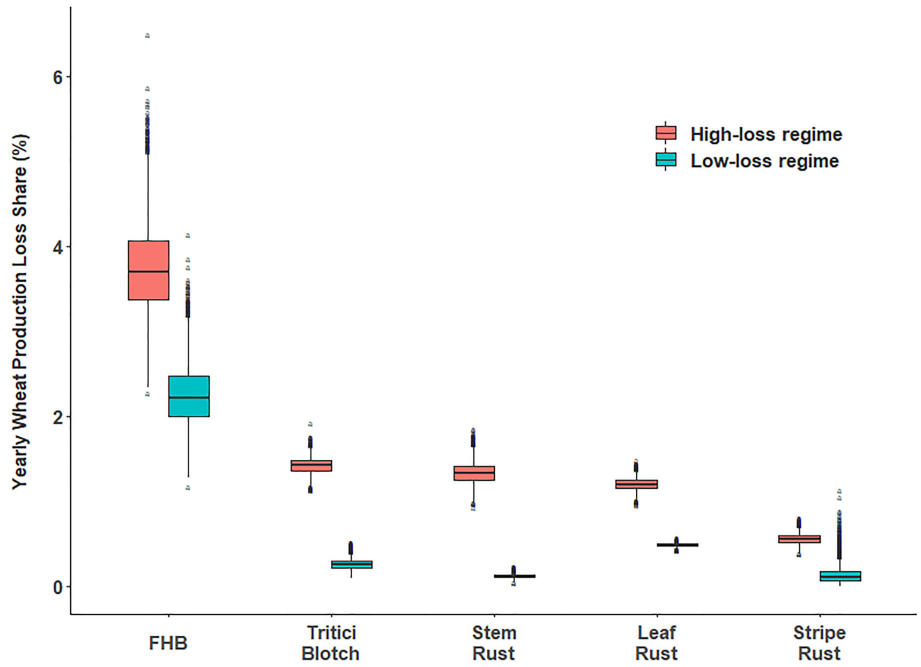

FIGURE 3
Distribution of simulated global yearly wheat production loss percentage attributable to selected wheat fungal diseases. Note: For the box plot, the lower and upper hinges correspond to the first and third quartiles (the 25th and 75th percentiles) with the middle line corresponds to the median from the distribution of yield losses. The upper (lower) whiskers extend from the upper (lower) hinge to the largest (smallest) value no further than 1.5 times of the inter-quartile range (distance between the first and third quartiles). Outliers are marked by black dots.

R&D worldwide, according to findings by Rao et al., 2020) would require investing between $350 million (based on the low-loss regime) and $974 million (high-loss regime) on research for just these five fungal diseases of wheat, let alone the other biotic threats affecting wheat and other crops (Figure 4, right-hand column). For comparison, the two left-hand bars in Figure 4 shows the estimated annual investment in public wheat research worldwide averaged over the period of 1980-2015 was $540 million per year for "non-pest & disease" R&D and $185 million per year for "pest & disease" related research, both in 2018 prices. Thus, our estimate implies that current spending on agricultural R&D for crop disease resistance is woefully inadequate and justifies a significant increase in funding on disease-related R&D for wheat by at least 2- to 5-fold.

Discussion

Fungal diseases have substantial negative consequences for global wheat production. Large shares of the world's wheat growing area are at risk from infection by each of the fungi, and the multi-peril risk is high, with around 75% of the area at risk of infection from at least four of the five fungal diseases in this study. The multi-peril risks are particularly high in Latin America and even more so in sub-Saharan Africa. Although sub-Saharan Africa produced only 1.1% of the world's wheat crop in 2019, that year it accounted for 5.4% of worldwide wheat consumption. It is also where large numbers of the world's poor and food insecure people now reside, and increasingly so in the decades ahead if we fail to promote the region's economic growth in general, and agricultural growth in particular. Here we estimate losses of upwards of $10.8 billion (2018 prices) on average, year in and year out for just this one crop and the specific set of biological threats we evaluated. Preventing these losses could provide sufficient calories to feed an additional 173 million people every year (for the high-loss regime), assuming per person calorie consumption at the 2018 global average rate reported by the U.N.'s Food and Agricultural Organization (2001 and 2021). Fungal and other pathogens also cause significant losses in other major food crops, such as corn, rice, and potato (Ristaino et al., 2021).

There is a large amount of economic literature on the rates-of-return to agricultural R&D. Rao et al. (2020) reviewed 3,426 estimates taken from 492 different studies and reported an overall benefit-cost ratio of 10:1 on average (i.e., every dollar invested in agricultural R&D returned a stream of benefits with a present value of 10 dollars). A benefit-cost ratio significantly greater than 1:1 indicates that governments would have profited

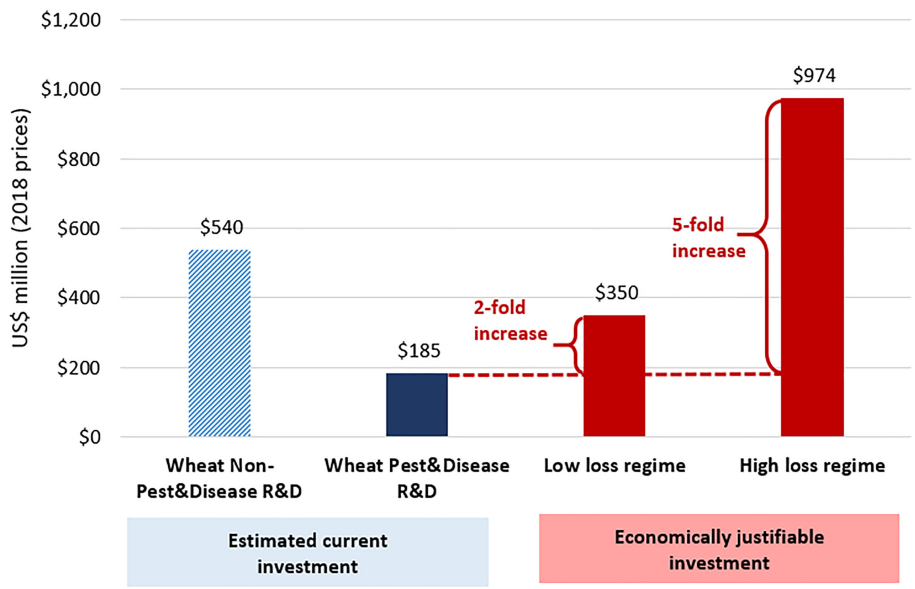

FIGURE 4
The Investment Bottom Line. All dollar estimates represent average annual values expressed in 2018 prices.

society by doing more agricultural R&D, compared with investment opportunities normally available to them. Alston et al. (2020, p. vi) argued that the totality of the considerable evidence on the size and nature of the payoffs, and the potential for future payoffs (see, e.g., Alston and Pardey, 2021) "… supports at least a doubling of the overall investment in agricultural R&D performed both in national and international agencies." Our results support a 2- to 5-fold increase in (public) R&D to mitigate fungal wheat pathogens, which at face value also implies placing a greater emphasis on reducing the risks associated with crop pests within the expanded portfolio of wheat research.

While the private sector accounts for an increasing share of agri-food R&D in aggregate (Pardey et al., 2016), the private presence is comparatively small in many low- and middle-income countries. Moreover, wheat improving research worldwide still has a significant public presence. For example, data underlying Chai et al. (2022) study of all the commercially grown wheat varieties in the U.S over the past century reveals that a large share of these varieties were bred by public agencies, and plant varietal improvement in Canada is still a largely public affair (Gray et al., 2017). And while the private sector has made significant in-roads to wheat breeding in Europe and the U.K. (see, e.g., Galushko and Gray, 2014), in Australia the shift towards privately-led crop improvement still involves complex collaborative research, funding and even co-ownership arrangements with public entities (Alston and Gray, 2013). Nonetheless, much of the fundamental and longer-term R-gene discovery and more basic research related to wheat diseases is conducted by public non-profit agencies throughout the world.

Other important investment questions involve who should pay for this increase in R&D funding, and how. Alston and Pardey (1996 and 2021) review many of the economic issues involved in these types of decisions, but from a global perspective, the bottom line is that the entire world's wheat crop is highly vulnerable to these fungal diseases, so all the world's wheat producers and consumers share in the benefits from dealing with these diseases. Thus, irrespective of whether the research is performed by national or international agencies, the funding is generating wheat innovations that have global collective value. And, similar to the COVID crisis still afflicting human health worldwide, crop pests that undermine plant health are capable of travelling great distances through wind patterns and *via* international trade and travel. Thus, solving the problem for, say, wheat stem rust infestations that impact farmers in the U.S. or Africa, means that solutions can be deployed for farmers elsewhere in the world. From an economic perspective, the R&D funding should be directed to the innovative efforts that are likely to deliver effective fungal resistance technologies the fastest and cheapest. However, given proper attention to technology access and use details, particular governments or donor agencies can be assured that funding this type of disease resistance research, even if the research is carried out by institutes or individuals located elsewhere in the world, will bear positive returns to local producers and consumers given the worldwide nature of many disease problems: a classic case of doing well by doing good (Tribe, 1991).

Of course, for these innovations to find their way onto farmers' fields requires much more than investing in the (pre-breeding) R&D required to produce durable disease resistance solutions. In stark contrast to COVID vaccine solutions that have worldwide applicability, genetic technologies that confer crop disease resistance must be bred into a myriad of locally adapted wheat varieties that are best suited to the diverse agroecological environments in which the crop is grown (see, e.g., Chai et al., 2022). Crucially, it is those myriad varieties, safeguarded with disease resistance, that must then find their way into the hands of the millions of farmers who grow the crop. Thus, complementary investments in rural infrastructure, epidemiological tracking of pest outbreaks, education, and timely and accurate information to farmers, input suppliers and crop breeders (who all play complementary roles in mitigating the impacts of reoccurring or newly emerging pest outbreaks) are crucial components of the innovation package required to achieve durable crop diseases resistance on the ground.

Methods

Assessing the spatial extent of multiperil pest risk

Based on prior work by GEMS Informatics personnel and collaborators over the past decade, we assembled and spatially concorded global maps of the climate suitability of a given locale to sustain each of the following five fungal wheat diseases: stem, stripe and leaf rust, fusarium head blight (FHB), and septoria tritici blotch (STB). Specifically, we drew on previously reported CLIMEX models for four fungal diseases, including stem rust (Pardey et al., 2013), stripe rust (Beddow et al., 2015), leaf rust (Chai et al., 2020), and FHB (Turkington et al., 2016). Additionally, a CLIMEX model for STB was developed under the auspices of the HarvestChoice initiative (see, e.g., Koo and Pardey, 2020). All five CLMEX model outputs used for this study are openly accessible on the Data Repository for U of MN (DRUM) system (see Data Availability). CLIMEX models map the suitability of the climate at a given locale to support the survival (for at least one generation) of each wheat pest (see, e.g., Sutherst and Maywald, 1985; Kriticos et al., 2015). The models represent each climate-suitable locale at 10 arc minute spatial grids (or 18.5 x 18.5 km pixel along the equator), for which we have 141,681 pixels representing the spatialized extent of wheat production worldwide sourced from Yu et al. (2020). We then calculated the extent of the spatial concordance of wheat area that was pest-free—in the sense that these pixels had climates considered unsuitable to sustain any of our five fungal diseases—and those pixels that may sustain at least one, two, three, and so on up to five of our target diseases. We report these as climate co-suitability counts to provide a straightforward indication of the multi-peril pest risk faced by wheat farmers around the world.

Assessing the probabilistic consequences of multiperil crop losses

In this study, estimating the *probabilistic* losses worldwide associated with each of the five fungal pathogens, as well as the likely combined losses from all five, is conceptually equivalent to comparing a no-disease yield distribution with yield distributions under different disease pressure and management practices. Specifically, as illustrated in Figure 2, differences between the red vs green distributions represent the high-loss (counterfactual) regime where crop protection is absent, while differences between the blue vs green distributions represent the low-loss (counterfactual) regime where certain crop protection measures were implemented, albeit not all entirely effective in eliminating all pest-induced losses. Practical implementation of these complex counterfactual regimes is impaired by limited and incomplete data, but we assembled or created the best available data sets and proceeded as follows.

To develop our statistical representation of the yield loss *distributions* for each of the diseases we sourced data from the USDA-Cereal Disease Laboratory (2020) for stem, stripe, and leaf rust; for FHB we used Crop Protection Network (2020), supplemented with Nganje et al. (2004); and for STB we also sourced data from Crop Protection Network (2020). Using these loss data, we applied a maximum goodness-of-fit estimation method implemented in the fitdist function in R (Delignette-Muller and Dutang, 2015) to estimate the probabilistic beta-distribution of losses associated with each of these diseases. The resulting disease-specific beta distributions are plotted in Supplementary Figure S1, where the vertical axis indicates the likelihood of a given yield loss as revealed along the horizontal axis. The general shape, but notably not the position, of each distribution is similar, indicating a high frequency of little to low losses in a given year, and low odds of especially high yield losses.

High-loss and low-loss regimes

Stem rust loss distribution: Following Pardey et al. (2013), we estimated two loss regimes for stem rust (caused by *Puccinia graminis*) to capture the high-loss distribution in the U.S. before 1960, a period subject to frequent stem rust epidemics, and a low-loss distribution in the U.S. spanning the post-1960 period when the deployment of resistant wheat varieties effectively mitigated crop losses associated with this pathogen.

Stripe rust loss distribution: In the U.S., losses from stripe rust (caused by *Puccinia striiformis f.* sp. *tritici*) were not significant prior to 1960 (Line, 2002; Beddow et al., 2015). From the 1960s to the early 2000s, stripe rust losses occurred

mainly in the Pacific Northwest region of the U.S. Beginning around 2000, there appeared to be an increase in stripe rust losses in the central U.S. states and a spread into the (south) eastern part of the country (Beddow et al., 2015). For stripe rust, we estimated two yield loss distributions, one based on yield loss data before 1960 (designated a low-loss regime), and one based on yield loss data after 1960 (a high-loss regime).

Leaf rust loss distribution: Following Chai et al. (2020), there are no obvious shifts in the frequency and magnitude of losses due to leaf rust (caused by *Puccinia triticina*) in the U.S. over the past century. Thus, to estimate a high-loss distribution for leaf rust we used the yield loss data reported by USDA-CDL for the entire 1919-2020 time period. To construct a low-loss distribution, we drew all the observations from the subset of 1919-2020 losses that were below 1%, with the assumption that under a low-loss regime leaf rust losses would not exceed 1%.

Fusarium head blight (FHB) loss distribution: In the U.S., we obtained two sets of state-level yield loss data for FHB (caused by *Fusarium graminearum*). For the period 1993-2001, Nganje et al. (2004) reported state-level wheat FHB losses for nine FHB affected states growing three wheat classes (hard red spring, durum, and soft red winter), where major yield losses began in 1993 and continued through 2001. Beginning in 2018, the Crop Protection Network (2020) report wheat disease losses throughout the U.S. and Canada, from which we sourced state-level FHB yield losses for the period 2018-2020. In the U.S., FHB losses in wheat during the 1990s were comparatively high as a result of substantial FHB outbreaks (Nganje et al., 2004), and were thus used to construct our high-loss regime, while losses since 2018 were relatively low according to the Fusarium Head Blight newsletters from the U.S. Wheat & Barley Scab Initiative (USWBSI, 2022), and thus used to construct our low-loss regime.

Septoria tritici blotch loss distribution: The distribution of losses from septoria tritici blotch (caused by *Zymoseptoria tritici*, also known as *Mycosphaerella graminicola*) in the U.S. was estimated using state-level data for the 2018-2020 period reported by the Crop Protection Network (2021). State-level loss data for the entire 2018-2020 period were used to represent the low-loss regime because the U.S. losses reported for septoria tritici blotch during this period were generally low. We then used the subset of losses above 1% to represent a hypothetical high-loss regime.

Probabilistic monte carlo simulations

Following Saari and Prescott (1985), we segmented the world into 15 epidemiological zones, with largely independent climatological patterns such that an epidemic in a given zone is likely to occur independently of epidemics in other zones (Beddow et al., 2013). Within each epidemiological zone, we geospatially intersected the HarvestChoice Spatial Allocation Model (SPAM) results for wheat with CLIMEX models for our targeted wheat fungal diseases to calculate the share of each zone, z, deemed suitable for wheat fungal disease d as

$$\beta_{x,d} = \frac{\left[\alpha_z'(GI_{z,d,i} \circ I_z) - \alpha_z'(GI_{z,d,n} \circ (I_z - 1))\right]}{\alpha_z' 1}$$

where $\boldsymbol{\alpha_z}$ is a vector of the total wheat production area in zone z's cells; $\boldsymbol{GI_{z,d,i}}$ is a vector of binary seasonal suitability indicators in zone z for disease d under an irrigation scenario (1 if suitable; 0 otherwise); $\boldsymbol{GI_{z,d,n}}$ is a vector of binary seasonal suitability indicators in zone z for disease d under the non-irrigated scenario (1 if suitable; 0 otherwise); $\boldsymbol{I_z}$ is a vector of binary indicators set to one if any wheat area in the corresponding cell was irrigated and zero otherwise; $\mathbf{1}$ is a vector of ones of the appropriate length, and " ∘ " is the operator indicating an element-by-element vector product.

With the disease-suitable area share $\beta_{z,d}$ identified, we then apply the loss distribution for each disease estimated above. Specifically, the proportional yield loss attributable to disease d can be represented by a random draw from their corresponding beta-distribution $l_d \sim Beta(a_d, b_d)$ and the overall yield loss from a set of multiple wheat fungal diseases can be calculated as:

$$l_z = 1 - \prod_d (1 - \beta_{z,d} l_d)$$

If the observed yield for zone z during year t is $Y_z^a t$ and the total proportional yield loss from all wheat fungal diseases is $l_{z,t}$, then the potential yield $Y_z^p t$ (i.e., the counterfactual yield absent all wheat fungal diseases) can be calculated as:

$$Y_{z,t}^p = \frac{Y_{z,t}^a}{1 - l_{z,t}}$$

The production losses for zone z and year t can then be calculated as:

$$L_{z,t} = (Y_{z,t}^p - Y_{z,t}^a) A_{z,t}$$

where $A_{z,t}$ is the wheat production area in zone z and year t.

Using projected zonal wheat production for the period 2010-2050 from the International Agricultural Prospects (*i*AP) model (Pardey et al., 2014), we applied two alternative loss regimes with different combinations of loss distributions. Using this procedure, we obtain probabilistic estimates of the global production losses attributable to the five wheat fungal diseases during the period 2020-2050 benchmarked on the two alternative loss regimes.

Economically justified R&D investment

To estimate the economically justifiable investment in R&D focused on avoiding the long-run crop losses associated with

these wheat fungal diseases, we drew on the modified internal rate of return (MIRR) concept presented by Hurley et al. (2014). Specifically, we estimated the annual investment in R&D for the period 1990-2050 that achieved at least a 10% MIRR per year with a probability of 95%. Mathematically, we find the value V that solves:

$$V(i^r, i^c, i^m) = max\left\{ v : Pr\left(\sqrt[60]{\frac{\sum_{t=2000}^{2050} p_t L_t^R (1+i^r)^{2050-t}}{\sum_{t=1990}^{2050} v(1+i^c)^{1990-t}}} - 1 \geq i^m \right) > 0.95 \right\}$$

where p_t is the price of wheat in year t, i^r is the reinvestment rate, i^c is the cost of capital, and i^m is the modified internal rate of return (MIRR). Here, we assume a 10-year research adoption lag to account for the latency in the adoption of new rust resistant wheat varieties. This equation calculates the annual investment amount for 1990 to 2050 that yields a MIRR of at least i^m (targeting 10 percent per year) with a probability of 0.95. Based on the MIRR method in Pardey et al. (2013), the underlying reinvestment rate i^r is taken to be 3 percent per year and the cost of capital rate i^c is set at 10 percent per year.

Data availability statement

Publicly available datasets were analyzed in this study. This data can be found here: The CLIMEX model outputs used for all five wheat fungal diseases are openly accessible through the Data Repository for U of MN (DRUM) system at https://doi.org/10.13020/0QSZ-W114; Yield losses from rust diseases in the U.S. were downloaded from https://www.ars.usda.gov/midwest-area/stpaul/cereal-disease-lab/docs/small-grain-losses-due-to-rust/small-grain-losses-due-to-rust/; Yield losses in the U.S. for other wheat diseases were sourced from https://loss.cropprotectionnetwork.org/crops/wheat-diseases; Other datasets generated during and/or analyzed as part of the current study are maintained on the GEMS Informatics Platform and can be requested from the corresponding author YC for use to replicate the findings of this study.

Author contributions

YC and PP co-led and designed the study. SS and YC compiled and processed the CLIMEX models for wheat fungal diseases. YC performed the numerical analyses. YC, PP, and DH contributed to the writing. All authors contributed to the article and approved the submitted version.

Funding

This work received funding support from 2Blades, the University of Minnesota's GEMS Informatics Center, and CIMMYT, the International Maize and Wheat Improvement Center. Prior work on the development of CLIMEX models received support from the International Science and Technology Practice and Policy (InSTePP) Center at the University of Minnesota and the Bill and Melinda Gates Foundation Grant # OPPGD1450 by way of the HarvestChoice initiative.

Acknowledgments

We thank Michael Kelleher from the 2Blades for his comments and edits. We thank Connie Chan-Kang of the GEMS Informatics Center for her research assistance.

Conflict of interest

The authors declare that the research was conducted in the absence of any commercial or financial relationships that could be construed as a potential conflict of interest.

Publisher's note

Supplementary material

The Supplementary Material for this article can be found online at: https://www.frontiersin.org/articles/10.3389/fpls.2022.1034600/full#supplementary-material

References

Alston, J. M., and Gray, R. S. (2013). Wheat research funding in Australia: The rise of public–private–producer partnerships. *Eurochoices* 12 (1), 30–34. doi: 10.1111/1746-692X.12017

Alston, J. M., and Pardey, P. G. (1996). *Making science pay: The economics of agricultural R&D policy* (Washington D.C: American Enterprise Institute Press).

Alston, J. M., and Pardey, P. G. (2021). "The economics of agricultural innovation," in *Handbook of agricultural economics*, vol. 5 . Eds. C. B. Barrett and D. R. Just (Amsterdam: Elsevier).

Alston, J. M., Pardey, P. G., and Rao, X. (2020). *The payoff to investing in CGIAR research* (Arlington, VA: SoAR Foundation).

Bebber, D. P., Ramotowski, M. A. T., and Gurr, S. J. (2013). Crop pests and pathogens move polewards in a warming world. *Nat. Clim. Change* 3, 985–988. doi: 10.1038/nclimate1990

Beddow, J. M., Hurley, T. M., Kriticos, D. J., and Pardey, P. G. (2013). "Measuring the global occurrence and probabilistic consequences of wheat stem rust," in *HarvestChoice technical note* (St. Paul, MN: HarvestChoice). Available at: http://www.croppest.org/purl/20131.

Beddow, J. M., Pardey, P. G., Chai, Y., Hurley, T. M., Kriticos, D. J., Braun, H.-J., et al. (2015). "Research investment implications of shifts in the global geography of wheat stripe rust". *Nat. Plants.* 1 (10), 15132. doi: 10.1038/nplants.2015.132

Chai, Y., Pardey, P. G., Hurley, T. M., Senay, S. D., and Beddow, J. M. (2020). A probabilistic bio-economic assessment of the global consequences of wheat leaf rust. *Phytopathology*. 110 (12), 1886–1996 doi: 10.1094/PHYTO-02-20-0032-R

Chai, Y., Pardey, P. G., and Silverstein, K. A. T. (2022). "Scientific selection: A century of increasing crop varietal diversity in U.S. wheat," in *Staff paper P22-05*. (St Paul, MN: International science and technology practice and policy (InSTePP) center and department of applied economics, University of Minnesota).

Chaloner, T. M., Gurr, S. J., and Bebber, D. P. (2021). Plant pathogen infection risk tracks global crop yields under climate change. *Nat. Climate Change* 11 (8), 710–715. doi: 10.1038/s41558-021-01104-8

Crop Protection Network (2020) *Estimates of corn, soybean, and wheat yield losses due to disease: an online tool*. Available at: https://loss.cropprotectionnetwork.org/.

Delignette-Muller, M. L., and Dutang, C. (2015). Fitdistrplus: An r package for fitting distributions. *J. Stat. Software.* 64 (4), 1–34. doi: 10.18637/jss.v064.i04

FAO (2020) *FAOSTAT statistics database: Food balance sheets*. Available at: http://www.fao.org/faostat/en/#data/FBS (Accessed April 25th, 2022).

Figueroa, M., Hammond-Kosack, K. E., and Solomon, P. S. (2018). A review of wheat diseases-a field perspective: A review of wheat diseases. *Mol. Plant Pathol.* 19 (6), 1523–1536. doi: 10.1111/mpp.12618

Galushko, V., and Gray, R. (2014). Twenty five years of private wheat breeding in the UK: Lessons for other countries. *Sci. Public Policy* 41, 765–779. doi: 10.1093/scipol/scu004

Gray, R. S., Kingwell, R. S., and Galushko and K. Bolek, V. (2017). Intellectual property rights and Canadian wheat breeding for the 21st century. *Can. J. Agric. Econ.* 65, 667–691. doi: 10.1111/cjag.12142

Hurley, T. M., Rao, X., and Pardey, P. G. (2014). Re-examining the reported rates of return to food and agricultural research and development. *Am. J. Agric. Econ.* 96 (5), 1492–1504. doi: 10.1093/ajae/aau047

Joglekar, A. B., Pardey, P. G., and Wood-Sichra, U. (2016). *Where in the world are crops grown*? HarvestChoice Brief (St. Paul, MN, HarvestChoice).

Khoury, C. K., Achicanoy, H. A., Bjorkman, A. D., Navarro-Racines, C., Guarino, L., Flores-Palacios, X., et al. (2016). Origins of food crops connect countries worldwide. *Proc. R. Soc. B.* 283, 20160792. doi: 10.1098/rspb.2016.0792

Koo, J., and Pardey, P. G. (2020). *HarvestChoice: Supporting strategic investment choices in agricultural technology development and adoption* (Washington, D.C: International Food Policy Research Institute). doi: 10.2499/p15738coll2.133807

Kriticos, D., Maywald, G., Yonow, T., Zurcher, E., Herrmann, N., and Sutherst, B. (2015). *CLIMEX version 4: Exploring the effects of climate on plants, animals and diseases* (Canberra: CSIRO).

Line, R. F. (2002). Stripe rust of wheat and barley in north America: a retrospective historical review. *Annu. Rev. Phytopathol.* 40 (1), 75–118. doi: 10.1146/annurev.phyto.40.020102.111645

Nganje, W. E., Kaitibie, S., Wilson, W. W., Leistritz, F. L., and Bangsund, D. A. (2004). *Economic impacts of fusarium head blight in wheat and barley: 1993-2001*. In Agribusiness and Applied Economics Report No 538. (Fargo, ND: Department of Agribusiness and Applied Economics, North Dakota State University of Minnesota). doi: 10.22004/ag.econ.23627

Oerke, E.-C. (2006). Crop losses to pests. *J. Agric. Sci.* 144 (1), 31–43. doi: 10.1017/S0021859605005708

Pardey, P. G., and Beddow, J. M. (2013). *Agricultural innovation: The united states in a changing global reality* (CCGA Report Chicago Council on Global Affairs). doi: 10.1126/science.122970

Pardey, P. G., Beddow, J. M., Hurley, T. M., Beatty, T. K. M., and Eidman, V. R. (2014). A bounds analysis of world food futures: global agriculture through to 2050. *Aust. J. Agric. Resour. Econ.* 58 (4), 571–589. doi: 10.1111/1467-8489.12072

Pardey, P. G., Beddow, J. M., Kriticos, D. J., Hurley, T. M., Park, R. F., Duveiller, E., et al. (2013). Right-sizing stem-rust research. *Science* 340 (6129), 147–148.

Pardey, P. G., Chan-Kang, C., Dehmer, S. P., and Beddow, J. M. (2016). Agricultural R&D is on the move. *Nature* 15 (537), 301–303. doi: 10.1038/537301a

Pardey, P. G., Joglekar, A., Chan-Kang, C., Liebenberg, F., Luby, I., Senay, S. D., et al. (2022). "What do we know about (procured) input use in African agriculture?," in *InSTePP working paper* (St Paul, MN: Department of Applied Economics, University of Minnesota).

Rao, X., Hurley, T. M., and Pardey, P. G. (2020). Recalibrating the reported returns to agricultural R&D: what if we all heeded griliches? *Aust. J. Agric. Resour. Econ.* 64 (3), 977–1001. doi: 10.1111/1467-8489.12388

Reynolds, M. P., Braun, H.-J., Pietragalla, J., and Ortiz, R. (2007). Challenges to international wheat breeding. *Euphytica* 157 (3), 281–285. doi: 10.1007/s10681-007-9505-4

Ristaino, J. B., Anderson, P. K., Bebberd, D. P., Braumane, K. A., Cunniffe, N. J., Fedoroff, N. V., et al. (2021). The persistent threat of emerging plant disease pandemics to global food security. *PNAS* 118 (23), e2022239118. doi: 10.1073/pnas.2022239118

Saari, E. E., and Prescott, J. M. (1985). "World distribution in relationship to economic losses," in *The cereal rusts. volume II. disease, distribution, epidemiology, and control*. Eds. A. P. Roelfs and W. R. Bushnell (Orlando: Academic Press), 257.

Savary, S., Willocquet, L., Pethybridge, S. J., Esker, P., McRoberts, N., and Nelson, A. (2019). The global burden of pathogens and pests on major food crops. *Nat. Ecol. Evol.* 3 (3), 430. doi: 10.1038/s41559-018-0793-y

Sheahan, M., and Barrett, C. B. (2017). Ten striking facts about agricultural input use in Sub-Saharan Africa. *Food Policy* 67, 12–25. doi: 10.1016/j.foodpol.2016.09.010

Sutherst, R. W., and Maywald, G. F. (1985). A computerised system for matching climates in ecology. *Agricult. Ecosyst. Environ.* 13 (3), 281–299. doi: 10.1016/0167-8809(85)90016-7

Thompson, J. N., and Burdon, J. J. (1992). Gene-for-Gene coevolution between plants and parasites. *Nature* 360, 121–125. doi: 10.1038/360121a0

Tribe, D. E. (1991). *Doing well by doing good: agricultural research: feeding and greening the world* (Leichhardt, N.S.W.: Parkville, Vic: Pluto Press; Crawford Foundation for International Agricultural Research).

Turkington, T. K., Petran, A., Yonow, T., and Kriticos, D. J. (2016). "Fusarium graminearum (Fusarium head blight)," in *HarvestChoice pest geography* (St. Paul, MN: InSTePP-HarvestChoice).

U.N. Department of Economic and Social Affairs, Population Division (2022). *World population prospects 2022: Summary of results* (New York: United Nations).

U.N. Food and Agricultural Organization (2001). *Food balance sheets-annex food composition tables* (Rome: FAO). Available at: http://www.fao.org/3/x9892e/x9892e00.pdf.

U.N. Food and Agricultural Organization (2021). *FAOSTAT* (Rome: FAO). Available at: http://www.fao.org/faostat/en/#data/FBS.

USDA-Cereal Disease Laboratory (2020). "*Small grain losses due to Rust: USDA ARS*," in Small grain losses due to rust. (St. Paul, MN, Cereal Disease Lab) Available at: https://www.ars.usda.gov/midwest-area/stpaul/cereal-disease-lab/docs/small-grain-losses-due-to-rust/small-grain-losses-due-to-rust/.

USDA-NASS (2018). *2017 agricultural chemical use survey: Wheat. no 2018-5* (Washington, D.C: USDA, National Agricultural Statistical Service). Available at: https://www.nass.usda.gov/Surveys/Guide_to_NASS_Surveys/Chemical_Use/2012_Wheat_Highlights/.

USDA-RMA (2021). *United states department of agriculture risk management agency summary of business* (Washington, D.C: USDA, Agriculture Risk Management Agency). Available at: https://www.rma.usda.gov/SummaryOfBusiness.

USWBSI (2022) *US Wheat & barley scab initiative newsletters*. Available at: https://www.scabusa.org/news#newsletters.

Yu, Q., You, L., Wood-Sichra, U., Ru, Y., Joglekar, A. K. B., Fritz, S., et al. (2020). A cultivated planet in 2010 – part 2: The global gridded agricultural-production maps. *Earth Syst. Sci. Data* 12 (4), 3545–3572. doi: 10.5194/essd-12-3545-2020

frontiers | Frontiers in Microbiology

TYPE Original Research
PUBLISHED 11 November 2022
DOI 10.3389/fmicb.2022.1045796

OPEN ACCESS

EDITED BY
Paul Christiaan Struik,
Wageningen University and Research,
Netherlands

REVIEWED BY
Antonin Dreiseitl,
Agricultural Research Institute Kromeriz,
Czechia
Hongjie Li,
Institute of Crop Sciences (CAAS),
China

*CORRESPONDENCE
Wei Liu
wliusdau@163.com
Jieru Fan,
fanjieru@caas.cn

SPECIALTY SECTION
This article was submitted to
Microbe and Virus Interactions with Plants,
a section of the journal
Frontiers in Microbiology

RECEIVED 16 September 2022
ACCEPTED 25 October 2022
PUBLISHED 11 November 2022

CITATION
Zhang M, Wang A, Zhang C, Xu F, Liu W, Fan J, Ma Z and Zhou Y (2022) Key infection stages defending heat stress in high-temperature-resistant *Blumeria graminis* f. sp. *tritici* isolates.
Front. Microbiol. 13:1045796.
doi: 10.3389/fmicb.2022.1045796

Key infection stages defending heat stress in high-temperature-resistant *Blumeria graminis* f. sp. *tritici* isolates

Meihui Zhang[1,2], Aolin Wang[1], Cheng Zhang[1,3], Fei Xu[1,4], Wei Liu[1]*, Jieru Fan[1]*, Zhanhong Ma[2] and Yilin Zhou[1]

[1]State Key Laboratory for Biology of Plant Diseases and Insect Pests, Institute of Plant Protection, Chinese Academy of Agricultural Sciences, Beijing, China, [2]Department of Plant Pathology, College of Plant Protection, China Agricultural University, Beijing, China, [3]Department of Plant Protection, College of Agriculture and Foresty Science and Technoloy, Hebei North University, Zhangjiakou, China, [4]Institute of Plant Protection, Henan Academy of Agricultural Sciences, Key Laboratory of Integrated Pest Management on Crops in Southern Part of North China, Ministry of Agriculture and Rural Affairs of the People's Republic of China, Zhengzhou, China

With the increase of temperature in the winter wheat-growing regions in China, the high-temperature-resistant *Blumeria graminis* f. sp. *tritici* (*Bgt*) isolates developed in the fields. To clarify the key infection stages and the roles of heat shock protein (HSP) genes of high-temperature-resistant *Bgt* isolates defending high temperature, 3 high-temperature-resistant and 3 sensitive *Bgt* isolates were selected from 55 isolates after determination of temperature sensitivity. And then they were used to investigate the infection stages and the expression levels of *HSP* genes, including *Bgthsp60*, *Bgthsp70*, *Bgthsp90,* and *Bgthsp104*, at 18°C and 25°C. The formation frequency of abnormal appressoria and inhibition rate of haustoria formation of high-temperature-resistant isolates at 25°C were lower than those of high-temperature-sensitive isolates, while major axis of microcolonies of high-temperature-resistant isolates was higher than those of high-temperature-sensitive isolates at 25°C. The results indicated that haustoria formation and hyphal expansion were the key infection stages of defense against heat stress in high-temperature-resistant isolates. Further analyses of *HSP* genes found the expression levels of *Bgthsp60* and *Bgthsp70c* were upregulated at 24 and 72h post-inoculation in high-temperature-resistant isolates, while no significant difference was observed for *Bgthsp90* and *Bgthsp104* genes. Taken together, the basis of high-temperature-resistant *Bgt* isolates is associated with induced expression of *Bgthsp60* and *Bgthsp70c* response to heat stress in haustoria formation and hyphal expansion stages.

KEYWORDS

***Blumeria graminis* f. sp. *tritici*, high-temperature-resistant isolate, infection stage, histological observation, expression level, heat shock protein**

Introduction

Temperature is an important abiotic factor influencing several plant pathogens as various features, such as geographical range, growth rates in population, infection stages, and ability to spread, ultimately affects the prevalence of the disease (Coakley et al., 1999; Velásquez et al., 2018). For example, severity and frequency of wheat yellow rust caused by *Puccinia striiformis* f. sp. *tritici* (*Pst*) increased in association with increased winter temperatures and lower spring temperatures in the USA (Coakley, 1979). Prevalence of *Pst* was decreased with increased average annual temperatures from 1950 to 1995 (Luck et al., 2011). Increased severity of wheat spot blotch caused by *Cochliobolus sativus* was associated with increased average night-time temperatures in South Asia (Sharma et al., 2007). Needle blight of pine caused by *Dothistroma septosporum* was moving north with increasing temperature and precipitation in Canada (Woods et al., 2005). To survive temperature increasing, organisms, including plant pathogens, have developed the ability to adapt changing environment by constantly adjusting their phenotype on biological, ecological, and evolutionary processes (Knies et al., 2006; Knies and Kingsolver, 2010). For instance, high temperature affected conidia germination of *Pst*, *P. recondita* f. sp. *tritici*, *Beauveria bassiana*, and *Leveillula taurica* (de Vallavieille-Pope et al., 1995; Guzman-Plazola et al., 2003; Devi et al., 2005), appressoria formation in *Colletotrichum gloeosporioides* (Estrada et al., 2000), germ tube elongation of *L. taurica* (Guzman-Plazola et al., 2003), and haustoria formation in *Oidium heveae, Podosphaera xanthii*, and *Golovinomyces orontii* (Trecate et al., 2019; Cao et al., 2021). In molecular level, heat shock proteins (HSPs) resisted the effects of heat stress by protecting proteins from aggregation and degradation in many fungi (Tiwari et al., 2015). *HSP* genes in fungi played important roles when subjected to heat stress, such as HSP60 in *Aspergillus fumigatus* and *A. terreus* (Raggam et al., 2011), HSP70 in *Trichoderma harzianum* (Montero-Barrientos et al., 2008), HSP90 in *Fusarium graminearum* (Bui et al., 2016), and HSP104 in *Saccharomyces cerevisiae* (Parsell et al., 1994).

Wheat powdery mildew is a regionally epidemic disease, caused by the parasitic fungus *Blumeria graminis* f. sp. *tritici* (*Bgt*), which over-summer in cool, high-altitude wheat-growing areas in China. As the mean monthly atmospheric temperature of the major wheat-growing areas in China had increased from 1970 to 2012 by a mean 0.329°C per decade (Tang et al., 2017), the minimum altitude for over-summering of *Bgt* decreased during the disease survey (Li et al., 2013), suggesting that high-temperature-resistant isolates exist in the fields. Wan's data proved this hypothesis, temperature sensitivity distribution of *Bgt* isolates in the fields in China was abnormal (Wan et al., 2010). However, the key infection stages of defense against heat stress in high-temperature-resistant *Bgt* isolates and the role of *HSP* genes in key infection stages remain unknown.

In this study, conidia germination, appressoria formation, haustoria formation, and hyphal expansion of *Bgt* isolates with different temperature sensitivity at 18°C and 25°C were investigated. And then expression levels of *HSP* genes were analyzed in these infection stages, including *Bgthsp60*, *Bgthsp70*, *Bgthsp90,* and *Bgthsp104*. The purposes of the present study were to clarify the key infection stages of *Bgt* isolates affected by high temperature and roles of *HSP* genes in response to heat stress. These results will help us to understanding the molecular basis of high thermal resistance mechanism in *Bgt*.

Materials and methods

Isolates and cultivation

Bgt-infected wheat leaves were collected from fields in Beijing, Shaanxi, Henan, and Yunnan province/city in China. After isolation and purification as described previously (Xu et al., 2014), 55 isolates were used in this study (Table 1). These isolates were reproduced on seedlings of highly susceptible wheat cultivar 'Jingshuang16', which has no effective genes against Chinese *Bgt* isolates. Briefly, seeds were sown in a Φ 5 cm glass tube covered with 5 layers of gauze to prevent accidental contamination. Conidia of *Bgt* isolates were used to inoculate on seedlings at one-leaf stage and incubated in a growth chamber (Panasonic, Ehime-ken, Japan, temperature fluctuation range: ±0.5°C) with a 16-h-light/8-h-dark cycle at 18°C.

Temperature sensitivity test

Temperature sensitivity was tested using seedling sensitivity assays. Briefly, conidia of *Bgt* isolates were used to inoculate on wheat seedlings and incubated in growth chamber at 18°C, 22°C, 24°C, 26°C, and 28°C, respectively, with 18°C as the reference incubation temperature. For each temperature, 15 wheat seedlings (one leaf seedling stage) were inoculated. Disease severity (percentage of diseased area to total leaf area) was recorded at 10 days post inoculation (dpi). Disease inhibition rate (DIR) was calculated by (1−average disease severity in treatment temperature/average disease severity at 18°C) × 100%. The linear regression equation was constructed with culture temperature (X) as dependent variables and DIR (Y) as independent variables as follows:

$$Y = a\,X + b$$

ET_{50} represented the temperature at which the DIR (Y) reached 50%.

TABLE 1 Information of *Blumeria graminis* f. sp. *tritici* isolates used in this study.

Number	Name of isolate	Collection site	Latitude	Longitude	Altitude / m	Collection date
1	13–14–7-2-2	Shaanxi (12)	34°11′	107°40′	669	2012.12.26
2	13–14–7-1-1		34°11′	107°40′	669	2012.12.26
3	13–14–1-3-1		34°34′	108°03′	581	2012.12.26
4	13–14–3-1-1		34°52′	109°56′	352	2012.12.26
5	13–14–1-2		35°14′	110°13′	662	2012.12.26
6	13–14–3-3		34°52′	109°56′	352	2012.12.26
7	13–14–1-3-2		34°52′	109°56′	352	2012.12.26
8	13–14–2-6-1		34°52′	109°56′	413	2012.12.26
9	13–14–2-1		34°52′	109°56′	413	2012.12.26
10	13–14–1-1-1		35°14′	110°13′	662	2012.12.26
11	13–14–8-2-2		34°11′	104°40′	669	2012.12.26
12	13–14–9-1		35°51′	109°30′	473	2012.12.26
13	13–1–5-5-1-2	Yunnan (11)	25°12′	100°18′	1,695	2013.04.06
14	13–1–1-1		23°54′	100°05′	1,455	2013.02.25
15	13–1–1-3		23°54′	100°05′	1,455	2013.02.25
16	13–1–2-1		25°06′	102°71′	–	2013.02.25
17	13–1–4-1-1-1		25°08′	99°11′	1,658	2013.04.05
18	13–1–4-1-2-2		25°08′	99°11′	1,658	2013.04.05
19	13–1–3-1		23°54′	100°05′	1,455	2013.02.25
20	13–1–4-1-1-2		25°08′	99°11′	1,658	2013.04.05
21	13–1–2-2		25°06′	102°71′	-	2013.02.25
22	13–1–5-5-1-1		25°12′	100°18′	1,695	2013.04.06
23	13–1–4-1-3-1		25°08′	99°11′	1,658	2013.04.05
24	13–11–4-2-2-2	Henan (15)	34°21′	110°45′	678	2013.04
25	13–11–4-2-2-1		34°21′	110°45′	678	2013.04
26	13–11–3-1-2-1		34°40′	113°12′	343	2013.04
27	13–11–1-2-3		34°40′	113°12′	343	2013.04
28	13–11–2-1-1		34°21′	110°45′	678	2012.12.28
29	Z-13–11–31–1-1		34°48′	114°21′	76	2012.5.24
30	13–11–1-2-2		34°40′	113°12′	343	2013.04
31	13–11–3-1-1-1		34°41′	113°13′	213	2013.04
32	13–11–4-2-1-1		34°21′	110°45′	678	2013.04
33	13–11–4-2-1-3		34°21′	110°45′	678	2013.04
34	13–11–2-2-3		34°21′	110°45′	678	2013.04
35	13–11–1-1-3		34°40′	113°12′	343	2013.04
36	13–11–2-3-2		34°21′	110°45′	678	2013.04
37	13–11–1-1-2		34°40′	113°12′	303	2012.12.25
38	13–11–2-2-2		34°21′	110°45′	678	2013.04
39	13–10–11–1-2	Beijing (17)	39°34′	115°42′	115	2013.05.31
40	13–10–2-3-1		39°34′	115°42′	115	2013.05.31
41	13–10–11–1-1		39°34′	115°42′	115	2013.05.31
42	13–10–2-2-3		39°34′	115°42′	115	2013.05.31
43	13–10–5-3-2		39°34′	115°42′	115	2013.05.31
44	13–10–2-3-2		39°34′	115°42′	115	2013.05.31
45	13–10–5-2-2		39°34′	115°42′	115	2013.05.31
46	13–10–2-1-2		39°34′	115°42′	115	2013.05.31
47	13–10–3-1-2		39°34′	115°42′	115	2013.05.31
48	Z-13–10-1-6-1		39°34′	115°42′	115	2013.05.31
49	13–10–2-2-2		39°34′	115°42′	115	2013.05.31
50	13–10–5-3-1		39°34′	115°42′	115	2013.05.31

(Continued)

TABLE 1 (Continued)

Number	Name of isolate	Collection site	Latitude	Longitude	Altitude / m	Collection date
51	13–10–5-1-1		39°34′	115°42′	115	2013.05.31
52	13–10–3-2-3		39°34′	115°42′	115	2013.05.31
53	13–10–3-2-1		39°34′	115°42′	115	2013.05.31
54	13–10–3-2-2		39°34′	115°42′	115	2013.05.31
55	13–10–2-2-1		39°34′	115°42′	115	2013.05.31

The system of screening high-temperature-sensitive and resistant isolates

To screen the high-temperature-sensitive and resistant *Bgt* isolates, ET_{50} and DIR at 26°C were used as two indictors. First, *Bgt* isolates with the ET_{50} less than 24°C and more than 25°C were classified as candidate high-temperature-sensitive and candidate high-temperature-resistant isolates, respectively. Then, the candidate isolates with high DIR at 26°C were considered high-temperature-sensitive isolates, and those with low DIR at 26°C were considered high-temperature-resistant isolates.

Reaction of *Bgt* high-temperature-sensitive and resistant isolates to high temperature at infection stages

The temperature ranging from 15°C to 22°C is considered the optimum temperature for development of *Bgt* (Last, 1963), while *Bgt* is rarely grown at 26°C on each leaf segment. Therefore, 25°C, a sublethal high temperature was used as the heat stress treatment, and 18°C was used as the reference temperature in histological observation and *HSPs* expression analyses. For histological observation assay of *Bgt* during infection stages, one-leaf seedlings were cut into 3.5 cm-long segments. Ninety-six leaf segments were floated on a water agar amended with 60 μg/ml benzimidazole in 10 × 10 cm plates. Two plates were evenly inoculated with around 40 mg of conidia (collected and quantified to 100 μl using a 1.5 ml Eppendorf tube) of a single isolate using a settling tower. Plates were incubated at 18°C and 25°C, respectively. Conidia germination, appressoria formation (normal and abnormal appressoria formation), haustoria formation, and hyphal expansion were examined at 8, 24, 48, and 72 h post-inoculation (hpi). Glass slide was used to catch spores during inoculation to estimate the inoculation density.

To test conidia germination, about 100 *Bgt* conidia on each leaf segment were randomly selected and the number of conidia with primary germ tubes was counted at 8 hpi. For testing appressoria formation, the number of normal and abnormal appressoria was recorded for about 100 germinated conidia on each leaf segment at 24 hpi. In addition, the length of appressorial germ tube (AGT; 24 hpi) was measured using CellSens Dimension software. The formation frequency of haustoria was calculated by the percentage of the number of haustoria to the number of inoculated spores on each leaf segment (80 mm^2 areas) at 48 hpi. Inhibition rate of haustoria formation was calculated according to the following formula:

$$\text{Inhibition rate of haustoria formation}(\%) = \left(1 - \text{formation frequencies of haustoria at } 25°C / \text{formation frequencies of haustoria at} 18°C\right) \times 100.$$

The major axis of the microcolonies was presented by the average hyphal expansion width of 30 microcolonies on each leaf segment at 72 hpi using a microscope at 100× magnification. Disease severities of five leaf segments were measured at 10 dpi. Three independent repeats were performed for statistical analysis.

Staining and histological observation

For histological observation assay of *Bgt* during infection stages, infected leaf segments by *Bgt* isolates were stained with Wheat germ agglutinin (WGA) conjugated to fluorescein isothiocyanate (Sigma-Aldrich, St. Louis, MO, USA) as described previously (Ayliffe et al., 2011). After decolorating in ethanol/acetic acid (1:1 v/v), infected leaf segments were cleared in saturated chloral hydrate until translucent, followed by soaking in 1 M KOH for 1 h and neutralized in 50 mM Tris–HCl (pH 7.5). These samples were stained with a 20 μg/ml solution of WGA, followed by rinsing with distilled water. Histological observation was conducted on fluorescence microscope Olympus BX61 (Olympus Corporation, Tokyo, Japan) with blue light excitation (450–480 nm).

Identification of *hsp60*, *hsp70*, *hsp90*, and *hsp104* genes in *Bgt*

To identify *HSP* genes of *Bgt*, amino acid sequences of HSP60, HSP70, HSP90, and HSP104 of *Saccharomyces cerevisiae* and *Aspergillus nidulans* were employed as queries to search the *Bgt* genome under the NCBI accession GCA_900519115.1 (Wicker et al., 2013). All the sequences were submitted to Conserved

Domains Database (CDD) to confirm the conserved domains of HSP family in *Bgt*.[1] WoLF PSORT was used to predict protein subcellular localization.[2]

RNA isolation and quantitative real-time PCR

To analyze gene expressions of *Bgthsp60*, *Bgthsp70* (*Bgthsp70a*, *Bgthsp70b,* and *Bgthsp70c*), *Bgthsp90*, and *Bgthsp104* (*Bgthsp104a* and *Bgthsp104b*), the detached leaf segments were inoculated with conidia and incubated at 18°C and 25°C, respectively, and then collected and snap frozen in liquid nitrogen at 0, 24, 48, and 72 hpi. Total RNA was extracted with Trizol reagent (Invitrogen, Camarillo, CA, United States). The first-strand cDNA was synthesized with FastKing One-Step RT-PCR Kit (TIANGEN, Beijing, China). Real-time PCR amplifications were conducted with TranStart Top Green qPCR SuperMix (TRANSGEN BIOTECH, Beijing, China) and performed on ABI 7500 real-time PCR system (Applied Biosystems Inc., Foster City, CA, United States). Relative expressions were calculated using the $2^{-\triangle\triangle CT}$ method (Livak and Schmittgen, 2001) with β-tubulin as reference gene and 0 hpi of the one independent repeats of 13–10–3-2-2 as reference sample. The primers used for quantitative PCR were listed in Table 2. Three independent repeats were performed for statistical analysis.

Data analysis

Two-way analysis of variance (ANOVA) with SAS software version 9.4 (SAS Institute Inc., Cary, NC, USA) was used to assess the difference in conidia germination frequencies, formation frequencies of appressoria and abnormal appressoria, haustoria formation frequencies, lengths of AGT, major axis of the microcolonies, disease severity, and genes expression levels between two culture temperatures or high-temperature-sensitive and resistant isolates. One-way ANOVA was used to test the effect of temperature on inhibition rate of haustoria formation.

Results

Assessments of high-temperature-sensitive and resistant isolates

Temperature sensitivity tests showed that ET_{50} of the 55 *Bgt* isolates ranged from 22.20°C to 25.77°C, and mean ET_{50} was 24.57 ± 0.71°C (Table 3). Depending on the discrimination system, 11 isolates with ET_{50} less than 24°C were classified as candidates of high-temperature-sensitive isolates, and 18 isolates with ET_{50} greater than 25°C were classified as candidates of high-temperature-resistant isolates. The DIR at 26°C of those candidate high-temperature-sensitive isolates ranged from 51.54% to 98.78%, while those candidate high-temperature-resistant isolates ranged from 20.91% to 82.64% (Figure 1). Three isolates with more than 85% DIR at 26°C were selected as high-temperature-sensitive isolates, and three isolates with less than 60% DIR at 26°C were selected as high-temperature-resistant isolates (Table 3). And then, the six isolates were used in histological observation.

Histological observation of infection stages of *Bgt* isolates

For both high-temperature-sensitive and resistant isolates incubated at 18°C, conidia germination started at 30 min post inoculation, but most of the conidia completed germination at 8 hpi, and the average germination frequency reached about 76.46% (Supplementary Table S1). About 85.22% germinated conidia had formed appressoria at 24 hpi (Figure 2A; Supplementary Table S1), after that about 12.06% appressoria were deformed (Supplementary Table S1). The abnormal appressoria were usually multi-lobed or absence of AGT hooking leading to elongation of the AGT (Figures 2B,C). Totally, around 8.46% appressoria developed to form primary haustoria (Figure 2D; Supplementary Table S1) and developed into mature haustoria with a finger-like structure at 48 hpi (Figure 2E). Then, the secondary hyphae developed from the appressoria and expanded to form microcolonies at 72 hpi (Figure 2F).

TABLE 2 Primers used in this study.

Gene name	Primer name	Primer sequence (5′-3′)
Bgthsp60	RT-*Bgt hsp60a*-F	CCGAAACAGTCAAGAATGTGG
	RT-*Bgt hsp60a*-R	CGCTCGTCGTGATGTCTC
Bgthsp70a	RT-*Bgt hsp70a*-F	CCCTTCATTACAGCAGACTCTTC
	RT-*Bgt hsp70a*-R	CATCCTTCAGTGCCTTTCG
Bgthsp70b	RT-*Bgt hsp70b*-F	GCTTACTTCAACGATTCGCA
	RT-*Bgt hsp70b*-R	CCTTCTTCAATGGTCAACAGG
Bgthsp70c	RT-*Bgt hsp70c*-F	GGTGCTGCTGTTCAGGGTG
	RT-*Bgt hsp70c*-R	CGGTGTTTCTTGGGATGAGC
Bgthsp90	RT-*Bgt hsp90a*-F	CCCTCTGACATCAACGCTG
	RT-*Bgt hsp90a*-R	TTGGGCACGAATAGGATTG
Bgthsp104a	RT-*Bgt hsp104a*-F	CAACGACTTTAGCAGAATACCG
	RT-*Bgt hsp104a*-R	CCTCGCAGGATAGACACCG
Bgthsp104b	RT-*Bgt hsp104b*-F	GCGACCTACAGCAATCGG
	RT-*Bgt hsp104b*-R	TGCGGCTTCTTCCTGACA
β-tubulin	β-tubulin-F	GACACTGTTGTTGAGCCATACA
	β-tubulin-R	GACATTACGGCAGACACCAA

1 https://www.ncbi.nlm.nih.gov/cdd

2 https://wolfpsort.hgc.jp/

TABLE 3 ET_{50} and disease inhibition rate (DIR) at 26°C of 55 *B. graminis* f. sp. *tritici* isolates.

Number	Collection site	Name of isolate	ET_{50}/°C	Disease inhibition rate/%	Number	Collection site	Name of isolate	ET_{50}/°C	Disease inhibition rate/%
1	Yunnan	13–1–5-5-1-2	23.94	79.49	29	Shannxi	**13–14–7-2-2**	**23.44**	**88.35**
2		13–1–1-1	23.57	79.81	30		13–14–7-1-1	24.28	81.08
3		13–1–1-3	24.86	60.14	31		13–14–1-3-1	24.31	69.16
4		13–1–2-1	23.51	62.16	32		13–14–3-1-1	24.38	82.61
5		**13–1–4-1-1-1**	**25.29**	**57.41**	33		13–14–1-2	24.46	64.29
6		13–1–4-1-2-2	25.19	49.21	34		13–14–3-3	24.48	77.48
7		13–1–3-1	24.43	52.82	35		13–14–1-3-2	24.56	69.64
8		13–1–4-1-1-2	24.84	53.42	36		13–14–2-6-1	24.97	69.03
9		13–1–2-2	25.00	54.35	37		13–14–2-1	25.21	64.86
10		13–1–5-5-1-1	24.56	48.46	38		13–14–1-1-1	25.27	20.91
11		13–1–4-1-3-1	24.85	37.97	39		**13–14–8-2-2**	**25.33**	**59.62**
12	Beijing	13–10–11–1-2	24.31	95.69	40		13–14–9-1	25.77	34.26
13		13–10–2-3-1	24.37	92.80	41	Henan	13–11–4-2-2-2	23.90	98.78
14		**13–10–11–1-1**	**23.52**	**85.71**	42		**13–11–4-2-2-1**	**24.75**	**95.80**
15		13–10–2-2-3	24.22	78.54	43		13–11–3-1-2-1	25.19	82.64
16		13–10–5-3-2	22.97	82.78	44		13–11–1-2-3	24.89	82.84
17		13–10–2-3-2	24.63	74.34	45		13–11–2-1-1	24.87	79.55
18		13–10–5-2-2	25.17	73.91	46		Z-13–11–31–1-1	24.70	82.81
19		13–10–2-1-2	24.09	80.38	47		13–11–1-2-2	24.02	80.47
20		13–10–3-1-2	24.42	69.30	48		13–11–3-1-1-1	25.52	73.68
21		Z-13–10-1-6-1	23.79	73.38	49		13–11–4-2-1-1	25.38	75.00
22		13–10–2-2-2	25.21	66.96	50		13–11–4-2-1-3	25.35	70.00
23		13–10–5-3-1	23.71	70.68	51		13–11–2-2-3	25.09	72.37
24		13–10–5-1-1	23.52	72.98	52		13–11–1-1-3	25.18	70.00
25		13–10–3-2-3	25.17	48.60	53		13–11–2-3-2	25.35	71.14
26		13–10–3-2-1	24.66	51.69	54		13–11–1-1-2	25.17	65.28
27		**13–10–3-2-2**	**25.01**	**53.91**	55		13–11–2-2-2	24.57	53.55
28		13–10–2-2-1	22.20	51.54	Mean			24.57 ± 0.71	68.98 ± 15.79

High-temperature-sensitive and resistant isolates were shown in bold.

Impact of high temperature on infection stages of high-temperature-sensitive and resistant *Bgt* isolates

There were no significant differences in conidia germination frequencies and appressoria formation frequencies among high-temperature-sensitive and resistant *Bgt* isolates at 25°C (Figures 3A,B). However, the formation frequencies of abnormal appressoria of high-temperature-resistant isolates were significantly lower than those of two high-temperature-sensitive isolates at 25°C (Figure 3C). In addition, there was no significant effect of high temperature on the length of AGT (Figure 3D). Furthermore, for all the high-temperature-sensitive and resistant *Bgt* isolates, about 11.30% conidia developed haustoria at 18°C, while only around 5.62% conidia developed haustoria at 25°C (Figure 3E). And the inhibition rates of haustoria formation at 25°C in high-temperature-resistant isolates (except 13–1–4-1-1-1) were significantly reduced compared with the high-temperature-sensitive isolates (Figure 3F). Moreover, major axis of microcolonies of high-temperature-resistant isolates at 25°C were higher in comparison with high-temperature-sensitive isolates (Figure 3G), which suggests that the hyphal extension of high-temperature-resistant isolates is much more easily at high temperature. Notably, disease severities of all isolates were significantly decreased at 25°C in comparison with those at 18°C; furthermore, disease severities of high-temperature-sensitive isolates were decreased more than those of high-temperature-resistant isolates at 25°C (Figure 3H).

Identification of *Bgthsp60*, *Bgthsp70*, *Bgthsp90,* and *Bgthsp104* genes in *Bgt*

Totally, 1 *hsp60* gene, 3 homologous *hsp70* genes (*Bgthsp70a*, *Bgthsp70b,* and *Bgthsp70c*), 1 *hsp90* gene, and 2 homologous *hsp104* genes (*Bgthsp104a* and *Bgthsp104b*) were identified in the *Bgt* genome. The conserved domains of HSPs were confirmed using CDD database. There is a GroEL domain in *Bgthsp60* gene,

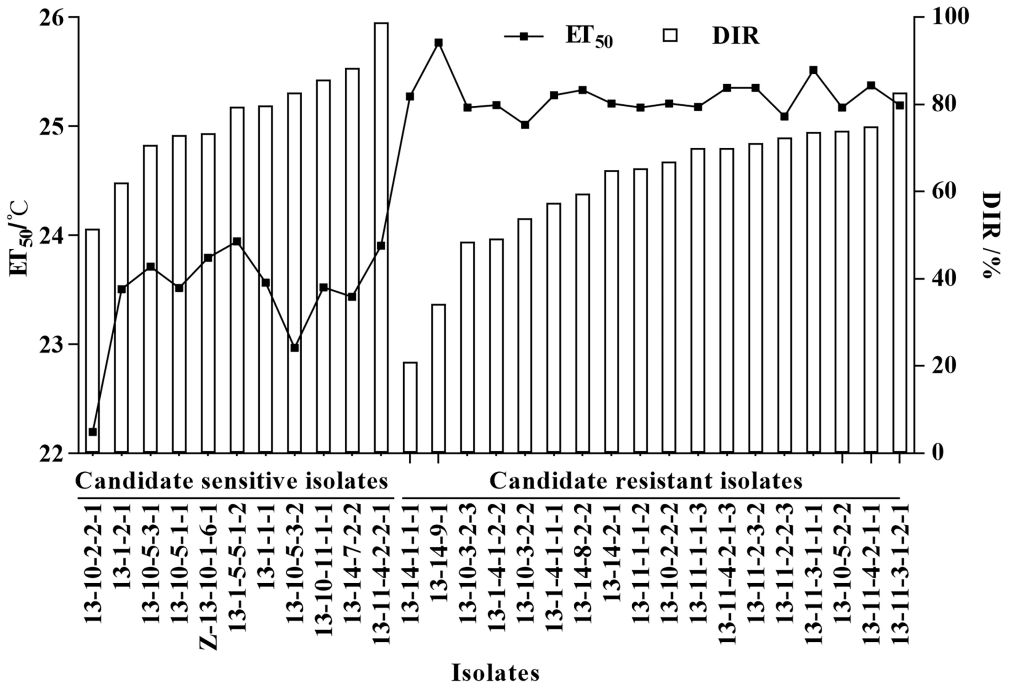

FIGURE 1
ET_{50} and disease inhibition rate (DIR) at 26°C of 11 high-temperature-sensitive and 18 high-temperature-resistant candidate isolates of *Blumeria graminis* f. sp. *tritici*. Line chart depicted the ET_{50}, and bar chart depicted the DIR at 26°C.

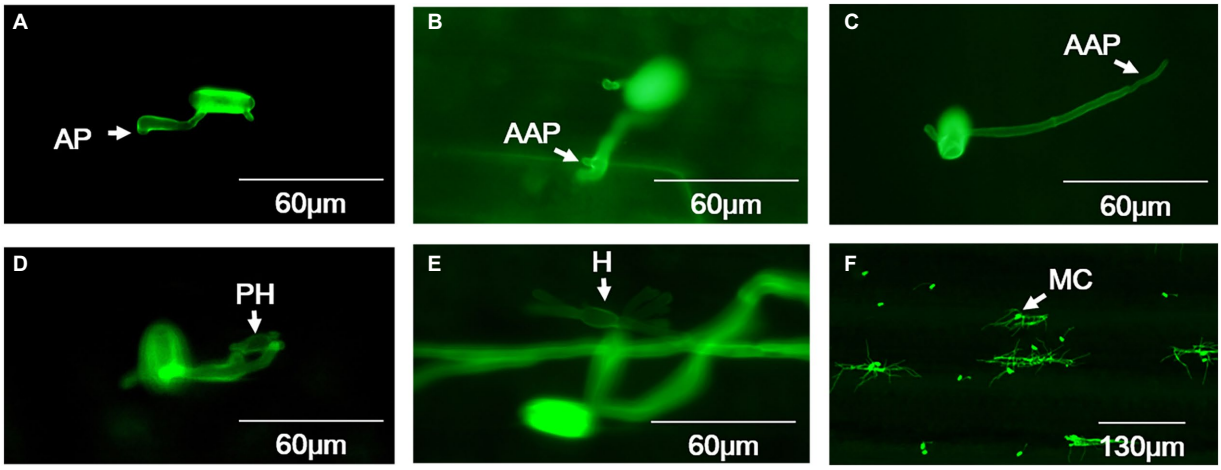

FIGURE 2
Histological observation on key infection stages of *B. graminis* f. sp. *tritici* isolates at 18°C. **(A)** Appressorium, **(B,C)** Abnormal appressoria, **(D)** Primary haustoria, **(E)** Finger-like matured haustoria, **(F)** Microcolony. AP=appressorium; AAP=abnormal appressorium; PH=primary haustorium; H=haustorium; MC=microcolony. A-E bars=60μm, F bar=130μm.

a DnaK domain in 3 homologous *Bgthsp70* genes, a HSP83 domain in *Bgthsp90* gene, and a ClpB domain in both 2 homologous *Bgthsp104* genes. Subcellular localization prediction by WoLF PSORT showed that HSP60 was localized in mitochondria, and HSP70a, HSP70b, HSP90, HSP104a, and HSP104b were localized in cytoplasm, while HSP70c was localized in endoplasmic reticulum (ER; Table 4).

Expression levels of *HSP* genes of *Bgt* under different temperature

Two high-temperature-sensitive isolates, 13–14–7-2-2 and 13–11–4-2-2-1, and two high-temperature-resistant isolates, 13–10–3-2-2 and 13–14–8-2-2, were used to analyze the *HSP* genes expression levels at 24, 48, and 72 hpi at 18°C and 25°C. At

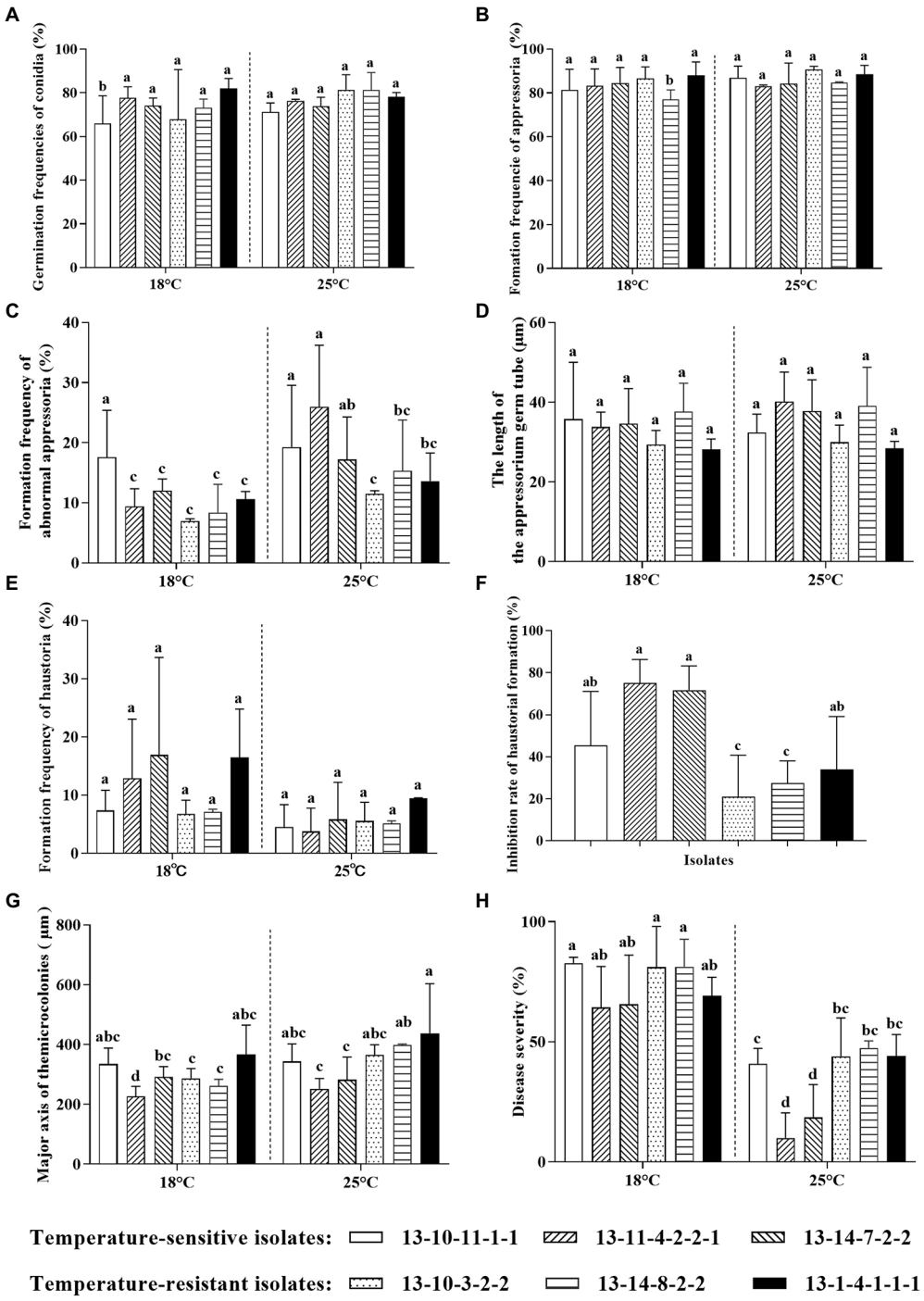

FIGURE 3
Differences in infection stages of high-temperature-sensitive and resistant isolates of *B. graminis* f. sp. *tritici* at 18°C and 25°C. **(A)** Germination frequencies of conidia; **(B)** Formation frequencies of appressoria; **(C)** Formation frequencies of abnormal appressoria; **(D)** Lengths of appressorial germ tube (AGT); **(E)** Formation frequencies of haustoria; **(F)** Inhibition rate of haustoria formation; **(G)** Major axis of microcolonies; **(H)** Disease severity. The inhibition rate of haustoria formation was analyzed by one-way analysis of variance (ANOVA), while other data were analyzed using two-way ANOVA with Duncan's multiple range test. The error bar showed standard error of three independent repeats. The different letters above the error bars indicated significant differences ($p \leq 0.05$).

24 hpi, the expression levels of *Bgthsp60*, *Bgthsp70a*, *Bgthsp70c*, *and Bgthsp104a* in high-temperature-resistant *Bgt* isolates were increased at 25°C, while the expression levels of *Bgthsp70a*, *Bgthsp70c*, and *Bgthsp104a* were decreased in high-temperature-sensitive isolates at 25°C in comparison with those at 18°C (Figure 4A). At 48 hpi, expression levels of *Bgthsp60* in all *Bgt*

TABLE 4 Features of heat shock protein gens identified in *B. graminis* f. sp. *tritici*.

Gene name	Sequence ID	ORF length (bp)	Length (aa)	Subcellular location
Bgthsp60	EPQ64594	1,847	498	Mitochondria
Bgthsp70a	EPQ65390	1,536	511	Cytoplasm
Bgthsp70b	EPQ67700	1,991	648	Cytoplasm
Bgthsp70c	EPQ62600	2,172	578	Endoplasmic reticulum
Bgthsp90	EPQ66372	2,152	701	Cytoplasm
Bgthsp104a	EPQ63989	2,787	928	Cytoplasm
Bgthsp104b	EPQ65860	2,685	802	Cytoplasm

isolates were increased at 25°C in comparison with those at 18°C (Figure 4B). At 72 hpi, expression levels of *Bgthsp60, Bgthsp70c, Bgthsp90, Bgthsp104a,* and *Bgthsp104b* in all *Bgt* isolates were increased at 25°C in comparison with those at 18°C (Figure 4C).

At 25°C, the expression levels of *Bgthsp60* were upregulation in high-temperature-resistant isolates at 48 and 72 hpi, while no difference or down-regulation in high-temperature-sensitive isolates was observed (Figure 5A). At 25°C, the expression levels of *Bgthsp70c* in high-temperature-resistant isolates were greatly increased at 24 and 72 hpi and higher than those of high-temperature-sensitive isolates at 24 hpi (Figure 5B).

Discussion

To survive climatic warming, plant pathogens evolved to adapt changing temperature by adjusting the biology, ecology, and evolutionary processes. Although the life cycle of *Pst* will be limited by increasing temperatures, new isolates of *Pst* better adapted to high temperatures than the isolates collected before 2000 that dominated the pathogen population in south central USA (Milus et al., 2006, 2009). High-temperature-resistant *Bgt* isolates had existed in the fields in 2008 and accounted for 17.7% (20/113; Wan et al., 2010). Furthermore, the parasitic fitness of high-temperature-resistant isolates was higher than that of high-temperature-sensitive isolates under higher temperatures (Wan et al., 2012). In this research, three high-temperature-resistant and sensitive *Bgt* isolates were selected in 55 *Bgt* isolates to clarify the high parasitic fitness of high-temperature-resistant isolates at cytological and molecular levels under higher temperatures.

Haustoria formation is the key infection stage defending heat stress in high-temperature-resistant isolates

Temperature is an important abiotic factor having a critical influence, positive, or negative, on infection stages of plant pathogens, such as conidia germination, appressoria formation, germ tube elongation, and haustoria formation in *Pst*, *Puccinia recondita* f. sp. *tritici*, *Colletotrichum acutatum*, *Leveillula taurica, Oidium neolycopersici*, *O. heveae, Podosphaera xanthii*, and *Golovinomyces orontii* (Guzman-Plazola et al., 2003; Leandro et al., 2003; Mieslerová and Lebeda, 2010; Trecate et al., 2019; Cao et al., 2021). This research showed that conidia germination of two types isolates was not affected at 25°C, which indicates that 25°C was not unfavorable temperature for conidia germination of *Bgt*. This is consistent with previous reports that temperatures between 15°C and 25°C were favorable for conidia germination of *B. graminis* f. sp. *hordei* on plain agar substrate (Yarwood et al., 1954). In addition, the optimum temperatures of appressorial formation of *C. acutatum* ranged from 17.6°C to 26.5°C, while this formation was inhibited until 30°C (Leandro et al., 2003). In this research, there were no significant differences in the formation frequencies of appressoria in two types isolates between 18°C and 25°C. This indicates that 25°C is favorable temperature as 18°C for appressorial formation of *Bgt*. These results also suggest that 25°C, a sublethal high temperature, has little effect on the precede penetration of *Bgt*.

Although the formation frequency of abnormal appressoria was increased at 25°C in comparison with at 18°C for high-temperature-sensitive and resistant isolates, the abnormal appressoria formation of high-temperature-resistant isolates was lower than that of high-temperature-sensitive isolates at 25°C, indicating that the high-temperature-resistant isolates were better adapted to high temperature. Previous research showed that the abnormal appressoria were caused by the failure of appressoria penetrating host cells (Nonomura et al., 2010), and finally resulted in the failure of haustoria formation. Although high temperature has little effect on the quantity of appressoria formation, it significantly increased abnormal morphology of appressoria, such as absence of AGT hooking and multi-lobed appressoria, followed by dramatically decreased haustoria formation frequency. A previous report also found that temperature significantly affected haustoria formation of *O. heveae* (Cao et al., 2021). In addition, the inhibition rate of haustoria formation in high-temperature-resistant *Bgt* isolates was lower than the high-temperature-sensitive isolates, suggesting that the haustoria formation of high-temperature-sensitive isolates was more severely inhibited by 25°C than high-temperature-resistant isolates. Moreover, the hyphal extension of high-temperature-resistant isolates was much more easily at 25°C than that of high-temperature-sensitive isolates. These results suggest that haustoria formation and hyphal expansion are key infection stages for high-temperature-resistant isolates defending heat stress.

Bgthsp60 and *Bgthsp70c* play important roles on defending heat stress in high-temperature-resistant isolates

In this study, 7 HSPs were identified in *Bgt*, of which *Bgthsp60* and *Bgthsp70c* in high-temperature-resistant isolates played important roles at 25°C in the stage of haustoria formation and hyphal expansion.

10.3389/fmicb.2022.1045796

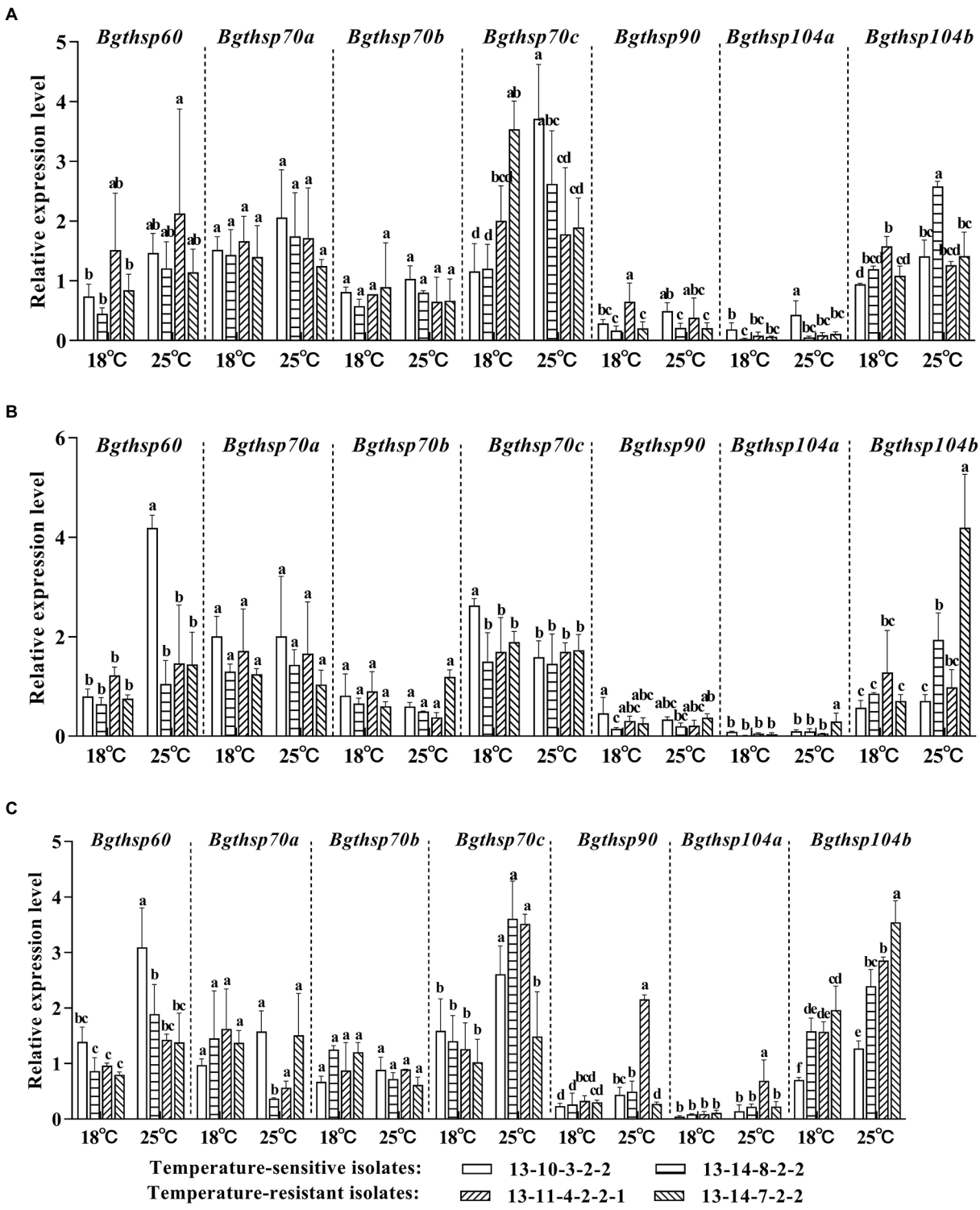

FIGURE 4
Expression levels of *Bgthsp60*, *Bgthsp70*, *Bgthsp90* and *Bgthsp104* under different temperature conditions at **(A)** 24h post-inoculation (hpi), **(B)** 48 hpi, **(C)** 72 hpi. β-tubulin was used as reference gene and 0 hpi of the one independent repeat of 13–10–3-2-2 as reference sample. The error bar showed standard error of three independent repeats. Data were analyzed by two-way ANOVA with Duncan's multiple range test. The different letters above the error bars indicated significant differences ($p \leq 0.05$).

Bgthsp60 was localized in mitochondria and significantly upregulated only in high-temperature-resistant *Bgt* isolates at 25°C compared with 18°C in the stage of hyphal expansion (Figure 4C). This suggests that upregulation of *Bgthsp60* was associated with hyphal expansion to defend heat stress in high-temperature-resistant *Bgt* isolates. Similar results were also

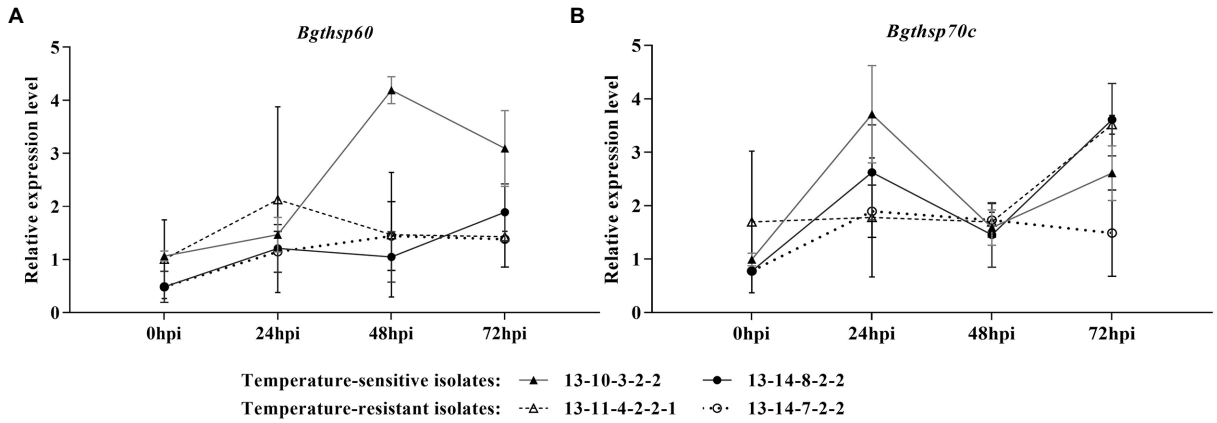

FIGURE 5
Time course of gene expression level of *Bgthsp60* **(A)** and *Bgthsp70c* **(B)** in high-temperature-sensitive and resistant isolates at 25°C. Infected leaf segments by *B. graminis* f. sp. *tritici* isolates were collected at 0, 24, 48, and 72h post-inoculation (hpi). β-tubulin was used as reference gene and 0 hpi of the one independent repeat of 13–10–3-2-2 as reference sample. The error bar showed standard error of three independent repeats.

obtained in *Aspergillus fumigatus* and *A. terreus*, the expression levels were upregulation 5.9-fold and 6.7-fold at high temperature of 40°C compared with that at regular temperature of 25°C (Raggam et al., 2011). HSP60 was required for maintaining mitochondrial protein homeostasis together with the co-chaperonin Hsp10 by preventing protein aggregation, and mediating folding and refolding under heat stress (Martin et al., 1992; Caruso Bavisotto et al., 2020). In addition, heat stress usually increased the number of interaction proteins with HSP60, which were related to metabolism demanded to proliferate in *B. graminis* (Both et al., 2005), including amino acid and protein metabolism and carbohydrate metabolism (Guimarães et al., 2011). These results suggest that *Bgthsp60* were induced by high temperature, and play a part in the process of defending high temperatures, but it remains to verify how HSP60 work in high-temperature-resistant *Bgt* isolates.

Bgthsp70c was identified as an ER lumenal HSP70, and upregulated in all isolates at 25°C compared with 18°C in the stage of haustoria formation and hyphal expansion. Especially, in the stage of haustoria formation, the levels of *Bgthsp70c* expression of high-temperature-resistant isolates were more than that of high-temperature-sensitive isolates at 25°C (Figure 5B). The result shows that *Bgthsp70c* of high-temperature-resistant isolates could contribute to tolerance to heat stress in the stage of haustoria formation. ER HSP70 proteins as molecular chaperones played key roles in protein transport into the ER and proper protein folding in the ER lumen, such as Kar2p and Lhs1p in fungi (Brodsky et al., 1995; Craven et al., 1996). In addition, Lhs1 was necessary for proper growth, conidiation, and pathogenicity in fungi, such as *Magnaporthe oryzae*, *Beauveria bassiana*, and *Fusarium pseudograminearum* (Yi et al., 2009; Chen et al., 2019; Wang et al., 2020). Particularly, Lhs1 properly processed of secreted proteins, including effectors, was requisite for successful disease development in *F. pseudograminearum* and *M. oryzae* (Yi et al., 2009; Chen et al., 2019). Binding protein (Bip) is also a member of the ER HSP70 family (Denecke et al., 1991). When plants were subjected to heat stress, *BiP* genes were upregulated *via* the unfolded protein response pathway, in *Arabidopsis* (Deng et al., 2011), and pepper (*Capsicum annuum L.*; Wang et al., 2017). The silencing of *CaBiP1* decreased the tolerance of pepper to heat stress. Conversely, overexpression of *CaBiP1* increased the tolerance of *Arabidopsis* (Wang et al., 2017). Therefore, it is supposed that overexpressed *Bgthsp70c* reduced the number of misfolded proteins in the stage of haustoria formation in high-temperature-resistant isolates at high temperature.

HSP90 in *F. graminearum* and HSP104 in *Saccharomyces cerevisiae* were thermotolerance factors. Deletion of *hsp90* stopped growing after heat shock (48°C for 30 min), whereas the wild-type isolates showed slightly delayed growth in *F. graminearum* (Bui et al., 2016). The ability of *S. cerevisiae* to withstand high temperatures was reduced when *hsp104* was knockout (Parsell et al., 1994). However, the expression levels of *hsp90*, *hsp104a,* and *hsp104b* showed no difference in high-temperature-resistant *Bgt* isolates at 25°C compared with that at 18°C, indicating that these genes could not be thermotolerance factors in *Bgt*.

In this research, it is confirmed that haustoria formation and hyphal expansion were key infection stages for high-temperature-resistant isolates to defend heat stress. In addition, upregulation of *Bgthsp60* and *Bgthsp70c* is associated with heat stress in high-temperature-resistant isolates in these stages. It is supposed that *Bgthsp60* and *Bgthsp70c* of high-temperature-resistant *Bgt* isolates could play a role in the process of defending high temperatures. However, the high thermal resistance mechanism of *Bgt* in haustoria formation and hyphae needs a deeper understanding.

Data availability statement

The datasets presented in this study can be found in online repositories. The names of the repository/repositories and

accession number(s) can be found in the article/ Supplementary material.

Author contributions

MZ, WL, and JF contributed to conception and design of the experiments. MZ and CZ performed the experiments. MZ, AW, WL, FX, ZM, and YZ analyzed the data. MZ wrote the manuscript. All authors contributed to the article and approved the submitted version.

Funding

This research was financially supported by the National Natural Science Foundation of China (31972226).

Acknowledgments

The authors thank D. W. HU (Zhejiang University, Hangzhou, China) for his help in the histological study of *Blumeria graminis* f. sp. *tritici* and Y. LUO (University of California-Davis, California, USA) and F. P. CHEN (Fujian Agriculture and Forestry University, Fujian, China) for their helps to advice on revision of manuscript.

Conflict of interest

The authors declare that the research was conducted in the absence of any commercial or financial relationships that could be construed as a potential conflict of interest.

Publisher's note

All claims expressed in this article are solely those of the authors and do not necessarily represent those of their affiliated organizations, or those of the publisher, the editors and the reviewers. Any product that may be evaluated in this article, or claim that may be made by its manufacturer, is not guaranteed or endorsed by the publisher.

Supplementary material

The Supplementary material for this article can be found online at: https://www.frontiersin.org/articles/10.3389/fmicb.2022.1045796/full#supplementary-material

References

Ayliffe, M., Devilla, R., Mago, R., White, R., Talbot, M., Pryor, A., et al. (2011). Nonhost resistance of rice to rust pathogens. *Mol. Plant-Microbe Interact.* 24, 1143–1155. doi: 10.1094/MPMI-04-11-0100

Both, M., Csukai, M., Stumpf, M. P., and Spanu, P. D. (2005). Gene expression profiles of *Blumeria graminis* indicate dynamic changes to primary metabolism during development of an obligate biotrophic pathogen. *Plant Cell* 17, 2107–2122. doi: 10.1105/tpc.105.032631

Brodsky, J. L., Goeckeler, J., and Schekman, R. (1995). BiP and Sec63p are required for both co-and posttranslational protein translocation into the yeast endoplasmic reticulum. *Proc. Natl. Acad. Sci. U. S. A.* 92, 9643–9646. doi: 10.1073/pnas.92.21.9643

Bui, D. C., Lee, Y., Lim, J. Y., Fu, M., Kim, J. C., Choi, G. J., et al. (2016). Heat shock protein 90 is required for sexual and asexual development, virulence, and heat shock response in *Fusarium graminearum*. *Sci. Rep.* 6, 1–11. doi: 10.1038/srep28154

Cao, X. R., Xu, X. M., Che, H. Y., West, J. S., and Luo, D. Q. (2021). Effects of temperature and leaf age on conidial germination and disease development of powdery mildew on rubber tree. *Plant Pathol.* 70, 484–491. doi: 10.1111/ppa.13281

Caruso Bavisotto, C., Alberti, G., Vitale, A. M., Paladino, L., Campanella, C., Rappa, F., et al. (2020). Hsp60 post-translational modifications: functional and pathological consequences. *Front. Mol. Biosci.* 7:95. doi: 10.3389/fmolb.2020.00095

Chen, L., Geng, X., Ma, Y., Zhao, J., Chen, W., Xing, X., et al. (2019). The ER lumenal Hsp70 protein FpLhs1 is important for conidiation and plant infection in *Fusarium pseudograminearum*. *Front. Microbiol.* 10:1401. doi: 10.3389/fmicb.2019.01401

Coakley, S. M. (1979). Climate variability in the Pacific northwest and its effect on stripe rust disease of winter wheat. *Clim. Chang.* 2, 33–51. doi: 10.1007/bf00138225

Coakley, S. M., Scherm, H., and Chakraborty, S. (1999). Climate change and plant disease management. *Annu. Rev. Phytopathol.* 37, 399–426. doi: 10.1146/annurev.phyto.37.1.399

Craven, R. A., Egerton, M., and Stirling, C. J. (1996). A novel Hsp70 of the yeast ER lumen is required for the efficient translocation of a number of protein precursors. *EMBO J.* 15, 2640–2650. doi: 10.1002/j.1460-2075.1996.tb00624.x

de Vallavieille-Pope, C., Huber, L., Leconte, M., and Goyeau, H. (1995). Comparative effects of temperature and interrupted wet periods on germination, penetration, and infection of *Puccinia recondita* f. sp. *tritici* and *P. striiformis* on wheat seedlings. *Phytopathology* 85, 409–415. doi: 10.1094/phyto-85-409

Denecke, J., Goldman, M., Demolder, J., Seurinck, J., and Botterman, J. (1991). The tobacco luminal binding protein is encoded by a multigene family. *Plant Cell* 3, 1025–1035. doi: 10.1105/tpc.3.9.1025

Deng, Y., Humbert, S., Liu, J. X., Srivastava, R., Rothstein, S. J., and Howell, S. H. (2011). Heat induces the splicing by IRE1 of a mRNA encoding a transcription factor involved in the unfolded protein response in *Arabidopsis*. *Proc. Natl. Acad. Sci. U. S. A.* 108, 7247–7252. doi: 10.1073/pnas.1102117108

Devi, K. U., Sridevi, V., Mohan, C. M., and Padmavathi, J. (2005). Effect of high temperature and water stress on in vitro germination and growth in isolates of the entomopathogenic fungus *Beauveria bassiana* (Bals.) Vuillemin. *J. Invertebr. Pathol.* 88, 181–189. doi: 10.1016/j.jip.2005.02.001

Estrada, A., Dodd, J. C., and Jeffries, P. (2000). Effect of humidity and temperature on conidial germination and appressorium development of two Philippine isolates of the mango anthracnose pathogen *Colletotrichum gloeosporioides*. *Plant Pathol.* 49, 608–618. doi: 10.1046/j.1365-3059.2000.00492.x

Guimarães, A. J., Nakayasu, E. S., Sobreira, T. J., Cordero, R. J., Nimrichter, L., Almeida, I. C., et al. (2011). Histoplasma capsulatum heat-shock 60 orchestrates the adaptation of the fungus to temperature stress. *PLoS One* 6:e14660. doi: 10.1371/journal.pone.0014660

Guzman-Plazola, R. A., Davis, R. M., and Marois, J. J. (2003). Effects of relative humidity and high temperature on spore germination and development of tomato powdery mildew (*Leveillula taurica*). *Crop Prot.* 22, 1157–1168. doi: 10.1016/s0261-2194(03)00157-1

Knies, J. L., Izem, R., Supler, K. L., Kingsolver, J. G., and Burch, C. L. (2006). The genetic basis of thermal reaction norm evolution in lab and natural phage populations. *PLoS Biol.* 4:e201. doi: 10.1371/journal.pbio.0040201

Knies, J. L., and Kingsolver, J. G. (2010). Erroneous Arrhenius: modified Arrhenius model best explains the temperature dependence of ectotherm fitness. *Am. Nat.* 176, 227–233. doi: 10.1086/653662

Last, F. (1963). Effect of temperature on cereal powdery mildews. *Plant Pathol.* 12, 132–133. doi: 10.1111/j.1365-3059.1963.tb00232.x

Leandro, L., Gleason, M., Nutter, F. Jr., Wegulo, S., and Dixon, P. (2003). Influence of temperature and wetness duration on conidia and appressoria of *Colletotrichum acutatum* on symptomless strawberry leaves. *Phytopathology* 93, 513–520. doi: 10.1094/phyto.2003.93.4.513

Li, B., Cao, X., Chen, L., Zhou, Y., Duan, X., Luo, Y., et al. (2013). Application of geographic information systems to identify the oversummering regions of *Blumeria graminis* f. sp. *tritici* in China. *Plant Dis.* 97, 1168–1174. doi: 10.1094/pdis-10-12-0957-re

Livak, K. J., and Schmittgen, T. D. (2001). Analysis of relative gene expression data using real-time quantitative PCR and the $2^{-\Delta\Delta CT}$ method. *Methods* 25, 402–408. doi: 10.1006/meth.2001.1262

Luck, J., Spackman, M., Freeman, A., Tre Bicki, P., Griffiths, W., Finlay, K., et al. (2011). Climate change and diseases of food crops. *Plant Pathol.* 60, 113–121. doi: 10.1111/j.1365-3059.2010.02414.x

Martin, J., Horwich, A. L., and Hartl, F. U. (1992). Prevention of protein denaturation under heat stress by the chaperonin Hsp60. *Science* 258, 995–998. doi: 10.1126/science.1359644

Mieslerová, B., and Lebeda, A. (2010). Influence of temperature and light conditions on germination, growth and conidiation of *Oidium neolycopersici*. *J. Phytopathol.* 158, 616–627. doi: 10.1111/j.1439-0434.2009.01663.x

Milus, E. A., Kristensen, K., and Hovmøller, M. S. (2009). Evidence for increased aggressiveness in a recent widespread strain of *Puccinia striiformis* f. sp. *tritici* causing stripe rust of wheat. *Phytopathology* 99, 89–94. doi: 10.1094/phyto-99-1-0089

Milus, E., Seyran, E., and McNew, R. (2006). Aggressiveness of *Puccinia striiformis* f. sp. *tritici* isolates in the south-Central United States. *Plant Dis.* 90, 847–852. doi: 10.1094/pd-90-0847

Montero-Barrientos, M., Hermosa, R., Nicolás, C., Cardoza, R. E., Gutiérrez, S., and Monte, E. (2008). Overexpression of a *Trichoderma* HSP70 gene increases fungal resistance to heat and other abiotic stresses. *Fungal Genet. Biol.* 45, 1506–1513. doi: 10.1016/j.fgb.2008.09.003

Nonomura, T., Nishitomi, A., Matsuda, Y., Soma, C., Xu, L., Kakutani, K., et al. (2010). Polymorphic change of appressoria by the tomato powdery mildew *Oidium neolycopersici* on host tomato leaves reflects multiple unsuccessful penetration attempts. *Fungal Biol.* 114, 917–928. doi: 10.1016/j.funbio.2010.08.008

Parsell, D. A., Kowal, A. S., Singer, M. A., and Lindquist, S. (1994). Protein disaggregation mediated by heat-shock protein Hspl04. *Nature* 372, 475–478. doi: 10.1038/372475a0

Raggam, R. B., Salzer, H. J., Marth, E., Heiling, B., Paulitsch, A. H., and Buzina, W. (2011). Molecular detection and characterisation of fungal heat shock protein 60. *Mycoses* 54, e394–e399. doi: 10.1111/j.1439-0507.2010.01933.x

Sharma, R., Duveiller, E., and Ortiz-Ferrara, G. (2007). Progress and challenge towards reducing wheat spot blotch threat in the eastern Gangetic Plains of South Asia: is climate change already taking its toll? *Field Crop Res.* 103, 109–118. doi: 10.1016/j.fcr.2007.05.004

Tang, X., Cao, X., Xu, X., Jiang, Y., Luo, Y., Ma, Z., et al. (2017). Effects of climate change on epidemics of powdery mildew in winter wheat in China. *Plant Dis.* 101, 1753–1760. doi: 10.1094/pdis-02-17-0168-re

Tiwari, S., Thakur, R., and Shankar, J. (2015). Role of heat-shock proteins in cellular function and in the biology of fungi. *Biotechnol. Res. Int.* 2015:132635, 1–11. doi: 10.1155/2015/132635

Trecate, L., Sedláková, B., Mieslerová, B., Manstretta, V., Rossi, V., and Lebeda, A. (2019). Effect of temperature on infection and development of powdery mildew on cucumber. *Plant Pathol.* 68, 1165–1178. doi: 10.1111/ppa.13038

Velásquez, A. C., Castroverde, C. D. M., and He, S. Y. (2018). Plant–pathogen warfare under changing climate conditions. *Curr. Biol.* 28, R619–R634. doi: 10.1016/j.cub.2018.03.054

Wan, Q., Ding, K., Duan, X., and Zhou, Y. (2010). Sensitivity of population of *Blumeria graminis* f. sp. *tritici* isolates to temperature in 2008. *Acta Pharmacol. Sin.* 40, 106–109. doi: 10.13926j.cnki.apps.2010.01.008

Wan, Q., Ding, K., Zhou, Y., Duan, X., and Zou, Y. (2012). Parasitic fitness of *Blumeria graminis* f. sp. *tritici* isolates with different sensitivity to temperature. *Acta Pharmacol. Sin.* 42, 186–194. doi: 10.13926/j.cnki.apps.2012.02.011

Wang, J., Chen, J., Hu, Y., Ying, S., and Feng, M. (2020). Roles of six *Hsp70* genes in virulence, cell wall integrity, antioxidant activity and multiple stress tolerance of *Beauveria bassiana*. *Fungal Genet. Biol.* 144:103437. doi: 10.1016/j.fgb.2020.103437

Wang, H., Niu, H., Zhai, Y., and Lu, M. (2017). Characterization of *BiP* genes from pepper (*Capsicum annuum L.*) and the role of *CaBiP1* in response to endoplasmic reticulum and multiple abiotic stresses. *Front. Plant Sci.* 8:1122. doi: 10.3389/fpls.2017.01122

Wicker, T., Oberhaensli, S., Parlange, F., Buchmann, J. P., Shatalina, M., Roffler, S., et al. (2013). The wheat powdery mildew genome shows the unique evolution of an obligate biotroph. *Nat. Genet.* 45, 1092–1096. doi: 10.1038/ng.2704

Woods, A., Coates, K. D., and Hamann, A. (2005). Is an unprecedented Dothistroma needle blight epidemic related to climate change? *Bioscience* 55, 761–769. doi: 10.1641/0006-3568(2005)055[0761:iaudnb]2.0.co;2

Xu, Z., Duan, X. Y., Zhou, Y. L., Guo, Q. Y., Yao, Q., and Cao, S. Q. (2014). Population genetic analysis of *Blumeria graminis* f. sp. *tritici* in Qinghai Province, China. *J Integr. Agric.* 13, 1952–1961. doi: 10.1016/s2095-3119(13)60591-2

Yarwood, C., Sidky, S., Cohen, M., and Santilli, V. (1954). Temperature relations of powdery mildews. *Hilgardia* 22, 603–622. doi: 10.3733/hilg.v22n17p603

Yi, M., Chi, M. H., Khang, C. H., Park, S. Y., Kang, S., Valent, B., et al. (2009). The ER chaperone LHS1 is involved in asexual development and rice infection by the blast fungus *Magnaporthe oryzae*. *Plant Cell* 21, 681–695. doi: 10.1105/tpc.107.055988

frontiers | Frontiers in Plant Science

TYPE Original Research
PUBLISHED 08 December 2022
DOI 10.3389/fpls.2022.1043171

OPEN ACCESS

EDITED BY
Maria Rosa Simon,
National University of La Plata, Argentina

REVIEWED BY
Marta Cabello,
Instituto Spegazzini, Comisión de Investigaciones Científicas de La Provincia de Buenos Aires (CIC-PBA), La Plata, Argentina
Anton Hartmann,
Ludwig Maximilian University of Munich, Germany

*CORRESPONDENCE
Zengwen Liang
ysny2000@163.com
Hui Cao
hui5232@163.com

SPECIALTY SECTION
This article was submitted to Plant Pathogen Interactions, a section of the journal Frontiers in Plant Science

RECEIVED 13 September 2022
ACCEPTED 28 October 2022
PUBLISHED 08 December 2022

CITATION
Ji C, Chen Z, Kong X, Xin Z, Sun F, Xing J, Li C, Li K, Liang Z and Cao H (2022) Biocontrol and plant growth promotion by combined *Bacillus* spp. inoculation affecting pathogen and AMF communities in the wheat rhizosphere at low salt stress conditions.
Front. Plant Sci. 13:1043171.
doi: 10.3389/fpls.2022.1043171

Biocontrol and plant growth promotion by combined *Bacillus* spp. inoculation affecting pathogen and AMF communities in the wheat rhizosphere at low salt stress conditions

Chao Ji[1,2,3,4], Zhizhang Chen[5], Xuehua Kong[6], Zhiwen Xin[1,2], Fujin Sun[1,4], Jiahao Xing[1,2], Chunyu Li[1,2], Kun Li[7,8], Zengwen Liang[1,2,3]* and Hui Cao[1,2,3]*

[1]College of Seed and Facility Agricultural Engineering, Weifang University, Weifang, Shandong, China, [2]Key Laboratory of Biochemistry and Molecular Biology in University of Shandong Province, Weifang University, Weifang, Shandong, China, [3]Shandong Yongsheng Agricultural Development Co., Ltd. Yongsheng (Shouguang) Vegetable Technology Research Institute Co., Ltd, Shandong Engineering Research Center, Weifang, Shandong, China, [4]Runxin Fruit and Vegetable Cultivation Cooperative of Weifang Economic Development Zone, Weifang Agricultural Bureau, Weifang, Shandong, China, [5]College of Foreign Languages, Weifang University, Weifang, Shandong, China, [6]Weifang Hanting Vestibule School, Weifang Education Bureau, Weifang, Shandong, China, [7]College of Forestry, Shandong Agriculture University, Taian, Shandong, China, [8]Taishan Forest Ecosystem Research Station, Key Laboratory of State Forestry Administration for Silviculture of the Lower Yellow River, Shandong Agricultural University, Taian, Shandong, China

Applying plant growth-promoting rhizobacteria (PGPR) improves the efficiency of soil-borne disease control and is considered a sustainable practice. However, the effect of PGPR on the fungal community, especially pathogenic fungi and arbuscular mycorrhizal fungi (AMF), remains unclear. In this study, we examined the effects of a compound microbial agent (consisting of *Bacillus subtilis* HG-15 and *Bacillus velezensis* JC-K3) on the incidence and yield of wheat under low salt stress, as well as compared the diversity and community composition of the rhizosphere fungal and AMF communities of wheat in the CK (not inoculated bacterial agent) and BIO (inoculated with a bacterial agent) groups. Chlorophyll relative content (SPAD), net photosynthesis rate (*Pn*), transpiration rate (*Tr*), leaf water use efficiency (WUE_L), grains per spike and wheat yield in the BIO group increased more than in the CK group. The number of diseased plants and disease incidence was observed to be reduced. The relative efficacy reached 79.80%. We classified 1007 fungal operational taxonomic units (OTU) based on Miseq sequencing data: 11 phyla, 173 families, 319 genera, and 521 species. Fifty-four OTUs were classified from the AMF effective sequences, including 1 phylum, 3 families, 3 genera, and 17 species. The inoculation of bacterial agents reduced the relative abundance of pathogen genera such as *Gibberella*, *Fusarium*, *Cladosporium*, and *Alternaria* in wheat rhizosphere. It increased the relative abundance of AMF species such as Glomus-group-B-Glomus-lamellosu-VTX00193, Glomus-

viscosum-VTX00063, and Glomus-Glo2-VTX00280. In addition, pH, EC, exchangeable K, available N, total N, organic matter, and olsen P were the main driving forces for shaping wheat rhizosphere fungi. The pH value was positively correlated with the relative abundance of fungal communities in soil, especially *Gibberella*, *Cladosporium*, *Fusarium*, and *Alternaria*. In summary, inoculation with *Bacillus subtilis* HG-15 and *Bacillus velezensis* JC-K3 affected wheat yield, incidence, rhizosphere soil chemical properties, rhizosphere fungi, and AMF fungal diversity and community. The findings may provide a theoretical foundation and strain support for constructing efficient PGPR-community and clarifying its mechanism of pathogenic bacteria inhibition.

KEYWORDS

salt stress, microbial inoculants, plant growth-promoting rhizobacteria, arbuscular mycorrhizal fungi, community structure, wheat yield, disease control

Introduction

Salt stress is one of the major abiotic stresses limiting crop production in arid and semi-arid regions; salinity threatens at least 20% of the world's cropland to varying degrees (Zhu et al., 2011). Salt stress causes osmotic, ion toxicity, and oxidative stress, disrupting the integrity of cell membrane systems and ultrastructure in photosynthetic systems. The structure and function of inter-root soil microbial communities are also susceptible to significant changes because of salt stress, directly affecting crop growth and yield (Munns and Tester, 2008). Although plants can produce some yield in saline soil habitats, most crops and tree species are not highly salt tolerant, with major food crops such as wheat, maize, rice, and barley suffering yield losses of up to 70% because of salt stress (Acquaah, 2007). With the intensification of population growth, land and food conflicts, and climate change, improving the soil environment and promoting crop yields in low salt-stressed soils are crucial for promoting economic development, ensuring food security, relieving population pressure, and maintaining ecological balance.

Crop diseases caused by soil-borne pathogens are another important constraint to high-quality, high-yielding food and sustainable agricultural development worldwide. The sexual stage of *Fusarium* is often *Gibberella*, which can cause crown rot, stem rot, and blast rot in wheat (Javad et al., 2006); more seriously, *Fusarium* can cause wilt and root rot in over 100 crops (Li et al., 2015), such as wheat wilt caused by *Fusarium graminearum* (Drakopoulos et al., 2020); and rice blight caused by *Fusarium moniliforme* (Alam et al., 2010). The *Gibberella*, on the other hand, causes fusarium head blight in wheat, barley, and other cereal crops (Oliver et al., 2008).

Salt-tolerant PGPR has probiotic properties, such as the production of phytohormones, siderophores, ACC deaminase (ACCD), and compatible solutes like proline, which directly reduce the level of plant stress hormone ethylene and are involved in the conversion and cycling of carbon (C), nitrogen (N), and phosphorus (P), as well as other substances and energy in the soil (Singh et al., 2015; Delgado-Baquerizo et al., 2016). These mechanisms are related to improving plant salt tolerance and induced system tolerance (IST), which can effectively reduce salt stress damage in plants, promote crop growth, and suppress pathogen proliferation (Etesami and Beattie, 2018). Arbuscular mycorrhizal fungi (AMF) can form symbiotic relationships with most crops. They can improve salt tolerance and disease resistance to soil-borne diseases by promoting plant growth, water uptake, and initiating host plant defense responses, besides improving soil nutrient acquisition (Cameron et al., 2013; Ruiz-Lozano et al., 2016; Despina et al., 2018; Bennett and Groten, 2022). Although AMF may not be "sustainable saviors" for agricultural intensification (Thirkell et al., 2017), AMF does have the potential to aid in the nutritional assimilation of grains (Thirkell et al., 2020). Most studies have focused on the pro-growth effects of exogenous inoculation of PGPR or AMF on host plants. In contrast, little research has been done on the synergistic effects of salt-tolerant PGPR with other microorganisms in the root zone on saline soils and crops. There is a specific lack of research on the response of AMF communities to salt-tolerant PGPR.

The rational application of microorganisms in modern agriculture can maximize yields while minimizing inputs under anticipated environmental perturbations (Vries et al., 2020). *Bacillus subtilis* HG-15 and *Bacillus velezensis* JC-K3, the strains used in this study, are salt-tolerant bacteria obtained, respectively, from the rhizoplane and inside the roots of wheat in the saline soil of Yellow River Delta; the strains did not inhibit each other and were able to colonize stably in the inter-root of

saline wheat, both with the properties of producing ACC deaminase, IAA, Siderophore, and proline. The strains have been demonstrated to promote wheat seedling growth, reduce salt stress damage, and improve photosynthesis and osmoregulation in pot experiments (Ji et al., 2021; Ji et al., 2022). More studies have shown that combined bacterial inoculum has higher environmental adaptability, biological viability, and synergistic metabolism levels than single strains and has a greater impact on soil-plant material cycling (Dombrowski et al., 2018). Therefore, this study will investigate the effects of combined biocontrol agents composed of these two strains on fungi, especially the AMF community in wheat rhizosphere soil, as well as the relationship between microbial community response, wheat yield, and disease resistance. The results of this study may provide a theoretical foundation and data support to clarify further the mechanisms of PGPR and AMF promotion and disease prevention under salt stress, as well as a reference point for future research on how to mobilize indigenous AMF.

Materials and methods

Biocontrol strain and culture medium

The microbial inoculant is a compound agent of *Bacillus subtilis* HG-15 and *Bacillus velezensis* JC-K3. Both strains exhibit efficient antagonistic activity and other growth-promoting characteristics, as described in our previous studies (Ji et al., 2021; Ji et al., 2022). Luria-Bertani liquid medium was used as a seed and fermentation medium. When the spore formation rate in the fermentation liquid was greater than 95%, diatomite was sterilized at a high temperature (121 °C, 20 min) and added at a concentration of 10% to the fermented liquid. The bacteria were allowed to adsorb to the diatomite. The suspension was centrifuged at 3,100 × *g* for 20 min. The supernatant was removed, and the sediment was stored at −40 °C for 48 h before being placed in a lyophilizer (Labconco FreeZone® Plus 4.5 L; Kansas City, MO, USA) and treated at −48 °C and 9 Pa for 48 h (Ji et al., 2020). The density of HG-15 and JC-K3 in the resultant solid microbial agent was 472 × 10^8 CFU g^{-1} and 511 × 10^8 CFU g^{-1}, respectively. The bacterial preparations were mixed with sterile diatomite and diluted to 20 × 10^8 CFU g^{-1}.

Experimental design

Between October 2021 and July 2022, an experimental plot system was established in the Weifang Changyi area of Shandong Province, China (119°31′55″E, 36°38′47″N). The soil in the experimental area was mildly salinized alluvial, and the surface soil texture was medium loam. The chemical properties of initial soil were pH 8.11, EC 316 μs cm^{-1}, organic matter 23.51 g kg^{-1}, total nitrogen 1.792 g kg^{-1}, available nitrogen 79.35 mg kg^{-1}, Olsen P 18.83 mg kg^{-1}, and exchangeable potassium 97.06 mg kg^{-1}. Nutrient Agar (NA) medium and Potato Dextrose Agar (PDA) medium were used to isolate and count culturable bacteria and fungi in rhizosphere soil, respectively. The number of culturable bacteria and fungi in soil was 5.73 × 10^4 and 2.34 × 10^3 CFU g^{-1} dry weight of soil, respectively. This study used a completely randomized block design with three replicates per treatment (CK and BIO), with each replicate consisting of an area of 40 m^2 (8 m length × 5 m width) insulated with a buffer zone.

Wheat seeds (CV. *Jimai* 22) were surface-sterilized with 1% sodium hypochlorite for 5 min, washed 3–5 times with sterile water, and sown artificially on the plot at 0.6 kg per 40 m^2 on October 12, 2021. At the jointing stage, wheat seedlings in the treatment groups were first irrigated with bacterial preparations (previously dissolved in water at 5.0 kg per 40 m^2) on February 20, 2022, and then on March 08, 2022; wheat seedlings in the control group were irrigated with the same volume of tap water. Before replanting, a basal fertilizer (45% Yangfeng compound fertilizer, N14-P16-K15; 1.2 kg per 40 m^2) was used; the nitrogen fertilizer (urea, 1.5 kg per 40 m^2) was used during the green-up period.

Rhizosphere soil sampling and analysis

The bulk of the soil at the root of the wheat was removed by gentle shaking, leaving only rhizosphere soil; and the soil that remained adhered to the roots was considered rhizosphere soil. The residual soil was collected from the roots using a sterile brush (Smalla et al., 1993). Soil samples for the determination of microbial communities were quick-frozen in liquid nitrogen and stored in a refrigerator at -80°C until they were extracted and analyzed. Soil samples for chemical determination were stored at 4 °C. Soil pH and EC values were analyzed using digital pH (FE20) and EC (FE930) meters (Mettler Toledo, Switzerland), respectively, with soil-water ratios of 1:2.5 and 1:5. The organic matter content in the soil was determined with a method described in Aj and Black (1934). Olsen P was determined using the method proposed by Olsen (1954). The total N was determined using the Bremner (2009) method. Available N and exchangeable potassium values were obtained using a method described in Jackson (1979).

Chlorophyll relative content (SPAD) and photosynthetic parameters

Five flag leaves were randomly selected from each plot at 9:00–11:00 a.m. on 0, 10, 20, and 30 days after the flowering of winter wheat. The SPAD value was measured using a portable chlorophyll tester (SPAD 502, Minolta Camera Co., Ltd., Japan).

Net photosynthetic rate (*Pn*) and transpiration rate (*Tr*) were measured using an LI-6800XT portable photosynthetic instrument (Li-COR, Lincoln, NE, USA). The measuring time, date, and leaf position were all consistent with the wheat SPAD value. The photon flux was set to 1,200 μmol m^{-2} s^{-1}, the blade temperature to 25 °C, the humidity to 55%, and the flow rate to 500 μmol s^{-1}. Each treatment consisted of five leaves. Leaf water use efficiency (WUE_L) was calculated using the following equation:

$$WUE_L = Pn/Tr$$

Effects of microbial inoculants on disease

At the end of grouting, the main disease characteristics of white heads in wheat were investigated. Each treatment had three replicates, and each replicate had three sampling sites chosen at random. A total of 100 wheat seedlings were surveyed for each sampling point. The number of white spikes was counted, and the relative biocontrol effect was calculated using the following formula (Moussa et al., 2013).

$$\text{Disease incidence} = \frac{\text{The number of diseased plants}}{\text{Total number of wheat seedling}} \times 100\%$$

$$\text{Relative efficacy} = \frac{\text{Disease incidence in control} - \text{disease incidence in treatment}}{\text{Disease incidence in control}} \times 100\%$$

Grain filling rate and yield

Ten wheat spikes were randomly collected from each plot at 7, 14, 21, 28, and 35 days after flowering. They were placed in the oven at 105°C for 30 min and dried to constant weight at 75°C for 72 h. The filling rate was calculated as grain weight/filling duration (Deng et al., 2021). For wheat maturity, each plot randomly selected 1 m^2 to investigate the number of spikes per unit area, selected 100 spikes to investigate the number of grains per spike, harvested 4 m^2 threshing, and weighed after natural air drying (grain moisture content is approximately 12.5%), calculated yield per unit area, and investigated 1000-grain weight. The procedure was repeated five times for each treatment.

DNA preparation and polymerase chain reaction-based amplification

Soil genomic DNA was extracted from 0.5 g soils with a FastDNA SPIN Kit for Soil (MP, California, USA) according to the manufacturer's instructions. The DNA quality was examined using 1.0% agarose gel electrophoresis, and the DNA concentration was quantified using a NanoDrop 2000 UV–Vis spectrophotometer (Wilmington, USA) (Zeng et al., 2021).

The fungal rDNA-ITS gene was amplified from the total soil genomic DNA using primers ITS1F (5′-barcode-CTTGGTCATTTAGAGGAAGTAA-3′)/2043R (5′-GCTGCGTTCTTCATCGATGC-3′). PCR was performed in triplicates in a 20-μL reaction tube containing 4 μL of 5× FastPfu Buffer, 2 μL of 2.5 mmol dNTPs, 0.8 μL of each primer (5 μmoL), 0.4 μL FastPfu Polymerase, 10 ng template DNA, and adding ddH_2O to a final volume of 20 μL.

Nested PCR was conducted to amplify fragments of AMF 18S rRNA gene with high specific amplification. The first PCR step was conducted in a 20 μL reaction tube containing 1 μL of genomic DNA (approximately 10 ng), 2 μL of 2.5 mM dNTPs, 0.4 μL of FastPfu DNA Polymerase (5 U μL^{-1}), 0.4 μL of each primer (10 μM; AML1 (5′-ATCAACTTTCGATGGTAGGATAGA-3′)/AML2 (5′-GAACCCAAACACTTTGGTTTCC-3′) primer pair), 4 μL of 5-fold Fastpfu DNA Buffer (Takara, Dalian, China), and molecular-grade water. In the second PCR amplification, the products of first PCR step (with approximately 10 ng used as the template) were amplified in a 50-μL reaction tube with the primers AMV4.5NF (5′-AAGCTCGTAGTTGAATTTCG-3′) and AMDGR (5′-CCCAACTATCCCTATTAATCAT-3′), as described for the first PCR step. The thermal cycling conditions for both PCR steps were as follows: initial denaturation at 95 °C for 3 min; 27 cycles of 30 s of denaturation at 95 °C, 30 s of annealing at 55 °C, and 45 s of elongation at 72 °C; and final elongation at 72 °C for 10 min. PCR products were extracted using 2% agarose gels and purified using an AxyPrep DNA Gel Extraction Kit (Axygen, USA) according to manufacturer's protocol and quantified using a QuantiFluor ST instrument (Promega, USA).

Illumina MiSeq and bioinformatics analyses

Qualified and purified PCR products were sent to Majorbio BioPharm Technology Co., Ltd. (Shanghai, China) for sequencing on an Illumina MiSeq PE300 instrument (San Diego, USA). The raw sequences were deposited in NCBI Sequence Read Archive (SRA) database (accession number PRJNA869482). The forward and reverse raw sequences were merged using FLASH (Mago and Salzberg, 2011) by overlapping paired-end reads using a required overlap length of >10 base pairs (bp) and quality-controlled using Trimmomatic software (Bolger et al., 2014); low-quality sequences (average quality score< 20) containing ambiguous bases, sequences with no valid primer sequence or barcode sequence, and sequences with a read length< 50 bp were excluded. Moreover, the permitted maximum error ratio of overlapping sequences was

0.2, which was established as the basis for screening overlapping sequences.

After the sequences were merged and subjected to quality control, non-repeating sequences were extracted, and individual sequences that did not repeat were removed using Usearch 7.0 (Edgar, 2013); the sequences were subsequently clustered into operational taxonomic units (OTUs) with a 97% similarity cut-off using QIIME software (Caporaso et al., 2010). After the sequences were clustered, the taxonomy of each OTU was classified from the domain level to the OTU level using RDP Classifier algorithm against the MaarjAM database (Maarjam 081) (ÖPik et al., 2010), with a default confidence threshold of 0.7.

Statistical analyses

Data analysis was performed using IBM SPSS 19.0. Plant and soil parameters followed a normal distribution. A student's t-test and one-way ANOVA were used for parameter differences among plant parameters ($P< 0.05$). Redundancy analysis (RDA) was performed to examine the relationships between the relative abundance of fungal, AMF taxa and the chemical properties of soil samples by using Canoco 4.5.1 (Microcomputer Power, Ithaca, USA) software. The non-parametric factorial Kruskal-Wallis (KW) sum-rank test of the LEfSe software was used to detect the characteristics of significant abundance differences, and the groups with significant differences in abundance were found. LEfSe uses linear discriminant analysis (LDA) to estimate the effect of each component (species) abundance on the difference.

Results

The soil's nutritional status was analyzed for the plant growth study. To evaluate the effect of microbial agents, we performed a student's t-test ($P< 0.05$). The EC (5.50%), exchangeable potassium (10.24%), Olsen P (5.68%), total N (7.22%), available N (10.16%), and organic matter (12.31%) of wheat rhizosphere soil treated with BIO were significantly higher than those treated with CK group ($P< 0.05$). The pH of CK group was significantly higher than that of the BIO treatment (2.04%, $P< 0.05$) (Table 1).

The SPAD content of wheat after flowering decreased as the growth process progressed in both treatments. Under the same treatment, no significant difference was observed in the SPAD content of wheat after flowering between days 0 and 10, but it decreased significantly on days 20 and 30 ($P< 0.05$). At each time point, the SPAD content of BIO treatment was significantly higher than that of the CK treatment ($P< 0.05$) (Figure 1A). With the advancement of growth process, *Pn* and *Tr* decreased significantly ($P< 0.05$). On days 10, 20, and 30, the *Pn* of the BIO treatment was significantly higher than that of the CK treatment ($P< 0.05$). On day 20, the *Tr* of the BIO treatment was significantly higher than that of the CK treatment ($P< 0.05$) (Figures 1B, C). Under both treatments, WUE_L decreased significantly on days 20 and 30 ($P< 0.05$). On days 10, 20, and 30, the WUE_L of the BIO treatment was significantly higher than that of the CK treatment (Figure 1D).

The fitting curve (Figure 2) shows that the grain filling rate of CK group reached peaked on day 20 after flowering. The BIO group peaked on day 25 after flowering and was higher than the CK treatment during 30–35 days after flowering. The incidence of wheat disease was determined at the end of grain filling. Diseased wheat plants (79.24%) and disease incidence (79.84%) in the BIO group were significantly lower than those in the CK group ($P< 0.05$). The relative efficacy was 79.80% (Table 2). Inoculation with compound bacteria did not significantly change the spike number or thousand-grain weight of wheat. However, the grain number per spike (10.43%) and yield (8.77%) of the BIO group were significantly higher than those of the CK group ($P< 0.05$) (Table 3).

Wheat rhizosphere soil samples of the CK and BIO groups were analyzed to determine their community structure. A total of 759029 effective ITS sequences and 254269 effective AMF sequences were obtained, which accounted for 82.54% and 97.83% of the raw sequences, respectively, and their average lengths were 237 and 216, respectively. As the number of sequences increases, so does the microbial diversity index. At the final stage, the dilution curve became flat, indicating that the sequencing data for this study reached saturation and could cover most microbial communities in rhizosphere soil (Figures 3A–D). Based on a 97% similarity score, 1007 OTUs

TABLE 1 Effects of the inoculation with combined PGPR inoculation (BIO) compared to control (CK) on the chemical properties of wheat rhizosphere soil.

Treatment	EC(μs/cm)	Exchangeable K(mg/kg)	Olsen-P(mg/kg)	Total N(g/kg)	Available N(mg/kg)	Organic matter(g/kg)	pH
CK	342.0 ± 2.92b	101.52 ± 1.88b	18.49 ± 0.15b	1.94 ± 0.07b	85.41 ± 2.40b	26.49 ± 0.59b	7.99 ± 0.06a
BIO	360.8 ± 4.38a	111.92 ± 2.67a	19.54 ± 0.23a	2.08 ± 0.06a	94.09 ± 1.58a	29.75 ± 0.99a	7.83 ± 0.03b

Data are means ± standard deviation (SD) (n = 5). The small letters in the table represent the significant difference between the indexes of uninoculated and inoculated compound microbial agent wheat, P < 0.05.

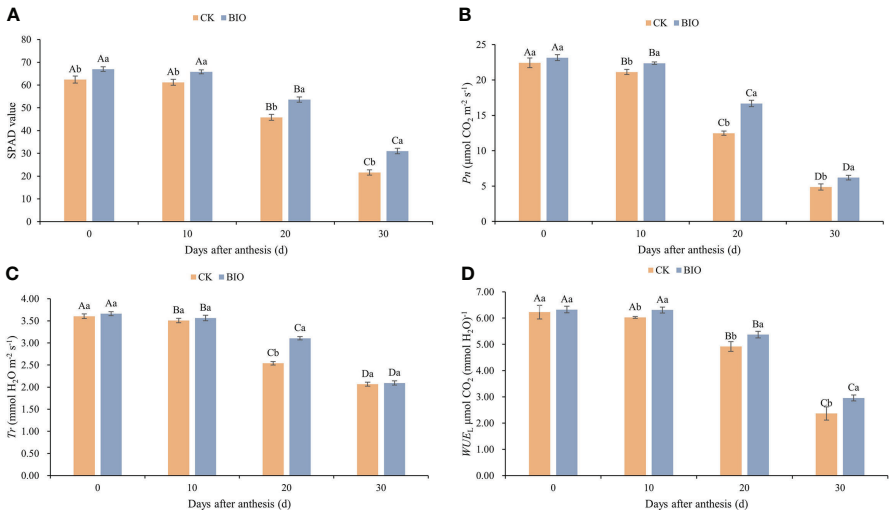

FIGURE 1
Effects of compound microbial agents on SPAD and photosynthetic parameters in flag leaf. CK and BIO represent the control and combined biocontrol agents inoculated plants, respectively. **(A)** SPAD: Chlorophyll relative content. **(B)** Pn: Net photosynthesis rate. **(C)** Tr: Transpiration rate. **(D)** WUEL: Leaf water use efficiency. Capital letters indicated significant differences between groups (one-way ANOVA, P < 0:05), whereas small letters indicate significant differences among control (CK) and compound microbial agents inoculated (BIO) plants at the same time point (student's t-test, P < 0.05), respectively. The smaller bars are standard errors.

were classified from the effective fungal sequences: 11 phyla, 173 families, 319 genera, and 521 species (Figure 3E). 54 OTUs were classified from the AMF effective sequences, including 1 phylum, 3 families, 3 genera, and 17 species (Figure 3F). The Sobs, Chao, and ACE indexes represent species richness indexes. The higher the index value, the more diverse the microbial community composition. The Shannon and Simpson indexes represent microbial diversity indexes. The higher the Shannon index or lower the Simpson index, the more diverse the microbial community composition. Inoculation with the PGPR significantly increased the richness of fungal community in wheat rhizosphere soil, decreased the diversity of AMF community, increased fungal diversity ($P< 0.05$), and had no significant effect on AMF diversity (Table 4).

In terms of fungi community information in the rhizosphere at the genus level. The relative abundance of *Apodus,*

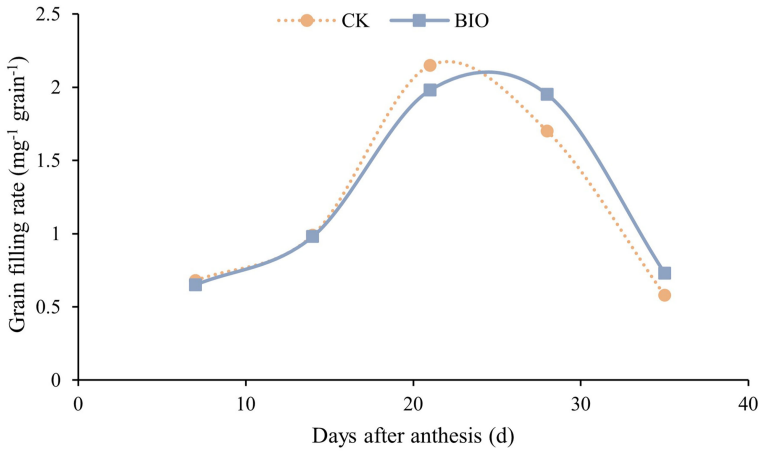

FIGURE 2
Effects of compound microbial agents on grain filling rate. CK and BIO represent the control and combined biocontrol agents inoculated plants, respectively.

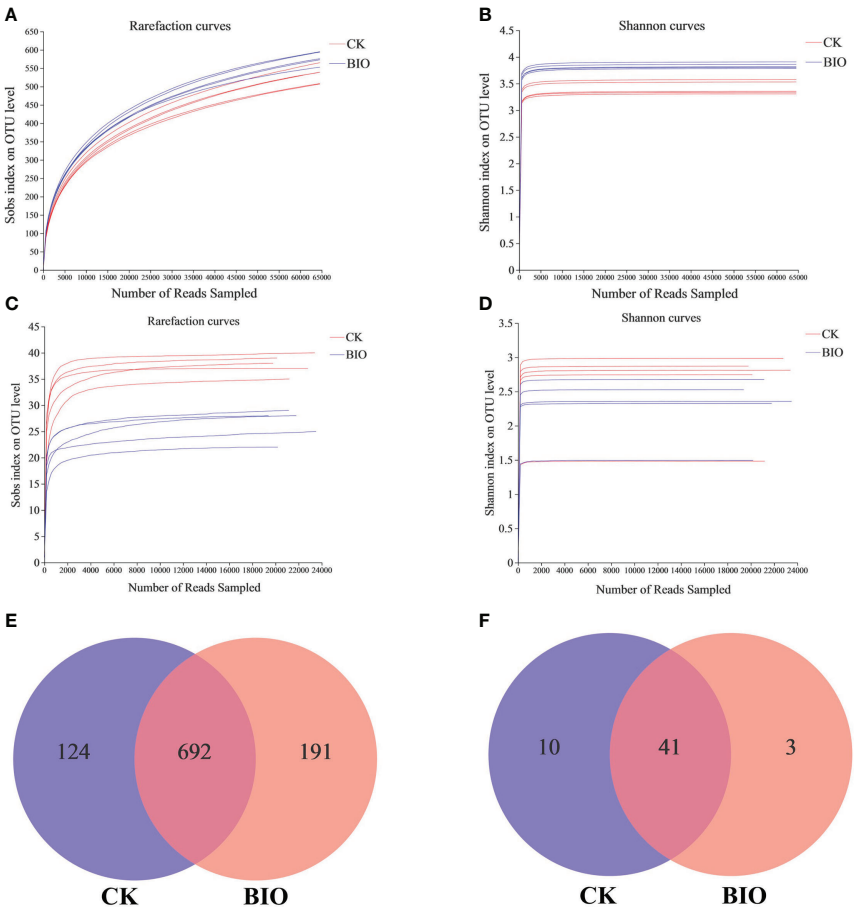

FIGURE 3
Different treatment samples generate microbial rarefaction curves, Shannon curves, and venn diagrams based on OTU level. **(A)** Fungi rarefaction curves; **(B)** fungi Shannon curves. **(C)** AMF rarefaction curves; **(D)** AMF Shannon curves. **(E)** The unique and shared fungal OTUs in CK and BIO groups; **(F)** the unique and shared AMF OTUs in CK and BIO groups. CK and BIO represent the control and combined biocontrol agents inoculated plants, respectively.

Acremonium, *Sarocladium*, *Coprinopsis*, *Schizothecium*, *Chaetomium* in the BIO treatment (12.01%, 22.15%, 5.24%, 3.65%, 1.66%, and 2.02%, respectively) was higher than that in the CK group (10.91%, 0.74%, 3.92%, 0.89%, 0.01%, 1.37%, and 0.91%, respectively). The relative abundance of *Penicillium*, *Gibberella*, *Mortierella*, *Fusarium*, *Cladosporium*, *Alternaria*, *Filobasidium* in the CK group (23.06%, 8.19%, 5.54%, 7.98%, 5.76%, 4.06%, and 4.53%, respectively) was higher than that in the BIO group (1.08%, 2.86%, 5.2%, 2.17%, 2.77%, 2.27%, and 1.41%, respectively). The relative abundance of *Arachnomyces* and *Candida* in the BIO group (2.10% and 1.55%, respectively) was higher than that in the CK group (both<0.01%). The relative abundance of *Epicoccum* and *Pyrenochaetopsis* in the CK group was 2.89% and 1.37%, respectively, but both accounted for<0.01% in the BIO group (Figure 4A). Regarding AMF community information in the wheat rhizosphere soil at the species level. The relative abundance of Glomus-group-B-Glomus-lamellosu-VTX00193, Glomus-viscosum-VTX00063, Glomus-sp.-VTX00304, Glomus-MO-G17-VTX00114, Glomus-intraradices-VTX00105, Glomus-acnaGlo2-VTX00155 in the BIO group

TABLE 2 Disease prevention efficacy by microbial inoculants.

Treatment	Total number of wheat seedlings	Diseased plants	Disease incidence	Relative efficacy
CK	300	79 ± 5.3a	26.30%a	—
BIO	300	16 ± 5.1b	5.30%b	79.80%

Data are means ± standard deviation (SD) (n = 5). CK and BIO represent the control and combined biocontrol agents inoculated plants, respectively. The small letters in the table represent the significant difference between the indexes of uninoculated and inoculated compound microbial agent wheat, $P < 0.05$.

TABLE 3 Effects of different treatments on grain yield and yield components in winter wheat.

Treatment	Spike number($\times10^4$ hm^{-2})	Grain number per spike	1000-grain weight(g)	Yield(kg hm^{-2})
CK	653.14 ± 6.72a	34.53 ± 2.31b	42.17 ± 3.41a	7469.37 ± 357.6b
BIO	657.62 ± 6.84a	38.13 ± 2.06a	42.94 ± 2.11a	8124.52 ± 277.8a

Data are means ± standard deviation (SD) (n = 5). CK and BIO represent the control and combined biocontrol agents inoculated plants, respectively. The small letters in the table represent the significant difference between the indexes of uninoculated and inoculated compound microbial agent wheat, P < 0.05.

(15.44%, 9.44%, 8.88%, 5.34%, 4.18%, and 1.36%, respectively) was higher than that in the CK group (14.55%, 5.47%, 2.81%, 4.10%, 2.12%, and 0.46%, respectively). The relative abundance of Glomus-mosseae-VTX000679, Glomus-caledonium-VTX00065, Glomus-sp.-VTX00301 in the CK group (8.40%, 18.65%, and 1.81%, respectively) was higher than that in BIO group (8.16%, 12.98%, and 1.75%, respectively). The relative abundance of Glomus-Glo2-VTX00280 in BIO group (1.38%) was higher than that in CK group (<0.01%). The relative abundance of Glomus-Glo-C-VTX00323 in CK group (1.42%) was higher than in the BIO group (< 0.01%) (Figure 4B).

RDA results revealed that the fungal communities of different treatments were significantly separated, but AMF community was not significantly separated. EC, exchangeable K, available N, total N, organic matter, and Olsen P, primarily *Acremonium* and *Apodus*, were positively correlated with changes in the fungal community in wheat rhizosphere soil under CK group. A positive correlation was observed between pH and the change in the fungal community in BIO treatment, including *Gibberella* and *Mortierella*. *Penicillium* was less affected by the soil's chemical properties (Figure 5A). The interaction between soil chemical properties and the AMF community revealed that Glomus-caledonium-VTX00065 was significantly positively correlated with pH and EC. Glomus-mosseae-VTX00067, Glomus-sp.-VTX00304, Glomus-viscosum-VTX00063, Glomus-group-B-Glomus-lamellosu-VTX00193 were positively correlated with exchangeable K, available N, total N, organic matter, and Olsen P (Figure 5B).

The fungal communities of two groups were classified and analyzed using a microecological guild. The relative abundance of plant pathogen, animal pathogen, and soil saprotroph functional guilds in wheat rhizosphere soil fungi in the CK group was higher than in the BIO group (Figure 6). The fungal genera directly related to the pathogen: *Gibberella*, *Cladosporium*, *Fusarium*, *Alternaria*, and *Bipolaris* (Table S1). The co-occurrence networks were used to explore the co-occurrence relationships between fungal genera and AMF species. The fungal collinear network contained five phyla: Ascomycota, Mortierellomycota, Basidiomycota, Olpidiomycota, and Chytridiomycota. There are 37 genera with more than 30 nodes, including *Panaeolus*, *Epicoccum*, *Coniothyrium*, and *Sistotrema*, *Gibberella* (Figure 7A). The AMF collinear network includes Glomeromycota. Glomus-MO-G17-VTX00114s, Glomus-acnaGlo2-VTX00155, and Glomus-viscosum-VTX00063 are important nodes (Figure 7B).

The relative abundance of *Penicillium*, *Fusarium*, *Gibberella*, *Filobasidium*, and *Cladosporium* in the CK group was significantly higher than in the BIO group ($P< 0.05$). The relative abundance of *Acremonium*, *Coprinopsis*, and *Bipolaris* in the BIO group was significantly higher than that in the CK group ($P< 0.05$) (Figure 8A). The relative abundance of AMF species, such as Glomus-Glo-C-VTX00323, in the CK group was significantly higher than that in the BIO group ($P< 0.05$). The relative abundance of Glomus in the BIO group was significantly higher than that in the CK group ($P< 0.05$) (Figure 8B).

Discussion

Agricultural development in ecologically fragile areas is hampered by geographical location, natural conditions, and other factors and is confronted with severe challenges of salt stress. The climatic conditions with a high evaporation-precipitation ratio and a scarcity of freshwater resources are prone to salinization, which is the main natural limiting factor for land use in most countries (Ashraf et al., 2018). Effectively improving the quality of crop rhizosphere soil can ensure improved wheat yield and quality under biotic and abiotic stresses (Simón et al., 2020). Non-salt-tolerant PGPRs are susceptible to synergistic metabolism and antagonism by indigenous microbial community in saline-alkaline soils, their

TABLE 4 Diversity index of fungi and AMF in wheat rhizosphere soil samples under different treatments.

	Sample	sobs	shannon	simpson	ace	chao	coverage
Fungi	CK	531.60 ± 24.43b	3.42 ± 0.12b	0.09 ± 0.01a	658.75 ± 45.93a	666.88 ± 46.01a	0.997962b
	BIO	578.20 ± 17.31a	3.83 ± 0.05a	0.06 ± 0.01b	677.42 ± 27.74a	671.27 ± 18.28a	0.998104a
AMF	CK	37.60 ± 1.67a	2.58 ± 0.62a	0.16 ± 0.18a	37.90 ± 1.76a	37.60 ± 1.67a	0.999969a
	BIO	26.40 ± 2.88b	2.28 ± 0.46a	0.17 ± 0.11a	28.04 ± 3.45b	26.80 ± 3.03b	0.999938a

Data are means ± standard deviation (SD) (n = 5). CK and BIO represent the control and combined biocontrol agents inoculated plants, respectively. The small letters in the table represent the significant difference between the indexes of uninoculated and inoculated compound microbial agent wheat, P < 0.05.

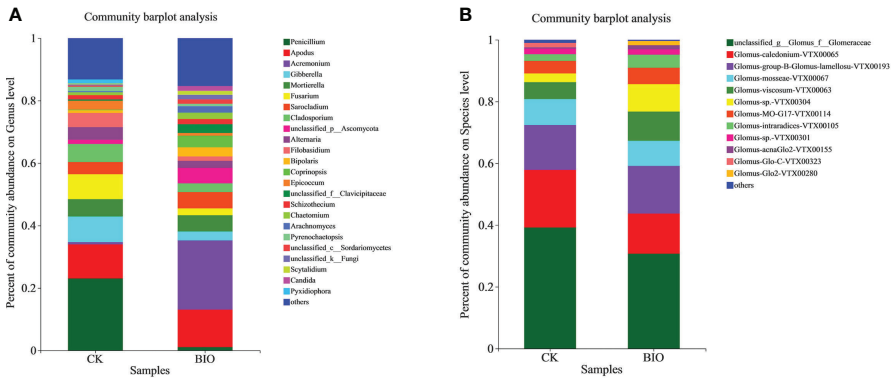

FIGURE 4
Relative abundance of fungal and AMF communities in wheat rhizosphere soil. **(A)** Relative abundance of fungal community in wheat rhizosphere soil at the genus level. **(B)** Relative abundance of AMF community in wheat rhizosphere soil at the species level. Different colors represent different species, and the rectangular area represents the percentage of species. CK and BIO represent the control and combined biocontrol agents inoculated plants, respectively.

ecological functions are limited, or they gradually lose colonization and plant growth promoting (PGP) properties with increasing salinity (Etesami and Beattie, 2018). Therefore, exploring microbial improvement measures that meet the requirements of soil quality improvement and health conservation in saline-alkali land is challenging and urgent.

Small molecular organic acids and siderophores secreted by salt-tolerant PGPR can decompose insoluble minerals *via* chelation, ion exchange, and acidification, thereby increasing the availability of nutrients in the soil, lowering pH, and alleviating Na^+ stress in wheat (Delvasto et al., 2006; Chang and Yang, 2009; Saha et al., 2016; Ramakrishna et al., 2019). Both strains used in this study were salt-tolerant bacteria that can tolerate at least 12% (w/v) NaCl stress (Ji et al., 2021; Ji et al., 2022). This will greatly improve the strain's ability to colonize in saline-alkali land and maintain high biological activity. The EC, exchangeable potassium, olsen P, total N, available N, and organic matter of wheat rhizosphere soil in BIO group were significantly higher than those in the CK group ($P< 0.05$) (Table 1). The finding demonstrates that both strains have competitive advantages in microbial-microbial interactions and can achieve mutual benefit in plant-microbial interactions. Similarly, previous studies have shown that strain salt tolerance and ACC deaminase-producing activity directly influence the effects of bacterial agents on saline agricultural fields. For example, under salt stress, ACCD-producing *Pseudomonas fluorescens* N3 and *Pseudomonas putida* Q7 strains increased maize root growth by 330% and plant height by 230%, respectively (Kausar and Shahzad, 2006). *Azospirillum brasilense* FP2 can reduce ACC oxidase expression and promote

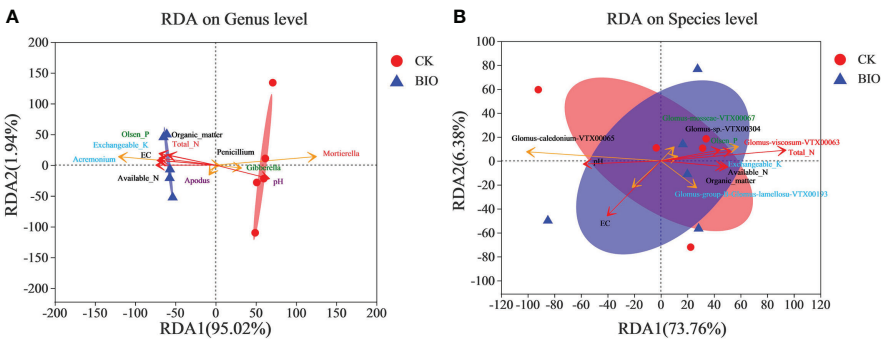

FIGURE 5
Redundancy Analysis (RDA) of AMF community based on Bray-Curtis distances. **(A)** fungal communities. **(B)** AMF communities. CK and BIO represent the control and combined biocontrol agents inoculated plants, respectively.

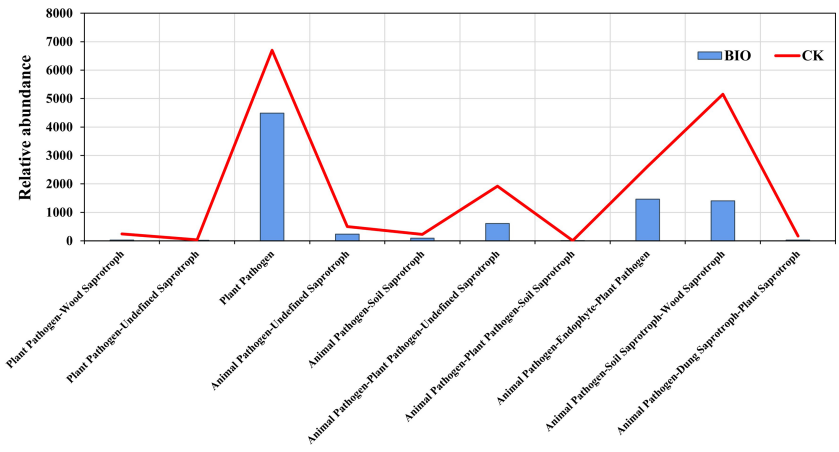

FIGURE 6
Variations in the composition of fungal functional groups inferred by FUNGuild. CK and BIO represent the control and combined biocontrol agents inoculated plants, respectively.

root growth in wheat plants (Camilios-Neto et al., 2014). Inoculation of salt-tolerant PGPB *Micrococcus yunnanensis*, *Planococcus rifietoensis*, and *Variovorax paradoxus* into sugar beet (*Beta vulgaris* L.) can increase seed germination and plant biomass, enhance photosynthesis, and significantly reduce stress-induced ethylene content (Zhou et al., 2017). Klebsiella, Pseudomonas, Agrobacterium, and Ochrobactrum strains isolated from the roots of *Arthrocnemum indicum* were *nifH*-positive and were able to produce indole-3 acetic acid (ranging from 11 to 19.1μg mL^{-1}). In nutrient broth medium, all isolates showed tolerance to NaCl ranging from 4 to 8%. Under salt stress, inoculated peanut seedlings maintain ionic balance, accumulate less reactive oxygen species (ROS), and show enhanced growth compared to uninoculated seedlings (Sharma et al., 2016).

Inoculation of PGPR under salt stress improves the efficiency of plants to absorb selective ions by regulating the expression of ion transporter (High-affinity K^+ Transporter, *HKT1*) to maintain a high K^+/Na^+ ratio, reduce the accumulation of Na^+ and Cl^- ions, and regulate the balance of macronutrients and micronutrients in plants and soils (Islam et al., 2016; Etesami and Beattie, 2018). Inoculation with ACCD-producing *Bacillus licheniformis* HSW-16 can protect wheat plants from growth inhibition caused by NaCl and increase plant growth (6-38%) in terms of root length, shoot length, fresh weight, and dry weight. Ionic analysis of plant samples showed that bacterial inoculation decreases the accumulation of Na^+ content (51%) and increases K^+ (68%) and Ca^{2+} content (32%) in plants treated with different concentrations of NaCl (Singh and Jha., 2016). Additionally, AMF communities have been shown to induce sugar accumulation in plant roots further, leading to more organic acids being secreted into the soil, lowering plant ion toxicity, and enhancing antioxidant and detoxification defense systems (Abdelgawad et al., 2022). These effects may be the direct cause of higher EC in the BIO group than in the CK group (Table 1).

Photosynthesis is the basis of dry matter production and the driving force behind final yield. PGPR affects the expression of multiple proteins involved in plant photosynthesis, antioxidant processes, transmembrane transport, and pathogenesis (Cheng et al., 2012). In this study, the photosynthetic characteristics of wheat after flowering were significantly reduced on days 20 and 30 ($P< 0.05$), but the SPAD, *Pn*, and WUE_L of wheat in the BIO group were significantly higher than those in the CK group ($P< 0.05$) (Figure 1). This may be related to the characteristics that both strains can produce siderophores and proline. The siderophore can specifically and strongly bind Fe^{3+} to form an absorbable organic chelate. The enriched Fe is an integral part of key enzymes involved in plant respiration, photosynthesis, and other reactions (Kobayashi and Nishizawa, 2012). Osmoregulation substances such as proline can protect the structure and function of biological macromolecules, scavenge free radicals, and buffer the redox potential of cells to reduce enzyme inactivation caused by salt stress and ensure physiological activities such as photosynthesis (Ashraf and Foolad, 2007; Kohler et al., 2009). In this study, the grain number and yield of wheat in the BIO group were significantly higher than those in the CK group (Table 3). The main reason may be increased rhizosphere soil nutrients (Yadav et al., 2021). Concurrently, PGPR and AMF synergistically increase nutrient absorption, enhance photosynthesis, optimize rhizosphere bacteria, and improve soil health. The factors above can

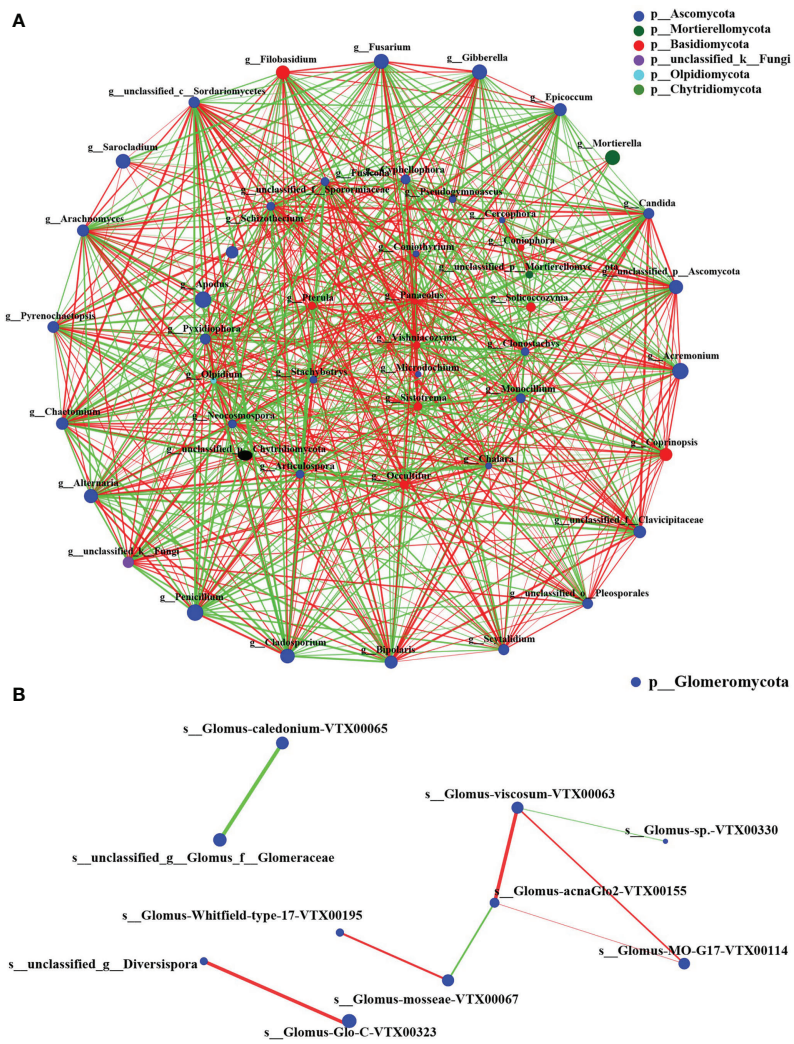

FIGURE 7
The co-occurrence network on virtual taxon level of fungi and AMF. **(A)** The genus-level fungal correlation. **(B)** The species level AMF correlation. The size of nodes in the figure represents the abundance of species, and different colors represent different species. The color of connection represents positive and negative correlation; red represents positive correlation; green represents negative correlation; the thickness of line indicates the size of correlation coefficient. The thicker the line, the higher the correlation between species. The more lines, the closer the relationship between the species and other species. Species with $P< 0.05$ are shown by default in the figure.

improve plant development, biofortification, and grain yield, consistent with previous studies (Smith and Sally, 2008; Cameron et al., 2013; Singh and Prasanna, 2020).

Wheat root rot and basal stem rot are soil-borne diseases caused by pathogens such as *Alternaria*, *Fusarium*, and *Gibberella*, which can cause seed decay and seedling death during wheat planting, basal stem browning at the adult stage, and white spike disease in severe cases, seriously affecting wheat yield and quality (Yuan et al., 2012; Gaju et al., 2014). To cope with climate change and increased abiotic stress in cultivated land, it is crucial to control disease occurrence and enhance crop stress resistance to achieve long-term sustainable agricultural development (Simón et al., 2021). Lowering the number of pathogens in soil by inoculating PGPR is an effective biological control measure (Ju et al., 2021; Vogel et al., 2021; Wang et al., 2022). As a major member of PGPR, *Bacillus* has a higher affinity for iron, which can deprive pathogenic microorganisms of nutrients and inhibit their pathogenesis (Radhakrishnan et al., 2017). *Bacillus amyloliquefaciens* subsp. *Plantarum* XH-9 has potential as a biocontrol agent when applied to local arable land to prevent the damage caused by *Fusarium oxysporum* and other phytopathogens (Wang et al., 2018). AMF not only competes for a niche with pathogens and produces mechanical defense barriers to reduce the number of pathogens such as *Fusarium*

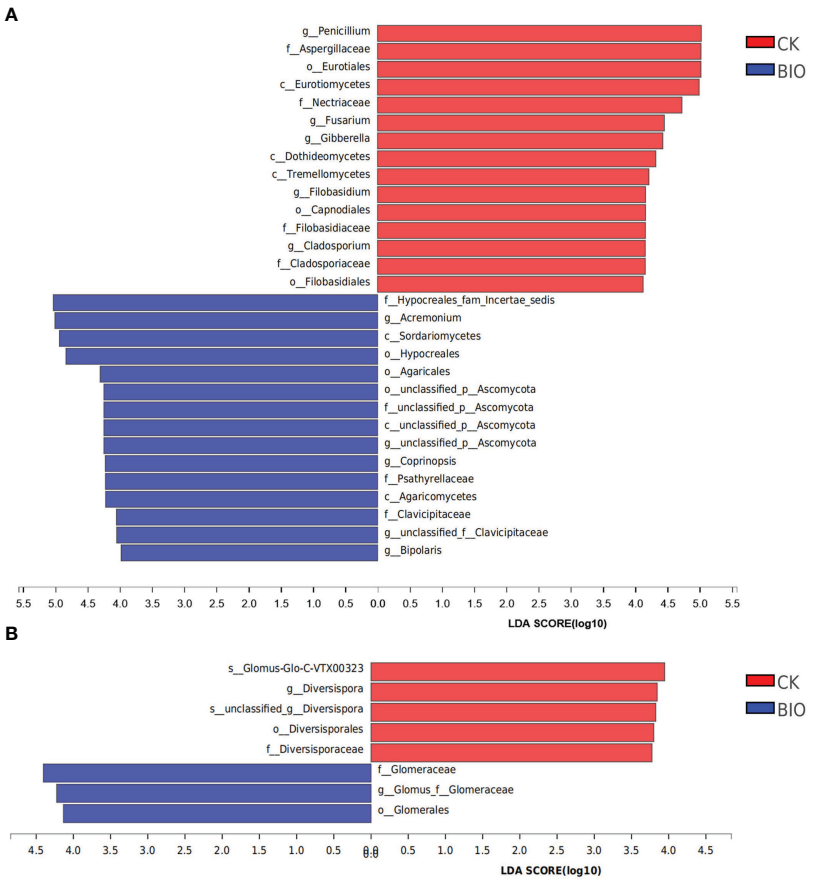

FIGURE 8
Discriminant analysis of multi-level species differences in CK and BIO groups. Indicator fungi and AMF with LDA scores of 3 or greater in communities associated with soil from CK and BIO groups. **(A)** fungal communities. **(B)** AMF communities. CK and BIO represent the control and combined biocontrol agents inoculated plants, respectively. Different-colored regions represent different constituents (red, CK; blue, BIO). The greater the LDA score, the greater the effect of species abundance on the difference. Class (c), Order (o), Family (f), Genus (g), Species (s).

(Hao et al., 2010); AMF can also induce plants to produce protective enzymes and regulate root exudates/secondary metabolites, reduce root damage caused by pathogens, induce systemic defense systems in crops, and further enhance nutrient and water absorption (Geel et al., 2017). It is unclear how the application of antagonistic bacteria affects wheat rhizosphere fungi, especially AMF. In this study, diseased plants (79.24%) and disease incidence (79.84%) in the BIO group were significantly lower than those in the CK group ($P< 0.05$), and relative efficacy was 79.80% (Table 2). Our results showed that inoculation of antagonistic bacteria into the rhizosphere of plants could significantly alter the microbial community structure of arbuscular mycorrhizal fungi in the wheat rhizosphere (Figure 4), which may explain why plants produce 'induced systemic tolerance'. Differences in fungal community function between the BIO and CK groups confirmed this result (Figure 6). All these findings demonstrate that combined *Bacillus* spp. inoculation can effectively control soil-borne diseases.

The biocontrol effect of microbial agents is easily affected by many biological and non-biological factors. In this study, salt stress and pathogens increased the complexity of PGPR biocontrol mechanisms in the field. Illumina MiSeq sequencing results revealed that microbial agents increased the richness and diversity of fungi (Table 4). The relative abundance of *Apodus*, *Acremonium*, *Sarocladium*, *Coprinopsis*, *Schizothecium*, and *Chaetomium* in the BIO group was higher than in the CK group. *Chaetomium* is widely used and studied because it produces a variety of secondary metabolites with antibacterial effects (Shanthiyaa et al., 2013). The relative abundance of *Penicillium*, *Gibberella*, *Mortierella*, *Fusarium*, *Cladosporium*, *Alternaria*, and *Filobasidium* in the CK group

was higher than that in the BIO group (Figures 4A, 8A). *Gibberella* and *Mortierella* were positively correlated with soil pH (Figure 5A), which may be attributed to the weakened inhibitory effect of combined *Bacillus* spp. inoculation at high pH. Although *Penicillium* has an antibacterial effect (Larena et al., 2018), its inhibitory effect on *Gibberella, Fusarium, Alternaria*, and other pathogens was not demonstrated in this study. We speculate that *Penicillium* is inhibited by the inoculated compound microbial agent or that it cannot produce enough antibacterial metabolites under salt stress.

Glomus is a major AMF fungus infecting plants (Landwehr et al., 2002). Previous studies have demonstrated that inoculation with Glomus helps stimulate plant growth and biomass (Campos-Soriano et al., 2010; Naseer et al., 2022). However, glomus's mycelial growth is susceptible to salt stress (Juniper and Abbott, 2006). In this study, Glomus was the most common AMF genus in the CK and BIO groups (Figure 4B), but not among all fungi (Figure 4A). In the BIO group, Glomus-group-B-Glomus-lamellosu-VTX00193, Glomus-viscosum-VTX00063, Glomus-sp.-VTX00304, Glomus-MO-G17-VTX00114, Glomus-intraradices-VTX00105, Glomus-acnaGlo2-VTX00155, Glomus-Glo2-VTX00280 were the most common bacteria. Their relative abundance in the BIO group was higher than in the CK group (Figure 4). Glomus-group-B-Glomus-lamellosu-VTX00193, Glomus-viscosum-VTX00063 and Glomus-sp.-VTX00304 were positively correlated with organic matter, total N, exchangeable K, Olsen P (Figure 5B). Not only PGPR directly influenced AMF community structure and function, but also the changes in rhizosphere soil chemical properties have a selective effect on community composition. AMF has broad-spectrum benefits and potential application value under adverse conditions (Guo et al., 2022). The effect of AMF on plant growth was negatively correlated with the complexity of symbiotic network (Vannini et al., 2016; Pawlowska et al., 2018). In this study, AMF strains did not exhibit a complex symbiotic network (Figure 7B), indicating that AMF may strongly affect wheat. Current studies have confirmed that the combination of PGPR and AMF can exert greater growth-promoting characteristics to stimulate plant growth, which is better than inorganic fertilizer (Yadav et al., 2020; Yadav et al., 2021). Therefore, because of the universality of AMF and its potential impact on plant nutrient uptake and growth, it is crucial to verify the effect of biocontrol agents on AMF communities in the field.

Conclusion

Our experiments established that a compound bacterial agent (consisting of *Bacillus subtilis* HG-15 and *Bacillus velezensis* JC-K3) improved wheat plant growth and yield under salt stress. They improved soil chemical properties, enhanced wheat photosynthesis, and WUE_L, and significantly reduced wheat disease incidence. Illumina MiSeq sequencing results confirmed the inhibitory effect of combined *Bacillus* spp. inoculation on pathogens in wheat rhizosphere soil. Concurrently, the AMF community structure in the soil responded to combined *Bacillus* spp. inoculation, and multiple AMFs were correlated with soil chemical properties. This study deepens research on the ecological function of PGPR in the wheat rhizosphere in saline-alkali land. However, more research on the functions of different AMF strains and communities is required to fully understand the complexity and succession of the microbial community structure or the directional regulation of the AMF community.

Data availability statement

The datasets presented in this study can be found in online repositories. The names of the repository/repositories and accession number(s) can be found in the article/Supplementary Material.

Author contributions

CJ, ZC, and XK conceived the ideas and designed the experiment. CJ, ZC, XK, and ZX collected and analysed the samples. CJ, FS, CL, and JX analysed the data. CJ, ZC, KL, ZL, and HC prepared the figures and wrote the manuscript. CJ, ZL and HC revised and edited the draft. All authors made significant contributions to the draft and gave final approve for publication.

Funding

This work was supported by the National Natural Science Foundation of China (32072518), Shandong Provincial Natural Science Foundation (ZR2022QC155), Key Research and Development Project of Shandong Province (2018GNC2306), Weifang University Doctor Initiation Fund Project (208-44121013), Horizontal Topic (208-40121141).

Acknowledgments

We would like to thank Weifang University, Shandong Agriculture University, Key Laboratory of State Forestry Administration for Silviculture of the Lower Yellow River for supporting this work.

Conflict of interest

Author CJ, HC and ZL are employed by Shandong Yongsheng Agricultural Development Co., Ltd. Yongsheng (Shouguang) Vegetable Technology Research Institute Co., Ltd.

The remaining authors declare that the research was conducted in the absence of any commercial or financial relationships that could be construed as a potential conflict of interest.

Publisher's note

All claims expressed in this article are solely those of the authors and do not necessarily represent those of their affiliated organizations, or those of the publisher, the editors and the reviewers. Any product that may be evaluated in this article, or claim that may be made by its manufacturer, is not guaranteed or endorsed by the publisher.

Supplementary material

The Supplementary Material for this article can be found online at: https://www.frontiersin.org/articles/10.3389/fpls.2022.1043171/full#supplementary-material

SUPPLEMENTARY TABLE 1
Normalized relative abundance of assigned fungal functional guilds with treatment

References

Abdelgawad, H., El-Sawah, A. M., Mohammed, A. E., Alotaibi, M. O., Yehia, R. S., Selim, S., et al. (2022). Increasing atmospheric CO_2 differentially supports arsenite stress mitigating impact of arbuscular mycorrhizal fungi in wheat and soybean plants. *Chemosphere* 296, 134044. doi: 10.1016/j.chemosphere.2022.134044

Acquaah, G. (2007). *Principles of plant genetics and breeding* (Oxford: Blackwell Publishing Ltd).

Aj, W., and Black, I. (1934). An examination of the degtjareff method for determining soil organic matter, and a proposed modification of the chromic acid titration method. *Soil Sci.* 37, 29–38. doi: 10.1097/00010694-193401000-00003

Alam, M., Chourasia, H. K., Sattar, A., and Janardhanan, K. K. (2010). Collar rot and wilt: a new disease of Java citronella (*Cymbopogon winterianus*) caused by *Fusarium moniliforme* Sheldon. *Plant Pathol.* 43, 1057–1061. doi: 10.1111/j.1365-3059.1994.tb01659.x

Ashraf, M., and Foolad, M. R. (2007). Roles of glycine betaine and proline in improving plant abiotic stress resistance. *Environ. Exp. Bot.* 59, 206–216. doi: 10.1016/j.envexpbot.2005.12.006

Ashraf, M., Shahzad, S. M., Imtiaz, M., Rizwan, M. S., Arif, M. S., and Kausar, R. (2018). Nitrogen nutrition and adaptation of glycophytes to saline environment: a review. *Arch. Agron. Soil Sci.* 1419571, 1–26. doi: 10.1080/03650340.2017.1419571

Bennett, A., and Groten, K. (2022). The costs and benefits of plant–arbuscular mycorrhizal fungal interactions. *Annu. Rev. Plant Biol.* 73, 649–672. doi: 10.1146/annurev-arplant-102820-124504

Bolger, A. M., Marc, L., and Bjoern, U. (2014). Trimmomatic: a flexible trimmer for illumina sequence data. *Bioinformatics* 30, 2114–2120. doi: 10.1093/bioinformatics/btu170

Bremner, J. M. (2009). Determination of nitrogen in soil by the kjeldahl method. *J. Agric. Sci.* 55, 11–33. doi: 10.1017/S0021859600021572

Cameron, D. D., Neal, A. L., Wees, S., and Ton, J. (2013). Mycorrhiza-induced resistance: More than the sum of its parts? *Trends Plant Sci.* 18, 539–545. doi: 10.1016/j.tplants.2013.06.004

Camilios-Neto, D., Bonato, P., Wassem, R., Tadra-Sfeir, M. Z., Brusamarello-Santos, L. C., Valdameri, G., et al. (2014). Dual RNA-seq transcriptional analysis of wheat roots colonized by *Azospirillum brasilense* reveals up-regulation of nutrient acquisition and cell cycle genes. *BMC Genomics* 15, 378. 1–378.13. doi: 10.1186/1471-2164-15-378

Campos-Soriano,, Garcia-Garrido, J. M., San,, and Segundo, (2010). Activation of basal defense mechanisms of rice plants by glomus intraradices does not affect the arbuscular mycorrhizal symbiosis. *New Phytol.* 188 (2), 597–614. doi: 10.1111/j.1469-8137.2010.03386.x

Caporaso, J. G., Kuczynski, J., Stombaugh, J., Bittinger, K., Bushman, F. D., Costello, E. K., et al. (2010). QIIME allows analysis of high-throughput community sequencing data. *Nat. Methods* 7, 335–336. doi: 10.1038/nmeth.f.303

Chang, C. H., and Yang, S. S. (2009). Thermo-tolerant phosphate-solubilizing microbes for multi-functional biofertilizer preparation. *Bioresource Technol.* 100, 1648–1658. doi: 10.1016/j.biortech.2008.09.009

Cheng, Z., Woody, O. Z., Mcconkey, B. J., and Glick, B. R. (2012). Combined effects of the plant growth-promoting bacterium *Pseudomonas putida* UW4 and salinity stress on the *Brassica napus* proteome. *Appl. Soil Ecol.* 61, 255–263. doi: 10.1016/j.apsoil.2011.10.006

Delgado-Baquerizo, M., Grinyer, J., Reich, P. B., and Singh, B. K. (2016). Relative importance of soil properties and microbial community for soil functionality: insights from a microbial swap experiment. *Funct. Ecol.* 30, 1–12. doi: 10.1111/1365-2435.12674

Delvasto, P., Valverde, A., Ballester, A., Igual, J. M., Muñoz, J. A., González, F., et al. (2006). Characterization of brushite as a re-crystallization product formed during bacterial solubilization of hydroxyapatite in batch culture. *s. Soil Biol. Biochem.* 38, 2645–2654. doi: 10.1016/j.soilbio.2006.03.020

Deng, Y., Liu, R., Wang, Z., Zhang, L., and Diao, J. (2021). The stereoselectivity of metconazole on wheat grain filling and harvested seeds germination: implication for the application of triazole chiral pesticides. *J. Hazardous Materials* 416, 125911. doi: 10.1016/j.jhazmat.2021.125911

Despina, B., Cotton, T. E. A., Daniell, T. J., Bidartondo, M. I., Cameron, D. D., and Evans, K. L. (2018). The effects of arbuscular mycorrhizal fungal colonisation on nutrient status, growth, productivity, and canker resistance of apple (*Malus pumila*). *Front. Microbiol.* 9 (1461), 1–14. doi: 0.3389/fmicb.2018.01461

Dombrowski, N., Teske, A., and Baker, B. (2018). Expansive microbial metabolic versatility and biodiversity in dynamic guaymas basin hydrothermal sediments. *Nat. Commun.* 9, 1–13. doi: 10.1038/s41467-018-07418-0

Drakopoulos, D., Kgi, A., Gimeno, A., Six, J., and Vogelgsang, S. (2020). Prevention of *Fusarium* head blight infection and mycotoxins in wheat with cut-and-carry biofumigation and botanicals. *Field Crops Res.* 246 (107681), 1–9. doi: 10.1016/j.fcr.2019.107681

Edgar, R. C. (2013). UPARSE: highly accurate OTU sequences from microbial amplicon reads. *Nat. Methods* 10, 996–998. doi: 10.1038/nmeth.2604

Etesami, H., and Beattie, G. (2018). Mining halophytes for plant growth-promoting halotolerant bacteria to enhance the salinity tolerance of non-halophytic crops. *Front. Microbiol.* 9 148, 1–20. doi: 10.3389/fmicb.2018.00148

Gaju, O., Allard, V., Martre, P., Gouis, J. L., Moreau, D., Bogard, M., et al. (2014). Nitrogen partitioning and remobilization in relation to leaf senescence, grain yield and grain nitrogen concentration in wheat cultivars. *Field Crops Res.* 155, 213–223. doi: 10.1016/j.fcr.2013.09.003

Geel, M. V., Jacquemyn, H., Plue, J., Saar, L., and Ceulemans, T. (2017). Abiotic rather than biotic filtering shapes the arbuscular mycorrhizal fungal communities of European seminatural grasslands. *New Phytol.* 220, 1–11. doi: 10.1111/nph.14947

Guo, X., Wang, P., Wang, X., Li, Y., and Zhang, J. (2022). Specific plant mycorrhizal responses are linked to mycorrhizal fungal species interactions. *Front. Plant Sci. 13* 930069, 1–15. doi: 10.3389/fpls.2022.930069

Hao, W. Y., Ren, L. X., Ran, W., and Shen, Q. R. (2010). Allelopathic effects of root exudates from watermelon and rice plants on *Fusarium oxysporum* f.sp. *niveum*. *Plant Soil* 336, 485–497. doi: 10.1007/s11104-010-0505-0

Islam, F., Yasmeen, T., Arif, M. S., Ali, S., Ali, B., Hameed, S., et al. (2016). Plant growth promoting bacteria confer salt tolerance in *Vigna radiata* by up-regulating antioxidant defense and biological soil fertility. *Plant Growth Regul.* 80, 23–36. doi: 10.1007/s10725-015-0142-y

Jackson, M. L. (1979). *Soil chemical analysis - advanced course* (Prentice- Hall, Englewood Cliffs, NJ: UW-Madison Libraries Parallel Press).

Javad, N., Etebarian, H. R., and Gholam, K. (2006). Biological control of *Fusarium graminearum* on wheat by antagonistic bacteria. *Songklanakarin J. Sci. Technol.* 28, 29–38. Available at: https://www.researchgate.net/publication/26469827.

Ji, C., Tian, H., Wang, X., Song, X., Ju, R., Li, H., et al. (2022). *Bacillus subtilis* HG-15, a halotolerant rhizoplane bacterium, promotes growth and salinity tolerance in wheat (*Triticum aestivum*). *BioMed. Res. Int.* 9506227, 1–16. doi: 10.1155/2022/9506227

Ji, C., Wang, X., Song, X., Zhou, Q., Li, C., Chen, Z., et al. (2021). Effect of *Bacillus velezensis* JC-K3 on endophytic bacterial and fungal diversity in wheat under salt stress. *Front. Microbiol.* 12 (802054). doi: 10.3389/fmicb.2021.802054/full

Ji, C., Wang, X., Tian, H., Hao, L., Wang, C., Zhou, Y., et al. (2020). Effects of *Bacillus methylotrophicus* M4-1 on physiological and biochemical traits of wheat under salinity stress. *J. Appl. Microbiol.* 129, 1–17. doi: 10.1111/jam.14644

Ju, Y., Kou, M., Zhong, R., Christensen, M. J., and Zhang, X. (2021). Alleviating salt stress on seedings using plant growth promoting rhizobacteria isolated from the rhizosphere soil of *Achnatherum inebrians* infected with *Epichloë gansuensis* endophyte. *Plant Soil* 465, 349–366. doi: 10.1007/s11104-021-05002-y

Juniper, S., and Abbott, L. K. (2006). Soil salinity delays germination and limits growth of hyphae from propagules of arbuscular mycorrhizal fungi. *Mycorrhiza* 16, 371–379. doi: 10.1007/s00572-006-0046-9

Kausar, R., and Shahzad, S. M. (2006). Effect of ACC-deaminase containing rhizobacteria on growth promotion of maize under salinity stress. *J. Agric. Soc. Sci.* 2, 216–218.

Kobayashi, T., and Nishizawa, N. K. (2012). Iron uptake, translocation, and regulation in higher plants. *Annu. Rev. Plant Biol.* 63, 131–152. doi: 10.1146/annurev-arplant-042811-105522

Kohler, J., Hernández, J. A., Caravaca, F., and Roldán, A. (2009). Induction of antioxidant enzymes is involved in the greater effectiveness of a PGPR versus AM fungi with respect to increasing the tolerance of lettuce to severe salt stress. *Environ. Exp. Bot.* 65, 245–252. doi: 10.1016/j.envexpbot.2008.09.008

Landwehr, M., Hildebrandt, U., Wilde, P., Nawrath, K., Tóth, T., Biró, B., et al. (2002). The arbuscular mycorrhizal fungus *Glomus geosporum* in European saline, sodic and gypsum soils. *Mycorrhiza* 12, 199–211. doi: 10.1007/s00572-002-0172-y

Larena, I., Espeso, E. A., Villarino, M., Melgarejo, P., and Cal, A. D. (2018). Molecular techniques to register and commercialize a *Penicillium rubens* strain as a biocontrol agent. *New Future Developments Microbial Biotechnol. Bioengineering* 5, 97–117. doi: 10.1016/B978-0-444-63501-3.00005-3

Li, E., Ling, J., Wang, G., Xiao, J., Yang, Y., Mao, Z., et al. (2015). Comparative proteomics analyses of two races of *Fusarium oxysporum* f. sp. *conglutinans* that differ in pathogenicity. *Sci. Rep. 5* 13663, 1–21. doi: 10.1038/srep13663

Mago, T., and Salzberg, S. L. (2011). FLASH: Fast length adjustment of short reads to improve genome assemblies. *Bioinformatics* 27 (17), 2597–2963. doi: 10.1093/bioinformatics/btr507

Moussa, T. A. A., Almaghrabi, O. A., and Abdel-Moneim, T. S. (2013). Biological control of the wheat root rot caused by *Fusarium graminearum* using some PGPR strains in Saudi Arabia. *Ann. Appl. Biol.* 163, 72–81. doi: 10.1111/aab.12034

Munns, R., and Tester, M. (2008). Mechanisms of salinity tolerance. *Annu. Rev. Plant Biol.* 59, 651–681. doi: 10.1146/annurev.arplant.59.032607.092911

Naseer, M., Zhu, Y., Li, F. M., Yang, Y. M., Wang, S., and Xiong, Y. C. (2022). Nano-enabled improvements of growth and colonization rate in wheat inoculated with arbuscular mycorrhizal fungi. *Environ. pollut. 295* 118724, 1–12. doi: 10.1016/j.envpol.2021.118724

Oliver, R. E., Cai, X., Friesen, T. L., Halley, S., Stack, R. W., and Xu, S. S. (2008). Evaluation of *Fusarium* head blight resistance in tetraploid wheat (*Triticum turgidum* l.). *Crop Sci.* 48, 213–222. doi: 10.2135/cropsci2007.03.0129

Olsen, S. R. (1954). Estimation of available phosphorus in soils by extraction with sodium bicarbonate. *Miscellaneous Paper Institute Agric. Res. Samaru* 939, 18–19.

ÖPik, M., Vanatoa, A., Vanatoa, E., Moora, M., Davison, J., Kalwij, J. M., et al. (2010). The online database MaarjAM reveals global and ecosystemic distribution patterns in arbuscular mycorrhizal fungi (*Glomeromycota*). *New Phytol.* 188, 223–241. doi: 10.1111/j.1469-8137.2010.03334.x

Pawlowska, T. E., Gaspar, M. L., Lastovetsky, O. A., Mondo, S. J., Imperio, R. R., Evaniya, S., et al. (2018). Biology of fungi and their bacterial endosymbionts. *Annu. Rev. Phytopathol.* 56, 289–309. doi: 10.1146/annurev-phyto-080417-045914

Radhakrishnan, R., Hashem, A., and Abd_Allah, E. F. (2017). *Bacillus*: a biological tool for crop improvement through bio-molecular changes in adverse environments. *Front. Physiol.* 8, 667. doi: 10.3389/fphys.2017.00667

Ramakrishna, W., Yadav, R., and Li, K. (2019). Plant growth promoting bacteria in agriculture: Two sides of a coin. *Appl. Soil Ecol.* 138, 10–18. doi: 10.1016/j.apsoil.2019.02.019

Ruiz-Lozano, J. M., Aroca, R., Zamarre?, O.Á., Molina, S., Andreo-Jiménez, B., Porcel, R., et al. (2016). Arbuscular mycorrhizal symbiosis induces strigolactone biosynthesis under drought and improves drought tolerance in lettuce and tomato. *Plant Cell Environ.* 39, 441–452. doi: 10.1111/pce.12631

Saha, M., Sarkar, S., Sarkar, B., Sharma, B. K., Bhattacharjee, S., and Tribedi, P. (2016). Microbial siderophores and their potential applications: a review. *Environ. Sci. pollut. Res.* 23, 3984–3999. doi: 10.1007/s11356-015-4294-0

Shanthiyaa, V., Saravanakumar, D., Rajendran, L., Karthikeyan, G., and Raguchander, T. (2013). Use of *Chaetomium globosum* for biocontrol of potato late blight disease. *Crop Prot.* 52, 33–38. doi: 10.1016/j.cropro.2013.05.006

Sharma, S., Jayant, K., and Bhavanath, J. (2016). Halotolerant rhizobacteria promote growth and enhance salinity tolerance in peanut. *Front. Microbiol.* 7, 1600. 1–11. doi: 10.3389/fmicb.2016.01600

Simón, M., Brner, A., and Struik, P. C. (2021). Editorial: fungal wheat diseases: etiology, breeding, and integrated management. *Front. Plant Sci.* 12, 1–5. doi: 10.3389/fpls.2021.671060

Simón, M., Fleitas, M. C., Castro, A. C., and Schierenbeck, M. (2020). How foliar fungal diseases affect nitrogen dynamics, milling, and end-use quality of wheat. *Front. Plant Sci.* 11, 1–23. doi: 10.3389/fpls.2020.569401

Singh, R. P., and Jha., N. P. (2016). A halotolerant bacterium *Bacillus licheniformis* HSW-16 augments induced systemic tolerance to salt stress in wheat plant (*Triticum aestivum*). *Front. Plant Sci.* 7, 1890. 1–18. doi: 10.3389/fpls.2016.01890

Singh, D., and Prasanna, R. (2020). Potential of microbes in the biofortification of zn and fe in dietary food grains. a review. *Agron. Sustain. Dev.* 40 (15), 1–21. doi: 10.1007/s13593-020-00619-2

Singh, R. P., Shelke, G. M., Kumar, A., and Jha, P. N. (2015). Biochemistry and genetics of ACC deaminase: a weapon to "stress ethylene" produced in plants. *Front. Microbiol.* 6, 937. doi: 10.3389/fmicb.2015.00937

Smalla, K., Cresswell, N., Mendonca-Hagler, L. C., Wolters, A., and Elsas, J. D. V. (1993). Rapid DNA extraction protocol from soil for polymerase chain reaction-mediated amplification. *J. Appl. Microbiol.* 74, 78–85. doi: 10.1111/j.1365-2672.1993.tb02999.x

Smith,, and Sally, E. (2008). *Mycorrhizal symbiosis || structure and development of ectomycorrhizal roots* (New York: Academic Press), 191–268.

Thirkell, T., Charters, M., Elliott, A., Sait, S., and Field, K. (2017). Are mycorrhizal fungi our sustainable saviours? considerations for achieving food security. *J. Ecol.* 105, 921–929. doi: 10.1111/1365-2745.12788

Thirkell, T. J., Pastok, D., and Field, K. J. (2020). Carbon for nutrient exchange between arbuscular mycorrhizal fungi and wheat varies according to cultivar and changes in atmospheric carbon dioxide concentration. *Global Change Biol.* 26, 1-14. doi: 10.1111/gcb.14851

Vannini, C., Carpentieri, A., Salvioli, A., Novero, M., Marsoni, M., Testa, L., et al. (2016). An interdomain network: the endobacterium of a mycorrhizal fungus promotes antioxidative responses in both fungal and plant hosts. *New Phytol.* 211, 265–275. doi: 10.1111/nph.13895

Vogel, C., Potthoff, D., Schäfer, M., Barandun, N., and Vorholt, J. (2021). Protective role of the *Arabidopsis* leaf microbiota against a bacterial pathogen. *Nat. Microbiol.* 6, 1537–1548. doi: 10.1038/s41564-021-00997-7

Vries, F., Griffiths, R., Knight, C., Nicolitch, O., and Williams, A. (2020). Harnessing rhizosphere microbiomes for drought-resilient crop production. *Science* 368, 270–274. doi: 10.1126/science.aaz5192

Wang, Y., Pruitt, R. N., Nürnberger, T., and Wang, Y. (2022). Evasion of plant immunity by microbial pathogens. *Nat. Rev. Microbiol.* 20, 449–464. doi: 10.1038/s41579-022-00710-3

Wang, X. H., Wang, C. D., Li, Q., Zhang, J. M., Ji, C., Sui, J. K., et al. (2018). Isolation and characterization of antagonistic bacteria with the potential for biocontrol of soil-borne wheat diseases. *J. Appl. Microbiol.* 125, 1868–1880. doi: 10.1111/jam.14099

Yadav, R., Ror, P., Beniwal, R., Kumar, S., and Ramakrishna, W. (2021). *Bacillus* sp. and arbuscular mycorrhizal fungi consortia enhance wheat nutrient and yield in the second-year field trial: Superior performance in comparison with chemical fertilizers. *J. Appl. Microbiol.* 132, 2203–2219. doi: 10.1111/jam.15371

Yadav, R., Ror, P., Rathore, P., Kumar, S., and Ramakrishna, W. (2020). *Bacillus subtilis* CP4, isolated from native soil in combination with arbuscular mycorrhizal fungi promotes biofortification, yield and metabolite production in wheat under field conditions. *J. Appl. Microbiol.* 131, 339–359. doi: 10.1111/jam.14951

Yuan, J., Raza, W., Shen, Q., and Huang, Q. (2012) Antifungal activity of *Bacillus amyloliquefaciens* NJN-6 volatile compounds against *Fusarium oxysporum* f. sp. *cubense Appl. Environ. Microbiol.* 78, 5942–5944. doi: 10.1128/AEM.01357-12

Zeng, H., Yu, L., Liu, P., Wang, Z., and Wang, J. (2021). Nitrogen fertilization has a stronger influence than cropping pattern on AMF community in maize/soybean strip intercropping systems. *Appl. Soil Ecol.* 167, 104034. 1–11. doi: 10.1016/j.apsoil.2021.104034

Zhou, N., Zhao, S., and Tian, C. Y. (2017). Effect of halotolerant rhizobacteria isolated from halophytes on the growth of sugar beet (*Beta vulgaris* l.) under salt stress. *FEMS Microbiol. Lett.* 364, fnx091. 1–8. doi: 10.1093/femsle/fnx091

Zhu, F., Qu, L., Hong, X., and Sun, X. (2011). Isolation and characterization of a phosphate-solubilizing halophilic bacterium *Kushneria* sp. YCWA18 from daqiao saltern on the coast of yellow Sea of China. *Evidence-Based Complementary Altern. Med.* 615032, 1–6. doi: 10.1155/2011/615032

frontiers | Frontiers in Plant Science

TYPE Original Research
PUBLISHED 09 December 2022
DOI 10.3389/fpls.2022.1040752

OPEN ACCESS

EDITED BY
Paul Christiaan Struik,
Wageningen University and Research, Netherlands

REVIEWED BY
Mohammed Magdy Hamed,
Arab Academy for Science, Technology and Maritime Transport (AASTMT), Egypt
Emerson Del Ponte,
Universidade Federal de Viçosa, Brazil

*CORRESPONDENCE
Kwang-Hyung Kim
sospicy77@snu.ac.kr

SPECIALTY SECTION
This article was submitted to Plant Pathogen Interactions, a section of the journal Frontiers in Plant Science

RECEIVED 09 September 2022
ACCEPTED 23 November 2022
PUBLISHED 09 December 2022

CITATION
Jung J-Y, Kim J-H, Baek M, Cho C, Cho J, Kim J, Pavan W and Kim K-H (2022) Adapting to the projected epidemics of Fusarium head blight of wheat in Korea under climate change scenarios.
Front. Plant Sci. 13:1040752.
doi: 10.3389/fpls.2022.1040752

Adapting to the projected epidemics of Fusarium head blight of wheat in Korea under climate change scenarios

Jin-Yong Jung[1], Jin-Hee Kim[2], Minju Baek[1], Chuloh Cho[3], Jaepil Cho[4], Junhwan Kim[5], Willingthon Pavan[6,7] and Kwang-Hyung Kim[1]*

[1]Department of Agricultural Biotechnology, Seoul National University, Seoul, South Korea, [2]National Center for Agro-Meteorology, Seoul National University, Seoul, South Korea, [3]Wheat Research Team, National Institute of Crop Science, Wanju, South Korea, [4]Convergence Center for Watershed Management, Integrated Watershed Management Institute, Suwon, South Korea, [5]Korea National University of Agriculture and Fisheries, Jeonju, South Korea, [6]International Fertilizer Development Center, Muscle Shoals, AL, United States, [7]Graduate Program in Applied Computing, University of Passo Fundo, Passo Fundo, RS, Brazil

Fusarium head blight (FHB) of wheat, mainly caused by *Fusarium graminearum* Schwabe, is an emerging threat to wheat production in Korea under a changing climate. The disease occurrence and accumulation of associated trichothecene mycotoxins in wheat kernels strongly coincide with warm and wet environments during flowering. Recently, the International Panel for Climate Change released the 6th Coupled Model Intercomparison Project (CMIP6) climate change scenarios with shared socioeconomic pathways (SSPs). In this study, we adopted GIBSIM, an existing mechanistic model developed in Brazil to estimate the risk infection index of wheat FHB, to simulate the potential FHB epidemics in Korea using the SSP245 and SSP585 scenarios of CMIP6. The GIBSIM model simulates FHB infection risk from airborne inoculum density and infection frequency using temperature, precipitation, and relative humidity during the flowering period. First, wheat heading dates, during which GIBSIM runs, were predicted over suitable areas of winter wheat cultivation using a crop development rate model for wheat phenology and downscaled SSP scenarios. Second, an integrated model combining all results of wheat suitability, heading dates, and FHB infection risks from the SSP scenarios showed a gradual increase in FHB epidemics towards 2100, with different temporal and spatial patterns of varying magnitudes depending on the scenarios. These results indicate that proactive management strategies need to be seriously considered in the near future to minimize the potential impacts of the FHB epidemic under climate change in Korea. Therefore, available wheat cultivars with early or late heading dates were used in the model simulations as a realistic adaptation measure. As a result,

wheat cultivars with early heading dates showed significant decreases in FHB epidemics in future periods, emphasizing the importance of effective adaptation measures against the projected increase in FHB epidemics in Korea under climate change.

KEYWORDS

wheat, fusarium head blight, shared socioeconomic pathway, CMIP6, climate change, adaptation measure

1 Introduction

Fusarium head blight (FHB), also known as wheat scab, is mainly caused by *Fusarium graminearum* Schwabe and is a deadly fungal disease affecting staple crops, such as wheat, barley, and rice, in many countries (Bai and Shaner, 2004; Kim Y et al., 2018). Under favorable conditions for disease occurrence, FHB deteriorates crop quality and reduces yield, resulting in the economic loss (Parry et al., 1995). Grains infected with FHB can also be contaminated with various mycotoxins produced by the fungal pathogen, posing a health risk to humans and animals (Salgado et al., 2014). Therefore, FHB outbreaks can cause serious socioeconomic disruption. Previous studies report that FHB caused economic losses worth approximately $2.7 billion in the United States over the 20 years since the early 1990s (McMullen et al., 2012). Further, wheat- and barley-growing regions of South America reported a similar trend of increased FHB epidemic frequency and resultant losses in the 1990s (Del Ponte et al., 2009; Moschini et al., 2013; Duffeck et al., 2020). Fusarium head blight also poses a threat to wheat and barley production in many other countries, including China and Canada (Zhu et al., 2019).

Fusarium head blight is a major wheat disease in Korea (Ryu and Lee, 1990; Shin et al., 2018). In South Korea, wheat is cultivated mainly in the southern region; however, it is gradually expanding to the northern provinces, possibly owing to the recent warming climate. In 1963, the first major FHB outbreak devastated the southern region of the country, reducing the wheat yield by 40–80%. Since then, regular outbreaks have been reported approximately every ten years (Chung, 1975). However, owing to abnormal weather patterns and the expansion of wheat cultivation areas, the frequency of the disease outbreak has increased in the last two decades (Park et al., 2012). While severe outbreaks in 2002 resulted in up to 59% of the FHB incidence, the incidence in the southern provinces varied over the years, ranging from 0.1% to 16% (Shim and Gang, 2018), indicating that the occurrence of FHB is indeed affected by the annual variation in weather conditions during critical crop growth stages, including heading and flowering.

The wheat FHB causes distinct symptoms, such as premature bleaching of spikelets or blank heads and accumulation of mycotoxins, such as deoxynivalenol (DON), nivalenol (NIV), and zearalenone (ZEA), that have adverse effects on humans and animals. The FHB pathogen infects wheat anthers through wind dispersal or rain-splash during the flowering period from mid-April to mid-May. Since FHB is a monocyclic disease, the quantity of the primary inoculum is a key factor influencing its incidence. Overwintering pathogens on the crop residue are the main inoculum sources causing new infections during the following spring. Airborne ascospores, produced outside the field, could initiate disease by traveling long distances (Köhl et al., 2007). The FHB infection is greatly affected by weather conditions. During the flowering period, if the environmental conditions are optimal (16 to 30°C along with > 95% relative humidity for 2–3 days), the disease can spread rapidly (Parry et al., 1995). Owing to these epidemiological characteristics, FHB is considered a major plant disease influenced by abnormal weather events under climate change conditions.

A climate change impact assessment study of the FHB epidemic was conducted in Scotland (Skelsey and Newton, 2015). Decreasing risks of FHB epidemics with both limited and non-limited primary inocula were assessed for the 2040s and the 2080s. Similarly, Boland et al. (2004) estimated a possible reduction of FHB epidemics caused by the decreased rates of disease progression due to a projected decrease in rain and leaf wetness in Ontario, Canada. However, a contrary projection was made in Sweden (Roos et al., 2011), showing an increase in mycotoxin contamination owing to a more humid climate in the future. Another study in China simulated the projected increases of FHB epidemics in wheat by inputting the estimated anthesis dates and climate change scenario data into an FHB forecasting model (Zhang et al., 2014). Moschini et al. (2013) also showed an increase in the number of years with moderate or severe FHB incidence under the future climate change scenario in Argentina. These contrasting assessment studies indicate that climate change has complex impacts on FHB depending on the region and thus demand sophisticated impact assessments in future studies (Juroszek and von Tiedemann, 2013).

To conduct a climate change impact assessment on FHB, an ecophysiological model that considers environmental conditions affecting FHB infection and transmission can be used. Several models simulating the epidemics of FHB have been developed for Argentina (Moschini and Fortugno, 1996), Belgium (Detrixhe et al., 2003), Canada (Hooker et al., 2002), Italy (Rossi et al., 2003), the United States (De Wolf et al., 2003; Shah et al., 2013), and China (Xiao et al., 2020). Moschini and Fortugno (1996) developed empirical equations to predict FHB incidence in Argentina using accumulated degree-days and two-day window values of precipitation and relative humidity variables. Detrixhe et al. (2003) developed an ecophysiological model of FHB for winter wheat in Belgium, which predicts FHB infection based on the interpolation of weather radar data and uses the estimation of leaf wetness duration instead of relative humidity. In Canada, three equations using rainfall and temperature data as input variables for 4–7 days before heading were developed to predict the production of DON in mature wheat grains (Hooker et al., 2002). Rossi et al. (2003) developed a dynamic simulation model for FHB infection in wheat in Italy. This model calculates two daily indices, the infection risk of FHB and the mycotoxin content of kernels, based on a systems analysis that includes factors such as sporulation, spore dispersal, and infection of the host tissue (Leffelaar and Ferrari, 1989). In the United States, logistic regression models were developed using weather variables for seven days prior and ten days post anthesis (De Wolf et al., 2003). Other logistic regression models using weather variables before and after anthesis have also been developed in the US (Shah et al., 2013). Xiao et al. (2020) used a dynamic remote sensing technique to predict FHB infections in China.

Among existing FHB models, we used the GIBSIM to simulate the potential epidemics of FHB in wheat in Korea, as it better reflects the environmental conditions affecting the development of FHB during the flowering period (Del Ponte et al., 2005). The GIBSIM model was first developed in Brazil and used as a web-based FHB forecasting system (Fernandes et al., 2007) and a climate variability impact assessment of FHB in southern Brazil (Del Ponte et al., 2009). The GIBSIM model calculates FHB infection risk by combining the effects of multiple epidemiological factors, such as the host, inoculum, and environment. It simulates the accumulated infection index (GIB%) by obtaining the proportional value of each epidemiological factor and then multiplying them. The proportion of host factors is the proportion of susceptible tissue obtained by calculating the anthers extruded in the head emerging at the heading date. The proportion of the inoculum factor reflects the inoculum pressure with daily relative humidity and is a dummy variable for consecutive rainy days. Daily precipitation and relative humidity were used to determine the conducive conditions for FHB infection and the proportion of possible infection events.

The GIBSIM model requires information on the wheat heading date as a key input to simulate FHB infection risk. Since the heading date could change due to the increasing temperature under climate change, the potential FHB epidemic can be predicted realistically by integrating the simulation of wheat heading dates into the modeling process with the GIBSIM in this study. Many phenological models, including empirical models based on the accumulation of thermal time and mechanistic models simulating the emission of leaves and spike primordia at the shoot apex, have been used to predict wheat phenology (Bogard et al., 2014). We adopted the development rate (DVR) model introduced by Maruyama et al. (2010) to estimate the wheat heading date for each simulation site and period.

Wheat is not the main staple crop in Korea, and most of the wheat consumed in Korea is imported from the United States, Canada, and Australia (Statistics Korea, 2022). Therefore, the self-sufficiency rate of wheat production in South Korea is at a meager 0.5%. However, owing to food security issues due to the recent COVID-19 pandemic and international conflicts limiting the trade of food and natural resources, the importance of wheat production in Korea is increasing. In addition, considering the recurring food crisis due to rapid global and climate change and the modest self-sufficiency rate (20.2% as of 2020) of grain crops in South Korea, the government has been trying to increase domestic wheat production by implementing the "wheat industry development basic plan" policy aimed at achieving a 10% wheat self-sufficiency rate by 2030. Wheat is currently cultivated only in the southern region of South Korea. Wheat cultivation areas, benefiting from government support and the warming winter temperatures, are likely to expand northward. Therefore, assessing the projected impacts of climate change on the FHB epidemic in Korea is necessary. In this study, we determined the areas suitable for wheat cultivation at present and in the future based on the guidelines of the Rural Development Administration (RDA) of South Korea, predicted wheat heading dates for each area using the DVR model, and then simulated the future FHB epidemics using the GIBSIM over the suitable areas and during the predicted heading periods from the respective models. Finally, we examined the projected FHB epidemics in alternative wheat cultivars with early or late heading dates as an adaptation strategy to climate change.

2 Materials and methods

2.1 Study area and climate data

The target area of this study was the entire Korean Peninsula (latitude 37°31' N, longitude 127°01' E), including both South and North Korea (Figure 1). The spatial variability in climate over the peninsula is influenced by topography, consisting of mountains (57.4%) and plains (35.1%). In addition, the climate differs dramatically from north to south, spanning approximately 11 degrees of latitude (approximately 1100 km distance). South Korea experiences a relatively warm and wet

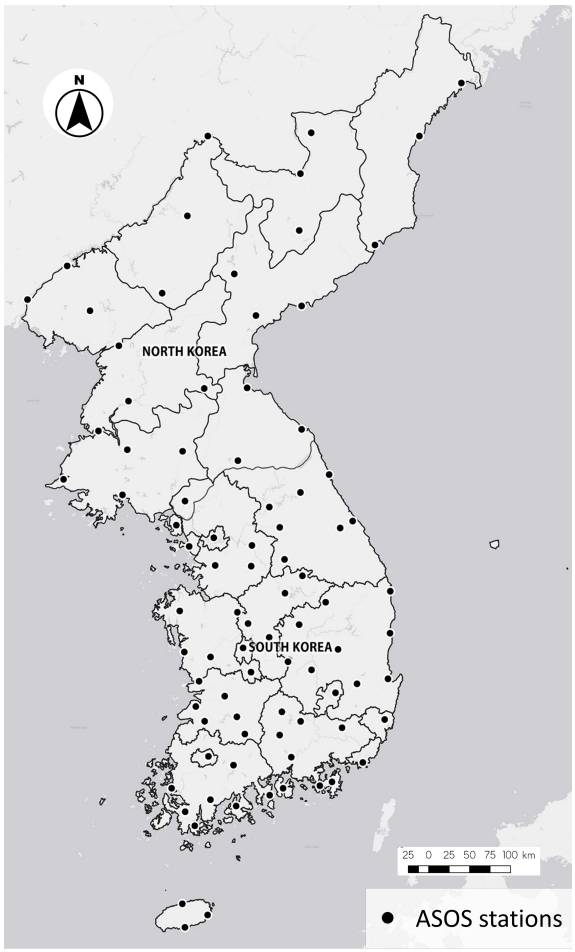

FIGURE 1
The Korean Peninsula with the location information of the 87 Automatic Synoptic Observation System (ASOS) stations used in the study.

climate affected by the warm East Korea Warm Current, whereas North Korea experiences a colder and, to some extent, an inland climate similar to that of the continent. A recent climate change assessment report published by the Korea Meteorological Administration (KMA) showed that the historical records of air temperature over the Korean Peninsula show a faster rise than the global mean trend. Further, the seasonal precipitation variability considerably increased over the past few years (Korea Meteorological Administration, 2020).

Daily weather data, such as maximum and minimum air temperature (°C), precipitation (mm), relative humidity (%), and solar radiation (W m^{-2}), from 1981 to 2021, were obtained from 87 Automatic Synoptic Observation System (ASOS) stations. These stations are evenly distributed over the Korean Peninsula (Figure 1), representing most of the local climate of the peninsula. The ASOS data are quality-controlled by the KMA and can be downloaded from the Open Meteorological Data Portal (https://data.kma.go.kr). In this study, the ASOS weather data for 1981–2010 were used as the observation weather data (hereafter, the observation data) for bias-correction of or comparison with climate change scenario data (hereafter, the scenario data) from global climate models (GCM). Owing to considerable missing solar radiation data in the ASOS data, we used daily climatological averages of solar radiation from 1993 to 2021, obtained from the National Aeronautics and Space Administration–Prediction Of Worldwide Energy Resources (NASA–POWER), for each ASOS station (Sayago et al., 2020).

The Shared Socioeconomic Pathways (SSP) scenario data from the sixth phase of the Coupled Model Intercomparison Project (CMIP6) by the Intergovernmental Panel on Climate Change (IPCC) were used in this study. The SSP scenarios include new social and economic factors along with the Representative Concentration Pathway (RCP), thus allowing the projection of future changes in energy and land use based on adaptation and mitigation scenarios (O'Neill et al., 2017; Wang et al., 2018). The

SSP scenarios are divided into five main groups (SSP119, SSP126, SSP245, SSP370, and SSP585) based on future mitigation and adaptation efforts considering future socioeconomic changes and various radiative forcings in the Fifth Assessment Report (AR5). Among them, two scenarios, SSP245 and SSP585, were used as future climate change scenarios in this study. As the current emissions are comparable to the RCP8.5 pathway (Schwalm et al., 2020), these two scenarios are thought to be the most relevant for policymakers to develop policy interventions for climate change in Korea (Lee et al., 2022b). For example, SSP245 assumes a scenario in which a range of technologies and strategies for reducing greenhouse gas emissions are employed in Korea, resulting in stabilized anthropogenic radiative forcing at 4.5 W m^{-2} in 2100. If the "net-zero" emissions or carbon neutrality policy are realized, as pledged by the South Korean government in 2020 (Ministry of Environment, http://eng.me.go.kr), the SSP245 scenario is highly likely to occur in the future. On the contrary, SSP585 corresponds to a nominal anthropogenic forcing of 8.5 W m^{-2} by 2100, assuming a continuously increasing trend of greenhouse gas emissions owing to limited global/national policy intervention in the future (Olivier et al., 2017).

CMIP6 scenario data are available from the Earth System Grid Federation (Williams et al., 2016). In this study, daily weather variables of maximum and minimum air temperatures, relative humidity, precipitation, and solar radiation from 1981 to 2100 were collected from 18 GCMs for two scenarios: SSP245 and SSP585 (Table 1). For the subsequent model simulation, the scenario data from 18 GCMs were divided into three periods:1981–2010, 2041–2070, and 2071–2100. Scenario data from 1981 to 2010 were used to represent the historical period, whereas scenario data for 2041–2070 were used for the near future period and 2071–2100 for the distant future period.

The scenario data obtained from the GCMs deviated significantly from the observation data obtained from the ASOS stations. Therefore, using them directly as inputs in impact modeling is challenging. In particular, agricultural impact models, such as crop growth, phenology, and pest and disease models, are highly sensitive to systemic bias in scenario data from GCMs (Ines and Hansen, 2006; Laux et al., 2021). The simple quantile mapping (SQM) method was used for bias correction in this study. SQM is a non-parametric bias correction method that uses empirical quantile mapping to

TABLE 1 18 GCMs for the CMIP6 climate change scenarios.

Model	Origin	Country	Resolution	Reference
GFDL-ESM4	Geophysical Fluid Dynamics Laboratory	USA	360 * 180	(John et al., 2018)
MRI-ESM2-0	Meteorological Research Institute	Japan	320 * 160	(Yukimoto et al., 2019)
CNRM-CM6-1 CNRM-EMS2-1	Centre National de Recherches Meteorologiques	France	24572 grids over 128 latitude circles	(Voldoire, 2019) (Seferian, 2019)
IPSL-CM6A-LR	Institute Pierre-Simon Laplace	France	144 * 143	(Boucher et al., 2019)
MPI-ESM1-2-HR MPI-ESM1-2-LR	Max Planck Institute for Meteorology	Germany	384 * 192 192 * 96	(Schupfner et al., 2019) (Wieners et al., 2019)
UKESM1-0-LL	Met Office Hadley Centre	UK	192 * 144	(Good et al., 2019)
ACCESS-CM2	Commonwealth Scientific and Industrial Research Organisation, Australian Research Council Centre of Excellence for Climate System Science	Australia	192 * 144	(Dix et al., 2019)
ACCESS-ESM1-5	Commonwealth Scientific and Industrial Research Organisation	Australia	192 * 145	(Ziehn et al., 2019)
CanESM5	Canadian Centre for Climate Modelling and Analysis	Canada	128 * 64	(Swart et al., 2019)
INM-CM4-8 INM-CM5-0	Institute for Numerical Mathematics	Russia	180 * 120 180 * 120	(Volodin et al., 2019a) (Volodin et al., 2019b)
EC-Earth3	EC-Earth-Consortium		512 * 256	EC-Earth Consortium (EC-Earth) (2019)
MIROC6 MIROC-ES2L	Japan Agency for Marine-Earth Science and Technology, Atmosphere and Ocean Research Institute, National Institute for Environmental Studies, RIKEN Center for Computational Science	Japan	256 * 128 128 * 64	(Shiogama et al., 2019) (Tachiiri et al., 2019)
NorESM2-LM	NorESM Climate modeling Consortium consisting of CICERO	Norway	144 * 96	(Seland et al., 2019)
KACE-1-0-G	National Institute of Meteorological Sciences, Korea Meteorological Administration	Korea	192 * 144	(Byun et al., 2019)

estimate the bias between the observation data for each quantile and the scenario data from GCMs. It is capable of minimizing the overestimation that may be caused by the theoretical cumulative distribution function (CDF) equation. To conduct bias correction, we used 30 years of observation data for 1981–2010 obtained from the ASOS stations as a reference for the SQM. The scenario data from 18 GCMs were bias-corrected and spatially downscaled to 87 weather station points for three simulation periods (historical, near future, and distant future) using the rSQM package of the R programming language (R version 4.2.1) (Cho et al., 2018). More details on the SQM implementation for the bias correction of GCM data are available in previous studies by Cho et al. (2020) and Lee et al., (2022b).

The reproducibility of the bias-corrected and downscaled CMIP6 scenarios from 18 GCMs was evaluated based on spatial comparisons between the observation and scenario weather data for the historical period (1981–2010). The reproducibility test was conducted for three weather variables (average air temperature, total precipitation, and average relative humidity) in April and May because the flowering of wheat—corresponding to the simulation period of the FHB epidemic—took place during these months of the historical period (1981–2010). Solar radiation was omitted because the NASA–POWER averages were used in the ASOS data. The monthly average values of the corresponding weather variables were compared, and the percentage differences between the scenario and observation data were visualized to examine the reproducibility of the scenario data from the GCMs. Reasonably good agreement for the percent difference maps of all three weather variables is shown in Supplementary Figure S1. The reproducibility tests indicate that the bias-corrected and downscaled CMIP6 scenarios are comparable to the observation data, allowing their use for the subsequent analyses of impact assessment and adaptation studies using the DVR model for simulating wheat heading date and GIBSIM for simulating the FHB epidemic.

2.2 Models

2.2.1 The DVR model to predict the heading date of wheat

The developmental rate (DVR) model, introduced by Maruyama et al. (2010), was used to predict the heading date of the Geumgang cultivar for winter wheat. The Geumgang cultivar is cultivated in over 70% of wheat areas in South Korea. The DVR model estimates phenological development based on the numerical relationship between DVR and daily weather data and has been widely used for several crops (Sameshima, 2000; Maruyama et al., 2010; Zhang and Tao, 2013). The DVR model can predict major growth stages relatively accurately and with lesser effort, according to the weather information of the crop growth period. The phenological stage of wheat is represented by the developmental index (DVI). Starting from the sowing date (DVI = 0), the point at which the accumulated DVR value reached 1 was considered the heading date (DVI = 1) (Eq. 1).

$$DVI_n = \sum_{i=1}^{n} DVR_i \tag{1}$$

where DVI_n is the developmental index on day n, and DVR_i is the developmental rate on day i.

The DVR values were calculated using Eq. (2), which requires two weather variables, the daily mean air temperature (T) and daily photoperiod (L), and five parameters, including the minimum number of days from emergence to heading (G_v), temperature when the DVR value becomes half of the maximum rate (T_{hv}), critical photoperiod (L_c), temperature parameter (A_v), and photoperiod parameter (B). Further information on the definition and response of the model parameters is described in detail by Maruyama et al. (2010). Kim et al. (2022) determined five parameters using the observed heading dates of the Geumgang cultivar collected from eight distinct agroclimatic sites in Korea from 2011 to 2021.

$$\begin{aligned} DVR &= \frac{1}{G_v} \times \frac{1-exp\{-B(L-L_c)\}}{1+exp\{-A_v(T-T_{hv})\}}, \quad for \;\; B(L-L_c) \geq 0 \\ &= \; 0, \qquad\qquad\qquad\qquad\quad for \;\; B(L-L_c) \geq 0 \end{aligned} \tag{2}$$

The air temperature variable (T) was obtained either from the ASOS data or from the CMIP6 scenario data of the 18 GCMs used in the study, and the photoperiod variable (L) was estimated using Eq. (3) (Allen et al., 1998)

$$L = \frac{24}{\pi}\left[\cos^{-1}(-\tan\phi \tan\delta)\right] \tag{3}$$

where ϕ is the latitude, and δ is the declination of the sun.

The average prediction errors for the estimated heading date using the DVR model were as follows: ME = 0.9, RMSE = 5.1 (day), and the coefficient of determination (R^2) = 0.56. In the study, with the DVR model, heading dates of the Geumgang cultivar were estimated for all 87 ASOS stations using either the observation data from the ASOS stations or scenario data from the 18 GCMs.

Suitable areas for winter wheat were determined based on official guidelines published by the RDA in Korea (Rural Development Administration, 2020). The RDA guideline instructs that winter wheat can grow where the daily minimum temperature in January ranges from −9 °C to 10 °C. Therefore, the suitable areas were determined as follows: the ASOS observation data and the GCM scenario data were divided into decadal (10-year) periods, and decadal averages of daily minimum temperature in January were calculated and used for the determination of suitable areas in every decadal interval. The sowing date was predicted only for the selected suitable areas by using the quadratic equations in Eq. (4) and Eq. (5), based on the

relationship between the average minimum temperature in January and the optimal sowing date for each area under distinct elevations, either below or above 100 m from the sea surface.

$$[Below\ \ 100m]\quad y = -0.1017x^2 + 2.2899x + 305.98 \qquad (4)$$

$$[More\ \ than\ \ 100m]\quad y = \ -0.081x^2 + 2.2603x + 299.35 \qquad (5)$$

where x is the daily minimum temperature in January averaged over 10 years, and y is the estimated sowing date of winter wheat.

As a result, the sowing dates of the Geumgang cultivar for the 87 ASOS stations were calculated for the historical (1981–2010) and two future periods (2041–2070 and 2071–2100) using the ASOS observation data and the scenario data of two SSP245 and SSP585 scenarios from 18 GCMs. Using the same weather input data and DVR model (Eq. 1, 2, and 3), heading dates were predicted from the estimated sowing dates.

2.2.2 The GIBSIM model used to predict the FHB epidemics

The GIBSIM, an FHB infection risk model (Del Ponte et al., 2005), was used to simulate the FHB epidemics at the 87 ASOS stations. Daily weather variables, average air temperature, total precipitation, and average relative humidity were used as input data for the model simulation.

The GIBSIM was first developed and successfully used for FHB early warning and climate variability studies in Brazil (Del Ponte et al., 2005; Fernandes et al., 2007; Del Ponte et al., 2009). The model considers three epidemiological factors related to FHB infection: host, inoculum, and environmental factors. The final output of the model is the accumulated infection index (GIB%; hereafter, FHB risk index) as a function of the proportion of susceptible tissue (ST), infection frequency (INF), and FHB spore cloud density (GZ). Individual equations to determine the level of contributions from each epidemiological factor are available in detail in the study by Del Ponte et al. (2005). In addition, Supplementary Figure S2 also provides the diagram for the modeling structure of the GIBSIM, adopted from Figure 1 in Del Ponte et al. (2005), and the details of simulation mechanisms and equations used in the study.

Del Ponte et al. (2005) estimated disease incidence values using linear regression adjusted to the observed FHB incidence data collected in the experimental fields in Brazil. Similarly, to estimate FHB incidence from the FHB risk index of GIBSIM in Korea, we fitted a linear regression model between the FHB risk index and the actual FHB incidence in Korea. For this, the observed FHB incidence data (N=52) collected from major wheat and barley fields in Korea for 2015–2021 were used, and the GIBSIM was run to generate the corresponding FHB risk index using the observed data from the nearest ASOS stations for individual FHB survey data. The linear regression analysis using the observed FHB incidence data and the simulated FHB risk index resulted in a regression equation of $y = 4.06\ x + 1.19$ (y: FHB incidence; x: FHB risk index) and an R^2 of 0.55 (Supplementary Figure S3). This equation was used to estimate the ballpark figure of disease incidences from the FHB risk indices of GIBSIM throughout the study. This is because the risk index is a theoretical value for FHB infection risk, which hinders the readers from intuitively understanding the magnitudes of climate change impact and adaptation assessment results in the study.

2.3 Climate change impact and adaptation assessments

We used the GIBSIM to simulate FHB epidemics in the Korean Peninsula using *in situ* observations (the observation data) from 87 ASOS stations and climate change scenarios (the scenario data) from 18 GCMs of the CMIP6. Daily weather variables, such as maximum air temperature, minimum air temperature, total precipitation, average relative humidity, and average solar radiation, were used as input data for the model simulation. The predicted heading dates from the DVR model were used to initiate the GIBSIM simulations for each individual season. All GIBSIM simulations were run from the initial heading date (five days before the predicted heading date) to the date when susceptible tissues no longer existed, indicating that the simulation duration for each year was automatically determined in the model. The average duration of the model simulation was very similar for all periods: for example, 38.7, 38.3, and 39.4 days for the historical, near future, and distant future periods, respectively, in the SSP585 scenario.

To assess the climate change impact on FHB epidemics in Korea, GIBSIM was simulated for 87 ASOS stations based on two emission scenarios (SSP245 and SSP585) of CMIP6. Scenario data from 18 GCMs of the CMIP6 that were bias-corrected using the SQM were used as input data for the model simulation. The resulting simulation results were divided into three periods (1981–2010 for the historical, 2041–2070 for the near future, and 2071–2100 for the distant future). To visualize the results on the map, we created a multi-model ensemble (MME) using 30-year simulations for each period. Briefly, for a given GCM at each ASOS station, the average FHB risk indices over the 30-year GIBSIM simulations were calculated. The resultant one average value per GCM was then averaged for the 18 GCMs for each emission scenario (SSP245 or SSP585) to calculate the MME means. The MMEs of the FHB risk index were then converted into FHB incidences using the regression equation between the simulated FHB risk indices and the actual FHB incidences, shown in the 2.2.2 section. These were then visualized on the maps by spatially interpolating the 87 ASOS point values over the Korean Peninsula using the kriging method (Nelson et al., 1999).

Based on the GIBSIM simulations, we also proposed a possible adaptation strategy using wheat cultivars with different heading

dates. The underlying assumption of using alternative cultivars with different heading dates is that early or late heading dates will avoid environmental conditions conducive to FHB infection. Changing planting dates or using cultivars of different maturity to avoid high disease pressure periods is a popular adaptation strategy to mitigate the projected impacts of climate change on plant diseases (Nouri et al., 2017; Kim and Koh, 2019). A series of GIBSIM simulations were run to determine the effect of the changed (early or late) heading date on the FHB risk index. Briefly, the heading dates of the wheat cultivars released in South Korea were collected, and the relative differences to those of Geumgang, a cultivar used in the impact assessment, were used to determine the ranges of heading date adjustment in the GIBSIM simulation. The heading dates of the additional cultivar were ranged from 10 days earlier (−10) to 10 days later (+10), compared to the one of Geumgang. Simulations were conducted by adjusting the predicted heading dates from the DVR model at 5-day intervals (−10, −5, 0, + 5, and +10 days) and using the scenario data from 18 GCMs for future periods (2041–2070 and 2071–2100) of the SSP585 scenario. The simulation results were converted into FHB incidences using the regression equation in the 2.2.2 section and then summarized as the average FHB incidences of the entire Korean Peninsula for each future period.

To investigate whether the differences in the simulated risks from changing heading dates with different wheat cultivars were related to projected changes in each weather variable under climate change, we calculated the mean temperature, total precipitation, number of rainy days with more than 0.3 mm precipitation, and mean relative humidity for the simulation duration of the GIBSIM for each run. The number of rainy days over 0.3 mm was selected as it was used to determine the GZ (the daily relative density of an airborne FHB spore cloud) in the model. We conducted this analysis using only the SSP585 scenario data for the distant future period, as it showed the most considerable differences between different heading dates. The results were plotted using a box plot to compare the distribution of the projected changes in each weather variable, representing non-adaptation (using heading dates of the Geumgang) versus the early (−10 days) and the late (+10 days) heading dates, representing adaptation using different cultivars. In addition, a regression analysis with FHB incidences as a dependent variable and four weather variables as an explanatory variable was conducted to statistically understand the relative contribution of individual weather variables to the simulated FHB incidences.

3 Results

3.1 Suitable areas for winter wheat cultivation with the predicted heading dates from the DVR model

Prior to the impact assessment of future changes in FHB epidemics, the reproducibility of the essential weather variables (air temperature, precipitation, and relative humidity) from the CMIP6 scenario data was evaluated for April and May, corresponding to the duration of the GIBSIM simulations for the historical period (Supplementary Figure S1). With respect to average air temperature, the spatial distribution produced using the observation data showed similar results to the scenario data from 18 GCMs. The difference (%) between the observation and scenario data for the air temperature in April ranged from –9.8 to +8.9% (less than 0.63°C in absolute terms) over the Korean Peninsula. Mountainous areas in North Korea showed relatively higher differences (%) between the observation and scenario temperature data in April, with the maximum difference (–9.8%) in Baekdu-san, the highest mountain in Korea. Other than this specific case (air temperature in April), the reproducibility tests of other variables in both April and May resulted in smaller differences (%). While the air temperature in May ranged from –0.19 to +5.35%, the precipitation in April and May ranged from –0.56 to +1.64% and –0.49 to +3.46%, respectively. Further, the relative humidity in April and May ranged from –1.81 to +0.06% and –1.03 to +0.05%, respectively. The SQM used for the bias correction of the CMIP6 scenario tended to overestimate the precipitation in North Korea while underestimating it in South Korea. In addition, the SQM tended to underestimate the relative humidity throughout the Korean Peninsula, as shown in the difference (%) maps in Supplementary Figure S1. Consequently, based on these results, the bias-corrected scenario data from 18 GCMs showed reasonably good reproducibility to be used as input data for the models to simulate the wheat heading date and FHB risk index in the study.

Climatic suitability maps for wheat cultivation in the Korean Peninsula were generated based on the climatic conditions of the SSP245 and SSP585 scenarios for three periods (1981–2010 for historical, 2041–2070 for the near future, and 2071–2100 for the distant future). The projected spatiotemporal changes in the suitable areas for wheat cultivation (uncolored area indicates 'Not suitable' and colored area indicates 'Suitable') for each administrative area are indicated in Figure 2. The simulated suitable areas for the historic period show a good agreement with the actual wheat-growing areas in Korea for 2018–2022 (Korean Statistical Information Service, http://kosis.kr). Despite numerous factors, such as crop rotation, abiotic and biotic stresses, and socioeconomic factors, that affect actual areas for wheat cultivation, these results indicate that the climatic conditions used in this study can be used as a representative of the actual wheat cultivation conditions.

With climate change, the geographical areas that can support wheat cultivation will gradually expand from the present coastal and southern areas to higher inland and northern areas by 2100. In the historical period, more than 50% of the Korean Peninsula appears to be 'Not suitable' for wheat cultivation. However, in the distant future, more than 80% of the areas can be marked as 'Suitable' (Figure 2). This result strengthens the rationale for this study; new environments in the future, either from the

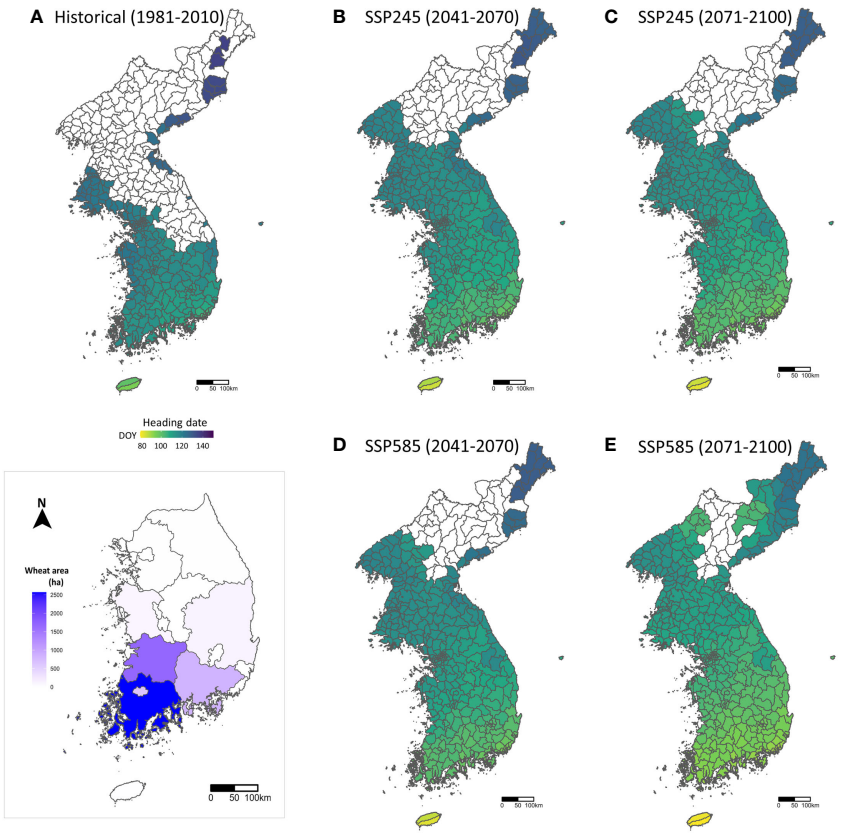

FIGURE 2
Areas suitable for wheat cultivation and the day of year (DOY) of the predicted heading dates on the maps of the Korean Peninsula in 1981-2010 **(A)** for the historical period, 2041–2070 **(B)** and 2071–2100 **(C)** under the SSP245 scenario, and 2041–2070 **(D)** and 2071–2100 **(E)** under the SSP585 scenario for the future periods. The colored areas indicate suitable wheat cultivation areas, and the DOY of the heading dates is expressed in color. The bottom left map (inset) shows the actual wheat cultivation areas **(ha)** in the provinces of South Korea for 2018–2022, obtained from the Korean Statistical Information Service (https://kosis.kr).

expansion of suitable areas or owing to climate change, will introduce new challenges, such as sudden FHB outbreaks, to wheat growers in Korea. Comparing the two SSP scenarios, the suitable areas for wheat cultivation in the near future are similar. In contrast, in the distant future period, wheat cultivation becomes possible in a larger area in the SSP585 scenario than in SSP245 due to an increase in minimum temperature in January.

For areas suitable for wheat cultivation, the heading dates of the Geumgang cultivar were predicted using the DVR model. The day of year (DOY) of the predicted heading dates shown on the maps indicate that the heading dates occur earlier in the south and later in the north, primarily because of the temperature-dependent development rate in phenology development. The average heading date for the historical period is 116 DOY, which, in the distant future period (2071–2100), advances to 108 DOY and 102 DOY in the SSP245 and SSP585 scenarios, respectively. This result suggests that increasing temperatures due to climate change significantly affect the phenological development of wheat in Korea.

3.2 Predicting climate change impacts on FHB epidemics using the GIBSIM

On suitable wheat cultivation areas and using the predicted heading dates (Figure 2), the effects of climate change on the FHB epidemics were assessed based on the SSP245 and SSP585 scenarios, and the MME (30-year average of the GIBSIM simulations using 18 GCM scenario data) of the FHB incidences for individual administrative areas were calculated and interpolated on the maps (Figure 3). In the historical period (1981–2010), most areas suitable for wheat showed relatively mild incidences of FHB epidemics, with an average incidence rate of 5.1%. This was consistent with the observed FHB incidence in the field. In fact, the epidemics of FHB in South

Korea have been below an economical threshold level, despite varying from 0.1% to 16% since 2002 due to the annual variation in weather conditions in the past years. However, the projected FHB incidences across the Korean Peninsula tended to be more severe towards future periods: 5.1%, 7.2%, and 9.2% of the average FHB incidences for the historical, near future, and distant future periods, respectively, in the SSP585 scenario. Notably, in the SSP245 scenario, a few areas in Korea showed slightly decreased FHB incidences (up to 11.3%) in the distant future period compared to the ones in the near future (data not shown).

Comparing South and North Korea, the incidence of FHB is projected to be relatively higher in North Korea than in South Korea; the average incidences of FHB in South and North Korea in the SSP585 scenario are 6.9% and 7.7%, respectively, for the near future, and 9.0% and 9.5% for the distant future period. These differences indicate that climate conditions in North Korea will become more conducive to FHB epidemics due to climate change. In particular, Hamgyeongbuk-do, the mountainous province in North Korea, showed the highest incidence of FHB, up to 21.8% in the distant future period. In most areas, the FHB incidence was relatively higher in SSP585 than in SSP245. Notably, in the distant future, the incidence of FHB will significantly increase in the coastal areas of the Korean Peninsula.

3.3 Adapting to the projected FHB epidemics

A possible adaptation strategy to the projected FHB epidemics was suggested using currently available wheat cultivars, either with earlier or later heading dates than the Geumgang cultivar. The underlying assumption is that advancing or delaying the timing of susceptible stages of wheat may help avoid environmental conditions conducive to FHB infection. Indeed, changing heading dates from −10 to +10 days at 5-day intervals compared to those of the Geumgang cultivar resulted in significant changes in FHB incidences (Table 2). The cultivars with an earlier heading date had a lower FHB incidence than the Geumgang cultivar, whereas the cultivars with a later heading date had a higher FHB incidence. Wheat cultivars with 10 days earlier heading dates showed a more substantial reduction in FHB incidences compared to those with 5 days earlier heading dates, despite limited availability for the cultivars with 10 days earlier heading dates, as shown in Table 2. Cultivars

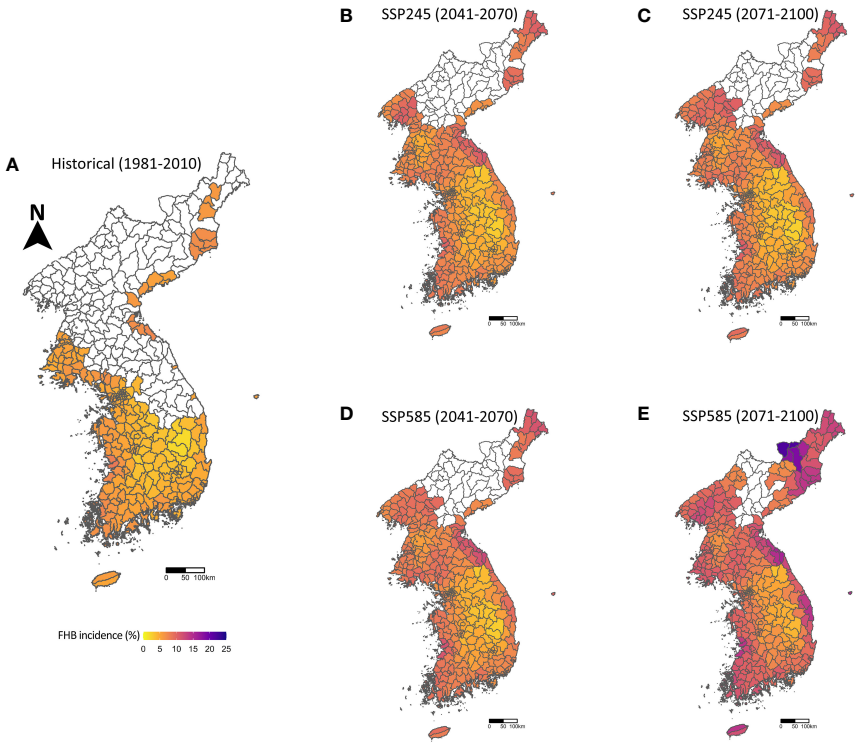

FIGURE 3
Projected FHB epidemics over the Korean Peninsula in 1981–2010 **(A)** for the historical period, 2041–2070 **(B)** and 2071–2100 **(C)** under the SSP245 scenario, and 2041–2070 **(D)** and 2071–2100 **(E)** under the SSP585 scenario for the future periods. The impact of climate change on FHB incidences was assessed for the suitable wheat cultivation areas using the predicted heading dates, as shown in Figure 2.

with early heading dates showed reductions of 17.3% (5 days earlier heading date) and 32.1% (10 days earlier heading date) in the average incidence of FHB in the near future, whereas the extent of risk reduction was decreased in the distant future. In contrast, later heading dates resulted in higher incidences of FHB in the near future: 19.5% with 5 days later heading date and 40.7% with 10 days later heading date. However, no further increase in FHB incidence was simulated in the near future. Instead, slightly decreased FHB incidences were recorded in the near future period. Overall, our adaptation analysis suggested that the Arijinheuk, Baekgang, Hwanggeumal, Joeun, Jogyeong, Johan, Jojung, Jonong, Jopum, and Saeol cultivars could be selected as alternatives for coping with the projected FHB epidemics in the future by replacing the Geumgang, a major wheat cultivar, in South Korea.

To understand the key weather variables affecting the projected changes in FHB incidences with varying heading dates, we extracted and analyzed the weather data used to simulate the GIBSIM (Figure 4). Graphical comparisons of the ranges of four weather variables (average air temperature, total precipitation, number of rainy days with more than 0.3 mm of precipitation, and average relative humidity) between the cultivars with different heading dates (before and after 10 days) indicated that the average air temperature and FHB incidences had the most similar box plot distribution. Thus, the temperature was the main factor that changed with a shift in the heading dates. Although the median values of the other three variables showed a similar increasing trend (from before to after 10 days) to the ones of FHB incidence, the heights of their box plots considerably overlapped, making the graphical interpretation of the FHB incidence and these weather variables interaction difficult.

Therefore, to further understand the relative contribution of individual weather variables, a regression analysis was conducted with FHB incidence as a dependent variable and four weather variables as an explanatory variable (Supplementary Figure S4). The linear regression results showed that with 0.83 of the coefficient of determination (R^2), the average air temperature had a relatively pronounced positive effect (coefficient: +1.28) with a confidence level of 99%, followed by the average relative humidity with a positive effect (coefficient: +0.30) with a confidence level of 99%, and the number of rainy days with a positive effect (coefficients: +0.22) with a confidence level of 99%. In contrast, total precipitation showed a very minimal positive effect (coefficient: +0.004) with no statistical significance in the regression result. These results indicated that the changes in air temperature, relative humidity, and rainy days significantly affected the resulting FHB incidences when the heading date was changed. Overall, our findings suggest that adopting alternatives or breeding new cultivars with early heading dates can be an effective adaptation strategy to manage the FHB epidemics better under climate change conditions in the Korean Peninsula.

4 Discussion and conclusions

We performed a series of modeling studies on wheat phenology and FHB epidemics in response to climatic conditions and successfully evaluated the impacts of climate change by sequentially integrating the modeling results. The integrated modeling approach, combining all results of wheat suitability, heading dates, and FHB incidences, showed gradual but continuous increases in the FHB incidence towards 2100, with different temporal and spatial patterns of varying magnitudes depending on the two SSP scenarios. To counter the projected increases in FHB incidence in the Korean Peninsula, a practical adaptation strategy utilizing currently available wheat cultivars, either with earlier or later heading dates compared to the Geumgang cultivar used in the study, was investigated. Replacing the Geumgang cultivar with the ones

TABLE 2 Manipulating the FHB risks for the near future (2041–2070) and the distant future (2071–2100) periods under the SSP585 scenario, through an adaptive measure of introducing alternative wheat cultivars with early or late heading dates (–10 to +10 days from the heading date of the Geumgang cultivar).

Heading Date	Cultivar	Future Period	Incidence (%)	Percent Change in Incidence (%)
Before 10 days (-10)	Arijinheuk	2041–2071	4.9	-32.1
		2071–2100	6.8	-26.1
Before 5 days (-5)	Baekgang, Hwanggeumal, Joeun, Jogyeong, Johan, Jojung, Jonong, Jopum, Saeol	2041–2071	6.0	-17.3
		2071–2100	7.9	-14.7
0	Dabun, Geumgang, Jeokjung, Joa, Jungmo2008	2041–2071	7.2	0
		2071–2100	9.2	0
After 5 days (+5)	Anbaek, Baekchal, Baekjung, Cheonggye, Dajung, Gobun, Goso, Hanbaek, Hojung, Jinpum, Milseong, Namhae, Ol, Olgeuru, Seodun, Sinmichal1, Suan, Sugang, Tapdong, Uju, Uri, Yeonbaek	2041–2071	8.6	19.5
		2071–2100	10.9	18.1
After 10 days (+10)	Alchan, Dahong, Eunpa, Geuru, Saegeumgang, Sinmichal, Taejung	2041–2071	10.2	40.7
		2071–2100	12.9	39.7

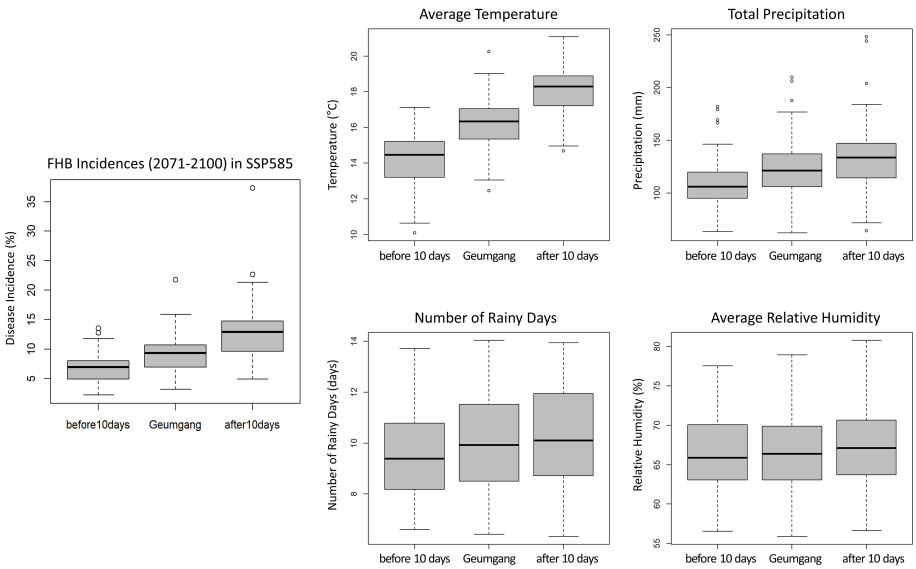

FIGURE 4
Comparisons of the adaptation strategy using early (before 10 days) or late (after 10 days) heading dates for the projected FHB incidences and the corresponding weather conditions of average air temperature, total precipitation, number of rainy days, and average relative humidity during the duration of GIBSIM simulations. Box plots were made with the results from multiple wheat-suitable areas based on the SSP585 scenario for the distant future period (2071-2100).

with an earlier heading date resulted in a substantial reduction in FHB incidence in future periods.

4.1 Simulation of suitable areas and heading dates for winter wheat in the Korean Peninsula

Based on the optimal climatic conditions for wheat cultivation, we simulated the potential expansion of areas suitable for wheat cultivation under climate change. This suitability mapping for areas where wheat fields are likely to be located in the future is a prerequisite to making the subsequent FHB risk projections more realistic and reasonable. Nevertheless, current wheat cultivation areas in the Korean Peninsula may not be+ the same as the simulated suitable areas. This is because wheat cultivation in Korea involves many factors besides climate. Thus, in several instances, wheat is not grown even if the area is climatically suitable for cultivation. Owing to the recent COVID-19 pandemic, frequent conflicts between countries, and the resultant surge in international wheat price, the South Korean government has been trying to increase domestic wheat production by implementing the "wheat industry development basic plan" policy aimed at achieving a 10% wheat self-sufficiency rate by 2030. These ongoing efforts may encourage the expansion of wheat cultivation areas to the simulated suitable areas in the near future.

A potential but more realistic FHB risk projection under climate change was derived by linking the GIBSIM with the DVR model to realize the actual field interactions of wheat and FHB during the flowering period of wheat. In this study, the DVR model was adopted to predict the heading date of the Geumgang cultivar. The simulations of heading date using the DVR model resulted in an advancing trend over future periods, reflecting the temperature rise under climate change. The GCMs of the SSP245 and SSP585 scenarios used in this study predicted that global mean temperature would rise by 3.02°C and 5.20°C by 2100, respectively (Sung et al., 2021). Our results showed a reasonable shift in the wheat heading date affected by this projected temperature increase. Considering that the existing ecophysiological models were able to predict the heading date of wheat with good accuracy with root mean square errors as low as 4 to 7 days (Asseng et al., 1998; White et al., 2008; Zheng et al., 2013; Bogard et al., 2014), the performance of the DVR model (5.1 days of RMSE) used in this study is reasonably good in predicting the heading date of the Geumgang cultivar (Kim et al., 2022). Nevertheless, to apply the GIBSIM model to other cultivars currently grown in Korea, adopting a mechanistic phenology model, such as the Sirius model (Jamieson et al., 1998), for the prediction of heading date should be considered. This is because mechanistic models consider the interactions between environment and genotype, represented by 'genetic

parameters' reflecting genetic variation among cultivars (Bogard et al., 2014).

4.2 Lack of the GIBSIM model calibration in the context of Korea

The regression equation between the simulated FHB risk indices of GIBSIM and the actual FHB incidences collected in the wheat fields of Korea showed that the GIBSIM simulations explain only 55% of the variation in the observed FHB incidences. Although similar levels of goodness-of-fit between the observed and simulated values is often found in many previous studies with plant disease or growth models (Burleigh et al., 1972; Hooker et al., 2002; Rossi et al., 2003; Liang et al., 2016; Jevtić et al., 2017), further effort should be made to improve the model performance. There are three possible reasons for the relatively low correlation between the observed FHB incidences and GIB% from the GIBSIM. First, some of the parameters and embedded algorithms of the GIBSIM are empirically developed based on the observations in Brazil (Del Ponte et al., 2005). This indicates these original parameters and algorithms may need to be calibrated or modified, respectively, to reflect the local-specific characteristics of the environment, pathogen strains, and wheat cultivars in Korea. In fact, this kind of model localization is required to minimize uncertainty and generate optimal model performance when adopting an existing model developed in other countries or regions (Andrade-Piedra et al., 2005; Kim KH et al., 2018; Rotter et al., 2012). Secondly, the quality of the observed FHB incidence data was low, as the spatial resolution of the data was low at the district (*si* or *gun* in Korea) level. Lastly, the corresponding weather data to run GIBSIM were obtained from the nearest ASOS weather station; thus, they might not represent the local weather conditions where the FHB incidence data were collected. To support the calibration study of GIBSIM in a future study, the corresponding metadata, such as coordinates and data collection dates, should be collected and used with the FHB incidence data (Donatelli et al., 2017). Location-specific, long-term, FHB occurrence data should be systematically collected, with the corresponding metadata, to enable further statistical modeling (Lee et al., 2022a) or process-based model calibration and validation (Kim KH et al., 2018). High-resolution grid products, such as the 1-km interpolated weather observation data from the KMA (https://data.kma.go.kr), need to be evaluated for the accuracy of the weather variables needed for the GIBSIM simulation. Although weather conditions largely determine the occurrence of FHB, agronomic factors also significantly influence FHB. Potential factors to be considered in future modeling efforts with GIBSIM include fungicide treatment, crop rotation system (with rice), weed management, and host plant resistance in Korea (Schaafsma and Hooker, 2007; Landschoot et al., 2011).

4.3 Adaptation strategies to the projected impacts of FHB in the Korean Peninsula

Impact assessments of FHB epidemics in the future indicate that the incidence of FHB in the Korean Peninsula is projected to increase in the future, and the projected incidence of FHB is slightly higher in North Korea than that in South Korea. Graphical comparisons for four essential weather variables between North and South Korea showed that air temperature and relative humidity were higher (favorable to FHB epidemics) in North Korea (Supplementary Figure S5). Wheat-suitable areas have expanded northward, covering much of the North Korean area in the distant future, indicating that more wheat cultivation may be possible in North Korea. Because of the economic sanctions and border closures due to COVID-19 over the last few years, North Korea is aggressively promoting wheat cultivation to fight for food security these days (news articles not shown). Considering the inevitable vulnerability of wheat cultivation due to the rapid expansion of wheat cultivation and the projected increase of FHB epidemics from this study, proactive, adaptive measures, supported by international humanitarian efforts supplying diverse wheat cultivars and essential agricultural inputs, should be prepared prior to actual cultivation of wheat in North Korea.

A possible adaptation strategy to the projected epidemics of FHB is suggested in this study, which uses alternative wheat cultivars with earlier heading dates compared with the Geumgang cultivar. Changing planting dates or using cultivars with different maturity to avoid the high disease pressure period is one of the most popular adaptation strategies to mitigate the projected impacts of climate change on plant diseases. In the study, wheat cultivars with 10 days earlier heading date showed a larger reduction in FHB incidences compared to those with 5 days earlier heading dates. However, cultivars with 10 days earlier heading dates, such as Arijinheuk (Table 2), have very limited availability on the market. However, the Baekgang, Hwanggeumal, Joeun, Jogyeong, Johan, Jojung, Jonong, Jopum, and Saeol cultivars, with 5 days earlier heading date, can also be an alternative as they reduce the projected risk for the near future period by 17.3%. Nevertheless, applying this adaptation strategy is not simple, as there are other factors to consider selecting alternative cultivars, such as stress tolerance, length of maturity, socioeconomic factor, and preference in the market. In addition, the assumption of a phenophase date for a plant is difficult to apply to annual crops, such as rice and wheat, which are more significantly affected by human-dependent planting and cultivation activities. In Korea, wheat is generally grown in crop rotation with rice, wherein winter wheat is grown after the rice harvest. Therefore, the possible period of wheat growth should not interfere with the rice cultivation period. Considering these potential conflicts, an integrated modeling solution that includes both wheat and rice growth models should be developed. Overall,

these indicate that reasonable adaptation strategies are difficult to implement even if they are properly presented.

4.4 Management of uncertainty in the climate change impact and adaptation study and the way forward

In addition to the projected FHB epidemics using only climatic factors, we expect that the epidemics of FHB will be more complicated in the future because of the complex interaction of climatic, genetic, and agronomic factors. This indicates that continuous studies are needed to get a clearer picture of uncertain climate change and the resulting disease risks in Korea. First, reducing the uncertainty level by removing or quantifying uncertain factors and better understanding used-to-be uncertain factors must be pursued through active research and development. For example, using 18 GCMs for each SSP scenario compensates for some systematic uncertainty inherent in GCMs (Mathukumalli et al., 2016; Ouma et al., 2016). Further, uncertainty in individual ecophysiological models, which leads to low reliability of the model, must be addressed. As mentioned previously, the main sources of model uncertainty include insufficient integration of non-climatic confounding factors in modeling and poor calibration and validation due to limited ground-truth data. As more location-specific ground-truth data are obtained through long-term and regular surveys, more reliable models can be used for impact studies. In addition, significant uncertainties account for all factors influencing plant disease epidemics, some of which cannot be predicted with the currently available knowledge and techniques. Various environmental factors not directly considered in the model, such as elevated CO_2 levels, soil nutrients, and other weather variables, can also influence future ecophysiological interactions (Velásquez et al., 2018). Therefore, a comprehensive process-based and integrated modeling approach that includes the ecophysiological responses of a plant, its interactions with pathogens, and environmental factors may be considered for future studies.

In this study, we presented an impact assessment and adaptation study of wheat FHB epidemics using an integrated modeling approach with multiple models. To alleviate projected increases in the FHB epidemic over the next 30 to 60 years, we used an integrated modeling solution to investigate a scientifically informed, long-term adaptation strategy replacing the original cultivar with a disease-resistant cultivar or a cultivar that can avoid high disease pressure by shortening the duration before the heading date. In addition, the impact assessment in each administrative district of the Korean Peninsula also needs to develop localized adaptation strategies for local government units in the local context. For example, an early warning system using short-term (2–3 days) to mid-term (7–15 days) weather forecasts and an FHB infection model would be useful for wheat growers to implement timely preventive controls of FHB. As this type of integrated modeling platform is developed and continuously improved with more quality-controlled data and more reliable modeling algorithms, policymakers and agricultural stakeholders will be able to prepare more realistic, rational adaptation strategies to deal with the upcoming climate change threat based on evidence-based scientific results. Many follow-up studies are needed in the near future, as indicated by the findings of this study.

Data availability statement

The original contributions presented in the study are included in the article/Supplementary Material. Further inquiries can be directed to the corresponding author.

Author contributions

J-YJ, J-HK, K-HK conceived and initiated the study and led the manuscript preparation. CC, JC collected and managed the required data for the analysis. J-YJ, J-HK, MB, JK conducted modelling and analysed the results. WP sourced the GIBSIM and provided advice and guidance for the study. All authors contributed to the article and approved the submitted version.

Funding

This work was supported by the National Research Foundation of Korea (NRF) grant funded by the Korean government (MSIT) (No. 500-20220247).

Conflict of interest

The authors declare that the research was conducted in the absence of any commercial or financial relationships that could be construed as a potential conflict of interest.

Publisher's note

Supplementary material

The Supplementary Material for this article can be found online at: https://www.frontiersin.org/articles/10.3389/fpls.2022.1040752/full#supplementary-material

References

Allen, R. G., Pereira, L. S., Raes, D., and Smith, M. (1998). *Crop evapotranspiration-guidelines for computing crop water requirements-FAO irrigation and drainage paper 56* Vol. 300 (Rome: FAO), D05109.

Andrade-Piedra, J. L., Forbes, G. A., Shtienberg, D., Grunwald, N. J., Chacon, M. G., Taipe, M. V., et al. (2005). Qualification of a plant disease simulation model: performance of the LATEBLIGHT model across a broad range of environments. *Phytopathology* 5, 1412–1422. doi: 10.1094/PHYTO-95-1412

Asseng, S., Keating, B., Fillery, I. R., Gregory, P., Bowden, J., Turner, N., et al. (1998). Performance of the APSIM-wheat model in Western Australia. *Field Crops Res.* 57, 163–179. doi: 10.1016/s0378-4290(97)00117-2

Bai, G., and Shaner, G. (2004). Management and resistance in wheat and barley to fusarium head blight. *Annu. Rev. Phytopathol.* 42, 135–161. doi: 10.1146/annurev.phyto.42.040803.140340

Bogard, M., Ravel, C., Paux, E., Bordes, J., Balfourier, F., Chapman, S. C., et al. (2014). Predictions of heading date in bread wheat (*Triticum aestivum* l.) using QTL-based parameters of an ecophysiological model. *J. Exp. Bot.* 65 (20), 5849–5865. doi: 10.1093/jxb/eru328

Boland, G. J., Melzer, M. S., Hopkin, A., Higgins, V., and Nassuth, A. (2004). Climate change and plant diseases in Ontario. *Can. J. Plant Pathol.* 26 (3), 335–350. doi: 10.1080/07060660409507151

Boucher, O., Denvil, S., Levavasseur, G., Cozic, A., Caubel, A., Foujols, M. A., et al. (2019). *IPSL IPSL-CM6A-LR model output prepared for CMIP6 ScenarioMIP* (Earth System Grid Federation). doi: 10.22033/ESGF/CMIP6.1532

Burleigh, J. R., Eversmeyer, M. G., and Roelfs, A. P. (1972). Development of linear equations for predicting wheat leaf rust. *Phytopathology* 62, 947–953. doi: 10.1094/Phyto-62-947

Byun, Y. H., Lim, Y. J., Shim, S., Sung, H. M., Sun, M., Kim, J., et al. (2019). *NIMS-KMA KACE1.0-G model output prepared for CMIP6 ScenarioMIP* (Earth System Grid Federation). doi: 10.22033/ESGF/CMIP6.2242

Cho, J., Cho, W., and Jung, I. (2018) *rSQM: Statistical downscaling toolkit for climate change scenario using non-parametric quantile mapping for CMIP5, CMIP6, and CORDEX*. Available at: https://CRAN.R-project.org/package=rSQM.

Cho, J. P., Kim, J. U., Choi, S. K., Hwang, S. W., and Jung, H. C. (2020). Variability analysis of climate extreme index using downscaled multi-models and grid-based CMIP5 climate change scenario data. *J. Clim. Change Res.* 11 (2), 123–132. doi: 10.15531/ksccr.2020.11.2.123

Chung, H. S. (1975). Cereal scab causing mycotoxicosis in Korea and present status of mycotoxin researches. *Korean J. Mycol.* 3, 31–36.

Del Ponte, E. M., Fernandes, J. M. C., and Pavan, W. (2005). A risk infection simulation model for fusarium head blight of wheat. *Fitopatologia Bras.* 30 (6), 634–642. doi: 10.1590/S0100-41582005000600011

Del Ponte, E. M., Fernandes, J. M. C., Pavan, W., and Baethgen, W. E. (2009). A model-based assessment of the impacts of climate variability on fusarium head blight seasonal risk in southern Brazil. *J. Phytopathol.* 157, 675–681. doi: 10.1111/j.1439-0434.2009.01559.x

Detrixhe, P., Chandelier, A., Cavelier, M., Buffet, D., and Oger, R. (2003). Development of an agrometeorological model integrating leaf wetness duration estimation to assess the risk of head blight infection in wheat. *Asp. Appl. Biol.* 68, 199–204.

De Wolf, E. D., Madden, L. V., and Lipps, P. E. (2003). Risk assessment models for wheat fusarium head blight epidemics based on within-season weather data. *Phytopathology* 93 (4), 428–435. doi: 10.1094/PHYTO.2003.93.4.428

Dix, M., Bi, D., Dobrohotoff, P., Fiedler, R., Harman, I., Law, R., et al. (2019). *CSIRO-ARCCSS ACCESS-CM2 model output prepared for CMIP6 ScenarioMIP* (Earth System Grid Federation). doi: 10.22033/ESGF/CMIP6.2285

Donatelli, M., Magarey, R. D., Bregaglio, S., Willocquet, L., Whish, J. P., and Savary, S. (2017). Modelling the impacts of pests and diseases on agricultural systems. *Agric. Syst.* 155, 213–224. doi: 10.1016/j.agsy.2017.01.019

Duffeck, M. R., dos Santos Alves, K., Machado, F. J., Esker, P. D., and Del Ponte, E. M. (2020). Modeling yield losses and fungicide profitability for managing fusarium head blight in Brazilian spring wheat. *Phytopathology* 110 (2), 370–378. doi: 10.1094/PHYTO-04-19-0122-R

EC-Earth Consortium (EC-Earth) (2019). *EC-Earth-Consortium EC-Earth3 model output prepared for CMIP6 ScenarioMIP* (Earth System Grid Federation). doi: 10.22033/ESGF/CMIP6.251

Fernandes, J. M. C., Del Ponte, E. M., Pavan, W., and Cunha, G. D. (2007). *Web-based system to true-forecast disease epidemics–case study for fusarium head blight of wheat* (Berlin, Heidelberg: Climate Prediction and Agriculture, Springer), 265–271. doi: 10.1007/978-3-540-44650-7_25

Good, P., Sellar, A., Tang, Y., Rumbold, S., Ellis, R., Kelley, D., et al. (2019). *MOHC UKESM1.0-LL model output prepared for CMIP6 ScenarioMIP* (Earth System Grid Federation). doi: 10.22033/ESGF/CMIP6.1567

Hooker, D. C., Schaafsma, A. W., and Tamburic-Ilincic, L. (2002). *Using weather variables pre- and post-heading to predict deoxynivalenol content in winter wheat* (Erlanger, KY, USA: Anais, National Fusarium Head Blight Forum), 165. doi: 10.1094/pdis.2002.86.6.611

Ines, A. V., and Hansen, J. W. (2006). Bias correction of daily GCM rainfall for crop simulation studies. *Agric. For. Meteorol.* 138 (1-4), 44–53. doi: 10.1016/j.agrformet.2006.03.009

Jamieson, P. D., Semenov, M. A., Brooking, I. R., and Francis, G. S. (1998). Sirius: a mechanistic model of wheat response to environmental variation. *Eur. J. Agron.* 8 (3-4), 161–179. doi: 10.1016/s1161-0301(98)00020-3

Jevtić, R., Župunski, V., Lalošević, M., and Župunski, L. (2017). Predicting potential winter wheat yield losses caused by multiple disease systems and climatic conditions. *Crop Prot.* 99, 17–25. doi: 10.1016/j.cropro.2017.05.005

John, J. G., Blanton, C., McHugh, C., Radhakrishnan, A., Rand, K., Vahlenkamp, H., et al. (2018). *NOAA-GFDL GFDL-ESM4 model output prepared for CMIP6 ScenarioMIP* (Earth System Grid Federation). doi: 10.22033/ESGF/CMIP6.1414

Juroszek, P., and von Tiedemann, A. (2013). Climate change and potential future risks through wheat diseases: A review. *Eur. J. Plant Pathol.* 136 (1), 21–33. doi: 10.1007/s10658-012-0144-9

Kim, Y., Kang, I. J., Shin, D. B., Roh, J. H., Heu, S., and Shim, H. K. (2018). Timing of fusarium head blight infection in rice by heading stage. *Mycobiology* 46 (3), 283–286. doi: 10.1080/12298093.2018.1496637

Kim, J. H., Kim, D. J., Yun, E. J., Kim, H. S., and Shim, K. M. (2022). "Prediction of heading and maturity dates in winter wheat "Geumgang" using phenological model," in *Proceedings of The Korean Society of Agricultural and Forest Meteorology Conference*, Vol. 116.

Kim, K. H., and Koh, Y. J. (2019). An integrated modeling approach for predicting potential epidemics of bacterial blossom blight in kiwifruit under climate change. *Plant Pathol. J.* 35 (5), 459. doi: 10.5423/ppj.oa.05.2019.0140

Kim, K.-H., Son, K. I., and Koh, Y. J. (2018). Adaptation of the new Zealand 'Psa risk model' for forecasting kiwifruit bacterial canker in Korea. *Plant Pathol.* 67 (5), 1208–1219. doi: 10.1111/ppa.12810

Köhl, J., de Haas, B. H., Kastelein, P., Burgers, S. L. G. E., and Waalwijk, C. (2007). Population dynamics of *Fusarium* spp. and *Microdochium nivale* in crops and crop residues of winter wheat. *Phytopathology* 97 (8), 971–978. doi: 10.1094/phyto-97-8-0971

Korea Meteorological Administration (2020). *Korean Climate change assessment report 2020: The physical science basis*, Vol. 48 (Seoul: Korea Meteorological Administration).

Landschoot, S., Audenaert, K., Waegeman, W., Pycke, B., Bekaert, B., De Baets, B., et al. (2011). Connection between primary fusarium inoculum on gramineous weeds, crop residues and soil samples and the final population on wheat ears in Flanders, Belgium. *Crop Prot.* 30 (10), 1297–1305. doi: 10.1016/j.cropro.2011.05.018

Laux, P., Rötter, R. P., Webber, H., Dieng, D., Rahimi, J., Wei, J., et al. (2021). To bias correct or not to bias correct? an agricultural impact modelers' perspective on regional climate model data. *Agric. For. Meteorol* 304, 108406. doi: 10.1016/j.agrformet.2021.108406

Lee, K. T., Han, J., and Kim, K. H. (2022a). Optimizing artificial neural network-based models to predict rice blast epidemics in Korea. *Plant Pathol. J.* 38 (4), 395–402. doi: 10.5423/PPJ.NT.04.2022.0062

Lee, K. T., Jeon, H. W., Park, S. Y., Cho, J., and Kim, K. H. (2022b). Comparison of projected rice blast epidemics in the Korean peninsula between the CMIP5 and CMIP6 scenarios. *Clim. Change.* 173 (1–2), 12. doi: 10.1007/s10584-022-03410-2

Leffelaar, P. A., and Ferrari, T. J. (1989). "Some elements of dynamic simulation," in *Simulation and systems management in crop protection* Wageningen: Pudoc, 19–45.

Liang, H., Hu, K., Batchelor, W. D., Qi, Z., and Li, B. (2016). An integrated soil-crop system model for water and nitrogen management in north China. *Sci. Rep.* 6 (1), 25755. doi: 10.1038/srep25755

Maruyama, A., Kurose, Y., and Ohba, K. (2010). Modeling of phenological development in winter wheat to estimate the timing of heading and maturity based on daily mean air temperature and photoperiod. *J. Agric. Meteorol.* 66 (1), 41–50. doi: 10.2480/agrmet.66.1.7

Mathukumalli, S. R., Dammu, M., Sengottaiyan, V., Ongolu, S., Biradar, A. K., Kondru, V. R., et al. (2016). Prediction of *Helicoverpa armigera* hubner on pigeonpea during future climate change periods using MarkSim multimodel data. *Agric. For. Meteorol.* 228, 130–138. doi: 10.1016/j.agrformet.2016.07.009

McMullen, M., Bergstrom, G., De Wolf, E., Dill-Macky, R., Hershman, D., Shaner, G., et al. (2012). A unified effort to fight an enemy of wheat and barley: Fusarium head blight. *Plant Dis.* 96, 1712–1728. doi: 10.1094/PDIS-03-12-0291-FE

Moschini, R. C., and Fortugno, C. (1996). Predicting wheat head blight incidence using models based on meteorological factors in pergamino, Argentina. *Eur. J. Plant Pathol.* 102 (3), 211–218. doi: 10.1007/bf01877959

Moschini, R. C., Martínez, M. I., and Sepulcri, M. G. (2013). "Modeling and forecasting systems for fusarium head blight and deoxynivalenol content in wheat in Argentina," in *Fusarium head blight in Latin America* (Dordrecht: Springer Netherlands), 205–227. doi: 10.1007/978-94-007-7091-1_13

Nelson, M. R., Orum, T. V., Jaime-Garcia, R., and Nadeem, A. (1999). Applications of geographic information systems and geostatistics in plant disease epidemiology and management. *Plant Dis.* 83 (4), 308–319. doi: 10.1094/pdis.1999.83.4.308

Nouri, M., Homaee, M., Bannayan, M., and Hoogenboom, G. (2017). Towards shifting planting date as an adaptation practice for rainfed wheat response to climate change. *Agric. Water Manage.* 186, 108–119. doi: 10.1016/j.agwat.2017.03.004

Olivier, J. G., Schure, K. M., and Peters, J. A. H. W. (2017). *Trends in global CO2 and total greenhouse gas emissions: 2017 report* (The Hague: PBL Netherlands Environmental Assessment Agency).

O'Neill, B. C., Kriegler, E., Ebi, K. L., Kemp-Benedict, E., Riahi, K., Rothman, D. S., et al. (2017). The roads ahead: Narratives for shared socioeconomic pathways describing world futures in the 21st century. *Global Environ. Change.* 42, 169–180. doi: 10.1016/j.gloenvcha.2015.01.004

Ouma, P. O., Odera, P. A., and Mukundi, J. B. (2016). Spatial modelling of weather variables for plant disease applications in mwea region. *J. Geosci. Environ. Prot.* 4 (5), 127–136. doi: 10.4236/gep.2016.45013

Park, J. M., Shin, S. H., Kang, C. S., Kim, K. H., Cho, K. M., Choi, J. S., et al. (2012). Fungicide effects *in vitro* and in field trials on fusarium head blight of wheat. *Res. Plant Dis.* 18 (3), 194–200. doi: 10.5423/rpd.2012.18.3.194

Parry, D. W., Jenkinson, P., and McLeod, L. (1995). Fusarium ear blight (scab) in small grain cereals-a review. *Plant Pathol.* 44, 207–238. doi: 10.1111/j.1365-3059.1995.tb02773.x

Roos, J., Hopkins, R., Kvarnheden, A., and Dixelius, C. (2011). The impact of global warming on plant diseases and insect vectors in Sweden. *Eur. J. Plant Pathol.* 129 (1), 9–19. doi: 10.1007/s10658-010-9692-z

Rossi, V., Giosuè, S., Pattori, E., Spanna, F., and Del Vecchio, A. (2003). A model estimating the risk of fusarium head blight on wheat*: A model estimating the risk of fusarium head blight on wheat. *EPPO Bull.* 33 (3), 421–425. doi: 10.1111/j.1365-2338.2003.00667.x

Rotter, R. P., Palosuo, T., Kersebaum, K. C., Angulo, C., Bindi, M., Ewert, F., et al. (2012). Simulation of spring barley yield in different climatic zones of northern and central Europe: a comparison of nine crop models. *Field Crops Res.* 133, 23–36. doi: 10.1016/j.fcr.2012.03.016

Rural Development Administration (2020). *Agricultural technology Guide_Wheat* (Jeonju: Rural Development Administration of Korea), 141–170. Jeonju: Rural Development Administration.

Ryu, J. G., and Lee, Y. W. (1990). Mycotoxins produced by fusarium isolates from barley in Korea. *Plant Pathol. J.* 6, 21–27.

Salgado, J. D., Madden, L. V., and Paul, P. A. (2014). Quantifying the effects of fusarium head blight on grain yield and test weight in soft red winter wheat. *Phytopathology* 105 (3), 295–306. doi: 10.1094/PHYTO-08-14-0215-R

Sameshima, R. (2000). Modeling soybean growth and development responses to environmental factors. *Bull. Nat. Agric. Res. Cent.* 32, 1–119.

Sayago, S., Ovando, G., Almorox, J., and Bocco, M. (2020). Daily solar radiation from NASA-POWER product: assessing its accuracy considering atmospheric transparency. *Int. J. Remote Sens* 41 (3), 897–910. doi: 10.1080/01431161.2019.1650986

Schaafsma, A. W., and Hooker, D. C. (2007). Climatic models to predict occurrence of fusarium toxins in wheat and maize. *Int. J. Food Microbiol.* 119 (1-2), 116–125. doi: 10.1016/j.ijfoodmicro.2007.08.006

Schupfner, M., Wieners, K. H., Wachsmann, F., Steger, C., Bittner, M., Jungclaus, J., et al. (2019). *DKRZ MPI-ESM1.2-HR model output prepared for CMIP6 ScenarioMIP* (Earth System Grid Federation). doi: 10.22033/ESGF/CMIP6.2450

Schwalm, C. R., Glendon, S., and Duffy, P. B. (2020). RCP8. 5 tracks cumulative CO2 emissions. *Proc. Natl. Acad. Sci. U.S.A.* 117 (33), 19656–19657. doi: 10.1073/pnas.2007117117

Seferian, R. (2019). *CNRM-CERFACS CNRM-ESM2-1 model output prepared for CMIP6 ScenarioMIP* (Earth System Grid Federation). doi: 10.22033/ESGF/CMIP6.1395

Seland, Ø., Bentsen, M., Oliviè, D. J. L., Toniazzo, T., Gjermundsen, A., Graff, L. S., et al. (2019). *NCC NorESM2-LM model output prepared for CMIP6 ScenarioMIP* (Earth System Grid Federation). doi: 10.22033/ESGF/CMIP6.604

Shah, D. A., Molineros, J. E., Paul, P. A., Willyerd, K. T., Madden, L. V., and De Wolf, E. D. (2013). Predicting fusarium head blight epidemics with weather-driven pre- and post-anthesis logistic regression models. *Phytopathology* 103 (9), 906–919. doi: 10.1094/PHYTO-11-12-0304-R

Shim, H. K., and Gang, I. J. (2018). Development of monitoring and management technology for fusarium head blight. *Natl. Institute Crop Sci.* 2, 1593–1666.

Shin, S., Son, J. H., Park, J. C., Kim, K. H., Yoon, Y. M., Cheong, Y. K., et al. (2018). Comparative pathogenicity of fusarium graminearum isolates from wheat kernels in Korea. *Plant Pathol. J.* 34 (5), 347. doi: 10.5423/PPJ.OA.01.2018.0013

Shiogama, H., Abe, M., and Tatebe, H. (2019). *MIROC MIROC6 model output prepared for CMIP6 ScenarioMIP* (Earth System Grid Federation). doi: 10.22033/ESGF/CMIP6.898

Skelsey, P., and Newton, A. C. (2015). Future environmental and geographic risks of fusarium head blight of wheat in Scotland. *Eur. J. Plant Pathol.* 142 (1), 133–147. doi: 10.1007/s10658-015-0598-7

Statistics Korea (2022). *SDGs in the republic of Korea: Progress report 2022* (Daejon: Statistics Korea), 22.

Sung, H. M., Kim, J., Shim, S., Seo, J., Kwon, S. H., Sun, M. A., et al. (2021). Climate change projection in the twenty-first century simulated by NIMS-KMA CMIP6 model based on new GHGs concentration pathways. *Asia-Pac. J. Atmos. Sci.* 57 (4), 851–862. doi: 10.1007/s13143-021-00225-6

Swart, N. C., Cole, J. N. S., Kharin, V. V., Lazare, M., Scinocca, J. F., Gillett, N. P., et al. (2019). *CCCma CanESM5 model output prepared for CMIP6 ScenarioMIP* (Earth System Grid Federation). doi: 10.22033/ESGF/CMIP6.1317

Tachiiri, K., Abe, M., Hajima, T., Arakawa, O., Suzuki, T., Komuro, Y., et al. (2019). *MIROC MIROC-ES2L model output prepared for CMIP6 ScenarioMIP* (Earth System Grid Federation). doi: 10.22033/ESGF/CMIP6.936

Velásquez, A. C., Castroverde, C. D. M., and He, S. Y. (2018). Plant–pathogen warfare under changing climate conditions. *Cur. Biol.* 28 (10), R619–R634. doi: 10.1016/j.cub.2018.03.054

Voldoire, A. (2019). *CNRM-CERFACS CNRM-CM6-1 model output prepared for CMIP6 ScenarioMIP* (Earth System Grid Federation). doi: 10.22033/ESGF/CMIP6.1384

Volodin, E., Mortikov, E., Gritsun, A., Lykossov, V., Galin, V., Diansky, N., et al. (2019a). *INM INM-CM4-8 model output prepared for CMIP6 ScenarioMIP* (Earth System Grid Federation). doi: 10.22033/ESGF/CMIP6.12321

Volodin, E., Mortikov, E., Gritsun, A., Lykossov, V., Galin, V., Diansky, N., et al. (2019b). *INM INM-CM5-0 model output prepared for CMIP6 ScenarioMIP* (Earth System Grid Federation). doi: 10.22033/ESGF/CMIP6.12322

Wang, M., Zhang, D. Q., Su, J., Dong, J. W., and Tan, S. K. (2018). Assessing hydrological effects and performance of low impact development practices based on future scenarios modeling. *J. Cleaner Prod.* 179, 12–23. doi: 10.1016/j.jclepro.2018.01.096

White, J. W., Herndl, M., Hunt, L. A., Payne, T. S., and Hoogenboom, G. (2008). Simulation-based analysis of effects of and loci on flowering in wheat. *Crop Sci.* 48, 678. doi: 10.2135/cropsci2007.06.0318

Wieners, K. H., Giorgetta, M., Jungclaus, J., Reick, C., Esch, M., Bittner, M., et al. (2019). *MPI-m MPIESM1.2-LR model output prepared for CMIP6 ScenarioMIP* (Earth System Grid Federation). doi: 10.22033/ESGF/CMIP6.793

Williams, D. N., Balaji, V., Cinquini, L., Denvil, S., Duffy, D., Evans, B., et al. (2016). A global repository for planet-sized experiments and observations. *Bull. Am. Meteorol. Soc* 97 (5), 803–816. doi: 10.1175/BAMS-D-15-00132.1

Xiao, Y., Dong, Y., Huang, W., Liu, L., Ma, H., Ye, H., et al. (2020). Dynamic remote sensing prediction for wheat fusarium head blight by combining host and habitat conditions. *Remote Sens.* 12 (18), 3046. doi: 10.3390/rs12183046

Yukimoto, S., Koshiro, T., Kawai, H., Oshima, N., Yoshida, K., Urakawa, S., et al. (2019). *MRI MRI-ESM2.0 model output prepared for CMIP6 ScenarioMIP* (Earth System Grid Federation). doi: 10.22033/ESGF/CMIP6.638

Zhang, X., Halder, J., White, R. P., Hughes, D. J., Ye, Z., Wang, C., et al. (2014). Climate change increases risk of fusarium ear blight on wheat in central China: Fusarium and climate change in China. *Ann. Appl. Biol.* 164 (3), 384–395. doi: 10.1111/aab.12107

Zhang, S., and Tao, F. (2013). Modeling the response of rice phenology to climate change and variability in different climatic zones: Comparisons of five models. *Eur. J. Agron.* 45, 165–176. doi: 10.1016/j.eja.2012.10.005

Zhu, Z., Hao, Y., Mergoum, M., Bai, G., Humphreys, G., Cloutier, S., et al. (2019). Breeding wheat for resistance to fusarium head blight in the global north: China, USA, and Canada. *Crop J.* 7, Issue 6, 730–738. doi: 10.1016/j.cj.2019.06.003

Zheng, B., Biddulph, B., Li, D., Kuchel, H., and Chapman, S. (2013). Quantification of the effects of VRN1 and ppd-D1 to predict spring wheat (*Triticum aestivum*) heading time across diverse environments. *J. Exp. Bot.* 64, 3747–3761. doi: 10.1093/jxb/ert209

Ziehn, T., Chamberlain, M., Lenton, A., Law, R., Bodman, R., Dix, M., et al. (2019). *CSIRO ACCESS-ESM1.5 model output prepared for CMIP6 ScenarioMIP* (Earth System Grid Federation). doi: 10.22033/ESGF/CMIP6.2291

frontiers | Frontiers in Plant Science

TYPE Original Research
PUBLISHED 18 January 2023
DOI 10.3389/fpls.2022.1036064

OPEN ACCESS

EDITED BY
Maria Rosa Simon,
National University of La Plata,
Argentina

REVIEWED BY
Deepmala Sehgal,
Syngenta, United Kingdom
Sunil S. Gangurde,
University of Georgia, United States
Shasidhar Yaduru,
International Crops Research Institute for the Semi-Arid Tropics (ICRISAT), India

*CORRESPONDENCE
Pushpendra Kumar Gupta
pkgupta36@gmail.com

SPECIALTY SECTION
This article was submitted to Plant Pathogen Interactions, a section of the journal Frontiers in Plant Science

RECEIVED 03 September 2022
ACCEPTED 28 December 2022
PUBLISHED 18 January 2023

CITATION
Singh S, Gaurav SS, Vasistha NK, Kumar U, Joshi AK, Mishra VK, Chand R and Gupta PK (2023) Genetics of spot blotch resistance in bread wheat (*Triticum aestivum* L.) using five models for GWAS. *Front. Plant Sci.* 13:1036064. doi: 10.3389/fpls.2022.1036064

Genetics of spot blotch resistance in bread wheat (*Triticum aestivum* L.) using five models for GWAS

Sahadev Singh[1], Shailendra Singh Gaurav[1], Neeraj Kumar Vasistha[2], Uttam Kumar[3], Arun Kumar Joshi[4], Vinod Kumar Mishra[5], Ramesh Chand[6] and Pushpendra Kumar Gupta[1,3,7]*

[1]Molecular Biology Laboratory, Department of Genetics and Plant Breeding, Chaudhary Charan Singh University, Meerut, India, [2]Department of Genetics-Plant Breeding and Biotechnology, Dr Khem Singh Gill, Akal College of Agriculture, Eternal University, Sirmaur, India, [3]Borlaug Institute for South Asia (BISA), Ludhiana, India, [4]The International Maize and Wheat Improvement Center (CIMMYT), Borlaug Institute for South Asia (BISA), G-2, B-Block, NASC Complex, DPS Marg, New Delhi, India, [5]Department of Genetics and Plant Breeding, Indian Institute of Agricultural Science, Banaras Hindu University, Varanasi, India, [6]Department of Mycology and Plant Pathology, Indian Institute of Agricultural Science Banaras Hindu University, Varanasi, India, [7]Murdoch's Centre for Crop & Food Innovation, Murdoch University, Murdoch, WA, Australia

Genetic architecture of resistance to spot blotch in wheat was examined using a Genome-Wide Association Study (GWAS) involving an association panel comprising 303 diverse genotypes. The association panel was evaluated at two different locations in India including Banaras Hindu University (BHU), Varanasi (Uttar Pradesh), and Borlaug Institute for South Asia (BISA), Pusa, Samastipur (Bihar) for two consecutive years (2017-2018 and 2018-2019), thus making four environments (E1, BHU 2017-18; E2, BHU 2018-19; E3, PUSA, 2017-18; E4, PUSA, 2018-19). The panel was genotyped for 12,196 SNPs based on DArT-seq (outsourced to DArT Ltd by CIMMYT); these SNPs included 5,400 SNPs, which could not be assigned to individual chromosomes and were therefore, described as unassigned by the vendor. Phenotypic data was recorded on the following three disease-related traits: (i) Area Under Disease Progress Curve (AUDPC), (ii) Incubation Period (IP), and (iii) Lesion Number (LN). GWAS was conducted using each of five different models, which included two single-locus models (CMLM and SUPER) and three multi-locus models (MLMM, FarmCPU, and BLINK). This exercise gave 306 MTAs, but only 89 MTAs (33 for AUDPC, 30 for IP and 26 for LN) including a solitary MTA detected using all the five models and 88 identified using four of the five models (barring SUPER) were considered to be important. These were used for further analysis, which included identification of candidate genes (CGs) and their annotation. A majority of these MTAs were novel. Only 70 of the 89 MTAs were assigned to individual chromosomes; the remaining 19 MTAs belonged to unassigned SNPs, for which chromosomes were not known. Seven MTAs were selected on the basis of minimum P value, number of models, number of environments and location on chromosomes with respect to QTLs reported earlier. These 7 MTAs, which included

five main effect MTAs and two for epistatic interactions, were considered to be important for marker-assisted selection (MAS). The present study thus improved our understanding of the genetics of resistance against spot blotch in wheat and provided seven MTAs, which may be used for MAS after due validation.

KEYWORDS

Triticum aestivum L, GWAS, MTA, epistasis, candidate genes

Introduction

Wheat is the third most important crop world-wide, next only to rice and maize, contributing ~20% of total dietary calories and proteins worldwide (Shiferaw et al., 2013). Although the global production of wheat has been able to keep pace with the demand and consumption during the last more than five decades, the decline in rate of annual production from 3% in the past during green revolution to <1% in recent years has been a cause of alarm, since 18% increase in global wheat production will be needed by the year 2050, according to some available estimates (Alexandratos and Bruinsma, 2012). Therefore, there is a need to improve the productivity and production of wheat to meet future demands. In this connection, it is relevant to recognize that the productivity of wheat has been constantly under threat due to a variety of biotic and abiotic stresses. Among biotic stresses, several diseases cause major yield losses to wheat crop everywhere in the world. Spot blotch has its own share in this loss in productivity. According to some estimates, globally spot blotch affects >25 million ha, representing 12% of the total wheat area (Duveiller et al., 2005). Geographically, this affected area includes parts of South Asia (including North-Eastern Plain Zone of India, Bangladesh, and Tarai Region of Nepal), South-East Asia (including Thailand, Philippines, Indonesia, and China), Latin America (including North East part of Argentina, Bolivia, warmest area of Brazil, Paraguay) and Africa (including Tanzania and Zambia) (Joshi et al., 2002; Joshi et al., 2007b; Chatrath et al., 2007; Juliana et al., 2022). According to different estimates, yield losses due to SB, in different years, ranged from 0% to 100% in different parts of the world (Sharma and Duveiller, 2006; Siddique et al., 2006; Juliana et al., 2022); complete destruction of the crop leading to 100% loss occurs only under conditions, favourable for the pathogen, (Mehta, 1985; Saari, 1998). The end-use quality of harvested grain is also affected, since the pathogen infects the spikes and the grain (Singh et al., 2015; Gupta et al., 2018a; Gupta et al., 2018b; Kumar et al., 2019).

It is widely known that the use of resistant cultivars is the safest means to safeguard against yield losses and is also environmentally safe. A knowledge of the genetics of resistance in the host is necessary for the development of these resistant cultivars. Therefore, a large number of studies for the study of the genetics of resistance have been undertaken in the past. The early inheritance studies suggested monogenic to polygenic resistance with the involvement of dominant as well as recessive genes. The availability of dominant as well as recessive nature of disease resistance in these different studies has been attributed to the use of parents with different genetic constitutions and the possibility of same genes behaving as dominant in one genetic background and recessive in the other (for a review, see Gupta et al., 2018a).

For identification of the genes involved in resistance to SB in wheat, the trait has been treated as a qualitative trait in some studies and as a quantitative trait in some other relatively recent studies. While treating it as a quantitative trait, QTL analysis involved either interval mapping or genome-wide association studies (GWAS) (Kumar et al., 2009; Kumar et al., 2010; Marone et al., 2013; French et al., 2016; Juliana et al., 2022). As a qualitative trait, two different classes of genes were identified, the first having four Sb genes, which follow a gene-for-gene (GFG) relationship (Flor, 1955), and the second with a solitary sensitivity gene *Tsn1*, which follows an inverse gene-for-gene relationship (IGFG). The four Sb genes in the former category included the following: *Sb1* (7DS), *Sb2* (5BL), *Sb3* (3BS) and *Sb4* (4BL) (Lillemo et al., 2013; Kumar et al., 2015; Lu et al., 2016; Zhang et al., 2020), but no corresponding avirulence (Avr) genes is known for any of these four genes. But for sensitivity gene *Tsn1* in the second category, the corresponding virulence gene *ToxA* is known (Navathe et al., 2020).

A number of interval mapping studies for the identification of QTLs and GWA studies for identification of MTAs have also been conducted (for a review, see Gupta et al., 2018a). These QTLs and MTAs are listed in "WheatQTLdatabase" that was recently developed at our centre (Singh et al., 2021; Singh et al., 2022). The most comprehensive recent GWA study, however, involved six association panels from a large set of 6,736 advanced bread wheat breeding lines from the International Maize and Wheat Improvement Center (CIMMYT) (Juliana et al., 2022). A meta-QTL analysis involving QTLs for resistance against spot blotch and other related diseases has also been conducted at our centre, leading to the identification of 30 M-QTLs based on 87 of the 241 QTLs identified so far using interval mapping (our unpublished results).

The pathogen (*B. sorokiniana*) has also been studied for occurrence of races/pathotypes and identification of genes involved in pathogenesis. In several studies, isolates have been collected from specific geographical regions and differentials suggested for classification of these isolates into groups, sometimes erroneously described as pathotypes (Aggarwal et al., 2009; Chauhan et al., 2017; also see reviews by Gupta et al., 2018a and Navathe et al., 2022). So far, no physiological races or pathotypes have been identified and described, although a virulence gene has been identified (*VHv1* in barley and *VTa1* in wheat; Zhong et al., 2002). However, no avirulence (Avr) gene for any Sb gene following GFG model and/or effector molecule derived from the pathogen (*B. sorokinaia*) has been identified. However, a virulence gene *ToxA* in the pathogen and its

sensitivity gene *Tsn1* in the host following IGFG for spot blotch was identified recently (McDonald et al., 2018), although this pair of genes for other necrotrophic diseases like Septoria blotch and tan spot was known for quite some time (Gupta et al., 2022 for a review). Prevalence of *ToxA* in wheat genotypes and that of *Tsn1* in pathogen isolates has also been examined. For instance, Navathe et al. (2020) reported occurrence of *ToxA* gene in 70% isolates (77 of 110 Indian isolates) and *Tsn1* gene in 36.8% of wheat genotypes (81 of 220 wheat genotypes). Whole genome sequence of the pathogen (*B. sorokiniana*) has also been worked out recently and putative avirulence genes suggested, but these genes need to be validated through further investigations (Aggarwal et al., 2022).

Despite the progress outlined above, we feel convinced that the available genes/QTLs/MTAs do not represent the entire repertoire of gene loci or QTLs that may be involved in providing resistance against spot blotch, and that there is a scope for finding additional novel MTAs using additional germplasm. Keeping this in view, a GWA study was undertaken using five different models to identify novel marker trait association (MTAs) and to detect loci which provide spot blotch resistance through a novel association panel (never used earlier). As expected, many novel MTAs involved in spot blotch resistance were identified in the present study. The results of the study are presented and discussed in this communication.

Material and methods

Association panel and experimental design

The GWAS panel consisted of 303 diverse wheat accessions (a set of Spring Wheat Reference Set also known as SWRS population which procured from CIMMYT gene bank, Mexico; for details of 303 genotypes, see Supplementary Table 1) and was genotyped for 12,160 (with MAF of <5%) of the 17, 937 SNPs that were generated using NGS-based DArT-seq using Illumina platform under the "Seed for Discovery" project of CIMMYT Mexico (outsourced by CIMMYT to Diversity Array Technology Pvt. Ltd. Australia). Of these 12,160 SNPs, 5,400 SNPs were described as unassigned, since these SNPs could not be assigned to specific chromosomes.

Following alignment, filtering was applied in order to detect the best assignment/anchorage to a physical position on the reference genome using the default criteria of Bowtie 2: The following criteria were used for filtering: (i) unique mapping to an unambiguous locus; (ii) maximum 1 bp mismatch to the marker sequence, and (iii) markers with multiple alignment options discarded, if the second-best hit showed < 3 bp mismatch to the marker sequence, i.e. markers with 2 or more hits (loci) were discarded if there was not at least 3 bp difference between the best and second-best hit. (iv) Monomorphic markers were discarded as well as (v) SNPs with MAF (Minor Allele Frequency less than 5% and more than 5% missing data).

The panel was raised in a CRBD with two replications in each of the following four environments: E1 (2017-2018) and E2 (2018-2019) at Agriculture Research Farm, BHU, Varanasi, UP, E3 (2017-2018) and E4 (2018-2019) at BISA Agriculture farm, Pusa, Samastipur, Bihar. Recommended crop management practices were followed (i.e., 200 kg/ha fertilizer; N: P: K = 8: 8: 8). Each genotype in a replication was represented by a plot of 3 rows of 1m each, with a row-to-row distance of 0.25 m.

Inoculation and recording of phenotypic data

Pure culture of a highly aggressing isolate of the pathogen (HD 3069, BHU, Varanasi, India) was multiplied on sorghum grain and used for inoculation following Chaurasia et al. (1999). Development of spot blotch was ensured through use of agronomic practices (including frequent irrigations) to create environment conducive for the pathogen. Phenotypic data were recorded on the following three disease related traits: (i) Area Under Disease Progress Curve (AUDPC; 00-99, double digit data). (ii) Incubation Period (IP; in days). (iii) Lesion number (LN).

For AUDPC, disease severity (%) was recorded in three different growth stages (GS), GS 63 (beginning of anthesis to half complete), GS 69 (anthesis complete) and GS 77 (late milking). Disease severity was assessed by the formula [(1/9 (D1×D2) ×100] using the double-digit scale (DD, 00–99) (Saari and Prescott, 1975). The first digit (D1) refers to vertical disease progress on the plant, whereas the second digit (D2) was the disease severity score in the affected leaves. Thus, disease severity was used to estimate the AUDPC by following formula (Sharma and Duveiller, 2007).

$$AUDPC = \sum 1/2 \times \left(Y_i + Y_{(i+1)}\right) * \left(t_{(i+1)} - t_i\right)$$

Where Y_i and $Y_{(i+1)}$ = disease severity at time t_i and $t_{(i+1)}$, respectively; $t_{(i+1)}$—t_i = time interval (number of days) between two disease scores assessed.

IP was recorded as the duration (in number of days) from inoculation to the appearance of visible symptoms on five randomly tagged plants in each plot (Parlevliet, 1979). Similarly, for LN, five random flag leaves were each divided into four parts with a marker pen and the number of lesions on each part was counted. The number of spots from each part were added and the total number of spots was used as LN (Roumen, 1992).

Statistical analysis and frequency distribution

ANOVA and correlation coefficients were obtained using Agricolae package in R studio. Violin plots for phenotypic data were developed for each of the four individual environments and BLUP values. For this purpose, BLUP values were obtained using the 'lme4' in R (Bates et al., 2015). Descriptive statistics including mean, standard deviation, coefficient of variation (CV) was obtained using SPSS v. 17.0 (SPSS Inc 2008).

Principal components, population structure and kinship matrix

Genotype data were available for 17,937 SNPs, but only 12,160 markers remained after filtering out those with a marker allele

frequency (MAF) of less than 5%. These 12,160 SNPs were then employed in PCA/population structure analysis and GWAS.

The principal component (PC) analysis using genotypic data was conducted for the development of population structure (Q matrix) and relatedness (K matrix) using tools available in GAPIT (Lipka et al., 2012); Q and K matrices were obtained using default set of parameters (VanRaden, 2008; Lipka et al., 2012). The first three PCs were used to produce a 3D scatter plot showing distribution of genotypes into sub-groups.

Population structure involving 210 SNPs (ten SNPs from each chromosome) was examined using the software STRUCTURE version 2.3.4 (Pritchard et al., 2000). The details of the procedure followed are available in an earlier publication from our lab, where the same association panel with minor differences was employed (Kumar et al., 2018).

Identification of marker trait associations

Following five different models were used for GWAS: (i) Compressed mixed linear model (CMLM; Zhang et al., 2010); (ii) Settlement of MLM Under Progressively Exclusive Relationship (SUPER; Wang et al., 2014); (iii) Multi locus mixed-model (MLMM; Segura et al., 2012); (iv) Fixed and random model Circulating Probability Unification (FarmCPU; Liu et al., 2016); (v) Bayesian-information and Linkage-disequilibrium Iteratively Nested Keyway (BLINK; Huang et al., 2018). The first two models are single locus models and the remaining three are multi-locus models. These models are freely available in Latest version of Genomic Association and Prediction Integrated Tool (GAPIT V.3) (Wang and Zhang, 2021). Default significance threshold value implemented by GAPIT was FDR<0.05. But since the FDR implemented in GAPIT seems to be very stringent/conservative, no significant MTAs could be identified for any of the traits; therefore, GWAS using P<0.001 was also conducted, as also done earlier in wheat (Wang et al., 2017) and other cereals including rice (Feng et al., 2016). Significant MTAs were identified at a stringent probability value of P<0.001 and MTAs were represented in the form of maps using MAPCHART software (Voorrips, 2002).

Epistasis analysis (SNP×SNP interaction)

PLINK provides several alternatives for selecting the pairs of SNPs to be used for epistatic interactions, which means either we can use all available pairs of SNPs or select only a limited number of pairs, using any one of the several criteria provided. In the present study, epistatic interactions were identified using all the possible pairs of SNPs (12,160 SNPs give 73,926,720 pairs) was carried out by using PLINK[2] (Purcell et al., 2007). It is freely available and command-based package of tools for whole genome association analysis. Significant interactions were filtered at p-value $<1\times10^{-8}$ (Purcell et al., 2007; Jan et al., 2019). The SNPs involved in epistatic interactions were described as E-QTNs.

Identification of putative candidate genes

The most significant MTAs detected were also used for identification of CGs through alignment of sequences associated with MTAs with wheat genome assembly IWGSC v.1 (International Wheat Genome Sequencing Consortium (IWGSC) et al., 2018) that is hosted on the Ensembl database[3]. Highly significant annotated CGs were retrieved from a 200 kb window for each MTA. IWGSC[4] was used for gene ontology (GO) annotation information of these CGs.

Results

Violin plots showing variation for three spot blotch traits in four individual environments and BLUP are depicted in Figure 1. The results of the analysis of variance (ANOVA) are presented in Table 1.

Principal components analysis and population structure

The results for the first three PCs (PC1, PC2 and PC3) are presented in Figure 2, suggesting the presence of three sub-groups in the association panel. Following population structure analysis using 210 unlinked markers, 303 genotypes were placed in four

FIGURE 1
Violin plots for three traits in four environments and BLUP; means are shown by vertical solid black bars with means shown as white dots within the bars.

10.3389/fpls.2022.1036064

TABLE 1 ANOVA for three traits: (i) area under disease progress curve (AUDPC), (ii) incubation period (IP) and (iii) lesion number (LN).

Source of variation	Df	Mean sum of squares		
		AUDPC	IP	LN
Env	1	430117*	0.0	23144*
Year	1	8332	1.3*	1524*
Genotype	302	36805*	0.3*	735*
Rep	1	7.6	1.4*	30.5
Env × Genotype	302	35972*	0.3*	342*
Year × Genotype	302	2817	0.1	11.5

*Significant at the p-value (P<0.01) probability level; Df, degrees of freedom.

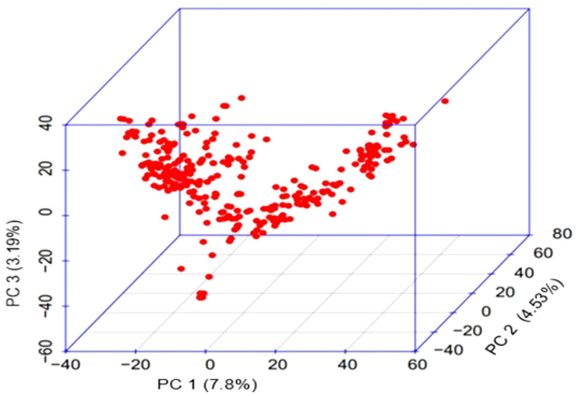

FIGURE 2
3D PC scatter plot (3D PC) for genotypes based on the first three principal components (PC1, PC2 and PC3).

subgroups, with 75 genotypes in subgroup I, 11 genotypes in subgroup II, 42 in subgroup III and the remaining 175 in the admixture group IV (Figure 3). The information generated by population structure was used for developing Q matrix for GWAS.

GWAS and marker trait associations

A representative set of Manhattan plots and QQ plots based on BLUP data are depicted in Figure 4. Manhattan plots for all 60 combinations (3 traits, 4 environments and 5 models) are available in Supplementary Figures 1–12. The total number of MTAs involving three traits and five models were 306 (91 for AUDPC; 100 for IP and 115 for LN; Supplementary Tables 2–4). A summary of 89 MTAs including one MTA found in all the five models and 88 that were common among four models (except SUPER) is presented in Table 2 and Figure 5. These 89 MTAs include 33 for AUDPC, 30 for IP and 26 for LN. Among these MTAs, 12 MTAs occurred in more than one environment (four for AUDPC, two for IP, and six for LN) and 19 MTAs belongs to the category of unassigned SNPs. Assignment of

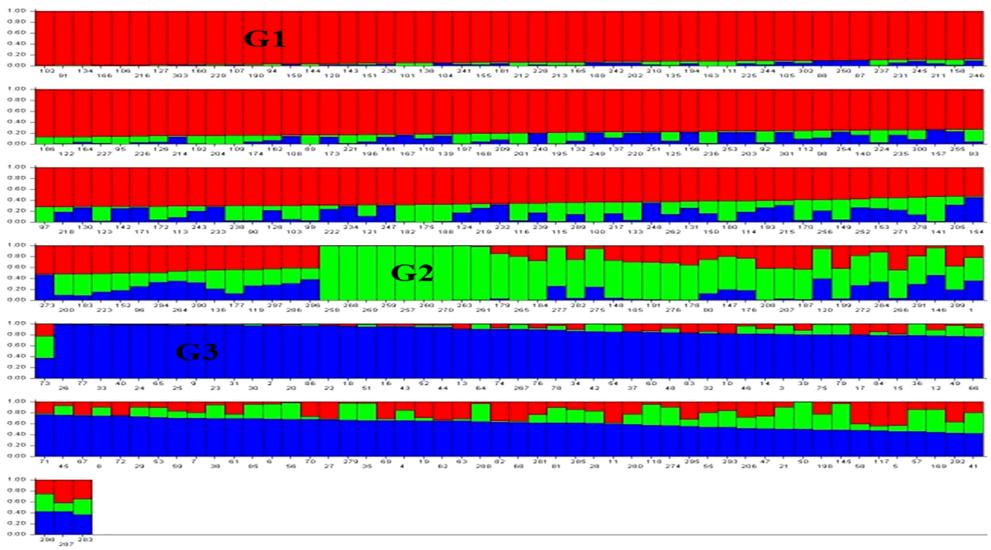

FIGURE 3
Population structure showing three sub-groups (G1, G2, G3) by three different colours (red, green, and blue); the subgroup IV representing admixture had genotypes with more than one color. Each bar represents one genotype.

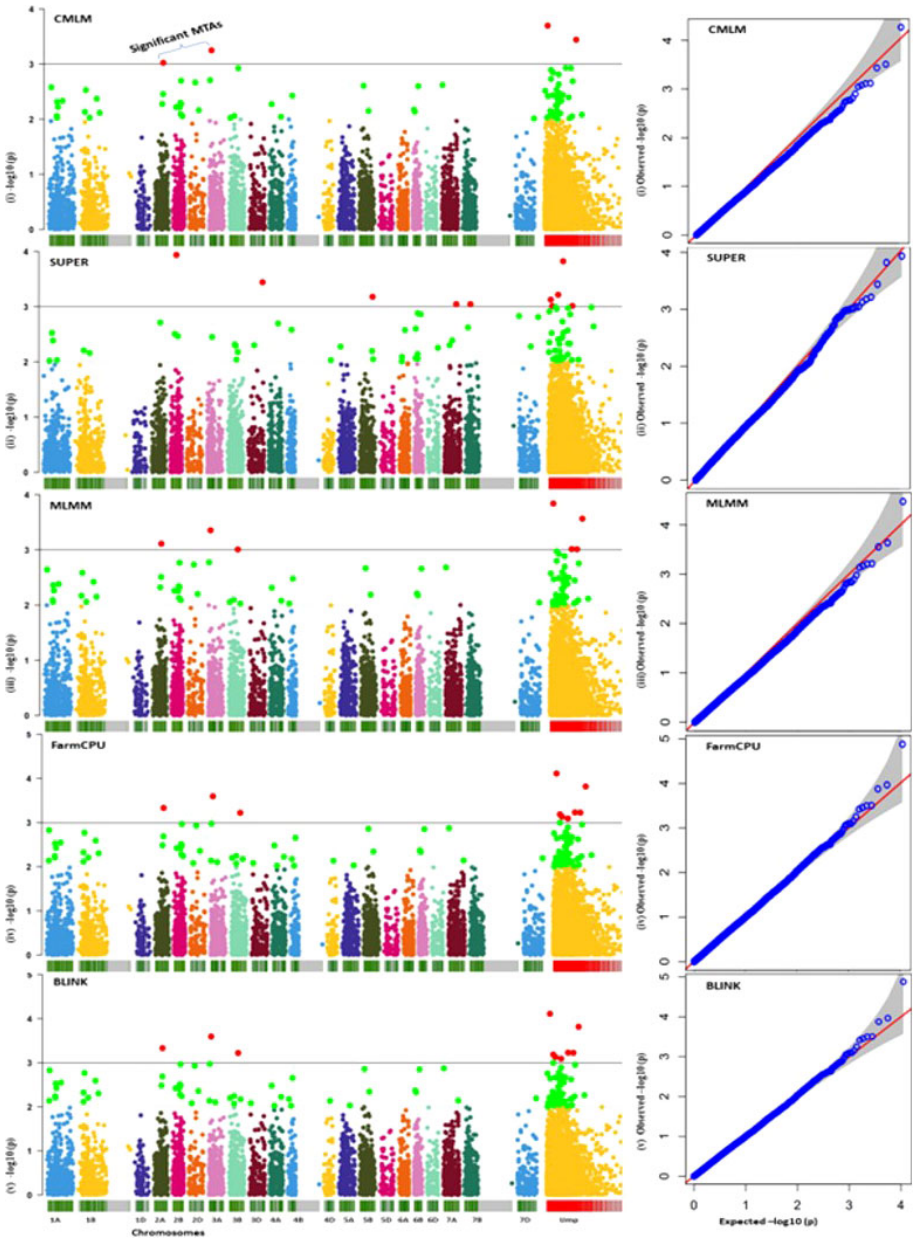

FIGURE 4
A set of representative Manhattan plots (left panel) and Q–Q plots (right panel; expected values shown as red line assuming no association) for five models (for only BLUP values for AUDPC); red dots above the horizontal line depict significant MTAs.

remained 57 MTAs; 18 for AUPDC (located on 13 chromosomes), 22 for IP (located on 13 chromosomes), 17 for LN (located on 13 chromosomes) on individual chromosomes is shown in Figure 5.

Epistatic interactions

MTAs representing 44 pairs of first-order epistatic interactions (SNP × SNP interactions) are listed in Supplementary Table 5. Eight major interactions (two for AUDPC, one for IP and five for LN) are listed in Table 3.

MTAs overlapping or occurring in the vicinity of known QTLs/MTAs

When compared with 84 known QTLs reported in earlier studies, only seven MTAs of the 70 (remaining 19 were unassigned) occurred within the QTL interval (in green colour) (one associated with AUDPC, four associated with IP and two associated with LN) and the other 12 occurred in the vicinity of the markers flanking (range from 0.4 to 22.7 Mb; in brown colour; three for AUDPC, seven for IP, and two for LN) the QTLs reported earlier (Supplementary Tables 6 and Figure 5); remained 38 MTAs were novel.

TABLE 2 A Summary of MTAs for each trait (one MTA in bold was detected by all the five models; the remaining MTAs were detected by four models except SUPER; NA=not available).

SNP	Chr.	Pos. of SNP tag (bp)	-log10 (P)	maf	SNP	Chr.	Pos. of SNP tag (bp)	-log10(P)	maf
AUDPC (E1:7; E2:4; E3:4; E4:7 and BLUP:11)									
E1									
M2266: A/G	1A	445269309-445269377	8.37E-04	0.445545	M1654: C/A	2B	797177741-797377809	2.36E-04	0.237624
M3799: T/A	3B	685318543-685318611	3.68E-04	0.065677	M4359: A/T	6B	22081357-22081425	6.66E-04	0.356304
M5103: G/C	2A	73179815-73179883	8.98E-04	0.227723	M8026: A/G	NA	NA	4.53E-04	0.236584
M6031: C/G	5A	672843173-672843241	5.36E-05	0.095215	M9772: A/G	3A	659038152-659038220	2.32E-04	0.285462
M7254: G/A	NA	NA	3.09E-04	0.11495	M10198: T/G	7A	35630453-35630518	6.17E-04	0.057574
M10592: G/C	NA	NA	7.72E-04	0.062706	M11870: C/T	NA	NA	2.70E-04	0.156617
M10876: G/A	4A	709908601-709908669	7.63E-04	0.235066	B				
E2					M763: C/G	1A	14161093-14161161	4.38E-04	0.462046
M5576: T/C	3A	23840923-23840991	5.63E-04	0.206254	M3226: T/C	6B	698461241-698461309	5.85E-04	0.321634
M6146: A/C	5B	598120554-598120622	3.61E-04	0.360264	M4359: A/T	6B	22081357-22081425	4.66E-04	0.356304
M8330: A/C	2A	700374249-700374317	9.51E-04	0.155116	M5019: C/T	7B	677430865-677430933	4.18E-04	0.326337
M10783: G/A	7D	490344136-490344204	2.01E-04	0.223531	M7025: T/C	NA	NA	7.40E-04	0.055941
E3					M7745: G/C	2D	35039085-35039153	2.89E-04	0.431749
M976: G/C	NA	NA	3.36E-04	0.257228	M9397: C/A	NA	NA	5.26E-04	0.116386
M1654: C/A	2B	797177741-797377809	4.09E-04	0.237624	M9772: A/G	3A	659038152-659038220	1.25E-04	0.285462
M8026: A/G	NA	NA	4.99E-04	0.236584	M10783: G/A	7D	490344136-490344204	1.82E-04	0.223531
M9772: A/G	3A	659038152-659038220	1.16E-04	0.285462	M11095: A/G	7A	700115446-700115514	7.88E-04	0.079076
E4					M11338: T/C	NA	NA	9.06E-04	0.459703
M976: G/C	NA	NA	5.54E-05	0.257228					
Incubation Period (E1:3; E2:2; E3:12; E4:6 and BLUP:7)									
E1									
M140: A/C	2B	91205274-91205342	4.95E-04	0.158416	M9264: G/C	NA	NA	7.62E-04	0.174719
M650: C/A	2B	79317077-79317117	4.37E-04	0.19802	M10907: G/T	7B	730875968-730876036	1.24E-04	0.278696
M11792: C/G	4B	647704512-647704580	2.46E-04	0.348878	E4				
E2					M4648: G/T	7A	94143005-94143073	2.78E-04	0.285132
M8531: T/C	NA	NA	9.08E-04	0.108812	M5996: A/C	3D	479617743-479617811	9.84E-04	0.370875
M11418: G/A	6A	443334314-443334382	8.30E-04	0.203663	M7433: T/C	3B	60372653-60372721	3.22E-04	0.17495
E3					M10241: G/T	3B	11646443-11646511	2.24E-04	0.051139
M119: A/G	5B	529608885-529608950	5.53E-04	0.064274	M11765: T/C	2A	107180183-107180251	3.43E-04	0.155116
M225: A/G	2A	143209405-143209473	8.46E-04	0.432343	M12439: G/C	NA	NA	8.90E-04	0.183828
M804: C/T	5A	582958870-582958938	3.90E-04	0.054406	B				
M3107: T/C	7B	196255937-196256005	5.85E-04	0.05264	**M876: G/C**	6B	27649755-27649823	8.16E-04	0.498548
M3962: C/T	5B	228277790-228277858	6.15E-04	0.318399	M2039: C/G	2A	81660284-81660352	1.32E-04	0.062706
M4648: G/T	7A	94143005-94143073	5.89E-05	0.285132	M2947: T/G	1B	170842706-170842774	7.09E-04	0.395776
M4837: T/C	NA	NA	1.86E-04	0.224422	M4089: T/A	6A	593657698-593657766	1.81E-04	0.159719
M4958: G/A	NA	NA	9.23E-04	0.113449	M7868: T/C	NA	NA	3.70E-04	0.156155
M5551: T/G	1D	452208385-452208453	8.56E-04	0.256997	M9665: C/T	3B	746854760-746854828	9.63E-04	0.154422

(Continued)

10.3389/fpls.2022.1036064

TABLE 2 Continued

SNP	Chr.	Pos. of SNP tag (bp)	-log10 (P)	maf	SNP	Chr.	Pos. of SNP tag (bp)	-log10(P)	maf
M8110: T/C	7B	553167382-553167450	7.43E-04	0.074868	M11765: T/C	2A	107180183-107180251	3.43E-04	0.155116
Lesion Number (E1:6; E2:4; E3:9; E4:6 and BLUP:1)									
E1									
M2326: T/C	5A	32743559-32743627	5.00E-04	0.235924	M6140: T/C	5B	522912127-522912195	3.24E-04	0.221023
M3426: A/G	2B	73990358-73990426	1.85E-04	0.480182	M6730: T/C	1A	20893697-20893765	5.11E-04	0.094604
M5696: T/G	5D	382494021-382494089	6.70E-04	0.287228	M9263: G/C	NA	NA	7.11E-04	0.440545
M8024: A/G	6A	585062562-585062630	8.90E-04	0.168944	M11585: G/A	7A	66298367-66298435	5.01E-04	0.17066
M8443: G/A	4D	134916786-134916854	3.98E-06	0.124752	M4854: T/G	4A	4A:200817628-200817696	8.44E-04	0.186056
M9994: G/C	NA	NA	4.57E-04	0.306931	M2010: T/C	3B	598995436-598995504	9.93E-04	0.359736
E2					E4				
M164: A/G	4B	538706787-538706855	5.74E-04	0.067607	M2771: A/C	4A	16997957-16998025	1.18E-04	0.308531
M992: C/T	NA	NA	7.62E-05	0.145017	M3928: G/C	2B	602182720-602182788	2.83E-04	0.438614
M3416: G/A	6A	596590906-596590974	6.52E-04	0.409373	M5313: T/C	2A	485122901-485122967	6.21E-04	0.135314
M9240: G/A	6D	467151830-467151898	2.54E-04	0.192327	M6140: T/C	5B	522912127-522912195	5.34E-04	0.221023
E3					M6730: T/C	1A	20893697-20893765	3.99E-04	0.094604
M2771: A/C	4A	16997957-16998025	6.62E-04	0.308531	M11585: G/A	7A	66298367-66298435	5.37E-04	0.17066
M3928: G/C	2B	602182720-602182788	2.12E-04	0.438614	B				
M5313: T/C	2A	485122901-485122967	4.94E-04	0.135314	M5928: T/C	6A	33188097-33188165	5.94E-04	0.250957

Candidate genes

Genomic regions within a window of 200 kb of each MTA (100 kb on each side), when subjected to identification of CGs, gave 163 CGs (61 for AUDPC, 54 for IP and 48 for LN). These CGs were associated with only 72 MTAs (AUDPC: 26; IP: 28; and LN: 18); the remaining 21 MTAs gave no CGs. These CGs, when screened for the identification of genes already known to be involved in different pathways of pathogen–host interactions and pathogenesis, gave 64 CGs, which included 25 CGs for AUDPC, 23 for IP and 16 for LN (Supplementary Table 7). These CGs encoded the following 14 major proteins that are relevant to pathogenesis and pathogen–host interactions: (i) NBS-LRR domain superfamily; (ii) F-box domain superfamily; (iii) Kinase-like domain superfamily; (iv) DEAD/DEAH box helicase domain; (v) P-loop containing nucleoside triphosphate hydrolase; (vi) Senescence-associated family protein; (vii) Zinc finger like domain; (viii) Transcription factor GRAS; (ix) Helix-loop-helix DNA-binding domain superfamily; (x) Basic-leucine zipper domain; (xi) DPBB domain; (xii) Transcription factor, MADS-box superfamily; (xiii) Cytochrome P450 superfamily and (xiv) GDSL lipase/esterase-like, plant SGNH hydrolase superfamily. CGs encodes proteins which are directly or indirectly involved in host-pathogen response and are the targets for future functional genomics research focus to understand the significance of these CGs for resistance to spot blotch.

Discussion

In the present study, an association panel comprising global collection of 303 diverse genotypes (procured from CIMMYT, Mexico) was evaluated for variation in spot blotch resistance at two different locations of India, which represented regions with warm humid climate, suitable for the spot blotch disease. The study allowed identification of genomic regions carrying markers associated with functional loci for SB resistance. High level of variability (as revealed by descriptive statistics) for each of the three traits suggested that the panel was suitable for a study of the genetics of quantitative traits. The same panel was earlier utilized by us in GWAS for several other traits including the following: (i) yield related traits (Sehgal et al., 2017; Malik et al., 2021a; Malik et al., 2021b; Malik et al., 2022); (ii) Fe, Zn, β-carotene, GPC content (Kumar et al., 2018); and, (iii) drought tolerance (Gahlaut et al., 2019).

The genotyping data for 210 SNP markers (distributed on 21 chromosomes) suggested a low level of population structure in the association panel (Figure 2), which is a desirable feature for GWAS, as also shown in our earlier studies involving the same association panel with minor differences (Kumar et al., 2018; Gahlaut et al., 2019; Malik et al., 2021a; Malik et al., 2021b; Malik et al., 2022). In earlier studies involving different association panels also, the number of sub-populations ranged from three (for example, Wang et al., 2017; Rahimi et al., 2019) to six (for example, Li et al., 2016; Qaseem et al., 2018; Jamil et al., 2019), suggesting that in majority of studies in wheat, the level of

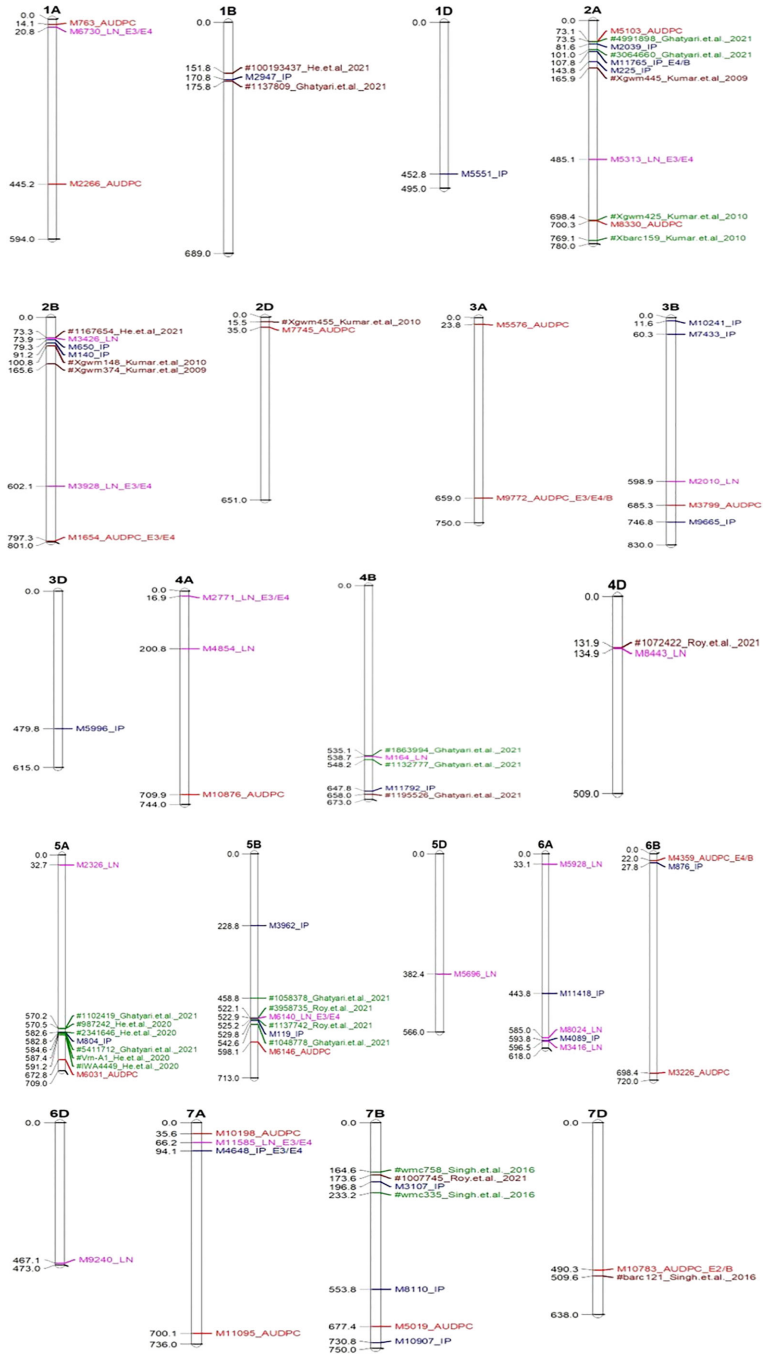

FIGURE 5
Significant MTAs associated with QTLs reported earlier (Green and Brown colour) mapped on different chromosome. In the above figures significant MTAs for AUDPC indicated by red colour; IP by blue colour & LN by pink colour; E1-Enivironment 1; E2-Enivironment 2; E3-Enivironment 3; E4-Enivironment 4; B-BLUP.

population structure is low. It has been shown that population structure and relatedness due to ancestry are two important confounding factors in GWAS, which were initially addressed in mixed linear model, MLM (Yu et al., 2006). In this model, the problem of population structure and relatedness were addressed though development and use of Q and K matrices (Sui et al., 2018). However, MLM had several weaknesses including computational demand, multiple testing, and background effect. Therefore, during the last 15 years, about a dozen models were proposed to address these problems. Five of these improved models were used in the present study to evaluate their relative merits.

In the present study, 306 MTAs were identified using one or more of the five models used in the present study. There was a solitary MTA (M876, present on chromosome 6), which was detected by all the five models. The remaining 305 MTAs were first placed in two groups, those identified using SUPER and those common to all the remaining four models. The MTAs other than 88 MTAs common to four

TABLE 3 Epistatic interactions for different traits in three environments.

SNP1; SNP Allele	Ch: Pos. of SNP Tag	SNP2; SNP Allele	Ch: Pos. of SNP Tag	p- Value
AUDPC				
M238; A>G	2B: 67247748-67247765	M1164; A>C	7A: 94495522-94495590	1.27E-03
M4326; C>G	7A: 640669196-640669264	M11844; T>C	3B: 581263393-581263461	1.07E-03
IP				
M3711; G>C	1B: 499899181-499899249	M4228; T>C	7B: 572536722-572536790	4.02E-03
LN				
M921; G>A	3A: 509934375-509934443	M8709; G>A	6B: 48479624-48479692	1.57E-03
M1998; C>T	3A:12868494-12868562	M8278; G>C	6A: 606427410-606427478	7.26E-03
M7467; C>G	3D: 556059162-556059230	M12122; C>G	7D: 3854256-3854324	9.14E-03
M9322; G>T	2A: 16016622-16016690	M3401; G>A	7A: 27478985-27479053	7.55E-03
M9496; G>A	3A: 17528445-17528513	M9267; T>C	3B: 683764839-683764907	2.00E-03

Ch, Chromosome; Pos, position.

models, were then classified into MTAs common to three models, two models and those unique to individual models (see Supplementary Tables 2–4).

One of the major issues in GWAS, is the control of both false positives as well as false negatives. The false positives are the result of occurrence of LD due to reasons other than linkage, including selection, genetic drift, etc. To control these false positives, use of Bonferroni correction and FDR were recommended. However, it has been repeatedly reported that these measures, although control false positives, but lead to false negatives, which is equally undesirable (Narum, 2006; Kaler and Purcell, 2019; White et al., 2019; Kaler et al., 2020). For the identification of significant MTAs, stringent criteria (p-value <0.001) were used. Bonferroni correction was also used in the form of built-in facility in FarmCPU and BLINK. The 88 MTAs highlighted in the present study represented those, which were detected using four of the five models (excluding SUPER), such that these MTAs do not suffer from any weaknesses of the two single locus models CMLM, SUPER and the multi-locus model MLMM. These were all identified by FarmCPU and BLINK, thus suggesting that all MTAs were valid even after Bonferroni correction. Otherwise, Bonferroni correction is widely known to give many undesirable false negatives.

The above results can be examined in light of the results of QTL analysis studies conducted (including interval mapping and GWAS) in the last three decades. A variety of molecular markers and statistical tools were utilized for the earlier studies involving all major crops. At least >30,000 QTLs for different traits including yield and tolerance to biotic and abiotic stresses are already available in wheat (for wheat QTL database, see Singh et al., 2021; Singh et al., 2022). Of these ~600 QTLs/MTAs (84 QTLs using interval mapping + 516 MTAs using GWAS) were available for resistance against spot blotch and related diseases.

Among linkage-based interval mapping studies, eleven studies were conducted for spot blotch (Kumar et al., 2009; Kumar et al., 2010; Lillemo et al., 2013; Zhu et al., 2014; Kumar et al., 2015; Singh et al., 2016; Singh et al., 2018; He et al., 2020; Roy et al., 2021; Gahtyari et al., 2021 and Kaur et al., 2021). Similarly, about a dozen GWA studies (ten studies) were also conducted for spot blotch (Adhikari et al., 2012; Gurung et al., 2014; Ahirwar et al., 2018; Ayana et al., 2018; Jamil et al., 2018; Juliana et al., 2019; Bainsla et al., 2020; Tomar et al., 2021; Juliana et al., 2022; Lozano-Ramirez et al., 2022). The present study is yet another attempt, adding 36 novel MTAs to the ever-growing list of markers associated with resistance against spot blotch. Some of these are recommended for use in MAS (see later).

At least a dozen models are now available showing significant improvement in GWAS. In the recent past several genome wide association studies have been conducted, where several models have been used and the results compared (Ayana et al., 2018; Ward et al., 2019; Chaurasia et al., 2020; Alemu et al., 2021; Malik et al., 2021a; Sandhu et al., 2021; Soumya et al., 2021). In this study, we selected five models for identification of main effect MTAs and PLINK for epistatic interactions. The merits and demerits of these models have been widely discussed (Gupta et al., 2014, Gupta et al., 2019; Kaler et al., 2020). Among these models, till recently, FarmCPU was a preferred model since it involves the use of Fixed Effect Model (FEM) and a Random Effect Model (REM) iteratively, and thus eliminates confounding problems arising due to kinship, population structure, multiple testing. However, FarmCPU is a model, which is based on unrealistic assumption that quantitative trait nucleotides (QTNs) are evenly distributed throughout the genome. BLINK approximates the maximum likelihood using Bayesian Information Content (BIC) in a fixed-effect model to eliminate the computational burden. In BLINK, REM is replaced with FEM to eliminate the requirement that QTNs are evenly distributed throughout the genome, which further improved the statistical power over FarmCPU, in addition to reduced computing time, so that in BLINK, the computational time is reduced from approximately one week in FarmCPU (Huang et al., 2018) to three hours in BLINK. The detailed difference among models is discussed by Gupta et al. (2019).

The single locus single trait analysis (used in CMLM and SUPER) has several limitations (Gupta et al., 2014). These two models were used in the present study mainly for the purpose of comparing their results with the three other improved multi-locus models that were used in parallel in this study. These new approaches included MLMM,

TABLE 4 A summary of most important MTAs common in four GWAS models (CMLM, MLMM, FarmCPU & BLINK; MTAs with SUPER not included).

Marker: SNP	Chr*	Pos*. of SNP tag (bp)	P. value	Description
AUDPC				
M1654: C/A	2B	797177741-797377809	4.09E-04	E3, E4
M4359: A/T	6B	22081AU357-22081425	6.66E-04	E4, B
M9772: A/G	3A	659038152-659038220	1.16E-04	E3, E4, B
M10783: G/A	7D	490344136-490344204	2.01E-04	E2, B
M8330#: A/C	2A	700374249-700374317	9.51E-04	QSb.bhu-2A
IP				
M4648: G/T	7A	94143005-94143073	5.89E-05	E3, E4
M11765: T/C	2A	107180183-107180251	3.55E-04	E4, B
LN				
M2771: A/C	4A	16997957-16998025	1.18E-04	E3, E4
M3928: G/C	2B	602182720-602182788	2.12E-04	E3, E4
M5313: T/C	2A	485122901-485122967	4.94E-04	E3, E4
M6140: T/C	5B	522912127-522912195	5.34E-04	E3, E4
M6730: T/C	1A	20893697-20893765	5.11E-04	E3, E4
M11585: G/A	7A	66298367-66298435	5.01E-04	E3, E4

*Chr, Chromosome; Pos, Position; bp, base pair #Lying within QTL interval of QSb.bhu-2A (Kumar et al., 2010).

FarmCPU and BLINK (Segura et al., 2012; Liu et al., 2016 and Huang et al., 2018). These models were also used in earlier studies, although BLINK was only sparingly used (Ayana et al., 2018; Bainsala et al., 2020; and Tomar et al., 2021). These five approaches (two for single locus; three for multi-locus) for GWAS used in the present study take into consideration the genetic background and epistatic interaction.

Epistatic interactions are often ignored in GWAS, although recently studied for the following traits: (1) flowering time (Reif et al., 2011; Langer et al., 2014), (2) stem rust resistance (Yu et al., 2011), (3) agronomic traits (Sehgal et al., 2017), (iv) yield related traits, micronutrients, and grain morphology (Jaiswal et al., 2016; Kumar et al., 2018; Malik et al., 2021a, Malik et al., 2022). Epistatic interactions were also detected through interval mapping (Li et al., 2011; Xu et al., 2012; Rouse et al., 2014; Boeven et al., 2020). However, epistatic MTAs have been sparingly used in MAS for crop improvement (Kao et al., 1999; Reif et al., 2011; Langer et al., 2014; Jaiswal et al., 2016; Sehgal et al., 2017; Kumar et al., 2018). We believe that all epistatic QTLs and MTAs, including those detected in this study, should be examined for their possible use in MAS.

MTAs for MAS

Among the MTAs identified in this study, 13 MTAs suitable for marker-assisted selection (MAS) were initially selected using the following criteria: (1) lowest P-value, (2) identified by more than one models, (3) identified in more than one environment, (4) reported in earlier studies. These 13 MTAs included five MTAs for AUDPC, two MTAs for IP, six MTAs for LN (Table 4). Surprisingly, no multi-trait MTA was detected for more than one trait. Therefore, we need to consider the relative importance of three traits. Due to proven value of AUDPC in majority of past studies on genetics and breeding for SB, we like to recommend only five MTAs for AUPDC and ignore those for IP and LN. Since epistatic QTLs are also important, we like to add two MTAs only for AUDPC (Table 3) involving epistatic interaction. In this manner, we recommend that seven MTAs including five main effect MTAs and two epistatic interactions (four markers) should be examined for their use in MAS (or preferably marker assisted recurrent selection).

Candidate genes

Among the candidate genes identified in this study, genes encoding proteins with NBS-LRR domain superfamily are the most important, since these are the most common disease resistance genes (Lee and Yeom, 2015; Dubey and Singh, 2018; Tomar et al., 2021). Nine CGs (Supplementary Table 7) identified are known to be involved in defense response of wheat to *Puccinia triticina* causing leaf rust (Wang et al., 2019), *Zymoseptoria tritici* causing septoria tritici blotch (STB) and some other fungal diseases (He et al., 2018). The genes encoding proteins with F-box family are also known to mediate responses to biotic (Kim and Delaney, 2002) and abiotic stresses (Calderon-Villalobos et al., 2007); these genes are also known to control leaf senescence (Woo et al., 2001), stay-green trait (Tomar et al., 2021) and leaf blight resistance (Joshi et al., 2007a; Rosyara et al., 2008). Three CGs were associated with the genomic region, which encode proteins with Zinc finger domain and are known to take part in several traits including the following: (i) ABA/gibberellin stress response (Lin et al., 2011); (ii) seed germination (Kim et al., 2008);

(iii) pathogen-associated molecular pattern-triggered immune (PTI) responses (Maldonado-Bonilla et al., 2013); (iv) salt stress response (Sun et al., 2007).

Conclusions

The MTAs for three SB resistance traits i.e., AUDPC, IP and LN identified in the present study may be useful for MAS in breeding programs involving improvement in spot blotch resistance. These MTAs may be validated for use in MAS and may also be used for post-GWAS or joint linkage and association mapping (JLAM; Gupta et al., 2019). The information of the CGs may also be useful for the development of CG-based functional markers. The CGs identified in the present study may also be used for CG based association mapping and functional genomics in future research.

Web links

[1] Wheat QTL database (http://wheatqtldb.net/)
[2] PLINK (https://zzz.bwh.harvard.edu/plink/index.shtml)
[3] Ensembl database (http://www.ensembl.org/info/docs/tools/vep/index.html)
[4] IWGSC (http://www.wheatgenome.org)

Data availability statement

The original contributions presented in the study are included in the article/Supplementary Material. Further inquiries can be directed to the corresponding author.

Author contributions

SS performed the analyses and drafted the manuscript. PG, SG and NV designed the experiments and supervised the analysis. AJ, UK, RC and VM were involved in spot blotch phenotyping. All authors reviewed the article and approved the submitted version.

Acknowledgments

SS received financial support in the form of an Inspire Fellowship from Department of Science & Technology (DST), Govt. of India. Head, Genetics and Plant Breeding, CCS University, Meerut provided the facilities. AJ, BISA farm, CIMMYT, India provided field facility at both location (BHU & BISA). RC providing SB inoculum and other departmental facility and Manish Kumar providing all facility at the BISA farm. CIMMYT gene bank is sincerely acknowledged for providing seed material and genotypic data for the present research.

Conflict of interest

The authors declare that the research was conducted in the absence of any commercial or financial relationships that could be construed as a potential conflict of interest.

Publisher's note

Supplementary material

The Supplementary Material for this article can be found online at: https://www.frontiersin.org/articles/10.3389/fpls.2022.1036064/full#supplementary-material

SUPPLEMENTARY FIGURE 1
Manhattan and Q-Q plots for AUDPC in E1, for all five models.

SUPPLEMENTARY FIGURE 2
Manhattan and Q-Q plots for AUDPC in E2, for all five models.

SUPPLEMENTARY FIGURE 3
Manhattan and Q-Q plots for AUDPC in E3, for all five models.

SUPPLEMENTARY FIGURE 4
Manhattan and Q-Q plots for AUDPC in E4, for all five models.

SUPPLEMENTARY FIGURE 5
Manhattan and Q-Q plots for IP in E1, for all five models.

SUPPLEMENTARY FIGURE 6
Manhattan and Q-Q plots for IP in E2, for all five models.

SUPPLEMENTARY FIGURE 7
Manhattan and Q-Q plots for IP in E3, for all five models.

SUPPLEMENTARY FIGURE 8
Manhattan and Q-Q plots for IP in E4, for all five models.

SUPPLEMENTARY FIGURE 9
Manhattan and Q-Q plots for LN in E1, for all five models.

SUPPLEMENTARY FIGURE 10
Manhattan and Q-Q plots for LN in E2, for all five models.

SUPPLEMENTARY FIGURE 11
Manhattan and Q-Q plots for LN in E3, for all five models

SUPPLEMENTARY FIGURE 12
Manhattan and Q-Q plots for LN in E4, for all five models.

References

Adhikari, T. B., Gurung, S., Hansen, J. M., Jackson, E. W., and Bonman, J. M. (2012). Association mapping of quantitative trait loci in spring wheat landraces conferring resistance to bacterial leaf streak and spot blotch. *Plant Genome* 5, 1–16. doi: 10.3835/plantgenome2011.12.0032

Aggarwal, R., Agarwal, S., Sharma, S., Gurjar, M. S., Bashyal, B. M., Rao, A. R., et al. (2022). Whole-genome sequence analysis of *Bipolaris sorokiniana* infecting wheat in India and characterization of *ToxA* gene in different isolates as pathogenicity determinants. *3 Biotech.* 12 (7), 1–15. doi: 10.1007/s13205-022-03213-3

Aggarwal, R., Singh, V. B., Gurjar, M. S., Gupta, S., and Srinivas, P. (2009). Intraspecific variations in Indian isolates of *Bipolaris sorokiniana* infecting wheat based on morphological, pathogenic, and molecular characters. *Indian Phytopathol.* 62 (4), 449–460.

Ahirwar, R. N., Mishra, V. K., Chand, R., Budhlakoti, N., Mishra, D. C., Kumar, S., et al. (2018). Genome-wide association mapping of spot blotch resistance in wheat association mapping initiative (WAMI) panel of spring wheat (*Triticum aestivum* l.). *PloS One* 13 (12), e0208196. doi: 10.1371/journal.pone.0208196

Alemu, A., Suliman, S., Hagras, A., Thabet, S., Al-Abdallat, A., Abdelmula, A. A., et al. (2021). Multi-model genome-wide association and genomic prediction analysis of 16 agronomic, physiological, and quality related traits in ICARDA spring wheat. *Euphytica* 217 (11), 1–22. doi: 10.1007/s10681-021-02933-6

Alexandratos, N., and Bruinsma, J. (2012). World agriculture towards 2030/2050: the 2012 revision (Rome: FAO). ESA Working paper No. 12-03. doi: 10.22004/ag.econ.288998

Ayana, G. T., Ali, S., Sidhu, J. S., Gonzalez Hernandez, J. L., Turnipseed, B., and Sehgal, S. K. (2018). Genome-wide association study for spot blotch resistance in hard winter wheat. *Front. Plant Sci.* 9. doi: 10.3389/fpls.2018.00926

Bainsla, N. K., Phuke, R. M., He, X., Gupta, V., Bishnoi, S. K., Sharma, R. K., et al. (2020). Genome-wide association study for spot blotch resistance in afghan wheat germplasm. *Plant Pathol.* 69, 1161–1171. doi: 10.1111/ppa.13191

Bates, D., Maechler, M., Bolker, B., and Walker, S. (2015). Mixed-effects models using lme4. *J. Stat. Software* 67, 1–48. doi: 10.48550/arXiv.1406.5823

Boeven, P. H., Zhao, Y., Thorwarth, P., Liu, F., Maurer, H. P., Gils, M., et al. (2020). Negative dominance and dominance-by-dominance epistatic effects reduce grain-yield heterosis in wide crosses in wheat. *Sci. Adv.* 6 (24), e4897. doi: 10.1126/sciadv.aay4897

Calderon-Villalobos, L. I. A., Nill, C., Marrocco, K., Kretsch, T., and Schwechheimer, C. (2007). The evolutionarily conserved *Arabidopsis thaliana* f-box protein AtFBP7 is required for efficient translation during temperature stress. *Gene* 392, 106–116. doi: 10.1016/j.gene.2006.11.016

Chatrath, R., Mishra, B., Ortiz Ferrara, G., Singh, S. K., and Joshi, A. K. (2007). Challenges to wheat production in south Asia. *Euphytica* 157, 447–456. doi: 10.1007/s10681-007-9515-2

Chauhan, P. K., Singh, D. P., and Karwasra, S. S. (2017). Morphological and pathogenic variability in *Bipolaris sorokiniana* causing spot blotch in wheat (*Triticum aestivum*, *T. durum, t. dicoccum*) in India. *Int. J. Curr. Microbiol. App. Sci.* 6 (11), 3499–3520. doi: 10.20546/ijcmas.2017.611.41

Chaurasia, S., Joshi, A. K., Dhari, R., and Chand, R. (1999). Resistance to foliar blight of wheat: a search. *Genet. Res. Crop Evol.* 46 (5), 469–475. doi: 10.1023/A:1008797232108

Chaurasia, S., Singh, A. K., Songachan, L. S., Sharma, A. D., Bhardwaj, R., and Singh, K. (2020). Multi-locus genome-wide association studies reveal novel genomic regions associated with vegetative stage salt tolerance in bread wheat (*Triticum aestivum* l.). *Genomics* 112 (6), 4608–4621. doi: 10.1016/j.ygeno.2020.08.006

Dubey, N., and Singh, K. (2018). "Role of NBS-LRR proteins in plant defense," in *Molecular aspects of plant-pathogen interaction*. Eds. A. Singh and I. K. Singh (Singapore: Springer), 115–138. doi: 10.1007/978-981-10-7371-7_5

Duveiller, E., Kandel, Y. R., Sharma, R. C., and Shrestha, S. M. (2005). Epidemiology of foliar blights (spot blotch and tan spot) of wheat in the plains bordering the Himalayas. *Phytopathology* 95, 248–256. doi: 10.1094/PHYTO-95-0248

Feng, Y., Lu, Q., Zhai, R., Zhang, M., Xu, Q., Yang, Y., et al. (2016). Genome wide association mapping for grain shape traits in indica rice. *Planta* 244 (4), 819–830. doi: 10.1007/s00425-016-2548-9

Flor, H. H. (1955). Host-parasite interaction in flax rust-its genetics and other implications. *Phytopathology* 45, 680–685.

French, E., Kim, B. S., and Iyer-Pascuzzi, A. S. (2016). Mechanisms of quantitative disease resistance in plants. *Cell Dev. Biol.* 56, 201–208. doi: 10.1016/j.semcdb.2016.05.015

Gahlaut, V., Jaiswal, V., Singh, S., Balyan, H. S., and Gupta, P. K. (2019). Multi-locus genome wide association mapping for yield and its contributing traits in hexaploid wheat under different water regimes. *Sci. Rep.* 9 (1), 1–15. doi: 10.1038/s41598-019-55520-0

Gahtyari, N. C., Roy, C., He, X., Roy, K. K., Reza, M., Hakim, M. A., et al. (2021). Identification of QTLs for spot blotch resistance in two bi-parental mapping populations of wheat. *Plants* 10 (5), 973. doi: 10.3390/plants10050973

Gupta, P. K., Chand, R., Vasistha, N. K., Pandey, S. P., Kumar, U., Mishra, V. K., et al. (2018b). Spot blotch disease of wheat: the current status of research on genetics and breeding. *Plant Pathol.* 67, 508–531. doi: 10.1111/ppa.12781

Gupta, P. K., Kulwal, P. L., and Jaiswal, V. (2014). Association mapping in crop plants: opportunities and challenges. *Adv. Genet.* 85, 109–147. doi: 10.1016/B978-0-12-800271-1.00002-0

Gupta, P. K., Kulwal, P. L., and Jaiswal, V. (2019). Association mapping in plants in the post-GWAS genomics era. *Adv. Genet.* 104, 75–154. doi: 10.1016/bs.adgen.2018.12.001

Gupta, V., Sheoran, S., Singh, C., Tyagi, B. S., Singh, G. P., and Singh, G. (2022). "Breeding for spot blotch resistance in wheat," in *New horizons in wheat and barley research* (Singapore: Springer), 307–330. doi: 10.1007/978-981-16-4449-8_13

Gupta, P. K., Vasistha, N. K., Aggarwal, R., and Joshi, A. K. (2018a). Biology of *B. sorokiniana* (syn. *Cochliobolus sativus*) in genomics era. *J. Plant Biochem. Biotechnol.* 27 (2), 123–138. doi: 10.1007/s13562-017-0426-6

Gurung, S., Mamidi, S., Bonman, J. M., Xiong, M., Brown-Guedira, G., and Adhikari, T. B. (2014). Genome-wide association study reveals novel quantitative trait loci associated with resistance to multiple leaf spot diseases of spring wheat. *PloS One* 9, e108179. doi: 10.1371/journal.pone.0108179

He, X., Dreisigacker, S., Sansaloni, C., Duveiller, E., Singh, R. P., and Singh, P. K. (2020). Quantitative trait loci mapping for spot blotch resistance in two biparental mapping populations of bread wheat. *Phytopathology* 110 (12), 1980–1987. doi: 10.1094/PHYTO-05-20-0197-R

He, H., Zhu, S., Zhao, R., Jiang, Z., Ji, Y., Ji, J., et al. (2018). *Pm21*, encoding a typical CC-NBS-LRR protein, confers broad-spectrum resistance to wheat powdery mildew disease. *Mol. Plant* 11, 879–882. doi: 10.1016/j.molp.2018.03.004

Huang, M., Liu, X., Zhou, Y., Summers, R. M., and Zhang, Z. (2018). BLINK: a package for the next level of genome-wide association studies with both individuals and markers in the millions. *Gigascience* 8 (2), giy154. doi: 10.1093/gigascience/giy154

International Wheat Genome Sequencing Consortium (IWGSC), Appels, R., Eversole, K., Stein, N., Feuillet, C., Keller, B., et al. (2018). Shifting the limits in wheat research and breeding using a fully annotated reference genome. *Science* 361 (6403), e7191. doi: 10.1126/science.aar7191

Jaiswal, V., Gahlaut, V., Meher, P. K., Mir, R. R., Jaiswal, J. P., Rao, A. R., et al. (2016). Genome wide single locus single trait, multi-locus and multi-trait association mapping for some important agronomic traits in common wheat (*T. aestivum* l.). *PloS One* 11 (7), 1–25. doi: 10.1371/journal.pone.0159343

Jamil, M., Ali, A., Gul, A., Ghafoor, A., Ibrahim, A. M. H., and Mujeeb-Kazi, A. (2018). Genome-wide association studies for spot blotch (*Cochliobolus sativus*) resistance in bread wheat using genotyping-by-sequencing. *Phytopathology* 108, 1307–1314. doi: 10.1094/PHYTO-02-18-0047-R

Jamil, M., Ali, A., Gul, A., Ghafoor, A., Napar, A. A., Ibrahim, A. M., et al. (2019). Genome-wide association studies of seven agronomic traits under two sowing conditions in bread wheat. *BMC Plant Biol.* 19 (1), 1–18. doi: 10.1186/s12870-019-1754-6

Jan, H. U., Guan, M., Yao, M., Liu, W., Wei, D., Abbadi, A., et al. (2019). Genome-wide haplotype analysis improves trait predictions in brassica napus hybrids. *Plant Sci.* 283, 157–164. doi: 10.1016/j.plantsci.2019.02.007

Joshi, A. K., Chand, R., and Arun, B. (2002). Relationship of plant height and days to maturity with resistance to spot blotch in wheat. *Euphytica* 123, 221–228. doi: 10.1023/A:1014922416058

Joshi, A. K., Kumari, M., Singh, V. P., Reddy, C. M., Kumar, S., Rane, J., et al. (2007a). Stay green trait: variation, inheritance, and its association with spot blotch resistance in spring wheat (*Triticum aestivum* l.). *Euphytica* 153 (1), 59–71. doi: 10.1007/s10681-006-9235-z

Joshi, A. K., Ortiz-Ferrara, G., Crossa, J., Singh, G., Alvarado, G., Bhatta, M. R., et al. (2007b). Associations of environments in south Asia based on spot blotch disease of wheat caused by cochliobolus sativus. *Crop Sci.* 47 (3), 1071–1081. doi: 10.2135/cropsci2006.07.0477

Juliana, P., Poland, J., Huerta-Espino, J., Shrestha, S., Crossa, J., Crespo-Herrera, L., et al. (2019). Improving grain yield, stress resilience and quality of bread wheat using large-scale genomics. *Nat. Genet.* 51, 1530–1539. doi: 10.1038/s41588-019-0496-6

Juliana, P., Xinyao, H., Poland, J., Shrestha, S., Joshi, A. K., Huerta-Espino, J., et al. (2022). Genome-wide association mapping indicates quantitative genetic control of spot blotch resistance in bread wheat and the favourable effects of some spot blotch loci on grain yield. *Front. Plant Sci.* 13. doi: 10.3389/fpls.2022.835095

Kaler, A. S., Gillman, J. D., Beissinger, T., and Purcell, L. C. (2020). Comparing different statistical models and multiple testing corrections for association mapping in soybean and maize. *Front. Plant Sci.* 10. doi: 10.3389/fpls.2019.01794

Kaler, A. S., and Purcell, L. C. (2019). Estimation of a significance threshold for genome-wide association studies. *BMC Genom* 20, 618. doi: 10.1186/s12864-019-5992-7

Kao, C. H., Zeng, Z. B., and Teasdale, R. D. (1999). Multiple interval mapping for quantitative trait loci. *Genetics* 152, 1203–1216. doi: 10.1093/genetics/152.3.1203

Kaur, J., Kaur, J., Dhillon, G. S., Kaur, H., Singh, J., Bala, R., et al. (2021). Characterization and mapping of spot blotch in *Triticum durum-aegilops speltoides* introgression lines using SNP markers. *Front. Plant Sci.* 12. doi: 10.3389/fpls.2021.650400

Kim, H. S., and Delaney, T. P. (2002). Arabidopsis SON1 is an f-box protein that regulates a novel induced defense response independent of both salicylic acid and systemic acquired resistance. *Plant Cell* 14, 1469–1482. doi: 10.1105/tpc.001867

Kim, D. H., Yamaguchi, S., Lim, S., Oh, E., Park, J., Hanada, A., et al. (2008). SOMNUS, a CCCH-type zinc finger protein in arabidopsis, negatively regulates light-dependent seed germination downstream of PIL5. *Plant Cell* 20, 1260–1277. doi: 10.1105/tpc.108.058859

Kumar, U., Joshi, A. K., Kumar, S., Chand, R., and Roder, M. S. (2009). Mapping of resistance to spot blotch disease caused by *Bipolaris sorokiniana* in spring wheat. *Theor. Appl. Genet.* 118 (4), 783–792. doi: 10.1007/s00122-008-0938-5

Kumar, U., Joshi, A. K., Kumar, S., Chand, R., and Roder, M. S. (2010). Quantitative trait loci for resistance to spot blotch caused by *Bipolaris sorokiniana* in wheat (*T.*

aestivum l.) lines 'Ning 8201' and 'Chirya 3.'. *Mol. Breed.* 26, 477–491. doi: 10.1007/s11032-009-9388-2

Kumar, U., Kumar, S., Prasad, R., Roder, M. S., Kumar, S., Chand, R., et al. (2019). Genetic gain on resistance to spot blotch of wheat by developing lines with near immunity. *Crop Breed. Genet. Genom.* 1, e190017. doi: 10.20900/cbgg20190017

Kumar, S., Roder, M. S., Tripathi, S. B., Kumar, S., Chand, R., and Joshi, A. K. (2015). Mendelization and fine mapping of a bread wheat spot blotch disease resistance QTL. *Mol. Breed.* 35, 218. doi: 10.1007/s11032-015-0411-5

Kumar, J., Saripalli, G., Gahlaut, V., Goel, N., Meher, P. K., and Mishra, K. K. (2018). Genetics of fe, zn, β-carotene, GPC, and yield traits in bread wheat (*Triticum aestivum* l.) using multi-locus and multi-traits GWAS. *Euphytica* 214 (11), 1–17. doi: 10.1007/s10681-018-2284-2

Langer, S. M., Longin, C. F. H., and Wurschum, T. (2014). Flowering time control in European winter wheat. *Front. Plant Sci.* 5. doi: 10.3389/fpls.2014.00537

Lee, H. A., and Yeom, S. I. (2015). Plant NB-LRR proteins: tightly regulated sensors in a complex manner. *Brief. Funct. Genomics* 14, 233–242. doi: 10.1093/bfgp/elv012

Lillemo, M., Joshi, A. K., Prasad, R., Chand, R., and Singh, R. P. (2013). QTL for spot blotch resistance in bread wheat line Saar co-locate to the biotrophic disease resistance loci *Lr34* and *Lr46*. *Theor. Appl. Genet.* 126, 711–719. doi: 10.1007/s00122-012-2012-6

Lin, P. C., Pomeranz, M. C., Jikumaru, Y., Kang, S. G., Hah, C., Fujioka, S., et al. (2011). The arabidopsis tandem zinc finger protein AtTZF1 affects ABA and GA-mediated growth, stress, and gene expression responses. *Plant J.* 65, 253–268. doi: 10.1111/j.1365-313X.2010.04419.x

Lipka, A. E., Tian, F., Wang, Q., Peiffer, J., Li, M., Bradbury, P. J., et al. (2012). GAPIT: genome association and prediction integrated tool. *Bioinformatics* 28 (18), 2397–2399. doi: 10.1093/bioinformatics/bts444

Liu, X., Huang, M., Fan, B., Buckler, E. S., and Zhang, Z. (2016). Iterative usage of fixed and random effect models for powerful and efficient genome-wide association studies. *PloS Genet.* 12 (2), e1005767. doi: 10.1371/journal.pgen.1005767

Li, W. H., Wei, L. I. U., Li, L. I. U., You, M. S., Liu, G. T., and Li, B. Y. (2011). QTL mapping for wheat flour color with additive, epistatic, and QTL x environmental interaction effects. *Agric. Sci. China* 10 (5), 651–660. doi: 10.1016/S1671-2927(11)60047-3

Li, G., Xu, X., Bai, G., Carver, B. F., Hunger, R., Bonman, J. M., et al. (2016). Genome-wide association mapping reveals novel QTL for seedling leaf rust resistance in a worldwide collection of winter wheat. *Plant Genome* 9 (3), 51. doi: 10.3835/plantgenome2016.06.0051

Lozano-Ramirez, N., Dreisigacker, S., Sansaloni, C. P., He, X., Sandoval-Islas, J. S., Pérez-Rodríguez, P., et al. (2022). Genome-wide association study for spot blotch resistance in synthetic hexaploid wheat. *Genes* 13 (8), 1387. doi: 10.3390/genes13081387

Lu, P., Liang, Y., Li, D., Wang, Z., Li, W., Wang, G., et al. (2016). Fine genetic mapping of spot blotch resistance gene *Sb3* in wheat (*Triticum aestivum*). *Theor. Appl. Genet.* 129, 577–589. doi: 10.1007/s00122-015-2649-z

Maldonado-Bonilla, L. D., Eschen-Lippold, L., Gago-Zachert, S., Tabassum, N., Bauer, N., Scheel, D., et al. (2013). The arabidopsis tandem zinc finger 9 protein binds RNA and mediates pathogen-associated molecular pattern-triggered immune responses. *Plant Cell Physiol.* 55, 412–425. doi: 10.1093/pcp/pct175

Malik, P., Kumar, J., Sharma, S., Meher, P. K., Balyan, H. S., Gupta, P. K., et al. (2022). GWAS for main effects and epistatic interactions for grain morphology traits in wheat. *Physiol. Mol. Biol. Plants* 28 (3), 651–668. doi: 10.1007/s12298-022-01164-w

Malik, P., Kumar, J., Sharma, S., Sharma, R., and Sharma, S. (2021b). Multi-locus genome-wide association mapping for spike-related traits in bread wheat (*Triticum aestivum* l.). *BMC Genomics* 22 (1), 1–21. doi: 10.1186/s12864-021-07834-5

Malik, P., Kumar, J., Singh, S., Sharma, S., Meher, P. K., Sharma, M. K., et al. (2021a). Single-trait, multi-locus, and multi-trait GWAS using four different models for yield traits in bread wheat. *Mol. Breed.* 41 (7), 1–21. doi: 10.1007/s11032-021-01240-1

Marone, D., Russo, M. A., Laidò, G., De Vita, P., Papa, R., Blanco, A., et al. (2013). Genetic basis of qualitative and quantitative resistance to powdery mildew in wheat: from consensus regions to candidate genes. *BMC Genomics* 14, 562. doi: 10.1186/1471-2164-14-562

McDonald, M. C., Ahren, D., Simpfendorfer, S., Milgate, A., and Solomon, P. S. (2018). The discovery of the virulence gene *ToxA* in the wheat and barley pathogen *Bipolaris sorokiniana*. *Mol. Plant Pathol* 19 (2), 432–9. doi: 10.1111/mpp.12535

Mehta, Y. R. (1985). "Breeding wheats for resistance to helminthosporium spot blotch," in *Wheats for more tropical environments: A proceedings of the international symposium*. Eds. R. L. Villareal and A. R. Klatts (Mexico: CIMMYT), 135–144.

Narum, S. R. (2006). Beyond bonferroni: less conservative analyses for conservation genetics. *Conserv. Genet.* 7 (5), 783–787. doi: 10.1007/s10592-005-9056-y

Navathe, S., Yadav, P. S., Chand, R., Mishra, V. K., Vasistha, N. K., Meher, P. K., et al. (2020). ToxA–Tsn1 interaction for spot blotch susceptibility in Indian wheat: An example of inverse gene-for-gene relationship. *Plant Dis.* 104 (1), 71–81. doi: 10.1094/PDIS-05-19-1066-RE

Navathe, S., Yashavanthakumar, K. J., Pandey, A. K., Patil, R. M., Baviskar, V. S., and Chand, R. (2022). "Leaf blight disease of wheat and barley: Past, present and future," in *Eds new horizons in wheat and barley research* (Singapore: Springer), 77–105. doi: 10.1007/978-981-16-4134-3_3

Parlevliet, J. E. (1979). Components of resistance that reduce the rate of epidemic development. *Annu. Rev. Phytopathol.* 17 (1), 203–222. doi: 10.1146/annurev.py.17.090179.001223

Pritchard, J. K., Stephens, M., and Donnelly, P. (2000). Inference of population structure using multilocus genotype data. *Genetics* 155 (2), 945–959. doi: 10.1093/genetics/155.2.945

Purcell, S., Neale, B., Todd-Brown, K., Thomas, L., Ferreira, M. A., Bender, D., et al. (2007). PLINK: a tool set for whole-genome association and population-based linkage analyses. the. *Annu. Rev. Phytopathol.* 81 (3), 559–575. doi: 10.1086/519795

Qaseem, M. F., Qureshi, R., Muqaddasi, Q. H., Shaheen, H., Kousar, R., and Roder, M. S. (2018). Genome-wide association mapping in bread wheat subjected to independent and combined high temperature and drought stress. *PloS One* 13 (6), e0199121. doi: 10.1371/journal.pone.0199121

Rahimi, Y., Bihamta, M. R., Taleei, A., Alipour, H., and Ingvarsson, P. K. (2019). Genome-wide association study of agronomic traits in bread wheat reveals novel putative alleles for future breeding programs. *BMC Plant Biol.* 19 (1), 1–19. doi: 10.1186/s12870-019-2165-4

Reif, J. C., Maurer, H. P., Korzun, V., Ebmeyer, E., Miedaner, T., and Wurschum, T. (2011). Mapping QTLs with main and epistatic effects underlying grain yield and heading time in soft winter wheat. *Theor. Appl. Genet.* 123 (2), 283–292. doi: 10.1007/s00122-011-1583-y

Rosyara, U. R., Khadka, K., Subedi, S., Sharma, R. C., and Duveiller, E. (2008). Heritability of stay green traits and association with spot blotch resistance in three spring wheat populations. *J. Genet. Breed.* 62, 75–82. doi: 10.1007/s00122-011-1583-y

Roumen, E. C. (1992). Effect of leaf age on components of partial resistance in rice to leaf blast. *Euphytica* 63 (3), 271–279. doi: 10.1007/BF00024554

Rouse, M. N., Talbert, L. E., Singh, D., and Sherman, J. D. (2014). Complementary epistasis involving *Sr12* explains adult plant resistance to stem rust in thatcher wheat (*Triticum aestivum* l.). *Theor. Appl. Genet.* 127, 1549–1559. doi: 10.1007/s00122-014-2319-6

Roy, C., Gahtyari, N. C., He, X., Mishra, V. K., Chand, R., Joshi, A. K., et al. (2021). Dissecting quantitative trait loci for spot blotch resistance in south Asia using two wheat recombinant inbred line populations. *Front. Plant Sci.* 12. doi: 10.3389/fpls.2021.641324

Saari, E. E. (1998). "Leaf blight disease and associated soil-borne fungal pathogens of wheat in south and south East Asia," in *Helminthosporium blights of wheat: Spot blotch and tan spot*. Eds. E. Duveiller, H. J. Dubin, J. Reeves and A. McNab (Mexico: CIMMYT).

Saari, E. E., and Prescott, J. M. (1975). A scale for appraising the foliar intensity of wheat diseases. *Plant Dis. Rep.* 59, 377–380.

Sandhu, K. S., Mihalyov, P. D., Lewien, M. J., Pumphrey, M. O., and Carter, A. H. (2021). Genomic selection and genome-wide association studies for grain protein content stability in a nested association mapping population of wheat. *Agronomy* 11 (12), 2528. doi: 10.3390/agronomy11122528

Segura, V., Vilhjalmsson, B. J., Platt, A., Korte, A., Seren, U., Long, Q., et al. (2012). An efficient multi-locus mixed-model approach for genome-wide association studies in structured populations. *Nat. Genet.* 44 (7), 825–830. doi: 10.1038/ng.2314

Sehgal, D., Autrique, E., Singh, R., Ellis, M., Singh, S., and Dreisigacker, S. (2017). Identification of genomic regions for grain yield and yield stability and their epistatic interactions. *Sci. Rep.* 7 (1), 1–12. doi: 10.1038/srep41578

Sharma, R. C., and Duveiller, E. (2006). Spot blotch continues to cause substantial grain yield reductions under resource-limited farming conditions. *J. Phytopathol.* 154, 482–488. doi: 10.1111/j.1439-0434.2006.01134.x

Sharma, R. C., and Duveiller, E. (2007). Advancement toward new spot blotch resistant wheats in south Asia. *Crop Sci.* 47 (3), 961–968. doi: 10.2135/cropsci2006.03.0201

Shiferaw, B., Smale, M., Braun, H. J., Duveiller, E., Reynolds, M., and Muricho, G. (2013). Crops that feed the world 10. past successes and future challenges to the role played by wheat in global food security. *Food Secur.* 5 (3), 291–317. doi: 10.1007/s12571-013-0263-y

Siddique, A. B., Hossain, M. H., Duveiller, E., and Sharma, R. (2006). Progress in wheat resistance to spot blotch in Bangladesh. *C J. Phytopathol.* 154, 16–22. doi: 10.1111/j.1439-0434.2005.01049.x

Singh, K., Batra, R., Sharma, S., Saripalli, G., Gautam, T., Singh, R., et al. (2021). WheatQTLdb: a QTL database for wheat. *Mol. Genet. Genom.* 296 (5), 1051–1056. doi: 10.1007/s00438-021-01796-9

Singh, P. K., He, X. Y., Sansaloni, C. P., Philomin, J., Dreisigacker, S., Duveiller, E., et al. (2018). Resistance to spot blotch in two mapping populations of common wheat is controlled by multiple QTL of minor effects. *Int. J. Mol. Sci.* 19 (12), 4054. doi: 10.3390/ijms19124054

Singh, K., Saini, D. K., Saripalli, G., Batra, R., Gautam, T., Singh, R., et al. (2022). WheatQTLdb V2. 0: A supplement to the database for wheat QTL. *Mol. Breed.* 42, 56. doi: 10.21203/rs.3.rs-1379009/v1

Singh, V., Singh, G., Chaudhury, A., Ojha, A., Tyagi, B. S., Chowdhary, A. K., et al. (2016). Phenotyping at hot spots and tagging of QTLs conferring spot blotch resistance in bread wheat. *Mol. Biol. Rep.* 43 (11), 1293–1303. doi: 10.1007/s11033-016-4066-z

Singh, P. K., Zhang, Y., He, X., Singh, R. P., Chand, R., Mishra, V. K., et al. (2015). Development and characterization of the 4th CSISA-spot blotch nursery of bread wheat. *Eur. J. Plant Pathol.* 143 (3), 595–605. doi: 10.1007/s10658-015-0712-x

Soumya, P. R., Burridge, A. J., Singh, N., Batra, R., Pandey, R., Kalia, S., et al. (2021). Population structure and genome-wide association studies in bread wheat for phosphorus efficiency traits using 35 K wheat breeder's affymetrix array. *Sci. Rep.* 11 (1), 1–17. doi: 10.1038/s41598-021-87182-2

Sui, J. H., Martin, L. S., and Eskin, E. (2018). Population structure in genetic studies: Confounding factors and mixed models. *PloS Genet.* 14 (12), e1007309. doi: 10.1371/journal.pgen.1007309

Sun, J., Jiang, H., Xu, Y., Li, H., Wu, X., Xie, Q., et al. (2007). The CCCH-type zinc finger proteins AtSZF1 and AtSZF2 regulate salt stress responses in arabidopsis. *Plant Cell Physiol.* 48 (8), 1148–1158. doi: 10.1093/pcp/pcm088

Tomar, V., Singh, D., Dhillon, G. S., Singh, R. P., Poland, J., Joshi, A. K., et al. (2021). New QTLs for spot blotch disease resistance in wheat (*Triticum aestivum* l.) using genome-wide association mapping. *Front. Genet.* 11. doi: 10.3389/fgene.2020.61321

VanRaden, P. M. (2008). Efficient methods to compute genomic predictions. *J. Dairy Sci.* 91 (11), 4414–4423. doi: 10.3168/jds.2007-0980

Voorrips, R. (2002). MapChart: software for the graphical presentation of linkage maps and QTLs. *J. Hered.* 93 (1), 77–78. doi: 10.1093/jhered/93.1.77

Wang, Q., Tian, F., Pan, Y., Buckler, E. S., and Zhang, Z. (2014). A SUPER powerful method for genome wide association study. *PloS One* 9 (9), e107684. doi: 10.1371/journal.pone.0107684

Wang, Y., Wei, F., Zhou, H., Liu, N., Niu, X., Yan, C., et al (2019). TaCAMTA4, a calmodulin-Interacting protein, involved in defense response of wheat to Puccinia triticina. *Sci. Rep.* 9, 641. doi: 10.1038/s41598-018-36385-1

Wang, J., and Zhang, Z. (2021). GAPIT version 3: boosting power and accuracy for genomic association and prediction. *Genom. Proteom. Bioinform.* 19 (4), 629–640. doi: 10.1016/j.gpb.2021.08.005

Wang, S. X., Zhu, Y. L., Zhang, D. X., Shao, H., Liu, P., Hu, J. B., et al. (2017). Genome-wide association study for grain yield and related traits in elite wheat varieties and advanced lines using SNP markers. *PloS One* 12, e0188662. doi: 10.1371/journal.pone.0188662

Ward, B. P., Brown-Guedira, G., Kolb, F. L., Van Sanford, D. A., Tyagi, P., Sneller, C. H., et al. (2019). Genome-wide association studies for yield-related traits in soft red winter wheat grown in Virginia. *PloS One* 14 (2), e0208217. doi: 10.1371/journal.pone.0208217

White, T., van der Ende, J., and Nichols, T. E. (2019). Beyond bonferroni revisited: concerns over inflated false positive research findings in the fields of conservation genetics, biology, and medicine. *Conserv. Genet.* 20 (4), 927–937. doi: 10.1007/s10592-019-01178-0

Woo, H. R., Chung, K. M., Park, J. H., Oh, S. A., Ahn, T., Hong, S. H., et al. (2001). ORE9, an f-box protein that regulates leaf senescence in arabidopsis. *Plant Cell* 13 (8), 1779–1790. doi: 10.1105/TPC.010061

Xu, Y., An, D., Liu, D., Zhang, A., Xu, H., and Li, B. (2012). Molecular mapping of QTLs for grain zinc, iron, and protein concentration of wheat across two environments. *Field Crops Res.* 138, 57–62. doi: 10.1016/j.fcr.2012.09.017

Yu, L. X., Lorenz, A., Rutkoski, J., Singh, R. P., Bhavani, S., Huerta-Espino, J., et al. (2011). Association mapping and gene–gene interaction for stem rust resistance in CIMMYT spring wheat germplasm. *Theor. Appl. Genet.* 123 (8), 1257–1268. doi: 10.1007/s00122-011-1664-y

Yu, J., Pressoir, G., Briggs, W. H., Vroh Bi, I., Yamasaki, M., Doebley, J. F., et al. (2006). A unified mixed-model method for association mapping that accounts for multiple levels of relatedness. *Nat. Genet.* 38 (2), 203–208. doi: 10.1038/ng1702

Zhang, Z., Ersoz, E., Lai, C. Q., Todhunter, R. J., Tiwari, H. K., Gore, M. A., et al. (2010). Mixed linear model approach adapted for genome-wide association studies. *Nat. Genet.* 42 (4), 355–360. doi: 10.1038/ng.546

Zhang, P., Guo, G., Wu, Q., Chen, Y., Xie, J., Lu, P., et al. (2020). Identification and fine mapping of spot blotch (*Bipolaris sorokiniana*) resistance gene *Sb4* in wheat. *Theor. Appl. Genet.* 133, 2451–2459. doi: 10.1007/s00122-020-03610-3

Zhong, S., Steffenson, B. J., Martinez, J. P., and Ciuffetti, L. M. (2002). A molecular genetic map and electrophoretic karyotype of the plant pathogenic fungus *Cochliobolus sativus*. *Mol. Plant Microbe Interact.* 15, 481–492. doi: 10.1094/MPMI.2002.15.5.481

Zhu, Z., Bonnett, D., Ellis, M., Singh, P., Heslot, N., Dreisigacker, S., et al. (2014). Mapping resistance to spot blotch in a CIMMYT synthetic-derived bread wheat. *Mol. Breed.* 34 (3), 1215–1228. doi: 10.1007/s11032-014-0111-6

frontiers | Frontiers in Microbiology

TYPE Original Research
PUBLISHED 01 February 2023
DOI 10.3389/fmicb.2023.1040605

OPEN ACCESS

EDITED BY
Maria Rosa Simon,
National University of La Plata,
Argentina

REVIEWED BY
Paul M. Severns,
University of Georgia,
United States
Matías Schierenbeck,
Leibniz Institute of Plant Genetics and Crop Plant Research (IPK), Germany

*CORRESPONDENCE
Musrat Zahan Surovy
✉ msurovy@gwdg.de
Andreas von Tiedemann
✉ atiedem@gwdg.de

SPECIALTY SECTION
This article was submitted to Microbe and Virus Interactions with Plants, a section of the journal Frontiers in Microbiology

RECEIVED 09 September 2022
ACCEPTED 09 January 2023
PUBLISHED 01 February 2023

CITATION
Surovy MZ, Islam T and von Tiedemann A (2023) Role of seed infection for the near and far distance dissemination of wheat blast caused by *Magnaporthe oryzae* pathotype *Triticum*. *Front. Microbiol.* 14:1040605. doi: 10.3389/fmicb.2023.1040605

Role of seed infection for the near and far distance dissemination of wheat blast caused by *Magnaporthe oryzae* pathotype *Triticum*

Musrat Zahan Surovy[1,2]*, Tofazzal Islam[2] and Andreas von Tiedemann[1]*

[1]Division of Plant Pathology and Crop Protection, Department of Crop Sciences, Georg-August-Universität Göttingen, Göttingen, Germany, [2]Institute of Biotechnology and Genetic Engineering, Bangabandhu Sheikh Mujibur Rahman Agricultural University, Gazipur, Bangladesh

Magnaporthe oryzae pathotype *Triticum* (MoT) is a devastating fungal phytopathogen causing wheat blast disease which threatens wheat production particularly in warmer climate zones. Effective disease control is hampered by the limited knowledge on the life cycle, epidemiology, and pathogenicity of MoT. Since MoT mainly infects and colonizes the inflorescences of wheat, infection, invasion routes and colonization of MoT on wheat ears and in wheat seeds were investigated in order to assess potential seed transmission pathways. MoT was spray inoculated on two wheat cultivars (Sumai 3, susceptible and Milan, resistant) at three ear maturity stages [full ear emergence, growth stage (GS) 59; mid flowering, GS 65; and end of flowering, GS 69]. Incidence of MoT on Sumai 3 seeds was 100% and 20–25% on Milan. MoT sporulation rate on Sumai 3 contaminated seeds was more than 15 times higher than on Milan. Repeated washes of seed samples for removing paraffin fixation hampers seed microscopy. To overcome the damage of seed samples, we used hand-sectioned seed samples instead of paraffin-fixed microtome samples to facilitate microscopy. The colonization of MoT within various seed tissues was followed by light and confocal laser scanning microscopy (CLSM). Invasion of MoT in seeds predominantly occurred in the caryopsis germ region, but entry *via* other seed parts was also observed, confirming the potential of intense colonization of MoT in wheat grains. Fungal spread in wheat plants growing from MoT infected seeds was monitored through plating, microscopic and molecular techniques. Under greenhouse conditions, no spread of MoT from infected seeds to seedlings later than GS 21 or to ears was detected, neither in Milan nor in Sumai 3. We therefore conclude, that MoT may not systemically contaminate inflorescences and seeds in neither susceptible nor resistant wheat cultivars. However, initial blast symptoms, only found on seedlings of Sumai 3 but not Milan, resulted in the formation of new conidia, which may serve as inoculum source for plant-to-plant dissemination by airborne infection of plant stands in the field (short distance spread). Ultimately the inoculum may infect young inflorescences in the field and contaminate seeds. Our findings again stress the risk of long-distance dissemination of wheat blast across continents through MoT-contaminated seeds. This underlines the importance of mandatory use of healthy seeds in strategies to control any further spread of wheat blast.

KEYWORDS

MoT, epidemiology, seed germ, seed transmission, healthy seeds

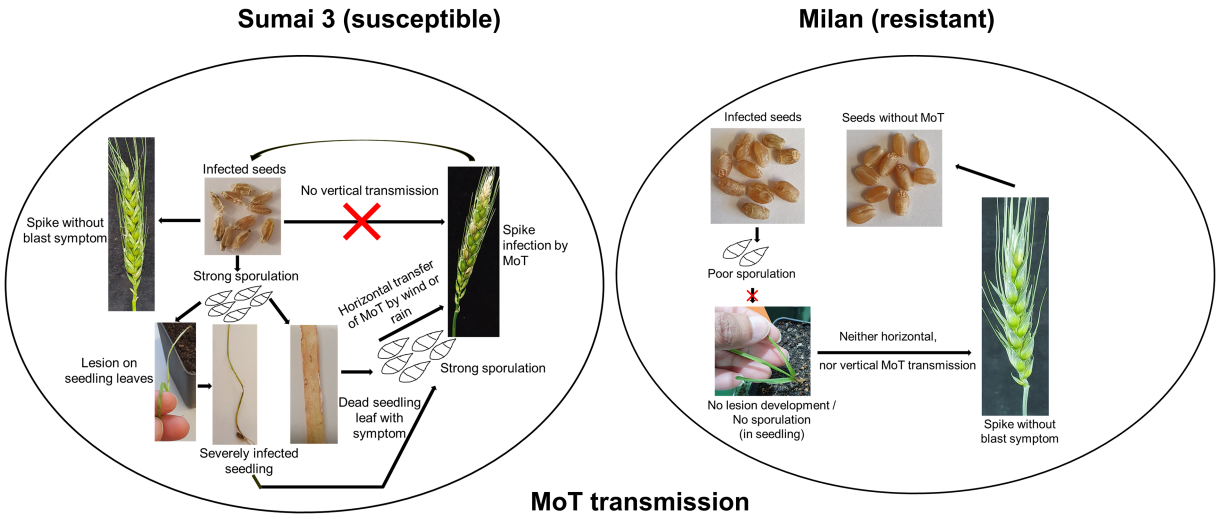

GRAPHICAL ABSTRACT

1. Introduction

Seeds are a main source of inoculum and the potential starting point of numerous diseases (Elmer, 2001). Besides seed-to-plant transmission, either by systemic infection of seedlings or by (horizontal) infection of neighbor plants by seed-borne spores, there also exists a (vertical) seed-to-seed transmission, which allows long-range spread of pathogens through seed trade (Baker and Smith, 1966; Shahzad et al., 2018; Nallathambi et al., 2021). The latter may lead to the introduction and establishment of a pathogen in a new region (Elmer, 2001). Hence, the potential role of seeds in spreading plant diseases is essential for understanding plant disease epidemiology and for assessing the risk of long distance dissemination (McGee, 1979).

Wheat is an important cereal food crop and grown on more than 200 million hectares of cropland worldwide (Tesfaye, 2021). It can grow under a wide range of climatic conditions (Shiferaw et al., 2013) and provides 20% of global dietary protein and calories (FAO, 2015), thus playing a crucial role in global food security. Fungal pathogens may threaten wheat production (Stokstad, 2007; Winston, 2015). The hemibiotrophic fungus *Magnaporthe oryzae* (anamorph *Pyricularia oryzae*) pathotype *Triticum* (MoT) causes wheat blast, a disease which may reduce yield up to 100% in susceptible cultivars (Islam et al., 2016, 2020). This disease first occurred in Brazil (Igarashi et al., 1985), then spread to Bolivia, Argentina, Paraguay, and more recently to Bangladesh and Zambia (Ceresini et al., 2019; Tembo et al., 2020; Singh et al., 2021). In 2016, Bangladesh imported a large amount of wheat from South America, which is supposed to have introduced wheat blast to Bangladesh (Ceresini et al., 2018; Mottaleb et al., 2018). Warm and humid weather is conducive for wheat blast epidemics as experienced by the extraordinary warm and humid weather conditions in 2016 which facilitated the wheat blast outbreak in Bangladesh (Islam et al., 2019).

The wheat blast pathogen MoT may infect leaves and stems, but ear infection is clearly prevailing in the field, whereas leaf symptoms are rarely observed (Urashima et al., 2004). Basal senescent wheat leaves may however produce conidia and play a role in the secondary distribution of wheat blast in the field (Cruz et al., 2015). Blast conidia may survive for 5 months in crop residues, like stems, rachis and leaves (Pizolotto et al., 2019) and for 3 years in rice stems and straw (Raveloson et al., 2018). In wheat seeds, MoT can survive for 19–22 months (Reis, 1995) maintaining a viability of 60% (Maciel, 2018). MoT inoculum is mainly dispersed by rain, and wind, but seeds have also been reported to play a role (Urashima et al., 2007; Islam et al., 2019). Barley (*Hordeum vulgare*), maize (*Zea mays*), oat (*Avena sativa*), swamp grass (*Leersia hexandra*), and goosegrass (*Eleusine indica L.*) are alternative hosts of MoT (Maciel et al., 2014; Cruz and Valent, 2017; Gupta et al., 2021). Conversely, the rice blast pathogen *Magnaporthe oryzae* pathotype *oryzae* (MoO) has been reported to occasionally infect wheat (Shizhen et al., 2021; Paul et al., 2022), while rice does not normally serve as a host for MoT (Monsur et al., 2016). However, Tingting (2014) reported that some MoT strains may also infect rice seedlings.

Ear infection results in deformed, shriveled, and discolored grains (Urashima et al., 2009; Cruz and Valent, 2017; Martínez et al., 2019; Surovy et al., 2020). It was reported that wheat blast infection deteriorated the grain quality by modulating the grain protein content (Surovy et al., 2020). Data from previous studies indicate that MoT infected seeds may cause more than 20% disease incidence in the offspring (Goulart et al., 1990; Goulart and Paiva, 2000). However, 42 days after sowing, MoT could not be isolated from wheat plants grown from infected seeds (Martinez et al., 2021). Taking previous reports together, the mode of disease transfer by seeds infected with MoT is not clear. There are two possible ways of seed transmission of MoT, (i) by superficial attachment on the seed surface and transmission by wind, rain, or other mechanical ways into the field (horizontal transfer), or (ii) by seeds internally producing systemically infected plants and MoT-infected grains (vertical transmission).

The detection of MoT from superficially or internally colonized seeds is possible through plating and microscopic techniques, but the symptomless internal colonization is quite difficult to detect only by these methods. Proper localization of MoT in the seeds, however, is crucial to understand the systemic transmission of MoT from seeds to plants or next-generation seeds. Previous studies investigating transmission of blast pathogens (Faivre-Rampant et al., 2013; Martinez et al., 2021) used visual identification followed by plating and fluorescence microscopy. Until today, a comprehensive study addressing

the potential of vertical seed-to-seed transmission of MoT in wheat and the localization of MoT in seeds is lacking. The present study combined plating, microscopy and quantitative polymerase chain reaction (qPCR) in order to address the following questions, (i) which parts of the seeds are preferentially colonized by MoT, (ii) is MoT transmitted vertically in a symptomless manner to infect next generation seeds, and (iii) how can infected seeds produce diseased plants with ear blast symptoms? The overall aim of this study was to investigate the role of infected wheat seeds in the dissemination of blast disease within a field (short distance) and from far away regions (long distance).

2. Materials and methods

2.1. Plant material

Two wheat cultivars, susceptible Sumai 3 and resistant Milan [CIMMYT wheat advanced line carrying 2NS/2AS translocation (Téllez et al., 2022)] were selected. Seeds were surface sterilized with 3% NaOCl for 1 min and subsequently washed three times with sterilized distilled water (SDW). Surface-sterilized seeds were kept in 90 mm Petri dishes for 48 h in humid conditions to facilitate germination. Pre-germinated seeds were sown in plastic pots (two per pot; 9 cm× 9 cm× 9.5 cm) filled with a mixture of compost, sand, and peat [2:1:1, volume basis (v/v/v)]. The plants were grown in a greenhouse at 14 h daylight, 25°C (±1), and 65–70% relative humidity (RH). Bottom watering was performed based on water demand. Hakaphos blue nutrient solution (3 g/l, COMPO, Muenster, Germany) was applied weekly beginning at GS 20 (tillering stage, Zadoks et al., 1974). One tiller per plant and two primary tillers in each pot were maintained.

2.2. Fungal isolate

Wheat blast isolate BTGP-6f was obtained through single conidia isolation method from the infected ears collected from a blast affected farmer's field in Meherpur of Bangladesh by the Institute of Biotechnology and Genetic Engineering (IBGE), Bangabandhu Sheikh Mujibur Rahman Agricultural University, Bangladesh (Gupta et al., 2020). The fungal isolate was cultured on 90 mm Petri dishes containing 5% V8 agar medium (50 ml V8 juice, 2 g $CaCO_3$, 15 g Agar, 950 ml water) supplemented with streptomycin (200 ppm) and incubated in a growth chamber (SANYO growth cabinet MLR 350, EWALD Innovationstechnik GmbH, Germany) at 25°C (±1) under continuous fluorescent light (fluorescent lamp 40 W, 20,000 lumens). The conidial suspension was prepared from 7-days old MoT cultures by adding 10 ml of 0.01% sterile Tween 20 aqueous solution per plate. The conidial density was adjusted to 1×10^5 conidia/ml using a Neubauer hemocytometer (Fuchs-Rosenthal, 0.0625 mm^2) (Surovy et al., 2022).

2.3. Inoculation procedure

Uniform ears were artificially inoculated with MoT (1×10^5 conidia/ml) at three different growth stages (GS 59, full ear emergence; GS 65, mid flowering; and GS 69, end of flowering) (Zadoks et al., 1974). An air compressor (Mini air compressor K17, Type N022 An. 18) was used for spray inoculation, and *ca.* 2 ml of conidial suspensions were sprayed per ear while distilled water was used as control (Ha et al., 2016). Twelve pots for each inoculation time point and each cultivar were prepared. Humidity was immediately maintained by covering inoculated ears with plastic bags. Plastic bags were removed 24 h after inoculation, and plants were kept in a climate chamber with a 12 h/12 h day-night photoperiod with 120 µmol m^{-2} s^{-1} (±5) light intensity (high-pressure sodium lamp) at 25°C (±1). Wheat plants were organized in a completely randomized design (CRD), and the ear samples were collected at GS 91 (grain hard). Two repetitive experiments were conducted.

2.4. Assessment of seed germination and MoT infection rate

Thirty randomly selected surface-sterilized seeds (single replicate) were placed in a 90 mm Petri dish containing PDA (4 g potato extract, 20 g dextrose, 15 g agar, 1,000 ml water, pH 5.6) to determine percentage of seed infection by MoT. Three replicates for each inoculation time point of each cultivar were assessed. Visual and microscopic observation for the presence of MoT conidia in seeds or grown mycelia were conducted to determine the MoT seed infection rate. The percentage seed infection was calculated 5 days after plating using the formula used by Surovy et al. (2020):

$$\text{Seed infection}\,(\%) = \left(\frac{\text{Number of seeds infected}}{\text{Total number of seeds used}}\right) \times 100\%$$

For assessment of seed germination, 25 randomly selected surface-sterilized seeds (single replication) from each inoculation time point of each cultivar were placed in a Petri dish containing sterilized distilled water-soaked filter paper (90 mm, Ref# 41255009, Glaswarenfabrik Karl Hecht GmBH & Co KG, Sondheim, Germany) for germination assay. Three replications were maintained. The percentage of germination was calculated 7 days after incubation following the formula used by Surovy et al. (2020):

$$\text{Seed germination}\,(\%) = \left(\frac{\text{Number of seeds germinated}}{\text{Total number of seeds used for germination}}\right) \times 100\%$$

2.5. Assessment of sporulation on seeds

Twenty seeds per replication were randomly selected from each inoculation time point of each cultivar for the MoT sporulation assay. Three replicates were prepared for each treatment. Surface sterilized seeds were placed in sterile micro-slides (76 × 26 mm, Glaswarenfabrik Karl Hecht GmbH and Co KG, Germany) in a 90 mm Petri dish (single seed placed in single slide) containing sterilized distilled water-soaked sterile filter paper to maintain humidity. Twenty-four to 48 h after incubation, seeds were observed under a stereomicroscope (Leica Wild M10) followed by a compound light microscope (Leica Leitz DM RB). The samples were photographed with a Leica DFC420 camera (version 2.8.0.0), and all images were processed using Leica Application Suite V4 (LAS V4) software

(version 4.9.0.129). Subsequently, a single infected seed presenting MoT conidia was placed in a 1.5 ml Eppendorf tube containing 1 ml of SDW and vortexed briefly. After vortexing, 5 µl of suspension was poured into each counting chamber of hemocytometer (Fuchs-Rosenthal, 0.0625 mm^2) to check the homogeneity of the conidial suspension before the conidia were counted. This procedure was repeated five times, and the average counts were multiplied by 200 to obtain the total number of conidia per seed.

2.6. Assessment of seed-to-seed transmission of MoT

Visually infected seeds from artificial inoculation assays were further used in greenhouse experiments to investigate seed-to-seed transmission of MoT. A composite mixed sample of seeds collected from all three inoculation time points was prepared from Sumai 3 and Milan. Randomly selected seeds from the composite mixture were washed with SDW and pre-germinated in 90 mm Petri dishes. Pre-germinated seeds were sown in plastic pots (one per pot; 7 cm × 7 cm × 8 cm) containing similar potting mixture described previously (see above 2.1). Each pot was treated as a replicate, and 60 replicates were used for each cultivar. Wheat plants were grown in a climate chamber, maintaining same conditions as described above (section 2.3). Seedlings were subjected to careful daily observation for disease symptoms, and the experiment was repeated once. Samples were taken for further analysis from seedling leaves, stems, and ears at GS 11, GS 14, GS 21, GS 55, GS 65, and GS 91.

2.7. Reisolation of conidia from the offspring of MoT-infected seeds

Plant samples were surface sterilized with 3% NaOCl and placed in a humid chamber for 24–48 h at 25°C (±1) for germination of MoT conidia. The presence of characteristic three–celled pyriform MoT conidia was examined under stereo and compound microscopes and also plated on synthetic nutrient-poor agar (SNA) (1 g KNO_3, 1 g KH_2PO_4, 0.5 g $MgSO_4 \times 7H_2O$, 0.5 g KCl, 0.2 g glucose, 0.2 g sucrose, 20 g agar, 1,000 ml H_2O) supplemented with streptomycin (200 ppm). Sporulation of MoT on SNA was again checked for further confirmation of MoT from plant samples.

2.8. Localization of MoT in infected seeds and plant samples by confocal laser scanning microscopy (CLSM)

Seed caryopsis samples for cytological analyses were collected from Sumai 3 and Milan ears at 10 and 14 days after MoT inoculation on ears. Seed samples were stored in ACE solution (25% ethanol: 75% chloroform, adjusted to pH 2.8 with 0.15% trichloroacetic acid). Ten to fifteen caryopses were transversely cross-sectioned by hand for microscopic analysis (30–40 sections from each inoculation time point of each cultivar).

Infected leaves and stems (at least six) of wheat plants derived from MoT contaminated seeds were also stored in ACE solution for further analysis. The leaf samples were cut into small pieces, whereas stems and seeds were cross-sectioned using razor blades (Wilkinson sword, Germany), and all samples were double-stained with Wheat Germ Agglutinin Alexa Fluor 488 conjugate, AF (ThermoFisher SCIENTIFIC, Catalogue number W11261), and propidium iodide, PI (SIGMA, Catalogue number P4170-10MG). For leaf and stem samples, AF was added (30 µl of 50 µg/ml) and vacuum infiltrated for 20 min. Later, PI was added (30 µl of 10 µg/ml) and again vacuum infiltrated for 10 min. Vacuum infiltration was done at 250 millibars (mbs) with a regular interval of every 5 min (Ha et al., 2016). The AF staining of seed samples was done for 2 h and PI for 30 min. After staining, the specimens were mounted immediately in 50% glycerol for observation or stored dark at 4°C for further analysis. The CLSM was carried out with a Leica TCS SP5 laser scanning microscope 510 (Leica Microsystems CMS GmbH, Germany). AF was excited using a 488 nm laser and collected at 500–540 nm. The fluorescence signal of PI was excited at 514, and emission recorded at 580–660 nm. CLSM images were processed using Leica Application Suite Advanced Fluorescence software (LAS AF), Version 2.6.3.8173.

2.9. Detection of MoT in plant samples by qPCR

Asymptomatic wheat seedlings and ear samples from Milan at different growth stages (GS 11, GS 14, GS 21, GS 55, GS 65, and GS 91) and ear samples from Sumai 3 collected at GS 55, GS 65, and GS 91 were used for qPCR analysis. At each time point, six ear samples were randomly selected for qPCR analysis for each cultivar.

Collected fresh samples were immediately frozen in liquid nitrogen and ground in a ball mixer mill (Mixer Mill MM400, Retsch). The DNA was extracted by the modified cetyltrimethylammonium bromide (CTAB) method with polyethylene glycol (PEG) precipitation (Ha et al., 2016; Alisaac et al., 2020). The extracted DNA was dissolved in 100 µl TE buffer (10 mM Tris, 1 mM EDTA, pH 8.0). The quality of DNA was checked in a 1.0% agarose gel electrophoresis. DNA concentration was measured using a microplate spectrophotometer (Epoch, Bio-tech) at 260 nm and controlled by the ratio of OD260/OD280. The target sequence was quantified by a thermal cycler (BioRad C1000 Touch™ Thermal Cycler, CFX384™Real-Time System), maintaining a standard curve of pure MoT DNA with 10-fold dilutions (from 1.0 ng to 0.01 pg./µl). The qPCR data were further analyzed with BioRad CFX Maestro 1.1 (Bio-Rad) software. The presence of MoT DNA was determined by species-specific primers [forward primer, *pfh2a* (5′-CGTCACACGTTCTTCAACC-3′) and reverse primer *pfh2b* (5′-CGTTTCACGCTTCTCCG-3′), synthesized by InvitrogenTM (Thermo Fisher Scientific)]. Briefly, the PCR was performed with an initial denaturation at 95°C for 3 min, followed by denaturation at 95°C for 15 s for 35 cycles, annealing at 58°C for 25 s, and elongation at 72°C for 45 s. The final elongation was carried out for 2 min at 72°C. Three technical replicates were performed for each biological replicate.

2.10. Statistical data analysis

All experimental data were analyzed by R software (version 4.0.5, accessed 31 March 2021) integrated with R studio (version 1.2.5001, accessed 31 March 2021). Linear models (LMs) and generalized linear models (GLMs) were used to analyze the relationship between explanatory variables (% seed infection, % reduction of seed germination, number of conidia per seed) and the effects of MoT on wheat cultivars. The model's dispersion and residuals were tested using the function test 'dispersion' and 'stimulatedResiduals' of the "DHARMa" package. These functions

are a simulation-based approach to create readily interpretable scaled residuals for the fitted linear models. Seed infection (%) and seed germination (%) were analyzed by using linear models (ANOVA), and the number of conidia per seed was analyzed by generalized linear models (GLMs) with negative binomial (link = log) family. For multiple comparisons "emmeans" package was used with "Tukey" function. The Spearman Rank correlation was performed to determine the relationship between seed infection percentage and reduction of seed germination percentage. For visualization of bar graphs, "ggplot2" package was used and to combine two or more graphs, "gridextra" package was used. The "ggpubr" function was used to visualize the Spearman Rank correlation data, and the staked graph was prepared using the Microsoft office excel program (Microsoft Office Professional Plus 2016, version 16.0.4266.1001).

3. Results

3.1. Effect of MoT inoculation on seed infection percentage

Magnaporthe oryzae pathotype *Triticum*-inoculated ears of susceptible Sumai 3 and resistant Milan were collected at GS 91 to determine percentage of seed infection by MoT. There were no significant interactions between cultivar and inoculation time points on MoT seed infection percentage ($F = 0.09$, $p = 0.914$). In all three inoculation time points, seed infection was significantly higher in Sumai 3 than in Milan ($F = 325.20$, $p < 0.001$), while no significant effects were found for different inoculation time points ($F = 1.022$, $p = 0.389$) (Table 1).

Seed phenotyping from the greenhouse experiment confirmed that, Sumai 3 was more susceptible to MoT, showing severely deformed, shriveled, and blackish grains, than Milan (Figure 1A). In both cultivars, no disease symptoms were recorded in mock-inoculated control seeds. Seed infection in Sumai 3 ranged from 74 to 100%, while in Milan, it ranged from 10 to 28% (Figures 1A,B).

3.2. Effect of MoT inoculation on seed germination

Parallel to the seed infection assessment, seeds collected at GS 91 were used for seed germination assay. Cultivars ($p < 0.001$), inoculation time points ($p = 0.001$) and their interactions ($p = 0.01$) had statistically significant effects on seed germination percentage. In all three inoculation time points, the seed germination rate of Sumai 3 was significantly lower than in Milan, varying from 80.7% on ears inoculated at GS 59, to 65.3% on ears inoculated at GS 69 (Figure 2). In contrast, there was no statistically significant difference in the reduction of seed germination at different inoculation time points for Milan.

TABLE 1 ANOVA for the effect of MoT on seed infection percentage.

Variables	df	*F* value	*p*-value
Cultivar (C)	1	325.20	<0.001
Inoculation time points (ITPs)	2	1.022	0.389
C: ITPs	2	0.09	0.914

3.3. Correlation between seed infection by MoT and seed germination

Based on Spearman Rank correlation analysis, seed infection by MoT was positively related to the reduction of seed germination percentage. Higher MoT infection in seeds resulted in less germination rates of seeds ($R = 82\%$), and these interactions were significantly different ($p < 0.001$) between cultivars (Figure 3).

3.4. Sporulation of MoT conidia from MoT-infected seeds

Sporulation of MoT was detected on seeds of both Sumai 3 and Milan collected from all inoculation time points (full ear emergence, GS 59; mid flowering, GS 65; and end of flowering stages, GS 69). The highest sporulation rate was consistently found in Sumai 3 which significantly differed from Milan ($p < 0.001$). Upon close inspection of seeds under a stereomicroscope, more MoT sporulation was noticed in the germ region than in other seed parts in both cultivars (Figure 4A).

In the susceptible cultivar Sumai 3, the number of conidia per seed ranged from 31,667 to 63,334. Number of conidia per seed did not significantly differ between ears inoculated at GS 65 (63,334 conidia/seed) and GS 59 (60,666 conidia/seed), however, the lowest number of conidia was found in seeds collected from GS 69 (31,667 conidia/seed), which was significantly different from GS 59 and GS 65.

In Milan, the number of conidia per seed ranged from 1,354 to 3,688. Like Sumai 3, the lowest number of conidia was recorded in seeds inoculated at GS 69 (1,354 conidia/seed), which significantly differed from GS 59 (3,688 conidia/seed) and GS 65 (2,729 conidia per seed) (Figure 4B).

3.5. Detection of MoT in seeds from inoculated ears through CLSM

In order to localize MoT in seeds from inoculated ears, CLSM microscopy was performed with seed sections. The internal tissues of the healthy caryopses of Sumai 3 and Milan were entirely free of MoT hyphae (Figures 5G,J). However, after MoT inoculation, the caryopsis pericarp was severely damaged and deformed in Sumai 3. Massive hyphal growth was detected in the caryopsis coat tissues and endosperm of Sumai 3 seeds. When MoT hyphae started to progress beyond the germ, they accumulated in the germ, causing loosening of the compacted starchy endosperm tissue (Figures 5Ai,B,C). However, when MoT hyphae progressed *via* seed coat rather than germ (Figure 5 Aii), the caryopsis endosperm were less damaged by MoT, and cell wall degradation started from the infection site (Figure 5D).

In Milan, MoT hyphae were mainly detected in the caryopsis coat tissues and in the germ part, with a prevalence of the germ region (Figures 5H,I). Due to the low infection rate in Milan, MoT hyphae only very slowly progressed toward the innermost endosperm (Figure 5).

3.6. Vertical seed-to-seed transmission of MoT

About half of the seedlings from infected seeds obtained from Sumai 3 ears inoculated at different maturity stages in the greenhouse

10.3389/fmicb.2023.1040605

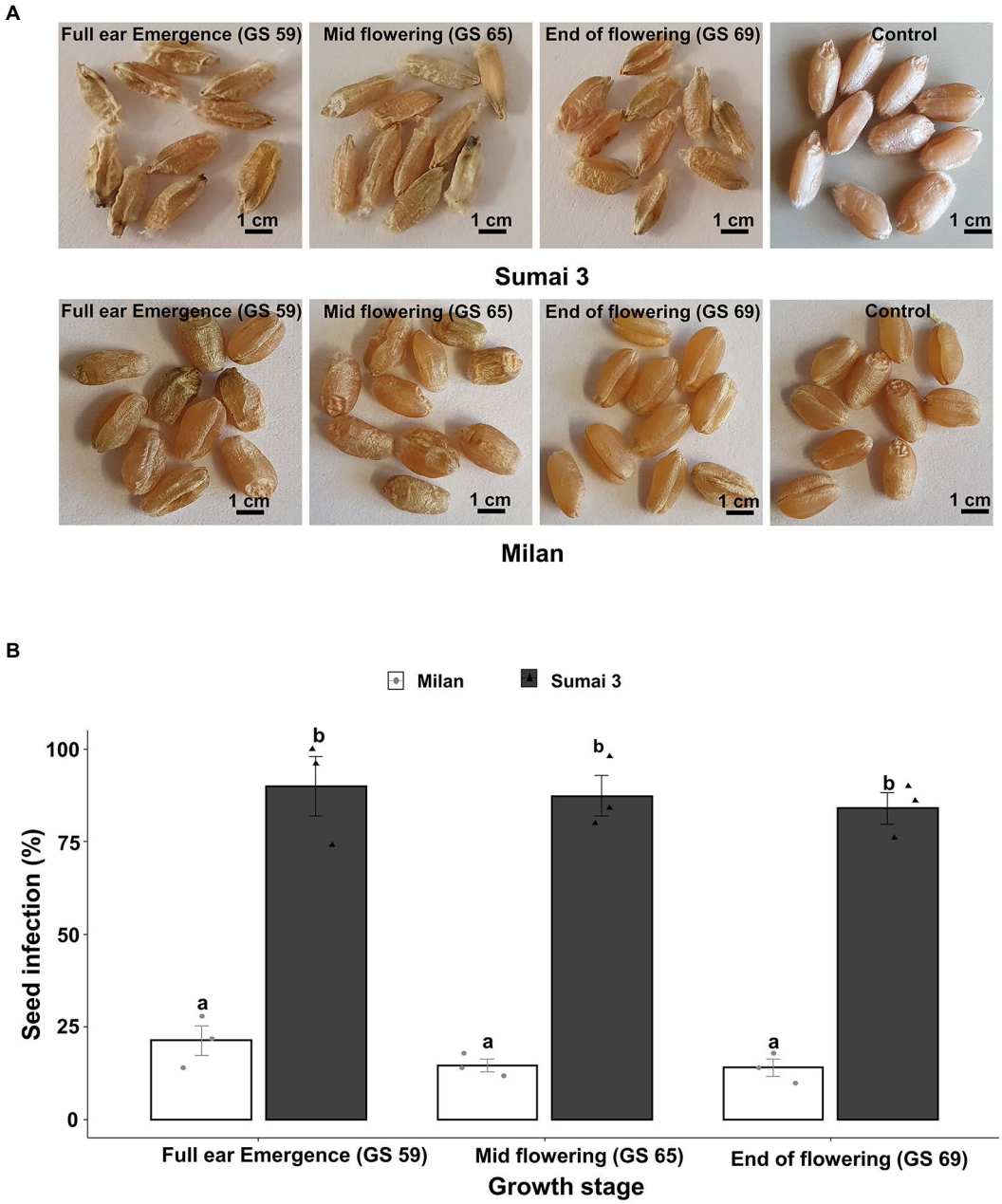

FIGURE 1
Effect of MoT inoculation of wheat ears on MoT seed infection of Sumai 3 and Milan in greenhouse conditions. **(A)** Mature seeds of Sumai 3 and Milan were collected from ears inoculated at three different ear maturity stages (GS 59, full ear emergence; GS 65, mid flowering; and GS 69, end of flowering); **(B)** Seed infection with MoT in Sumai 3 and Milan cultivars assessed by plating assay under greenhouse conditions. Surface sterilized seeds were incubated on PDA at 25°C for 5days. The mean (±standard error) of seed infection (%) of each ear inoculation time point is represented by each bar. ANOVA with Tukey test was performed, and treatments with the same letters at the cultivar level were not significantly different ($n=3$; one replication contained 30 seeds of each cultivar at each inoculation time point; $p=0.05$). Each data point represents one replicate consisting of 30 randomly selected seeds.

showed symptoms on seedling leaves. At GS 11 (first leaf emerged), Sumai 3 seedlings showed symptoms on their first leaves (Figures 6A,B), about 36% of plants had characteristic blast symptoms on seedling stems (Figure 6D), and 10% were asymptomatic. Symptomatic leaves and stems were randomly collected, and MoT was reisolated from all infected samples. Interestingly, disease symptoms on ears were absent (Figures 6I,K). Due to severe blast severity, 45% of Sumai 3 seedlings were dead at GS 14 (emergence of the 4th leaves) (Figures 6G, 7).

At GS 21 (main stem with one tiller), 20% of seedlings showed blast symptoms on lower leaves (Figure 6H), and the rest were entirely asymptomatic. Surprisingly, after GS 21, no blast symptoms were observed in any parts of Sumai 3 plants, and MoT was also not detected by qPCR.

No visual blast symptoms were recorded in Milan from seedling to maturity stages, and no MoT was detected by CLSM, plating, and qPCR techniques (Figures 6, 7).

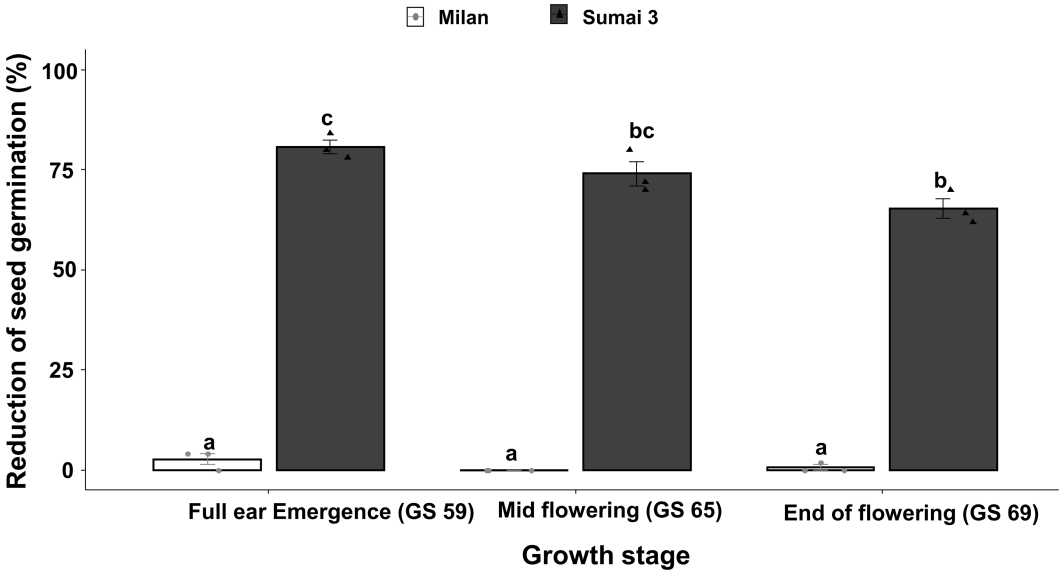

FIGURE 2
Effect of different MoT inoculation time points on the reduction of (%) seed germination of Sumai 3 and Milan in greenhouse conditions. The wheat ears were inoculated with a conidial suspension of 1×10^5 conidia/ml at GS 59, full ear emergence; GS 65, mid flowering; and GS 69, end of flowering stages. For each cultivar, the mean (± standard error) of reduction of seed germination (%) of each ear inoculation time point is represented by a bar. ANOVA with Tukey test was performed, and treatments with the same letters at the cultivar level were not significantly different (n=3; one replication contained 25 seeds of each cultivar at each inoculation time point; p=0.05). Each data point represents one replicate consisting of 25 randomly selected seeds.

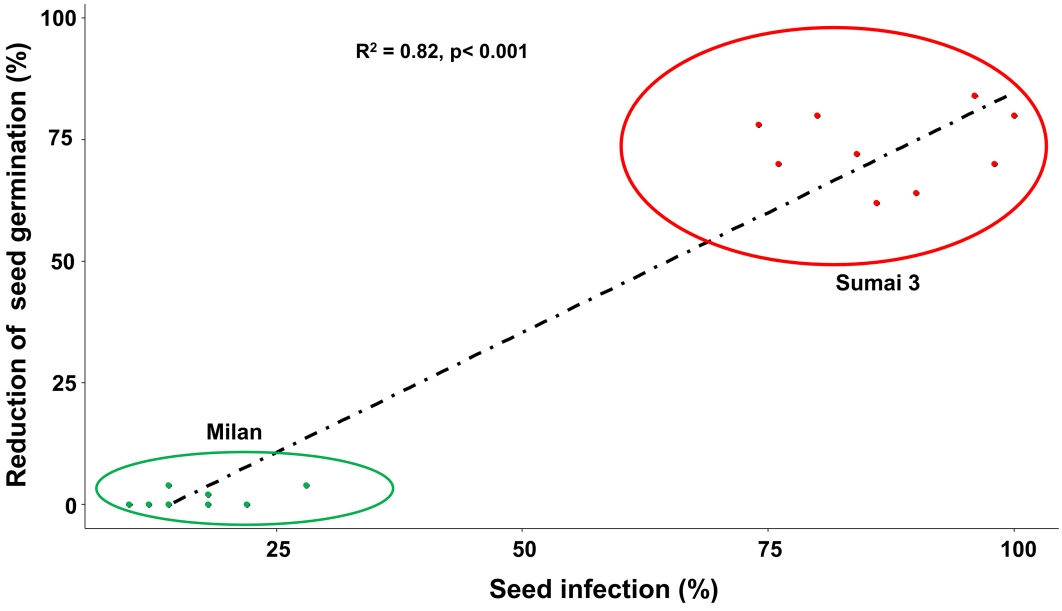

FIGURE 3
Relationship between MoT seed infection (%) and reduction of seed germination (%) of Sumai 3 (red) and Milan (green). Spearman Rank correlation analysis was performed to visualize the correlation data.

4. Discussion

Seeds are the primary units for crop production but may also play a key role in transmitting pathogens within a field or from one region to another. Neither the systemic growth of MoT from seed to seed nor the potential spread of MoT by seeds at the local, regional or long distance scale have been so far explored in-depth. In a previous study MoT could not be detected by reisolation from infected wheat plants (susceptible cultivar Apogee) later than 42 days after sowing (Martinez et al., 2021). In addition, till today, the role of cultivar resistance in the transmission and dissemination of MoT and its localization in seeds is not known.

The present study, conducted under controlled greenhouse and climate chamber conditions confirmed that MoT was able to establish in seeds after inoculation of ears at different flowering stages but there was

10.3389/fmicb.2023.1040605

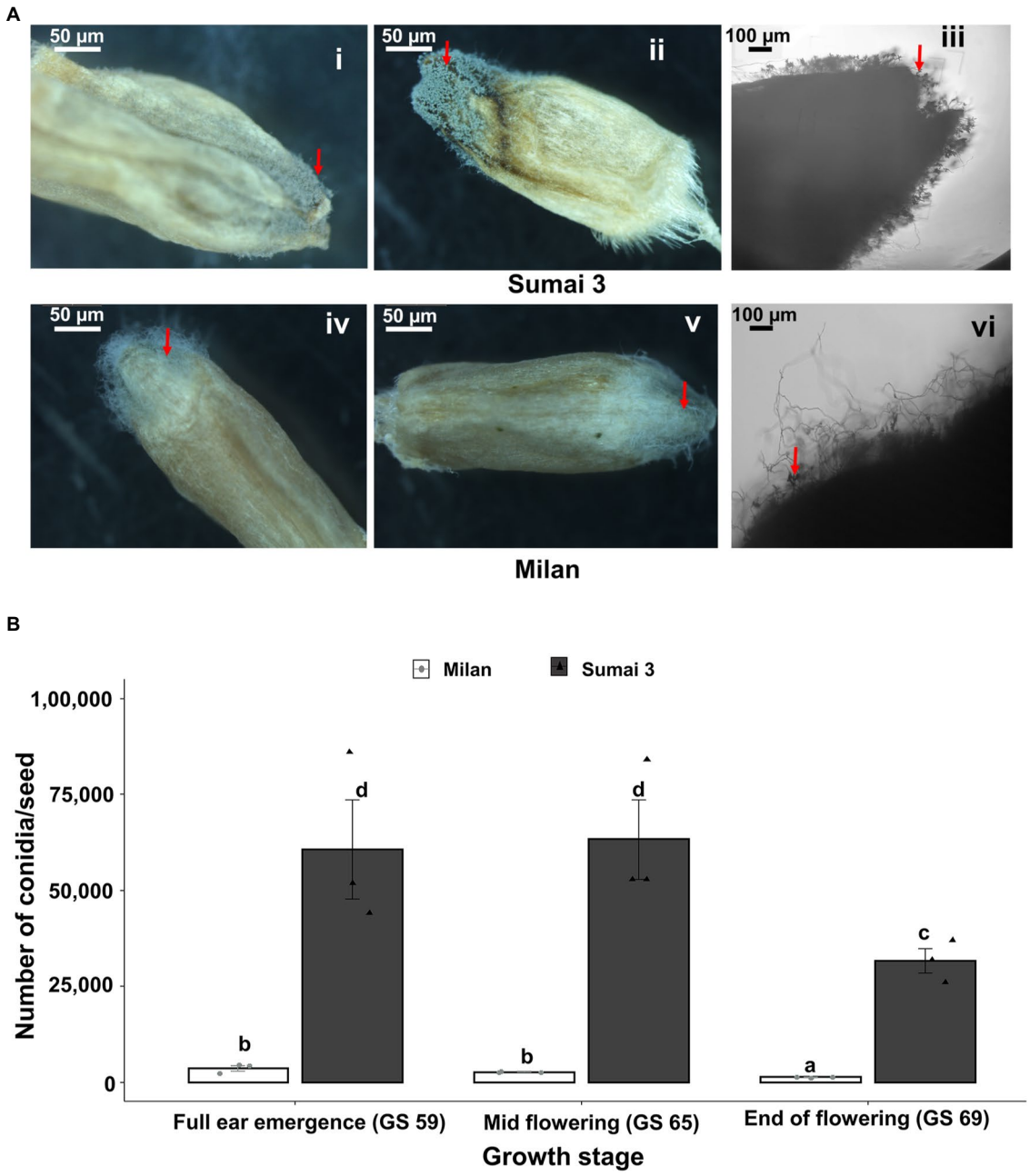

FIGURE 4
Sporulation rate of MoT in seeds from wheat plants spray inoculated with a MoT conidial suspension of 1×10^5 conidia/ml on ears at three different flowering stages. **(A)** MoT conidia on representative seeds of Sumai 3 and Milan. The red arrow indicates the sporulation of MoT conidia on the seeds. **Ai**, **Aii**, **Aiv**, **Av** (scale bar 50µm) were photographed under a stereomicroscope, **Aiii** and **Avi** were photographed under a compound light microscope (scale bar 100µm). **(B)** Number of MoT conidia per seed in Sumai 3 and Milan seeds collected from different inoculation time points. For each cultivar, bars represent the mean (± standard error) of total number of conidia per seed of each ear inoculation time point. ANOVA with Tukey test was performed, and treatments with the same letters at the cultivar level were not significantly different (n=3; one replicate contained 20 seeds of each cultivar at each inoculation time point; p=0.05). Each data point represents one replicate consisting of 20 randomly selected seeds.

no systemic (vertical) transmission detected to the next generation seeds (seed-to-seed). This was ensured through manually removing all infected leaves and dead plant parts in our trials immediately after observing any signs or symptoms of disease. The reason was to avoid cross-contamination of MoT from infected leaves or seedlings to ears or healthy plants. However, on plants grown from seeds of a susceptible cultivar, the pathogen caused symptoms on leaves and stems up to GS 21 from where it was reisolated indicating the potential of a local (horizontal) spread in the field originating from sowing infected seeds. In contrast, no such local spread of MoT was detectable in any stages of the resistant cultivar Milan.

Blast disease at ear maturity stages may have a significant economic impact on wheat production by producing a higher amount of abnormally formed seeds. In our greenhouse experiments, at all MoT inoculation time points, seed infection was almost 100% in Sumai 3 and 20–25% in Milan, resulting in poor quality grains. Previous studies on effects of MoT infection in wheat have demonstrated a positive

10.3389/fmicb.2023.1040605

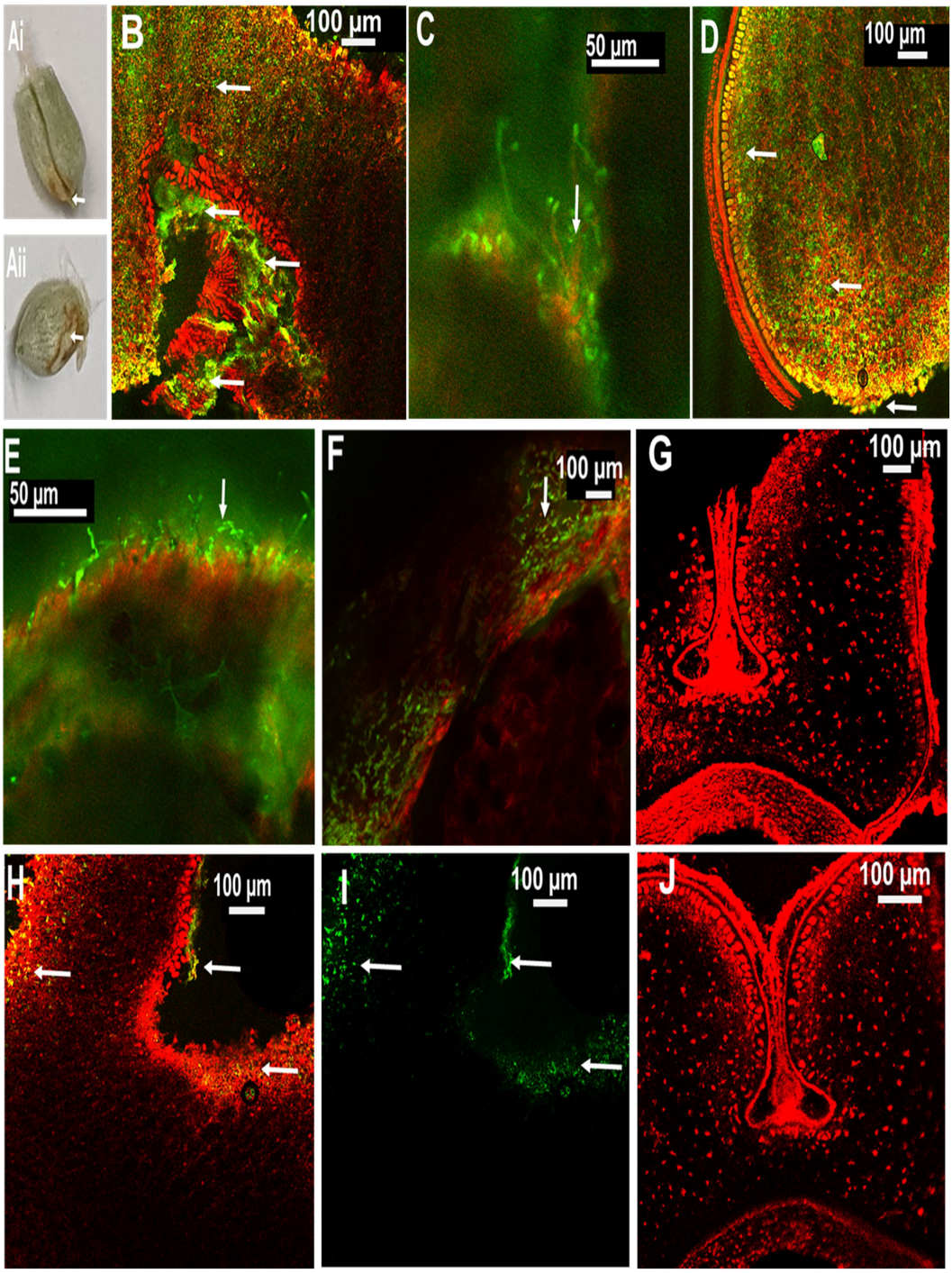

FIGURE 5
Localization of MoT on wheat seeds by confocal laser scanning microscopy (CLSM) using Alexa Flour 488 (AF), staining fungal material green and Propidium Iodide (PI) staining plant tissue red. **(A)** Seeds of wheat cv. Sumai 3 infected with MoT, where **(Ai)** inoculated at mid flowering stage, GS 65 and sampled at 10dpi and **(Aii)** inoculated at the end of flowering stage, GS 69 and sampled at 10dpi. **(B)** Overlay image of a cross-section of the germ region of an infected Sumai 3 seed (inoculated at GS 65 and sampled at 14dpi). **(C)** MoT hyphae in germ endosperm (enlarged view from **B**). **(D)** Cross-section of MoT infected caryopsis of Sumai 3 (infected at seed coat region) (inoculated at GS 69 and sampled at 10dpi); **(E)** MoT hyphae in the caryopsis coat tissue of Sumai 3 (inoculated at GS 69 and sampled at 10dpi). **(F)** MoT hyphae within seed pericarp and testa region (enlarged view from **B**). **(G)** Cross-section of Sumai 3 healthy caryopsis. **(H)** Overlay image of a cross-section of the germ region of infected Milan seed (inoculated at GS 65 and sampled at 14dpi). **(I)** MoT hyphae in infected Milan caryopsis germ region-single channel excitation (inoculated at GS 65 and sampled at 14dpi). **(J)** Cross-section of a healthy caryopsis of Milan. The scale bar of images **(B,C,E)** is 50µm, and the rest is 100µm. White arrows indicate presence of MoT hyphae.

correlation between MoT infection and grain quality (Goulart and Paiva, 2000; Islam et al., 2016; Singh et al., 2016; Surovy et al., 2020). Higher seed infection caused malformed seeds with lower protein content (Supplementary Figure S2). The grain protein content is essential for germination, and endosperm protein increases the seed water and oxygen uptake capacity. It also triggers faster germination and

10.3389/fmicb.2023.1040605

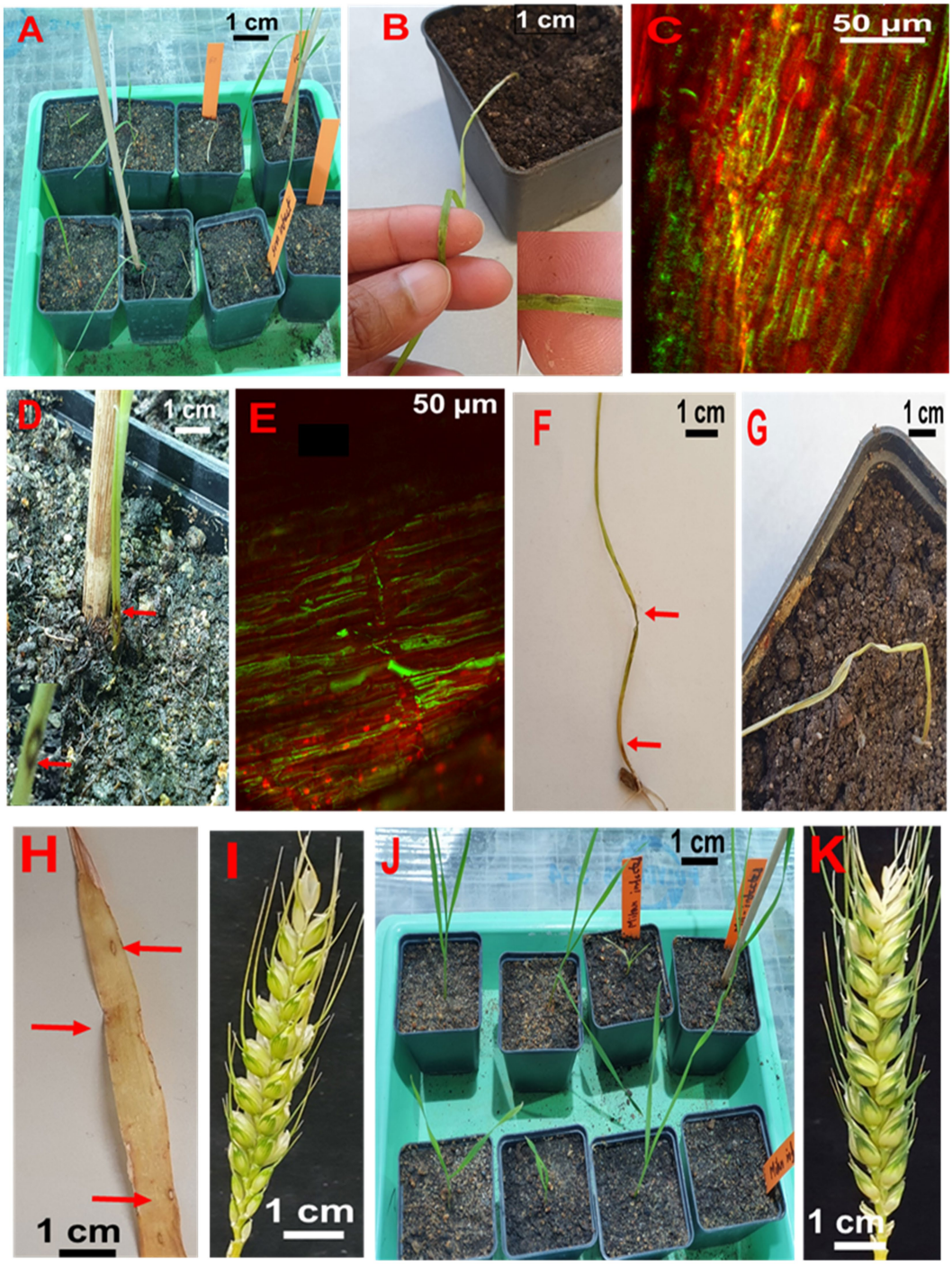

FIGURE 6
Testing seed-to-seed transmission of MoT. **(A)** Seedlings from infected Sumai 3 seeds in the climate chamber. **(B)** Characteristic eye-shaped blast symptoms on the first leaf of a Sumai 3 seedling (GS 11). **(C)** Fungal hyphae in infected Sumai 3 seedling leaf tissue visualized through CLSM. **(D)** Typical eye-shaped blast symptom on the stem of Sumai 3 (GS 11). **(E)** Longitudinal section of infected Sumai 3 stem displaying fungal growth in infected stem tissue by CLSM (GS 11). **(F)** Severely infected Sumai 3 seedling developed from MoT infected seed. **(G)** Sumai 3 seedling killed through MoT infection (GS 14). **(H)** Characteristic blast symptoms on older leaves of Sumai 3 (GS 21). **(I)** Asymptomatic ear from infected seeds of Sumai 3 (GS 65). **(J)** Seedlings from infected seeds of Milan (GS 11). **(K)** Asymptomatic ear from infected Milan seeds (GS 65).

larger seedlings with high dry matter contents (Lopez and Grabe, 1973; Bulisani and Warner, 1980). Infection by *F. graminearum* (Nightingale et al., 1999; Prange et al., 2005; Gärtner et al., 2007; Arata et al., 2022), stripe rust (Devadas et al., 2014; Rozo-Ortega et al., 2021), leaf rust, septoria blotch (Castro et al., 2018), and tan spot (Fleitas et al., 2018) in wheat may also reduce grain protein content like MoT. Contrary to our results, some studies also showed that MoT-infected seeds contained higher protein content than healthy seeds (Urashima et al., 2009; Martínez et al., 2019).

When MoT conidia are spray inoculated on wheat ears, conidia start to germinate and infect the earlets (Ha et al., 2016). After infection at early ear emergence stage, MoT was found in husks and rachis, progressing

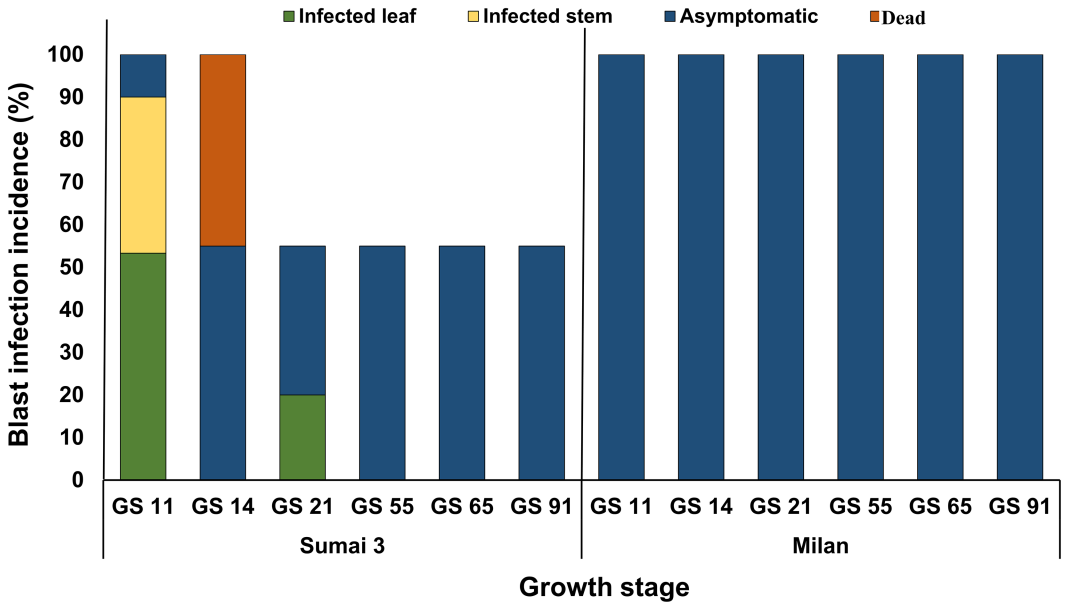

FIGURE 7
MoT infection incidence (%) in wheat plants grown from MoT infected seeds of Sumai 3 and Milan in the climate chamber. Sampling was performed at GS 11 (first leaf emerged), GS 14 (emergence of the 4th leaves), GS 21 (main stem with one tiller), GS 55 (half of the ear emerged above flag leaf ligule), GS 65 (mid flowering), and GS 91 (grain hard).

toward the rachilla, colonizing the caryopsis germ region, and spreading in the endosperm. MoT present in the seed coat further progressed toward endosperm *via* penetrating the aleuric layer. Progression of MoT inside the wheat caryopsis was slower in Milan than in Sumai 3. Through CLSM, Ha et al. (2016) showed that disease progression was faster through the ear rachilla than palea in a susceptible cultivar.

The seed germ region plays a crucial role in reproducing new wheat plants. Most blast-infected seeds were tiny, low in weight, deformed, or showed black discoloration of their germ region. In the MoT sporulation assay with seeds, we found that most MoT conidia germinated from the germ region. Commonly, germs are a natural sink for essential amino acids, vitamins, fatty acids, minerals, phytosterols, and tocopherols (Zia Sherrell, 2021). As a result, MoT may prefer to colonize the wheat germ in order to get access to and utilize these nutrients. Our study confirmed that the MoT-infected wheat germ region is a preferred tissue where MoT can survive and sporulate for further dissemination. Rice blast-infected seeds also preferentially colonized the germ region (Manandhar et al., 1998; Long et al., 2001). Additionally, seeds from MoT-infected ears of both Sumai 3 and Milan produced MoT conidia which can serve as primary inoculum to spread blast disease into new areas or within a field after sowing. This is in partial contrast to previous reports explaining that only seeds from infected ears of susceptible cultivars but not from resistant cultivars may be a source of inoculum (Bernaux and Berti, 1981; Guerber and TeBeest, 2006).

The seed CLSM analyses revealed that MoT colonized the Sumai 3 seed germ region significantly stronger than in Milan. The localization of MoT inside the seeds was more difficult to track compared to leaves or stems. Producing thin seed sections of mature seeds with the microtome was quite challenging and paraffin fixation (Höch et al., 2021) followed by repeated washing caused damage to seed sections. Therefore, instead of paraffin fixation and sectioning with a microtome, we used razor blades (Wilkinson sword, Germany) for manual sectioning of wheat seeds. The AF and PI double staining easily distinguished plant tissue and fungal hyphae, after optimization of the staining time of AF (2 h) for seed samples. This double staining method is an effective and reliable method to visualize the presence of MoT hyphae inside the seed. AF is a specific chitin-binding dye and directly binds with the fungal cell wall. On the other hand, PI is specific for staining the nucleic acids. The concentration of AF was higher than of PI, as higher concentration of AF inhibits the binding of PI to fungal cells. As a result, AF stained fungal cells green and PI stained plant cells red. The CLSM examinations allowed us to analyze the presence of MoT hyphae within seeds, even in thicker cross-sectioned samples. Double staining with AF and PI has been previously used to localize *Fusarium* spp. in wheat, barley, and rye seeds (Jansen et al., 2005; Jin et al., 2021).

When MoT infected seeds were sown in the greenhouse, characteristic blast symptoms were observed at GS 11in younger leaves and stems of Sumai 3. The presence of MoT in infected leaves and stems was confirmed by observing the presence of conidia in infected parts by microscopy and agar plating methods. Severely infected seedlings died in later stages. Interestingly, after GS 21, no visual symptoms were observed in Sumai 3 plants, while no symptoms at all were noted on seedlings or ears derived from blast-infected Milan seeds. The disease incidence on seedlings of Sumai 3 grown from infected seeds ranged up to 64%, causing necrosis and death of seedlings. In contrast, Martinez et al. (2021) did not detect blast symptoms 41 days after sowing infected wheat seeds. Cruz et al. (2015) stated that old basal leaves are the initial inoculum source of wheat blast, and sampling at anthesis from the lower three senescent leaves resulted in recovery of MoT conidia. In their study, only four different susceptible cultivars were used and high numbers of MoT conidia were recovered from the lower basal leaves of all cultivars. However, in our study, we also used a resistant cultivar in order to explore the variability in symptom development and conidia production in cultivars differing in resistance. Our studies demonstrate, that on a resistant cultivar, sporulation may occur on infected seeds but is lacking on seedlings and adult plants grown from such seeds.

This is the first in-depth systematic report on the potential role of MoT seed infection in the short and long-distance dissemination of MoT. Transmission of seed-borne pathogens may depend on plant age (Giorcelli et al., 1996), cultivar (Roderick and Clifford, 1995), plant nutritional status (Chowdhury et al., 2022), and plant growing conditions (Nopsa and Pfender, 2014).

The plumule and radicle emerge by rupturing the germ coat. During emergence and cell differentiation, MoT conidia transmitted to plumule and radicle at the early cell differentiation stages may result in transfer of MoT from seed to seedling (Baker and Smith, 1966). There are two possibilities to transmit MoT from seed to wheat plants, first, by vertical transmission of MoT from seed to seed in a systemic manner, second, by horizontal transmission by MoT conidia by rain or wind. In our case, we only found conidia in early stages but not in ears. So, a vertical transmission of MoT can be excluded. In our system conidia either formed on infected seeds or on leaves and stems of young plants. They may be the primary inoculum spreading the disease within a field and finally causing ear infection. During cultural management in the field, by rain or wind, MoT conidia from seeds, infected seedlings, or leaves may spread to new seedlings or healthy ears of neighboring plants. This may ultimately incite an epidemic resulting in ear infection without systemic transfer of the pathogen.

Plating is an easy and handy method, however, with a high chance of low detection rate and false negative results (Hariharan and Prasannath, 2021). On the other hand, slight damage to living cells or tissues may hamper the detection by CLSM (DeVree et al., 2021). An optimized qPCR with species-specific primers thus appears a more reliable and sensitive technique to detect and trace minimal amounts of fungal biomass *in situ* (Zheng et al., 2019). If MoT was transmitted vertically from seed to ear in an asymptomatic manner, even low levels of fungal biomass in wheat stems and ears should be traceable by qPCR. However, by qPCR analysis no MoT DNA was detected in Milan (from seedling to ear) and Sumai 3 (after GS 21). This is the first comprehensive study combining qPCR, microscopy, and plating methods to precisely trace MoT colonization in wheat in order to unveil a potential transmission of MoT from seed to seed.

The lower infection and sporulation rates of MoT in Milan indicate that breeding for MoT-resistant cultivars is an excellent strategy to reduce the risk of MoT epidemics. In addition, the current study provides evidence that safeguarding healthy seeds to stop seed transmission appears an equally important strategy. The effectiveness of seed treatment with chemicals or biologicals therefore needs to be improved to avoid horizontal dissemination from infected seeds. The results from the present study are particularly important for wheat-producing regions where MoT has not been recorded thus far.

Data availability statement

The raw data supporting the conclusions of this article will be made available by the authors, without undue reservation.

Author contributions

MS and AT conceptualization and funding. MS: investigation, data analysis, visualization, and writing-original draft preparation. AT: project administration, writing, reviewing, and editing. TI: contributed to the basic design and provided a wheat blast isolate for the study. All authors read and approved the final version of the manuscript.

Funding

The German academic exchange service (DAAD) funded MS for pursuing her Ph.D. degree at the Division of Plant Pathology and Crop Protection, Georg-August-Universität Göttingen, Germany. Lab consumables and Open Access publication fees were provided by the Division of Plant Pathology and Crop Protection, and the University Library (SUB) of the Georg-August-Universität Göttingen, Germany.

Acknowledgments

We are thankful to Maik Knobel, Evelin Vorbeck, and Dagmer Tacke for their outstanding technical support and Shahinoor Rahman for his assistance in sample preparation and data analysis. We also thank Anke Sirrenberg for linguistic editing of this manuscript.

Conflict of interest

The authors declare that the research was conducted in the absence of any commercial or financial relationships that could be construed as a potential conflict of interest.

Publisher's note

Supplementary material

The Supplementary material for this article van be found online at: https://www.frontiersin.org/articles/10.3389/fmicb.2023.1040605/full#supplementary-material

References

Alisaac, E., Rathgeb, A., Karlovsky, P., and Mahlein, A.-K. (2020). Fusarium head blight: effect of infection timing on spread of *Fusarium graminearum* and spatial distribution of deoxynivalenol within wheat spikes. *Microorganisms* 9:79. doi: 10.3390/microorganisms9010079

Arata, G. J., Martínez, M., Elguezábal, C., Rojas, D., Cristos, D., Dinolfo, M. I., et al. (2022). Effects of sowing date, nitrogen fertilization, and *Fusarium graminearum* in an Argentinean bread wheat: integrated analysis of disease parameters, mycotoxin contamination, grain quality, and seed deterioration. *J. Food Compost. Anal.* 107:104364. doi: 10.1016/j.jfca.2021.104364

Baker, K. F., and Smith, S. H. (1966). Dynamics of seed transmission of plant pathogens. *Annu. Rev. Phytopathol.* 4, 311–332. doi: 10.1146/annurev.py.04.090166.001523

Bernaux, P., and Berti, G. (1981). Évolution de la sensibilité des glumelles du riz à *Pyricularia oryzae* Cav. et à *Drechslera oryzae* (Br. de Haan) Sub. et Jain: conséquences pour la transmission des maladies. *Agronomie* 1, 261–264. doi: 10.1051/agro:19810402

Bulisani, E. A., and Warner, R. L. (1980). Seed protein and nitrogen effects upon seedling vigor in wheat. *Agron. J.* 72, 657–662. doi: 10.2134/agronj1980.00021962007200040021x

Castro, A. C., Fleitas, M. C., Schierenbeck, M., Gerard, G. S., and Simón, M. R. (2018). Evaluation of different fungicides and nitrogen rates on grain yield and bread-making quality in wheat affected by Septoria tritici blotch and yellow spot. *J. Cereal Sci.* 83, 49–57. doi: 10.1016/j.jcs.2018.07.014

Ceresini, P. C., Castroagudín, V. L., Rodrigues, F. Á., Rios, J. A., Aucique-Pérez, C. E., Moreira, S. I., et al. (2019). Wheat blast: from its origins in South America to its emergence as a global threat: wheat blast. *Mol. Plant Pathol.* 20, 155–172. doi: 10.1111/mpp.12747

Ceresini, P. C., Castroagudín, V. L., Rodrigues, F. Á., Rios, J. A., Eduardo Aucique-Pérez, C., Moreira, S. I., et al. (2018). Wheat blast: past, present, and future. *Annu. Rev. Phytopathol.* 56, 427–456. doi: 10.1146/annurev-phyto-080417-050036

Chowdhury, M. S. R., Rahman, M. A., Nahar, K., Dastogeer, K. M. G., Hamim, I., and Mohiuddin, K. M. (2022). Mineral nutrient content of infected plants and allied soils provide insight into wheat blast epidemics. *Heliyon* 8:e08966. doi: 10.1016/j.heliyon.2022.e08966

Cruz, C. D., Kiyuna, J., Bockus, W. W., Todd, T. C., Stack, J. P., and Valent, B. (2015). *Magnaporthe oryzae* conidia on basal wheat leaves as a potential source of wheat blast inoculum. *Plant Pathol.* 64, 1491–1498. doi: 10.1111/ppa.12414

Cruz, C. D., and Valent, B. (2017). Wheat blast disease: danger on the move. *Trop. Plant Pathol.* 42, 210–222. doi: 10.1007/s40858-017-0159-z

Devadas, R., Simpfendorfer, S., Backhouse, D., and Lamb, D. W. (2014). Effect of stripe rust on the yield response of wheat to nitrogen. *Crop J.* 2, 201–206. doi: 10.1016/j.cj.2014.05.002

DeVree, B. T., Steiner, L. M., Glazowska, S., Ruhnow, F., Herburger, K., Persson, S., et al. (2021). Current and future advances in fluorescence-based visualization of plant cell wall components and cell wall biosynthetic mechineries. *Biotechnol. Biofuels* 14:78. doi: 10.1186/s13068-021-01922-0

Elmer, W. H. (2001). Seeds as vehicles for pathogen importation. *Biol. Invasions* 3, 263–271. doi: 10.1023/A:1015217308477

Faivre-Rampant, O., Geniès, L., Piffanelli, P., and Tharreau, D. (2013). Transmission of rice blast from seeds to adult plants in a non-systemic way. *Plant Pathol.* 62, 879–887. doi: 10.1111/ppa.12003

Fleitas, M. C., Schierenbeck, M., Gerard, G. S., Dietz, J. I., Golik, S. I., and Simón, M. R. (2018). Breadmaking quality and yield response to the green leaf area dration caused by fluxapyroxad under three nitrogen rates in wheat affected with tan spot. *Crop Prot.* 106, 201–209. doi: 10.1016/j.cropprto.2018.01.004

Food and Agriculture Organization of the United Nations (2015). *FAO Statistical Pocketbook 2015: World Food and Agriculture*. Rome: Food and Agriculture Organization of the United Nations.

Gärtner, B. H., Munich, M., Kleijer, G., and Mascher, F. (2007). Characterisation of kernel resistance against Fusarium infection in spring wheat by baking quality and mycotoxin assessments. *Eur. J. Plant Pathol.* 120, 61–68. doi: 10.1007/s10658-007-9198-5

Giorcelli, A., Vietto, L., Anselmi, N., and Gennaro, M. (1996). Influence of clonal susceptibility, leaf age and inoculum density on infections by *Melampsora larici-Populina* races E1 and E3. *Eur. J. Plant Pathol.* 26, 323–331. doi: 10.1111/j.1439-0329.1996.tb01078.x

Goulart, A. C. P., and Paiva, F. A. (2000). Wheat yield losses due to *Pyricularia grisea*, in 1991 and 1992, in the state of Mato Grosso do Sul. *Summa Phytopathol.* 26, 279–282.

Goulart, A. C. P., Paiva, F. A., and De Mesquita, A. N. (1990). *Pyricularia oryzae* in wheat seeds: incidence, transmission and survival. *Annu. Wheat Newsl.* 36, 49–50.

Guerber, C., and TeBeest, D. O. (2006). Infection of rice seed grown in Arkansas by *Pyricularia grisea* and transmission to seedlings in the field. *Plant Dis.* 90, 170–176. doi: 10.1094/PD-90-0170

Gupta, D. R., Khanom, S., Rohman, M. M., Hasanuzzaman, M., Surovy, M. Z., Mahmud, N. U., et al. (2021). Hydrogen peroxide detoxifying enzymes show different activity patterns in host and non-host plant interactions with *Magnaporthe oryzae Triticum* pathotype. *Physiol. Mol. Biol. Plants* 27, 2127–2139. doi: 10.1007/s12298-021-01057-4

Gupta, D. R., Surovy, M. Z., Mahmud, N. U., Chakraborty, M., Paul, S. K., Hossain, M. S., et al. (2020). Suitable methods for isolation, culture, storage and identification of wheat blast fungus *Magnaporthe oryzae Triticum* Pathotype. *Phytopathol. Res.* 2:30. doi: 10.1186/s42483-020-00070-x

Ha, X., Koopmann, B., and von Tiedemann, A. (2016). Wheat blast and fusarium head blight display contrasting interaction patterns on ears of wheat genotypes differing in resistance. *Phytopathology* 106, 270–281. doi: 10.1094/PHYTO-09-15-0202-R

Hariharan, G., and Prasannath, K. (2021). Recent advances in molecular diagnostics of fungal plant pathogens: a mini review. *Front. Cell. Infect. Microbiol.* 10:600234. doi: 10.3389/fcimb.2020.600234

Höch, K., Koopmann, B., and von Tiedemann, A. (2021). Lignin composition and timing of cell wall lignification are involved in *Brassica napus* resistance to stem rot caused by *Sclerotinia sclerotiorum*. *Phytopathology* 111, 1438–1448. doi: 10.1094/PHYTO-09-20-0425-R

Igarashi, S., Utiamada, C. M., Igarashi, L. C., Kazuma, A. H., and Lopes, R. S. (1985). Pyricularia em trigo. 1. ocorrência de *Pyricularia* sp. no estado do Paraná. *Fitopatol. Bras.* 11, 351–352.

Islam, M. T., Croll, D., Gladieux, P., Soanes, D. M., Persoons, A., Bhattacharjee, P., et al. (2016). Emergence of wheat blast in Bangladesh was caused by a south American lineage of *Magnaporthe oryzae*. *BMC Biol.* 14:84. doi: 10.1186/s12915-016-0309-7

Islam, M. T., Gupta, D. R., Hossain, A., Roy, K. K., He, X., Kabir, M. R., et al. (2020). Wheat blast: a new threat to food security. *Phytopathol. Res.* 2:28. doi: 10.1186/s42483-020-00067-6

Islam, M. T., Kim, K.-H., and Choi, J. (2019). Wheat blast in Bangladesh: the current situation and future impacts. *Plant Pathol. J.* 35, 1–10. doi: 10.5423/PPJ.RW.08.2018.0168

Jansen, C., von Wettstein, D., Schafer, W., Kogel, K.-H., Felk, A., and Maier, F. J. (2005). Infection patterns in barley and wheat spikes inoculated with wild-type and trichodiene synthase gene disrupted *Fusarium graminearum*. *Proc. Natl. Acad. Sci.* 102, 16892–16897. doi: 10.1073/pnas.0508467102

Jin, Z., Solanki, S., Ameen, G., Gross, T., Poudel, R. S., Borowicz, P., et al. (2021). Expansion of internal hyphal growth in fusarium head blight–infected grains contributes to the elevated mycotoxin production during the malting process. *Mol. Plant Microbe Interact.* 34, 793–802. doi: 10.1094/MPMI-01-21-0024-R

Long, D. H., Correll, J. C., Lee, F. N., and TeBeest, D. O. (2001). Rice blast epidemics initiated by infested rice grain on the soil surface. *Plant Dis.* 85, 612–616. doi: 10.1094/PDIS.2001.85.6.612

Lopez, A., and Grabe, D. F. (1973). Effect of protein content on seed performance in wheat (*Triticum aestivum* L.). in Proceedings of the Association of Official Seed Analysts (Association of Official Seed Analysts and the Society of Commercial Seed Technologists (SCST), 106–116.

Maciel, J. L. N. (2018). "Diseases affecting wheat: wheat blast" in *Burleigh Dodds Series in Agricultural Science*. ed. R. Oliver (London: Burleigh Dodds Science Publishing), 155–169. doi: 10.19103/AS.2018.0039.08

Maciel, J. L. N., Ceresini, P. C., Castroagudin, V. L., Zala, M., Kema, G. H. J., and McDonald, B. A. (2014). Population structure and pathotype diversity of the wheat blast pathogen *Magnaporthe oryzae* 25 years after its emergence in Brazil. *Phytopathology* 104, 95–107. doi: 10.1094/PHYTO-11-12-0294-R

Manandhar, H. K., Jorgensen, H. J. L., Smedegaard-Petersen, V., and Mathur, S. B. (1998). Seedborne infection of rice by *Pyricularia oryzae* and its transmission to seedlings. *Plant Dis.* 82, 1093–1099. doi: 10.1094/PDIS.1998.82.10.1093

Martínez, S. I., Sanabria, A., Fleitas, M. C., Consolo, V. F., and Perelló, A. (2019). Wheat blast: aggressiveness of isolates of *Pyricularia oryzae* and effect on grain quality. *J. King Saud Univ. Sci.* 31, 150–157. doi: 10.1016/j.jksus.2018.05.003

Martinez, S. I., Wegner, A., Bohnert, S., Schaffrath, U., and Perelló, A. (2021). Tracing seed to seedling transmission of the wheat blast pathogen *Magnaporthe oryzae* pathotype *Triticum*. *Plant Pathol.* 70, 1562–1571. doi: 10.1111/ppa.13400

McGee, D. C. (1979). Epidemiological aspects of seed disease control. *J. Seed Tech.* 4, 96–98.

Monsur, M., Ahmed, M., Haque, A., Jahan, Q., Ansari, T., Latif, M., et al. (2016). Cross infection between rice and wheat blast pathogen *Pyricularia oryzae*. *Bangladesh Rice J.* 20, 21–29. doi: 10.3329/brj.v20i2.34125

Mottaleb, K. A., Singh, P. K., Sonder, K., Kruseman, G., Tiwari, T. P., Barma, N. C. D., et al. (2018). Threat of wheat blast to South Asia's food security: an ex-ante analysis. *PLoS One* 13:e0197555. doi: 10.1371/journal.pone.0197555

Nallathambi, P., Umamaheswari, C., Sandeep, K. L., Manjunatha, C., and Berliner, J. (2021). "Mechanism of seed transmission and seed infection in major agricultural crops in India" in *Seed-Borne Diseases of Agricultural Crops: Detection, Diagnosis and Management*. eds. R. Kumar and A. Gupta (Singapore: Springer Nature Singapore Pte Ltd. 2020), 749–791.

Nightingale, M. J., Marchylo, B. A., Clear, R. M., Dexter, J. E., and Preston, K. R. (1999). Fusarium head blight: effect of fungal proteases on wheat storage proteins. *Cereal Chem.* 76, 150–158. doi: 10.1094/CCHEM.1999.76.1.150

Nopsa, J. F. H., and Pfender, W. F. (2014). A latent period duration model for wheat stem rust. *Plant Dis.* 98, 1358–1363. doi: 10.1094/PDIS-11-13-1128-RE

Paul, S. K., Mahmud, N. U., Gupta, D. R., Rani, K., Kang, H., Wang, G. L., et al. (2022). *Oryzae* pathotype of *Magnaporthe oryzae* can cause typical blast disease symptoms on both leaves and spikes of wheat under a growth room condition. *Phytopathol. Res.* 4:9. doi: 10.1186/s42483-022-00114-4

Pizolotto, C. A., Maciel, J. L. N., Fernandes, J. M. C., and Boller, W. (2019). Saprotrophic survival of *Magnaporthe oryzae* in infested wheat residues. *Eur. J. Plant Pathol.* 153, 327–339. doi: 10.1007/s10658-018-1578-5

Prange, A., Birzele, B., Krämer, J., Meier, A., Modrow, H., and Köhler, P. (2005). Fusarium-inoculated wheat: deoxynivalenol contents and baking quality in relation to infection time. *Food Control* 16, 739–745. doi: 10.1016/j.foodcont.2004.06.013

Raveloson, H., Ratsimiala Ramonta, I., Tharreau, D., and Sester, M. (2018). Long-term survival of blast pathogen in infected rice residues as major source of primary inoculum in high altitude upland ecology. *Plant Pathol.* 67, 610–618. doi: 10.1111/ppa.12790

Reis, E. M. (1995). Sobrevivência de *Pyricularia oryzae*, associada as sementes de trigo. *Summa Phytopathol.* 21:43.

Roderick, H. W., and Clifford, B. C. (1995). Variation in adult plant resistance to powdery mildew in spring oats under field and laboratory conditions. *Plant Pathol.* 44, 366–373. doi: 10.1111/j.1365-3059.1995.tb02789.x

Rozo-Ortega, G. P., Serrago, R. A., Lo Valvo, P. J., Fleitas, M. C., Simón, M. R., and Miralles, D. J. (2021). Grain yield, milling and breadmaking quality responses to foliar diseases in old and modern Argentinean wheat cultivars. *J. Cereal Sci.* 99:103211. doi: 10.1016/j.jcs.2021.103211

Shahzad, R., Khan, A. L., Bilal, S., Asaf, S., and Lee, I.-J. (2018). What is there in seeds? Vertically transmitted endophytic resources for sustainable inprovement in plant growth. *Front. Plant Sci.* 9:24. doi: 10.3389/fpls.2018.00024

Shiferaw, B., Smale, M., Braun, H.-J., Duveiller, E., Reynolds, M., and Muricho, G. (2013). Crops that feed the world 10. Past successes and future challenges to the role played by wheat in global food security. *Food Sec.* 5, 291–317. doi: 10.1007/s12571-013-0263-y

Shizhen, W., Jiaoyu, W., Zhen, Z., Zhongna, H., Xueming, Z., Rongyao, C., et al. (2021). The risk of wheat blast in rice–wheat co-planting regions in China: MoO strains of *Pyricularia oryzae* cause typical symptom and host reaction on both wheat leaves and spikes. *Phytopathology* 111, 1393–1400. doi: 10.1094/PHYTO-10-20-0470-R

Singh, P. K., Gahtyari, N. C., Roy, C., Roy, K. K., He, X., Tembo, B., et al. (2021). Wheat blast: a disease spreading by intercontinental jumps and its management strategies. *Front. Plant Sci.* 12:710707. doi: 10.3389/fpls.2021.710707

Singh, R. P., Singh, P. K., Rutkoski, J., Hodson, D. P., He, X., Jørgensen, L. N., et al. (2016). Disease impact on wheat yield potential and prospects of genetic control. *Annu. Rev. Phytopathol.* 54, 303–322. doi: 10.1146/annurev-phyto-080615-095835

Stokstad, E. (2007). Deadly wheat fungus threatens world's breadbaskets. *Science* 315, 1786–1787. doi: 10.1126/science.315.5820.1786

Surovy, M. Z., Dutta, S., Mahmud, N. U., Gupta, D. R., Farhana, T., Paul, S. K., et al. (2022). Probiotic *Bacillus* species: promising biological control agents for managing worrisome wheat blast disease. *Preprints*. doi: 10.20994/preprints202211.0382.v1

Surovy, M. Z., Mahmud, N. U., Bhattacharjee, P., Hossain, M. S., Mehebub, M. S., Rahman, M., et al. (2020). Modulation of nutritional and biochemical properties of wheat grains infected by blast fungus *Magnaporthe oryzae Triticum* Pathotype. *Front. Microbiol.* 11:1174. doi: 10.3389/fmicb.2020.01174

Téllez, L. C., Chavez, A., Estigarribia, P. P., Reyes, M., Cazal, C., Heesacker, A., et al. (2022). Caninde2/Milan: promising wheat line to discover novel genes for resistant to wheat blast. *Crop Breed. Appl. Biotechnol.* 22:e40032221. doi: 10.1590/1984-70332022v22n2a11

Tembo, B., Mulenga, R. M., Sichilima, S., M'siska, K. K., Mwale, M., Chikoti, P. C., et al. (2020). Detection and characterization of fungus (*Magnaporthe oryzae* pathotype *Triticum*) causing wheat blast disease on rain-fed grown wheat (*Triticum aestivum* L.) in Zambia. *PLoS One* 15:e0238724. doi: 10.1371/journal.pone.0238724

Tesfaye, K. (2021). Climate change in the hottest wheat regions. *Nat. Food* 2, 8–9. doi: 10.1038/s43016-020-00218-0

Tingting, W. (2014). Epidemiology, phytopathological and molecular differentiation and leaf infection process of diverse strains of *Magnaporthe* spp. on wheat and rice. Ph. D. dissertation. Göttingen: Georg-August-Universität Göttingen.

Urashima, A. S., Grosso, C. R. F., Stabili, A., Freitas, E. G., Silva, C. P., Netto, D. C. S., et al. (2009). "Effect of *Magnaporthe grisea* on seed germination, yield and quality of wheat" in *Advances in Genetics, Genomics and Control of Rice Blast Disease*. eds. G. L. Wang and B. Valent (Dordrecht: Springer), 267–277. doi: 10.1007/978-1-4020-9500-9_27

Urashima, A. S., Lavorent, N. A., Goulart, A. C. P., and Mehta, Y. R. (2004). Resistance spectra of wheat cultivars and virulence diversity of *Magnaporthe grisea* isolates in Brazil. *Fitopatol. Bras.* 29, 511–518. doi: 10.1590/S0100-41582004000500007

Urashima, A. S., Leite, S. F., and Galbieri, R. (2007). Eficiência da disseminação aérea em *Pyricularia grisea*. *Summa Phytopathol.* 33, 275–279. doi: 10.1590/S0100-54052007000300011

Winston, J. (2015). Aggressive Plant Fungus Threatens Wheat Production. Available a: https://www.biomedcentral.com/about/press-centre/science-press-releases/27-02-2015 ().

Zadoks, J. C., Chang, T. T., and Konzak, C. F. (1974). A decimal code for the growth stages of cereals. *Weed Res.* 14, 415–421. doi: 10.1111/j.1365-3180.1974.tb01084.x

Zheng, X., Lopisso, D. T., Eseola, A. B., Koopmann, B., and Tiedemann, A. (2019). Potential for seed transmission of *Verticillium longisporum* in oilseed rape (*Brassica napus*). *Plant Dis.* 103, 1843–1849. doi: 10.1094/PDIS-11-18-2024-RE

Zia Sherrell, M. (2021). Look out, wheaties — wheat germ might be the new breakfast of health champs. *Nutrition*

frontiers | Frontiers in Plant Science

TYPE Review
PUBLISHED 29 March 2023
DOI 10.3389/fpls.2023.1023824

OPEN ACCESS

EDITED BY
Andreas Börner,
Leibniz Institute of Plant Genetics and Crop Plant Research (IPK), Germany

REVIEWED BY
Rita Armoniene,
Lithuanian Research Centre for Agriculture and Forestry, Lithuania
Morten Lillemo,
Norwegian University of Life Sciences, Norway

*CORRESPONDENCE
Pushpendra Kumar Gupta
pkgupta36@gmail.com

SPECIALTY SECTION
This article was submitted to Plant Pathogen Interactions, a section of the journal Frontiers in Plant Science

RECEIVED 20 August 2022
ACCEPTED 28 February 2023
PUBLISHED 29 March 2023

CITATION
Gupta PK, Vasistha NK, Singh S and Joshi AK (2023) Genetics and breeding for resistance against four leaf spot diseases in wheat (*Triticum aestivum* L.). *Front. Plant Sci.* 14:1023824. doi: 10.3389/fpls.2023.1023824

Genetics and breeding for resistance against four leaf spot diseases in wheat (*Triticum aestivum* L.)

Pushpendra Kumar Gupta[1,2,3]*, Neeraj Kumar Vasistha[1,4], Sahadev Singh[1] and Arun Kumar Joshi[3,5]

[1]Department of Genetics and Plant Breeding, Chaudhary Charan Singh University, Meerut, India, [2]Murdoch's Centre for Crop and Food Innovation, Murdoch University, Murdoch, WA, Australia, [3]Borlaug Institute for South Asia (BISA), National Agricultural Science Complex (NASC), Dev Prakash Shastri (DPS) Marg, New Delhi, India, [4]Department of Genetics-Plant Breeding and Biotechnology, Dr Khem Singh Gill, Akal College of Agriculture, Eternal University, Baru Sahib, Sirmour, India, [5]The International Maize and Wheat Improvement Center (CIMMYT), National Agricultural Science Complex (NASC), Dev Prakash Shastri (DPS) Marg, New Delhi, India

In wheat, major yield losses are caused by a variety of diseases including rusts, spike diseases, leaf spot and root diseases. The genetics of resistance against all these diseases have been studied in great detail and utilized for breeding resistant cultivars. The resistance against leaf spot diseases caused by each individual necrotroph/hemi-biotroph involves a complex system involving resistance (R) genes, sensitivity (S) genes, small secreted protein (SSP) genes and quantitative resistance loci (QRLs). This review deals with resistance for the following four-leaf spot diseases: (i) Septoria nodorum blotch (SNB) caused by *Parastagonospora nodorum*; (ii) Tan spot (TS) caused by *Pyrenophora tritici-repentis*; (iii) Spot blotch (SB) caused by *Bipolaris sorokiniana* and (iv) Septoria tritici blotch (STB) caused by *Zymoseptoria tritici*.

KEYWORDS

wheat, pathogens, sensitivity genes, resistance genes, necrotrophic effectors, PR proteins

Introduction

Wheat (*Triticum aestivum* L.) is the third most important staple food crop worldwide (the other two being maize and rice). According to FAO, during 2021-22, the total global wheat grain production was 778.6 million tonnes as against ~697 million tonnes in the year 2011-12, and 756.5 million tonnes in 2016-17 giving an annual increase of a mere 1.24% over the last 10 years and 0.83% over the last five years showing a decline in annual growth rate as against the desired rate of ~1.5% - 2% to meet the demand of growing world population. A variety of biotic and abiotic stresses are responsible for this bottleneck. The biotic stresses mainly include pathogens like fungi, viruses, bacteria, and nematodes, which cause a variety of diseases. Among these pathogens, fungal pathogens cause diseases like

rusts, mildew, blast, bunts, and blights, which are responsible for 15-20% yield loss (Figueroa et al., 2018). Among major classes of wheat diseases, the following are the four important leaf spot diseases, which are also described as blotch diseases (Figure 1): (i) Septoria nodorum blotch (SNB) caused by *Parastagonospora nodorum*, (ii) Tan spot (TS) caused by *Pyrenophora tritici-repentis*, (iii) Spot blotch (SB) caused by *Bipolaris sorokiniana* and (iv) Septoria tritici blotch (STB) caused by *Zymoseptoria tritici*. Among these four pathogens, *P. nodorum* and *P. tritici-repentis* are necrotrops, while *B. sorokiniana* and *Z. tritici* are hemi-biotrophs, since these are believed to need living tissue initially and later kill the host tissues and then feed and survive on the dead tissues of the host. The hemi-biotrophic nature of *Z. tritici* has, however, been recently questioned (Sanchez-Vallet et al., 2015; Friesen and Faris, 2021).

It has been shown that for most diseases in all crops including wheat, a gene-for-gene (GFG) model holds good between individual R genes of the host and the matching Avr genes in the pathogen (Flor, 1942; Flor, 1956). As a result, in the absence of a matching avirulance (Avr) gene in the prevalent race of the pathogen, the R gene can not provide resistance (Figure 2A). In contrast, the inverse gene-for-gene (IGFG) model (Fenton et al., 2009) assumes that a compatible interaction requires the presence of a matching susceptibility/S gene in the host and the corresponding necrotrphhic effector (NE) gene in the pathogen, so that in the absence of matching S gene in the host, an infection can not occur (Figure 2B; Friesen et al., 2007). Current knowledge suggests that in the same crop, both GFG and IGFG systems may operate synergistically, although this has not been widely discussed. Another class of genes include small secreted protein (SSP) genes, which have recently been shown to provide resistance against *Z. tritici* (Zhou et al., 2020); these SSP genes in wheat for other diseases have yet to be discovered. Quantitative disease resistance (QDR) may also occur together with S genes, R genes and SSP genes, although in some cases, one or more quantitative resistance loci (QRLs) have also been shown to represent S/R genes (for QRLs, see later). This makes the genetic systems for resistance against individual necrotrophs and hemi-biotrophs rather complex, but an interesting subject for research.

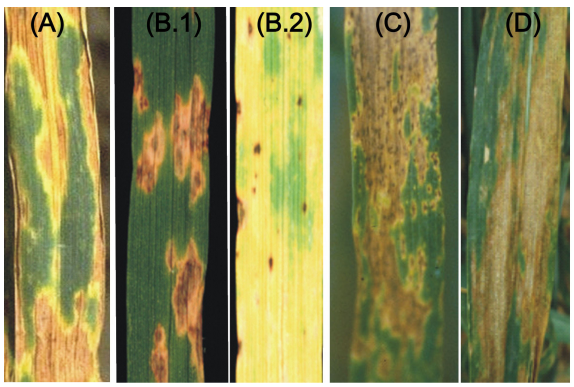

FIGURE 1
The visual symptoms of four necrotrophic and hemibiotrophic diseases. **(A)** SNB; **(B)** TS (**B.1** and **B.2** showing necrosis and chlorosis); **(C)** SB and **(D)** STB.

A number of studies have also been conducted on QDR against each of the above four diseases. These studies mainly include identification of either the QRLs using linkage-based interval mapping, often involving biparental mapping populations [sometimes also involving multi-parent advanced generation inter-cross (MAGIC) populations] or the marker-trait associations (MTAs) using LD-based genome-wide association studies (GWAS) using association panels. In some cases, a QRL identified through interval mapping may also overlap a resistance R gene, as shown in the case of one or more of the four R genes (*Sb1-Sb4*) for resistance against *B. sorokiniana* (Kumar et al., 2015; Gupta et al., 2018a). The relative roles of QRLs/R genes and the sensitivity S genes have also been assessed, and it was shown that QRLs/R and not the S genes are the major source of resistance, although in certain parts of the world, resistance has also been found to be associated with absence of S genes like *Tsn1* (Cowger et al., 2020).

The occurrence of multiple disease resistance (MDR) involving resistance against more than one disease has also been reported (Zwart et al., 2010; Mago et al., 2011; Singh et al., 2012; Jighly et al., 2016; Pal et al., 2022). As an example, MDR for SNB and TS has been reported in some winter wheat cultivars, suggesting that MDR may be associated with winter habit and that diverse sources of resistance for multiple diseases can be made to hybridize to achieve MDR (Ali et al., 2008; Gurung et al., 2009; Gurung et al., 2014). Association among resistance to two or three diseases, namely SNB, SB, and STB has also been observed (Gurung et al., 2014). Such an association involving MDR could also be the result of unconscious selection for resistance to multiple diseases during wheat breeding programmes. GWAS-based MTAs, each associated with more than one disease, have also been identified, suggesting occurrence of either the pleiotropic genes or closely linked loci providing resistance to more than one disease (Gurung et al., 2014).

Meta-QTLs involving diseases caused by more than one necrotroph have also been recently identified (Saini et al., 2022). However, while the available literature on interactions between S genes and necrotrophic effectors (NEs), and also on cloning and characterization of the sensitivity genes in the host and the NE genes in the pathogen has been the subject of several reviews, the literature on the complex genetic system for disease resistance involving S genes, R genes, SSP genes and QRLs associated with more than one disease caused by necrotrophs has not been adequately reviewed (Cowger et al., 2020). However, it has been shown that durable resistance against the pathogen is generally achieved through a quantitative genetic system and that interactions between the products of the recessive alleles of S genes and the NEs play a minor role in providing resistance (Cowger et al., 2020). The S genes, S QTLs, R genes, and resistance QTLs identified through QTL interval mapping and GWAS are sown in Supplementary Figures S1, S2.

The present review is intended to provide an overview of the complex genetic system of resistance in wheat against each of the four different pathogens, mentioned above. While doing so, we recognize that the work involving GFG in biotrophs is widely known and regularly reviewed (Van Der Biezen and Jones, 1998;

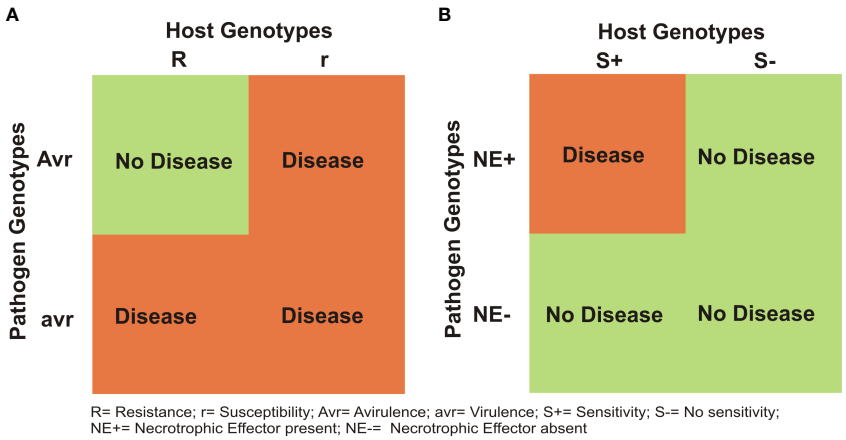

FIGURE 2
Two different models for host- pathogen interactions in plants: **(A)** gene-for gene (GFG) model, proposed by Flor (1956) and **(B)** an inverse gene-for gene (IGFG) model that was discovered recently in a number of necrotrophic diseases in wheat.

Kaur et al., 2021). Therefore, in this review, emphasis will be on the NEs and S genes involved in IGFG. In each case, the disease is caused by an interaction between NEs encoded by host-specific toxin (HST) genes of the pathogens and the proteins encoded by the corresponding S genes in the host, but resistance is largely quantitative in nature. The recent information on the genomics of all four pathogens will also be included in this review since whole genome sequences are now available for all four pathogens; this became possible only due to the availability of high through-put next-generation sequencing (NGS) technology (Syme et al., 2013; Moolhuijzen et al., 2018; Plissonneau et al., 2018; Richards et al., 2018; Syme et al., 2018; Aggarwal et al., 2019; Aggarwal et al., 2022). The present review on genetics and breeding for resistance against four leaf spot diseases in wheat should prove useful for geneticists, breeders and pathologists for further research targeted towards development of high yielding cultivars, resistant to these four foliar leaf spot diseases.

Pathosystems and genetics of disease resistance

As mentioned above, among the four pathosystems selected for this review, two pathosystems involve necrotrophs, while the other two involve hemi-biotrophs. The major differences between biotrophs and necrotrophs are listed in Table 1. The details of the

TABLE 1 A comparison of characteristics of biotrophs and necrotrophs (based on the link http://www.davidmoore.org.uk/21st_Century_Guidebook_to_Fungi_PLATINUM/Ch14_10.htm).

Biotroph pathogens	Necrotroph pathogens
Appressoria or haustoria produced	Appressoria/haustoria normally not produced
Resistance is controlled by SA-dependent host-defense pathways	Resistance controlled by SA, JA and Et-dependent host-defense pathways
Gene-for-gene (GFG) relationship	Inverse gene-for-gene (IGFG) relationship
Difficult to culture	Easy to culture
Entry, direct or through natural openings	Entry via wounds or natural openings
Survive on living tissues or as dormant propagules	Survive on living/dead tissue or as competitive saprotrophs
Host cells not killed rapidly; hypersensitive reaction (HR) in resistant genotype	Host cells killed rapidly; no hypersensitive reaction in resistant genotype
Few lytic enzymes/toxins are produced	Cell-wall-degrading (lytic) enzymes/toxins are produced
Often systemic	Seldom systemic
Attack vigorous plants; any stage	Attack weak, young/damaged plants
Narrow host range	Wide host range
Intercellular/Intracellular growth of pathogen	Intercellular/Intracellular growth of pathogen
Effectors: Avr proteins recognized by matching resistance (R) proteins	Effectors: host-specific or host-selective toxins (HST)
Disease caused by suppressing PTI/ETI	Disease caused either by suppressing PTI/ETI or by activation of sensitivity genes

four important pathogens (necrotrophs/hemi-biotrophs) and the wheat diseases caused by them are listed in Table 2. For each of the four diseases, S genes, R genes and QRLs identified either through interval mapping or through GWAS are summarised in Supplemantery Table S1, which also includes information on SSP genes for resistance against STB. More details for each of the four pathosystems under review along with genetics of disease susceptibility/resistance as well as interactions between S genes and NE genes are presented in this section.

P. nodorum-wheat pathosystem

The *P. nodorum*-wheat pathosystem involved in the disease SNB is the most extensively studied pathosystem involving necrotrophs. Therefore, it is also used as a model to study host-pathogen interactions involving NEs previously referred to as host selective toxins (HSTs), released by the pathogen and the products of S genes in the host. The disease SNB includes both leaf blotch and glume blotch (Figure 1A) that are common in warm and humid areas of the world, causing ~16% yield losses, which sometimes approach 60% under severe infection/epidemic conditions (Bhathal et al., 2003; Ficke et al., 2018; Shankar et al., 2021). The disease is particularly common in Australia, USA, parts of Europe and southern Brazil. The short incubation period enables the pathogen for multiple infection cycles within a season. The fungus can reproduce through asexual conidia as well as through sexual reproduction due to the availability of both mating types (MAT1-1 and MAT1-2).

NE genes, S genes, and the interactions

P. nodorum produces NEs, which contribute to variation in aggressiveness. The infection occurs only when a specific S gene of the host responds to the presence of a NE encoded by a gene in the pathogen. Nine S genes in the host and eight NE genes in the pathogen have been identified, which are involved in the following nine interactions: (i) *Tsn1*-SnToxA; (ii) *Snn1*-SnTox1; (iii) *Snn2*-SnTox2; (iv) *Snn3B1*-SnTox3; (v) *Snn3D1*-SnTox3 (vi) *Snn4*-SnTox4; (vii) *Snn6*-SnTox6; (viii) *Snn7*-SnTox7; (ix) *Tsn1*-SnToxA. A new NE named SnTox267, was later shown to represent three previously characterized NEs, namely SnTox2, SnTox6 and SnTox7, hence the name SnTox267 (Richards et al., 2021). Among the above nine interactions, the following interactions have been subjected to relatively detailed studies because the S genes and the NE genes involved in these interactions have all been cloned and characterized: *Tsn1-SnToxA, Snn1-SnTox1* and *Snn3-D1-SnTox3*.

The distribution of S genes involved in SNB in wheat populations differs in different wheat-growing regions of the world. However, maximum data is available from the USA, Europe (including UK and Norway) and Western Australia. The distribution of three NE genes (*SnToxA*, *SnTox1* and *SnTox3*) in a globally diverse collection of pathogen isolates, was reported by McDonald et al. (2013); the results are summarised in Table 3. These results, suggested that the gene *SnTox1* is the most widely distributed gene, occurring in 95.4% isolates from the USA (as above) and in 84% isolates worldwide. Similar frequencies (85%) were reported for the corresponding S gene *Snn1* in wheat germplasm; this was also confirmed in some independent surveys conducted for the distribution of different S genes in wheat cultivars (Tan et al., 2014; Phan et al., 2018; Hafez et al., 2020).

Cloning of S genes and NE genes

Three S genes (*Tsn1*, *Snn1*, and *Snn3-D1*) and five NE genes (*SnToxA*, *SnTox1*, *SnTox3*, *SnTox5*, *SnTox267*) have also been cloned and characterized thus permitting a study of interactions between the products of sensitivity genes and NEs at the molecular level. Efforts are also underway for cloning of *Tsc1* gene. For this purpose, in a recent study, 58 molecular markers were identified delineating a 1.4 cM genetic interval spanning 184kb on chromosome 1AS, carrying *Tsc1* gene (Running et al., 2022). This short region carried only nine candidate genes that were mainly related to NB-ARC, protein kinase, LRR, retinal pigment epithelial membrane protein and pseudo-gliadin proteins. The information with details of the cloned S genes and NE genes is available in a number of individual original papers (Ciuffetti et al., 1997; Liu et al., 2009; Faris et al., 2010; Liu et al., 2012; Liu et al., 2016; Shi et al., 2016a; Shi et al., 2016b; Kariyawasam et al., 2021; Zhang et al., 2021) and summarized in several recent reviews (Wang et al., 2014; McDonald and Solomon, 2018; Faris and Friesen, 2020; Friesen and Faris, 2021; Lin and Lillemo, 2021; Peters Haugrud et al., 2022). The information is also summarized in Table 4 and Supplementary Figure S3.

TABLE 2 Necrotrophs and hemibiotrophs causing diseases in wheat.

Pathogen (teleomorph)	Pathogen (anamorph)	Disease caused	Reference
Parastagonospora nodorum (Berk.) Quaedvlieg, Verkley & Crous	*Stagonospora nodorum* [Berk.] Castellani & E.G. Germano)	Septoria nodorum blotch (SNB)	Weber, 1922; Sprague, 1950; King et al., 1983; Scharen et al., 1985
Pyrenophora tritici-repentis (Died.) Drechsle	*Drechslera tritici-repentis* (Died.) Shoemaker	Tan spot	Drechsler, 1923; Shoemaker, 1959; Shoemaker, 1962
Cochliobolus sativus (S. Ito & Kurib.) Drechsler ex Dastur	*Bipolaris sorokiniana* (Sorokin) Shoemaker	Spot Blotch (SB)	Dastur, 1942; Shoemaker, 1959
Mycosphaerella graminicola (Fuckel) J. Schröt.	*Zymoseptoria tritici* (Desm.) Quaedvlieg & Crous	Septoria tritici blotch (STB)	Desmazieres, 1842; Schroter, 1894

TABLE 3 Distribution (%) of three Tox genes among isolates of *P. nodorum* and sensitivity genes in wheat.

Distribution (%) of three Tox genes in *P. nodorum*				
Region	*SnToxA*	*SnTox1*	*SnTox3*	Reference
Fertile Crescent	95.0	97.0	72.0	Ghaderi et al., 2020
Norwegian	67.9	46.1	47.9	Lin et al., 2020b
Canada	69.2	80.7	76.9	Hafez et al., 2020
Norwegian	69.0	53.0	76.0	Ruud et al., 2018
World-wide collection	18.0	26.0	22.0	McDonald et al., 2013
Europe	12.0	89.0	67.0	McDonald et al., 2013
South-eastern United States	15.0	74.0	39.0	Crook et al., 2012
Distribution (%) of three sensitivity related genes in wheat				
	Tsn1	*Snn1*	*Snn3*	
Norwegian	30.0	7.6	15.3	Lin et al., 2020b
Canada	59.0	32.9	56.9	Hafez et al., 2020
Norwegian	45.0	12.0	55.0	Ruud et al., 2018
Russia	29.3	26.8	51.2	Phan et al., 2018
Kazakhstan	27.7	28.6	63.6	Phan et al., 2018
India	66.7	58.3	77.8	Phan et al., 2018
Pakistan	59.4	71.9	68.8	Phan et al., 2018
British French, German and Dutch	9.1	28.0	42.0	Downie et al., 2018
Australia	63.0	71.7	91.3	Tan et al., 2014
USA	32.0	0.0	64.0	Bertucci et al., 2014

Genetics of resistance

There are at least three genetic systems, which provide resistance against SNB, as also in other pathosystems; these three systems include the following: (i) recessive alleles or loss of S genes, (ii) classical R genes and (iii) QTLs/MTAs identified through interval mapping and GWAS. Some details of these three systems will be described.

S genes for resistance.

According to Cowger et al. (2020), some evidence is available, which suggests that during breeding programs, perhaps unconscious selection for resistance has been exercised against S genes (*Snn* genes in the case of *P. nodorum*) due to their role in conferring susceptibility. It is also assumed that some S genes were R-genes, which provided resistance against pathogens, but have

TABLE 4 A summary of cloned sensitivity and NE genes involved in SNB.

Gene/chromosome	Length (bp)	Protein (aa)	Reference	Figure
Sensitivity genes (wheat, *T. aestivum*)				
Tsn1 (5BL)	10,581	S/TPK-NBS-LRR	Faris et al., 2010	Supplementary Figures S3A, B
Snn1 (1BS)	13,045	GUB-WAK, EGF_CA, TM, PK	Shi et al., 2016b	Supplementary Figures S3C–F
Snn3–D1 (5DS)	1,977	PKMSP	Zhang et al., 2021	Supplementary Figure S3G
NE Genes (*P. nodorum*)				
SnToxA	534	13 kD	Ciuffetti et al., 1997	Supplementary Figure S3H
SnTox1	7,600	10.3 kD	Liu et al., 2012	Supplementary Figures S3I, J
SnTox3	693	25.8 kD	Liu et al., 2009	Supplementary Figures S3L, M
SnTox5	654	16.26 kDa	Kariyawasam et al., 2021	Supplementary Figure S3K
Sn267	2,086	74.5 kDa	Richards et al., 2021	Supplementary Figure S3N

been hijacked/corrupted by necrotrophs to provide susceptibility, thus becoming S genes (Nagy and Bennetzen, 2008; Faris et al., 2010; Gilbert and Wolpert, 2013; Shi et al., 2016b). For instance, during the cloning of *Tsn1* and *Snn1* genes, it was concluded that necrotrophs hijacked the R genes involved in resistance to biotrophs and altered them for their own benefit (Faris et al., 2010; Shi et al., 2016b). During interval mapping also, some QTLs were found to be located in the genomic regions occupied by S genes, thus suggesting that QTLs may also sometimes represent R genes hijacked by the pathogens.

Possible R genes

Wheat genome sequences were also utilized for the identification of R genes associated with the genomic regions occupied by QTLs that were earlier identified and mapped on 1BS and 5BL. The annotation of intervals in the reference sequence allowed identification and mapping of 13 R genes on 1BS and 12 R-genes on 5BL (Li D. et al., 2021), although no evidence was available showing that these R genes were involved in providing resistance against SNB. The analysis of R genes, however, resolved co-located QTL on 1BS into the following two distinct but linked loci: (i) *NRC1a* and *TFIID* mapped in one QTL on 1BS, and (ii) *RGA* and *Snn1* mapped in the linked locus; all these genes were found to be associated with SNB resistance, but only in one environment. Similarly, *Tsn1* and *WK35* were mapped on the same QTL on 5BL, with NETWORKED 1A and RGA genes mapped in the linked QTL interval.

QTLs/MTAs for SNB resistance (leaf blotch, and glume blotch)

As mentioned above, *P. nodorum* is responsible for two SNB diseases in wheat, *i.e.*, leaf blotch and glume blotch (involving flag leaf for leaf blotch and spikes for glume blotch). The inheritance pattern for resistance against the two diseases differs (Wicki et al., 1999; Xu et al., 2004; Shankar et al., 2008; Chu et al., 2010). However, in several genetic studies, no distinction was made between leaf blotch and glume blotch. QTLs for resistance against SNB have also been identified following both linkage-based interval mapping and LD-based GWAS.

Interval mapping involved both bi-parental and multi-parental (MAGIC) mapping populations, and resulted in the identification of ~170 QTLs including ~30 major QTLs, each explaining >20% of the phenotypic variation (Supplementary Table 2). These studies included the following: Czembor et al., 2003; Schnurbusch et al., 2003; Arseniuk et al., 2004; Liu et al., 2004a; Aguilar et al., 2005; Reszka et al., 2007; Uphaus et al., 2007; Shankar et al., 2008; Friesen et al., 2009; Gonzalez-Hernandez et al., 2009; Francki et al., 2011; Abeysekara et al., 2012; Shatalina et al., 2014; Ruud et al., 2017; Francki et al., 2018; Czembor et al., 2019; Singh et al., 2019; Lin et al., 2020a; Lin et al., 2021; (for a recent review, also see Downie et al., 2021).

The above QTL studies also included two recent major studies, each involving an independent MAGIC population, one used by Lin et al. (2020a) and the other used by Lin et al. (2021). Using these two MAGIC populations, 17 QTLs on the following chromosomes were identified: 2A, 2D, 5A, 5B, 6A, 7B and 7D. In these two studies, two QTLs, namely *QSnb.niab-2A.3* (UK MAGIC population, Lin et al., 2020a) and *QSnb.nmbu-2A.1* (German MAGIC population, Lin et al., 2021) were found in a short interval on chromosome 2A; these two QTLs could represent a hot spot controlling resistance against SNB. A QTL (*QSnb.niab-5B.2*) overlapping *Tsn1* was also identified on 5BL (Lin et al., 2020a; Lin et al., 2021).

The GWA studies for resistance to SNB were undertaken both at the seedling stage and adult plant stage (flag leaf and spike for glume blotch) and resulted in identification of MTAs on almost all 21 chromosomes. However, more studies were conducted at the seedling stage than at the adult stage (glume blotch). These association studies largely included the following: Adhikari et al., 2011; Korte and Farlow, 2013; Gurung et al., 2014; Gao et al., 2016; Pascual et al., 2016; Downie et al., 2018; Phan et al., 2018; Halder et al., 2019; Ruud et al., 2019; Francki et al., 2020; Phan et al., 2021; Lin et al., 2022). After due validation, the markers associated with QTLs and MTAs can be utilized for marker assisted selection (MAS) for resistance breeding.

High-resolution fine-mapping has also been undertaken for sensitivity genes. For this purpose, a high-density genetic linkage map was developed for a chromosome 2D region, which narrowed down the *Snn2* gene to a 4 cM region, thus facilitating the discovery of closely linked molecular markers for breeding and positional cloning of the *Snn2* gene (Zhang et al., 2009). Phenotypic variation (PV) for the disease was 47% for the interaction *Snn2-SnTox2*, 20% for *Tsn1-SnToxA*, and 66% for both interactions taken together, suggesting the utility of these interactions for breeding (Friesen et al., 2008).

Epistatic interactions among fungal NE genes.

Epistatic interactions involving suppression of *SnTox3* by *SnTox1* in the pathogen were also demonstrated (Phan et al., 2016). In this study, the mapping population consisted of 177 double haploid (DH) lines, and an aggressive isolate (Sn15) of the pathogen with genes for three NEs, namely *SnToxA*, *SnTox1* and *SnTox3* and its two deletions (tox1-6 with a deletion for *SnTox1*, and toxa13 with deletion for all the three NE genes) were used; mutant strain toxa13 retained pathogenicity and necrosis-inducing activities in the culture filtrate (Tan et al., 2015); the virulence of this toxa13 on the mapping population at the seedling stage was comparable with that of Sn15.

The following observations also suggested epistatic suppression of *SnTox3* by *SnTox1* and that of *SnToxA* by *SnTox3* in the pathogen: (i) The mapping population segregated for S genes *Snn1* and *Snn3*, since parents of the mapping population differed for these two genes; (ii) When Sn15 was used for infection, *SnToxA–Snn1* interaction was most important for SNB development on both seedlings and adult plants, suggesting that *SnToxA* always functioned; no effect of the *SnTox3–Snn3* interaction was observed under Sn15 infection. (iii) When tox1-6 strain was used for inoculation, *SnTox3–Snn3* interaction was observed; (iv) When toxa13 strain was used for infection, it unmasked a significant SNB QTL on 2DS, where *Snn2* is located. This QTL was not observed in Sn15 and tox1-6 infections, thus

suggesting that *SnToxA* and/or *SnTox3* were epistatic. Additional QTLs responding to SNB sensitivity were detected on 2AS1 and 3AL.

Seedling and adult plant field resistance

In each above case, resistance has generally been examined at the seedling stage under controlled conditions using single isolates of the pathogen, but often also examined and compared with those under field conditions (with a mixture of isolates) at the adult plant stage. However, caution should be exercised during evaluation of resistance at the seedling stage for developing resistance under field conditions. Several studies have shown comparable results at the seedling and adult plant stages, when using the same isolate or mix of isolates. However, since the natural infections in the field involve complex pathogen populations with a mixture of isolates, care must be taken to choose representative isolates (see Ruud and Lillemo, 2018 and Peters Haugrud et al., 2022 for recent discussions on this topic).

Genetics and genomics of *P. nodorum*

Genetic variation among naturally occurring isolates and population genetics of *P. nodorum* has also been examined both at the national level in Sweden (Blixt et al., 2008), Western Australia (Murphy et al., 2000) and Norway (Lin et al., 2020b), and at the global level (Stukenbrock et al., 2005; Stukenbrock et al., 2006). Using RFLPs and SSRs as molecular markers for this purpose, it was shown that in general, *SnToxA* had a relatively higher frequency among *P. nodorum* isolates sampled in different studies (Lin et al., 2020b).

Whole genome sequencing has also been undertaken for *P. nodorum*. The pathogen is haploid with a genome size ranging from 28 Mb to 37 Mb with 23 chromosomes including an accessory chromosome, AC_{23} that is involved in virulence-related functions other than the functions assigned to NEs (Syme et al., 2013; Richards et al., 2018; Syme et al., 2018). A number of isolates, including the following four major isolates were used for genome sequencing: Sn15, Sn4, Sn2000, Sn79-1087. The number of genes in the genome was shown to range from 13,569 for the Sn15 reference genome to 13,294 in Sn79-1087 genome (Hane et al., 2007; Syme et al., 2013; Syme et al., 2016; Richards et al., 2018). Another study involved 197 isolates collected from durum wheat and spring/winter bread wheat from the USA (Richards et al., 2019). These studies together resolved a wide range of structural variations (SVs). A pangenome was also developed using multiple genome sequences (Syme et al., 2018).

P. tritici-repentis-wheat pathosystem

TS caused by *P. tritici-repentis* (Died.) Drechs. has been reported from different parts of the world, including Australia, Canada, the USA, Mexico, South America (Argentina and Brazil), Europe, Africa, and Central Asia (Kazakhstan and Tajikistan) (Singh et al., 2008; Ciuffetti et al., 2010). The epidemics for this disease have been reported to cause yield losses of up to ~50% (Rees et al., 1982). The disease is characterized by two distinct and independent symptoms, namely necrosis and chlorosis (Figures 1B.1, B.2).

NE genes, S genes, and interactions

There are three NE genes (*ToxA*, *ToxB* and *ToxC*) and three sensitivity genes (*Tsn1*, *Tsc2* and *Tsc1*) involved in TS. The sensitivity genes and the NEs encoded by three Tox genes are involved in the following three interactions: (i) *Tsn1*-ToxA interaction (this interaction is also known in two other pthosystems, namely wheat-*P. nodorum* and wheat-*B. sorokiniana* pathosystem). (ii) *Tsc2*-ToxB interaction; (iii) *Tsc1*-ToxC interaction (Ciuffetti et al., 2010).

There is strong evidence that *P. tritici-repentis* acquired the gene *ToxA* from *P. nodorum* through horizontal gene transfer (Friesen et al., 2006). Among the three NEs, *ToxA* causes necrosis, while *ToxB* causes chlorosis. However, *ToxC*, which also causes chlorosis, is not a protein but a non-ionic, polar, low molecular mass molecule (Effertz et al., 2002).

In the pathogen populations, eight races (races 1 to 8) have been recognized on the basis of the types of susceptibility lesions using six differential wheat genotypes (chlorosis or necrosis) and HSTs/NEs produced (Lamari et al., 2003; Ciuffetti et al., 2010; Table 5). Each race produces one or more NEs in a combination, which differs for different races. For instance, races 1, 6, and 7 produce two NEs each (race 1 with ToxA and ToxC, race 6 with ToxB and ToxC and race 7 with ToxA and ToxB). Races 2, 3, and 5 each produce only one NE (race 2 with ToxA, race 3 with ToxC and race 5 with ToxB); race 8 produces all the three NEs, while race 4 is known to produce none (Faris et al., 2013; Guo et al., 2018). In addition to the above three toxins, as many as 38 novel necrosis inducing toxins called 'triticones' have also been identified, although only triticone A and triticone B have been purified from Ptr (Rawlinson et al., 2019).

Geographic distribution of Ptr NE genes

The distribution of the genes encoding three different NEs (ToxA, ToxB and ToxC) and the wheat genotypes with corresponding S genes involved in interactions differs widely in different parts of the world. Of these, ToxA is the most widely distributed, present in ~80% of the world's Ptr isolates (Lamari et al., 1998; Ali and Francl, 2002; Friesen et al., 2006).

Cloned NE genes for TS

Among NE genes, the gene encoding PtrToxA (a 13.2-kDa protein) has been characterized by several independent research groups, and was the first to be cloned (Ballance et al., 1996; Ciuffetti et al., 1997). The gene encoding PtrToxB (6.61 kDa) occurs as multiple copies, and carries a 261-bp open reading frame (ORF) within its sequence (Martinez et al., 2001). PtrToxC has not been

TABLE 5 Reaction of eight races of *P. tritici-repentis* on four bread and two durum wheat differential lines.

Differential genotypes	Race (with Toxin) and reaction of six differential genotypes							
	1	2	3	4	5	6	7	8
	ToxA, C	ToxA	ToxC	None	ToxB	ToxB, C	ToxA, B	ToxA, B, C
Bread wheats								
Glenlea	S1	S1	R	R	R	R	S1	S1
6B662	R	R	R	R	S2	S2	S2	S2
6B365	S	R	S2	R	R	S2	R	S2
Salamouni	R	R	R	R	R	R	R	R
Durum wheats								
Coulter	S1	S1	S1	R	S1	S1	S1	S1
4B1149	R	R	R	R	R	R	R	R

R indicates resistant, S1 indicates susceptible (necrosis), and S2 indicates susceptible (chlorosis).

fully characterized and purified; the mode of action of this NE is also not known. However, its partial characterization has been done as low molecular weight, non-ionic polar molecule (Effertz et al., 2002).

Cloned sensitivity genes for TS

Tsn1 (common for susceptibility to three necrotrophs) was cloned and characterized rather early (Supplementary Figures S3A, B; Faris et al., 2010). The other two S genes, *Tsc1* and *Tsc2*, are yet to be cloned and characterized, but markers have been developed for these two other sensitivity genes also (Supplementary Table S1). The variety 'Maris Dove' was also identified as the historical source of *Tsc2* alleles in the wheat germplasm (Corsi et al., 2020). A minor S QTL was also identified on chromosome 2A (Corsi et al., 2020) in this line. The marker developed in this study can be used for MAS to select insensitive genotypes exhibiting disease resistance (Corsi et al., 2020).

Attempts are also underway to clone *Tsc1* gene. For this purpose, in a recent study, two biparental populations were used leading to the delineation of *Tsc1* candidate gene region to a 1.4 centiMorgan (cM) interval, which spanned 184 kb region on the short arm of chromosome 1A. Mapping of the chlorotic phenotype, development of genetic markers, both for genetic mapping and MAS, and the identification of *Tsc1* candidate genes in this study provide a foundation for map-based cloning of *Tsc1* (Running et al., 2022)

Genetics of resistance

Assessment of sensitivity

In a recent study, 40 Australian spring wheat varieties were examined for sensitivity to ToxA and disease response to a race 1 specific wild-type Ptr isolate carrying *ToxA* and *ToxC* (See et al., 2018). *ToxA* sensitivity was generally associated with disease susceptibility (compatible interaction) but did not always produce symptoms (See et al., 2018). When wild type and *toxA* mutant isolates were used for infection, most *Tsn1* varieties exhibited low disease scores with *toxA* mutants (as expected). However, several varieties exhibited no distinct differences between wild-type and *toxA* mutant (See et al., 2018). This pattern suggested that ToxA is not the sole major cause of TS disease and that the appearance of the disease partly also depends on the background of the host (See et al., 2018). It is thus apparent that ToxA may need additional factors to cause infection (See et al., 2018).

R genes for resistance

Resistance genes (R genes or major QTLs) providing resistance against TS have also been identified. Most studies on the genetics of TS are based on bi-parental mapping populations (Faris et al., 2013). Among R genes, *Tsr7* locus was also identified in tetraploid wheat using a set of Langdon durum-wild emmer (*Triticum turgidum* ssp. *dicoccoides*) disomic chromosome substitution lines (Faris et al., 2020). Four user-friendly SNP-based semi-thermal asymmetric reverse PCR (STARP) markers co-segregated with *Tsr7* and should be helpful for MAS (Faris et al., 2020).

QTLs for resistance

Several QTLs have been identified, mainly corresponding to the available S-genes (Liu et al., 2020a). The QTL studies resulted in the identification of as many as >160 QTLs; a number of these QTLs explained >20% phenotypic variation (Supplementary Table S2). A meta-QTL analysis was also conducted, leading to the identification of 19 meta-QTLs derived from the results of 104 QTL studies (Liu et al., 2020a; Liu et al., 2020b). Three race nonspecific meta-QTLs were also identified, one each on chromosomes 2A, 3B and 5A. These three meta-QTLs had large phenotypic effects, each responsible for resistance to multiple races infecting bread and durum wheat races, thus suggesting their utility for marker-assisted selection (MAS).

GWAS for resistance

A number of GWA studies involving the identification of MTAs for TS resistance are also available (Patel et al., 2013; Kollers et al., 2014; Liu et al., 2015; Juliana et al., 2018; Dinglasan et al., 2019; Galagedara et al., 2020; Kokhmetova et al., 2020; Muqaddasi et al., 2021). These studies led to the identification of >240 MTAs, although many of these could be false positives (Supplementary Table S3). Candidate genes were found for 16 out of 19 meta-QTLs; the candidate genes for each meta-QTL ranged from 2 to 85, with most of them being on chromosome 2B. Many of these potential genes encoded NBS- and/or LRR-like proteins and were found near the *Tsc2* S gene (Liu et al., 2020a). However, none of these candidate genes could be actual *Tsc2* gene, because the genomic sequence used to identify candidate genes belonged to Chinese spring (CS) wheat, insensitive to Ptr ToxB. (Liu et al., 2020a).

Genetic studies at seedling and adult plant stage under field conditions

The genetics of resistance against TS in wheat has been examined both at the seeding and adult plant stages. For instance, in a study of ~300 accessions from Vavilov collection, seedling but not adult plant disease response corresponded with ToxA sensitivity; ToxA-sensitive accessions that were susceptible at the seedling stage, carried adult-plant resistance (APR) (Dinglasan et al., 2017). In a follow-up GWAS, they identified 11 QTL, of which were associated as follows: 5 with seedling resistance, 3 with all-stage resistance, and 3 with APR. Interestingly, the novel APR QTL was effective even in the presence of host sensitivity gene *Tsn1* (Dinglasan et al., 2019).

Genetics and genomics of *P. tritici-repentis*

The genetic studies on isolates of *P. tritici-repentis* from different parts of the world have also been conducted using molecular markers. It was shown in several studies including one from Oklahoma in USA that race 1 was the predominant race in most regions (Ali and Francl, 2003; Friesen et al., 2005; Kader et al., 2022).

The Ptr genome is 40.9 Mb in size and has already been fully sequenced (Moolhuijzen et al., 2018). As much as 98% of the genome has been mapped on 10 or more chromosomes, carrying 13,797 annotated genes (Moolhuijzen et al., 2018). The *Ptr ToxA* is a single copy gene (Ballance et al., 1989; Tomas et al., 1990; Tuori et al., 1995; Ballance et al., 1996; Zhang et al., 1997; Ballance et al., 1998), producing a 19.7 kD protein precursor (Ballance et al., 1996; Ciuffetti et al., 1997). *Ptr ToxB*, on the other hand, is a multi-copy gene (1-3 Kb in length; Martinez et al., 2004) that encodes a 6.6 kDa host selective toxin (Strelkov et al., 1999; Martinez et al., 2004). When the genome of a race 5 Tox-B isolate was sequenced, ten identical *ToxB* gene copies were identified (Moolhuijzen et al., 2020). Multiple *ToxB* gene loci on chromosome 10 were separated by 31-66 kb long segments and exhibited an alternating pattern involving forward and reverse DNA strands. Also, the gene is flanked by transposable elements (Moolhuijzen et al., 2020; Supplementary Figure S4).

B. sorokiniana-wheat pathosystem

B. sorokiniana is a hemi-biotroph, which causes several important wheat diseases, namely SB (Figure 1C), common root rot (CRR), black point and crown rot; these diseases are responsible for significant yield losses in several parts of the world (Gupta et al., 2018a; Gupta et al., 2018b). The correlations between these diseases in wheat seem to be poor and mechanisms for resistance against these diseases seem to differ (Conner, 1990; Al-Sadi, 2021). However, we will restrict our discussion to only spot blotch.

The gene *ToxA* initially reported in *P. nodorum* and *P. tritici-repentis* (Tuori et al., 1995; Friesen et al., 2006), has also been identified in some *B. sorokiniana* isolates from USA (South Central Texas), Australia, India, and Mexico. It was also shown that a *B. sorokiniana* isolate harbouring *ToxA* (dominant alleles of S gene) is more virulent on wheat lines carrying the S gene *Tsn1* (McDonald et al., 2018; Navathe et al., 2020).

NE gene, S gene, and the interaction

A solitary sensitivity gene (*Tsn1*) in the host (wheat) and the corresponding NE gene (*ToxA*) in the pathogen are known for wheat-SB pathosystem. The presence of the *Tsn1* gene is generally but not always associated with susceptibility to the pathogen carrying the *ToxA* gene, as shown in the material surveyed in Australia and India (McDonald et al., 2018; Navathe et al., 2020). It was reported that sometimes an isolate lacking *ToxA* is still highly virulent on cultivars from Australia and India lacking *Tsn1*. In contrast, a cultivar containing *Tsn1* can still be resistant to isolates carrying the *ToxA* gene. These results suggest that there are additional factors in the wheat genome, which control resistance; these factors may include R genes and QTLs controlling resistance to SB (Navathe et al., 2020).

BsToxA differs from *SnToxA* and *PtrToxA*

The gene *BsToxA* is embedded in the 12-kb AT-rich region of the pathogen genome (McDonald et al., 2013; McDonald et al., 2018). Decay near the gene edges has been reported and is attributed to repeat-induced polymorphism (RIP) (Supplementary Figure S5; McDonald et al., 2018). Small indels have also been reported in the gene's promoter region; the size of indel in *BsToxA* (148 bp) differs from that, in *SnToxA* (43 bp) and *PtrToxA* (238 bp) (McDonald et al., 2012; McDonald et al., 2018; also see Supplementary Figure S5). The haplotype organization of *ToxA* genes in three pathogens (*BsToxA*, *PtrToxA* and *SnToxA*) also differed (McDonald et al., 2018). The frequencies of pathogen isolates carrying *BsToxA* and the wheat genotypes carrying *Tsn1* also differ in different parts of the world (Friesen et al., 2018; McDonald et al., 2018; Navathe et al., 2020; Wu et al., 2021).

Sensitivity-related QTLs against *B. sorokiniana* have also been identified in barley, where recessive alleles of *Rcs5* and *Rcs6/Scs2* provided resistance to SB (Gupta et al., 2018a; Leng et al., 2018).

Two additional QTLs (*QSbs-1H-P1* and *QSbs-7H-P1h*) for susceptibility to SB were also identified in barley; of these two QTLs, *QSbs-7H-P1* mapped to the same region as the *Rcs5* gene, but *QSbs-1H-P1* was a novel QTL later reported by Leng et al. (2020).

Genetics of resistance

R genes

Resistance to SB is mainly associated with one or more of the four major R genes (*Sb1-Sb4*) that were identified using classical methods of genetics for Mendelian traits. The genetics of resistance to spot blotch has also been studied, taking the disease as a quantitative trait (reviewed by Gupta et al., 2018a).

QTLs/MTAs

Using interval mapping, ~70 QTLs were identified, which included 14 major QTLs with PVE >20% (Supplementary Table S2). Some of the QTLs were inherited in a Mendelian manner and overlapped the known major Sb genes (Lillemo et al., 2013; Kumar et al., 2015; Lu et al., 2016; Zhang et al., 2020). Such QTLs were later designated as *Sb1* (*QSb.bhu-7DS*) and *Sb2* (*QSb.bhu-5BL*) in two independent studies (Lillemo et al., 2013; Kumar et al., 2015). *Sb1* gene is also associated with *Lr34*, an important gene for leaf rust resistance in wheat (Lillemo et al., 2013). Using GWAS also, ~80 MTAs were identified (Gupta et al., 2018a; Chand et al., 2021; Supplementary Table S3). These interval mapping studies and GWAS were generally conducted only at the adult plant stages.

Resistance at seedling and adult stages

Resistance against SB in wheat has generally been examined only at the adult plant stage. Only in a recent study, resistance at seedling and adult plants stages and its association with biochemical profiling was examined (Mahapatra et al., 2021).

Phylogeography and genomics of *B. sorokiniana*

The phylogeographic pattern of *B. sorokiniana* isolates was examined in a recent study involving 254 isolates from different parts of the world with the goal to elucidate the demographic history. In this study, 162 ITS, 18 GAPDH and 74 TEF-1a gene sequences from *B. sorokiniana* obtained from GenBank were utilized and 40 haplotypes were identified (Sharma et al., 2022). It was inferred that human-mediated dispersal perhaps played a major role in shaping the distribution of *B. sorokiniana*.

Genomic studies of *B. sorokiniana* include generation of a draft genome sequence followed by a refined genome sequence of an Indian isolate, namely *B. sorokiniana* strain BS_112. These genome sequemces were reported in two independent publications by Aggarwal et al. (2019), Aggarwal et al. (2022) from Indian Council of Agriculture Research-Indian Agriculture Research Institute (ICAR-IARI) in India. The genome size was estimated to be 35.64 Mb, with an average G/C content of 50.20%. A total of 10,460 genes were predicted with an average gene density of 250 to 300 genes/Mb, which covers around 98% of predicted genes. The lengths of genes ranged from 50 bp to 8,506 bp with an average length of 435 to 545 bp per gene.

Z. tritici-wheat pathosystem

Z. tritici (syn. *Septoria tritici*, *Mycosphaerella graminicola*) is an important apoplastic fungal pathogen causing STB, which is responsible for major yield losses, sometimes approaching 50% under severe epidemic conditions (Eyal, 1973; Eyal et al., 1987). The fungus has been shown to be a hemibiotroph (Fones and Gurr, 2015), with the following two main phases: (i) the initial symptomless biotrophic latent phase (typically lasting for about 10 to 12 days), during which the hyphae enter the leaves through stomata and colonize the leaf tissues (Kema et al., 1996), and (ii) the later necrotrophic phase (Hehir et al., 2018), when the host tissue begins to die, and the fungus feeds on dead tissue (Keon et al., 2007).

In wheat-*Z. tritici* pathosystem, the host secretes β-1,3-glucanase into the apoplast, which cleaves β-1,3-glucan in the pathogen's cell wall and prevents colonization of the pathogen (Shetty et al., 2009). The major R genes and QTLs for the STB disease have been listed by Brown et al. (2015) and are also available on the Komugi database (https://shigen.nig.ac.jp/wheat/komugi/).

NEs, ZtNIP1/2, MgNLP and ZtSSPs

Hundreds of *Z. tritici* candidate effector genes have been identified through comparative genomics and transcriptomics (Gohari, 2015; Rudd et al., 2015; Kettles et al., 2017; Palma-Guerrero et al., 2017; Plissonneau et al., 2018). Three well characterized LysM effector genes (NE genes), namely *Mg3LysM*, *Mg1LysM* and *Mgx1LysM* have also been identified (Marshall et al., 2011; Tian et al., 2021). Initially, only two LysM effectors, namely Mg1LysM and Mg3LysM, were known. Among these two effectors, Mg3LysM, but not Mg1LysM, was shown to suppress the response of the host immune system at the level of pattern triggered immunity (PTI) (Figure 3).

The host's immune system involves synthesis of chitinases, which destroy fungal cell wall chitin that causes virulence. A third LysM gene, which was initially believed to be a pseudogene, was later shown to encode a LysM effector, named Mgx1LysM, also named Zt3LysM (Zhang, 2022). Later Zt3LysM effector was also shown to contribute to *Z. tritici* virulence, and to protect fungal hyphae against hydrolysis by chitinases of the host. All three LysM effectors display partial functional redundancy (Tian et al., 2021).

In addition to three LysMs as above, *Z. tritici* also secretes many rapidly evolving, small secreted proteins (ZtSSPs), which function as effectors and help the pathogen to colonize plant tissue. In a recent study, while working with the pathogen's SSPs, ZtSSP2 was found to express throughout *Z. tritici* infection phase in wheat, with

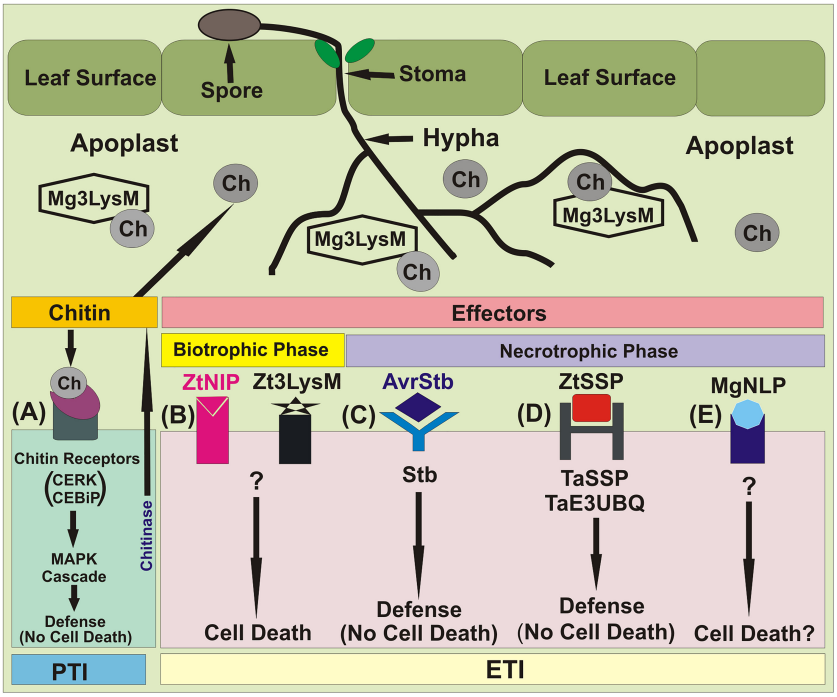

FIGURE 3
Major molecular events during *Z. tritici*–wheat interactions. **(A)** Fungal PAMP chitin is recognized by the host receptors Chitin Elicitor Binding Protein (CEBiP) and Chitin Elicitor Receptor Kinase 1 (CERK1), triggering MAP kinase cascades and immune activation. Multi-functional LysM-domain containing effector Mg3LysM scavenges chitin to suppress immunity and protects fungal hyphae from wheat chitinases. **(B)** 'Necrotrophic' effectors (NEs), Necrosis-Inducing Protein 1/2 (ZtNIP1/2) and and LysM effector (Zt3LysM) induce host cell death. **(C)** *Stb* gene-specified resistance, presumably triggered following recognition of cognate fungal effectors (AvrStb) secreted into the apoplast. This results in arrest of pathogen growth *via* an unknown mechanism that does not involve HR. **(D)** The NEP1-like effector protein MgNLP (unknown *Z. triticini* effector, predicted by bioinformatics analysis) has an unknown function(s) during wheat infection, but triggers cell death in dicots. **(E)** Small secreted proteins (ZtSSPs) of *Z. tritici*, which act as an effector. The TaE3UBQ synthesize in the wheat and interacts with the ZtSSPs resulting inhibition of the growth of *Z. tritici* pathogen.

the highest levels observed early during infection. A study of the interaction between ZtSSP2 and wheat E3 ubiquitin ligase (TaE3UBQ) further confirmed that down-regulation of the gene encoding TaE3UBQ using virus-induced gene silencing increased the susceptibility of wheat to STB, suggesting that ZtSSPs also function as effectors. These results also suggested that the wheat TaE3UBQ plays a role in plant immunity and helps the host to achieve defense against *Z. tritici*.

No S gene for STB

Despite major search and extensive studies in wheat–*Z. tritici* pathosystem, no S gene for compatible interaction between wheat and *Z. tritici* has been discovered so far. Earlier, till a few years ago, the same was true for *B. sorokiniana*, till McDonald et al. (2018) discovered the occurrence of *Tsn1* gene interacting with ToxA of the pathogen *B. sorokiniana*. It is, therefore, possible that a S gene for STB may also be discovered in the future, although it seems unlikely in view of the relatively extensive studies already conducted on wheat–*Z. tritici* pathosystem.

Genetics of resistance

TaSSPs and TaE3UBQ genes for resistance

As in the case of many other pathogens, in addition to LysM effectors, *Z. tritici* also secretes many SSPs, which can block plant defense and permit pathogens to colonize plant tissue (Zhou et al., 2020). It has also been shown that there are also independent TaSSP loci in the host associated with resistance to STB at seedling as well as at the adult plant stages.

In a recent study involving wheat genomics, an SSP-discovery pipeline was developed and 6,998 TaSSPs (each with <250 AA) were identified, which included 141 *Z. tritici* – responsive TaSSPs. A subset of these TaSSPs also had a functional signal peptide, which could interact with *Z. tritici* SSPs. It was also shown that the synthesis of TaSSPs was induced during pathogen attack. In a wheat cultivar named Stigg, two of these TaSSPs, namely *TaSSP6* and *TaSSP7*, when silenced using virus induced gene silencing (VIGS) led to susceptibility, thus confirming the role of TaSSPs in defense against *Z. tritici* (Zhou et al., 2020). ZtSSP2 was also shown to interact with wheat E3 ubiquitin ligase (TaE3UBQ) thus confirming that down-regulation of this wheat E3 ligase using

VIGS increased the susceptibility of wheat to STB. These results suggested that perhaps TaE3UBQ gene also plays a role in providing resistance against *Z. tritici* (Karki et al., 2021).

R (Stb) genes for resistance

In the germplasm of wheat, which included landraces, wild wheat species, and synthetic hexaploid wheat, 22 major R genes (named Stb genes) have been identified and characterised (Saintenac et al., 2021; Supplementary Table S1). Most of these Stb genes are genotype-specific, each providing short-term resistance against only a few *Z. tritici* isolates. Among these 22 Stb genes, *Stb6* and *Stb16q* are the two major genes, which exhibit GFG relationship, each providing broad spectrum resistance against a majority of *Z. tritici* isolates; both these genes have been cloned and characterized. *Stb6* gene was shown to code for a wall-associated kinase (WAK), which represents a subfamily of receptor-like kinases (RLKs), which are involved in GFG of resistance against isolates carrying the matching *AvrStb6* gene (Saintenac et al., 2018). Similarly, the gene *Stb16q* encodes a plasma membrane cysteine-rich receptor like kinase (CRK, also a member of the RLK family of kinases). There is evidence that this gene (*Stb16q)* is derived from *Ae. tauschii via* synthetic wheat and has now become a part of wheat genome. This origin of *Stb16q*, also suggested the importance of wild relatives of wheat in the improvement of disease resistance in wheat cultivars (Saintenac et al., 2021).

AvrStb6–Stb6 interaction provides early defense

An avirulence locus called *AvrStb6* was also identified using diverse *Z. tritici* populations. The corresponding wheat locus *TaStb6* was also shown to be associated with qualitative resistance on multiple wheat cultivars (Kema et al., 2000; Brading et al., 2002; Chartrain et al., 2005c). The *AvrStb6* gene confers a GFG interaction with the *TaStb6* gene of wheat (Zhong et al., 2017; Kema et al., 2018). No direct interaction between the *AvrStb6* and *Stb6* proteins has been reported, and no typical hypersensitive resistance (HR) was noticed during the resistance response, indicating that programmed cell death (PCD) was not the mode of resistance in this case (Friesen and Faris, 2021).

Stb7 is another important R gene, which is recognised by the *Avr3D1* gene of the pathogen, triggering a strong defence response, but without preventing pathogen infection. In an important study, *Avr3D1* gene was found to be present in all 132 strains of *Z. tritici* that were used in the study and provided a strong fitness advantage (Meile et al., 2018). Allelic differences at the locus of *Avr3D1* are responsible for maintaining the gene but still evading recognition by the host harbouring *Stb7* (Friesen and Faris, 2021). The *Avr3D1* gene is upregulated during biotrophic phase but downregulated in the necrotrophic phase, thus permitting early colonisation (Meile et al., 2018).

QTLs/GWAS for resistance

Quantitative resistance against STB is controlled by QTLs, each with a small to moderate effect, thus providing relatively durable resistance. Relative to Stb genes, these QTLs have weak specificity. According to a review by Brown et al. (2015), till 2015, 89 genomic regions carrying quantitative trait loci (QTLs) or meta-QTLs were known. Some of these QTLs have also been mapped at or near Stb genes like *Stb6* and *Stm16q*, which are each present in many genotypes.

Many interval mapping studies involving identification of QTLs have already been conducted (Adhikari et al., 2015; Stadlmeier et al., 2019; Tamburic-Ilincic and Rosa, 2019; Riaz et al., 2020). These studies suggested that host-pathogen interaction is complex and can-not be explained by simple R–Avr interactions. Additive epistatic interactions were also reported for more minor and significant qualitative effects that govern virulence for *Z. tritici* (Jones and Dangl, 2006; Meile et al., 2018; Stewart et al., 2018). The role of necrosis inducing protein 1 (ZtNIP1) of *Z. tritici* has been shown to trigger PCD. This protein is also expressed during 8 and 12 dpi and correlates with necrotic phase symptoms (Ben M'Barek et al., 2015). The 'Necrosis and Ethylene-Inducing Peptide 1' (NEP1) is also involved in causing necrosis (Kettles and Kanyuka, 2016).

A number of GWA studies for identification of MTAs (QTLs) for resistance against STB have also been conducted. The results of four such studies are summarized in Supplementary Table S3.

Seedling vs adult plant resistance

Majority of the 22 Stb genes contribute to STB resistance independently of the plant growth stage, although resistance can also be effective only in seedlings or only in adult plants. In a recent QTL mapping study on seedling and adult plant resistance, Piaskowska et al. (2021) reviewed the literature on this subject and reported identification of a new QTL (*QStb.ihar-2B.4*) for resistance at the seedling stage (PV upto 70.0%), thus proving its utility in breeding programs. In another recent study, Yang et al. (2022) reported identification of new QTLs for seedling resistance and APR, also described as multi-stage resistance (MSR) QTLs. Two of these new QTLs included *QStb.wai.6A.2* for APR and *QStb.wai.7A.2* for MSR.

Genetics and genomics of *Z. tritici*

Population genetics of *Z. tritici* from northern France, Iran, UK, Canada, and Ethiopia was also examined using molecular markers (generally SSR markers). Significant genetic diversity was reported in all these studies; the latest of these studies by Mekonnen et al. (2020) described an average of 2.5 alleles per SSR locus, although in some earlier reports a higher level of diversity was also reported.

The genome of *Z. tritici* carries 21 chromosomes, which include 13 core chromosomes and 8 dispensable/accessory chromosomes (Croll and McDonald, 2012). The genome size varies from 32 to 40 Mb, and the pangenome carries a core set of 9,149 genes (McDonald and Martinez, 1991; Mehrabi et al., 2007; Romdhane, 2011). Genome sequences of *Z. tritici* indicated the following important features (Stukenbrock et al., 2010); (i) The essential and dispensable chromosomes evolved differently and

independently, the former being syntenic, while the latter carrying many structural rearrangements. (ii) The average synonymous substitution rate in dispensable chromosomes is considerably lower than in essential chromosomes, whereas the average non-synonymous substitution rate is three times higher. (iii) As many as 43 candidate genes showed evidence of positive selection, one of these genes encoding a potential pathogen effector protein.

Similarities and differences among four pathosystems

The four pathosystems involved in four leaf spot diseases of wheat discussed above have several similarities and differences. Among similarities, the pathogens involved in these four pathosystems are all fungal pathogens belonging to the phylum Ascomycota, and all are either necrotrophs or hemibiotrophs, there being a thin cryptic line of distinction between necrotrophs and hemibiotrophs (Rajarammohan, 2021). The hemibiotrophic nature of *Z. tritici* has also been questioned (Sanchez-Vallet et al., 2015). Following are some other similarities: (i) occurrence of both GFG relationship involving R genes of the host and Avr genes of the pathogen and IGFG relationship, involving sensitivity (Tsn/Snn) genes of the host and NE genes of the pathogen. In this respect, the pathosystem involved in STB is the only exception. The pathogens also exhibit similar modes of reproduction involving asexual reproduction through conidia and sexual reproduction involving a mating system and producing ascospores. In this respect, *B. sorokiniana* is an exception being an anamoporph (its sexual form being teleomorph, described as *Cochliobolus sativus*). Another major difference includes homothallic nature of sexual forms: *P. nodorum* and *P. tritici-repentis* are homothallic, as against heterothallic nature of *B. sorokiniana* and *Z. tritici*. The availability of sexual reproduction also has a bearing on the diversity of the pathogen, the frequent sexual reproduction leading to higher level of diversity. Other differences include the number of known sensitivity (S) genes, R genes and QTL/QRL in the host and NE/Avr genes in the pathogen, there being nine S genes in the host and eight NE genes in the pathogen for SNB involved in nine interactions, three S genes and three NE genes for TS, only one S gene (*Tsn1*) and one NE gene (*ToxA*) for SB, and there being no known S gene for STB. The pathosystem involving STB also differs for the occurrence of a relatively large number of R genes (22 Stb genes) in the host and ZtSSP genes in the pathogen for virulence and the TaSSP genes for resistance/defence in the host.

Based on the occurrence of R/SSP genes and QTLs/QRLs for resistance and S genes for susceptibility in the wheat genome and the corresponding Avr/NE/SSP genes in the pathogen, one can perhaps try to study the interactions among these genes and plan strategies for developing resistance involving each of the four pathosystems. One such project for SB has already been planned by the authors of this review.

Breeding strategies

S genes, R genes and QTLs for resistance

The sensitivity (S) genes in bread wheat as the host are the most important source of susceptibility involving compatible interaction between the host and the pathogen, so that apparently the loss of these genes or use of their recessive alleles or mutant alleles should be the major sources of resistance. The interactions between S genes of the host and the NE genes of the pathogens for four diseases are summarised earlier in this review. All these cases represent examples of IGFG, where the pathogen can-not cause the disease, unless the host carries the corresponding S gene, which is recognized by the pathogen-derived effector.

There are examples, where a loss-of function mutations in S genes may either occur naturally, or else may be induced through mutagenesis. The most important example of such a loss of function mutations is the loss-of function of the *Mlo* gene in barley and many important cereals (including wheat and rice), vegetables (tomato, pepper, cucumber, and melon), legumes (peas and lentils), fruit trees and shrubs (apples, grapevines, peaches, and strawberries), and flowers (petunia and roses) providing resistance to powdery mildew disease. It is still unknown whether all these Mlo homologs can act as susceptibility genes in their respective hosts (for details of References, see Phd Thesis of Pavan, S. 2011). However, the susceptibility gene *Mlo* differs from the S genes like *Tsn1* involved in diseases like SNB and TS and SB in wheat, although this difference is not apparent. Examples of actual use of recessive alleles or mutants of S genes for breeding wheat cultivars with resistance against a necrotroph are limited. In a recent review involving evaluation of the role of NE-S genes in development of resistant cultivars, it was shown that most of the wheat cultivars in Eastern USA, carried durable quantitative SNB resistance and that *Snn*–NE interactions had very little role in providing resistance (Cowger et al., 2020).

If S genes did not play any major role in resistance breeding, it is apparent that either classical R genes or QTLs must be the source of resistance as shown in several studies cited earlier in this review. These resistant cultivars apparently resulted by an unconscious selection of specific R genes or QTLs. Since R genes and QTLs are now known for each of the four necrotrophs under review, one may plan a strategy, where specific R genes or QTLs may be used for developing resistant cultivars. This should be possible because molecular markers associated with these R genes and QTLs are now available.

QTLs using interval mapping and MTAs associated with QTLs using association mapping have also been discovered for almost all nerotrophs and hemi-biotrophs. A list of known S genes, R genes and QTLs for the four diseases under review are listed in Supplementary Tables S1–S3 suggesting that all the three systems operate in necrotrophs as well as hemibiotrophs and can be exploited for imparting resistance against the corresponding diseases.

The distribution of different S genes in wheat cultivars and that of NE genes in the isolates of the pathogen *P. nodorum* causing SNB has also been examined in multiple locations in different parts of the world. The relative frequencies of S genes in wheat cultivars and those of races with three different Tox genes in the pathogen are summarized in Table 3. In some cases, races could be classified based on NE constitution. For instance, eight races for the TS pathogen have been characterized based on their NE constitution (Table 5). A holistic view of the management of four foliar diseases through genetic tools is also given in Figure 4.

Identification of effectors and effector-assisted breeding

It is widely known now that effectors that are produced by a variety of pathogens, targeing host cells causing diseases. Development of tools for identification and utilization of these effectors has consequently been recognized as a new resistance breeding strategy. During the last two decades, hundreds of these effectors have already been identified and genome-wide catalogues of effectors have become available, such that effectoromics has emerged as a new area for research. Effector-assisted breeding has also been shown to be successful for some crops (for a review, see Vleeshouwers and Oliver, 2014). The question therefore is, whether or not the disease resistance of new cultivars can be accurately predicted from the response to effectors of the input germplasm. Genetic analysis of the response to purified effectors allowed the identification of several wheat genetic loci that correspond to regions conferring susceptibility to the disease.

Methods are also available for the identification of effectors in the secretome using conserved domains, which are common among effector families. One such example is the presence of RXLR (Arg-X-Leu-Arg) motif. Other effector motifs, located in the C-terminal and N-terminal regions, include CRN, LysM, RGD, DELD, EAR, RYWT, Y/F/WXC or CFEM. Rapid identification of effectors using RXLR motif allowed development of a catalogue of effectors for *Phytophthora infestans*, which later enabled identification of R genes in potato, Arabidopsis, and lettuce. More recently, WAxR motif has been found in different effectors in races of *Puccinia striiformis* (yellow rust) and other rust races through screening of secretomes. The tool EffectorP 3.0 has also been utilized for the identification of effectors (Sperschneider and Dodds, 2022).

A high-throughput screening procedure for evaluating wheat genotypes through the infiltration of effectors like ToxA into wheat leaves has also been developed and used in Australia (Tan et al., 2014; Vleeshouwers and Oliver, 2014). This method helped in the quick elimination of *Tsn1* from commercial cultivars. As a result, the area sown with ToxA sensitive cultivars was reduced from 30.4% to 16.9% during the three-year period following the use of this screening system (Vleeshouwers and Oliver, 2014; Cockram et al., 2015). However, the application of this method to other pathogens could be more complicated because all three homoeologues of the susceptibility/sensitivity gene must be eliminated to achieve resistance. In addition, undiscovered effectors that can differ between different regional populations may occur in the pathogen. Notwithstanding this, effector-assisted selection can be an effective way for determining weak and environment-dependent QTL (Vleeshouwers and Oliver, 2014; Downie et al., 2018). Moreover, this method enables to dissect components of quantitative resistance, develop diagnostic markers and fine-map susceptibility genes. Such markers can be converted into Kompetitive Allele-Specific PCR (KASP) markers for the rapid selection of desirable alleles. Thus, using effector-assisted selection for developing diagnostic markers can increase the pace of resistance breeding in wheat against necrotrophs (Cockram et al., 2015; Downie et al., 2018).

Necrotrophic effectors from *P. nodorum* (Pn) and toxic proteins from *Z. tritici* have also been utilized to detect R genes/QTLs in wheat (Lebrun et al., 2016). These effector/toxin proteins were first produced in yeast and purified proteins were obtained. These proteins were then delivered to wheat leaves through syringe infiltration. Disease symptoms were then scored after a few days. Screening of 220 elite French wheat cultivars with Pn ToxA 1 and Pn ToxaA3 allowed the identification of cultivars that were insensitive to the three necrotrophic effectors, and only a few were sensitive, suggesting that breeding for field resistance against Pn during 1960-1980 led to the accumulation of insensitive alleles (recessive alleles). The insensitive genotypes can be tested against Pn isolates producing Tox1 and Tox3 effectors, and insensitivity loci

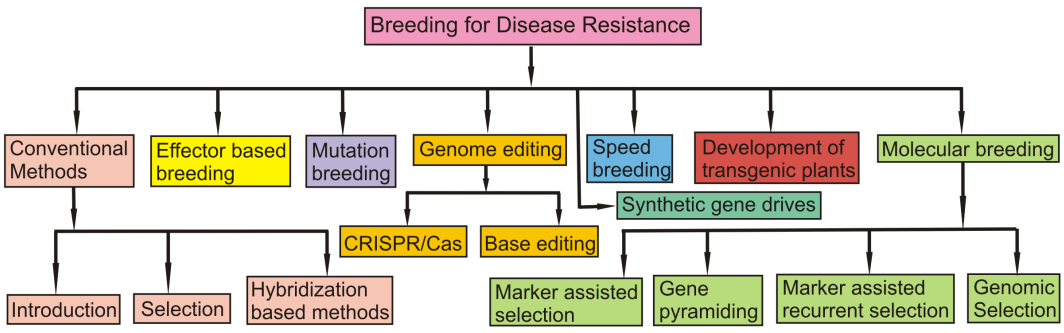

FIGURE 4
A schematic figure which shows a holistic view of the management of four foliar diseases through genetic tools.

can be mapped using GWAS and associated markers can be identified. This type of work will facilitate resistance breeding through MAS (For a review, see Li Q. et al., 2021).

In case of TS in Western Australia also, the elimination of a single effector, PtrToxA and the corresponding S gene *Tsn1*, has a dominating impact in breeding for disease resistance. The availability of ToxA to breeders has had a major impact on cultivar choice and breeding strategies. For *P. nodorum*, three effectors (SnToxA, SnTox1, and SnTox3) have been well characterized. Unlike TS, no one effector has a dominating role. Genetic analysis of various mapping populations and pathogen isolates has shown that different effectors have varying impact, and that epistatic interactions also occur. As a result of these factors, the deployment of these effectors for SNB resistance breeding is complex.

Tan et al. (2015) deleted genes encoding the three effectors in a strain of *P. nodorum* and measured effector activity and disease potential of a triple knockout mutant. The culture filtrate caused necrosis in several cultivars and the strain caused disease, albeit the overall levels are less than in the wild type. Modeling of the field disease resistance scores of cultivars from their reactions to the microbially expressed effectors SnToxA, SnTox1, and SnTox3 is significantly improved by including the response to the triple knockout mutant culture filtrate. This indicated that an additional one or more effectors are secreted into the culture filtrate. It was concluded that the *in vitro*-secreted necrotrophic effectors explain a very large part of the disease response of wheat germplasm and that this method of resistance breeding promises to reduce further the impact of these globally significant diseases. Thus, elimination of genotypes carrying *Tsn1* gene, inducing knockout mutants and introgression of QRLs are the three approaches that can be used for resistance breeding.

QTLs for resistance breeding

For diseases like SNB and TS, generally R genes are not known for breeding. In these cases, resistance is mainly quantitative in nature, governed by QTLs. Most QTLs had a limited effect that was hard to measure precisely and varied significantly from site to site and season to season.

In the late 1920s, A. E. Watkins collected ~7000 landrace cultivars (LCs) of bread wheat (*Triticum aestivum* L.) from 32 different countries around the world. Among these LCs, 826 LCs were viable and could be a valuable source of superior/favorable alleles to enhance disease resistance in wheat. Halder et al. (2019) used a core set of 121 LCs carrying the entire genetic diversity of Watkins collection, and evaluated them for identification of novel sources of resistance against SNB, TS and Fusarium Head Blight (FHB). Response for the three diseases, however, differed in 121 LCs, most of them being either moderately susceptible or susceptible to TS Ptr race 1 (84%) and FHB (96%), whereas a large number of LCs were either resistant or moderately resistant against TS Ptr race 5 (95%) and SNB (54%). Thirteen LCs were identified, which could be a valuable source for multiple resistance to TS Ptr races 1 and 5, and SNB, and another five LCs could be a potential source for FHB resistance.

GWA studies using 118 LCs were also carried out using disease phenotyping score and genotyping data using 8,807 SNPs data leading to identification of 30 significant MTAs (Halder et al., 2019). Ten, five, and five genomic regions were also found to be associated with resistance to TS Ptr race 1, race 5, and SNB, respectively in this study. In addition to *Tsn1*, several novel genomic regions were also identified, which included the following: (i) *Q.Ts1.sdsu-4BS* and *Q.Ts1.sdsu5BS* (TS Ptr race 1) and (ii) *Q.Ts5.sdsu-1BL*, *Q.Ts5.sdsu-2DL*, *Q.Ts5.sdsu-3AL*, and *Q.Ts5.sdsu-6BL* (TS Ptr race 5). These results indicated that these putative genomic regions contain several genes that play an important role in plant defence mechanisms. It was concluded that SNP markers linked to QTLs for SNB and TS resistance along with LCs harboring multiple disease resistance could be useful for future wheat breeding.

From QTLs to genes (R-Genes on 1BS and 5BL)

QTLs controlling response to SNB were initially identified on chromosomes 1BS and 5BL (although QTLs on other chromosomes are also known now). Li D. et al. (2021) conducted a study involving alignment of the genetic map with QTLs on 1BS and 5BS with the reference sequence of wheat. This allowed the identification of R-genes associated with SNB response, although correspondence of R genes with QTL was not shown. Alignment of QTL intervals allowed identification of significant genome rearrangements on 1BS between parents of the DH population (EGA Blanco, Millewa) and the reference sequence of Chinese Spring with subtle rearrangements on 5BL. Nevertheless, annotation of genomic intervals in the reference sequence allowed identification and mapping of 13 R-genes on 1BS and 12 R-genes on 5BL. R-genes discriminated co-located QTL on 1BS into following two distinct but linked loci, both associated with SNB resistance but in one environment only: (i) NRC1a and TFIID mapped in one QTL on 1BS, whereas (ii) RGA and *Snn1* mapped to QTL on 1BS. Similarly, *Tsn1* and *WK35* were mapped in one QTL on 5BL, with NETWORKED 1A and resistance gene analogs (RGA) genes mapped to the linked QTL interval. This study provided new insights on possible biochemical, cellular, and molecular mechanisms responding to SNB infection in different environments and also addressed limitations of using the reference sequence to identify the full complement of functional R-genes in modern varieties.

Multiple disease resistance

Since genotypes with multiple resistance and association among more than one disease have now been reported, it is also possible to plan a breeding programme for transfer of resistance for more than one disease using a single donor, as recommended by Gurung et al. (2014).

Possible molecular breeding approaches

As shown above, resistance against leaf spot diseases caused by necrotrophs in wheat is controlled by three different systems including S genes, R genes and QTLs. The genes belonging to all these three categories are now known for at least three of the four diseases (except for STB, for which S genes are not known; instead SSP genes are known). Markers associated with all these three systems are also known now. The number of markers for desirable genes will certainly be large (at least >20), thus making simple backcross or forward breeding approaches not suitable. Therefore, we recommend the use of either marker assisted recurrent selection (MARS) or QTL-based genomic selection (GS). Other possible molecular approaches include the use of genome editing, base/prime editing, and gene drive. The utility of these molecular approaches has already been demonstrated; these strategies are briefly described in this section.

Marker-assisted recurrent selection

MARS involving more than 20 markers and two or more than two cycles of recombination may be used as a suitable breeding strategy. Such an approach has already been successfully utilized by Rahman et al. (2020) for disease resistance involving crown rot disease in wheat. In this study, 22 markers could be recombined using two recombination cycles.

GS using QTLs and MTAs

In two recent studies, one each in maize and wheat, it has been shown that the prediction accuracy of genomic selection can be improved by using only those markers, which are known to be associated with QTLs or MTAs (Liu et al., 2019; Zaim et al., 2020). This strategy may be used for improvement of resistance against the four pathogens under review. Since we already have a large number of disease-associated markers, a selected set of polymorphic markers may be used in training population for estimation of breeding values, which may then be used for selecting desirable plants in the segregating breeding population.

Genome/base editing and synthetic gene drives

Genome editing, base editing and gene drives are three new approaches, which can also be used for resistance breeding. Several examples are available, where susceptibility genes in the host have been modified using CRISPR/Cas technology (for a review, see Borrelli et al., 2018; Tyagi et al., 2020; Paul et al., 2021; Negi et al., 2022). In wheat also, resistance against powdery mildew has been successfully achieved using this technology (Wang et al., 2014; Zhang et al., 2017). Base editing and prime editing are two other more efficient recent approaches, which have already been used for crop improvement (for a review, see Azameti and Dauda, 2021) and will certainly be used in future for disease resistance in wheat.

More recently, synthetic gene drives are being tried for creating bias in the inheritance of a particular DNA sequence, such that it can be used for increasing the frequency of genes/alleles that may spread and reduce the pathogen populations with virulence genes causing the diseases. The introduced gene/allele puts the pathogen at a disadvantage, and can be made to spread the altered desired trait throughout the population. Many such systems occur naturally, and will facilitate the development of new gene drives using synthetic biology techniques. For resistance breeding, synthetic gene drives may be used to modify either the susceptibility gene of the host or the virulence gene of the pathogen, so that either the host will lose susceptibility or the pathogen will lose virulence. If synthetically modified populations of the pathogen are released in wheat fields, this will soon spread in the pathogen population, and render the wheat cultivar resistant.

Disease management

In integrated management, resistant cultivars may be used along with cultural practices and fungicide application. Since infected seed and straw serve as the primary source of inoculum, seed treatment, crop rotation, and residue management may also prove useful in avoiding an epidemic in disease-prone areas. Also, since SNB infection causes the greatest yield losses at the adult plant stage, resistance screening may also be useful (Francki, 2013).

Conclusions and future perspectives

Disease resistance in plants, including wheat, can be race-specific or race-nonspecific, the latter sometimes also described as adult plant resistance. Both these types of disease resistance are generally controlled by R genes, which have been the subjects of detailed studies. The plant immunity involving these R genes has also been subjected to detailed studies at the molecular level, developing a zig-zag model involving PTI, effector triggered susceptibility (ETS) and effector triggered immunity (ETI) (Jones and Dangl, 2006). During the last >25 years, >300 R genes and several Avr genes have been cloned, thus providing an opportunity to study the interaction between the products of R genes of the host and the corresponding Avr genes in the pathogen at the molecular level (for a review, see Kourelis and van der Hoorn, 2018). However, studies on Avr genes have yet to be undertaken on a war scale to become comparable to those on R genes. In most examples of R genes, the GFG relationship proposed by Flor (1942), Flor (1956) holds good, although gene-for-gene models involving multiple genes have also been suggested (Sasaki, 2000; Fenton et al., 2009). However, disease resistance controlled by the absence (or presence of recessive alleles) of susceptibility/sensitivity genes like SWEET genes for bacterial blight (BB) in rice (Gupta, 2020) and S genes like *Tsn1* in wheat follow an inverse IGFG relationship with corresponding NE genes in the pathogen (Navathe et al., 2020).

This is an area of research on disease resistance, which has witnessed immense activity in recent years. As a result, several S genes in wheat for three of the four important diseases covered in this review, namely SNB, TS and SB and the corresponding NE genes in the form of NE producing genes or *Tox* genes) in the pathogens have been identified. Some of these genes (both S genes in the host and NE genes in the pathogen) have also been cloned and characterized, generating information about the molecular mechanism involved in plant immunity involving these pathosystems. In summary, perhaps only about a dozen NE genes and an equal number of corresponding S genes are now known. In future, more S genes in wheat and other crops and the corresponding NE Tox genes in the pathogens exhibiting IGFG may be discovered; it will be interesting to find out if S genes occur for STB also, although there is little chance, because despite detailed studies already undertaken, no S genes for STB have been discovered so far. It will, therefore, be interesting to find out the reasons for the absence of S gene and the implications of the presence of as many as 22 R (Stb) genes and many SSP genes for STB, both in the host and the pathogen.

We also believe and hope that the subject dealing with S genes following the IGFG model will receive more attention in future. For instance, although much is known about the pathosystems dealing with SNB and TS, the information about IGFG dealing with SB has just started being generated and hardly any work is available on pathosystems involving NEs causing the following diseases: (i) FHB caused by *F. graminearum*; (ii) eyespot caused by *Tapesia yallundae* (syn *Pseudocercosporella herpotrichoides*, W-type anamorph); (iii) STB caused by *Z. tritici* and their corresponding S related gene in the host. We also believe that for diseases like SB caused by hemibiotrophs, GFG and IGFG may operate in parallel. Further studies involving the scoring of allelic states of genes involved in GFG and IGFG models need to be undertaken. In a recent study on spot blotch involving analysis of *Tsn1-ToxA* system following IGFG, we discovered that the wheat genotypes carrying recessive allele of S gene (*tsn1*) could also be susceptible and vice versa. Variation in the SB caused by *ToxA* positive isolates was also noticed (Navathe et al., 2020). This suggests that the relationship between a S gene in the host and the corresponding NE genes in the pathogen is not so simple, offering scope for further detailed investigations.

Another interesting area of future research is to examine interactions and cooperation between dominant R genes, recessive alleles of S genes and QTLs for providing disease resistance. One such study for SB has been planned by the authors of the present review, with the hope that useful information will be generated through such a study, which should prove useful in planning future strategies for breeding cultivars that would be resistant against the four-leaf spot diseases covered in the present review. Use of gene editing and base editing involving CRISPR/Cas for disease resistance will also certainly receive more attention in future.

Author contributions

The subject of this review was conceived by PKG; All authors PKG, NKV, SS and AKJ contributed equally to this review.

Acknowledgments

The Department of Genetics and Plant Breeding, CCS University Meerut (India) primarily provided facilities to PG and NV for undertaking this work. NKV also received support from SERB-DST, India in the form of a Start UP Research Grant (SRG/2020/000091). PKG also held honorary positions at Murdoch University Australia and Borlaug Institute for South Asia (BISA). AKJ worked at CIMMYT, NASC Complex, DPS Marg, New Delhi 110012, India, and Borlaug Institute for South Asia (BISA), NASC Complex, DPS Marg, New Delhi 110018, India.

Conflict of interest

The authors declare that the research was conducted in the absence of any commercial or financial relationships that could be construed as a potential conflict of interest.

Publisher's note

Supplementary material

The Supplementary Material for this article can be found online at: https://www.frontiersin.org/articles/10.3389/fpls.2023.1023824/full#supplementary-material

References

Abeysekara, N. S., Faris, J. D., Chao, S., McClean, P. E., and Friesen, T. L. (2012). Whole-genome QTL analysis of stagonospora nodorum blotch resistance and validation of the SnTox4-*Snn4* interaction in hexaploid wheat. *Phytopathology* 102, 94–104. doi: 10.1094/PHYTO-02-11-0040

Adhikari, T. B., Jackson, E. W., Gurung, S., Hansen, J. M., and Bonman, J. M. (2011). Association mapping of quantitative resistance to *Phaeosphaeria nodorum* in spring wheat landraces from the USDA national small grains collection. *Phytopathology* 101, 1301–1310. doi: 10.1094/PHYTO-03-11-0076

Adhikari, T. B., Mamidi, S., Gurung, S., and Bonman, J. M. (2015). Mapping of new quantitative trait loci (QTL) for resistance to septoria tritici blotch in spring wheat (*Triticum aestivum* l.). *Euphytica* 205, 699–706. doi: 10.1007/s10681-015-1393-4

Aggarwal, R., Agarwal, S., Sharma, S., Gurjar, M. S., Bashyal, B. M., Rao, A. R., et al. (2022). Whole-genome sequence analysis of *Bipolaris sorokiniana* infecting wheat in India and characterization of *ToxA* gene in different isolates as pathogenicity determinants. *3 Biotech.* 12, 151. doi: 10.1007/s13205-022-03213-3

Aggarwal, R., Sharma, S., Singh, K., Gurjar, M. S., Saharan, M. S., Gupta, S., et al. (2019). First draft genome sequence of wheat spot blotch pathogen *Bipolaris sorokiniana* BS_112 from India, obtained using hybrid assembly. *Microbiol. Res. Announc.* 8, e00308–e00319. doi: 10.1128/MRA.00308-19

Aguilar, V., Stamp, P., Winzeler, M., Winzeler, H., Schachermayr, G., Keller, B., et al. (2005). Inheritance of field resistance to stagonospora nodorum leaf and glume blotch and correlations with other morphological traits in hexaploid wheat (*Triticum aestivum* l.). *Theor. Appl. Genet.* 111, 325–336. doi: 10.1007/s00122-005-2025-5

Ali, S., and Francl, L. J. (2002). Race structure of *Pyrenophora tritici*-repentis isolates obtained from wheat in south America. *Plant Prot. Sci.* 38, 302–304. doi: 10.17221/10473-PPS

Ali, S., and Francl, L. J. (2003). Population race structure of *Pyrenophora tritici-repentis* prevalent on wheat and noncereal grasses in the great plains. *Plant Dis.* 87, 418–422. doi: 10.1094/PDIS.2003.87.4.418

Ali, S., Singh, P. K., McMullen, M. P., Mergoum, M., and Adhikari, T. B. (2008). Resistance to multiple leaf spot diseases in wheat. *Euphytica* 159, 167–179. doi: 10.1007/s10681-007-9469-4

Al-Sadi, A. M. (2021). *Bipolaris sorokiniana*-induced black point, common root rot, and spot blotch diseases of wheat: a review. *Front. Cell Infect. Microbiol.* 11. doi: 10.3389/fcimb.2021.584899

Arseniuk, E., Czembor, P. C., Czaplicki, A., Song, Q., Cregan, P. B., Hoffman, D. L., et al. (2004). QTL controlling partial resistance to stagonospora nodorum leaf blotch in winter wheat cultivar alba. *Euphytica* 137, 225–231. doi: 10.1023/B:EUPH.0000041589.47544.de

Azameti, M. K., and Dauda, W. P. (2021). Base editing in plants: Applications, challenges, and future prospects. *Front. Plant Sci.* 12. doi: 10.3389/fpls.2021.664997

Ballance, G. M., Lamari, L., and Bernier, C. C. (1989). Purification and characterization of a host-selective necrosis toxin from *Pyrenophora tritici-repentis*. *Physiol. Mol. Plant Pathol.* 35, 203–213. doi: 10.1016/0885-5765(89)90051-9

Ballance, G. M., Lamari, L., Kowatsch, R., and Bernier, C. C. (1996). Cloning, expression, and occurrence of the gene encoding the ptr necrosis toxin from *Pyrenophora tritici-repentis*. *Mol. Plant Pathol.* doi: 10.1007/978-94-011-5218-1_21

Ballance, G. M., Lamari, L., Kowatsch, R., and Bernier, C. C. (1998). "The ptr necrosis toxin and necrosis toxin gene from pyrenophora tritici-repentis," in *Molecular genetics of host-specific toxins in plant disease*, vol. 13. Eds. K. Kohmoto and O. C. Yoder. (Netherland: Springer), 177–185.

Ben M'Barek, S., Cordewener, J. H., Tabib Ghaffary, S. M., van der Lee, T. A., Liu, Z., Gohari, A. M., et al. (2015). FPLC and liquid-chromatography mass spectrometry identify candidate necrosis-inducing proteins from culture filtrates of the fungal wheat pathogen *Zymoseptoria tritici*. *Fungal Genet. Biol.* 79, 54–62. doi: 10.1016/j.fgb.2015.03.015

Bertucci, M., Brown-Guedira, G., Murphy, J. P., and Cowger, C. (2014). Genes conferring sensitivity to *Stagonospora nodorum* necrotrophic effectors in stagonospora nodorum blotch-susceptible U.S. wheat cultivars. *Plant Dis.* 98, 746–753. doi: 10.1094/PDIS-08-13-0820-RE

Bhathal, J. S., Loughman, R., and Speijers, J. (2003). Yield reduction in wheat in relation to leaf disease from yellow (tan) spot and septoria nodorum blotch. *Eur. J. Plant Pathol.* 109, 435–443. doi: 10.1023/A:1024277420773

Blixt, E., Olson, Å., Högberg, N., Djurle, A., and Yuen, J. (2008). Mating type distribution and genetic structure are consistent with sexual recombination in the Swedish population of *Phaeosphaeria nodorum*. *Plant Pathol.* 57, 634–641. doi: 10.1111/j.1365-3059.2008.01826.x

Borrelli, V. M. G., Brambilla, V., Rogowsky, P., Marocco, A., and Lanubile, A. (2018). The enhancement of plant disease resistance using CRISPR/Cas9 technology. *Front. Plant Sci.* 9. doi: 10.3389/fpls.2018.01245

Brading, P. A., Verstappen, E. C. P., Kema, G. H. J., and Brown, J. K. M. (2002). A gene-for-gene relationship between wheat and *Mycosphaerella graminicola*, the *Septoria tritici blotch pathogen*. *Phytopathology* 92, 439–445. doi: 10.1094/PHYTO.2002.92.4.439

Brown, J. K., Chartrain, L., Lasserre-Zuber, P., and Saintenac, C. (2015). Genetics of resistance to *Zymoseptoria tritici* and applications to wheat breeding. *Fungal Genet. Biol.* 79, 33–41. doi: 10.1016/j.fgb.2015.04.017

Chand, R., Navathe, S., and Sharma, S. (2021). "Advances in breeding techniques for durable resistance to spot blotch in cereals," in *Achieving durable disease resistance in cereals* (Burleigh Dodds Series in Agricultural Science (London: Burleigh Dodds Science Publishing), 435–474. doi: 10.19103/AS.2021.0092.18

Chartrain, L., Brading, P. A., and Brown, J. K. M. (2005c). Presence of the Stb6 gene for resistance to septoria tritici blotch (*Mycosphaerella graminicola*) in cultivars used in wheat-breeding programmes worldwide. *Plant Pathol.* 54, 134–143. doi: 10.1111/j.1365-3059.2005.01164.x

Chu, C.-G., Chao, S., Friesen, T. L., Faris, J. D., Zhong, S., and Xu, S. S. (2010). Identification of novel tan spot resistance QTLs using an SSR-based linkage map of tetraploid wheat. *Mol. Breed.* 25, 327–338. doi: 10.1007/s11032-009-9335-2

Ciuffetti, L. M., Manning, V. A., Pandelova, I., Betts, M. F., and Martinez, J. P. (2010). Host-selective toxins. ptr ToxA and ptr ToxB, as necrotrophic effectors in the *Pyrenophora tritici-repentis*-wheat interaction. *New Phytol.* 187, 911–919. doi: 10.1111/j.1469-8137.2010.03362.x

Ciuffetti, L. M., Tuori, R. P., and Gaventa, J. M. (1997). A single gene encodes a selective toxin causal to the development of tan spot of wheat. *Plant Cell* 9, 135–144. doi: 10.1105/tpc.9.2.135

Cockram, J., Scuderi, A., Barber, T., Furuki, E., Gardner, K. A., Gosman, N., et al. (2015). Fine-mapping the wheat *Snn1* locus conferring sensitivity to the *Parastagonospora nodorum* necrotrophic effector SnTox1 using an eight founder multiparent advanced generation inter-cross population. *G3* 5, 2257–2266. doi: 10.1534/g3.115.021584

Conner, R. L. (1990). Interrelationship of cultivar reactions to common root rot, black point, and spot blotch in spring wheat. *Plant Dis.* 74, 224–227. doi: 10.1094/PD-74-0224

Corsi, B., Percival-Alwyn, L., Downie, R. C., Venturini, L., Iagallo, E. M., Campos Mantello, C. C., et al. (2020). Genetic analysis of wheat sensitivity to the ToxB fungal effector from *Pyrenophora tritici-repentis*, the causal agent of tan spot. *Theor. Appl. Genet.* 133, 935–950. doi: 10.1007/s00122-019-03517-8

Rivera-Burgos,L. A., Brown-Guedira,G., Johnson,J., Mergoum,M., and Cowger, C. (2022). Accounting for heading date gene effects allows detection of small-effect QTL associated with resistance to septoria nodorum blotch in wheat. *PloS One* 17, e0268546. doi: 10.1371/journal.pone.0268546

Cowger, C., Ward, B., Brown-Guedira, G., and Brown, J. K. M. (2020). Role of effector-sensitivity gene interactions and durability of quantitative resistance to septoria nodorum blotch in eastern U.S. wheat. *Front. Plant Sci.* 11. doi: 10.3389/fpls.2020.00155

Croll, D., and McDonald, B. A. (2012). The accessory genome as a cradle for adaptive evolution in pathogens. *PloS Pathog.* 8, e1002608. doi: 10.1371/journal.ppat.1002608

Crook, A. D., Friesen, T. L., Liu, Z. H., Ojiambo, P. S., and Cowger, C. (2012). Novel necrotrophic effectors from *Stagonospora nodorum* and corresponding host sensitivities in winter wheat germplasm in the southeastern united states. *Phytopathology* 102, 498–505. doi: 10.1094/PHYTO-08-11-0238

Czembor, P. C., Arseniuk, E., Czaplicki, A., Song, Q. J., Cregan, P. B., and Ueng, P. P. (2003). QTL mapping of partial resistance in winter wheat to stagonospora nodorum blotch. *Genome* 46, 546–554. doi: 10.1139/g03-036

Czembor, P. C., Arseniuk, E., Radecka-Janusik, M., Piechota, U., and Słowacki, P. (2019). Quantitative trait loci analysis of adult plant resistance to parastagonospora nodorum blotch in winter wheat cv. liwilla (*Triticum aestivum* l.). *Eur. J. Plant Pathol.* 155, 1001–1016. doi: 10.1007/s10658-019-01829-5

Dastur, J. F. (1942). Notes on some fungi isolated from "black point" affected kernels in the central provinces. *Ind. J. Agric. Sci.* 12, 731–742.

Desmazieres, J. B. H. J. (1842). Neuvieme notice sur quelques plantes cryptogames, la plupart inedites, recemment decouvertes en France, et que vont paraitre en nature dans la collection publiee par l'auteur. *Ann. Des. Sci. Nat. Bot. Ser.* 2, 91–107.

Dinglasan, E. G., Godwin, I. D., Phan, H. T. T., Tan, K.-C., Platz, G. J., and Hickey, L. T. (2017). Vavilov wheat accessions provide useful sources of resistance to tan spot (syn. yellow spot) of wheat. *Plant Pathol.* 67, 1076–1087. doi: 10.1111/ppa.12822

Dinglasan, E. G., Singh, D., Shankar, M., Afanasenko, O., Platz, G., Godwin, I. D., et al. (2019). Discovering new alleles for yellow spot resistance in the vavilov wheat collection. *Theor. Appl. Genet.* 132, 149–162. doi: 10.1007/s00122-018-3204-5

Downie, R. C., Bouvet, L., Furuki, E., Gosman, N., Gardner, K. A., Mackay, I. J., et al. (2018). Assessing European wheat sensitivities to *Parastagonospora nodorum* necrotrophic effectors and fine-mapping the *Snn3-B1* locus conferring sensitivity to the effector SnTox3. *Front. Plant Sci.* 9. doi: 10.3389/fpls.2018.00881

Downie, R. C., Lin, M., Corsi, B., Ficke, A., Lillemo, M., Oliver, R. P., et al. (2021). Septoria nodorum blotch of wheat: disease management and resistance breeding in the face of shifting disease dynamics and a changing environment. *Phytopathology* 11, 906–920. doi: 10.1094/PHYTO-07-20-0280-RVW

Drechsler, C. (1923). Some graminicolons species of *Helminthosporium*. *Int. J. Agric. Res.* 24, 614–670.

Effertz, R. J., Meinhardt, S. W., Anderson, J. A., Jordahl, J. G., and Francl, L. J. (2002). Identification of a chlorosis-inducing toxin from *Pyrenophora tritici*-repentis and the chromosomal location of an insensitivity locus in wheat. *Phytopathology* 92, 527–533. doi: 10.1094/PHYTO.2002.92.5.527

Eyal, Z. (1973). Physiologic specialization of *Septoria tritici*. *Phytopathology* 63, 1087–1091. doi: 10.1094/Phyto-63-1087

Eyal, Z., Scharen, A. L., Prescott, J. M., and van Ginkel, M. (1987). *The septoria diseases of wheat: Concepts and methods of disease management* (Mexico: CIMMYT).

Faris, J. D., and Friesen, T. L. (2020). Plant genes hijacked by necrotrophic fungal pathogens. *Curr. Opin. Plant Biol.* 56, 74–80. doi: 10.1016/j.pbi.2020.04.003

Faris, J. D., Liu, Z., and Xu, S. S. (2013). Genetics of tan spot resistance in wheat. *Theor. Appl. Genet.* 126, 2197–2217. doi: 10.1007/s00122-013-2157-y

Faris, J. D., Overlander, M. E., Kariyawasam, G. K., Carter, A., Xu, S. S., and Liu, Z. (2020). Identification of a major dominant gene for race-nonspecific tan spot resistance in wild emmer wheat. *Theor. Appl. Genet.* 133, 829–841. doi: 10.1007/s00122-019-03509-8

Faris, J. D., Zhang, Z., Lu, H. J., Lu, S. W., Reddy, L., Cloutier, S., et al. (2010). A unique wheat disease resistance-like gene governs effector-triggered susceptibility to necrotrophic pathogens. *Proc. Nat'l. Acad. Sci. U.S.A.* 107, 13544–13549. doi: 10.1073/pnas.1004090107

Fenton, A., Antonovics, J., and Brockhurst, M. A. (2009). Inverse-gene-for-gene infection genetics and coevolutionary dynamics. *Am. Nat.* 174, E230–E242. doi: 10.1086/645087

Ficke, A., Cowger, C., Bergstrom, G., and Brodal, G. (2018). Understanding yield loss and pathogen biology to improve disease management: Septoria nodorum blotch -a case study in wheat. *Plant Dis.* 102, 696–707. doi: 10.1094/PDIS-09-17-1375-FE

Figueroa, M., Hammond-Kosack, K. E., and Solomon, P. S. (2018). A review of wheat diseases: a field perspective. *Mol. Plant Pathol.* 19, 1523–1536. doi: 10.1111/mpp.12618

Flor, H. H. (1942). Inheritance of pathogenicity in melampsora lini. *Phytopathology* 32, 653–669.

Flor, H. H. (1956). The complementary genic systems in flax and flax rust. *Adv. Genet.* 8, 29–54. doi: 10.1016/S0065-2660(08)60498-8

Fones, H., and Gurr, S. (2015). The impact of septoria tritici blotch disease on wheat: an EU perspective. *Fungal Genet. Biol.* 79, 3–7. doi: 10.1016/j.fgb.2015.04.004

Francki, M. G. (2013). Improving *Stagonospora nodorum* resistance in wheat: a review. *Crop Sci.* 53, 355–365. doi: 10.2135/cropsci2012.06.0347

Francki, M. G., Shankar, M., Walker, E., Loughman, R., Golzar, H., and Ohm, H. (2011). New quantitative trait loci in wheat for flag leaf resistance to stagonospora nodorum blotch. *Phytopathology* 101, 1278–1284. doi: 10.1094/PHYTO-02-11-0054

Francki, M. G., Walker, E., Li, D. A., and Forrest, K. (2018). High-density SNP mapping reveals closely linked QTL for resistance to stagonospora nodorum blotch (SNB) in flag leaf and glume of hexaploid wheat. *Genome* 61, 145–149. doi: 10.1139/gen-2017-0203

Francki, M. G., Walker, E., McMullan, C. J., and Morris, W. G. (2020). Multi-location evaluation of global wheat lines reveal multiple QTL for adult plant resistance to septoria nodorum blotch (SNB) detected in specific environments and in response to different isolates. *Front. Plant Sci.* 11. doi: 10.3389/fpls.2020.00771

Friesen, T. L., Ali, S., Klein, K. K., and Rasmussen, J. (2005). Population genetic analysis of a global collection of *Pyrenophora tritici-repentis*, causal agent of tan spot of wheat. *Phytopathology* 95, 1144–1150. doi: 10.1094/PHYTO-95-1144

Friesen, T. L., Chu, C. G., Liu, Z. H., Xu, S. S., Halley, S., and Faris, J. D. (2009). Host-selective toxins produced by *Stagonospora nodorum* confer disease susceptibility in adult wheat plants under field conditions. *Theor. Appl. Genet.* 118, 1489–1497. doi: 10.1007/s00122-009-0997-2

Friesen, T. L., and Faris, J. D. (2021). Characterization of effector-target interactions in necrotrophic pathosystems reveals trends and variation in host manipulation. *Ann. Rev. Phytopathol.* 59, 77–98. doi: 10.1146/annurev-phyto-120320-012807

Friesen, T. L., Holmes, D. J., Bowden, R. L., and Faris, J. D. (2018). *ToxA* is present in the U.S. *Bipolaris sorokiniana* population and is a significant virulence factor on wheat harboring *Tsn1*. *Plant Dis.* 102, 2446–2452. doi: 10.1094/PDIS-03-18-0521-RE

Friesen, T. L., Meinhardt, S. W., and Faris, J. D. (2007). The *Stagonospora nodorum*-wheat pathosystem involves multiple proteinaceous host-selective toxins and corresponding host sensitivity genes that interact in an inverse gene-for-gene manner. *Plant J.* 51, 681–692. doi: 10.1111/j.1365-313X.2007.03166.x

Friesen, T. L., Stukenbrock, E. H., Liu, Z., Meinhardt, S., Ling, H., Faris, J. D., et al. (2006). Emergence of a new disease as a result of interspecific virulence gene transfer. *Nat. Genet.* 38, 953–956. doi: 10.1038/ng1839

Friesen, T. L., Zhang, Z., Solomon, P. S., Oliver, R. P., and Faris, J. D. (2008). Characterization of the interaction of a novel *Stagonospora nodorum* host-selective toxin with a wheat susceptibility gene. *Plant Physiol.* 146, 682–693. doi: 10.1104/pp.107.108761

Galagedara, N., Liu, Y., Fiedler, J., Shi, G., Chiao, S., Xu, S. S., et al. (2020). Genome-wide association mapping of tan spot resistance in a worldwide collection of durum wheat. *Theor. Appl. Genet.* 133, 2227–2237. doi: 10.1007/s00122-020-03593-1

Gao, Y., Liu, Z., Faris, J. D., Richards, J., Brueggeman, R. S., Li, X., et al. (2016). Validation of genome-wide association studies as a tool to identify virulence factors in *Parastagonospora nodorum*. *Phytopathology* 106, 1177–1185. doi: 10.1094/PHYTO-02-16-0113-FI

Ghaderi, F., Sharifnabi, B., Javan-Nikkhah, M., Brunner, P. C., and McDonald, B. A. (2020). SnToxA, SnTox1, and SnTox3 originated in *Parastagonospora nodorum* in the fertile crescent. *Plant Pathol.* 69, 1482–1491. doi: 10.1111/ppa.13233

Gilbert, B. M., and Wolpert, T. J. (2013). Characterization of the LOV1-mediated, victorin-induced, cell-death response with virus-induced gene silencing. *Mol. Plant Microbe Interact.* 26, 903–917. doi: 10.1094/MPMI-01-13-0014-R

Gohari, A. M. (2015). *Identification and functional characterization of putative virulence factors in the fungal wheat pathogen zymoseptoria tritici. [PhD thesis]* (Wageningen: Wageningen University).

Gonzalez-Hernandez, J. L., Singh, P. K., Mergoum, M., Adhikari, T. B., Kianian, S. F., Simsek, S., et al. (2009). A quantitative trait locus on chromosome 5B controls resistance of *Triticum turgidum* (L.) var. diccocoides to stagonospora nodorum blotch. *Euphytica* 166, 199. doi: 10.1007/s10681-008-9825-z

Guo, J., Shi, G., and Liu, Z. (2018). Characterizing virulence of the *Pyrenophora tritici-repentis* isolates lacking both *ToxA* and *ToxB* genes. *Pathogens* 7, 74. doi: 10.3390/pathogens7030074

Gupta, P. K. (2020). *SWEET* genes for disease resistance in plants. *Trends Genet.* 36, 901–904. doi: 10.1016/j.tig.2020.08.007

Gupta, P. K., Chand, R., Vasistha, N. K., Pandey, S. P., Kumar, U., Mishra, V. K., et al. (2018a). Spot blotch disease of wheat: the current status of research on genetics and breeding. *Plant Pathol.* 67, 508–531. doi: 10.1111/ppa.12781

Gupta, P. K., Vasistha, N. K., Aggarwal, R., and Joshi, A. K. (2018b). Biology of *B. sorokiniana* (syn. *Cochliobolus sativus*) in genomics era. *J. Plant Biochem. Biotechnol.* 27, 123–138. doi: 10.1007/s13562-017-0426-6

Gurung, S., Bonman, J. M., Ali, S., Patel, J., Myrfield, M., Mergoum, M., et al. (2009). New and diverse sources of multiple disease resistance in wheat. *Crop Sci.* 49, 1655–1666. doi: 10.2135/cropsci2008.10.0633

Gurung, S., Mamidi, S., Bonman, J. M., Xiong, M., Brown-Guedira, G., and Adhikari, T. B. (2014). Genome-wide association study reveals novel quantitative trait loci associated with resistance to multiple leaf spot diseases of spring wheat. *PloS One* 9, e108179. doi: 10.1371/journal.pone.0108179

Hafez, M., Gourlie, R., Despins, T., Turkington, T. K., Friesen, T. L., and Aboukhaddour, R. (2020). *Parastagonospora nodorum* and related species in Western Canada: genetic variability and effector genes. *Phytopathology* 110, 1946–1958. doi: 10.1094/PHYTO-05-20-0207-R

Halder, J., Zhang, J., Ali, S., Sidhu, J. S., Gill, H. S., Talukder, S. K., et al. (2019). Mining and genomic characterization of resistance to tan spot, stagonospora nodorum blotch (SNB), and fusarium head blight in Watkins core collection of wheat landraces. *BMC Plant Biol.* 19, 480. doi: 10.1186/s12870-019-2093-3

Hane, J. K., Lowe, R. G., Solomon, P. S., Tan, K. C., Schoch, C. L., Spatafora, J. W., et al. (2007). *Dothideomycete* plant interactions illuminated by genome sequencing and EST analysis of the wheat pathogen *Stagonospora nodorum*. *Plant Cell* 19, 3347–3368. doi: 10.1105/tpc.107.052829

Hehir, J. G., Connolly, C., O'Driscoll, A., Lynch, J. P., Spink, J., Brown, J. K. M., et al. (2018). Temporal and spatial field evaluations highlight the importance of the presymptomatic phase in supporting strong partial resistance in *Triticum aestivum* against *Zymoseptoria tritici*. *Plant Pathol.* 67, 573–583. doi: 10.1111/ppa.12780

Jighly, A., Alagu, M., Makdis, F., Singh, M., Singh, S., Emebiri, L. C., et al. (2016). Genomic regions conferring resistance to multiple fungal pathogens in synthetic hexaploid wheat. *Mol. Breed.* 36, 127. doi: 10.1007/s11032-016-0541-4

Jones, J. D., and Dangl, J. L. (2006). The plant immune system. *Nature* 444, 323–329. doi: 10.1038/nature05286

Juliana, P., Singh, R. P., Singh, P. K., Poland, J. A., Bergstrom, G. C., Huerta-Espino, J., et al. (2018). Genome-wide association mapping for resistance to leaf rust, stripe rust and tan spot in wheat reveals potential candidate genes. *Theor. Appl. Genet.* 131, 1405–1422. doi: 10.1007/s00122-018-3086-6

Kader, K. A., Hunger, R. M., Sreedharan, A., and Marek, S. M. (2022). Races, disease symptoms and genetic variability in *Pyrenophora tritici-repentis* isolates from Oklahoma that cause tan spot of winter wheat. *Cereal Res. Commun.* 50, 273–280. doi: 10.1007/s42976-021-00175-9

Kariyawasam, G. K., Richards, J. K., Wyatt, N. A., Running, K., Xu, S. S., Liu, Z., et al. (2021). The *Parastagonospora nodorum* necrotrophic effector SnTox5 targets the wheat gene *Snn5* and facilitates entry into the leaf mesophyll. *New Phytol.* 233, 409–426. doi: 10.1111/nph.17602

Karki, S. J., Reilly, A., Zhou, B., Mascarello, M., Burke, J., Doohan, F., et al. (2021). A small secreted protein from *Zymoseptoria tritici* interacts with a wheat E3 ubiquitin ligase to promote disease. *J. Exp. Bot.* 72, 733–746. doi: 10.1093/jxb/eraa489

Kaur, B., Bhatia, D., and Mavi, G. S. (2021). Eighty years of gene-for-gene relationship and its applications in identification and utilization of r genes. *J. Genet.* 100, 1–17. doi: 10.1007/s12041-021-01300-7

Kema, G. H. J., Gohari, A. M., Aouini, L., Gibriel, H. A. Y., Ware, S. B., van den Bosch, F., et al. (2018). Stress and sexual reproduction affect the dynamics of the wheat pathogen effector *AvrStb6* and *strobilurin* resistance. *Nat. Genet.* 50, 375–380. doi: 10.1038/s41588-018-0052-9

Kema, G. H. J., Verstappen, E. C. P., and Waalwijk, C. (2000). Avirulence in the wheat septoria tritici leaf blotch fungus *Mycosphaerella graminicola* is controlled by a single locus. *Mol. Plant Microbe Interact.* 13, 1375–1379. doi: 10.1094/MPMI.2000.13.12

Kema, G. H. J., Yu, D., Rijkenberg, F. H. J., Shaw, M. W., and Baayen, R. P. (1996). Histology of the pathogenesis of *Mycosphaerella graminicola* in wheat. *Phytopathology* 86, 777–786. doi: 10.1094/Phyto-86-777

Keon, J., Antoniw, J., Carzaniga, R., Deller, S., Ward, J. L., Baker, J. M., et al. (2007). Transcriptional adaptation of *Mycosphaerella graminicola* to programmed cell death (PCD) of its susceptible wheat host. *Mol. Plant Microbe Interact.* 20, 178–193. doi: 10.1094/MPMI-20-2-0178

Kettles, G. J., Bayon, C., Canning, G., Rudd, J. J., and Kanyuka, K. (2017). Apoplastic recognition of multiple candidate effectors from the wheat pathogen *Zymoseptoria tritici* in the nonhost plant *Nicotiana benthamiana*. *New Phytol.* 213, 338–350. doi: 10.1111/nph.14215

Kettles, G. J., and Kanyuka, K. (2016). Dissecting the molecular interactions between wheat and the fungal pathogen *Zymoseptoria tritici*. *Front. Plant Sci.* 7. doi: 10.3389/fpls.2016.00508

King, J. E., Cook, R. J., and Melville, S. C. (1983). A review of septoria diseases of wheat and barley. *Ann. Appl. Biol.* 103, 345–373. doi: 10.1111/j.1744-7348.1983.tb02773.x

Kokhmetova, A., Sehgal, D., Ali, S., Atishova, M., Kumarbayeva, M., Leonova, I., et al. (2020). Genome-wide association study of tan spot resistance in a hexaploid wheat collection from Kazakhstan. *Front. Genet.* 11. doi: 10.3389/fgene.2020.581214

Kollers, S., Rodemann, B., Ling, J., Korzun, V., Ebmeyer, E., Argillier, O., et al. (2014). Genome-wide association mapping of tan spot resistance (*Pyrenophora tritici-repentis*) in European winter wheat. *Mol. Breed.* 34, 363–371. doi: 10.1007/s11032-014-0039-x

Korte, A., and Farlow, A. (2013). The advantages and limitations of trait analysis with GWAS: a review. *Plant Methods* 9, 29. doi: 10.1186/1746-4811-9-29

Kourelis, J., and van der Hoorn, R. A. L. (2018). Defended to the nines: 25 years of resistance gene cloning identifies nine mechanisms for r protein function. *Plant Cell* 30, 285–299. doi: 10.1105/tpc.17.00579

Kumar, S., Roder, M. S., Tripathi, S. B., Kumar, S., Chand, R., Joshi, A. K., et al. (2015). Mendelization and fine mapping of a bread wheat spot blotch disease resistance QTL. *Mol. Breed.* 35, 218. doi: 10.1007/s11032-015-0411-5

Lamari, L., Gilbert, J., and Tekauz, A. (1998). Race differentiation in *Pyrenophora tritici-repentis* and survey of physiologic variation in western Canada. *Can. J. Plant Pathol.* 20, 396–400. doi: 10.1080/07060669809500410

Lamari, L., Strelkov, S. E., Yahyaoui, A., Orabi, J., and Smith, R. B. (2003). The identification of two new races of *Pyrenophora tritici-repentis* from the host center of diversity confirms a one-to-one relationship in tan spot of wheat. *Phytopathology* 93, 391–396. doi: 10.1094/PHYTO.2003.93.4.391

Lebrun, M. H., Langin, T., Kroj, T., Cockram, J., Oliver, R., Kema, G., et al (2016). "Wheat effector assisted breeding for resistance to fungal pathogens (WEAB)," in *(JJC)-11emes rencontres de phytopathologie-mycologie, societe française de phytopathologie (SFP)*, vol. 49Ed. J.J. Chevaugeon

Leng, Y., Zhao, M., Fiedler, J., Dreiseitl, A., Chao, S., Li, X., et al. (2020). Molecular mapping of loci conferring susceptibility to spot blotch and resistance to powdery mildew in barley using the sequencing-based genotyping approach. *Phytopathology* 110, 440–446. doi: 10.1094/PHYTO-08-19-0292-R

Leng, Y., Zhao, M., Wang, R., Steffenson, B. J., Brueggeman, R. S., and Zhong, S. (2018). The gene conferring susceptibility to spot blotch caused by *Cochliobolus sativus* is located at the mla locus in barley cultivar bowman. *Theor. Appl. Genet.* 131, 1531–1539. doi: 10.1007/s00122-018-3095-5

Li, D., Walker, E., and Francki, M. (2021). Genes associated with foliar resistance to septoria nodorum blotch of hexaploid wheat (*Triticum aestivum l.*). *In. J. Mol. Sci.* 22, 5580. doi: 10.3390/ijms22115580

Li, Q., Wang, B., Yu, J., and Dou, D. (2021). Pathogen-informed breeding for crop disease resistance. *J. Integr. Plant Biol.* 63, 305–311. doi: 10.1111/jipb.13029

Lillemo, M., Joshi, A. K., Prasad, R., Chand, R., and Singh, R. P. (2013). QTL for spot blotch resistance in bread wheat line Saar co-locate to the biotrophic disease resistance loci *Lr34* and *Lr46*. *Theor. Appl. Genet.* 126, 711–719. doi: 10.1007/s00122-012-2012-6

Lin, M., Corsi, B., Ficke, A., Tan, K. C., Cockram, J., and Lillemo, M. (2020a). Genetic mapping using a wheat multi-founder population reveals a locus on chromosome 2A controlling resistance to both leaf and glume blotch caused by the necrotrophic fungal pathogen *Parastagonospora nodorum*. *Theor. Appl. Genet.* 133, 785–808. doi: 10.1007/s00122-019-03507-w

Lin, M., Ficke, A., Cockram, J., and Lillemo, M. (2020b). Genetic structure of the Norwegian *Parastagonospora nodorum* population. *Front. Microbiol.* 11. doi: 10.3389/fmicb.2020.01280

Lin, M., Ficke, A., Dieseth, J. A., and Lillemo, M. (2022). Genome-wide association mapping of septoria nodorum blotch resistance in Nordic winter and spring wheat collections. *Theor. Appl. Genet.* 135, 4169–4182. doi: 10.1007/s00122-022-04210-z

Lin, M., and Lillemo, M. (2021). "Advances in genetic mapping of septoria nodorum blotch resistance in wheat and applications in resistance breeding" *Achieving durable disease resistance in cereals*", in *Burleigh Dodds Series in Agricultural Science*, (Cambridge: Burleigh Dodds Science Publishing)

Lin, M., Stadlmeier, M., Mohler, V., Tan, K. C., Ficke, A., Cockram, J., et al. (2021). Identification and cross-validation of genetic loci conferring resistance to septoria nodorum blotch using a German multi-founder winter wheat population. *Theor. Appl. Genet.* 134, 125–142. doi: 10.1007/s00122-020-03686-x

Liu, Z. H., El-Basyoni, I., Kariyawasam, G., Zhang, G., Fritz, A., Hansen, J., et al. (2015). Evaluation and association mapping of resistance to tan spot and stagonospora nodorum blotch in adapted winter wheat germplasm. *Plant Dis.* 99, 1333–1341. doi: 10.1094/PDIS-11-14-1131-RE

Liu, Z. H., Faris, J. D., Oliver, R. P., Tan, K. C., Solomon, P. S., McDonald, M. C., et al. (2009). SnTox3 acts in effector triggered susceptibility to induce disease on wheat carrying the *Snn3* gene. *PloS Pathog.* 5, e1000581. doi: 10.1371/journal.ppat.1000581

Liu, Z. H., Friesen, T. L., Rasmussen, J. B., Ali, S., Meinhardt, S. W., and Faris, J. D. (2004a). Quantitative trait loci analysis and mapping of seedling resistance to stagonospora nodorum leaf blotch in wheat. *Phytopathology* 94, 1061–1067. doi: 10.1094/PHYTO.2004.94.10.1061

Liu, Z. H., Gao, Y., Kim, Y. M., Faris, J. D., Shelver, W. L., de Wit, P.J.G.M, et al. (2016). SnTox1, a *Parastagonospora nodorum* necrotrophic effector, is a dual-function protein that facilitates infection while protecting from wheat-produced chitinases. *New Phytol.* 211, 1052–1064. doi: 10.1111/nph.13959

Liu, Y., Salsman, E., Wang, R., Galagedara, N., Zhang, Q., Fiedler, J. D., et al. (2020b). Meta-QTL analysis of tan spot resistance in wheat. *Theor. Appl. Genet.* 133, 2363–2375. doi: 10.1007/s00122-020-03604-1

Liu, X., Wang, H., Hu, X., Li, K., Liu, Z., Wu, Y., et al. (2019). Improving genomic selection with quantitative trait loci and nonadditive effects revealed by empirical evidence in maize. *Front. Plant Sci.* 10. doi: 10.3389/fpls.2019.01129

Liu, Z. H., Zhang, Z., Faris, J. D., Oliver, R. P., Syme, R., McDonald, M. C., et al. (2012). The cysteine rich necrotrophic effector SnTox1 produced by *Stagonospora nodorum* triggers susceptibility of wheat lines harboring *Snn1*. *PloS Pathog.* 8, e1002467. doi: 10.1371/journal.ppat.1002467

Liu, Y., Zhang, Q., Salsman, E., Fiedler, J. D., Hegstad, J. B., Liu, Z., et al. (2020a). QTL mapping of resistance to tan spot induced by race 2 of *Pyrenophora tritici-repentis* in tetraploid wheat. *Theor. Appl. Genet.* 133, 433–442. doi: 10.1007/s00122-019-03474-2

Lu, P., Liang, Y., Li, D., Wang, Z., Li, W., Wang, G., et al. (2016). Fine genetic mapping of spot blotch resistance gene *Sb3* in wheat (*Triticum aestivum*). *Theor. Appl. Genet.* 129, 577–589. doi: 10.1007/s00122-015-2649-z

Mago, R., Tabe, L., McIntosh, R. A., Pretorius, Z., Kota, R., Paux, E., et al. (2011). A multiple resistance locus on chromosome arm 3BS in wheat confers resistance to stem rust (*Sr2*), leaf rust (*Lr27*) and powdery mildew. *Theor. Appl. Genet.* 123, 615–623. doi: 10.1007/s00122-011-1611-y

Mahapatra, S. S., Navathe, S., Mishra, V. K., and Chand, R. (2021). Biochemical profiling of seedling and adult plant and its association with spot blotch resistance in bread wheat. *Russ. J. Plant Physiol.* 68, 1265–1275. doi: 10.1134/S1021443721060133

Marshall, R., Kombrink, A., Motteram, J., Loza-Reyes, E., Lucas, J., Hammond-Kosack, K. E., et al. (2011). Analysis of two in planta expressed LysM effector homologs from the fungus *Mycosphaerella graminicola* reveals novel functional properties and varying contributions to virulence on wheat. *Plant Physiol.* 156, 756–769. doi: 10.1104/pp.111.176347

Martinez, J. P., Oesch, N. W., and Ciuffetti, L. M. (2004). Characterization of the multiple-copy host-selective toxin gene, *ToxB*, in pathogenic and nonpathogenic isolates of *Pyrenophora tritici-repentis*. *Mol. Plant Microbe Interact.* 17, 467–474. doi: 10.1094/MPMI.2004.17.5.467

Martinez, J. P., Ottum, S. A., Ali, S., Franci, L. J., and Ciuffetti, L.M (2001) Characterization of the *ToxB* gene from *Pyrenophora tritici-repentis*. *Mol. Plant Microbe Interact.* 14, 675–677. doi: 10.1094/MPMI.2001.14.5.675

McDonald, M. C., Ahren, D., Simpfendorfer, S., Milgate, A., and Solomon, P. S. (2018). The discovery of the virulence gene *ToxA* in the wheat and barley pathogen *Bipolaris sorokiniana*. *Mol. Plant Pathol.* 19, 432–439. doi: 10.1111/mpp.12535

McDonald, B. A., and Martinez, J. P. (1991). Chromosome length polymorphisms in a *Septoria tritici* population. *Curr. Genet.* 19, 265–271. doi: 10.1007/BF00355053

McDonald, M. C., Oliver, R. P., Friesen, T. L., Brunner, P. C., and McDonald, B. A. (2013). Global diversity and distribution of three necrotrophic effectors in *Phaeosphaeria nodorum* and related species. *New Phytol.* 199, 241–251. doi: 10.1111/nph.12257

McDonald, M. C., Razavi, M., Friesen, T. L., Brunner, P. C., and McDonald, B. A. (2012). Phylogenetic and population genetic analyses of *Phaeosphaeria nodorum* and its close relatives indicate cryptic species and an origin in the fertile crescent. *Fungal Genet. Biol.* 49, 882–895. doi: 10.1016/j.fgb.2012.08.001

McDonald, M. C., and Solomon, P. S. (2018). Just the surface: advances in the discovery and characterization of necrotrophic wheat effectors. *Curr. Opin. Microbiol.* 46, 14–18. doi: 10.1016/j.mib.2018.01.019

McIntosh, R. A., Yamazaki, Y., Devos, K. M., Dubcovsky, J., Rogers, J., and Appels, R. (2007) *Catalogue of gene symbols for wheat: 2007 supplement. KOMUGI integrated wheat science database*. Available at: https://shigen.nig.ac.jp/wheat/komugi/genes/macgene/supplement2007.pdf.

McIntosh, R. A., Yamazaki, Y., Devos, K. M., Dubcovsky, J., Rogers, J., and Appels, R. (2008) *Catalogue of gene symbols for wheat:2008 supplement. KOMUGI integrated wheat science database*. Available at: https://shigen.nig.ac.jp/wheat/komugi/genes/macgene/supplement2008.pdf.

Mehrabi, R., Taga, M., and Kema, G. H. J. (2007). Electrophoretic and cytological karyotyping of the foliar wheat pathogen *Mycosphaerella graminicola* reveals many chromosomes with a large size range. *Mycologia* 99, 804–812. doi: 10.1080/15572536.2007.11832518

Meile, L., Croll, D., Brunner, P. C., Plissonneau, C., Hartmann, F. E., McDonald, B. A., et al. (2018). A fungal avirulence factor encoded in a highly plastic genomic region triggers partial resistance to septoria tritici blotch. *New Phytol.* 219, 1048–1061. doi: 10.1111/nph.15180

Mekonnen, T., Haileselassie, T., Goodwin, S. B., and Tesfayea, K. (2020). Genetic diversity and population structure of *Zymoseptoria tritici* in Ethiopia as revealed by microsatellite markers. *Fungal Genet. Biol.* 141, 103413. doi: 10.1016/j.fgb.2020.103413

Moolhuijzen, P., See, P. T., Hane, J. K., Shi, G., Liu, Z., Oliver, R. P., et al. (2018). Comparative genomics of the wheat fungal pathogen *Pyrenophora tritici-repentis* reveals chromosomal variations and genome plasticity. *BMC Genomics* 19, 279. doi: 10.1186/s12864-018-4680-3

Moolhuijzen, P., See, P. T., and Moffat, C. S. (2020). PacBio genome sequencing reveals new insights into the genomic organisation of the multi-copy *ToxB* gene of the wheat fungal pathogen *Pyrenophora tritici-repentis*. *BMC Genomics* 21, 645. doi: 10.1186/s12864-020-07029-4

Muqaddasi, Q. H., Kamal, R., Mirdita, V., Rodemann, B., Ganal, M. W., Reif, J. C., et al. (2021). Genome-wide association studies and prediction of tan spot (*Pyrenophora tritici-repentis*) infection in European winter wheat *via* different marker platforms. *Genes* 12, 490. doi: 10.3390/genes12040490

Murphy, N. E., Loughman, R., Appels, R., Lagudah, E. S., and Jones, M. G. K. (2000). Genetic variability in a collection of *Stagonospora nodorum isolates* from Western Australia. *Aus. J. Agric. Res.* 51, 679–684. doi: 10.1071/AR99107

Nagy, E. D., and Bennetzen, J. L. (2008). Pathogen corruption and site-directed recombination at a plant disease resistance gene cluster. *Genome Res.* 18, 1918–1923. doi: 10.1101/gr.078766.108

Navathe, S., Yadav, P. S., Chand, R., Mishra, V. K., Vasistha, N. K., Meher, P. K., et al. (2020). ToxA–*Tsn1* interaction for spot blotch susceptibility in Indian wheat: an example of inverse gene-for-gene relationship. *Plant Dis.* 104, 71–81. doi: 10.1094/PDIS-05-19-1066-RE

Negi, C., Vasistha, N. K., Singh, D., Vyas, P., and Dhaliwal, H. S. (2022). Application of CRISPR-mediated gene editing for crop improvement. *Mol. Biotechnol.* 64 (11), 1198–1217. doi: 10.1007/s12033-022-00507-y

Pal, N., Jan, I., Saini, D. K., Kumar, K., Kumar, A., Sharma, P. K., et al. (2022). Meta-QTLs for multiple disease resistance involving three rusts in common wheat (*Triticum aestivum* l.). *Theor. Appl. Genet.* 135, 2385–2405. doi: 10.1007/s00122-022-04119-7

Palma-Guerrero, J., Ma, X., Torriani, S. F. F., Zala, M., Francisco, C. S., Hartmann, F. E., et al. (2017). Comparative transcriptome analyses in *Zymoseptoria tritici* reveal significant differences in gene expression among strains during plant infection. *Mol. Plant Microbe Interact.* 30, 231–244. doi: 10.1094/MPMI-07-16-0146-R

Pascual, L., Albert, E., Sauvage, C., Duangjit, J., Bouchet, J. P., Bitton, F., et al. (2016). Dissecting quantitative trait variation in the resequencing era: complementarity of bi-parental, multi-parental, and association panels. *Plant Sci.* 242, 120–130. doi: 10.1016/j.plantsci.2015.06.017

Patel, J. S., Mamidi, S., Bonman, J. M., and Adhikari, T. B. (2013). Identification of QTL in spring wheat associated with resistance to a novel isolate of *Pyrenophora tritici-repentis*. *Crop Sci.* 53, 842–852. doi: 10.2135/cropsci2012.01.0036

Paul, N. C., Park, S. W., Liu, H., Choi, S., Ma, J., MacCready, J. S., et al. (2021). Plant and fungal genome editing to enhance plant disease resistance using the CRISPR/Cas9 system. *Front. Plant Sci.* 12. doi: 10.3389/fpls.2021.700925

Peters Haugrud, A. R., Zhang, Z., Friesen, T. L., and Faris, J. D. (2022). Genetics of resistance to septoria nodorum blotch in wheat. *Theor. Appl. Genet.* 135, 3685–3707. doi: 10.1007/s00122-022-04036-9

Phan, H. T. T., Furuki, E., Hunziker, L., Rybak, K., and Tan, K. C. (2021). GWAS analysis reveals distinct pathogenicity profiles of Australian *Parastagonospora nodorum* isolates and identification of marker-trait-associations to septoria nodorum blotch. *Sci. Rep.* 11, 10085. doi: 10.1038/s41598-021-87829-0

Phan, H. T. T., Rybak, K., Bertazzoni, S., Furuki, E., Dinglasan, E., Hickey, L. T., et al. (2018). Novel sources of resistance to septoria nodorum blotch in the vavilov wheat collection identified by genome-wide association studies. *Theor. Appl. Genet.* 131, 1223–1238. doi: 10.1007/s00122-018-3073-y

Phan, H. T. T., Rybak, K., Furuki, E., Breen, S., Solomon, P. S., Oliver, R. P., et al. (2016). Differential effector gene expression underpins epistasis in a plant fungal disease. *Plant J.* 87, 343–354. doi: 10.1111/tpj.13203

Piaskowska, D., Piechota, U., Radecka-Janusik, M., and Czembor, P. (2021). QTL mapping of seedling and adult plant resistance to septoria tritici blotch in winter wheat cv. mandub (*Triticum aestivum* l.). *Agronomy* 11, 1108. doi: 10.3390/agronomy11061108

Plissonneau, C., Hartmann, F. E., and Croll, D. (2018). Pangenome analyses of the wheat pathogen *Zymoseptoria tritici* reveal the structural basis of a highly plastic eukaryotic genome. *BMC Biol.* 16, 5. doi: 10.1186/s12915-017-0457-4

Rahman, M., Davies, P., Bansal, U., Pasam, R., Hayden, M., and Trethowan, R. (2020). Marker-assisted recurrent selection improves the crown rot resistance of bread wheat. *Mol. Breed.* 40, 28. doi: 10.1007/s11032-020-1105-1

Rajarammohan, S. (2021). Redefining plant-necrotroph interactions: the thin line between hemibiotrophs and necrotrophs. *Front. Microbiol.* 12. doi: 10.3389/fmicb.2021.673518

Rawlinson, C., See, P. T., Moolhuijzen, P., Li, H., Moffat, C. S., Chooi, Y. H., et al. (2019). The identification and deletion of the polyketide synthase-nonribosomal peptide synthase gene responsible for the production of the phytotoxic triticone A/B in the wheat fungal pathogen *Pyrenophora tritici-repentis*. *Environ. Microbiol.* 21, 4875–4886. doi: 10.1111/1462-2920.14854

Reddy, L., Friesen, T. L., Meinhardt, S. W., Chao, S., and Faris, J. D. (2008). Genomic analysis of the Snn1 locus on wheat chromosome arm 1BS and the identification of candidate genes. *Plant Genome* 1, 55–66. doi: 10.3835/plantgenome2008.03.0181

Rees, R. G., Platz, G. J., and Mayer, R. J. (1982). Yield losses in wheat from yellow spot: comparison of estimates derived from single tillers and plots. *Aus. J. Agric. Res.* 33, 899–908. doi: 10.1071/AR9820899

Reszka, E., Song, Q., Arseniuk, E., Cregan, P. B., and Ueng, P. P. (2007). The QTL controlling partial resistance to stagonospora nodorum blotch disease in winter triticale bogo. *Plant Pathol. Bull.* 16, 161–167.

Riaz, A., KockAppelgren, P., Hehir, J. G., Kang, J., Meade, F., Cockram, J., et al. (2020). Genetic analysis using a multi-parent wheat population identifies novel sources of septoria tritici blotch resistance. *Genes* 11, 887. doi: 10.3390/genes11080887

Richards, J. K., Kariyawasam, G. K., Seneviratne, S., Wyatt, N. A., Xu, S. S., Liu, Z., et al. (2021). A triple threat: the *Parastagonospora nodorum* SnTox267 effector exploits three distinct host genetic factors to cause disease in wheat. *New Phytol.* 233, 427–442. doi: 10.1111/nph.17601

Richards, J. K., Stukenbrock, E. H., Carpenter, J., Liu, Z., Cowger, C., Faris, J. D., et al. (2019). Local adaptation drives the diversification of effectors in the fungal wheat pathogen *Parastagonospora nodorum* in the united states. *PloS Genet.* 15, e1008223. doi: 10.1371/journal.pgen.1008223

Richards, J. K., Wyatt, N. A., Liu, Z., Faris, J. D., and Friesen, T. L. (2018). Reference quality genome assemblies of three *Parastagonospora nodorum* isolates differing in virulence on wheat. *G3* 8, 393–399. doi: 10.1534/g3.117.300462

Romdhane, S. B. M. B. (2011). *Genome structure and pathogenicity of the fungal wheat pathogen mycosphaerella graminicola. [PhD thesis]* (Wageningen: Wageningen University).

Rudd, J. J., Kanyuka, K., Hassani-Pak, K., Derbyshire, M., Andongabo, A., Devonshire, J., et al. (2015). Transcriptome and metabolite profiling of the infection cycle of *Zymoseptoria tritici* on wheat reveals a biphasic interaction with plant immunity involving differential pathogen chromosomal contributions and a variation on the hemibiotrophic lifestyle definition. *Plant Physiol.* 167, 1158–1185. doi: 10.1104/pp.114.255927

Ruud, A. K., Dieseth, J. A., Ficke, A., Furuki, E., Phan, H. T. T., Oliver, R. P., et al. (2019). Genome-wide association mapping of resistance to septoria nodorum leaf blotch in a Nordic spring wheat collection. *Plant Genome* 12, 1–15. doi: 10.3835/plantgenome2018.12.0105

Ruud, A. K., Dieseth, J. A., and Lillemo, M. (2018). Effects of three *Parastagonospora nodorum* necrotrophic effectors on spring wheat under Norwegian field conditions. *Crop Sci.* 58, 159–168. doi: 10.2135/cropsci2017.05.0281

Ruud, A. K., and Lillemo, M. (2018). "Diseases affecting wheat: septoria nodorum blotch," in *Burleigh dodds series in agricultural science* (Cambridge, UK: Burleigh Dodds Science Publishing Limited), 109–144. doi: 10.19103/AS.2018.0039.06

Ruud, A. K., Windju, S., Belova, T., Friesen, T. L., and Lillemo, M. (2017). Mapping of *SnTox3-Snn3* as a major determinant of field susceptibility to septoria nodorum leaf blotch in the SHA3/CBRD × naxos population. *Theor. Appl. Genet.* 130, 1361–1374. doi: 10.1007/s00122-017-2893-5

Saintenac, C., Cambon, F., Aouini, L., Verstappen, E., Ghaffary, S. M. T., Poucet, T., et al. (2021). A wheat cysteine-rich receptor-like kinase confers broad-spectrum resistance against septoria tritici blotch. *Nat. Commun.* 12, 433. doi: 10.1038/s41467-020-20685-0

Saintenac, C., Lee, W. S., Cambon, F., Rudd, J. J., King, R. C., Marande, W., et al. (2018). Wheat receptor-kinase-like protein *STB6* controls gene-for-gene resistance to fungal pathogen *Zymoseptoria tritici*. *Nat. Genet.* 50, 368–374. doi: 10.1038/s41588-018-0051-x

Sanchez-Vallet, A., McDonald, M. C., Solomon, P. S., and McDonald, B. A. (2015). Is *Zymoseptoria tritici* a hemibiotroph? *Fungal Genet. Biol.* 79, 29–32. doi: 10.1016/j.fgb.2015.04.001

Sasaki, A. (2000). Host–parasite coevolution in a multilocus gene-for-gene system. *Proc. R. Soc Lond. B.* 267, 2183–2188. doi: 10.1098/rspb.2000.1267

Scharen, A. L., Eyal, Z., Huffman, M. D., and Prescott, J. M. (1985). The distribution and frequency of virulence genes in geographically separated populations of *Leptosphaeria nodorum*. *Phytopathology* 75, 1463–1468. doi: 10.1094/Phyto-75-1463

Schnurbusch, T., Paillard, S., Fossati, D., Messmer, M., Schachermayr, G., Winzeler, M., et al. (2003). Detection of QTLs for stagonospora glume blotch resistance in Swiss winter wheat. *Theor. Appl. Genet.* 107, 1226–1234. doi: 10.1007/s00122-003-1372-3

Schroter, J. (1894). *Kryptogamen-flora von schlesien; im namen der schlesischen gesellschaft fur vaterlandische cultur* Vol. 3–2. Ed. K.-F. Cohn (Polland: J.U. Kern's verlag), 340.

See, P. T., Marathamuthu, K. A., Iagallo, E. M., Oliver, R. P., and Moffat, C. S. (2018). Evaluating the importance of the tan spot ToxA-*Tsn1* interaction in Australian wheat varieties. *Plant Pathol.* 67, 1066–1075. doi: 10.1111/ppa.12835

Shankar, M., Reeves, K., Bradley, J., Varischetti, R., and Loughman, R. (2021). Effect of varietal resistance on the yield loss function of wheat to nodorum blotch. *Plant Pathol.* 70, 745–759. doi: 10.1111/ppa.13317

Shankar, M., Walker, E., Golzar, H., Loughman, R., Wilson, R. E., and Francki, M. G. (2008). Quantitative trait loci for seedling and adult plant resistance to stagonospora nodorum in wheat. *Phytopathology* 98, 886–893. doi: 10.1094/PHYTO-98-8-0886

Shatalina, M., Messmer, M., Feuillet, C., Mascher, F., Paux, E., Choulet, F., et al. (2014). High-resolution analysis of a QTL for resistance to stagonospora nodorum glume blotch in wheat reveals presence of two distinct resistance loci in the target interval. *Theor. Appl. Genet.* 127, 573–586. doi: 10.1007/s00122-013-2240-4

Shetty, N. P., Jensen, J. D., Knudsen, A., Finnie, C., Geshi, N., Blennow, A., et al. (2009). Effects of β-1,3-glucan from *Septoria tritici* on structural defence responses in wheat. *J. Exp. Bot.* 60, 4287–4300. doi: 10.1093/jxb/erp269

Shi, G., Zhang, Z., Friesen, T. L., Bansal, U., Cloutier, S., Wicker, T., et al. (2016a). Marker development, saturation mapping, and high-resolution mapping of the septoria nodorum blotch susceptibility gene *Snn3-B1* in wheat. *Mol. Genet. Genomics* 291, 107–119. doi: 10.1007/s00438-015-1091-x

Shi, G., Zhang, Z., Friesen, T. L., Raats, D., Fahima, T., Brueggeman, R. S., et al. (2016b). The hijacking of a receptor kinase-driven pathway by a wheat fungal pathogen leads to disease. *Sci. Adv.* 2, e1600822. doi: 10.1126/sciadv.1600822

Shoemaker, R. A. (1959). Nomenclature of *Drechslera* and *Bipolaris*, grass parasites segregated from "*Helminthosporium*". *Can. J. Bot.* 37, 879–887. doi: 10.1139/b59-073

Shoemaker, R. A. (1962). *Drechslera* Ito. *Can. J. Bot.* 40, 809–836. doi: 10.1139/b62-075

Singh, S., Bockus, W. W., Sharma, I., and Bowden, R. L. (2008). A novel source of resistance in wheat to *Pyrenophora tritici-repentis* race 1. *Plant Dis.* 92, 91–95. doi: 10.1094/PDIS-92-1-0091

Singh, S., Hernandez, M. V., Crossa, J., Singh, P. K., Bains, N. S., Singh, K., et al. (2012). Multi-trait and multi-environment QTL analyses for resistance to wheat diseases. *PloS One* 7, e38008. doi: 10.1371/journal.pone.0038008

Singh, P. K., Singh, S., Deng, Z., He, X., Kehel, Z., and Singh, R. P. (2019). Characterization of QTLs for seedling resistance to tan spot and septoria nodorum blotch in the PBW343/Kenya nyangumi wheat recombinant inbred lines population. *Int. J. Mol. Sci.* 20, 5432. doi: 10.3390/ijms20215432

Sperschneider, J., and Dodds, P. N. (2022). EffectorP 3.0: prediction of apoplastic and cytoplasmic effectors in fungi and oomycetes. *Mol. Plant-Microbe Interact.* 35 (2), 146–156. doi: 10.1094/MPMI-08-21-0201-R

Sprague, R. (1950). *Diseases of cereals and grasses in north America* (New York: The Ronald Press).

Stadlmeier, M., Jørgensen, L. N., Corsi, B., Cockram, J., Hartl, L., and Mohler, V. (2019). Genetic dissection of resistance to the three fungal plant pathogens *Blumeria graminis*, *Zymoseptoria tritici*, and *Pyrenophora tritici-repentis* using a multiparental winter wheat population. *G3* 9, 1745–1757. doi: 10.1534/g3.119.400068

Stewart, E. L., Croll, D., Lendenmann, M. H., Sanchez-Vallet, A., Hartmann, F. E., Palma-Guerrero, et al. (2018). Quantitative trait locus mapping reveals complex genetic architecture of quantitative virulence in the wheat pathogen *Zymoseptoria tritici*. *Mol. Plant Pathol.* 19, 201–216. doi: 10.1111/mpp.12515

Strelkov, S. E., Lamari, L., and Ballance, G. M. (1999). Characterization of a host-specific protein toxin (Ptr ToxB) from *Pyrenophora tritici-repentis*. *Mol. Plant Microbe Interact.* 12, 728–732. doi: 10.1094/MPMI.1999.12.8.728

Stukenbrock, E. H., Banke, S., and McDonald, B. A. (2006). Global migration patterns in the fungal wheat pathogen *Phaeosphaeria nodorum*. *Mol. Ecol.* 15, 2895–2904. doi: 10.1111/j.1365-294X.2006.02986.x

Stukenbrock, E. H., Banke, S., Zala, M., Mcdonald, B. A., and Oliver, R. P. (2005). Isolation and characterization of EST-derived microsatellite loci from the fungal wheat pathogen *Phaeosphaeria nodorum*. *Mol. Ecol. Notes* 5, 931–933. doi: 10.1111/j.1471-8286.2005.01120.x

Stukenbrock, E. H., Jorgensen, F. G., Zala, M., Hansen, T. T., McDonald, B. A., and Schierup, M. H. (2010). Whole-genome and chromosome evolution associated with host adaptation and speciation of the wheat pathogen *Mycosphaerella graminicola*. *PloS Genet.* 6, e1001189. doi: 10.1371/journal.pgen.1001189

Syme, R. A., Hane, J. K., Friesen, T. L., and Oliver, R. P. (2013). Resequencing and comparative genomics of *Stagonospora nodorum*: sectional gene absence and effector discovery. *G3* 3, 959–969. doi: 10.1534/g3.112.004994

Syme, R. A., Tan, K. C., Hane, J. K., Dodhia, K., Stoll, T., Hastie, M., et al. (2016). Comprehensive annotation of the *Parastagonospora nodorum* reference genome using next-generation genomics, transcriptomics and proteogenomics. *PloS One* 11, e0147221. doi: 10.1371/journal.pone.0147221

Syme, R. A., Tan, K. C., Rybak, K., Friesen, T. L., McDonald, B. A., Oliver, R. P., et al. (2018). Pan-*Parastagonospora* comparative genome analysis-effector prediction and genome evolution. *Genome Biol. Evol.* 10, 2443–2457. doi: 10.1093/gbe/evy192

Tamburic-Ilincic, L., and Rosa, S. B. (2019). QTL mapping of fusarium head blight and septoria tritici blotch in an elite hard red winter wheat population. *Mol. Breed.* 39, 1–15. doi: 10.1007/s11032-019-0999-y

Tan, K. C., Phan, H. T., Rybak, K., John, E., Chooi, Y. H., Solomon, P. S., et al. (2015). Functional redundancy of necrotrophic effectors-consequences for exploitation for breeding. *Front. Plant Sci.* 6. doi: 10.3389/fpls.2015.00501

Tan, K. C., Waters, O. D. C., Rybak, K., Antoni, E., Furuki, E., and Oliver, R. P. (2014). Sensitivity to three *Parastagonospora nodorum* necrotrophic effectors in current Australian wheat cultivars and the presence of further fungal effectors. *Crop Pasture Sci.* 65, 150–158. doi: 10.1071/CP13443

Tian, H., MacKenzie, C. I., Rodriguez-Moreno, L., van den Berg, G. C. M., Chen, H., Rudd, J. J., et al. (2021). Three LysM effectors of *Zymoseptoria tritici* collectively disarm chitin-triggered plant immunity. *Mol. Plant Pathol.* 22, 683–693. doi: 10.1111/mpp.13055

Tomas, A., Feng, G. H., Reeck, G. R., Bockus, W. W., and Leach, J. E. (1990). Purification of a cultivar-specific toxin from *Pyrenophora tritici-repentis*, causal agent of tan spot of wheat. *Mol. Plant Microbe Interact.* 3, 221–224. doi: 10.1094/MPMI-3-221

Tuori, R. P., Wolpert, T. J., and Ciuffetti, L. M. (1995). Purification and immunological characterization of toxic components from cultures of *Pyrenophora tritici-repentis*. *Mol. Plant Microbe Interact.* 8, 41–48. doi: 10.1094/MPMI-8-0041

Tyagi, S., Kumar, R., Das, A., Won, S. Y., and Shukla, P. (2020). CRISPR-Cas9 system: a genome-editing tool with endless possibilities. *J. Biotechnol.* 319, 36–53. doi: 10.1016/j.jbiotec.2020.05.008

Uphaus, J., Walker, E., Shankar, M., Golzar, H., Loughman, R., Francki, M., et al. (2007). Quantitative trait loci identified for resistance to stagonospora glume blotch in wheat in the USA and Australia. *Crop Sci.* 47, 1813–1822. doi: 10.2135/cropsci2006.11.0732

Van Der Biezen, E. A., and Jones, J. D. (1998). Plant disease-resistance proteins and the gene-for-gene concept. *Trends Biochem. Sci.* 23, 454–456. doi: 10.1016/S0968-0004(98)01311-5

Vleeshouwers, V. G., and Oliver, R. P. (2014). Effectors as tools in disease resistance breeding against biotrophic, hemibiotrophic, and necrotrophic plant pathogens. *Mol. Plant Microbe Interact.* 27, 196–206. doi: 10.1094/MPMI-10-13-0313-IA

Wang, Y., Cheng, X., Shan, Q., Zhang, Y., Liu, J., Gao, C., et al. (2014). Simultaneous editing of three homoeoalleles in hexaploid bread wheat confers heritable resistance to powdery mildew. *Nat. Biotechnol.* 32, 947–951. doi: 10.1038/nbt.2969

Weber, G. F. (1922). Septoria diseases of cereals. II. septoria diseases of wheat. *Phytopathology* 12, 558–585.

Wicki, W., Winzeler, M., Schmid, J. E., Stamp, P., and Messmer, M. (1999). Inheritance of resistance to leaf and glume blotch caused by *Septoria nodorum* berk. in winter wheat. *Theor. Appl. Genet.* 99, 1265–1272. doi: 10.1007/s001220051332

Wu, L., He, X., Lozano, N., Zhang, X., and Singh, P. K. (2021). *ToxA*, a significant virulence factor involved in wheat spot blotch disease, exists in the Mexican population of *Bipolaris sorokiniana*. *Trop. Plant Pathol.* 46, 201–206. doi: 10.1007/s40858-020-00391-4

Xu, S. S., Friesen, T. L., and Mujeeb-Kazi, A. (2004). Seedling resistance to tan spot and stagonospora nodorum blotch in synthetic hexaploid wheats. *Crop Sci.* 44, 2238–2245. doi: 10.2135/cropsci2004.2238

Zaim, M., Kabbaj, H., Kehel, Z., Gorjanc, G., Filali-Maltouf, A., Belkadi, B., et al. (2020). Combining QTL analysis and genomic predictions for four durum wheat populations under drought conditions. *Front. Genet.* 11. doi: 10.3389/fgene.2020.00316

Zhang, F. (2022). Zt3LysM: a key effector protein in the fungal plant pathogen *Zymoseptoria tritici*. *Imp. Biol. Sci. Rev.*

Zhang, Y., Bai, Y., Wu, G., Zou, S., Chen, Y., Gao, C., et al. (2017). Simultaneous modification of three homoeologs of TaEDR1 by genome editing enhances powdery mildew resistance in wheat. *Plant J.* 91, 714–724. doi: 10.1111/tpj.13599

Zhang, H. F., Francl, L. J., Jordahl, J. G., and Meinhardt, S. W. (1997). Structural and physical properties of a necrosis-inducing toxin from *Pyrenophora tritici-repentis*. *Phytopathology* 87, 154–160. doi: 10.1094/PHYTO.1997.87.2.154

Zhang, Z., Friesen, T. L., Simons, K. J., Xu, S. S., and Faris, J. D. (2009). Development, identification, and validation of markers for marker-assisted selection against the *Stagonospora nodorum* toxin sensitivity genes *Tsn1* and *Snn2* in wheat. *Mol. Breed.* 23, 35–49. doi: 10.1007/s11032-008-9211-5

Zhang, P., Guo, G., Wu, Q., Chen, Y., Xie, J., Lu, P., et al. (2020). Identification and fine mapping of spot blotch (*Bipolaris sorokiniana*) resistance gene *Sb4* in wheat. *Theor. Appl. Genet.* 133, 2451–2459. doi: 10.1007/s00122-020-03610-3

Zhang, Z., Running, K. L. D., Seneviratne, S., Peters Haugrud, A. R., Szabo-Hever, A., Shi, G., et al. (2021). A protein kinase-major sperm protein gene hijacked by a necrotrophic fungal pathogen triggers disease susceptibility in wheat. *Plant J.* 106, 720–732. doi: 10.1111/tpj.15194

Zhong, Z., Marcel, T. C., Hartmann, F. E., Ma, X., Plissonneau, C., Zala, M., et al. (2017). A small secreted protein in *Zymoseptoria tritici* is responsible for avirulence on wheat cultivars carrying the *Stb6* resistance gene. *New Phytol.* 214, 619–631. doi: 10.1111/nph.14434

Zhou, B., Benbow, H. R., Brennan, C. J., Arunachalam, C., Karki, S. J., Mullins, E., et al. (2020). Wheat encodes small, secreted proteins that contribute to resistance to septoria tritici blotch. *Front. Genet.* 11. doi: 10.3389/fgene.2020.00469

Zwart, R. S., Thompson, J. P., Milgate, A. W., Bansal, U. K., Williamson, P. M., Raman, H., et al. (2010). QTL mapping of multiple foliar disease and root-lesion nematode resistances in wheat. *Mol. Breed.* 26, 107–124. doi: 10.1007/s11032-009-9381-9

frontiers | Frontiers in Plant Science

TYPE Original Research
PUBLISHED 12 June 2023
DOI 10.3389/fpls.2023.1166813

OPEN ACCESS

EDITED BY
Maria Rosa Simon,
National University of La Plata, Argentina

REVIEWED BY
Matías Schierenbeck,
Leibniz Institute of Plant Genetics and Crop Plant Research (IPK), Germany
Ana Carolina Castro,
National University of La Plata, Argentina

*CORRESPONDENCE
Sandiswa Figlan
figlas@unisa.ac.za

RECEIVED 15 February 2023
ACCEPTED 16 May 2023
PUBLISHED 12 June 2023

CITATION
Maserumule M, Rauwane M, Madala NE, Ncube E and Figlan S (2023) Defence-related metabolic changes in wheat (*Triticum aestivum* L.) seedlings in response to infection by *Puccinia graminis* f. sp. *tritici*. *Front. Plant Sci.* 14:1166813. doi: 10.3389/fpls.2023.1166813

Defence-related metabolic changes in wheat (*Triticum aestivum* L.) seedlings in response to infection by *Puccinia graminis* f. sp. *tritici*

Mercy Maserumule[1], Molemi Rauwane[1,2], Ntakadzeni E. Madala[3], Efficient Ncube[1] and Sandiswa Figlan[1]*

[1]Department of Agriculture and Animal Health, School of Agriculture and Life Sciences, College of Agriculture and Environmental Sciences, University of South Africa, Roodepoort, South Africa, [2]Department of Botany, Nelson Mandela University, Port Elizabeth, South Africa, [3]Department of Biochemistry and Microbiology, Faculty of Sciences, Agriculture and Engineering, University of Venda, Thohoyandou, Limpopo, South Africa

Stem rust caused by the pathogen *Puccinia graminis* f. sp. *tritici* is a destructive fungal disease-causing major grain yield losses in wheat. Therefore, understanding the plant defence regulation and function in response to the pathogen attack is required. As such, an untargeted LC-MS-based metabolomics approach was employed as a tool to dissect and understand the biochemical responses of Koonap (resistant) and Morocco (susceptible) wheat varieties infected with two different races of *P. graminis* (2SA88 [TTKSF] and 2SA107 [PTKST]). Data was generated from the infected and non-infected control plants harvested at 14- and 21- days post-inoculation (dpi), with 3 biological replicates per sample under a controlled environment. Chemo-metric tools such as principal component analysis (PCA), orthogonal projection to latent structures-discriminant analysis (OPLS-DA) were used to highlight the metabolic changes using LC-MS data of the methanolic extracts generated from the two wheat varieties. Molecular networking in Global Natural Product Social (GNPS) was further used to analyse biological networks between the perturbed metabolites. PCA and OPLS-DA analysis showed cluster separations between the varieties, infection races and the time-points. Distinct biochemical changes were also observed between the races and time-points. Metabolites were identified and classified using base peak intensities (BPI) and single ion extracted chromatograms from samples, and the most affected metabolites included flavonoids, carboxylic acids and alkaloids. Network analysis also showed high expression of metabolites from thiamine and glyoxylate, such as flavonoid glycosides, suggesting multi-faceted defence response strategy by understudied wheat varieties towards *P. graminis* pathogen infection. Overall, the study provided the insights of the biochemical changes in the expression of wheat metabolites in response to stem rust infection.

KEYWORDS

LC-MS, stem rust, *P. graminis* f. sp. *tritici*, primary and secondary metabolism, wheat metabolomics

1 Introduction

Wheat (*Triticum aestivum* L) is an important grain crop contributing 40% of the calorie intake and supporting 35% of the food intake of the global population (Grote et al., 2021). In the African continent, wheat has become one of the important staple food crops due to rapid population increases and changes in food habits. According to FAO (2017), Africa produces more than 25 million tons (MT) of wheat on 10 million hectares (Mha) of land, where sub-Saharan Africa (SSA) accounts for 40% of the produced wheat with 7.5 MT on a total area of 2.9 Mha. The most important wheat producing countries in SSA are Ethiopia, South Africa, Sudan, Kenya, Tanzania, Nigeria, Zimbabwe and Zambia (FAO, 2017). Ethiopia has the largest production at 1.7 Mha, followed by South Africa at 1.5 Mha. The production in the continent is regrettably not sufficient to meet the demands. As a result, from 2013 to 2019, African countries imported 16.9 MT of wheat at a cost of USD 6 billion, which exhaust inadequate foreign currency reserves of respective countries (FAO/WHO Human vitamin and mineral requirements, 2020).

According to Tadesse et al. (2018), the growing human population, rural-urban migration, inappropriate new agricultural policies and low adoption rates of new technologies remain major challenges for wheat production in developing countries. In addition, wheat production is constantly facing challenges such as climate change, increased inputs costs, abiotic (drought and heat) and biotic (diseases and pests) stresses. Among the biotic stresses, the most common diseases of wheat include wheat rusts, Fusarium head blight caused by *Fusarium graminearum* and powdery mildew caused by *Blumeria graminis* f. sp. *tritici* (Duveiller et al., 2007; Mondal et al., 2016; Deihimfard et al., 2022). Wheat rust such as stem rust caused by *Puccinia graminis* f. sp. *tritici* (*Pgt*), leaf rust (*P. triticina* Eriks. - *Pt*) and stripe rust (*P. striiformis* f. sp. *tritici* - *Pst*) are amongst the most destructive diseases of the crop. Great yield losses have been experienced worldwide, and these rust pathogens continue to evolve and threaten wheat production globally (Boshoff et al., 2018; Saunders et al., 2019; Davis et al., 2020; Li et al., 2022).

The emergence of a highly destructive wheat stem rust race, Ug99 (TTKSK) in Uganda in 1998 has threatened the global wheat production. A series of reviews by Singh et al. (2006); Singh et al. (2008); Singh et al. (2011); and Singh et al. (2015) have reported the significance, emergence, evolution and geographical spread of the Ug99 group. To date, there's a record of 15 known variants within the Ug99 lineage which have been identified in 14 countries (https://rusttracker.cimmyt.org/?page_id=22). South Africa was included on the Ug99 list in 2000, with currently five races of Ug99 present in the country (Terefe et al., 2019). The races include TTKSF (2SA88; Pretorius et al., 2000), TTKSP (2SA106; Pretorius et al., 2007), PTKST (2SA107; Visser et al., 2011), TTKSF+ (2SA88+; Visser et al., 2011) and PTKSK (2SA42; Terefe et al., 2021). These races vary from one another through virulence profiles against different wheat varieties with different resistant genes (Zhao et al., 2019). TTKSF and TTKSP are amongst the races that virulence was confirmed on wheat varieties that are known to possess the rust resistance genes such as *Sr31*, *Sr24* and *Sr36* that are now ineffective against the related races of Ug99 (Mondal et al., 2016). Thus, these studies highlighted the evolving pathogen potential and the need to develop stem rust resistant wheat varieties that will in turn boost productivity.

Improved host plant resistance is the most profitable and environmentally friendly control strategy to mitigate biotic stress (Kloppers and Pretorius, 1997; McCallum et al., 2016). Progress in understanding the underlying biochemical and molecular basis of rust diseases in wheat will facilitate resistance breeding through the use of biotechnology approaches. Omics studies such as metabolomics can assist in unravelling and better understanding metabolic responses of wheat to biotic stress for breeding programmes. Additionally, a combination of metabolomics and other omics studies may/can lead to the development of biomarkers for resistance/tolerance checks. In previous studies on oat (*Avena sativa*) (Li et al., 2022), sorghum (*Sorghum bicolor*) (Tugizimana et al., 2019), wheat (*Triticum aestivum* L), common bean (*Phaseolus vulgaris* L) (Makhumbila et al., 2023) among others, metabolomics has been used for comparative metabolomic phenotyping to identify biomarkers or metabolic signatures linked to varied response capacities shown in varieties with varied resistance potentials. Therefore, identifying biochemical changes of primary and especially secondary metabolites need to be considered when observing plant-pathogen interactions. Hence, this study aimed to identify the metabolomic changes of two wheat varieties (Koonap and Morocco) in response to infection by rust pathogen *P. graminis* at different time-points, using an untargeted LC-MS metabolomic approach.

2 Materials and methods

2.1 Plant and pathogen material

Seeds of two wheat varieties (Koonap and Morocco) used in this study were obtained from the Agricultural Research Council-Small Grain Institute (ARC-SGI, South Africa) germplasm bank (Table 1).

TABLE 1 Wheat varieties selected for stem rust screening.

Cultivar	Origin	Pedigree	Characteristic
Koonap	SGI (2010)	IP rights	Intermediate type, medium to high yield potential, medium to high growth length, excellent straw strength
Morocco*	Obscure; considered a North African cultivar	-	-

*Morocco (universal susceptible); IP, Intellectual Property.

The rust isolates (2SA88 and 2SA107) were also obtained from ARC-SGI for inoculation purposes.

2.2 Planting and inoculation

Wheat seeds (25 per pot) were sown in plastic pots of 10 cm diameter filled with steam-sterilised soil. Prior to planting, the soil was treated with water soluble fertiliser (10 g L^{-1}) containing nitrogen (15%), phosphorus (4.5%) and potassium (26.3%). After emergence, plants were fertilised twice with 10 g L^{-1} multi-feed (Nulandis, South Africa) water soluble fertiliser (19:8:16 NPK plus micronutrients). Seedlings were grown under light for 6 to 7 days in a temperature-controlled seedling room (22-25°C) and a rust-free environment prior inoculation.

For inoculation, urediniospores of stem rust isolates (2SA88 and 2SA107) stored at -80°C were heat-shocked in lukewarm water (about 40°C) for 10 minutes. Urediniospores were suspended in light mineral oil (Soltrol 170: Chevron Phillips, United State of America) at a concentration of 5 mg spores/mL (6x106 spores/mL) and sprayed onto the fully expanded primary leaves of wheat seedlings. For mock inoculation, Soltrol 170 (without the rust isolates) was also sprayed on control plants (Pretorius et al., 2000; Woldeab et al., 2017). Seedlings were incubated at 18°C in a dew chamber with relative humidity of 43% for 16 hours. Upon removal from the chamber, plants were exposed under fluorescent light for 3 hours. Inoculated plants were then placed in a greenhouse at a minimum temperature of 15°C and maximum of 25°C. Separate compartments in a greenhouse were used for different treatments. Each experiment was replicated 3 times, three different pots per variety were used to grow three biological replicates of each variety.

2.3 Disease scoring

Wheat seedlings were evaluated phenotypically and scored on a scale of 0 to 4 according to Stakman et al. (1962). Symptom severity was evaluated per plant whereby the scale of 0 - 2 represents low infection type, scale 3 – 4 represents high infection type. The symbols ';' representing macroscopic hypersensitive flecks, 'X' representing a mesothetic or mixed reaction, and '+' and '-' indicating 'more' or 'less', respectively, were also used. Infection recordings were taken at 14 days and 21 days post-inoculation (dpi).

2.4 Extraction and quantification of leaf tissue material

Metabolite extraction was carried out according to the modified version of Madala et al. (2014). One gram (1g) of each leaf sample was ground into powder with liquid nitrogen using a mortar and pestle. The sample was resuspended in 1.5 ml of 80% ice-cold methanol in a 2 ml centrifuge tube and vortexed for 30 sec. The sample was subjected to sonication for 30 min and centrifuged at 5000 ref per minute (rpm) for 5 min at 4°C. The supernatant (extract) was transferred to a new 2 ml Eppendorf tube and stored at 4°C for further analysis.

2.5 LC-qTOF-MS analysis

Samples were filtered with 0.22 µm nylon filters attached to 500 µL inserts (Thermo Fisher, Johannesburg, South Africa) to sieve the plant extract and transferred into HPLC glass vials. Plant extracts were analysed on liquid chromatography-quadrupole time-of flights tandem mass spectrometry instrument (LCMS-9030 qTOF, Shimadzu Corporation, Kyoto, Japan) for separation and detection of metabolites as described by Ramabulana et al. (2021). The chromatographic separation was performed on a Shim-pack Velox C18 column (100 mm x 2.1 mm with a particle size of 2.7 µm) (Shimadzu Corporation, Kyoto, Japan) housed inside a column oven set at 55°C. An injection volume of 3 µL was used for all samples, and a binary solvent system consisting of solvent A: 0.1% formic acid in Milli-Q water (both HPLC grade, Merck, Darmstadt, Germany) and solvent B: Methanol (UHPLC grade, Romil SpS, Cambridge, United Kingdom) with 0.1% formic acid pumped at a constant flow rate of 0.4 mL/min. A 20 min multiple gradient method was used to achieve the separation of metabolites. The starting condition were isocratic for 5% B for 3 min which was followed by gradual increase to 40% B for 2 min and later to 95% B for 7 min and kept isocratic at 95% B for 4 min, the conditions were then returned to 5% B in 2 min and kept constant for another 2 min at 5% B to re-equilibrate the column for the next injection. Chromatographic elution was monitored using qTOF high-definition mass spectrometer that was set to negative electrospray ionisation mode using data dependant acquisition (DDA) mode. Here, metabolic profiling was carried out in the negative electron ionization (ESI) mode (Figure 1), in order to better ionize phenolic compounds (such as flavonoids and carboxylic acids) (Hamany Djande et al., 2021). The subsequent parameters were set as follows: interface voltage (4.0 kV), interface temperature (300°C), nebulization and dry gas flow (3 L/min), heat block (400°C), DL temperature (280°C), detector voltage (1.8 kV), and flight tube temperature (42°C). Ion fragmentation was achieved using argon gas for collision induced dissociation (CID) experiments with energy of 30eV and 5 eV spread. NaI was used as a calibrant to ensure mass accuracy below 1 ppm.

2.6 Analysis of metabolites data

Extracts were converted to mzML files on Lab solutions (Shim-pack UFLC SHIMADZU CBM20A). The acquired raw datasets were processed using XCMS Online (http://XCMSOnline.scripps.edu/) (accessed on 10 July 2022). The data was processed with the following HPLC/UHD-qTOF parameters: feature detection was performed using the cent Wave method, maximal tolerated m/z was set to 30 ppm, signal-to-noise ratio was set to 10, the prefilter intensity and noise filter were set to 700 and 15, respectively. The retention time correction was performed using the ordered bijective

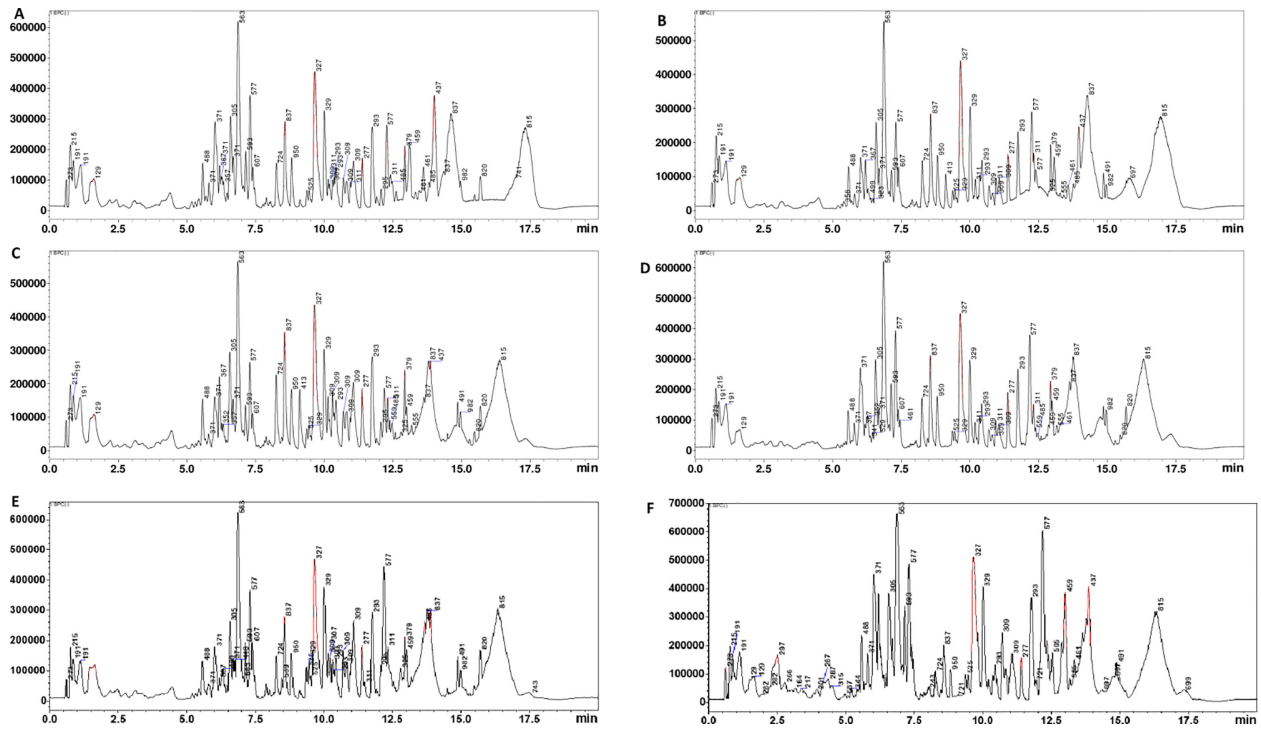

FIGURE 1
Representative UHPLC-QTOF-MS base peak intensity (BPI) chromatograms of Koonap cultivar methanolic-extracts. BPI MS chromatograms revealed differentially populated peaks for Koonap infected with rust race 2SA88 at 14- and 21- dpi (**A, B**, respectively), infected with rust race 2SA107 at 14- and 21 dpi (**C, D**, respectively) and control (**E, F**, respectively) each with unique m/z values, intensities and retention times (Rt's), representing the qualitative (presence/absence) and quantitative (intensity/concentration) detection of metabolites, thus providing a visual description of the similarities and differences between the selected wheat varieties.

interpolated warping (OBI-Warp method with a profStep of 0.4. Other parameters were set as bandwith = 0.5, minfrac (minimum fraction of sample in a group to be referred to as a feature) and mzwid (m/z width to determine peak groupings) of 0.020. The Kruskal–Wallis non-parametric method was used to perform the statistical test, *post-hoc* analysis was also performed, and the data was normalized using the median fold change. The resulting feature table with 2382 features was imported into SIMCA (soft independent modelling of class analogy) version 17.0 software (Sartorius, South Africa). The imported data were scaled using standard deviation by applying Pareto-scaling (Van den Berg et al., 2006). The models presented in this study are principal component analysis (PCA), Orthogonal projection to latent structures-discriminant analysis (OPLS–DA) and hierarchical cluster analysis (HCA). These are exploratory unsupervised models that assess the structure of a dataset highlighting trends or patterns within a dataset (Tugizimana et al., 2020). The explanation and description of these tools (PCA, OPLS-DA and HCA) have been detailed in literature (Saccenti et al., 2013; Saccenti et al., 2018; Saccenti et al., 2019). To complement the descriptive view provided by PCA modelling, orthogonal projection to latent structures-discriminant analysis (OPLS-DA) modelling of treated vs non-treated control samples was performed. The respective S-plots of the OPLS-DA score plots were also generated.

Metabolite annotation and identification were concomitantly carried out using the BPI, and single ion extracted chromatograms from Koonap and Morocco varieties. Chemo-metrically extracted metabolites were used to perform metabolic pathway analysis using MetaboAnalyst Pathway Analysis (MetPA) to reveal impactful metabolic pathways associated with the generated data across the two varieties. To inspect induction of biological events at the metabolic pathway level under stem rust infection, a KEGG pathway enrichment test was carried out. Pathway enrichment was used to identify the metabolic pathways to which the significantly changed metabolites are associated by mapping our metabolites data with the KEGG database.

3 Results

3.1 Phenotypic evaluation and scoring

The phenotypic evaluation and scoring of Koonap and Morocco varieties showed distinct differences between the infected and non-infected plants at different time-points (Figure 2). Koonap (resistant) showed low infection scores (0 – 2) for all three experiments at 14- and 21- dpi for the races as shown on Figure 2A (2SA88 at 14dpi) and 2B (2SA107 at 14dpi) as well as Figure 2D (2SA88 at 21dpi) and 2E (2SA107 at 21dpi). On the contrary, Morocco (susceptible) showed high infection scores (3 – 4) for both races at 14- and 21- dpi as shown on Figure 2G (2SA88 at 14dpi) and 2H (2SA107 at 14dpi) and 2J (2SA88 at 21dpi) and 2K

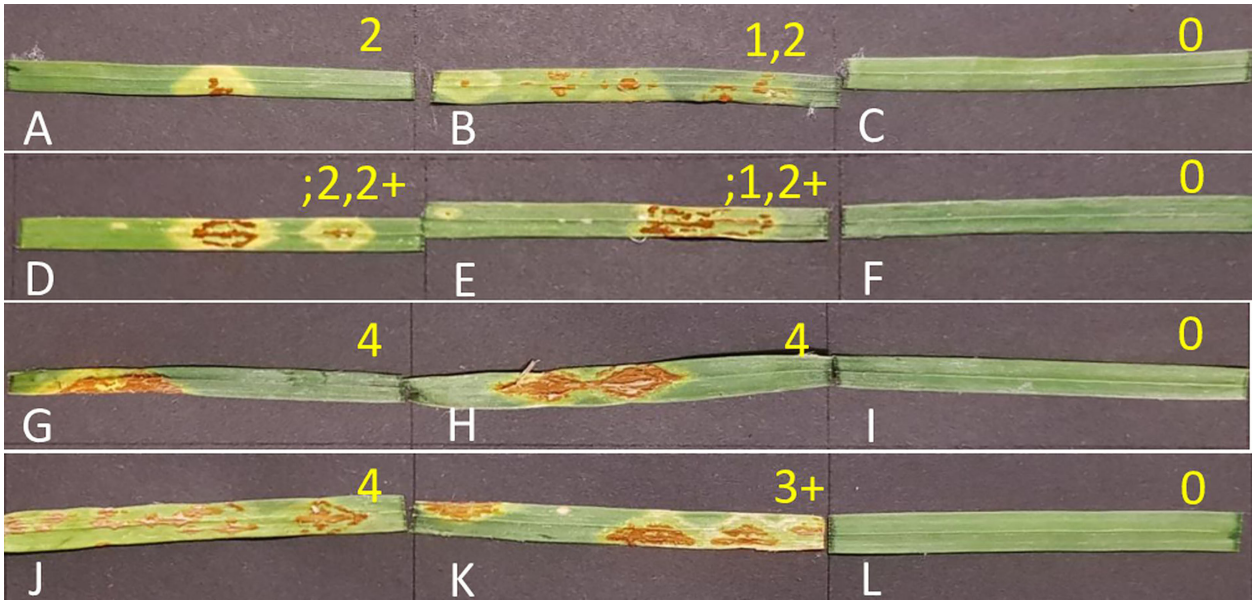

FIGURE 2
Stem rust response of Koonap and Morocco seedlings at different time-points. Koonap infected with rust races 2SA88, 2SA107 and control at 14dpi (**A–C**, respectively) and 21- dpi (**D–F**, respectively). Morocco infected with rust races 2SA88, 2SA107 and control at 14 dpi (**G–I**, respectively) and 21 dpi (**J–L**, respectively). Effective rust infection can be observed on the 2SA88 and 2SA107 treated plants relative to the control plants, where the appearance of the flecks (yellowing) and the spores (browning) appeared from 14 dpi and progressed (lesion elongation) over the days to 21 dpi. Infection types used to score wheat seedlings from 14 to 21 dpi. 0= immune,;= flecks, 1= minute uredinia, 2= small to medium sized uredinia, 3= large uredinia encircled by chlorosis, 4= large uredenia usually without any chlorosis.

(2SA107 at 21dpi), respectively. Figures 2C, F, I, L are the non-infected controls for both varieties, showing no symptoms of disease for both races at different time-points.

3.2 LC-qTOF-MS-analysis

Extracted LC chromatograms with distinct base peak intensities (BPI) revealed good chromatographic separation [Figure 1 (Koonap) and Supplementary Figure S1 (Morocco)]. The visual inspection of the extracted LC chromatograms displaying distinct BPI from ESI negative data shows chromatographic separation with slight or minor differences in some peak intensities of the metabolomes. The LC-qTOF-MS data sets were further analysed with explorative as well as predictive multivariate analyses to highlight the metabolic changes.

3.3 Multivariate data analysis

The PCA score scatterplot for Koonap and Morocco (Figures 3A, B, respectively) revealed differential clustering

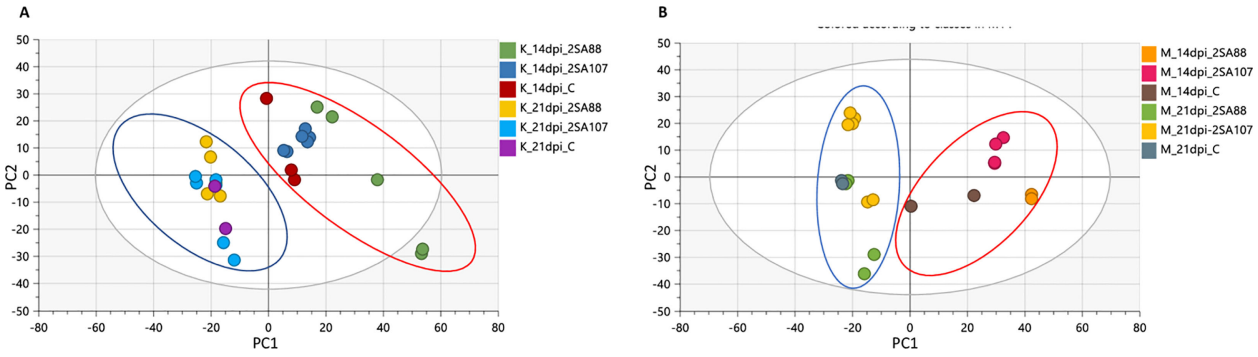

FIGURE 3
Unsupervised exploratory data analysis of ESI negative wheat cultivars classification data. Principal component analysis shows the grouping of *Pgt*-resistant Koonap cultivar **(A)**, while the susceptible Morocco cultivar **(B)** shows discriminant sample clustering coloured by time-point and race. The PCA scatter plots displayed a time-dependant response to infection. The diagnostic parameters of the score plot, generated from PC1 and PC2, are as follows; R^2 X (cum) = 88%, Q^2 (cum) = 73%.

between sample groups based on the races 2SA88, 2SA107 and the non-treated control at different time-points. The sample clustering was according to the 14- and 21- dpi time-points (as shown by blue and red circles on Figure 3), which is indicative of the different metabolite profile concentrations as the disease progressed. Also noteworthy, the differential clustering of the varieties reflected both differential quantitative distribution of each metabolite among the varieties as well as the qualitative makeup of metabolites.

The OPLS-DA further confirmed that the metabolite profiles in varieties were differentially regulated over time as evidenced in Figures 4, S2. This simply indicated that the data structures extracted by OPLS-DA modelling point to underlying differences in the measured metabolite profiles in the different sample groups. This observation was then further investigated by applying tools for annotating metabolites and performing quantitative assessments as shown and discussed below. The biomarkers as shown on the S-plots were also putatively annotated.

3.4 Metabolite annotation

Putative annotation of metabolites led to the identification of 51 metabolites of different classes originating from both primary and secondary metabolic pathways. A profile of these metabolites is illustrated in Table 2, listing the individual annotated metabolites commonly expressed within the two varieties or present as unique biomarkers. Metabolite annotation was performed to level 2 of the Metabolomics Standard Initiative (MSI) based on product ion spectral information formed by collision-induced dissociation (CID) of selected parent ions (Sumner et al., 2007). Molecular networking was used to confirm the classes of positively identified metabolites (Figure 5) and of these, significant classes are further discussed below.

4 Discussion

Two virulent races of 2SA88 (TTKSF) and 2SA107 (PTKST) were inoculated on Koonap and Morocco at seedling stage in which no complete resistance '0' was observed. The resistant wheat variety Koonap was noted having infection types ranging from ';' to '2+' for both races (Figure 2), indicating race-non-specific resistance in this variety. Previous research support this finding and have demonstrated that the variety Koonap confers long-lasting resistance to stem rust (Pretorius et al., 2000; Pretorius et al., 2007; Visser et al., 2011; Terefe et al., 2023). Our results of seedling tests against the two South African prevalent stem rust races also revealed that Koonap could be carrying effective seedling resistance metabolite biomarkers, as compared to Morocco where the vulnerability to Ug99 races on the variety was reported (Bajgain et al., 2016; Soko et al., 2018). The wheat variety Morocco is universally known to be relatively more susceptible to rust infection, which is in line with studies by Bender et al. (2016) that report on the large postules as indicators of the severity of the disease. The infection of the pathogen *P. graminis* seemingly spreads from 14 to 21 dpi for both races on the two varieties, indicating the disease progression between the two harvesting points. These findings provided further motivation to investigate

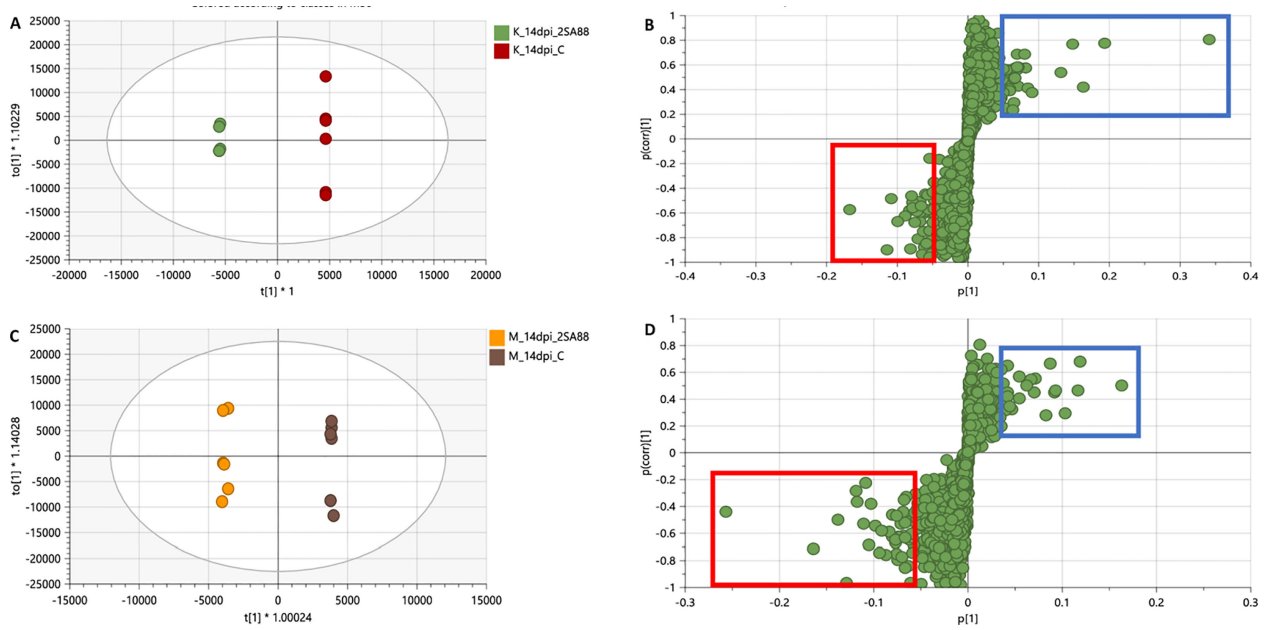

FIGURE 4
OPLS-DA modelling showing the selection of signatory biomarkers associated with response of rust race infections of 2SA88 and 2SA107. The OPLS-DA scores plot **(A, C)** showed clear discrimination between the treated samples and control whereas S-plots **(B, D)** allowed for the extraction of significant biomarkers. Extracted ions representing significant biomarkers responsible for the difference between the control at the top right corner (in the blue rectangle) and samples treated with *Pgt*. at the bottom left corner (in the red rectangle) for both Koonap and Morocco cultivars, respectively. The loading vector of the predictive component is on the y-axis, while the x-axis represents the modelled covariation.

TABLE 2 Summary of the putatively annotated metabolites from Koonap and Morocco wheat cultivars, untreated P(UT) and treated (PT), infected with 2SA88 and 2SA107 stem rust races at 14- and 21- dpi.

Metabolite	Experimental *m/z*	MW	MF	Rt	K14dpi 2SA88	K21dpi 2SA88	K14dpi 2SA107	K21dpi 2SA107	M14dpi 2SA88	M21dpi 2SA88	M14dpi 2SA107	M21dpi 2SA107	Biological role
Canrenone	339,2	340,5	$C_{22}H_{28}O_3$	15,51		P(T)							Flavanoid
Vicenin-3 I	563,13	564,5	$C_{26}H_{28}O_{14}$	7,35	P(UT)		P(UT)			P(UT)			Flavanoid
Guanosine	282,08	283,24	$C_{10}H_{13}N_5O_5$	2,05							P(T)		Hormone
2,6-Di-tert-butyl-4-nitrophenol	250,14	251,32	$C_{14}H_{21}NO_3$	11,96									Flavonoid
9,12,15-Octadecatrienoic acid, 3-(hexopyranosyloxy)-2-hydroxypropyl ester, (9Z,12Z,15Z)-	512,31	514,6	$C_{27}H_{46}O_9$	12,25									Fatty acid human
Canrenone	339,2	340,5	$C_{22}H_{28}O_3$	13,28									Flavonoid
Vicenin-2 I	593,15	594,5	$C_{27}H_{30}O_{15}$	7,07	P (UT)		P(UT)	P (T)					Flavanoid
(2E)-3-[4-({2-O-[(2S,3R,4R)-3,4-Dihydroxy-4-(hydroxymethyl)tetrahydro-2-furanyl]-beta-D-glucopyranosyl}oxy)-3-methoxyphenyl]acrylic acid	487,15	488,4	$C_{21}H_{28}O_{13}$	2,72									Hormone
Vicenin-3 II	563,18	564,5	$C_{26}H_{28}O_{14}$	6,86									Flavanoid
Vitexin-2-rhamnoside	577,15	578,5	$C_{27}H_{30}O_4$	7,29	P(UT)		P(UT)	P (T)		P(UT)	P(T)	P(UT)	Flavanoid
Chrysoeriol	299,06	300,26	$C_{16}H_{12}O_6$	11,08									Flavanoid
[(4E)-7-acetyloxy-6-hydroxy-2-methyl-10-oxo-2,3,6,7,8,9-hexahydrooxecin-3-yl] (E)-but-2-enoate	325,13	326,34	$C_{16}H_{22}O_7$	12,75		P(T)			P(T)		P(T)		Flavanoid
Saponarin I	593,15	594,5	$C_{27}H_{30}O_{15}$	6,77									Flavanoid
Orientin	447,09	448,4	$C_{21}H_{20}O_{11}$	12,31									Flavanoid
Decylbenzenesulfonic acid	297,15	298,4	$C_{16}H_{26}O_{3S}$	11,76	P(UT)				P(T)	P(UT)		P(UT)	Flavonoid
(10E,15E)-9,12,13-trihydroxyoctadeca-10,15-dienoic acid	327,42	328,4	$C_{18}H_{32}O_5$	14,03				P (T)					Fatty acid
Andrastin A	485,28	486,6	$C_{28}H_{38}0_7$	6,64				P (T)					Hormone
Glc-Glc-octadecatrienoyl-sn-glycerol	675,36	676,4	$C_{33}H_{56}O_{14}$	13,34	P (T)	P (T)	P (T)		P(T)			P(T)	Lipids
Apigenin-6-C-glucoside-7-O-glucoside	593,15	594,5	$C_{27}H_{30}O_{15}$	10,93						P(UT)		P(UT)	Flavanoid
4aR,5S,8aS,9aR)-9a-hydroxy-3,4a,5-trimethyl-5,6,7,8,8a,9-hexahydro-4H-benzo[f][1]benzofuran-2-one	249,11	250,33	$C_{15}H_{22}O_3$	10,15									Flavanoid
Thymol-beta-D-glucoside	311,11	312,4	$C_{16}H_{24}0_6$	12,3				P (T)		P(T)		P(T)	Flavanoid
[6-[3,4-dihydroxy-2,5-bis(hydroxymethyl)oxolan-2-yl]oxy-3,4,5-trihydroxyoxan-2-yl]methyl (E)-3-(4-hydroxy-3-methoxyphenyl)prop-2-enoate	517,15	518,5	$C_{22}H_{30}O_{14}$	6,57									Flavanoid
[5-hydroxy-6-[2-(4-hydroxy-3-methoxyphenyl)ethoxy]-2-(hydroxymethyl)-4-(3,4,5-trihydroxy-6-methyloxan-2-yl)oxyoxan-3-yl] (E)-3-(4-hydroxy-3-methoxyphenyl)prop-2-e	637,22	638,6	$C_{30}H_{30}O_{15}$	14,18	P (T)	P (T)	P(UT)	P (T)	P (T)	P(UT)			Flavanoid

(Continued)

10.3389/fpls.2023.1166813

TABLE 2 Continued

Metabolite	Experimental *m/z*	MW	MF	Rt	K14dpi 2SA88	K21dpi 2SA88	K14dpi 2SA107	K21dpi 2SA107	M14dpi 2SA88	M21dpi 2SA88	M14dpi 2SA107	M21dpi 2SA107	Biological role
Octyl-methoxycinnamate	290,4	291,16	$C_{18}H_{26}O_3$	11,76									Flavanoid
1-[2-methyl-6-[(2S,3R,4S,5S,6R)-3,4,5-trihydroxy-6-(hydroxymethyl)oxan-2-yl]oxyphenyl]ethanone	297,11	298,29	$C_{14}H_{18}O_8$	10,19		P(T)		P(UT)				P(T)	Flavanoid
9-OxoODE	293,18	294,4	$C_{18}H_{30}O_3$	12,75				P(UT)					Fatty acids
9-HOTrE	293,18	294,4	$C_{18}H_{30}O_3$	10,82	P (UT)	P (UT)		P(UT)					Fatty acids
PG(16:0/18:3)	743,48	744,56	$C_{40}H_{73}O_{10}P$	12,63	P (T)			P(UT)	P(UT)	P(UT)			Lipids
Norgestrel	311,19	312,4	$C_{21}H_{28}O_2$	12,18					P(T)				Flavanoid
2'-Deoxyguanosine	266,09	267,2	$C_{10}H_{13}N_{5O4}$	11,65	P(UT)		P(UT)		P(T)				Hormone
2-(4-Methyl-3-cyclohexen-1-yl)-2-propanyl 6-O-(6-deoxy-alpha-L-mannopyranosyl)-beta-D-glucopyranoside	461,2	462,5	$C_{22}H_{38}O_{10}$	13,56									Flavonoid
Dictamnoside D	449,28	450,5	$C_{21}H_{38}0_{11}$	13,08									Flavonoid
(3S)-5-[(1S,8aR)-2,5,5,8a-tetramethyl-4-oxo-4a,6,7,8-tetrahydro-1H-naphthalen-1-yl]-3-methylpentanoic acid	319,19	320,5	$C_{20}H_{32}O_3$	12,24									Flavonoid
2-[(1S,2S,4aR,8aS)-1-hydroxy-4a-methyl-8-methylidene-1,2,3,4,5,6,7,8a-octahydronaphthalen-2-yl]prop-2-enoic acid	249,15	250,33	$C_{15}H_{22}O_3$	10,98									Flavonoid
5,7-dihydroxy-2-(4-hydroxyphenyl)-8-[3,4,5-trihydroxy-6-(hydroxymethyl)oxan-2-yl]-6-(3,4,5-trihydroxyoxan-2-yl)chromen-4-one	563,16	564,5	$C_{26}H_{28}O_{14}$	6,83	P(UT)	P(T)		P (T)			P(T)		Flavonoid
PG(22:6/0:0)	555,28	554,3	$C_{26}H_{51}O_{10}P$	12,99	P(UT)		P(UT)		P(UT)	P(UT)	P(T)	P(UT)	Lipids
7-Glu tricin	491,12	492,4	$C_{23}H_{24}O_{12}$	13,23	P (T)							P(T)	Flavonoid
16-hydroxypalmitic acid	271,23	272,42	$C_{16}H_{32}O_3$	10,15									Fatty acid
[5-acetyloxy-3-(hydroxymethyl)-2-oxo-6-propan-2-ylcyclohex-3-en-1-yl] 3-methylpentanoate	339,14	340,4	$C_{18}H_{28}O_6$	10,46									Flavonoid
(2R)-5,8-dihydroxy-2-(2-hydroxyphenyl)-7-methoxy-2,3-dihydrochromen-4-one	301,12	302,28	$C_{16}H_{14}O_6$	3,07					P(T)				Lipids
PG(16:0/18:3)	744,48	745	$C_{40}H_{73}O_{10}P$	13	P (T)			P(UT)	P(UT)				Lipids
9-KODE	293,18	294,5	$C_{18}H_{30}O_3$	10,39			P (T)	P(UT)	P(UT)			P(T)	Fatty acid
Octyl-methoxycinnamate	291,16	290,4	$C_{18}H_{26}O_3$	9,87									Carboxylic Acids
6,7-dimethoxy-2,2-dimethyl-2h-1-benzopyran	235,15	236,26	$C_{13}H_{16}O_4$	11,55									Hormone
[5-acetyloxy-3-(hydroxymethyl)-2-oxo-6-propan-2-ylcyclohex-3-en-1-yl] ca	339,2	340,4	$C_{18}H_{28}O_6$	12,21					P(T)				Carboxylic Acids

(Continued)

10.3389/fpls.2023.1166813

10.3389/fpls.2023.1166813

TABLE 2 Continued

Metabolite	Experimental *m/z*	MW	MF	Rt	K14dpi 2SA88	K21dpi 2SA88	K14dpi 2SA107	K21dpi 2SA107	M14dpi 2SA88	M21dpi 2SA88	M14dpi 2SA107	M21dpi 2SA107	Biological role
2-[(4-adamantanylphenyl)carbonylamino]-3-indol-3-ylpropanoic acid	441,26	442,6	$C_{28}H_{30}N_2O_3$	12,65									Fatty acids
2,4-dihydroxyheptadec-16-enyl acetate	327,25	328,5	$C_{19}H_{36}O_4$	10,08				P(UT)	P(T)				Carboxylic Acids
Cyclopentaneacetic acid, 3-(hexopyranosyloxy)-2-[(2Z)-2-penten-1-yl]-	387,23	388,4	$C_{18}H_{28}O_9$	12,54									Carboxylic Acids
Vitexin 2''-O-rhamnoside II	593,15	594,5	$C_{27}H_{30}O_{14}$	7,78									Flavonoid
Ellipticine	246,31	247,17	$C_{17}H_{14}N_2$	11,49			P (T						Alkaloid
Silybin	481,14	482,44	$C_{25}H_{22}O_{10}$	11,39					P (T)	P (T)			Flavonoid

*The P(T) shaded in grey represent the identified metabolite found in treated sample at 14- and 21- dpi and the P(UT) shaded in blue represent identified metabolite found in non-treated control sample at 14- and 21- dpi. K14dpi = Koonap at 14 days post inoculation, K21dpi = Koonap at 21 days post inoculation, M14dpi = Morocco at 14 days post inoculation, M21dpi = Morocco at 21 days post inoculation.

the metabolites playing a role in *P. graminis* defence in the selected wheat varieties.

Quantified metabolic data can be explored for the determination of major metabolic differences between distinct wheat varieties as well as metabolic changes caused by *P. graminis* infection. In our study, the metabolomic profiles between the 2SA88 and 2SA107 infected wheat samples were almost similar (Figure 1), meaning that the genotype does not have a significant effect on the metabolite profile. The PCA model provided the virtual analysis of the effects of *P. graminis* treatments on wheat, mainly revealing clustering according to the time-points (Figure 3). This was indicative of the different metabolome profiles as the disease progressed (Mhlongo et al., 2020). The time-induced metabolomic changes following infection can be viewed in the context of metabolic pathways involved in the production of resistance related metabolites. The OPLS-DA score-plots further showed clear discrimination between the treated samples and control whereas S-plots allowed for the extraction of significant biomarkers (Figure 4). This observation is in agreement with previous works on wheat (Rudd et al., 2015; Cuperlovic-Culf et al., 2016; Duan et al., 2022; Mashabela et al., 2023), and other grains (Tugizimana et al., 2019; Li et al., 2022; Makhumbila et al., 2023). Overall, the separations observed gave insight into the chemistry and the differential metabolite profiles occurring in response to interactions with varying types of microbes. The biomarkers putatively annotated could serve in breeding programmes focusing on wheat improvement for rust resistance.

4.1 Role of annotated metabolites in defence against *P. graminis*

4.1.1 Flavonoids

Plants produce a wide variety of low-molecular weight secondary metabolites called flavonoids that serve a wide range of purposes including signalling between plants and microbes (Groenbaek et al., 2019), as well as defensive roles against biotic stress (Sukumaran et al., 2018). In this study, the flavonoids vicenin-2, vicenin-3; 2-[(1S,2S,4aR,8aS)-1-hydroxy-4a-methyl-8-methylidene-1,2,3,4,5,6,7,8a-octahydronaphthalen-2-yl]prop-2-enoic acid; 7-Glu tricin; (2E)-3-[4-({2-O-[(2S,3R,4R)-3,4-Dihydroxy-4-(hydroxymethyl)tetrahydro-2-furanyl]-beta-D-glucopyranosyl}oxy)-3-methoxyphenyl]acrylic acid; vitexin-2-rhamnoside were detected, whereas flavonoids such as chrysoeriol; saponarin I and others were detected but not identified under different time-points induced by stem rust infection (Table 2). Our findings demonstrate that the cellular metabolome is reprogrammed as a result of the response to stem rust infection, evident by the dynamic and distinct changes in metabolite profiles. Following the OPLS-DA analysis in Koonap vs. Morocco, vitexin-2-rhamnoside, dirhamnosyl linolenic acid, 6,8-di-C-glucosyl apigenin, and saponarin I (majority of flavonoids) were positively correlated to Koonap and negatively correlated to Morocco. These results are in support of the study conducted by Mashabela et al. (2022), wherein the variety Koonap was also enriched with flavonoid glycosides. The metabolite vitexin and its

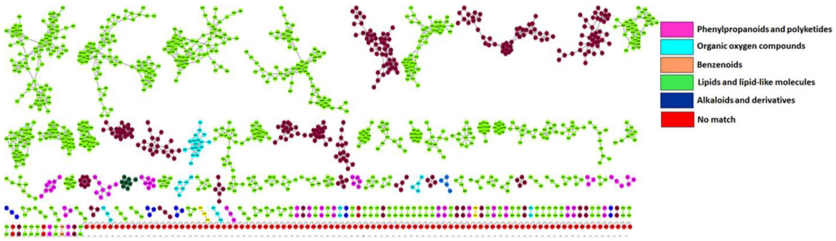

FIGURE 5
Molecular network of LC-MS spectra generated with MolNetEnhancer (in GNPS) giving a metabolome coverage and classes of extracted metabolites from *Pgt* treated and non-treated control plants. Each displayed node represents a metabolite, while each cluster of pooled nodes (coloured) depicts a class of chemically related and putatively annotated metabolites matched to GNPS libraries and databases. Red nodes represent unmatched spectral data.

derivatives is a natural flavonoid which is found in several plants including bamboo (Akter et al., 2021), mung bean (Wu et al., 2021), common buckwheat (Chua et al., 2020), hawthorn (Wu et al., 2021) and others. It has been shown to display antioxidant, anti-inflammatory, and anti-microbial effects (Noor et al., 2022). The other flavonoid glycosides detected in this study are shielding compounds that protect plants from oxidative damage caused by reactive oxygen species (ROSs) by slowing down oxidative degradation and scavenging free radicals (Groenbaek et al., 2019; Yang et al., 2020). In two separate studies reporting the metabolite profiling of wheat (Mashabela et al., 2022) and oat (Pretorius et al., 2022), varieties inoculated with *Puccinia triticina* and *Pseudomonas syringae* pv. Coronafaciens, respectively, elevated flavonoid glycosides production of dirhamnosyl linolenic acid, 6,8-di-C-glucosyl apigenin and others were also observed in response to inoculation with the two different plant pathogens. This is indicative of pathogen non-specificity of the detected flavonoid glycosides in protecting plants against diseases. A thorough dissection of the biosynthetic pathway and further investigation of the genes associated with the identified flavonoid glycosides could lead into the development of gene-based markers that can serve in breeding programs for rust resistance selection in wheat. Fractionation, isolation, purification and characterization of this group of biologically active secondary metabolites could also lead to a safer alternative to synthetic antifungal compounds or fungicides.

4.1.2 Fatty acids and lipids

Pathogen defence in plants is significantly influenced by fatty acids (FAs) metabolic pathways (Kachroo and Kachroo, 2009; Perincherry et al., 2019). Recent research, however, shows that FAs and the by-products of their breakdown play more direct roles in stimulating different plant defence mechanisms (Zhu et al., 2018; Yan et al., 2020; Sharma et al., 2021). In this study, oxooctadecadienoic (9-OxoODE), hydroxyoctadecatrienoic acid (9-HOTrE) and trihydroxyoctadecanoic annotated from treated samples for both time-points, i.e., 14 dpi and 21 dpi, have been previously reported to possess phytotoxic or antifungal properties (Rawlinson et al., 2019; Nigro et al., 2020; Elshazly et al., 2022). An analysis of the concentration of these two fatty acids as the infection progresses (from early to late stages) could assist in understanding their specific role and durability in wheat rust resistance. Octadecatrienoyl-glycerol on the other hand, a lipid that contributes to the physical barrier of the cell wall (Žilić, 2016) was annotated only at 14dpi. This could mean that the metabolite gets suppressed with the progression of the infection.

4.1.3 Carboxylic acids

Carboxylic acids or organic acids are compounds with a hydrocarbon radical with a carboxyl functional group connected to it (Kalgutkar and Daniels, 2010). These metabolites are often intermediating in amino acids-, lipids-, carbohydrates- and phenolic pathways (Xiao and Wu, 2014; Zhou et al., 2016). In order to produce molecules with a phenylpropane backbone under severe conditions, plants have exclusively acquired the ability to divert a significant quantity of carbon from the shikimic pathway into the different phenylpropanoid metabolism (Bhalla et al., 2005; Magazù et al., 2008; Vogt, 2010). The enzyme glucose-6-phosphate dehydrogenase (G6PDH), which transforms phosphate sugars to aromatic amino acids like phenylalanine, is mostly responsible for the formation of phenylpropanoids through the shikimic pathway. Later it is then used as the primary precursor and supplied into the phenylpropanoid biosynthesis pathway (Ali and Nozaki, 2007). In this current study, the carboxylic metabolites, cyclopentaneacetic acid, hydroxyamino, and dihydroxyheptadecane were differentially identified between the two wheat varieties, and thus could serve as biomarkers that distinguish between different genotypes (Rauf et al., 2021). The presence of these metabolites in the control and treated samples at both time-points is indicative of constitutive biosynthesis.

4.1.4 Sugars

Sugar molecules function as nutrients as well as regulators of metabolism, growth, stress responses (Sheen et al., 1999; Smeekens, 2000; Rolland et al., 2002; Rolland and Sheen, 2005; Rolland et al., 2006; O'Hara et al., 2013), and membrane stability under a variety of abiotic and biotic conditions (Koch, 1996; Hoekstra et al., 2001; Rosa et al., 2009; Lemoine et al., 2013). In addition to serving as metabolic intermediates, photosynthates including glucose, sucrose, and certain of their derivatives also function as signalling molecules that affect the metabolism of plant cells. These sugars act as substrates for the production of fatty acids. It is known that the processes such as pathogen attack, wounding, and ultimately activation and repression of defence genes related to these

processes are affected by glucose signalling through hexokinase dependent pathways (Tauzin and Giardina, 2014; Saddhe et al., 2021). Additionally, several studies where wheat was infected by a pathogen have demonstrated that *T. aestivum* may synthesize glucose and its glycosides as defence molecules (Brinkhaus et al., 2000; Satake and Kobuke, 2007; Shukri et al., 2011; Alqahtani et al., 2015). However, the present study did not find many of these compounds. Although hexopyranoside compound has been identified and biologically is categorized as sugar and was synthesised in the treated varieties at 21dpi (Table 3).

4.1.5 Nucleosides

G proteins, also referred to as guanine nucleotide-binding proteins, are a family of proteins that function as molecular switches within cells, conveying signals from a range of stimuli outside a cell to its interior (Gunnaiah and Kushalappa, 2014). A purine nucleoside such as guanosine, anchored on the cytoplasmic cell membrane were observed on the treated sample, Morocco at 14dpi and they are mediators for many cellular processes, including signal transduction, protein transport and growth regulation (Gogoi et al., 2001). According to Gunnaiah and Kushalappa (2014), G proteins are essential parts of plant defensive responses to pathogen challenge. Guanosine is a good signalling molecule that can reflect the metabolic and oxidative state of the cell due to its capacity to form complexes and its ease of metabolism in many cell compartments (Martínez-Reyes and Chandel, 2020). This finding suggested that guanosine and stem rust resistance may be tightly connected.

4.1.6 Alkaloids

Commonly, alkaloids are concentrated in specific organs like the leaves, bark, or roots. It has been proposed that alkaloids in plants serve as a defence mechanism against pathogenic pests owing to their bitter taste (Kaur and Arora, 2015). Alkaloids act as shielding compounds that protect plants by scavenging free radicals and thereby reducing cell stress (Debegnach et al., 2019). These protective qualities can be a potent strategy in the fight against resistant microorganisms. A pyridoindole alkaloid known as ellipticine was identified in Koonap variety at 21 dpi. The source of pyrrolidine alkaloids is l-ornithine. L-ornithine is first converted to putrescine by the enzyme ornithine decarboxylase (ODC), which is subsequently converted to methylputrescine by the enzyme putrescine N-methyltransferase (Docimo et al., 2012). Methylputrescine is deaminated and oxidized to generate 1-

TABLE 3 Significant metabolic pathways found to be active in *P. graminis*, inferred from Metabolomics Pathway Analysis (MetPA).

Pathway Name	Match Status	p	-log(p)	Holm p	FDR	Impact	Details
Thiamine metabolism	2/22	0.027694	1.5576	1.0	1.0	0.11561	KEGG
Folate biosynthesis	2/27	0.040612	1.3913	1.0	1.0	0.08748	KEGG
Alpha-Linolenic acid metabolism	2/27	0.040612	1.3913	1.0	1.0	0.22025	KEGG
Glyoxylate and dicarboxylate metabolism	2/29	0.046315	1.3343	1.0	1.0	0.10147	KEGG
Riboflavin metabolism	1/11	0.12592	0.89991	1.0	1.0	0.06667	KEGG
Cutin, suberine and wax biosynthesis	1/14	0.15758	0.80251	1.0	1.0	0.25	KEGG
Sulfur metabolism	1/15	0.16789	0.77498	1.0	1.0	0.06077	KEGG
Purine metabolism	2/63	0.17544	0.75588	1.0	1.0	0.0	KEGG
Tyrosine metabolism	1/18	0.19811	0.70309	1.0	1.0	0.0	KEGG
Glycerolipid metabolism	1/21	0.2273	0.6434	1.0	1.0	0.11765	KEGG
Biosynthesis of unsaturated fatty acids	1/22	0.2368	0.62561	1.0	1.0	0.0	KEGG
Valine, leucine and isoleucine biosynthesis	1/22	0.2368	0.62561	1.0	1.0	0.02145	KEGG
Pyruvate metabolism	1/22	0.2368	0.62561	1.0	1.0	0.075	KEGG
Tryptophan metabolism	1/23	0.2462	0.60871	1.0	1.0	0.27586	KEGG
Cyanoamino acid metabolism	1/26	0.27373	0.56267	1.0	1.0	0.0	KEGG
Glycolysis / Gluconeogenesis	1/26	0.27373	0.56267	1.0	1.0	0.00151	KEGG
Galactose metabolism	1/27	0.2827	0.54867	1.0	1.0	0.0	KEGG
Glutathione metabolism	1/27	0.2827	0.54867	1.0	1.0	0.07071	KEGG
Terpenoid backbone biosynthesis	1/29	0.30032	0.52241	1.0	1.0	0.1008	KEGG
Glycine, serine and threonine metabolism	1/33	0.33435	0.4758	1.0	1.0	0.21178	KEGG

The Thiamine metabolism, Folate biosynthesis, Alpha-Linolenic acid metabolism and Glyoxylate and dicarboxylate metabolism pathways were the most impactful among the different cultivars and showed the highest statistical significance (p-value < 0.05).

methylpyrrolinium, the precursor of all pyrrolidine alkaloids, under the catalysis of primary amine: oxygen oxidoreductase (AOC).

4.2 Pathway analysis

An interactive visualization of pathway enrichment analysis at the metabolome level was presented in Figures 6A, B. Twenty biological pathways (Table 3) were identified by pathway enrichment analysis as having a substantial influence on stem rust tolerance. The pathways in Figure 6C are linked to the annotated metabolites of the two different wheat varieties. The KEGG pathway of the model plant *Oryza sativa* was used to map the discovered metabolites, illustrating the function of various metabolites in distinct metabolic pathways. Based on matched metabolites from the data, the thiamine; folate biosynthesis; alpha linolenic acid metabolism; and glyoxylate and dicarboxylate metabolism pathways exhibited relatively substantial influence. The riboflavin; cutin, suberin and

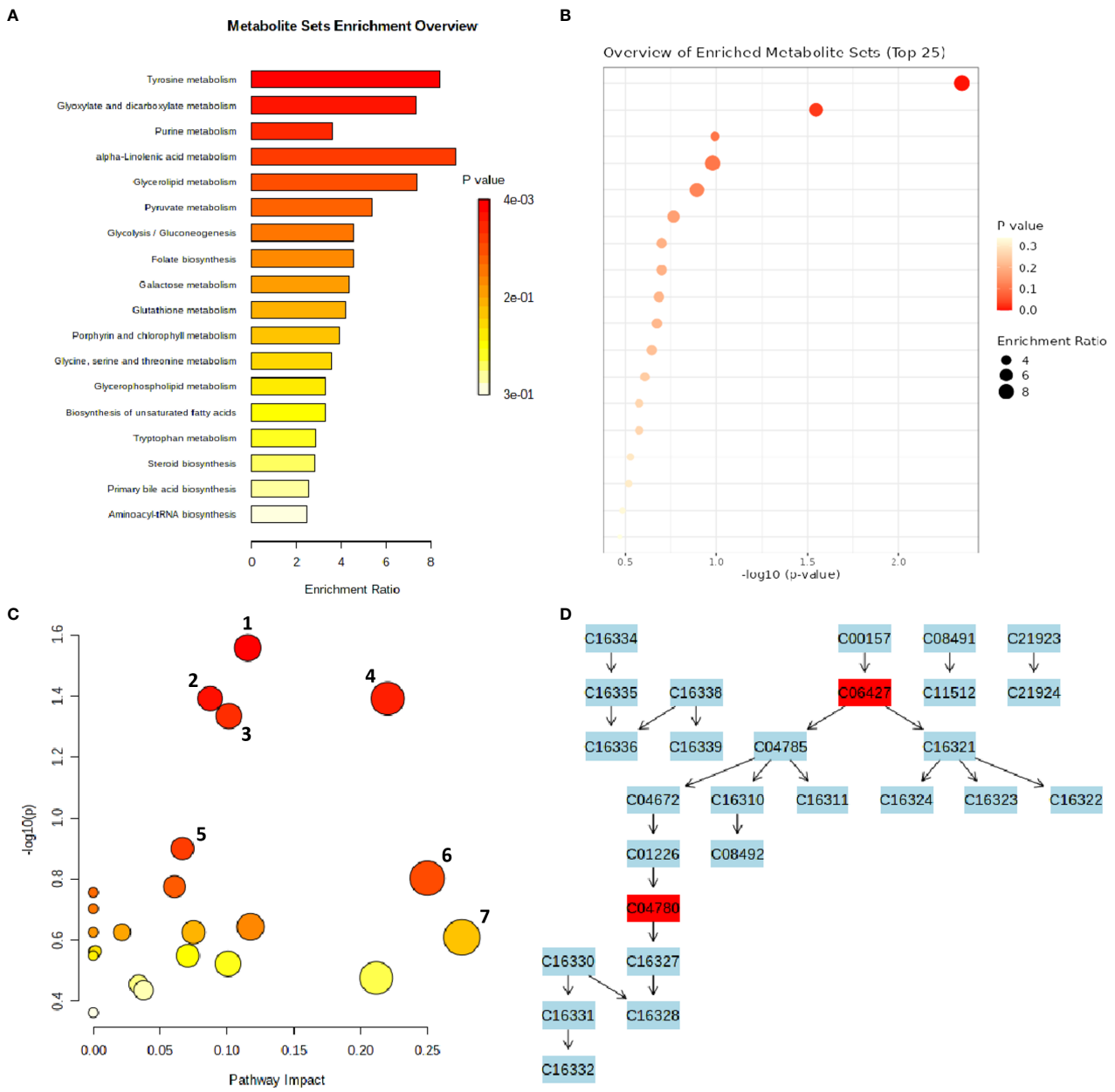

FIGURE 6
MetaboAnalyst-computed pathway analysis. **(A, B)** Representation of pathway enrichment analysis showing the metabolome view of the rust induced changes in different metabolic pathways. **(C)** Pathway view of statistically significant pathways flagged from the metabolome view based on matched metabolites, where the number represent 1) Thiamine pathway, 2) Folate biosynthesis, 3) Glyoxylate and dicarboxylate metabolism, 4) Alpha-Linolenic acid metabolism, 5) Riboflavin metabolism, 6) Cutin, suberine and wax biosynthesis, 7) Sulfur metabolism. **(D)** The diagram illustrates the integration and contribution of matched metabolites in the flagged Thiamine pathway.

wax biosynthesis; thiamine; folate; alpha linolenic metabolism; and glyoxylate and dicarboxylate metabolism pathways were the most statistically significant pathways.

Thiamine acts as a cofactor and activator to increase a plants' resistance to disease and stress (Rapala-Kozik et al., 2012). According to the metabolic pathway, the metabolites were used as precursors for thiamine pyrophosphate (TPP), a crucial molecule required for metabolic processes such acetyl-CoA biosynthesis, amino acid biosynthesis, the Krebs cycle, and the Calvin cycle (Dong et al., 2016). The integration and contribution of matched metabolites in the highlighted thiamine pathway are shown in Figure 6D. The KEGG IDs are used to match the metabolites (e.g., orientin: C10195). The glyoxylate and dicarboxylate metabolism pathways, which result in the formation of oxoglutarate, share a metabolic pathway with the matching metabolites that serve as thiamine intermediates (Figure 6D) in the thiamine pathway (Nigro et al., 2020). The other top enriched pathways in this study; folate biosynthesis is a component of the methylation reaction required for the production of lipids, proteins, chlorophyll, and lignin (Klaus et al., 2005). One of the most significant metabolic routes in plants, alpha-linolenic serves as the main energy source for cellular metabolism. Riboflavin metabolism directs photosynthesis to the phenylpropanoid pathway, which is involved in critical processes such as plant development and growth as well as the reduction of biotic and abiotic stress (Boubakri et al., 2013). In addition, suberin, a glycerol-phenol-lipid polymer, plays an important role in the resistance/tolerance response of plants to external factors such as drought, salt, pests, and disease stress. It acts as an apoplastic barrier, by impeding pathogen invasion and minimising water and nutrient movement across the cell wall (Ranathunge et al., 2011; Holbein et al., 2019). Therefore, in resistant genotypes of wheat, it is evident that there's enhanced accumulation of functional metabolic components such as thiamine, riboflavin, cutin, suberin, plant wax, and others, ensuring the normal growth and development of the plants.

5 Conclusion

The LC-qTOF-MS-based metabolomics approach revealed biomarkers associated with the wheat-pathogen interaction from four key classes of phenolic compounds such as flavonoids, hydroxycinnamic acid derivatives and polyphenols. The list also consists of fatty acids, carboxylic acids, and several sugars. In this study, it was discovered that the distributions of these metabolites varied depending on the differences between the two rust races and time-points. The findings further support the impact of differences based on a broader coverage of the metabolome and rich structural information from the interactions of the molecules in their natural environment. Overall, the riboflavin, cutin and suberin metabolism, thiamine, folate and alpha linolenic metabolism, and glyoxylate and dicarboxylate metabolism pathways were the most statistically significant pathways associated with the metabolites identified to be controlling wheat defence to *P. graminis*. Further investigations are however needed to better understand the mechanisms controlling these pathways, especially from the early to late stages of the infection. Moreover, studies on fractionation, isolation, purification and characterization of the detected biologically active group of secondary metabolites could lead to safer alternatives to synthetic antifungal compounds or fungicides. The potential for integrating metabolomics with other omics, such as genomics, transcriptomics, and proteomics, will aid in the discovery and characterization of significant candidate effectors in wheat pathogens at the molecular level and the development of novel molecular approaches for enhancing pathogen resistance in wheat. Additionally, crop breeders can use these tools to identify markers for desired traits, reintroduce genetic variation, and introduce desirable characteristics. The results from this study will pave a way to understand the mechanism of defence in wheat in response to rust pathogen infections.

Data availability statement

The raw data supporting the conclusions of this article will be made available by the authors, without undue reservation.

Author contributions

SF conceptualised and designed the experiment. MM, MR and SF conducted the plant growth experiments and applied the treatments. MM, MR and SF conducted the metabolite extractions. MM, MR, and EM conducted the LC-MS analysis. Data analysis was done by MM and EN. Revision of the manuscript was by MM, MR, EM, EN and SF. All authors contributed to the article and approved the submitted version.

Funding

This work was supported by the National Research Foundation Thuthuka research grant (TTK190323424245). The funders had no role in the study design, data collection and analysis. The decision to publish the prepared manuscript was solely by the authors.

Acknowledgments

We would like to acknowledge ARC-SGI (South Africa) for their provision of experimental facilities, pathogen material and germplasm. Ms. Joyce Mebalo and Ms. Tsepiso Hlongoane from ARC-SGI are acknowledged for technical assistance. Ms. Anza Ramabulana from the University of Venda is also acknowledged for assistance with LC-MS analysis.

Conflict of interest

The authors declare that the research was conducted in the absence of any commercial or financial relationships that could be construed as a potential conflict of interest.

Publisher's note

Supplementary material

The Supplementary Material for this article can be found online at: https://www.frontiersin.org/articles/10.3389/fpls.2023.1166813/full#supplementary-material

SUPPLEMENTARY FIGURE 1
Representative UHPLC-QTOF-MS base peak intensity (BPI) chromatograms of Morocco cultivar methanolic-extracts. BPI MS chromatograms revealed differentially populated peaks for Morocco infected with rust race 2SA88 at 14-, 21 dpi (**A, B**, respectively), infected with rust race 2SA107 at 14-, 21 dpi (**C, D**, respectively) and control (**E, F**, respectively) each with unique m/z values, intensities and retention times (Rt's), representing the qualitative (presence/absence) and quantitative (intensity/concentration) detection of metabolites, thus providing a visual description of the similarities and differences between the selected wheat varieties.

SUPPLEMENTARY FIGURE 2
OPLS-DA modelling showing the selection of signatory biomarkers associated with response of rust race infections of 2SA88 and 2SA107. The OPLS-DA scores plot **(A, C)** showed clear discrimination between the treated samples and control whereas S-plots **(B, D)** allowed for the extraction of significant biomarkers. Extracted ions representing significant biomarkers responsible for the difference between the control at the top right corner (in the blue rectangle) and samples treated with *Pgt.* at the bottom left corner (in the red rectangle) for both Koonap and Morocco cultivars at 21dpi, respectively.

References

Akter, R., Afrose, A., Rahman, M. R., Chowdhury, R., Nirzhor, S. S. R., Khan, R. I., et al. (2021). A comprehensive analysis into the therapeutic application of natural products as SIRT6 modulators in alzheimer's disease, aging, cancer, inflammation, and diabetes. *Int. J. Mol. Sci.* 22 (8), 4180. doi: 10.3390/ijms22084180

Ali, V., and Nozaki, T. (2007). Current therapeutics, their problems, and sulfur-containing-amino-acid metabolism as a novel target against infections by "amitochondriate" protozoan parasites. *Clin. Microbiol. Rev.* 20 (1), 164–187. doi: 10.1128/CMR.00019-06

Alqahtani, A., Tongkao-on, W., Li, K. M., Razmovski-Naumovski, V., Chan, K., and Li, G. Q. (2015). Seasonal variation of triterpenes and phenolic compounds in Australian *Centella asiatica* (L.) urb. *Phytochem. Anal.* 26 (6), 436–443. doi: 10.1002/pca.2578

Bajgain, P., Rouse, M. N., Tsilo, T. J., Macharia, G. K., Bhavani, S., Jin, Y., et al. (2016). Nested association mapping of stem rust resistance in wheat using genotyping by sequencing. *PloS One* 11 (5), e0155760. doi: 10.1371/journal.pone.0155760

Bender, C. M., Prins, R., and Pretorius, Z. A. (2016). Development of a greenhouse screening method for adult plant response in wheat to stem rust. *Plant Dis.* 100 (8), 1627–1633. doi: 10.1094/PDIS-02-16-0163-RE

Bhalla, R., Narasimhan, K., and Swarup, S. (2005). Metabolomics and its role in understanding cellular responses in plants. *Plant Cell Rep.* 24 (10), 562–571. doi: 10.1007/s00299-005-0054-9

Boshoff, W. H. P., Pretorius, Z. A., Terefe, T. G., Bender, C. M., Herselman, L., Maree, G. J., et al. (2018). Phenotypic and genotypic description of *Puccinia graminis* f.sp. *tritici* race 2SA55 in south Africa. *Eur. J. Plant Pathol.* 152, 783–789. doi: 10.1007/s10658-018-1527-3

Boubakri, H., Chong, J., Poutaraud, A., Schmitt, C., Bertsch, C., Mliki, A., et al. (2013). Riboflavin (Vitamin b 2) induces defence responses and resistance to plasmopara viticola in grapevine. *Eur. J. Plant Pathol.* 136, 837–855. doi: 10.1007/s10658-013-0211-x

Brinkhaus, B., Lindner, M., Schuppan, D., and Hahn, E. G. (2000). Chemical, pharmacological and clinical profile of the East Asian medical plant *Centella aslatica*. *Phytomedicine* 7 (5), 427–448. doi: 10.1016/S0944-7113(00)80065-3

Chua, L. S., Abdullah, F. I., and Awang, M. A. (2020). Potential of natural bioactive c-glycosyl flavones for antidiabetic properties. *Stu. N. Pro. Chem.* 64, 241–261. doi: 10.1016/B978-0-12-817903-1.00008-5

Cuperlovic-Culf, M., Wang, L., Forseille, L., Boyle, K., Merkley, N., Burton, I., et al. (2016). Metabolic biomarker panels of response to fusarium head blight infection in different wheat varieties. *PloS One* 11 (4), e0153642. doi: 10.1371/journal.pone.0153642

Davis, S. K., Kirk, D. A., Armstrong, L. M., Devries, J. H., and Fisher, R. J. (2020). Shifting from spring wheat to winter wheat: a potential conservation strategy for grassland songbirds in cultivated landscapes? *Biol. Conserv.* 245, 108530. doi: 10.1016/j.biocon.2020.108530

Debegnach, F., Patriarca, S., Brera, C., Gregori, E., Sonego, E., Moracci, G., et al. (2019). Ergot alkaloids in wheat and rye derived products in Italy. *Foods* 8 (5), 150. doi: 10.3390/foods8050150

Deihimfard, R., Rahimi-Moghaddam, S., Collins, B., and Azizi, K. (2022). Future climate change could reduce irrigated and rainfed wheat water footprint in arid environments. *Sci. Total Environ.* 807, 150991. doi: 10.1016/j.scitotenv.2021.150991

Docimo, T., Reichelt, M., Schneider, B., Kai, M., Kunert, G., Gershenzon, J., et al. (2012). The first step in the biosynthesis of cocaine in erythroxylum coca: the characterization of arginine and ornithine decarboxylases. *Plant Mol. Biol.* 78 (6), 599–615. doi: 10.1007/s11103-012-9886-1

Dong, W., Thomas, N., Ronald, P. C., and Goyer, A. (2016). Overexpression of thiamin biosynthesis genes in rice increases leaf and unpolished grain thiamin content but not resistance to *Xanthomonas oryzae* pv. *oryzae*. *Front. Plant Sci.* 7. doi: 10.3389/fpls.2016.00616

Duan, S., Jin, J., Gao, Y., Jin, C., Mu, J., Zhen, W., et al. (2022). Integrated transcriptome and metabolite profiling highlights the role of benzoxazinoids in wheat resistance against fusarium crown rot. *Crop J.* 10 (2), 407–417. doi: 10.1016/j.cj.2021.06.004

Duveiller, E., Singh, R. P., and Nicol, J. M. (2007). The challenges of maintaining wheat productivity: pests, diseases, and potential epidemics. *Euphytica* 157 (3), 417–430. doi: 10.1007/s10681-007-9380-z

Elshazly, E. H., Mohamed, A. K. S., Aboelmagd, H. A., Gouda, G. A., Abdallah, M. H., Ewais, E. A., et al. (2022). Phytotoxicity and antimicrobial activity of green synthesized silver nanoparticles using nigella sativa seeds on wheat seedlings. *J. Chem.* 2022, 1–9. doi: 10.1155/2022/9609559

FAO (2017) *FAOSTAT* (Rome: FAO). Available at: http://faostat.fao.org (Accessed 15 JanuarySeptember 2017).

FAO/WHO Human vitamin and mineral requirements (2020). *Report of a joint FAO/WHO expert consultation* (Rome, Italy: Bangkok, Thailand Food and Nutrition Division, FAO).

Gogoi, R., Singh, D. V., and Srivastava, K. D. (2001). Phenols as a biochemical basis of resistance in wheat against karnal bunt. *Plant Path.* 50 (4), 470–476. doi: 10.1046/j.1365-3059.2001.00583.x

Groenbaek, M., Tybirk, E., Neugart, S., Sundekilde, U. K., Schreiner, M., and Kristensen, H. L. (2019). Flavonoid glycosides and hydroxycinnamic acid derivatives in baby leaf rapeseed from white and yellow flowering cultivars with repeated harvest in a 2-years field study. *Front. Plant Sci.* 10. doi: 10.3389/fpls.2019.00355

Grote, U., Fasse, A., Nguyen, T. T., and Erenstein, O. (2021). Food security and the dynamics of wheat and maize value chains in Africa and Asia. *Front. Sustain. Food Syst.* 4. doi: 10.3389/fsufs.2020.617009

Gunnaiah, R., and Kushalappa, A. C. (2014). Metabolomics deciphers the host resistance mechanisms in wheat cultivar sumai-3, against trichothecene producing and non-producing isolates of *Fusarium graminearum*. *Plant Physiol. Biochem.* 83, 40–50. doi: 10.1016/j.plaphy.2014.07.002

Hamany Djande, C. Y., Piater, L. A., Steenkamp, P. A., Tugizimana, F., and Dubery, I. A. (2021). A metabolomics approach and chemometric tools for differentiation of barley cultivars and biomarker discovery. *Metabolites* 11 (9), 578. doi: 10.3390/metabo11090578

Hoekstra, F. A., Golovina, E. A., and Buitink, J. (2001). Mechanisms of plant desiccation tolerance. *Trends Plant Sci.* 6 (9), 431–438. doi: 10.1016/S1360-1385(01)02052-0

Holbein, J., Franke, R. B., Marhavý, P., Fujita, S., Górecka, M., Sobczak, M., et al. (2019). Root endodermal barrier system contributes to defence against plant-parasitic cyst and root-knot nematodes. *Plant J.* 100 (2), 221–236. doi: 10.1111/tpj.14459

Kachroo, A., and Kachroo, P. (2009). Fatty acid–derived signals in plant defence. *Annu. Rev. Phytopathol.* 47, 153–176. doi: 10.1146/annurev-phyto-080508-081820

Kalgutkar, A. S., and Daniels, J. S. (2010). Carboxylic acids and their bioisosteres. metabolism, pharmacokinetics and toxicity of functional groups: impact of chemical building blocks on ADMET 99–167.

Kaur, R., and Arora, S. (2015). Alkaloids-important therapeutic secondary metabolites of plant origin. *J. Crit. Rev.* 2 (3), 1–8.

Klaus, S. M., Wegkamp, A., Sybesma, W., Hugenholtz, J., Gregory, J. F., and Hanson, A. D. (2005). A nudix enzyme removes pyrophosphate from dihydroneopterin triphosphate in the folate synthesis pathway of bacteria and plants. *J. Biol. Chem.* 280 (7), 5274–5280. doi: 10.1074/jbc.M413759200

Kloppers, F. J., and Pretorius, Z. A. (1997). Effects of combinations amongst genes *Lr13, Lr34* and *Lr37* on components of resistance in wheat to leaf rust. *Plant Pathol.* 46 (5), 737–750. doi: 10.1046/j.1365-3059.1997.d01-58.x

Koch, K. E. (1996). Carbohydrate-modulated gene expression in plants. *Annu. Rev. Plant Biol.* 47 (1), 509–540. doi: 10.1146/annurev.arplant.47.1.509

Lemoine, R., Camera, S. L., Atanassova, R., Dédaldéchamp, F., Allario, T., Pourtau, N., et al. (2013). Source-to-sink transport of sugar and regulation by environmental factors. *Front. Plant Sci.* 4. doi: 10.3389/fpls.2013.00272

Li, Y., Lv, P., Mi, J., Zhao, B., and Liu, J. (2022). Integrative transcriptome and metabolome analyses of the interaction of oat–oat stem rust. *Agron.* 12 (10), 2353. doi: 10.3390/agronomy12102353

Madala, S., Satyanarayana, A. N. V., and Rao, T. N. (2014). Performance evaluation of PBL and cumulus parameterization schemes of WRF ARW model in simulating severe thunderstorm events over gadanki MST radar facility–case study. *Atmos. Res.* 139, 1–17. doi: 10.1016/j.atmosres.2013.12.017

Magazù, S., Migliardo, F., and Telling, M. T. F. (2008). Structural and dynamical properties of water in sugar mixtures. *Food Chem.* 106 (4), 1460–1466. doi: 10.1016/j.foodchem.2007.05.097

Makhumbila, P., Rauwane, M. E., Muedi, H. H., Madala, N. E., and Figlan, S. (2023). Metabolome profile variations in common bean (*Phaseolus vulgaris l.*) resistant and susceptible genotypes incited by rust (*Uromyces appendiculatus*). *Front. Genet.* 14 (258). doi: 10.3389/fgene.2023.1141201

Martínez-Reyes, I., and Chandel, N. S. (2020). Mitochondrial TCA cycle metabolites control physiology and disease. *Nat. Commun.* 11 (1), 1–11. doi: 10.1038/s41467-019-13668-3

Mashabela, M. D., Piater, L. A., Dubery, I. A., Tugizimana, F., and Mhlongo, M. I. (2022). Comparative metabolite profiling of wheat cultivars (*Triticum aestivum*) reveals signatory markers for resistance and susceptibility to stripe rust and aluminium (Al3+) toxicity. *Metabolites* 12 (2), 98. doi: 10.3390/metabo12020098

Mashabela, M. D., Tugizimana, F., Steenkamp, P. A., Piater, L. A., Dubery, I. A., Terefe, T., et al. (2023). Metabolomic evaluation of PGPR defence priming in wheat (*Triticum aestivum* l.) cultivars infected with *Puccinia striiformis* f. sp. *tritici* (stripe rust). *Front. Plant Sci.* 14. doi: 10.3389/fpls.2023.1103413

McCallum, B. D., Hiebert, C. W., Cloutier, S., Bakkeren, G., Rosa, S. B., Humphreys, D. G., et al. (2016). A review of wheat leaf rust research and the development of resistant cultivars in Canada. *Can. J. Plant Pathol.* 38 (1), 1–18. doi: 10.1080/07060661.2016.1145598

Mhlongo, M. I., Piater, L. A., Steenkamp, P. A., Labuschagne, N., and Dubery, I. A. (2020). Metabolic profiling of PGPR-treated tomato plants reveal priming-related adaptations of secondary metabolites and aromatic amino acids. *Metabolites* 10 (5), 210. doi: 10.3390/metabo10050210

Mondal, S., Rutkoski, J. E., Velu, G., Singh, P. K., Crespo-Herrera, L. A., Guzman, C., et al. (2016). Harnessing diversity in wheat to enhance grain yield, climate resilience, disease and insect pest resistance and nutrition through conventional and modern breeding approaches. *Front. Plant Sci.* 7. doi: 10.3389/fpls.2016.00991

Nigro, D., Grausgruber, H., Guzmán, C., and Laddomada, B. (2020). Phenolic compounds in wheat kernels: genetic and genomic studies of biosynthesis and regulations. *Wheat Qual. For Improving Process. And Hum. Health*, 225–253. doi: 10.1007/978-3-030-34163-3_1

Noor, K. K., Ijaz, M. U., Ehsan, N., Tahir, A., Yeni, D. K., Zihad, S. N. K., et al. (2022). Hepatoprotective role of vitexin against cadmium-induced liver damage in male rats: a biochemical, inflammatory, apoptotic and histopathological investigation. *Biomed. Pharmacother.* 150, 112934. doi: 10.1016/j.biopha.2022.112934

O'Hara, L. E., Paul, M. J., and Wingler, A. (2013). How do sugars regulate plant growth and development? new insight into the role of trehalose-6-phosphate. *Mol. Plant* 6 (2), 261–274. doi: 10.1093/mp/sss120

Perincherry, L., Lalak-Kańczugowska, J., and Stępień, Ł. (2019). Fusarium-produced mycotoxins in plant-pathogen interactions. *Toxins* 11 (11), 664. doi: 10.3390/toxins11110664

Pretorius, Z. A., Pakendorf, K. W., Marais, G. F., Prins, R., and Komen, J. S. (2007). Challenges for sustainable cereal rust control in south Africa. *Aust. J. Agric. Res.* 58 (6), 593–601. doi: 10.1071/AR06144

Pretorius, Z. A., Singh, R. P., Wagoire, W. W., and Payne, T. S. (2000). Detection of virulence to wheat stem rust resistance gene *Sr31* in *Puccinia graminis.* f. sp. *tritici* in Uganda. *Plant Dis.* 84 (2), 203–203. doi: 10.1094/PDIS.2000.84.2.203B

Pretorius, C. J., Steenkamp, P. A., Tugizimana, F., Piater, L. A., and Dubery, I. A. (2022). Metabolomic characterisation of discriminatory metabolites involved in halo blight disease in oat cultivars caused by *Pseudomonas syringae* pv. coronafaciens. *Metabolites* 12 (3), 248. doi: 10.3390/metabo12030248

Ramabulana, A. T., Petras, D., Madala, N. E., and Tugizimana, F. (2021). Metabolomics and molecular networking to characterize the chemical space of four momordica plant species. *Metabolites* 11 (11), 763. doi: 10.3390/metabo11110763

Ranathunge, K., Schreiber, L., and Franke, R. (2011). Suberin research in the genomics era–new interest for an old polymer. *Plant Sci.* 180 (3), 399–413. doi: 10.1016/j.plantsci.2010.11.003

Rapala-Kozik, M., Wolak, N., Kujda, M., and Banas, A. K. (2012). The upregulation of thiamine (vitamin B1) biosynthesis in arabidopsis thaliana seedlings under salt and osmotic stress conditions is mediated by abscisic acid at the early stages of this stress response. *BMC Plant Biol.* 12 (1), 1–14. doi: 10.1186/1471-2229-12-2

Rauf, M., Awais, M., Ud-Din, A., Ali, K., Gul, H., Rahman, M. M., et al. (2021). Molecular mechanisms of the 1-aminocyclopropane-1-carboxylic acid (ACC) deaminase producing *Trichoderma asperellum* MAP1 in enhancing wheat tolerance to waterlogging stress. *Front. Plant Sci.* 11. doi: 10.3389/fpls.2020.614971

Rawlinson, C., See, P. T., Moolhuijzen, P., Li, H., Moffat, C. S., Chooi, Y. H., et al. (2019). The identification and deletion of the polyketide synthase-nonribosomal peptide synthase gene responsible for the production of the phytotoxic triticone A/B in the wheat fungal pathogen pyrenophora tritici-repentis. *Environ. Microbiol.* 21 (12), 4875–4886. doi: 10.1111/1462-2920.14854

Rolland, F., Baena-Gonzalez, E., and Sheen, J. (2006). Sugar sensing and signaling in plants: conserved and novel mechanisms. *Annu. Rev. Plant Biol.* 57, 675–709. doi: 10.1146/annurev.arplant.57.032905.105441

Rolland, F., Moore, B., and Sheen, J. (2002). Sugar sensing and signaling in plants. *Plant Cell* 14(suppl_1), S185–S205. doi: 10.1105/tpc.010455.

Rolland, F., and Sheen, J. (2005). Sugar sensing and signalling networks in plants 269–271.

Rosa, M., Prado, C., Podazza, G., Interdonato, R., González, J. A., Hilal, M., et al. (2009). Soluble sugars: metabolism, sensing and abiotic stress: a complex network in the life of plants. *Plant Signal. Behav.* 4 (5), 388–393. doi: 10.4161/psb.4.5.8294

Rudd, J. J., Kanyuka, K., Hassani-Pak, K., Derbyshire, M., Andongabo, A., Devonshire, J., et al. (2015). Transcriptome and metabolite profiling of the infection cycle of zymoseptoria tritici on wheat reveals a biphasic interaction with plant immunity involving differential pathogen chromosomal contributions and a variation on the hemibiotrophic lifestyle definition. *Plant Physiol.* 167 (3), 1158–1185. doi: 10.1104/pp.114.255927

Rust Tracker (2021) *CIMMYT*. Available at: https://rusttracker.cimmyt.org/?page_id=22.

Saccenti, E., Gowda, G. N., Raftery, D., Alahmari, F., Jaremko, L., Jaremko, M., et al. (2019). NMR spectroscopy for metabolomics research. *Metabolites* 9 (7), 123. doi: 10.3390/metabo9070123

Saccenti, E., Hoefsloot, H. C., Smilde, A. K., Westerhuis, J. A., and Hendriks, M. M. (2013). Reflections on univariate and multivariate analysis of metabolomics data. *Metabolomics* 10 (3), 361–374. doi: 10.1007/s11306-013-0598-6

Saccenti, E., Smilde, A. K., and Camacho, J. (2018). Group-wise ANOVA simultaneous component analysis for designed omics experiments. *Metabolomics* 14 (6), 1–18. doi: 10.1007/s11306-018-1369-1

Saddhe, A. A., Manuka, R., and Penna, S. (2021). Plant sugars: homeostasis and transport under abiotic stress in plants. *Physiol. Plant* 171 (4), 739–755. doi: 10.1111/ppl.13283

Satake, A., and Kobuke, Y. (2007). Artificial photosynthetic systems: assemblies of slipped cofacial porphyrins and phthalocyanines showing strong electronic coupling. *Org. Biomol. Chem.* 5 (11), 1679–1691. doi: 10.1039/B703405A

Saunders, D. G., Pretorius, Z. A., and Hovmøller, M. S. (2019). Tackling the re-emergence of wheat stem rust in Western Europe. *Commun. Biol.* 2 (1), 1–3. doi: 10.1038/s42003-019-0294-9

Sharma, P., Jha, A. B., Dubey, R. S., and Pessarakli, M. (2021). "Reactive oxygen species generation, hazards, and defense mechanisms in plants under environmental (abiotic and biotic) stress conditions," in *Handbook of plant and crop physiology*. (London: Taylor and Francis Group), 617–658.

Sheen, J., Zhou, L., and Jang, J. C. (1999). Sugars as signaling molecules. *Curr. Opin. Plant Biol.* 2 (5), 410–418. doi: 10.1016/S1369-5266(99)00014-X

Shukri, R., Mohamed, S., Mustapha, N. M., and Hamid, A. A. (2011). Evaluating the toxic and beneficial effects of jering beans (Archidendronjiringa) in normal and diabetic rats. *J. Sci. Food Agric.* 91 (14), 2697–2706. doi: 10.1002/jsfa.4516

Singh, R. P., Hodson, D. P., Huerta-Espino, J., Jin, Y., Bhavani, S., Njau, P., et al. (2011). The emergence of Ug99 races of the stem rust fungus is a threat to world wheat production. *Annu. Rev. Phytopathol.* 49, 465–481. doi: 10.1146/annurev-phyto-072910-095423

Singh, R. P., Hodson, D. P., Huerta-Espino, J., Jin, Y., Njau, P., Wanyera, R., et al. (2008). Will stem rust destroy the world's wheat crop? *Adv. Agron.* 98, 271–278. doi: 10.1016/S0065-2113(08)00205-8

Singh, R. P., Hodson, D. P., Jin, Y., Huerta-Espino, J., Kinyua, M. G., Wanyera, R., et al. (2006). *Current status, likely migration and strategies to mitigate the threat to wheat production from race Ug99 (TTKS) of stem rust pathogen* Vol. 1 (CAB reviews: perspectives in agriculture, veterinary science, nutrition and natural resources), 1–13.

Singh, R. P., Hodson, D. P., Jin, Y., Lagudah, E. S., Ayliffe, M. A., Bhavani, S., et al. (2015). Emergence and spread of new races of wheat stem rust fungus: continued threat to food security and prospects of genetic control. *Phytopathology* 105 (7), 872–884. doi: 10.1094/PHYTO-01-15-0030-FI

Smeekens, S. (2000). Sugar-induced signal transduction in plants. *Annu. Rev. Plant Biol.* 51 (1), 49–81. doi: 10.1146/annurev.arplant.51.1.49

Soko, T., Bender, C. M., Prins, R., and Pretorius, Z. A. (2018). Yield loss associated with different levels of stem rust resistance in bread wheat. *Plant Dis.* 102 (12), 2531–2538. doi: 10.1094/PDIS-02-18-0307-RE

Stakman, E. C., Stewart, D. M., and Loegering, W. Q. (1962). *Identification of physiologic races of puccinia graminis var. tritici* (Washington: USDA).

Sukumaran, A., McDowell, T., Chen, L., Renaud, J., and Dhaubhadel, S. (2018). Isoflavonoid-specific prenyltransferase gene family in soybean: GmPT01, a pterocarpan 2-dimethylallyltransferase involved in glyceollin biosynthesis. *Plant J.* 96 (5), 966–981. doi: 10.1111/tpj.14083

Sumner, L. W., Amberg, A., Barrett, D., Beale, M. H., Beger, R., Daykin, C. A., et al. (2007). Proposed minimum reporting standards for chemical analysis. *Metabolomics* 3 (3), 211–221. doi: 10.1007/s11306-007-0082-2

Tadesse, W., Bishaw, Z., and Assefa, S. (2018). Wheat production and breeding in Sub-Saharan Africa: challenges and opportunities in the face of climate change. *Int. J. Clim. Change Strateg. Manag.* 11, 696–715 doi: 10.1108/IJCCSM-02-2018-0015

Tauzin, A. S., and Giardina, T. (2014). Sucrose and invertases, a part of the plant defense response to the biotic stresses. *Front. Plant Sci.* 5. doi: 10.3389/fpls.2014.00293

Terefe, T., Pretorius, Z. A., Visser, B., and Boshoff, W. H. P. (2019). First report of *Puccinia graminis* f. sp. *tritici* race PTKSK, a variant of wheat stem rust race Ug99 in south Africa. *Plant Dis.* 103 (6), 1421. doi: 10.1094/PDIS-11-18-1911-PDN

Terefe, T. G., Visser, B., Botha, W., Kozana, A., Roberts, R., Thompson, G. D., et al. (2021). Detection and molecular characterization of wheat stripe mosaic virus on wheat in south Africa. *Crop Prot.* 143, 105464. doi: 10.1016/j.cropro.2020.105464

Terefe, T. G., Visser, B., Pretorius, Z. A., and Boshoff, W. H. P. (2023). Physiologic races of puccinia triticina detected on wheat in south Africa from 2017 to 2020. *Eur. J. Plant Pathol.* 165 (1), 1–15. doi: 10.1007/s10658-022-02583-x

Tugizimana, F., Djami-Tchatchou, A. T., Steenkamp, P. A., Piater, L. A., and Dubery, I. A. (2019). Metabolomic analysis of defense-related reprogramming in *Sorghum bicolor* in response to *Colletotrichum sublineolum* infection reveals a functional metabolic web of phenylpropanoid and flavonoid pathways. *Front. Plant Sci.* 9, 1840. doi: 10.3389/fpls.2018.01840

Tugizimana, F., Engel, J., Salek, R., Dubery, I., Piater, L., and Burgess, K. (2020). "The disruptive 4IR in the life sciences: metabolomics," in *The disruptive fourth industrial revolution* (Cham: Springer), 227–256.

Van den Berg, R. A., Hoefsloot, H. C., Westerhuis, J. A., Smilde, A. K., and van der Werf, M. J. (2006). Centering, scaling, and transformations: improving the biological information content of metabolomics data. *BMC Genom.* 7 (1), 1–15. doi: 10.1186/1471-2164-7-142

Visser, B., Herselman, L., Park, R. F., Karaoglu, H., Bender, C. M., and Pretorius, Z. A. (2011). Characterization of two new puccinia graminis f. sp. tritici races within the Ug99 lineage in south Africa. *Euphytica* 179 (1), 119–127. doi: 10.1007/s10681-010-0269-x

Vogt, T. (2010). Phenylpropanoid biosynthesis. *Mol. Plant* 3 (1), 2–20. doi: 10.1093/mp/ssp106

Woldeab, G., Hailu, E., and Bacha, N. (2017). Protocols for race analysis of wheat stem rust (*Puccinia graminis f.* sp. *tritici*). 1–26.

Wu, J. Y., Wang, T. Y., Ding, H. Y., Zhang, Y. R., Lin, S. Y., and Chang, T. S. (2021). Enzymatic synthesis of novel vitexin glucosides. *Molecules* 26 (20), 6274. doi: 10.3390/molecules26206274

Xiao, M., and Wu, F. (2014). A review of environmental characteristics and effects of low-molecular weight organic acids in the surface ecosystem. *J. Environ. Sci.* 26 (5), 935–954. doi: 10.1016/S1001-0742(13)60570-7

Yan, M., Xue, C., Xiong, Y., Meng, X., Li, B., Shen, R., et al. (2020). Proteomic dissection of the similar and different responses of wheat to drought, salinity and submergence during seed germination. *J. Proteomics* 220, 103756. doi: 10.1016/j.jprot.2020.103756

Yang, D., Wang, T., Long, M., and Li, P. (2020). Quercetin: its main pharmacological activity and potential application in clinical medicine. *Oxid. Med. Cell. Longev.* 2020, 1–13. doi: 10.1155/2020/8825387

Zhao, W., Neyt, P., Van Lijsebettens, M., Shen, W. H., and Berr, A. (2019). Interactive and noninteractive roles of histone H2B monoubiquitination and H3K36 methylation in the regulation of active gene transcription and control of plant growth and development. *New Phytol.* 221 (2), 1101–1116. doi: 10.1111/nph.15418

Zhou, L., Liu, W., Xiong, Z., Zou, L., Chen, J., Liu, J., et al. (2016). Different modes of inhibition for organic acids on polyphenoloxidase. *Food Chem.* 199, 439–446. doi: 10.1016/j.foodchem.2015.12.034

Zhu, Q. F., Yan, J. W., Zhang, T. Y., Xiao, H. M., and Feng, Y. Q. (2018). Comprehensive screening and identification of fatty acid esters of hydroxy fatty acids in plant tissues by chemical isotope labeling-assisted liquid chromatography–mass spectrometry. *Anal. Chem.* 90 (16), 10056–10063. doi: 10.1021/acs.analchem.8b02839

Žilić, S. (2016). Phenolic compounds of wheat. their content, antioxidant capacity and bioaccessibility. *MOJ Food Process. Technol.* 2 (3), 37. doi: 10.15406/mojfpt.2016.02.00037

Frontiers in Plant Science

Cultivates the science of plant biology and its applications

The most cited plant science journal, which advances our understanding of plant biology for sustainable food security, functional ecosystems and human health.

Discover the latest Research Topics

See more →

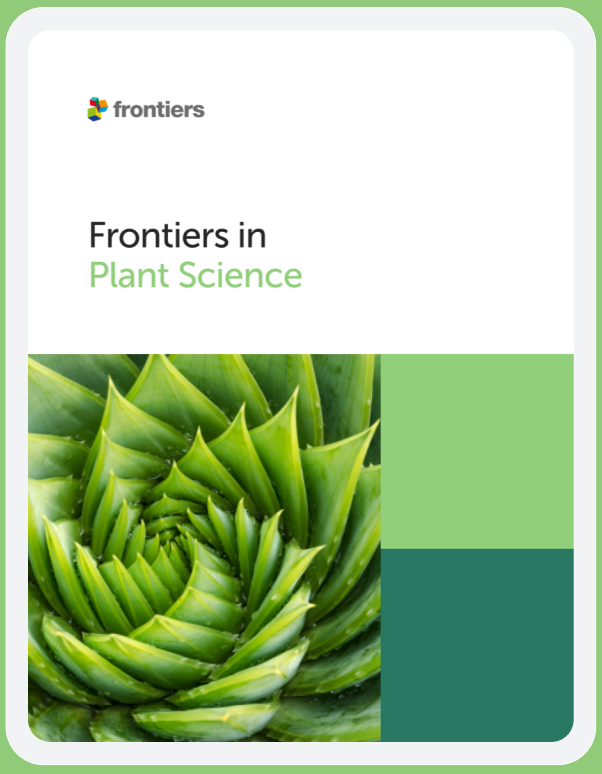

Frontiers

Avenue du Tribunal-Fédéral 34
1005 Lausanne, Switzerland
frontiersin.org

Contact us

+41 (0)21 510 17 00
frontiersin.org/about/contact